

Survey of Period Variations of Superhumps in SU UMa-Type Dwarf Novae

Taichi KATO,^{1*} Akira IMADA,² Makoto UEMURA,³ Daisaku NOGAMI,⁴ Hiroyuki MAEHARA,⁴ Ryoko ISHIOKA,⁵ Hajime BABA,⁶ Katsura MATSUMOTO,⁷ Hidetoshi IWAMATSU,¹ Kaori KUBOTA,¹ Kei SUGIYASU,¹ Yuichi SOEJIMA,¹ Yuuki MORITANI,¹ Tomohito OHSHIMA,¹ Hiroyuki OHASHI,¹ Junpei TANAKA,¹ Mahito SASADA,³ Akira ARAI,³ Kazuhiro NAKAJIMA,⁸ Seiichiro KIYOTA,⁹ Kenji TANABE,¹⁰ Kayuyoshi IMAMURA,¹⁰ Nanae KUNITOMI,¹⁰ Kenji KUNIHIRO,¹⁰ Hiroki TAGUCHI,¹⁰ Mitsuo KOIZUMI,¹⁰ Norimi YAMADA,¹⁰ Yuichi NISHI,¹⁰ Mayumi KIDA,¹⁰ Sawa TANAKA,¹⁰ Rie UEOKA,¹⁰ Hideki YASUL,¹⁰ Koichi MARUOKA,¹⁰ Arne HENDEN,¹¹ Arto OKSANEN,¹² Marko MOILANEN,¹² Petri TIKKANEN,¹² Mika AHO,¹² Berto MONARD,¹³ Hiroshi ITOH,¹⁴ Pavol A. DUBOVSKY,¹⁵ Igor KUDZEJ,¹⁵ Radka DANCIKOVA,¹⁶ Tonny VANMUNSTER,¹⁷ Jochen PIETZ,¹⁸ Greg BOLT,¹⁹ David BOYD,²⁰ Peter NELSON,²¹ Thomas KRAJCI,²² Lewis M. COOK,²³ Ken'ichi TORII,²⁴ Donn R. STARKEY,²⁵ Jeremy SHEARS,²⁶ Lasse-Teist JENSEN,²⁷ Gianluca MASI,²⁸ Tomáš HYNEK,²⁹ Rudolf NOVÁK,³⁰ Radek KOCIAN,²⁹ Lukáš KRÁL,²⁹ Hana KUČAKOVA,²⁹ Marek KOLASA,²⁹ Petr STASTNY,²⁹ Bart STAELS,^{11,31} Ian MILLER,³² Yasuo SANO,³³ Pierre de PONTIÈRE,³⁴ Atsushi MIYASHITA,³⁵ Tim CRAWFORD,³⁶ Steve BRADY,³⁷ Roland SANTALLO,³⁸ Tom RICHARDS,³⁹ Brian MARTIN,⁴⁰ Denis BUCZYNSKI,⁴¹ Michael RICHMOND,⁴² Jim KERN,⁴² Stacey DAVIS,⁴² Dustin CRABTREE,⁴² Kevin BEAULIEU,⁴² Tracy DAVIS,⁴² Matt AGGLETON,⁴² Etienne MORELLE,⁴³ Elena P. PAVLENKO,⁴⁴ Maksim ANDREEV,⁴⁵ Alexander BAKLANOV,⁴⁴ Michael D. KOPPELMAN,⁴⁶ Gary BILLINGS,⁴⁷ Ľubomír URBANČOK,⁴⁸ Yenel ÖGMEN,⁴⁹ Bernard HEATHCOTE,⁵⁰ Tomas L. GOMEZ,⁵¹ Alon RETTER,⁵² Krzysztof MULARCZYK,⁵³ Kamil ZŁOCZEWSKI,⁵⁶ Arkadiusz OLECH,⁵⁶ Piotr KEDZIERSKI,⁵³ Roger D. PICKARD,^{54,55} Chris STOCKDALE,⁵⁷ Jani VIRTANEN,⁵⁸ Koichi MORIKAWA,⁵⁹ Franz-Josef HAMBSCH,^{60,61,62} Gordon GARRADD,⁶³ Carlo GUALDONI,⁶⁴ Keith GEARY,¹¹ Toshihiro OMODAKA,⁶⁵ Nobuyuki SAKAI,⁶⁵ Raul MICHEL,⁶⁶ A. A. CÁRDENAS,⁶⁶ Kosmas D. GAZEAS,⁶⁷ Panos G. NIARCHOS,⁶⁷ A. V. YUSHCHENKO,⁶⁸ Franco MALLIA,⁶⁹ Marco FIASCHI,⁷⁰ Gerry A. GOOD,⁷¹ Stan WALKER,⁷² Nick JAMES,⁷³ Ken-ichi DOUZU,⁷ Wm Mack JULIAN II,⁷⁴ Neil D. BUTTERWORTH,⁷⁵ Sergey Yu. SHUGAROV,^{76,77} Igor VOLKOV,^{76,77} Drahomir CHOCHOL,⁷⁷ Natalia KATYSHEVA,⁷⁶ Alexander E. ROSENBUCH,⁷⁸ Maria KHRAMTSOVA,⁴⁵ Petri KEHUSMAA,⁷⁹ Maciej RESZELSKI,⁸⁰ James BEDIENT,¹¹ William LILLER,⁸¹ Grzegorz POJMAŃSKI,⁸² Mike SIMONSEN,⁸³ Rod STUBBINGS,⁸⁴ Patrick SCHMEER,⁸⁵ Eddy MUYLLAERT,⁸⁶ Timo KINNUNEN,⁸⁷ Gary POYNER,⁸⁸ Jose RIPERO,⁸⁹ Wolfgang KRIEBEL,^{61,90}

¹ Department of Astronomy, Kyoto University, Kyoto 606-8502

*tkato@kustastro.kyoto-u.ac.jp

² Okayama Astrophysical Observatory, National Astronomical Observatory of Japan, Asakuchi, Okayama 719-0232

³ Astrophysical Science Center, Hiroshima University, Kagamiyama, 1-3-1 Higashi-Hiroshima 739-8526

⁴ Kwasan and Hida Observatories, Kyoto University, Yamashina, Kyoto 607-8471

⁵ Subaru Telescope, National Astronomical Observatory of Japan, 650 North A'ohoku Place, Hilo, HI 96720, USA

⁶ Institute of Space and Astronautical Science, Japan Aerospace Exploration Agency, 3-1-1 Yoshinodai, Sagami-hara, Kanagawa 229-8510

⁷ Osaka Kyoiku University, 4-698-1 Asahigaoka, Osaka 582-8582

⁸ Variable Star Observers League in Japan (VSOLJ), 124 Isatotyo, Teradani, Kumano, Mie 519-4673

⁹ VSOLJ, 405-1003 Matsushiro, Tsukuba, Ibaraki 305-0035

¹⁰ Department of Biosphere-Geosphere Systems, Faculty of Informatics, Okayama University of Science, 1-1 Ridai-cho, Okayama, Okayama 700-0005

¹¹ American Association of Variable Star Observers, 49 Bay State Rd., Cambridge, MA 02138, USA

¹² Nyrola observatory, Jyvaskylan Sirius ry, Vertaalantie 419, FI-40270 Palokka, Finland

¹³ Bronberg Observatory, CBA Pretoria, PO Box 11426, Tiegerepoort 0056, South Africa

¹⁴ VSOLJ, 1001-105 Nishiterakata, Hachioji, Tokyo 192-0153

¹⁵ Vihorlat Observatory, Mierova 4, Humenne, Slovakia

¹⁶ Phillips Academy Andover, USA

¹⁷ Center for Backyard Astrophysics (Belgium), Walhostraat 1A, B-3401, Landen, Belgium

¹⁸ Nollenweg 6, 65510 Idstein, Germany

¹⁹ Camberwarra Drive, Craigie, Western Australia 6025, Australia

²⁰ Silver Lane, West Challow, Wantage, OX12 9TX, UK

²¹ RMB 2493, Ellinbank 3820, Australia

²² Center for Backyard Astrophysics New Mexico, PO Box 1351 Cloudcroft, New Mexico 83117, USA

²³ Center for Backyard Astrophysics (Concord), 1730 Helix Ct. Concord, California 94518, USA

²⁴ Department of Earth and Space Science, Graduate School of Science, Osaka University, 1-1 Machikaneyama-cho,

- Toyonaka, Osaka 560-0043*
- ²⁵ *DeKalb Observatory, H63, 2507 County Road 60, Auburn, Indiana 46706, USA*
- ²⁶ *“Pemberton”, School Lane, Bunbury, Tarporley, Cheshire, CW6 9NR, UK*
- ²⁷ *Sondervej 38, DK-8350 Hundslund, Denmark*
- ²⁸ *The Virtual Telescope Project, Via Madonna del Loco 47, 03023 Ceccano (FR), Italy*
- ²⁹ *Observatory and Planetarium of Johann Palisa, VSB – Technical University Ostrava, Trida 17. listopadu 15, Ostrava – Poruba 708 33, Czech Republic*
- ³⁰ *Institute of Computer Science, Faculty of Civil Engineering, Brno University of Technology, 602 00 Brno, Czech Republic*
- ³¹ *Center for Backyard Astrophysics (Flanders), American Association of Variable Star Observers (AAVSO), Alan Guth Observatory, Koningshofbaan 51, Hofstade, Aalst, Belgium*
- ³² *Furzehill House, Ilston, Swansea, SA2 7LE, UK*
- ³³ *VSOLJ, Nishi juni-jou minami 3-1-5, Nayoro, Hokkaido 096-0022*
- ³⁴ *American Association of Variable Star Observers (AAVSO), 15 rue Pré Mathy, 5170 Lesve (Profondeville), Belgium*
- ³⁵ *Seikei Meteorological Observatory, Seikei High School*
- ³⁶ *Arch Cape Observatory, 79916 W. Beach Road, Arch Cape, OR 97102*
- ³⁷ *5 Melba Drive, Hudson, NH 03051, USA*
- ³⁸ *Southern Stars Observatory, Po Box 60972, 98702 FAAA TAHITI, French Polynesia*
- ³⁹ *Woodridge Observatory, 8 Diosma Rd, Eltham, Vic 3095, Australia*
- ⁴⁰ *The King’s University College; Center for Backyard Astrophysics (Alberta), Edmonton, Alberta, Canada T6B 2H3*
- ⁴¹ *Conder Brow Observatory, Fell Acre, Conder Brow, Little Fell Lane, Scotforth, Lancs LA2 0RQ, England*
- ⁴² *Physics Department, Rochester Institute of Technology, Rochester, New York 14623, USA*
- ⁴³ *9 rue Vasco de GAMA, 59553 Lauwin Planque, France*
- ⁴⁴ *Crimean Astrophysical Observatory, 98409, Nauchny, Crimea, Ukraine*
- ⁴⁵ *Institute of Astronomy, Russian Academy of Sciences, 361605 Peak Terskol, Kabardino-Balkaria, Russia*
- ⁴⁶ *Department of Astronomy, University of Minnesota, MN, USA*
- ⁴⁷ *2320 Cherokee Drive NW, Calgary, Alberta, T2L 0X7 Canada*
- ⁴⁸ *Šíd Astronomical Observatory, Šíd 303, 986 01, The Slovak republic*
- ⁴⁹ *Green Island Observatory, Geçitkale, Magosa, via Mersin, North Cyprus*
- ⁵⁰ *Barfold Observatory, 165 Sievers Lane, Glenhope, 3444, Victoria, Australia*
- ⁵¹ *ICMAT (CSIC-UAM-UC3M-UCM), Serrano 113bis, 28006 Madrid, Spain*
- ⁵² *86a/6 Hamaccabim St., PO Box 4264, Shoham, 60850 Israel*
- ⁵³ *Warsaw University Observatory, Al. Ujazdowskie 4, 00-478 Warsaw, Poland*
- ⁵⁴ *The British Astronomical Association, Variable Star Section (BAA VSS), Burlington House, Piccadilly, London, W1J 0DU, UK*
- ⁵⁵ *3 The Birches, Shobdon, Leominster, Herefordshire, HR6 9NG, UK*
- ⁵⁶ *Nicolaus Copernicus Astronomical Center, Bartycka 18, 00-716 Warsaw, Poland*
- ⁵⁷ *8 Matta Drive, Churchill, Victoria 3842, Australia*
- ⁵⁸ *Ollilantie 98, 84880 Ylivieska, Finland*
- ⁵⁹ *468-3 Satoyamada, Yakage-cho, Oda-gun, Okayama 714-1213*
- ⁶⁰ *Groupe Européen d’Observations Stellaires (GEOS), 23 Parc de Levesville, 28300 Bailleau l’Evêque, France*
- ⁶¹ *Bundesdeutsche Arbeitsgemeinschaft für Veränderliche Sterne (BAV), Munsterdamm 90, 12169 Berlin, Germany*
- ⁶² *Vereniging Voor Sterrenkunde (VVS), Oude Bleken 12, 2400 Mol, Belgium*
- ⁶³ *PO Box 157, NSW 2340, Australia*
- ⁶⁴ *22100 Como, Italy*
- ⁶⁵ *Faculty of Science, Kagoshima University, 1-21-30 Korimoto, Kagoshima, Kagoshima 890-0065*
- ⁶⁶ *Instituto de Astronomía UNAM, Apartado Postal 877, 22800 Ensenada B.C., México*
- ⁶⁷ *Department of Astrophysics, Astronomy and Mechanics, University of Athens, Panepistimipolis, GR-157 84, Zografos, Athens, Greece*
- ⁶⁸ *Department of Astronomy and Astronomical Observatory, Odessa National University, Shevchenko Park, 270014 Odessa, Ukraine*
- ⁶⁹ *Campo Catino Astronomical Observatory, Via dei Siculi, 37, 04100 Latina, Italy*
- ⁷⁰ *Astronomical Observatory G. Colombo, Via Caltana 242, 35011 Campodarsego PD, Italy*
- ⁷¹ *Albuquerque, New Mexico, USA*
- ⁷² *Wharemaru Observatory, P.O. Box 13, Awanui 0552, New Zealand*
- ⁷³ *11 Tavistock Road, Chelmsford, Essex CM1 6JL, UK*
- ⁷⁴ *4597 Rockaway Loop, Rio Rancho, NM 87124, USA*
- ⁷⁵ *24 Payne Street, Mount Louisa, Queensland 4814, Australia*
- ⁷⁶ *Sternberg Astronomical Institute, Moscow University, Universitetsky Ave., 13, Moscow 119992, Russia*
- ⁷⁷ *Astronomical Institute of the Slovak Academy of Sciences, 05960, Tatranska Lomnica, the Slovak Republic*

⁷⁸ *Main Astronomical Observatory, Golosiiv, Kyiv-127, 03680, Ukraine*

⁷⁹ *Slope Rock Observatory, Uima-altaankatu 19, FIN-05820 Hyvinkaa, Finland*

⁸⁰ *Al. 1-go Maja 29/4, 64500 Szamotuly, Poland*

⁸¹ *Center for Nova Studies, Casilla 5022, Viña del Mar, Chile*

⁸² *Warsaw University Observatory, Al. Ujazdowskie 4, 00-478 Warsaw, Poland*

⁸³ *AAVSO, C. E. Scovill Observatory, 2615 S. Summers Rd., Imlay City, Michigan 48444, USA*

⁸⁴ *Tetoora Observatory, Tetoora Road, Victoria, Australia*

⁸⁵ *Bischmisheim, Am Probstbaum 10, 66132 Saarbrücken, Germany*

⁸⁶ *Vereniging Voor Sterrenkunde (VVS), Moffelstraat 13 3370 Boutersem, Belgium*

⁸⁷ *Sinirinnantie 16, SF-02660 Espoo, Finland*

⁸⁸ *BAA Variable Star Section, 67 Ellerton Road, Kingstanding, Birmingham B44 0QE, UK*

⁸⁹ *President of CAA (Centro Astronomico de Avila) and Variable and SNe Group M1, Buenavista 7, Ciudad Sto. Domingo, 28110 Algete/Madrid, Spain*

⁹⁰ *D-84072 Osterwaal Post Au, Germany*

(Received 200 0; accepted 200 0)

Abstract

We systematically surveyed period variations of superhumps in SU UMa-type dwarf novae based on newly obtained data and past publications. In many systems, the evolution of superhump period are found to be composed of three distinct stages: early evolutionary stage with a longer superhump period, middle stage with systematically varying periods, final stage with a shorter, stable superhump period. During the middle stage, many systems with superhump periods less than 0.08 d show positive period derivatives. We present observational characteristics of these stages and greatly improved statistics. Contrary to the earlier claim, we found no clear evidence for variation of period derivatives between superoutburst of the same object. We present an interpretation that the lengthening of the superhump period is a result of outward propagation of the eccentricity wave and is limited by the radius near the tidal truncation. We interpret that late stage superhumps are rejuvenized excitation of 3:1 resonance when the superhumps in the outer disk is effectively quenched. The general behavior of period variation, particularly in systems with short orbital periods, appears to follow the scenario proposed in Kato et al. (2008). We also present an observational summary of WZ Sge-type dwarf novae. Many of WZ Sge-type dwarf novae showed long-enduring superhumps during the post-superoutburst stage having periods longer than those during the main superoutburst. The period derivatives in WZ Sge-type dwarf novae are found to be strongly correlated with the fractional superhump excess, or consequently, mass ratio. WZ Sge-type dwarf novae with a long-lasting rebrightening or with multiple rebrightenings tend to have smaller period derivatives and are excellent candidate for the systems around or after the period minimum of evolution of cataclysmic variables.

Key words: accretion, accretion disks — stars: novae, cataclysmic variables — stars: dwarf novae

1. Introduction

Dwarf novae (DNe) are a class of cataclysmic variables (CVs), which are close binary systems consisting of a white dwarf and a red-dwarf secondary transferring matter via the Roche-lobe overflow. SU UMa-type dwarf novae, a subclass of DNe, show superhumps during their long, bright outbursts (superoutbursts) [see e.g. Vogt (1980); Warner (1985)]. The origin of superhumps is basically understood as a result of varying tidal dissipation in an eccentric accretion disk, whose eccentricity is excited by the 3:1 orbital resonance (Whitehurst 1988; Osaki 1989; Osaki 1996).

Until the mid-1990's, the period of superhumps (P_{SH}) had been considered to decrease during superoutburst (cf. Warner 1985), which was explained as a result of decreasing radius of the accretion disk during superoutburst (Osaki 1985). In recent years, the existence of objects with positive period derivatives ($P_{dot} = \dot{P}/P$) of super-

humps, particularly among systems with short orbital periods (P_{orb}) has been established (see e.g. Kato et al. 2001d). Since the superhump period, or its variation, is related to the radius of the accretion disk, or propagation of the eccentricity wave (see e.g. Hirose, Osaki 1990; Lubow 1991; Kato et al. 1998a), the period variation is expected to provide diagnostics of the dynamics in the outbursting accretion disk. A number of pieces of research have been issued in this perspective (e.g. Uemura et al. 2005; Imada et al. 2006a; Soejima et al. 2009). In particular, Uemura et al. (2005) reported markedly different P_{dot} 's between different superoutbursts of TV Crv. Uemura et al. (2005) proposed an interpretation that this difference is caused by the different mass (angular momentum) in the accretion disk at the onset of the superoutburst, following the theory by Osaki, Meyer (2003). If this is confirmed, P_{dot} is expected to provide an observational measure of the mass in the disk.

More recently, long-lasting superhumps with period un-

expectedly ($\sim 0.5\%$) longer than superhump periods during the slowly fading stage of WZ Sge-type superoutbursts have been established (Kato et al. 2008). Kato et al. (2008) suggested that they are superhumps arising from the disk matter outside the 3:1 resonance, or around the tidal truncation. Kato et al. (2008) also proposed the transient 2:1 resonance in the outer disk could regulate the excitation and propagation of the 3:1 resonance, leading to a novel interpretation of the variety of P_{dot} in different SU UMa-type dwarf novae.

Motivated by these suggestions, we present a new systematic survey of P_{dot} in SU UMa-type dwarf novae. The lack of published times of maxima in some of references having been one of the major obstacles in the research of period variations of superhumps, we present times of all measured superhumps for potential future analysis.

In section 2, we describe our observation and method of analysis. In section 3, we describe general properties of period variation in superhumps. General discussions are given in section 4. Section 5 is dedicated to WZ Sge-type dwarf novae. These sections are placed before section 6 (individual objects) because of the large amount of data presented in section 6. We finally give section 7 for a summary of new findings. The names of the objects are sometimes abbreviated in tables, figures and sections 3 and 4; for original names of these objects, refer to section 6. Alternative designations were sometimes used when the original names were difficult to abbreviate properly.

2. Observation and Analysis

The data were obtained under campaigns led by the VSNET Collaboration (Kato et al. 2004c). In some objects, we used archival data for published papers, and the public data from the AAVSO International Database¹ as a supplementary purpose. The majority of the data were acquired by time-resolved CCD photometry of with 30 cm-class telescopes, whose observational details on individual objects will be presented in separate papers dealing with in-depth analysis and discussion on individual objects.² We generally restricted our analysis to superoutburst plateau and rapid fading stage. In a few very well-observed cases, we dealt with post-superoutburst evolution of superhumps.

After correction for systematic differences between observers, and subtracting the general trend by fitting low-

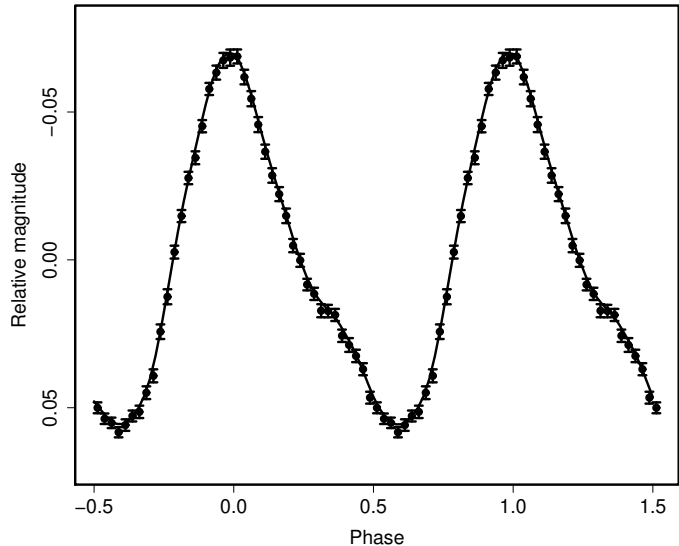


Fig. 1. Template light curve (phase-averaged light curve of superhumps in GW Lib).

order (typically three to five) polynomials, we extracted times of superhump maxima by numerically fitting a template superhump light curve around the times of observed maxima. We did not use the full superhump cycle but generally used phases -0.4 to 0.4 in order to minimize the contamination from potentially present secondary maxima. We employed a phase-averaged (and spline interpolated) light curve of superhumps of GW Lib as the template, which is one of the best-sampled object among all SU UMa-type dwarf novae (figure 1).

This usage of a fixed template has an advantage of much higher signal-to-noise and thereby higher precision in determining maxima than eye estimates (typically reducing the scatter by a factor of ~ 5) or than fitting using lower-quality template light curves prepared for individual objects. The usage of a fixed template, however, has a potential disadvantage of systematic errors caused by the variation in the superhump profile and the difference of the profile from the template. These potential effects have been examined by comparisons between previously reported times of maxima (referring to the same data) and those determined in the present work. No significant systematic differences were found to affect the determination of P_{dot} . In some cases, comparisons with other authors have yielded significant constant offsets (individually described in section 6), presumably caused by different methods in extracting maxima. These offsets were also found to be insensitive to determining P_{dot} after adjustment by constant offsets.

We generally used Phase Dispersion Minimization (PDM, Stellingwerf 1978) for determining mean superhump periods described in the text. The values determined using linear regressions to times of superhump maxima can be slightly different from those determined with the PDM. When segments (in E) are shown, these periods were derived from a linear regression of maxima times of

¹ <<http://www.aavso.org/data/download/>>.

² During this analysis, it became evident that the KU computer lost ntp connection between 2008 May 16 and November 25. The times of observations during this period have been corrected by correlating with other simultaneous observations. The maximum correction amounted to 0.005 d and estimated maximum error of correction 0.001 d. The details of the corrections and these effects will be discussed in Ohshima et al., in preparation. The objects affected were V466 And, VY Aqr, KP Cas, V1251 Cyg, V630 Cyg, HO Del, V699 Oph, PV Per, UW Tri, DO Vul, NSV 5285, SDSS J1627, OT J0211, OT J0238, OT J1631 and OT J1914. The maximum uncertainty caused by these corrections were 0.00001–0.00002 d for periods of V466 And, V1251 Cyg and PV Per, and less than 0.00001 d for other objects. The maximum uncertainty for P_{dot} was less than 1×10^{-5} .

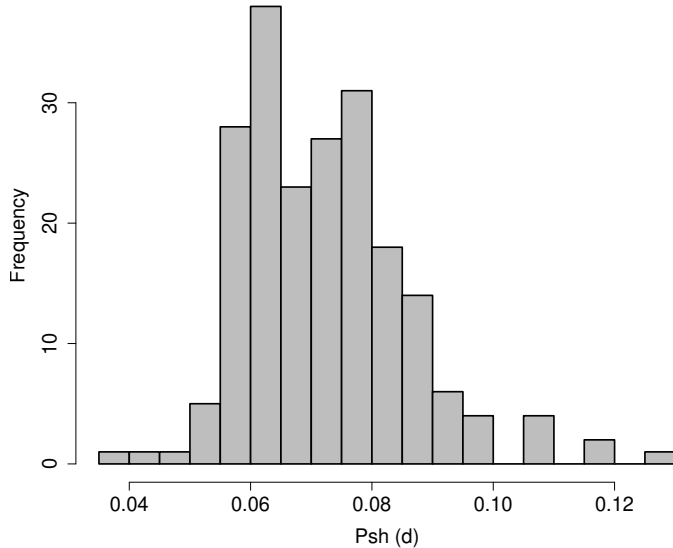


Fig. 2. Distribution of superhump periods in this survey.

superhumps unless otherwise noticed.

Since we mainly focus on period variations of superhumps, we only present superhump maxima and mostly omit individual light curves of outbursts, light curves of superhumps and results of PDM analysis to save space in section 6. Individual $O-C$ diagrams are not usually shown for the same reason; selected examples of $O-C$ diagrams are summarized in section 3. We, however, tried to include a comparison of $O-C$ diagrams if different superoutbursts of the same object were observed, and tried to include the result of period analysis and the superhump profile if they provide the first solid presentation. In section 6, we also included selected observations of several superoutbursts not sufficiently covered to determine P_{dot} , if the determination of P_{SH} is meaningful in itself or if the inclusion improves the statistical quality. We also included partially observed superoutbursts for completeness, and this inclusion for future research is justified by a suggestion that P_{dot} can be measured from a combination of different superoutbursts (subsection 3.8).

We also calculated superhump periods and derivatives when times of superhump maxima were available in the literature. We employed the same procedure as in the analysis of our own data. This work comprises the largest homogeneous survey of variation of superhumps in SU UMa-type dwarf novae.

3. General Properties

3.1. Distribution of Superhump Periods

Figure 2 shows the distribution of superhump periods in this survey. With the best statistics ever achieved, we can see the maximum of the distribution close to $P_{\text{SH}} = 0.06$ d and a monotonous decrease in population towards longer periods.

3.2. General Tendency in Period Variations

As already demonstrated by several authors (e.g. Olech et al. 2003; Soejima et al. 2009), short- P_{SH} SU UMa-type dwarf novae usually show three distinct stages of period evolution (figure 3): (A) early stage of superhump evolution having a longer P_{SH} , (B) middle segment with a stabilized period usually with a positive P_{dot} ,³ and (C) late stage with a shorter, stable superhump period. In well-observed systems, the transitions between stages A and B, and stages B and C are usually abrupt, associated with discontinuous period changes. Although Olech et al. (2003) referred these transitions to decreasing superhump periods, treating as if they are smooth variations, we adopted the above phenomenological staging because the transitions are usually discontinuous.

Figure 4 shows $O-C$ diagrams of representative systems taken from section 6 and from literature, in which systems all the three stages were observed. The figures are arranged in the increasing order of superhump periods (the periods given in the figures refer to the mean periods during the stage B). The thin lines are quadratic fits to the stage B. Note that the range of cycle counts (E) is different between figures and that the start of stage B was defined to be $E = 20$ for better visualization.

We can see the following general tendency on these figures: (1) the period derivative during the stage B becomes systematically smaller with increasing P_{SH} , and (2) the duration of the stage B becomes systematically shorter with increasing P_{SH} or the fractional superhump excess $\epsilon = P_{\text{SH}}/P_{\text{orb}} - 1$ (figures 5, 6).

The last four long- P_{SH} systems (SU UMa, DH Aql, SDSS J1556, UV Gem) and BZ Cir have nearly zero or negative P_{dot} , but are included in this sequence of figures because they have all the three distinct stages and because the behavior in these objects can be understood as a smooth extension of the tendency in shorter- P_{SH} systems.

Note also that a few historically controversial systems (V436 Cen: Semeniuk 1980, and Warner 1983 for a discussion; OY Car: Krzeminski, Vogt 1985, and Patterson et al. 1993 for a discussion) can well fit the present general tendency and no anomalies were apparent.

3.3. Transition to a Shorter Period

Following the stage B, most of well-observed objects showed a transition to a stage with a shorter P_{SH} . When stage A was not observed or non-existent, this transition on the $O-C$ diagram appears as a form of “period break”. The corresponding location of this break is shown in figure 3. Figure 7 shows $O-C$ diagrams of selected systems taken from section 6 and literature, in which systems this transition (stage B to stage C) was recorded, but stage A was not observed. The durations of the stage B in

³ This segment occasionally appears to be composed of two linear segments forming a “V”-shaped dip. Although this could suggest that the stage B may not be a continuous entity, we preserve the current staging for simplicity and for direct comparison with earlier works. Such instances will be individually discussed in section 6.

Table 1. List of Superoutbursts.

Subsection	Object	Year	Observers or references*
6.1	FO And	1994	Kato (1995b)
6.2	KV And	1994	Kato (1995a)
	KV And	2002	Tor, KU, Tan
6.3	LL And	1993	Kato (2004)
	LL And	2004	KU, AAVSO, Mhh, Njh
6.4	V402 And	2005	Mhh, AAVSO
	V402 And	2006	Mhh
	V402 And	2008	Mhh
6.5	V455 And	2007	BSt, Mhh, KU, DRS, Ioh, HHO, AAVSO, Kis, PIE, Njh, Mas, DPP, VAN, Nov, Nyr, OUS, GOT, RIT, BXS, DPV, LBr, CTX, Hid, Boy, Kop, MEV, MNi
6.6	V466 And	2008	KU, HHO, Njh, DPV, PIE, Mhh, OUS, URB, JSh, AAVSO, Nyr, RIT, CTX, Ost, BSt, MEV, Ter, VIR, DPP, Nov, Kis
6.7	DH Aql	2002	OUS, RIX, KU, Mor, MLF, Nel, Kis, San, Cac
	DH Aql	2003	KU, Tor
	DH Aql	2007	Kis
	DH Aql	2008	Kis
6.8	V725 Aql	1999	Uemura et al. (2001)
	V725 Aql	2005	AAVSO
6.9	V1141 Aql	2002	Olech (2003)
	V1141 Aql	2003	Hid, Kra, San
6.10	VY Aqr	1986	Patterson et al. (1993)
	VY Aqr	2008	MLF, Mhh, OUS, GBo, DPV, KU, GOT, Kis, Ioh, URB, PIE, DPP, Kag, SAN
6.11	EG Aqr	2006	Imada et al. (2008b)
	EG Aqr	2008	Mhh, Njh, Ogm
6.12	BF Ara	2002	Kato et al. (2003a)
6.13	V663 Ara	2004	MLF
6.14	V877 Ara	2002	Kato et al. (2003d)
6.15	BB Ari	2004	KU, Hid, Mhh, OUS, Nyr, VAN, COO
6.16	HV Aur	2002	Tor, OUS, Oud, KU, Nyr, DRS, Hid, Mas
6.17	TT Boo	2004	COO, PIE, Hid, Njh, Mhh, Bil, Suc, Olech et al. (2004a)
6.18	UZ Boo	1994	Oud
	UZ Boo	2003	OUS, Njh, VAN, OKU, Nyr, Mhh, Ost, Njh, AAVSO
6.19	NN Cam	2007	DPV, VAN
6.20	SY Cap	2008	Njh, Mhh, Nel, KU
6.21	AX Cap	2004	MLF, Chi, KU, Hid, GBo
–	OY Car	1980	Krzeminski, Vogt (1985)

*Key to observers: Ath (Athens Univ.), Bed[†](J. Bedient), Bil[†](G. Billings), Boy[†](D. Boyd), BSt[†](B. Staels), Buc (D. Buczynski), But (N. Butterworth), BXS (S. Brady), COO[†](L. Cook), CTX[†](T. Crawford), Chi (Concepcion), DPP[†](P. de Ponthiere), DPV (P. Dubovsky), DRS (D. Starkey), Fia (M. Fiaschi), GAR (G. Garradd), GBo (G. Bolt), GCO (C. Gualdoni), GGA (G. Good), GOT (T. Gomez), HHO (Higashi-Hiroshima Observatory), Hea (B. Heathcote), Hen[†](A. Henden), Hid (Hida Observatory), HMB (F. Hamsch), IMi (I. Miller), Ioh (H. Itoh), JDW (D. West), JEN[†](L. Jensen), JSh[†](J. Shears), JWM (W. M. Julian II), KU (Kyoto University, campus observatory), Kag (Kagoshima University), Keh (P. Kehusmaa), KGE[†](K. Geary), Kis (S. Kiyota), Kop[†](M. Koppelman), Kra[†](T. Krajci), Kry (T. Kryachko et al.), LBr (L. Brat), Lil[†](W. Liller), MEV[†](E. Morelle), MLF[†](B. Monard), MNi (M. Nicholson), Mar (B. Martin), Mas (G. Masi), Mhh (H. Maehara), Mor (K. Morikawa), Myy (M. Moriyama), NDJ (N. James), Nel (P. Nelson), Njh (K. Nakajima), Nov (R. Novák), Nyr[†](Nyrola and Hankasalmi Obs.), Ogm[†](Y. Ogmen), OKU (Osaka Kyoiku U.), Ost (Ostrava team), OUS (Okayama University of Science), Oud (Ouda station), PIE (J. Pietz), Pav (E. Pavlenko et al.), PXR[†](R. Pickard), RIT[†](M. Richmond), RIX[†](T. Richards), Res[†](M. Reszelski), Ret (A. Retter), Ros (A. Rosenbush), SAN (R. Santallo), SAC (Seikei High School), SPA (San Pedro de Atacama), SXN (M. Simonsen), San (Y. Sano), Shu (S. Shugarov), Sto (C. Stockdale), Suc (A. Sucker), Tan (K. Tanabe), Ter (Terskol Observatory), Tor (K. Torii), UNAM (UNAM, Mexico), URB (L. Urbancok), VAN[†](T. Vanmunster), VIR (J. Virtanen), Wal (S. Walker), War (Warsaw University), AAVSO (AAVSO database), ASAS (ASAS-3 data)

[†]includes observations from the AAVSO database.

Table 1. (continued) List of Superoutbursts.

Subsection	Object	Year	Observers or references
6.22	GX Cas	1994	Nogami et al. (1998c)
	GX Cas	1996	JEN
	GX Cas	1999	KU
	GX Cas	2006	KU, Njh
6.23	HT Cas	1985	Zhang et al. (1986)
6.24	KP Cas	2008	JSh, Boy, OUS, BSt, JWM, Nov, KU, Mhh, Njh
6.25	V452 Cas	1999	KU
	V452 Cas	2007	Shears et al. (2008d)
	V452 Cas	2008	Boy
6.26	V359 Cen	2002	Kato et al. (2002c)
–	V436 Cen	1978	Semeniuk (1980)
6.27	V485 Cen	1997	Olech (1997)
	V485 Cen	2001	KU, Ret
	V485 Cen	2004	Nel, Hea
6.28	V1040 Cen	2002	MLF, GBo
6.29	WX Cet	1989	O'Donoghue et al. (1991)
	WX Cet	1998	Kato et al. (2001b), JEN
	WX Cet	2001	KU, Sterken et al. (2007)
	WX Cet	2004	Mhh, Njh
–	Z Cha	1982	Warner, O'Donoghue (1988)
6.30	RX Cha	2009	Nel
6.31	BZ Cir	2004	MLF, Chi
6.32	CG CMa	1999	Kato et al. (1999b)
6.33	PU CMa	2003	Nel, MLF, SAN
	PU CMa	2005	Mhh, Njh, AAVSO
	PU CMa	2008	Nel, Njh, Kis, Mhh
6.34	YZ Cnc	2007	Njh
6.35	AK Cnc	1992	Kato (1994)
	AK Cnc	1999	JEN
	AK Cnc	2003	Tor, PIE, KU, Tan, Nyr, Mhh
6.36	CC Cnc	2001	Kato et al. (2002e)
–	EG Cnc	1996	Kato et al. (2004b), Patterson et al. (1998)
6.37	AL Com	1995	Nogami et al. (1997a), Howell et al. (1996), Pych, Olech (1995), Patterson et al. (1996)
	AL Com	2001	Ishioka et al. (2002)
	AL Com	2008	Uemura et al. (2008b)
6.38	GO Com	2003	Imada et al. (2005), Pav
	GO Com	2005	KU, Mhh, Njh, VAN, Boy
	GO Com	2006	Njh, Kis, Mhh, GOT
	GO Com	2008	Mhh, DPV
6.39	V728 CrA	2003	MLF, Nel, SAN
6.40	VW CrB	2001	Nogami et al. (2004b)
	VW CrB	2003	Nogami et al. (2004b)
	VW CrB	2006	AAVSO
6.41	TU Crt	1998	Mennickent et al. (1998)
	TU Crt	2001	KU, Kis
	TU Crt	2009	Njh, Kis
6.42	TV Crv	2001	Uemura et al. (2005)
	TV Crv	2003	Uemura et al. (2005)
	TV Crv	2004	Uemura et al. (2005)
6.43	V337 Cyg	2006	Kra, Boy, VAN
6.44	V503 Cyg	2002	KU, DRS, PIE
	V503 Cyg	2008	Njh, KU
6.45	V550 Cyg	2000	KU, Oud, PIE
6.46	V630 Cyg	1996	Nogami et al. (2001a)
	V630 Cyg	2008	KU, Mhh, Ioh

Table 1. (continued) List of Superoutbursts.

Subsection	Object	Year	Observers or references
6.47	V632 Cyg	2008	DPV, Njh, AAVSO, VIR, Mhh
6.48	V1028 Cyg	1995	Baba et al. (2000), AAVSO
	V1028 Cyg	1996	Oud, AAVSO
	V1028 Cyg	1999	KU, Buc
	V1028 Cyg	2001	Bil
	V1028 Cyg	2002	KU, OUS, Tor, Bil
	V1028 Cyg	2004	Njh, Nyr, DRS
	V1028 Cyg	2008	IMi, PXR
6.49	V1113 Cyg	1994	Kato et al. (1996c)
	V1113 Cyg	2008	Nov, Njh
6.50	V1251 Cyg	1991	Kato (1995c)
	V1251 Cyg	2008	Mhh, Njh, HHO, IMi, KU, Ioh, CTX, Mas, JSh, DPV, Keh, SAc
6.51	V1316 Cyg	2006	Boyd et al. (2008a)
6.52	V1454 Cyg	2006	Njh, AAVSO
6.53	V1504 Cyg	1994	Nogami, Masuda (1997)
	V1504 Cyg	2008	Mhh, Ioh
	V1504 Cyg	2009	KU
6.54	V2176 Cyg	1997	AAVSO, Novák et al. (2001), Kwast, Semeniuk (1998)
6.55	HO Del	1994	Kato et al. (2003c)
	HO Del	2001	Kato et al. (2003c)
	HO Del	2008	KU, DPV, Mhh, AAVSO, OUS, MEV, Kis
6.56	BC Dor	2003	Nel, RIX
6.57	CP Dra	2003	KU
	CP Dra	2009	IMi, Boy, Mhh, Bst, Nyr
6.58	DM Dra	2003	Tor, Tan, Hid
6.59	DV Dra	2005	Njh, VAN, Mhh, Hid
6.60	KV Dra	2002	KU, Tor, PIE, Nyr, OUS, DRS, COO, VAN, Bil
	KV Dra	2004	KU, Mhh, OUS, Boy
	KV Dra	2005	Mhh
	KV Dra	2009	DPV, Njh, Mhh, OUS, KU, Ioh, Hyn
6.61	MN Dra	2002a	Nogami et al. (2003b)
	MN Dra	2002b	Nogami et al. (2003b)
	MN Dra	2003	Nyr
	MN Dra	2008	MEV
–	IX Dra	2003	Olech et al. (2004b)
6.62	XZ Eri	2003a	Uemura et al. (2004)
	XZ Eri	2003b	KU, Njh
	XZ Eri	2007	SPA, Njh, Mhh
	XZ Eri	2008	AAVSO, Njh, Mhh, GBo, Kis
6.63	AQ Eri	1991	Kato (1991a)
	AQ Eri	1992	Oud
	AQ Eri	2006	Njh
	AQ Eri	2008	Njh, Ioh, OUS, DPV, Kis, Nel, KU
6.64	UV Gem	2003	Oud, KU, PIE, VAN, Nyr, Tan
	UV Gem	2008	Njh, KU
6.65	AW Gem	1995	Kato (1996b)
	AW Gem	2008	Mhh, OUS
	AW Gem	2009	Njh, AAVSO
6.66	CI Gem	2005	AAVSO, VAN, Njh
6.67	IR Gem	1991	Kato (2001a)
	IR Gem	2009	Njh, OUS, SAc
6.68	CI Gru	2004	MLF
–	V592 Her	1998	Kato et al. (2002f)
–	V660 Her	2004	Olech et al. (2005)

Table 1. (continued) List of Superoutbursts.

Subsection	Object	Year	Observers or references
6.69	V844 Her	1997	JEN
	V844 Her	1999	Oizumi et al. (2007)
	V844 Her	2002	Oizumi et al. (2007)
	V844 Her	2006	Oizumi et al. (2007)
	V844 Her	2008	KU, DPV, Mhh
6.70	V1108 Her	2004	AAVSO, VAN, KU, San, RIT, Hen, Kop, COO, Njh, Mhh, DRS, Boy, CTX
6.71	RU Hor	2003	MLF, GBo
	RU Hor	2008	MLF, GBo
6.72	CT Hya	1999	Kato et al. (1999a)
	CT Hya	2000	KU, Kis
	CT Hya	2002a	KU
	CT Hya	2002b	KU, Hid, Kis, Tor, Tan
	CT Hya	2009	Njh, OUS, Kis
6.73	MM Hya	1998	JEN, Oud
	MM Hya	2001	SAAO, KU
6.74	VW Hyi	1972	Vogt (1974)
	VW Hyi	2000	Lil
6.75	RZ Leo	2000	Ishioka et al. (2001), AAVSO
	RZ Leo	2006	Njh, Mhh, KU
6.76	GW Lib	2007	MLF, HHO, KU, Kis, Mhh, Njh, Nel, Ioh, San
6.77	RZ LMi	2004	Olech et al. (2008)
	RZ LMi	2005	COO
6.78	SS LMi	2006	Shears et al. (2008a)
6.79	SX LMi	1994	Nogami et al. (1997b)
	SX LMi	2001	KU
	SX LMi	2002	KU
6.80	BR Lup	2003	MLF, GBo, Nel
	BR Lup	2004	MLF, RIX
6.81	AY Lyr	1987	Udalski, Szymanski (1988)
	AY Lyr	2008	OUS, Ioh, Njh, SAc
	AY Lyr	2009	OUS, Njh
6.82	DM Lyr	1996	Nogami et al. (2003a)
	DM Lyr	1997	Nogami et al. (2003a)
	DM Lyr	2002	Tor, KU
6.83	V344 Lyr	1993	Kato (1993)
6.84	V358 Lyr	2008	KU, Njh, Mhh, Boy, AAVSO
6.85	V419 Lyr	1999	Nov, KU
	V419 Lyr	2006	Boy, DPV, Rutkowski et al. (2007)
6.86	V585 Lyr	2003	PIE, Nov, COO, KU, Tor, Kra, Nyr, Hid, Hen, War
–	TU Men	1980	Stolz, Schoembs (1984)
6.87	AD Men	2004	MLF
6.88	FQ Mon	2004	KU, Hid, Mas, Kis, MLF, PIE, Mhh, COO, Nyr
	FQ Mon	2006	Kis, KU, Mhh, Njh
	FQ Mon	2007	Njh, Mhh, Kis, GBo
6.89	AB Nor	2002	Kato et al. (2004a)
6.90	DT Oct	2003a	Kato et al. (2004a)
	DT Oct	2003b	Nel
	DT Oct	2008	RIX
6.91	V699 Oph	2003	San, Nel, Kra, DRS
	V699 Oph	2008	KU, GBo
6.92	V2051 Oph	1999	GAR, Wal, KU
	V2051 Oph	2003	Sto, SAN, Hea, Nel, MLF, San, Kis, Njh, Hid
	V2051 Oph	2009	Kis, KU
6.93	V2527 Oph	2004	MLF, GBo, Chi, Hid, Mhh, KU, Kis
	V2527 Oph	2006	Njh, Nel
	V2527 Oph	2008	Mhh, Ioh, Njh

Table 1. (continued) List of Superoutbursts.

Subsection	Object	Year	Observers or references
6.94	V1159 Ori	1993	Patterson et al. (1995)
	V1159 Ori	2002	KU, Kis, Tor, Tan, Oud
6.95	V344 Pav	2004	Uemura et al. (2004)
6.96	EF Peg	1991	Kato (2002b), Howell et al. (1993)
	EF Peg	1997	KU
6.97	V364 Peg	2004	Kra, VAN
6.98	V368 Peg	2000	KU, But, Nyr, Kra
	V368 Peg	2005	Mhh, Njh, GCO
	V368 Peg	2006	Njh, DPV
6.99	V369 Peg	1999	Kato, Uemura (2001b), JEN
6.100	UV Per	1991	Oud
	UV Per	2000	KU, Tor, Buc, Mas, PIE, Mar
	UV Per	2003	OUS, COO, AAVSO, VAN, PIE, Boy, Ost, Nyr, KU, Bil
	UV Per	2007	DPV, OUS, MEV
6.101	PU Per	2009	KU, Njh, Ioh, Mhh
6.102	PV Per	2008	KU, Mhh, Boy
6.103	QY Per	1999	KU, COO, Mar, VAN, Buc, JEN, AAVSO
	QY Per	2005	Mhh, KU, Njh, OUS
6.104	V518 Per	1992	Kato et al. (1995)
6.105	TY PsA	2008	Njh, Ioh, SAc
6.106	TY Psc	2005	Mhh
	TY Psc	2008	URB, Ost, Njh, OUS, Kis
6.107	EI Psc	2001	Uemura et al. (2002a), Skillman et al. (2002)
	EI Psc	2005	COO, Njh, Mhh
6.108	VZ Pyx	1996	Kato, Nogami (1997a)
	VZ Pyx	2000	Kis
	VZ Pyx	2004	Kis
	VZ Pyx	2008	Njh, Ioh, Kis
6.109	DV Sco	2004	MLF, Chi, GBo
	DV Sco	2008	MLF, GBo
6.110	MM Sco	2002	Kato et al. (2004a)
6.111	NY Ser	1996	Nogami et al. (1998b)
–	QW Ser	2000	Nogami et al. (2004a)
	QW Ser	2002	Nogami et al. (2004a)
6.112	RZ Sge	1994	Kato (1996a)
	RZ Sge	1996	Oud, Semeniuk et al. (1997a)
	RZ Sge	2002	KU
6.113	WZ Sge	1978	Patterson et al. (1981), Bohusz, Udalski (1979), Heiser, Henry (1979), Targan (1979)
	WZ Sge	2001	KU, Oud, Mas, Mar, RIT, PIE, VAN, Nyr, DRS, Nov, Mor, COO, Buc, UNAM, Ath, Kis, Kra, Hyn, GGA, San, Boy, Fia, Myy, JDW, Dou (Ishioka et al. 2002)
6.114	AW Sge	2000	Mas
	AW Sge	2006	Kra, JSh
6.115	V551 Sgr	2003	MLF, SAN, Nel, GBo, Sto, Hid
	V551 Sgr	2004	MLF
6.116	V4140 Sgr	2004	Chi, MLF, Ret
6.117	V701 Tau	1995	Oud
	V701 Tau	2005	Mhh, Boy, GCO, JSh, VAN
6.118	V1208 Tau	2000	KU, GAR, Mas, COO
	V1208 Tau	2002	Oud, Tan
6.119	KK Tel	2002	Kato et al. (2003d)
	KK Tel	2003	RIX
	KK Tel	2004	MLF
6.120	EK TrA	2007	MLF
–	FL TrA	2005	Imada et al. (2008a)
6.121	UW Tri	1995	Kato et al. (2001c)
	UW Tri	2008	KU, Ioh, Njh, Mhh, IMi, DRS, DPV, Bed, Nyr, Ogm, AAVSO

Table 1. (continued) List of Superoutbursts.

Subsection	Object	Year	Observers or references
6.122	WY Tri	2000	Vanmunster (2001), KU, Nov
6.123	SU UMa	1989	Udalski (1990)
	SU UMa	1999	KU, Buc, Mhh
6.124	SW UMa	1991	Oud
	SW UMa	1996	Semeniuk et al. (1997b), Nogami et al. (1998a)
	SW UMa	1997	JEN
	SW UMa	2000	KU, JEN, Nov, Buc, Mar, Pav, Mas, AAVSO
	SW UMa	2002	Tor, Tan
	SW UMa	2006	IMi, Mhh, Nyr, DPV, Njh, GOT, KU, AAVSO
6.125	BC UMa	2000	KU, Pav, NDJ
	BC UMa	2003	KU, Oud, Boy, PIE, Ost, Kis, Maehara et al. (2007)
6.126	BZ UMa	2007	VAN, PIE, AAVSO, Boy, Nyr, KU, Njh, Res, MEV, JSh, DRS, Kop, Kra, DPV, Mhh
6.127	CI UMa	2001	KU
	CI UMa	2003	Hid, KU, PIE, Nyr, Tan
	CI UMa	2006	DPV
6.128	CY UMa	1995	Harvey, Patterson (1995)
	CY UMa	1998	JEN
	CY UMa	1999	KU
	CY UMa	2009	DPV, BSt, Njh, HMB, Ioh, VIR, AAVSO
–	DI UMa	2007a	Rutkowski et al. (2008)
		2007b	Rutkowski et al. (2008)
6.129	DV UMa	1997	Patterson et al. (2000b), JEN, Nogami et al. (2001b)
	DV UMa	1999	KU, JEN
	DV UMa	2002	KU, Nyr
	DV UMa	2005	Mhh, Njh, KU
	DV UMa	2007	IMi, Njh, Mhh, DPP, PXR, AAVSO
6.130	ER UMa	1995	Kato et al. (2003b)
6.131	IY UMa	2000	Uemura et al. (2000), Patterson et al. (2000a)
	IY UMa	2002	KU, OUS, AAVSO
	IY UMa	2004	Mhh, Nyr, KU, DPP, KGE
	IY UMa	2006	Njh, Mhh, KU, Kra, DPV, RIT, Kop, AAVSO
	IY UMa	2007	Mhh
	IY UMa	2009	OUS, Njh, Ost, Ioh, SXN, Nyr
6.132	KS UMa	2003	VAN, Tor, KU, PIE, Njh, Mhh, Mar, Ost, Nyr, DRS, Olech et al. (2003)
	KS UMa	2007	HHO, Njh, KU
6.133	KV UMa	2000	Uemura et al. (2002c)
6.134	MR UMa	2002	KU, OUS
	MR UMa	2003	KU, Tor, PIE, Hid, Nyr, War
	MR UMa	2007	AAVSO
–	SS UMi	2004	Olech et al. (2006)
6.135	CU Vel	2002	Nel, GBo, Hea, RIX
6.136	HS Vir	1996	Kato et al. (1998b)
	HS Vir	2008	Nel
6.137	HV Vir	1992	Kato et al. (2001d)
	HV Vir	2002	Ishioka et al. (2003)
	HV Vir	2008	Njh, Kis, Mhh, KU, Ioh, Ros
6.138	OU Vir	2003	KU, Tor, MLF, Hid, Kis, Kra, Njh, Hea, VAN, Mar, PIE, DRS, Nyr
	OU Vir	2008	Ioh, DPV, Kis
6.139	QZ Vir	1993	Kato (1997), Lemm et al. (1993)
	QZ Vir	2005	Mhh, Njh, Ost
	QZ Vir	2007	Mhh, Njh, Kis (Ohshima et al. 2009)
	QZ Vir	2008	HHO, Njh, Kis, DPV, GBo, OUS (Ohshima et al. 2009)
	QZ Vir	2009	OUS, Njh, BSt, KU, Mhh, Ioh, HMB, Kis, Ogm (Ohshima et al. 2009)
6.140	RX Vol	2003	MLF, Nel, SAN
6.141	TY Vul	2003	KU, PIE, AAVSO
6.142	DO Vul	2008	KU, Mhh

Table 1. (continued) List of Superoutbursts.

Subsection	Object	Year	Observers or references	ID [‡]
6.143	NSV 4838	2005	PIE, VAN, Boy	
	NSV 4838	2007	Mhh, KU, Njh	
6.144	NSV 5285	2008	KU	
6.145	NSV 14652	2004	PIE	
6.146	1RXS J0232	2007	Nel, GBo, AAVSO	Pi of the Sky
6.147	1RXS J0423	2008	BXS, JSh, IMi, BSt, DPV, Ioh, Mhh	
6.148	1RXS J0532	2005	KGE, Mhh, DPP, VAN, Nyr, JSh, COO	Bernhard et al. (2005)
	1RXS J0532	2008	Njh, DPV, KU, Mhh	
6.149	2QZ J0219	2005	Imada et al. (2006b)	
	2QZ J0219	2009	Njh, Mhh, Ioh	
6.150	ASAS J0025	2004	Chi, COO, Mhh, MLF, Kis, KU, RIT, San, OUS, Nyr, Hid, DRS, PIE, Nel, Ret, Boy, GBo, Mas, PXR, Njh, Kop, VAN, Pav, CTX, AAVSO	
6.151	ASAS J0233	2006	Mhh, Kra, Njh, Kis, VAN, Boy, CTX, AAVSO	
6.152	ASAS J0918	2005	Mhh, Njh	
6.153	ASAS J1025	2006	Mhh, Kra, Njh, Kis, COO, MLF, AAVSO, Van, DPP, KU	
6.154	ASAS J1536	2004	KU, Kis, COO, Mhh, ASAS, Nyr, AAVSO	
6.155	ASAS J1600	2005	Soejima et al. (2009), MLF, Nel	
6.156	CTCV J0549	2006	Imada et al. (2008a)	
6.157	Ha 0242	2006	Kra, Mhh, MLF	
6.158	SDSS J0137	2003	Imada et al. (2006a)	
	SDSS J0137	2009	Njh, Mhh	
6.159	SDSS J0310	2004	MLF, Chi	
6.160	SDSS J0334	2009	Mhh, KU	
6.161	SDSS J0746	2009	KU, Njh, Mhh	
–	SDSS J0804	2006	Kato et al. (2009)	
6.162	SDSS J0812	2008	Mhh, Kis, Njh	
6.163	SDSS J0824	2007	Njh, Boy, Mhh, JSh, BXS (Boyd et al. 2008b)	
6.164	SDSS J0838	2007	VAN	
	SDSS J0838	2009	Mhh, BSt, KU, Ioh	
6.165	SDSS J1005	2009	Ioh, AAVSO, IMi, Mhh, Njh	
6.166	SDSS J1100	2009	KU, PIE	
6.167	SDSS J1227	2007	Mhh, DRS, Shears et al. (2008b)	
6.168	SDSS J1524	2009	Nov, AAVSO, DPV, Mhh, Pav, Ioh, BSt, Njh	
6.169	SDSS J1556	2007	Mhh, Njh, KU, Mas	
6.170	SDSS J1627	2008	JSh, Kra, BXS, KU, GBo, Ogm, BSt, Njh, Shears et al. (2008c)	
6.171	SDSS J1702	2005	Nyr, Boy, JSh, VAN, BXS (Boyd et al. 2006)	
6.172	SDSS J1730	2001	KU, Nyr	
	SDSS J1730	2002	KU	
	SDSS J1730	2004	KU, War, COO, Ost	
6.173	SDSS J2100	2007	Njh, Mhh	
6.174	SDSS J2258	2004	MLF, Kis	
	SDSS J2258	2008	Njh, Mhh, Ioh, OUS, SAc	
6.175	OT J0042	2008	KU, Mhh, Njh, Ioh, Kis	M31N 2008-11b
6.176	OT J0113	2008	Mhh	CSS080922:011307+215250
6.177	OT J0211	2008	OUS, Mhh, KU	CSS080130:021110+171624
6.178	OT J0238	2008	Mhh, Shugarov et al. (2008), KU, Njh	CSS081026:023839+355648
6.179	OT J0329	2006	Shafter et al. (2007), Kra, VAN, AAVSO, Boy, BXS	VS 0329+1250
6.180	OT J0406	2008	Mhh, OUS, GBo	Itagaki (Yamaoka et al. 2008a)

[‡]Original identifications or discoverers.

Table 1. (continued) List of Superoutbursts.

Subsection	Object	Year	Observers or reference	ID
6.181	OT J0557	2006	Uemura et al. (2009), Boy, VAN, Nyr	Kloehr et al. (2006)
6.182	OT J0747	2008	Kis, GBo, Njh, Mhh, Nel, BXS, DPP, JSh, CTX, Ioh, AAVSO	Itagaki (Yamaoka et al. 2008f)
6.183	OT J0807	2007	Mhh, HHO, Kra, Njh, Kis, DPV	Itagaki
6.184	OT J0814	2008	URB, DPV, Njh, KU	CSS080409:081419–005022
6.185	OT J0845	2008	Njh, Kis, Mhh	Itagaki (Yamaoka et al. 2008c)
6.186	OT J0902	2008	KU, Mhh	CSS080304:090240+052501
6.187	OT J1021	2006	Uemura et al. (2008a), AAVSO	Christensen (2006)
6.188	OT J1026	2009	Njh	Itagaki (Yamaoka, Itagaki 2009)
6.189	OT J1028	2009	GBo, KU, Mhh, Kis	CSS090331:102843–081927
6.190	OT J1112	2007	Ioh, GBo, Mhh, Kis	Pi of the Sky
6.191	OT J1300	2008	GBo, Mhh, PIE	CSS080702:130030+115101
6.192	OT J1440	2009	IMi, Mhh, KU, OUS	CSS090530:144011+494734
6.193	OT J1443	2009	Njh, Ioh, Mhh, GBo, KU, Kis	CSS090418:144342–175550
6.194	OT J1631	2008	DPV, PIE, Mhh, KU, Njh	CSS080505:163121+103134
6.195	OT J1914	2008	Mhh, KU, Njh, DPV, Nyr, AAVSO	Itagaki (Yamaoka et al. 2008d)
6.196	OT J1959	2005	VAN, KU, Njh	Renz et al. (2005)
6.197	OT J2131	2008	Mhh, Ioh, SAc	Itagaki (Yamaoka et al. 2008e)
6.198	OT J2137	2008	GBo, Mhh, Njh, DPV, SAc, Kis, Kry	Itagaki
6.199	TSS J0222	2005	Imada et al. (2006c)	Quimby et al. (2005)

these systems were not as exactly defined as in the objects treated in subsection 3.2.

Combined with the objects in subsection 3.2, this transition found to be quite generally, if not always, seen in many SU UMa-type dwarf novae. In many well-observed objects, the periods of superhumps varied little after this transition, in contrast to the systematic variation seen during the stage B.

3.4. Global Period Derivatives

Several authors, including us, have pointed out that P_{dot} in SU UMa-type dwarf novae has a strong correlation with P_{SH} (e.g. Kato et al. 2001d; Kato et al. 2003d; Uemura et al. 2005; Rutkowski et al. 2007). These works, however, were based on results from different segments of $O - C$ diagrams for extracting P_{dot} . On the other hand, Patterson et al. (1993) and their descendant papers calculated P_{SH} from the entire superoutburst (frequently consisting of stages A–C), and led to a conclusion that almost all P_{dot} 's were negative or zero (see also a discussion in Olech et al. 2003).

We nominally calculated P_{dot} for the entire superoutburst (restricting to $0 \leq E \leq 200$ to avoid contaminations from post-superoutburst variations) and simulated the treatment by Patterson et al. (1993). The results presented in figure 8⁴ indicate that more than half of systems below $P_{\text{SH}} = 0.065$ d have negative P_{dot} . The presence of systems with positive P_{SH} and the decreasing trend of P_{dot}

⁴ Individual values of P_{dot} are not presented because this analysis is meaningful only in the context of statistical comparison with previous research, and because globally determined P_{dot} 's on highly structured $O - C$'s are no better than nominal values. Better-defined P_{dot} for individual objects are discussed in 3.5 and later (sub)sections.

with increasing P_{SH} are already evident from this global determination.

3.5. Period Derivatives during Stage B

Since the stages B and C were better studied than the stage A in many systems, and since they have general properties common to the majority of superoutbursts, we first describe the stages B and C.

We determined P_{dot} for the stage B. This treatment corresponds to the analysis in Kato et al. (2001d) for short- P_{SH} systems. The values are listed in table 2 as well as other parameters discussed in subsection 3.6.⁵ The results are shown in figures 9 and 10. This figure is essentially an improvement of the corresponding figures presented in Kato et al. (2001d) and Kato et al. (2003d), in that the present samples do not include globally determined P_{dot} or locally determined P_{dot} around the transitions (stage A to B or stage B to C), and in that P_{dot} were (re-)determined in a homogeneous way from the times of superhump maxima, either published in the literature or re-examined in this paper. Note, in particular, that two unusual systems, V485 Cen and EI Psc, now have more usual P_{dot} in contrast to Kato et al. (2001d). This was caused by an error in estimating P_{dot} in the original paper (V485 Cen: Olech 1997) and a combination of two sets of published superhump maxima (EI Psc: Uemura et al. 2002a; Skillman et al. 2002). The figure indicates that systems with $P_{\text{SH}} < 0.08$ d have a general tendency of a positive P_{dot} during the stage B.

Figure 11 shows the relation between P_{dot} (for the stage

⁵ The intervals (E_1 and E_2) for the stages B and C given in the table sometimes overlap because of occasional observational ambiguity in determining the stages. The values of P_{orb} are taken from Ritter, Kolb (2003).

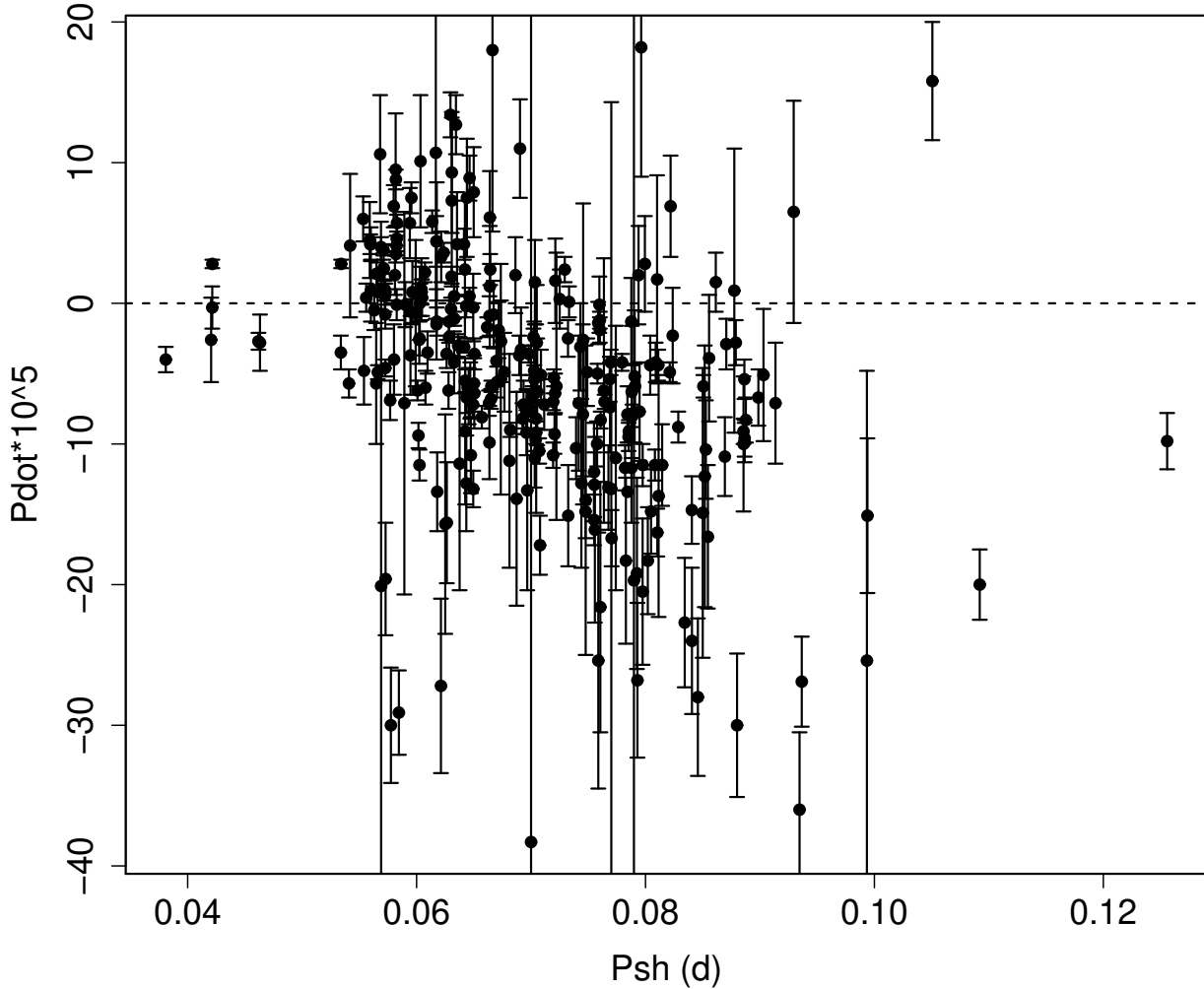


Fig. 8. Globally Determined $P_{\dot{\text{dot}}}$. Several objects with extremely negative $P_{\dot{\text{dot}}}$ (e.g. AX Cap: $-83.0(10.5) \times 10^{-5}$, $P_{\text{SH}} = 0.1131$ d, MN Dra: $-165.9(17.7) \times 10^{-5}$, $P_{\text{SH}} = 0.1077$ d, NY Ser: $-143.7(7.8) \times 10^{-5}$, 0.1072 d, GX Cas: $-66.3(15.2) \times 10^{-5}$, 0.0939 d, UV Gem: $-53.4(3.8) \times 10^{-5}$, 0.0931 d) are outside this figure.

B) versus ϵ . The period derivative has a strong correlation with ϵ , which is believed to be an excellent measure for the mass ratio $q = M_2/M_1$. It would be worth noting that two systems with unusually short P_{orb} (filled squares: EI Psc, V485 Cen) follow the same relation as the rest of systems, suggesting that $P_{\dot{\text{dot}}}$ is more dependent on q than on P_{orb} . $P_{\dot{\text{dot}}}$ reaches a maximum around $\epsilon = 0.025$ (equivalent to $q = 0.12$).

3.6. Superhump Periods during Stages B and C

Figure 12 summarizes fractional decrease of the superhump period between stage B (hereafter period P_1) and stage C (hereafter period P_2) versus P_{SH} . The superhump period usually decrease by $\sim 0.5\%$ during the transition from stage B to C. There appears to be a weak relation between the fractional decrease and P_{SH} : the decrease is larger in longer- P_{SH} systems.

Figure 13 shows the relation between the fractional superhump excess at the beginning of the stage B (calculated using the mean P_{SH} and $P_{\dot{\text{dot}}}$) versus P_{orb} . The figure was drawn for systems with a well-defined stage B (corre-

sponding to subsection 3.2) and with a known P_{orb} . The relation is tighter than the well-known relation between the global P_{SH} and P_{orb} (e.g. Molnar, Kobulnicky 1992). A linear regression to the data has yielded the following relation:

$$P_{\text{SH}(\text{start})}/P_{\text{orb}} - 1 = -0.033(6) + 0.87(9)P_{\text{orb}}. \quad (1)$$

Figure 14 shows the relation between the fractional superhump excess at the end of the stage B, i.e. the longest superhump period for positive- $P_{\dot{\text{dot}}}$ systems, versus mean P_{orb} . This fractional period excess has, in contrast to one at the beginning of the stage B, a fairly common value of ~ 0.03 (slightly increasing with increasing P_{orb} , equation 2) below the period gap. The difference in dependence to P_{orb} between these two periods is striking, and is most prominent at shorter P_{orb} except extreme WZ Sge-type dwarf novae (for WZ Sge-type dwarf novae, see description and discussion in section 5). This difference appears to determine the $P_{\dot{\text{dot}}} - P_{\text{SH}}$ relation (subsection 3.5).

$$P_{\text{SH}(\text{end})}/P_{\text{orb}} - 1 = 0.001(4) + 0.44(6)P_{\text{orb}}. \quad (2)$$

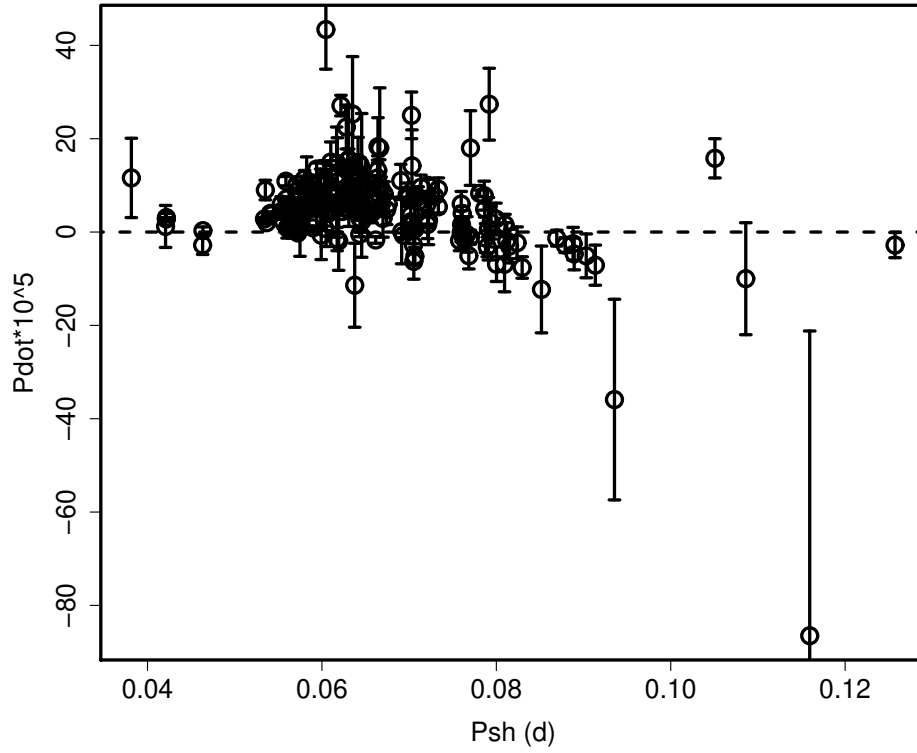


Fig. 9. $P_{\dot{d}}$ for stage B versus the mean P_{SH} during stage B.

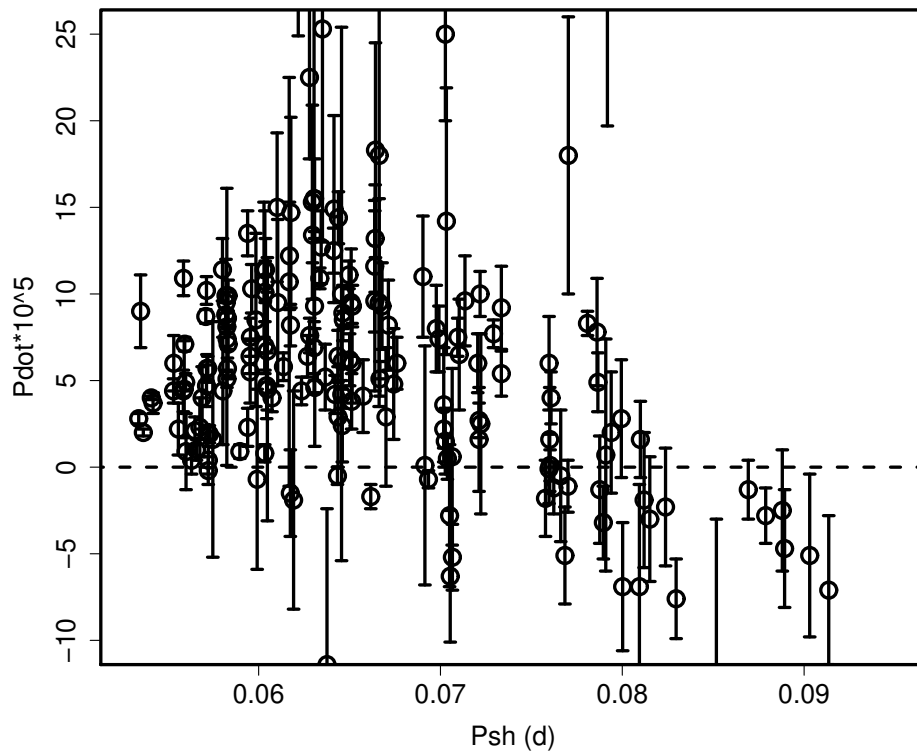


Fig. 10. $P_{\dot{d}}$ for stage B versus P_{SH} (enlarged).

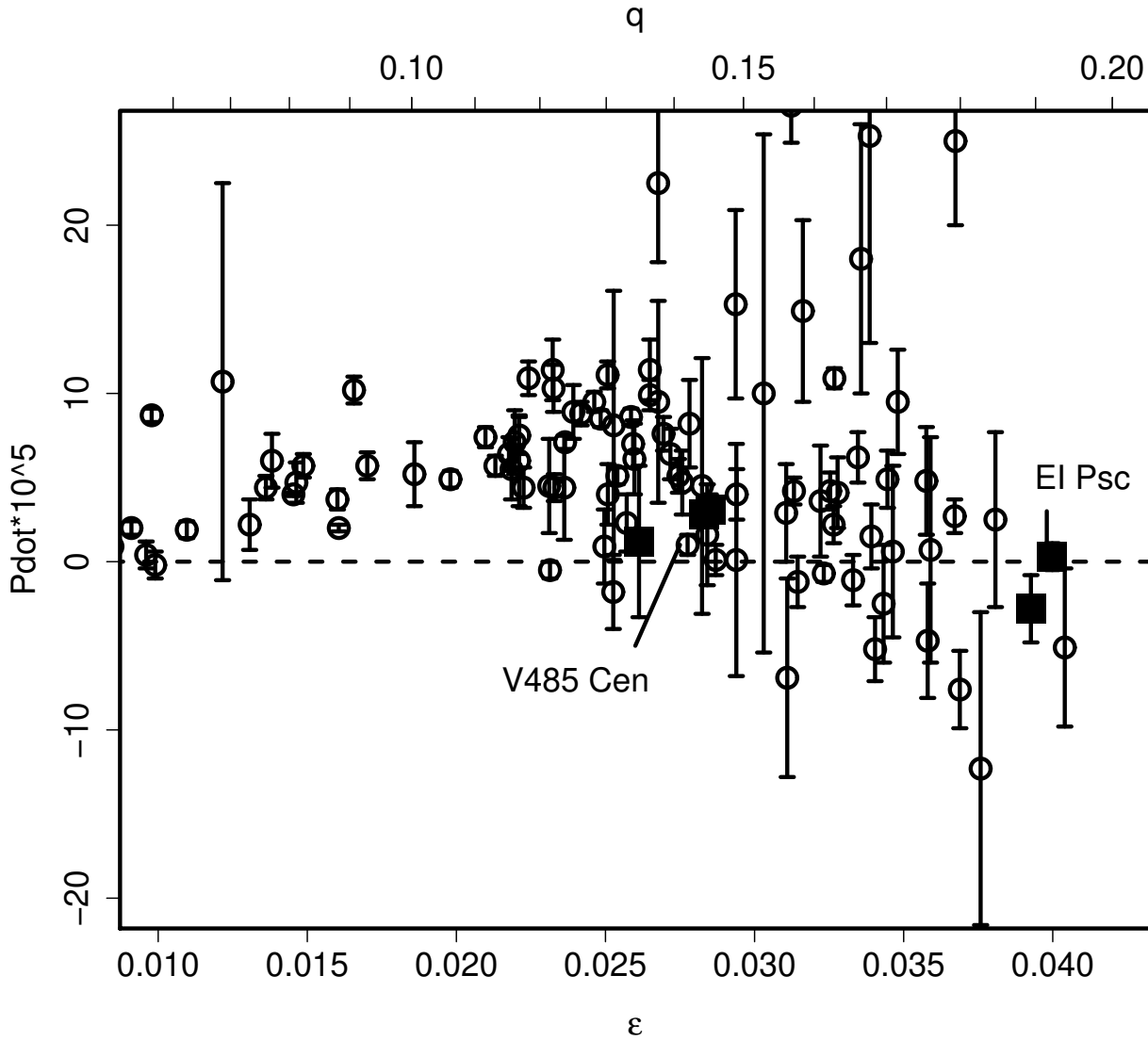


Fig. 11. P_{dot} (for stage B) versus ϵ . P_{dot} for stage B has a strong correlation with fractional superhump excess (ϵ), which is believed to be an excellent measure for q . The ϵ was determined from the mean P_{SH} during the stage B. Two systems with unusually short P_{orb} (filled squares: EI Psc, V485 Cen) follow the same relation as the rest of systems. One exceptionally large- ϵ object (TU Men: $\epsilon = 0.073$, $P_{\text{dot}} = -2.8(2.7) \times 10^{-5}$) is located outside this figure.

The superhump excesses (or periods) during the stage C are almost identical to those at the start of the stage B (figure 15).

For readers' convenience, we also provide relations between P_1 and P_{orb} (equation 3, the samples are the same as in figure 13) and P_2 and P_{orb} (equation 4).

$$P_1/P_{\text{orb}} - 1 = -0.017(7) + 0.66(10)P_{\text{orb}}. \quad (3)$$

$$P_2/P_{\text{orb}} - 1 = -0.012(4) + 0.56(5)P_{\text{orb}}. \quad (4)$$

These equations can be used for estimating P_{orb} (as in Ritter, Kolb 2003) when superhump periods for specific stages are known. The potential availability of P_2 for estimating P_{orb} would provide an excellent alternative to P_{SH} at the start of the stage B, since the break between the stages B and C is easier to detect than the start of the stage B, particularly when the superoutburst is detected during its later course.

The overall behavior of the stages B and C in positive- P_{dot} systems can be summarized:

- The superhumps during the stage B start with a short period, which is well correlated with P_{orb} .
- The superhumps evolve during the stage B toward a longer period, which commonly has a $\sim 3\%$ excess to P_{orb} .
- The superhump period return to the initial period during the stage C.

3.7. Superhump Periods during Stage A

The stage A usually constitutes ~ 20 superhump cycles. Table 3 and figure 16 summarize the recorded superhump periods during the stage A. Note, however, the periods during this stage were not very precisely determined because of the shortness of the interval, and because the

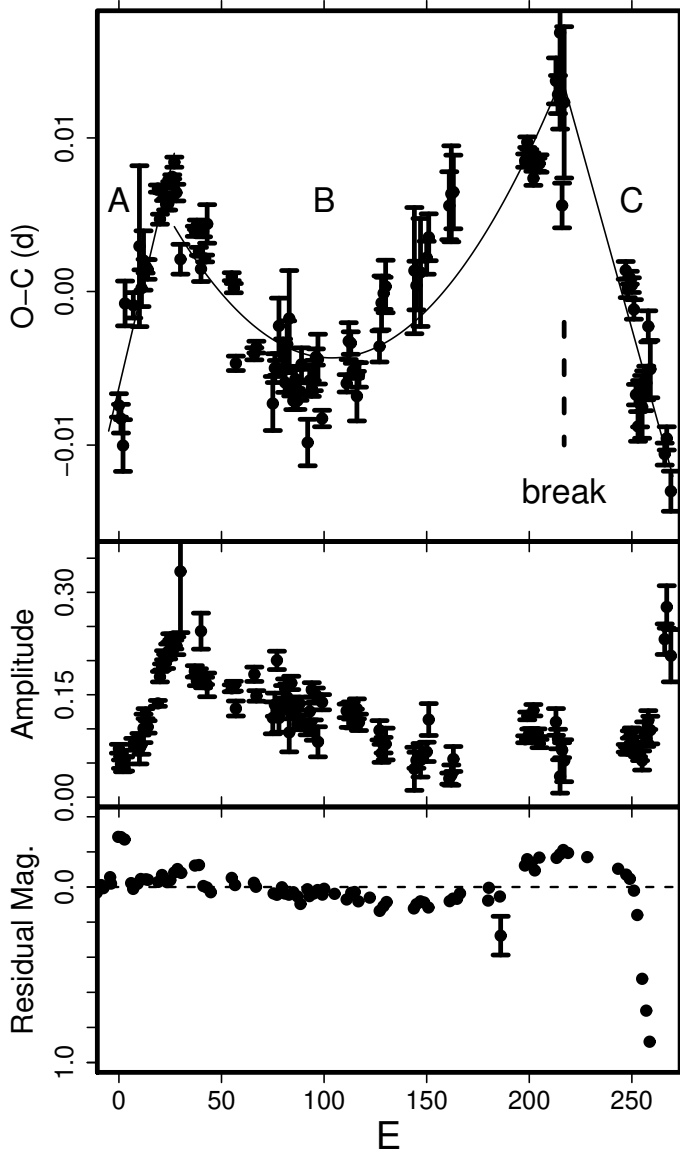


Fig. 3. Representative $O-C$ diagram showing three stages (A–C) of $O-C$ variation. The data were taken from the 2000 superoutburst of SW UMa. (Upper:) $O-C$ diagram. Three distinct stages (A – evolutionary stage, B – middle stage, and C – stage after transition to a shorter period) and the location of the period break between stages B and C are shown. (Middle:) Amplitude of superhumps. As shown in Soejima et al. (2009), the maximum amplitudes of superhumps coincide with transitions between stages (A to B and B to C). (Lower:) Deviations from linear decline during the superoutburst plateau. As seen in Soejima et al. (2009) and Kato et al. (2003c), rebrightening during the terminal plateau also corresponds to the transition from stage B to C.

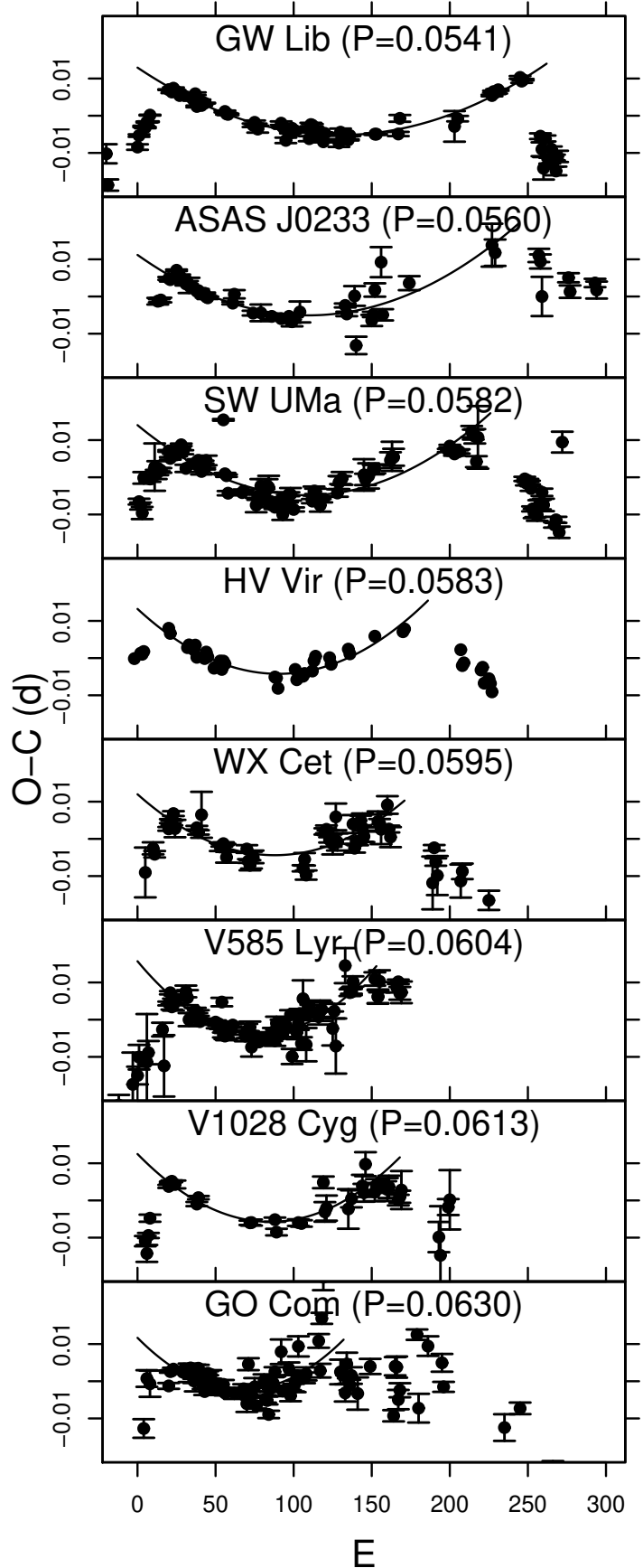


Fig. 4. $O-C$ diagrams of SU UMa-type dwarf novae showing three distinct stages.

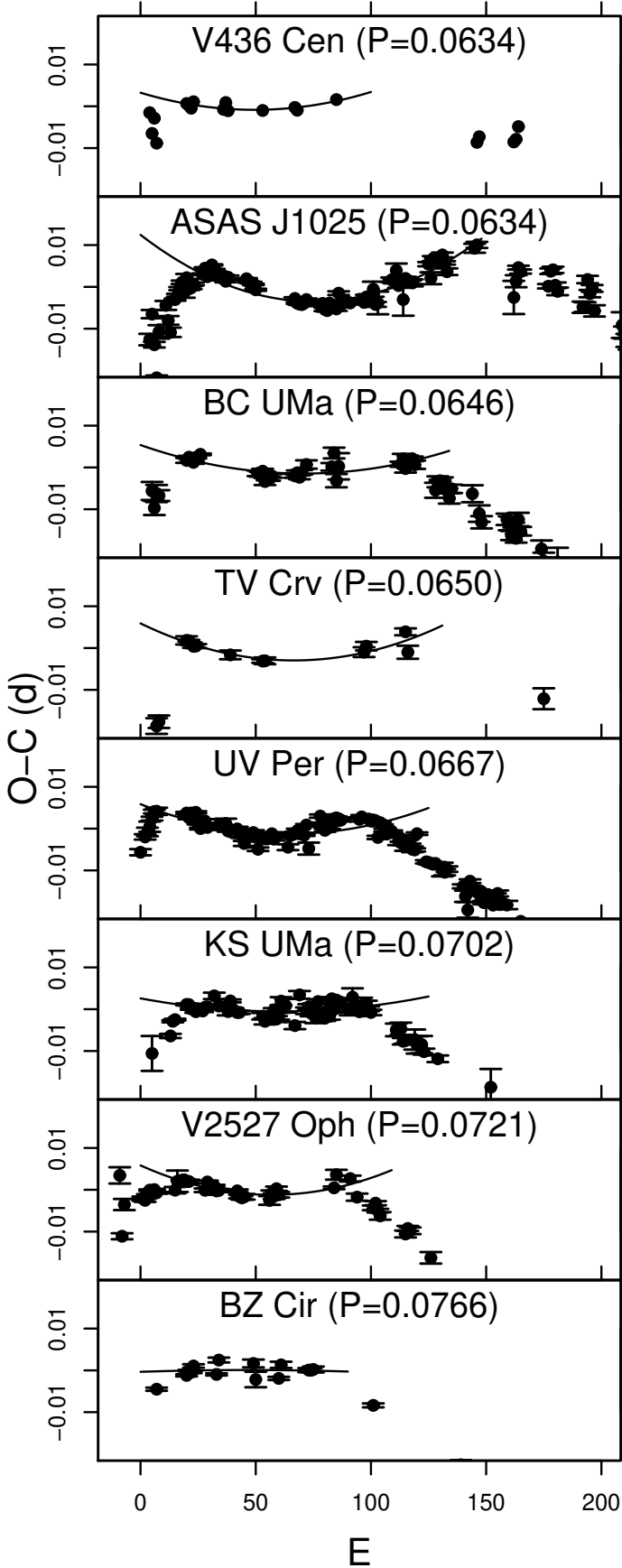


Fig. 4. $O-C$ diagrams of SU UMa-type dwarf novae showing three distinct stages (continued).

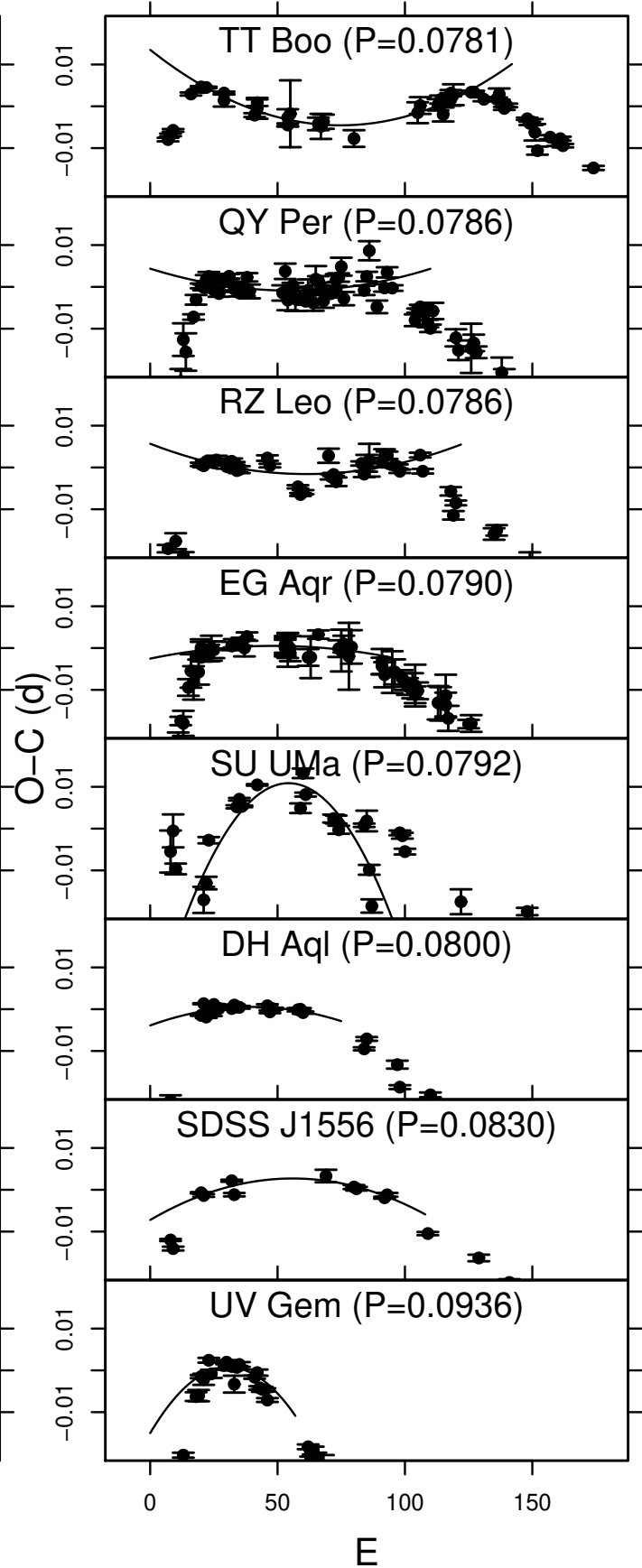


Fig. 4. $O-C$ diagrams of SU UMa-type dwarf novae showing three distinct stages (continued).

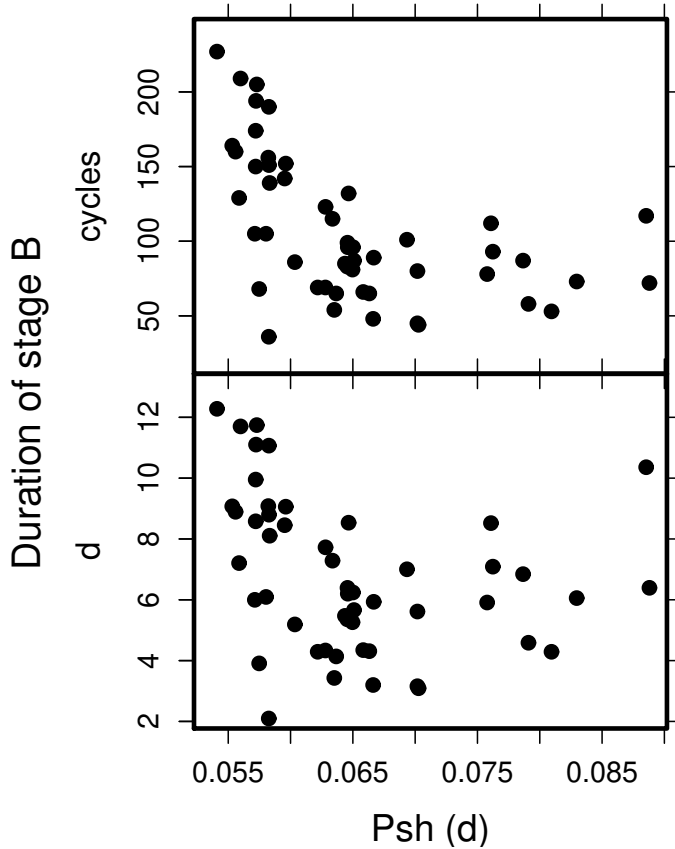


Fig. 5. Duration of stage B. The duration of stage B decreases with increasing P_{SH} both in cycle numbers (upper) and time in days (lower). We used mean P_{SH} during the stage B as the representative P_{SH} .

amplitudes of superhumps are still small. Fractional period excesses during this stage to the mean superhump period during the stage B tend to cluster around 1.0–1.5 %, with some exceptional systems having larger (~ 3 %) excesses.

3.8. Difference Between Different Superoutbursts

Uemura et al. (2005) reported significantly different P_{dot} 's between different superoutbursts of the same object, TV Crv. Several authors, however, have reported results contrary to this finding (e.g. Oizumi et al. 2007; Soejima et al. 2009; Ohshima et al. 2009).

We further examined different superoutbursts of the same objects, and found no convincing evidence for strong variation of P_{dot} between different superoutbursts. On the contrary, the behavior of superhump period in the same object appears to be similar between different superoutbursts (e.g. figure 17; figures in section 6). The difference reported in the past was apparently a result of observation of different stages of superoutbursts (A–C) and the insufficient coverage of the entire superoutburst.

A re-examination of the TV Crv case has also shown that the claim by Uemura et al. (2005) was not convincing (figure 18).

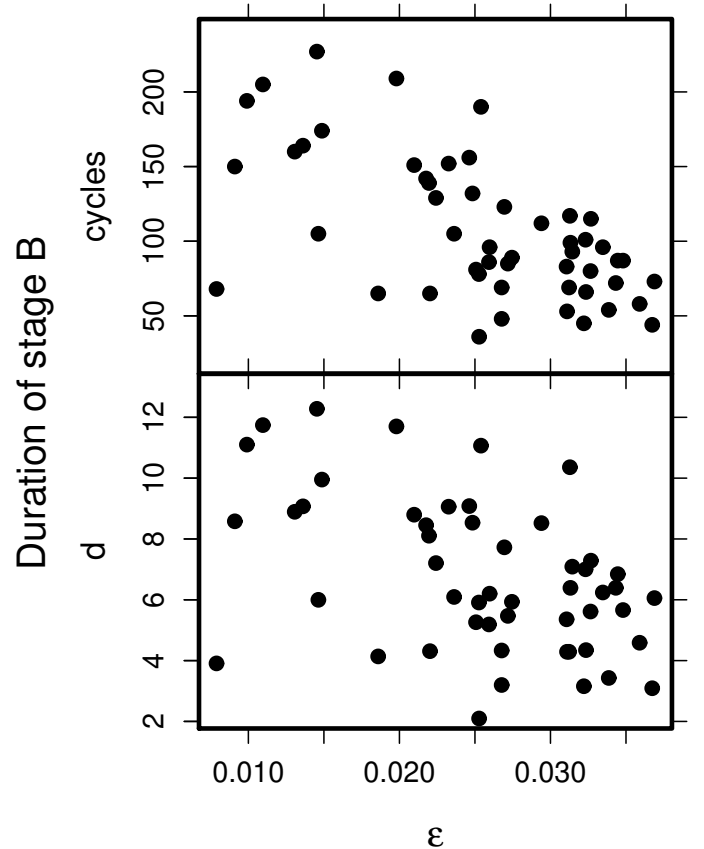


Fig. 6. Duration of stage B. The duration of stage B decreases with increasing ϵ both in cycle numbers (upper) and time in days (lower). We used mean P_{SH} during the stage B for evaluating ϵ .

During the 2004 superoutburst of V2527 Oph, no anomalous behavior in P_{dot} was observed even in the presence of a clear precursor outburst. Similar situations were observed in GO Com (2003), PU CMa (2008), AQ Eri (2009), QZ Vir (1993, 2009) and 1RXS J0532 (2005).⁶ The proposed relation between the presence of a precursor outburst and P_{SH} (Uemura et al. 2005) is not supported by these instances.

Although further work is needed to exclude the presence of different period behavior between different superoutbursts, the close agreement of the behavior between different superoutbursts in many objects might be used to construct a combined $O-C$ diagram and to determine P_{dot} from different superoutbursts even if observational coverage of each outburst is incomplete.

⁶ The period evolution during the 2008 superoutburst of 1RXS J0423, which was associated with a precursor, was slow (subsection 6.147). It is not clear whether the existence of a precursor is responsible in this instance.

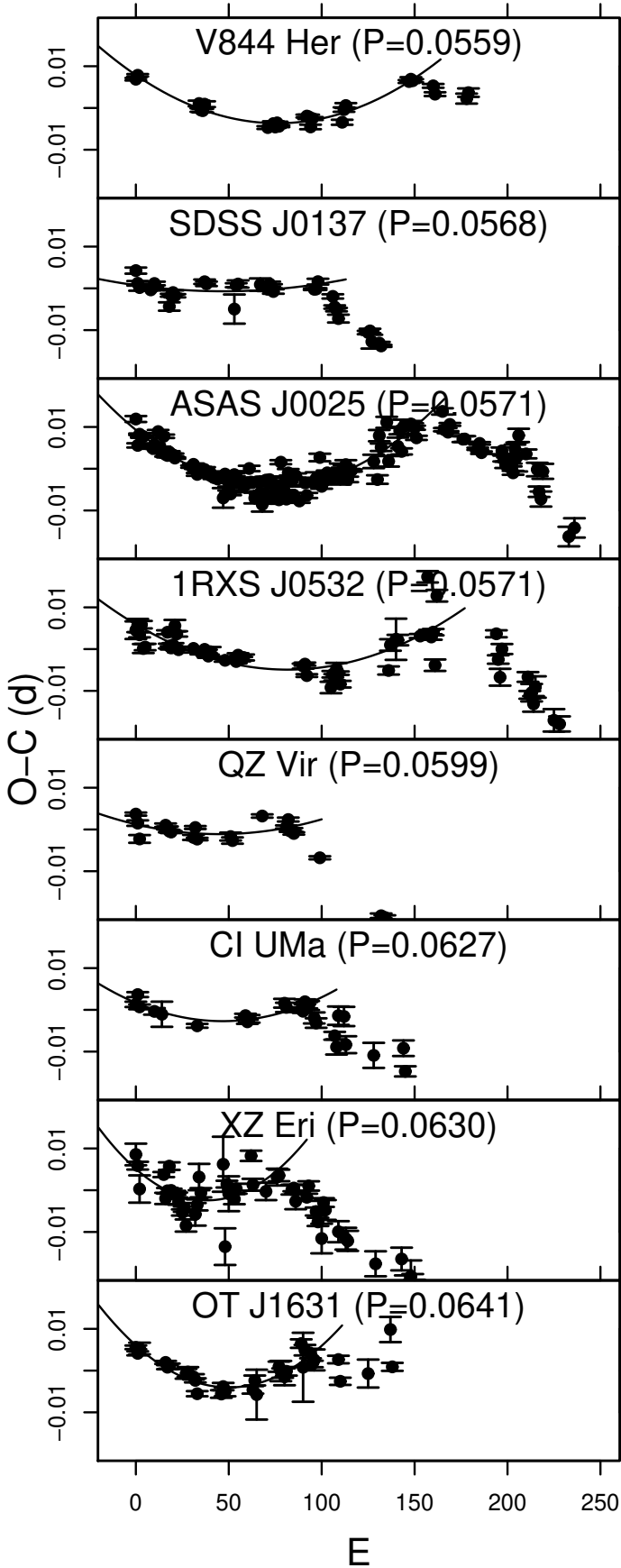


Fig. 7. $O-C$ diagrams of SU UMa-type dwarf novae showing transition in the superhump period.

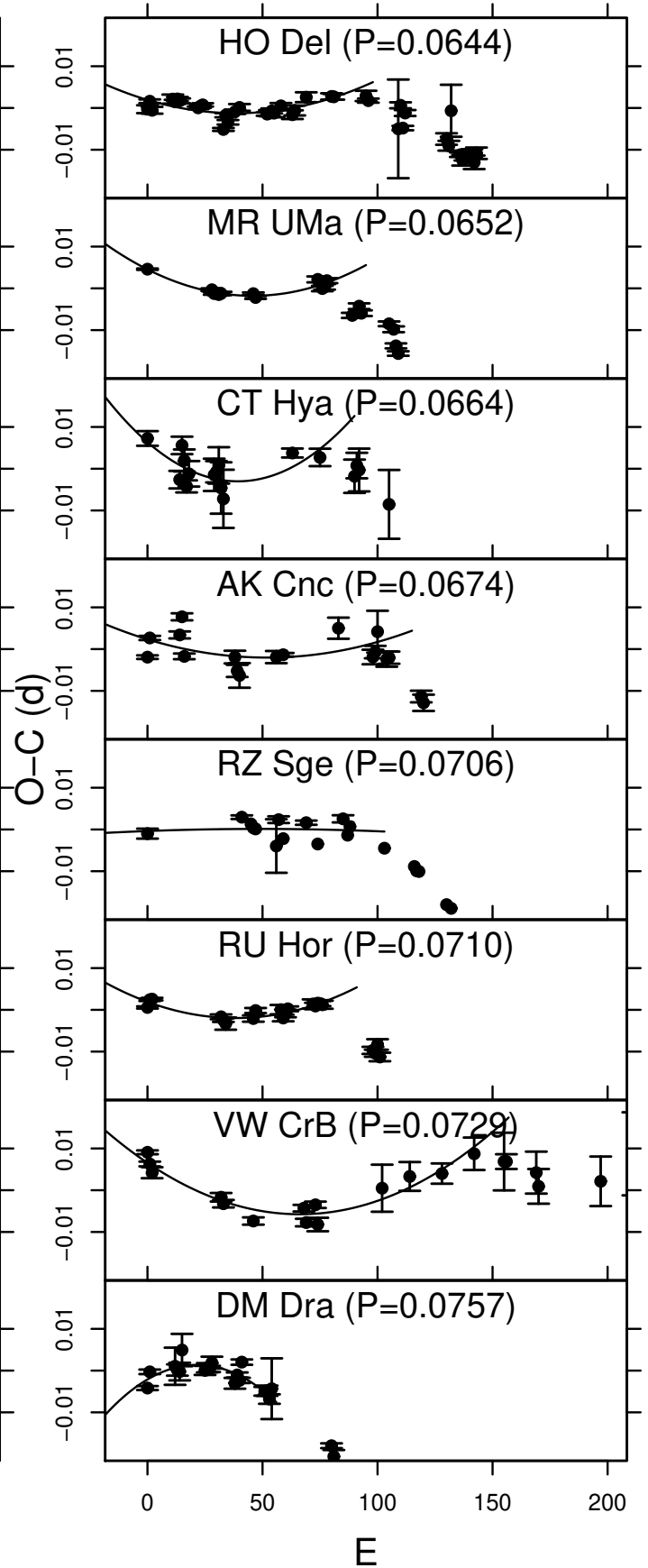


Fig. 7. $O-C$ diagrams of SU UMa-type dwarf novae showing transition in the superhump period (continued).

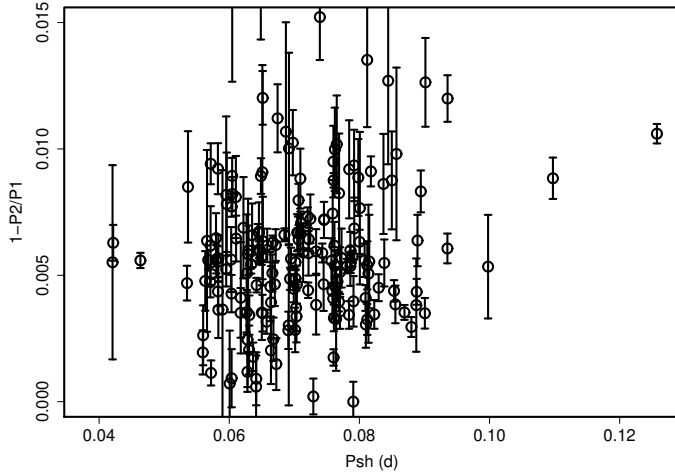


Fig. 12. Fractional decrease of superhump period between stages B and C versus P_{SH} .

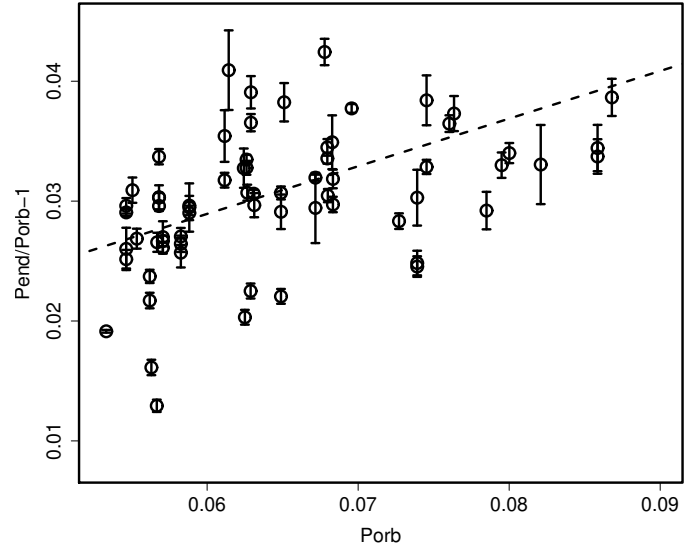


Fig. 14. Fractional superhump excess at the end of the stage B versus the mean P_{orb} . The dashed line represents equation 2. The figure is restricted to the displayed range for a comparison with figure 13.

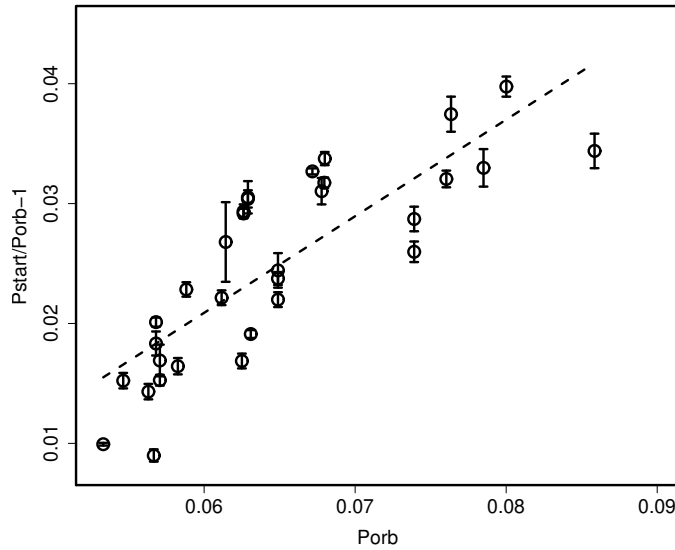


Fig. 13. Fractional superhump excess at the beginning of stage B versus mean P_{orb} . The dashed line represents equation 1.

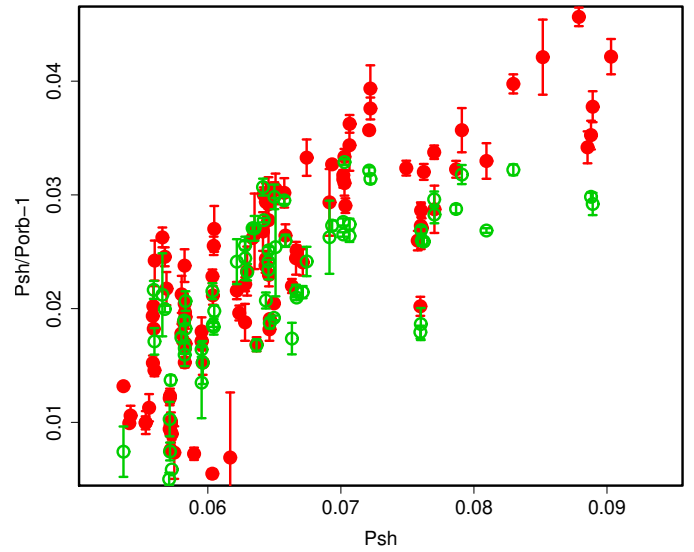


Fig. 15. Comparison of fractional superhump excesses between the stage C and the start of the stage B. The open and filled circles represent fractional superhump excesses in the stage C and at the start of the stage B, respectively. The superhump excesses during the stage C are almost identical to those at the start of the stage B. The figure is restricted to the displayed range for better visibility.

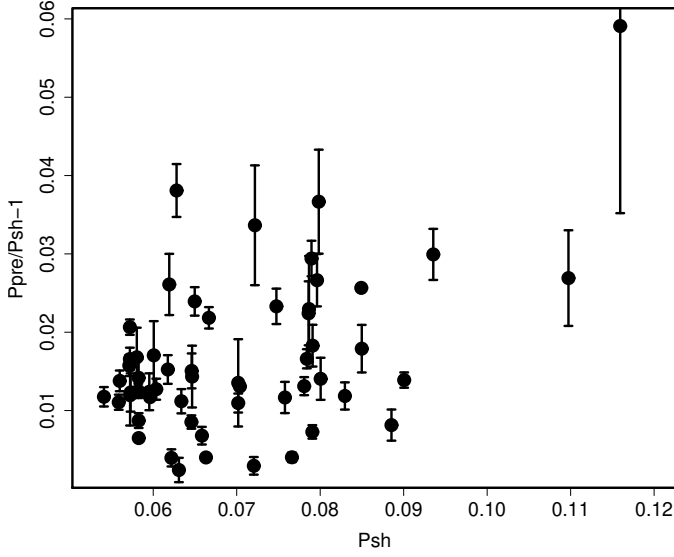


Fig. 16. Superhump periods during the stage A. Superhumps in this stage has a period typically 1.0–1.5 % longer than the one during the stage B. Some systems have still longer periods (~ 3 % longer than the one during the stage B).

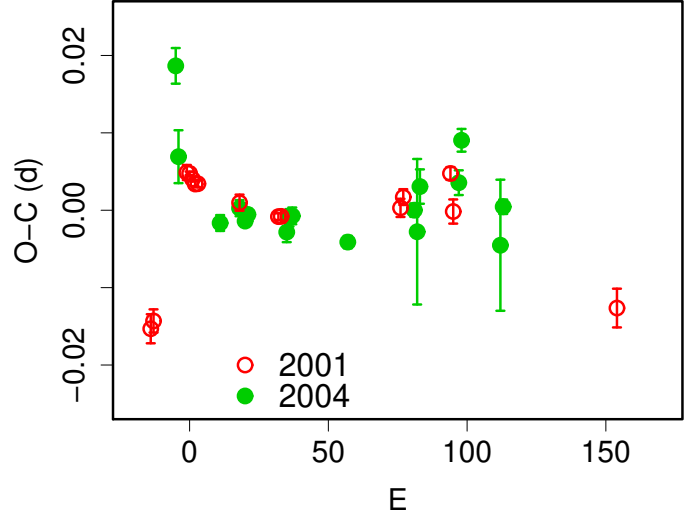


Fig. 18. Comparison of $O-C$ diagrams of TV Crv between 2001 and 2004 superoutbursts. $E=0$ corresponds to the start of the stage B.

4. Discussion

4.1. Existence of Stage B–C Transition

In section 3, we described that most of well-observed systems show stage B–C transitions. There are, however, some objects (or superoutbursts) without prominent stage B–C transitions even though the late stage of superoutbursts is well observed. WZ Sge-type dwarf novae with small P_{dot} , in particular, have tendency to lack the stage B–C transition (see also section 6).

We examined superoutbursts regarding the existence of stage B–C transitions. The sample was selected by criteria of “well-observed” quality (quality A or B) and observational coverage for at least 50 superhump cycles. As shown in figure 19, the existence of stage B–C transitions is most strongly correlated with ϵ . In systems with a small ϵ (typically $\epsilon < 0.015$), only a few superoutbursts showed stage B–C transitions. The result suggests that the appearance of this transition is strongly dependent on q .

In systems with $\epsilon > 0.02$, there are some superoutbursts without a clear transition to the stage C. The best observed example might be V844 Her in 2006 (Oizumi et al. 2007). During this superoutburst, there was no indication of a transition even after 146 superhump cycles, when the outburst just entered the rapid decline stage. In this case, however, the transition may have occurred after the termination of the observation since a transition was recorded during the rapid fading and subsequent stage during the 2008 superoutburst of the same object. The present statistical analysis may be similarly biased toward the lower detection rate of the transition for systems with long-lasting stage B, i.e. systems with a shorter P_{SH} or a smaller ϵ (subsection 3.2). Even considering this effect, the apparent rarity of the transition in small- P_{dot} WZ Sge-type dwarf novae is likely significant, since these objects were often observed even after the termination of their super-

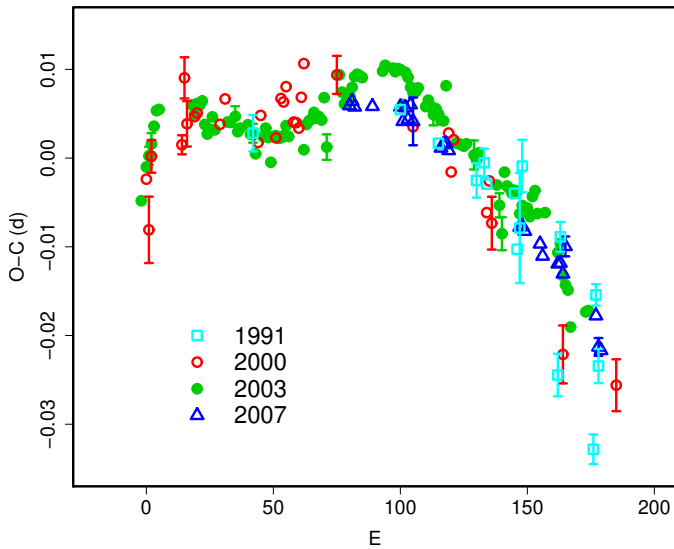


Fig. 17. Comparison of $O-C$ diagrams of UV Per between different superoutbursts.

Table 2. Superhump Periods and Period Derivatives

Object	Year	P_1 (d)	err	E_1^*	P_{dot}^\dagger	err †	P_2 (d)	err	E_2^*	P_{orb} (d)	Q ‡		
FO And	1994	0.074554	0.000052	0	14	–	–	0.074018	0.000012	13	27	0.07161	C
KV And	1994	0.074601	0.000122	0	55	–	–	0.074063	–	55	95	–	C
KV And	2002	0.074501	0.000045	0	41	–	–	0.074155	0.000064	41	82	–	C
LL And	1993	0.056900	0.000088	0	56	–	–	–	–	–	–	0.055055	C
LL And	2004	0.056583	0.000022	0	290	1.0	0.6	0.056223	0.000201	290	326	0.055055	C
V402 And	2005	0.063230	0.000058	0	41	–	–	–	–	–	–	–	C
V402 And	2006	0.063439	0.000062	0	79	12.7	2.1	–	–	–	–	–	C
V402 And	2008	0.063532	0.000029	0	95	4.2	3.7	–	–	–	–	–	CG
V455 And	2007	0.057133	0.000010	23	128	4.7	1.2	–	–	–	–	0.056309	A
V466 And	2008	0.057203	0.000015	20	194	5.7	0.7	0.057138	0.000024	208	349	0.056365	AE
DH Aql	2002	0.080020	0.000017	12	52	–6.9	3.7	0.079514	0.000034	76	128	–	A
DH Aql	2003	–	–	–	–	–	–	0.079593	–	49	120	–	C
DH Aql	2007	–	–	–	–	–	–	0.079527	0.000044	0	76	–	C
DH Aql	2008	–	–	–	–	–	–	0.079493	0.000043	0	38	–	C
V725 Aql	1999	–	–	–	–	–	–	0.099134	0.000141	0	54	–	C
V725 Aql	2005	0.098525	0.000080	0	30	–	–	–	–	–	–	–	C
V1141 Aql	2002	0.063076	0.000032	0	79	9.3	4.3	–	–	–	–	–	B
V1141 Aql	2003	0.062961	0.000023	0	70	13.4	1.6	–	–	–	–	–	B
VY Aqr	1986	0.064867	0.000041	0	31	–	–	0.064288	0.000020	30	155	0.06309	B
VY Aqr	2008	0.064657	0.000014	12	144	8.5	0.5	0.064272	0.000029	137	215	0.06309	A
EG Aqr	2006	0.078958	0.000014	12	71	–3.2	2.1	0.078505	0.000012	83	198	–	A
EG Aqr	2008	0.078760	0.000018	0	63	–1.3	3.1	–	–	–	–	–	C
BF Ara	2002	0.087887	0.000019	0	102	–2.8	1.6	–	–	–	–	0.08417	C
V663 Ara	2004	0.076420	0.000061	0	40	–	–	0.076170	0.000144	37	52	–	C
V877 Ara	2002	0.083928	0.000023	24	98	–5.7	2.9	–	–	–	–	–	CG2
BB Ari	2004	0.072122	0.000026	0	75	1.6	3.0	–	–	–	–	–	C2
HV Aur	2002	0.085563	0.000038	0	62	–3.5	5.0	–	–	–	–	–	CG
TT Boo	2004	0.078085	0.000018	13	120	8.3	0.7	0.077666	0.000013	120	218	–	A
UZ Boo	1994	0.061743	0.000038	0	178	–1.5	2.5	–	–	–	–	–	C
UZ Boo	2003	0.061922	0.000033	30	118	–1.9	6.3	–	–	–	–	–	C
NN Cam	2007	0.074292	0.000021	0	28	–	–	0.073855	0.000018	24	82	0.0717	B
OY Car	1980	0.064631	0.000026	0	126	8.9	1.6	–	–	–	–	0.063121	B
SY Cap	2008	0.063759	0.000022	0	49	–11.4	9.0	–	–	–	–	–	C
AX Cap	2004	0.115938	0.000356	8	34	–86.5	65.3	0.111432	0.000091	34	99	–	C
GX Cas	1994	–	–	–	–	–	–	0.092947	0.000064	0	65	–	C
GX Cas	1996	–	–	–	–	–	–	0.093042	0.000014	44	109	–	C
GX Cas	1999	0.093525	0.000050	21	44	–	–	0.092958	0.000023	42	108	–	B
GX Cas	2006	–	–	–	–	–	–	0.092761	0.000143	52	74	–	C
HT Cas	1985	0.075920	0.000020	1	14	–	–	–	–	–	–	0.073647	C2
KP Cas	2008	0.085529	0.000060	0	15	–	–	0.085200	0.000021	15	53	–	B
V452 Cas	1999	–	–	–	–	–	–	0.088561	0.000061	0	57	–	C
V452 Cas	2007	0.089434	0.000072	0	21	–	–	0.088690	0.000017	20	102	–	B
V452 Cas	2008	0.089319	0.000026	0	34	–	–	–	–	–	–	–	C
V359 Cen	2002	0.081210	0.000072	22	50	–	–	0.080772	0.000028	49	104	–	B
V436 Cen	1978	0.063663	0.000014	16	81	5.2	1.9	0.063550	0.000033	81	160	0.062501	B
V485 Cen	1997	0.042156	0.000008	0	188	2.8	0.3	–	–	–	–	0.040995	B
V485 Cen	2001	0.042066	0.000024	0	103	1.2	4.5	0.041834	0.000159	100	127	0.040995	C
V485 Cen	2004	0.042164	0.000010	0	167	3.1	0.9	0.041899	0.000028	166	190	0.040995	B
V1040 Cen	2002	0.062179	0.000034	17	86	27.1	2.2	0.061751	0.000119	85	103	0.060296	A
WX Cet	1989	0.059616	0.000050	33	185	10.3	1.4	0.059150	0.000110	184	201	0.058261	B

*Interval used for calculating the period (corresponding to E in section 6).

† Unit 10^{-5} .

‡ Data quality and comments. A: excellent, B: partial coverage or slightly low quality, C: insufficient coverage or observations with large scatter, G: P_{dot} denotes global P_{dot} , M: observational gap in middle stage, 2: late-stage coverage, the listed period may refer to P_2 , E: P_{orb} refers to the period of early superhumps. P: P_{orb} refers to a shorter stable periodicity recorded in outburst.

Table 2. Superhump Periods and Period Derivatives (continued)

Object	Year	P_1	err	E_1	$P_{\dot{}}$	err	P_2	err	E_2	P_{orb}	Q		
HO Del	1994	0.064559	0.000056	0	49	10.0	15.4	0.064128	0.000054	47	94	0.06266	C
HO Del	2001	0.064280	0.000120	0	2	–	–	–	–	–	–	0.06266	C
HO Del	2008	0.064363	0.000017	11	96	6.4	1.5	0.063958	0.000044	95	165	0.06266	B
BC Dor	2003	0.068473	0.000016	0	61	–	–	0.068021	0.000007	59	146	–	C
CP Dra	2003	0.083698	0.000028	0	15	–	–	0.082977	0.000162	36	49	–	C
CP Dra	2009	0.083822	0.000073	0	26	–	–	0.083362	0.000027	24	97	–	B
DM Dra	2003	0.075707	0.000051	0	40	–	–	0.075285	0.000044	38	81	–	C
KV Dra	2002	0.060295	0.000040	0	108	11.4	3.9	0.059956	0.000066	83	190	–	B
KV Dra	2004	0.060453	0.000076	0	96	43.4	8.5	0.059463	0.000208	94	118	–	B
KV Dra	2005	0.060341	0.000027	0	67	10.1	4.7	–	–	–	–	–	C
KV Dra	2009	0.060064	0.000061	7	42	–	–	0.060021	0.000110	105	124	–	CG
MN Dra	2002a	0.104351	0.000368	0	16	–	–	–	–	–	–	–	C
MN Dra	2002b	0.108606	0.000307	10	27	–10.0	12.0	0.105425	0.000191	27	51	–	B
MN Dra	2003	0.104796	0.000055	0	19	–	–	–	–	–	–	–	C
MN Dra	2008	0.105140	0.000135	0	10	–	–	–	–	–	–	–	C
IX Dra	2003	0.067003	0.000022	0	61	2.9	4.0	0.066692	0.000053	71	91	–	B
XZ Eri	2003a	0.062955	0.000043	0	77	15.3	5.6	0.062578	0.000044	77	150	0.061159	B
XZ Eri	2007	0.062807	0.000018	15	138	7.6	1.0	0.062653	0.000116	138	190	0.061159	B
XZ Eri	2008	0.062796	0.000044	23	92	22.5	4.7	0.062722	0.000023	91	163	0.061159	B
AQ Eri	1991	0.062250	–	–	–	–	–	–	–	–	–	0.06094	C
AQ Eri	1992	0.063810	0.000748	0	3	–	–	0.061634	0.000211	0	18	0.06094	C
AQ Eri	2006	0.061681	0.000126	0	97	10.7	11.8	–	–	–	–	0.06094	C
AQ Eri	2008	0.062359	0.000015	0	163	4.4	0.8	–	–	–	–	0.06094	A
UV Gem	2003	0.093547	0.000076	12	34	–35.9	21.5	0.092425	0.000040	33	81	–	A
UV Gem	2008	–	–	–	–	–	–	0.092758	0.000224	0	23	–	C
AW Gem	1995	0.079830	0.000113	12	25	–	–	0.079122	0.000044	25	51	0.07621	C
AW Gem	2008	0.078990	0.000138	0	52	–	–	–	–	–	–	0.07621	C
AW Gem	2009	–	–	–	–	–	–	0.078698	0.000056	63	114	0.07621	C
CI Gem	2005	0.119309	0.000590	0	17	–	–	0.108501	0.001404	16	26	–	C
IR Gem	1991	0.070821	0.000144	0	15	–	–	–	–	–	–	0.0684	C
IR Gem	2009	0.070925	0.000032	0	27	–	–	0.070299	0.000077	27	103	0.0684	C
CI Gru	2004	0.054020	0.000140	0	5	–	–	–	–	–	–	–	C
V592 Her	1998	0.056498	0.000013	0	152	2.1	0.8	–	–	–	–	–	C
V660 Her	2004	0.080994	0.000012	0	67	1.6	2.2	0.080747	0.000073	67	116	–	C
V844 Her	1997	0.056007	0.000024	0	160	0.9	2.2	–	–	–	–	0.054643	CM
V844 Her	1999	0.055906	0.000023	0	126	4.5	2.8	–	–	–	–	0.054643	C
V844 Her	2002	0.055859	0.000023	0	129	4.4	1.2	–	–	–	–	0.054643	C
V844 Her	2006	0.055868	0.000021	17	146	10.9	1.0	–	–	–	–	0.054643	A
V844 Her	2008	0.055935	0.000023	0	149	7.1	0.4	0.055826	0.000043	149	179	0.054643	B
V1108 Her	2004	0.057480	0.000034	29	97	1.6	6.8	–	–	–	–	0.05703	B2P
RU Hor	2003	0.070950	0.000017	0	76	7.5	1.1	0.070478	0.000059	76	101	–	A
RU Hor	2008	0.071032	0.000017	1	44	6.5	3.2	0.070530	0.000020	43	114	–	B
CT Hya	1999	0.066425	0.000062	0	75	18.3	6.2	0.066164	0.000072	63	105	–	B
CT Hya	2000	0.066390	0.000035	0	78	9.6	5.2	–	–	–	–	–	C
CT Hya	2002a	0.066384	0.000082	14	136	11.6	3.8	–	–	–	–	–	C
CT Hya	2002b	0.066408	0.000036	0	90	13.2	3.1	0.066273	0.000081	90	151	–	C
CT Hya	2009	0.066630	0.000065	0	61	18.0	12.9	–	–	–	–	–	C
MM Hya	1998	0.058960	0.000071	0	52	–	–	0.058745	0.000316	–	–	0.057590	C
VW Hyi	1972	0.076875	0.000033	0	65	–	–	0.076241	0.000177	65	79	0.074271	B
VW Hyi	2000	0.076986	0.000055	0	60	–	–	–	–	–	–	–	C
RZ Leo	2000	0.078658	0.000015	13	100	4.9	1.7	0.078225	0.000029	100	179	0.076038	A
RZ Leo	2006	0.078428	0.000058	0	127	–	–	–	–	–	–	0.076038	C
GW Lib	2007	0.054095	0.000010	51	278	4.0	0.1	–	–	–	–	0.05332	A
RZ LMi	2004	0.059394	0.000030	10	86	13.5	1.3	–	–	–	–	–	B
RZ LMi	2005	0.059396	0.000011	0	86	2.3	1.1	–	–	–	–	–	C

Table 2. Superhump Periods and Period Derivatives (continued)

Object	Year	P_1	err	E_1	$P_{\dot{}}$	err	P_2	err	E_2	P_{orb}	Q		
SX LMi	1994	0.069481	0.000017	0	45	–	–	0.069088	0.000025	45	118	0.06717	B
SX LMi	2001	0.069144	0.000033	0	85	0.1	6.9	0.068935	0.000216	84	113	0.06717	C
SX LMi	2002	0.069341	0.000004	14	115	–0.7	0.5	0.069004	0.000030	115	130	0.06717	C
BR Lup	2003	0.082284	0.000043	0	17	–	–	0.082000	0.000018	50	95	0.0795	C
BR Lup	2004	–	–	–	–	–	–	0.082193	0.000038	0	96	0.0795	C
AY Lyr	1987	0.075970	0.000018	0	92	–0.1	2.0	–	–	–	–	–	B
AY Lyr	2008	0.076232	0.000099	0	28	–	–	0.075471	0.000077	27	54	–	B
AY Lyr	2009	0.076161	0.000065	0	28	–	–	0.075691	0.000030	26	94	–	C
DM Lyr	1996	0.067085	0.000050	0	32	–	–	–	–	–	–	0.065409	C2
DM Lyr	1997	0.067205	0.000248	0	46	–	–	–	–	–	–	0.065409	C2
DM Lyr	2002	0.067230	0.000054	0	59	–	–	0.067130	0.000043	58	134	0.065409	C
V344 Lyr	1993	0.091354	0.000047	0	78	–7.1	4.3	–	–	–	–	–	C
V358 Lyr	2008	0.055629	0.000032	–	–	–	–	–	–	–	–	–	C
V419 Lyr	1999	0.090145	0.000140	3	38	–	–	0.089006	0.000073	36	78	–	C
V419 Lyr	2006	0.090060	0.000044	11	48	–	–	0.089745	0.000032	45	111	–	B
V585 Lyr	2003	0.060363	0.000018	32	150	10.7	1.2	0.060307	0.000067	150	181	–	A
TU Men	1980	0.125721	0.000035	0	96	–2.8	2.7	0.124388	0.000033	96	120	0.1172	B
AD Men	2004	0.096559	0.000228	–	–	–	–	–	–	–	–	–	C
FQ Mon	2004	0.073349	0.000035	0	111	9.2	2.4	0.072913	0.000054	109	205	–	B
FQ Mon	2006	0.073924	0.000103	0	51	–	–	0.072799	0.000071	51	134	–	C
FQ Mon	2007	0.073348	0.000022	0	124	5.4	1.3	0.073067	0.000083	122	164	–	B
AB Nor	2002	0.079620	0.000032	15	142	–8.1	2.7	–	–	–	–	–	BG
DT Oct	2003	0.074755	0.000019	21	118	–9.0	1.1	–	–	–	–	–	AG
DT Oct	2003b	0.074893	0.000075	0	14	–	–	–	–	–	–	–	C
DT Oct	2008	0.074554	0.000043	0	40	–	–	–	–	–	–	–	C2
V699 Oph	2003	0.070326	0.000038	0	43	14.2	7.7	0.070089	0.000061	42	68	–	B
V699 Oph	2008	0.070130	0.000014	14	87	–	–	0.069931	0.000060	87	129	–	C
V2051 Oph	1999	0.064367	0.000029	0	113	2.9	2.9	–	–	–	–	0.062428	C
V2051 Oph	2003	0.064850	0.000085	0	17	–	–	0.063801	0.000083	16	48	0.062428	C
V2051 Oph	2009	0.064179	0.000019	0	48	–	–	–	–	–	–	0.062428	C
V2527 Oph	2004	0.072050	0.000016	29	103	6.0	1.7	0.071522	0.000020	103	168	–	A
V2527 Oph	2006	0.071942	0.000019	0	97	–	–	–	–	–	–	–	C
V2527 Oph	2008	0.071943	0.000062	0	111	–	–	–	–	–	–	–	C
V1159 Ori	1993	0.064201	0.000014	0	116	4.2	1.1	0.063905	0.000012	124	194	0.062178	A
V1159 Ori	2002	0.064144	0.000049	0	63	14.9	5.4	0.064086	0.000046	93	249	0.062178	B
V344 Pav	2004	–	–	–	–	–	–	0.079667	0.000152	0	51	–	C
EF Peg	1991	0.086930	0.000018	23	111	–1.3	1.7	0.086623	0.000018	110	157	–	A
EF Peg	1997	0.087037	0.000025	0	91	–4.2	2.1	–	–	–	–	–	BG
V364 Peg	2004	0.085338	0.000032	0	28	–	–	–	–	–	–	–	C2
V368 Peg	2000	0.070380	0.000008	0	86	0.5	1.2	0.070054	0.000052	85	142	–	B
V368 Peg	2005	0.070381	0.000026	70	97	–	–	–	–	–	–	–	C
V368 Peg	2006	–	–	–	–	–	–	0.069945	0.000018	0	61	–	C
V369 Peg	1999	0.085694	0.000274	0	27	–	–	0.084854	0.000102	24	82	–	C
UV Per	2000	0.066627	0.000033	14	62	9.5	6.0	0.066288	0.000036	62	185	0.06489	B
UV Per	2003	0.066671	0.000010	20	109	5.1	1.0	0.066251	0.000015	107	176	0.06489	A
UV Per	2007	0.066319	0.000008	20	85	0.1	1.9	0.066017	0.000090	82	99	0.06489	BG
PU Per	2009	0.068707	0.000280	0	18	–	–	0.067973	0.000099	18	90	–	C
PV Per	2008	0.080801	0.000018	0	36	–	–	0.080349	0.000050	35	161	–	B
QY Per	1999	0.078611	0.000022	5	69	7.8	3.1	0.078140	0.000052	67	123	–	A
QY Per	2005	0.078609	0.000058	0	54	–	–	0.078188	0.000018	54	117	–	C
TY PsA	2008	0.087990	0.000017	0	34	–	–	0.087730	0.000030	46	91	0.0841	B
TY Psc	2005	0.070338	0.000013	0	43	1.5	3.0	–	–	–	–	0.06833	CG
TY Psc	2008	0.070656	0.000022	0	82	–5.2	1.9	0.070203	0.000034	82	133	0.06833	A
EI Psc	2001	0.046349	0.000007	0	141	0.3	0.8	0.046090	0.000012	162	382	0.044567	A
EI Psc	2005	0.046317	0.000007	0	73	–2.8	2.0	–	–	–	–	0.044567	B

Table 2. Superhump Periods and Period Derivatives (continued)

Object	Year	P_1	err	E_1	$P_{\dot{}}$	err	P_2	err	E_2	P_{orb}	Q		
VZ Pyx	1996	0.075754	0.000012	0	27	–	–	–	–	–	0.07332	C	
VZ Pyx	2000	–	–	–	–	–	0.075492	0.000016	0	94	0.07332	C	
VZ Pyx	2004	0.075875	0.000060	0	52	–	–	–	–	–	0.07332	C	
VZ Pyx	2008	0.076045	0.000021	0	27	–	0.075379	0.000006	54	80	0.07332	C	
DV Sco	2004	0.099776	0.000202	0	17	–	0.099243	0.000032	17	53	–	C	
MM Sco	2002	0.061324	0.000058	0	25	–	–	–	–	–	–	C	
NY Ser	1996	0.108610	–	–	–	–	0.105677	0.000304	18	37	–	C	
QW Ser	2000	0.077012	0.000014	0	79	–1.1	0.076737	0.000051	78	116	0.07453	B	
QW Ser	2002	0.077032	0.000049	0	52	18.0	0.076637	0.000057	51	91	0.07453	C	
RZ Sge	1994	0.070575	0.000028	0	42	–	0.070104	0.000037	41	100	0.06828	B	
RZ Sge	1996	0.070645	0.000028	0	88	0.6	0.070082	0.000036	88	173	0.06828	C	
RZ Sge	2002	0.070441	0.000023	27	128	–	0.069970	0.000046	128	171	0.06828	BG	
WZ Sge	1978	0.057232	0.000014	0	228	0.4	0.8	–	–	–	0.056688	B	
WZ Sge	2001	0.057204	0.000005	27	177	2.0	0.4	–	–	–	0.056688	A	
AW Sge	2000	0.074519	0.000192	0	13	–	–	–	–	–	–	C	
AW Sge	2006	0.074528	0.000032	0	44	–7.9	6.4	–	–	–	–	CG	
V551 Sgr	2003	0.067600	0.000022	22	126	6.0	1.5	–	–	–	–	A	
V4140 Sgr	2004	0.063510	0.000043	16	70	25.3	12.3	0.063092	0.000067	69	181	0.061430	C
V701 Tau	1995	0.069080	0.000050	0	60	–	–	0.068885	0.000010	58	159	–	C
V701 Tau	2005	0.069036	0.000036	0	79	11.0	3.5	–	–	–	–	B	
V1208 Tau	2000	0.070501	0.000032	0	80	–2.8	4.1	–	–	–	–	C	
V1208 Tau	2002	0.070537	0.000027	0	72	–6.3	3.8	–	–	–	–	B	
KK Tel	2002	0.087692	0.000066	22	47	–	–	–	–	–	–	C	
KK Tel	2003	0.087532	0.000050	0	13	–	–	–	–	–	–	C	
KK Tel	2004	0.087335	0.000068	0	14	–	–	–	–	–	–	CG	
EK TrA	2007	0.064335	0.000011	0	250	–0.5	0.5	–	–	–	0.06288	B	
FL TrA	2005	0.059850	0.000030	16	84	8.5	5.0	–	–	–	–	B	
UW Tri	2008	0.054194	0.000025	0	288	3.7	0.6	–	–	–	0.05334	BEM	
WY Tri	2000	0.078427	0.000045	0	40	–	–	0.077706	0.000144	37	58	–	B
SU UMa	1989	0.079209	0.000094	0	14	–	–	0.078666	0.000022	12	63	0.07635	B
SU UMa	1999	0.079091	0.000046	34	92	0.7	6.7	0.078777	0.000064	90	165	0.07635	A
SW UMa	1991	0.058251	0.000024	52	88	8.1	8.0	–	–	–	0.056815	C	
SW UMa	1996	0.058189	0.000017	0	120	8.8	0.7	–	–	–	0.056815	A	
SW UMa	1997	0.058284	0.000048	0	140	8.6	0.5	–	–	–	0.056815	C	
SW UMa	2000	0.058258	0.000012	27	217	5.1	0.5	0.057721	0.000057	217	269	0.056815	A
SW UMa	2002	0.058320	0.000021	0	142	9.9	0.9	0.057989	0.000049	142	228	0.056815	AM
SW UMa	2006	0.058214	0.000031	33	189	9.5	0.6	0.057892	0.000018	188	338	0.056815	B
BC UMa	2000	0.064555	0.000013	16	99	4.0	1.4	0.064121	–	99	116	0.06261	BG
BC UMa	2003	0.064571	0.000012	15	114	4.2	0.8	0.064183	0.000018	114	189	0.06261	A
BZ UMa	2007	0.070180	0.000014	19	64	3.6	3.3	0.069793	0.000013	72	138	0.06799	A
CI UMa	2001	0.062673	0.000098	0	32	–	–	0.062355	0.000108	31	65	–	C
CI UMa	2003	0.062688	0.000014	0	93	6.4	1.2	0.062466	0.000053	93	145	–	AM
CI UMa	2006	–	–	–	–	–	–	0.062479	0.000072	0	16	–	C
CY UMa	1995	0.072124	0.000009	0	73	2.7	1.0	0.071806	0.000020	70	153	0.06957	A
CY UMa	1998	0.072460	0.000067	0	56	–	–	0.071936	0.000020	52	154	0.06957	B
CY UMa	1999	0.072216	0.000032	0	43	–5.9	9.5	–	–	–	0.06957	CG	
CY UMa	2009	0.072219	0.000017	0	37	2.5	5.2	0.071755	0.000028	44	116	0.06957	B
DI UMa	2007a	0.055322	0.000015	18	182	4.4	0.7	–	–	–	0.054579	B	
DI UMa	2007b	0.055333	0.000022	0	126	6.0	1.6	–	–	–	0.054579	B	
DV UMa	1997	0.088800	0.000030	7	79	–2.5	3.5	0.088414	0.000034	100	184	0.085853	A
DV UMa	1999	0.088927	0.000032	0	80	–4.7	3.4	0.088360	0.000084	78	129	0.085853	B
DV UMa	2002	0.088743	0.000160	0	61	–	–	0.088404	0.000035	57	118	0.085853	B
DV UMa	2005	–	–	–	–	–	–	0.088356	0.000098	100	168	0.085853	C
DV UMa	2007	0.088539	0.000034	21	138	–4.8	2.4	–	–	–	0.085853	CG	
ER UMa	1995	0.065747	0.000024	0	123	4.1	2.1	0.065539	0.000020	–	–	0.06366	B

Table 2. Superhump Periods and Period Derivatives (continued)

Object	Year	P_1	err	E_1	$P_{\dot{d}ot}$	err	P_2	err	E_2	P_{orb}	Q		
IY UMa	2000	0.075776	0.000015	23	101	-1.8	2.2	-	-	-	0.073909	A	
IY UMa	2002	0.076009	0.000024	0	137	1.6	3.0	0.075287	0.000104	135	228	0.073909	C
IY UMa	2004	0.076030	0.000011	0	130	0.1	0.9	0.075897	0.000022	126	169	0.073909	C
IY UMa	2006	0.076082	0.000021	42	154	4.0	1.5	0.075830	0.000034	153	221	0.073909	C
IY UMa	2007	0.075849	0.000071	0	15	-	-	0.075517	0.000043	13	54	0.073909	C
IY UMa	2009	0.076233	0.000016	30	123	-1.2	1.5	0.075823	0.000027	122	189	0.073909	B
KS UMa	2003	0.070179	0.000009	15	95	2.2	1.1	0.069837	0.000021	95	147	0.06796	A
KS UMa	2007	0.070265	0.000016	0	73	1.5	1.9	-	-	-	-	0.06796	BM
MR UMa	2002	0.065157	0.000024	0	80	9.3	1.2	0.064743	0.000111	80	109	-	B
MR UMa	2003	0.065140	0.000018	0	84	6.0	2.3	0.064357	0.000066	84	144	-	B
MR UMa	2007	0.065115	0.000014	0	79	3.8	1.6	0.064887	0.000045	78	125	-	B
SS UMi	2004	0.070270	0.000062	13	57	25.0	5.0	0.070009	0.000017	55	113	0.06778	B
CU Vel	2002	0.080941	0.000038	22	75	-6.9	5.9	0.080609	0.000016	71	123	0.0785	B
HS Vir	1996	0.080056	0.000032	23	99	-	-	-	-	-	-	0.0769	C
HS Vir	2008	0.080028	0.000032	0	62	-	-	-	-	-	-	0.0769	C2
HV Vir	1992	0.058285	0.000017	0	165	5.7	0.6	-	-	-	-	0.057069	A
HV Vir	2002	0.058266	0.000017	22	173	7.4	0.6	0.058012	0.000029	172	229	0.057069	A
HV Vir	2008	0.058322	0.000027	18	157	7.1	1.9	0.058110	0.000059	157	226	0.057069	A
OU Vir	2003	0.074912	0.000017	0	217	-1.8	0.6	-	-	-	-	0.072706	CG
OU Vir	2008	0.074962	0.000132	0	24	-	-	-	-	-	-	0.072706	C
QZ Vir	1993	0.060345	0.000017	15	101	7.0	1.4	0.060087	0.000041	98	165	0.05882	B
QZ Vir	2005	0.060488	0.000050	0	50	-	-	-	-	-	-	0.05882	C
QZ Vir	2007	0.060481	0.000028	0	53	4.5	7.6	0.059984	0.000029	51	135	0.05882	BM
QZ Vir	2008	0.060442	0.000015	0	85	4.7	1.9	0.059902	0.000040	85	168	0.05882	A
QZ Vir	2009	0.060378	0.000022	0	91	11.4	1.8	0.059912	0.000010	88	251	0.05882	A
RX Vol	2003	0.061364	0.000017	0	134	5.8	0.8	-	-	-	-	-	A
TY Vul	2003	0.081196	0.000205	0	42	-	-	0.080098	0.000067	42	120	-	C
DO Vul	2008	0.058204	0.000037	0	156	9.9	2.1	-	-	-	-	-	B
NSV 4838	2005	-	-	-	-	-	-	0.069668	0.000086	0	86	-	C
NSV 4838	2007	0.069916	0.000028	0	101	7.4	1.9	0.069604	0.000024	101	189	-	B
NSV 5285	2008	0.087973	0.000086	0	34	-	-	-	-	-	-	-	C
NSV 14652	2004	0.081513	0.000016	0	50	-3.0	3.6	0.081061	0.000149	50	61	-	B
1RXS J0232	2007	0.066166	0.000011	0	106	-1.7	0.7	-	-	-	-	-	B2
1RXS J0423	2008	0.078399	0.000036	30	68	-	-	0.078130	0.000023	67	171	0.07632	B
1RXS J0532	2005	0.057156	0.000013	0	162	5.7	0.8	0.056618	0.000044	162	246	0.05620	A
1RXS J0532	2008	0.057131	0.000024	0	138	10.2	0.8	0.056778	0.000085	138	173	0.05620	A
2QZ J0219	2005	0.081199	0.000036	0	74	-1.9	3.9	0.080935	0.000034	74	123	-	B
2QZ J0219	2009	-	-	-	-	-	-	0.081004	0.000013	0	74	-	C
ASAS J0025	2004	0.057093	0.000012	0	151	8.7	0.4	0.056823	0.000032	151	236	0.056540	AP
ASAS J0233	2006	0.055987	0.000017	7	216	4.9	0.5	0.055840	0.000064	216	281	0.05490	AE
ASAS J0918	2005	0.062893	0.000067	0	32	-	-	0.062526	0.000120	32	79	-	C
ASAS J1025	2006	0.063365	0.000016	27	142	10.9	0.6	0.063021	0.000016	141	251	0.06136	AE
ASAS J1536	2004	0.064602	0.000024	30	139	2.4	2.1	-	-	-	-	-	A
ASAS J1600	2005	0.064970	0.000017	28	109	11.1	0.8	0.064597	0.000013	104	182	0.063381	AE
CTCV J0549	2006	0.084981	0.000157	23	36	-	-	0.084237	0.000049	35	119	-	B
Ha 0242	2006	0.077099	0.000022	0	43	-	-	-	-	-	-	0.074600	C
SDSS J0137	2003	0.056766	0.000013	0	98	2.3	1.7	0.056448	0.000016	98	231	0.055343	A
SDSS J0137	2009	-	-	-	-	-	-	0.056443	0.000008	0	160	0.055343	C
SDSS J0310	2004	0.068636	0.000037	0	161	2.0	2.7	-	-	-	-	-	CG
SDSS J0334	2009	0.074773	0.000052	0	54	-14.0	11.0	-	-	-	-	-	CG
SDSS J0746	2009	0.066786	0.000031	0	78	9.3	2.5	0.066621	0.000048	76	139	-	C
SDSS J0804	2006	0.059537	0.000031	0	40	-	-	-	-	-	-	0.059005	C
SDSS J0812	2008	0.084423	0.000095	0	60	-	-	0.083351	0.000259	59	95	-	B
SDSS J0824	2007	0.069770	0.000033	0	110	8.0	2.5	0.069055	0.000083	110	168	-	B
SDSS J0838	2009	-	-	-	-	-	-	0.071471	0.000023	101	155	-	CG

Table 2. Superhump Periods and Period Derivatives (continued)

Object	Year	P_1	err	E_1	$P_{\dot{}}$	err	P_2	err	E_2	P_{orb}	Q		
SDSS J1005	2009	–	–	–	–	–	0.077469	0.000021	0	49	–	C	
SDSS J1100	2009	0.067569	0.000025	0	64	–	–	–	–	–	–	C	
SDSS J1227	2007	0.064593	0.000022	33	129	6.1	2.1	–	–	–	0.062958	B	
SDSS J1524	2009	0.067136	0.000023	0	89	8.2	2.6	0.066720	0.000035	88	163	0.065319	B
SDSS J1556	2007	0.082961	0.000022	12	85	–7.6	2.3	0.082587	0.000038	85	145	0.08001	B
SDSS J1627	2008	0.109741	0.000087	15	50	–	–	0.108771	0.000022	49	150	–	A
SDSS J1702	2005	0.105065	0.000083	0	85	15.8	4.2	–	–	–	–	0.100082	B
SDSS J1730	2001	0.079413	0.000102	0	86	–	–	–	–	–	–	–	C2
SDSS J1730	2002	0.079390	0.000051	0	140	2.0	3.5	–	–	–	–	–	C2
SDSS J1730	2004	0.080068	0.000241	0	9	–	–	0.079455	0.000017	5	64	–	B
SDSS J2100	2007	0.086960	0.000150	44	56	–	–	–	–	–	–	–	C
SDSS J2258	2004	–	–	–	–	–	–	0.085900	0.000086	0	24	–	C
SDSS J2258	2008	–	–	–	–	–	–	0.086141	0.000025	0	98	–	B
OT J0042	2008	0.056892	0.000028	0	162	4.0	1.8	–	–	–	–	0.05550	BE
OT J0113	2008	0.094325	0.000076	0	43	–	–	–	–	–	–	–	C2
OT J0211	2008	0.081643	0.000313	0	14	–	–	–	–	–	–	–	C
OT J0238	2008	0.053658	0.000007	67	350	2.0	0.2	0.053202	0.000117	350	405	0.05281	BE
OT J0329	2006	0.053405	0.000006	0	139	2.8	0.3	–	–	–	–	–	B
OT J0406	2008	0.079947	0.000025	0	61	2.8	3.4	–	–	–	–	–	C2
OT J0557	2006	0.053509	0.000021	0	110	9.0	2.1	0.053258	0.000030	109	260	–	B
OT J0747	2008	0.060736	0.000009	0	109	4.0	0.8	–	–	–	–	–	B
OT J0807	2007	0.061050	0.000039	0	89	9.5	4.8	0.060656	0.000039	70	187	–	B
OT J0814	2008	0.076518	0.000021	0	79	–	–	0.075739	0.000145	79	141	–	C
OT J0845	2008	0.060473	0.000037	66	167	6.7	3.4	–	–	–	–	–	C
OT J1021	2006	0.056312	0.000012	0	240	0.4	0.8	0.056043	0.000065	237	298	–	B
OT J1026	2009	–	–	–	–	–	–	0.067520	0.000900	0	46	–	C
OT J1028	2009	0.038145	0.000025	0	59	11.6	8.5	–	–	–	–	–	C
OT J1112	2007	0.058965	0.000009	16	287	0.9	0.4	–	–	–	–	0.05847	BE
OT J1300	2008	0.064388	0.000036	14	109	14.4	1.5	–	–	–	–	–	C
OT J1440	2009	–	–	–	–	–	–	0.064736	0.000059	15	39	–	C
OT J1443	2009	0.072180	0.000028	12	112	10.0	1.3	0.071756	0.000057	110	180	–	B
OT J1631	2008	0.064125	0.000022	0	96	12.5	1.3	0.064087	0.000076	96	138	–	A
OT J1914	2008	0.071348	0.000028	0	82	9.6	2.6	0.070927	0.000078	82	168	–	B
OT J1959	2005	0.059919	0.000036	0	93	–0.7	5.2	–	–	–	–	–	C
OT J2131	2008	0.064630	0.000030	0	62	–	–	–	–	–	–	–	C
OT J2137	2008	0.099451	–	0	5	–	–	0.097675	0.000025	5	61	–	B
TSS J0222	2005	0.055585	0.000022	37	197	2.2	1.5	–	–	–	–	0.054868	BE

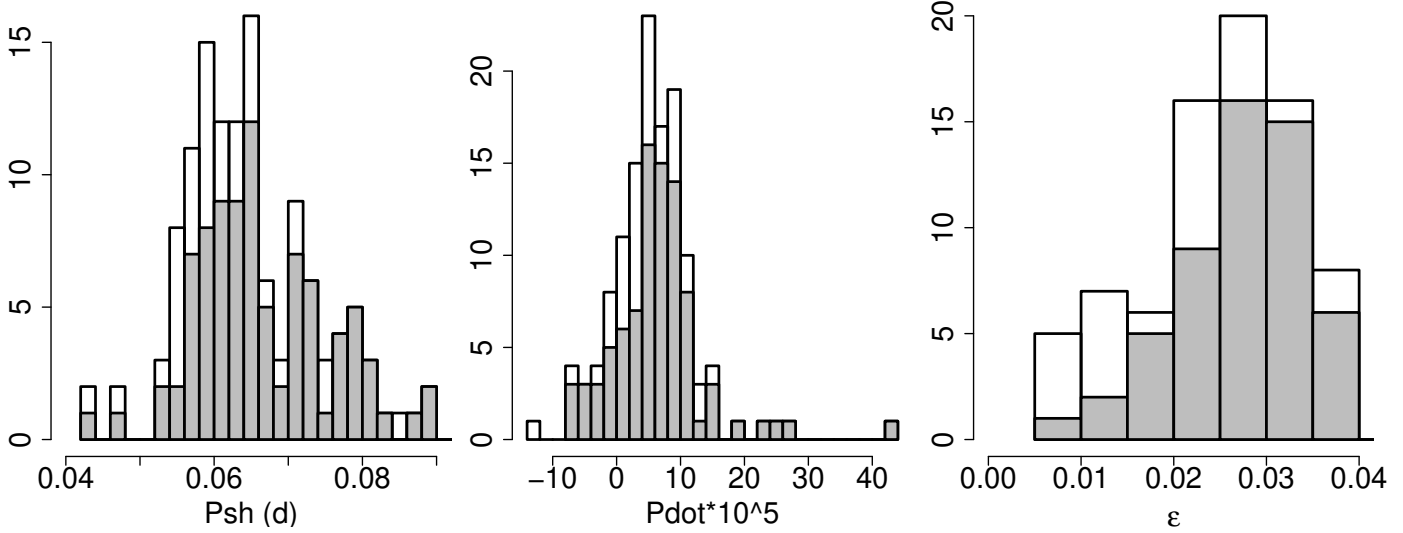


Fig. 19. Existence of stage B–C transition versus P_{SH} , P_{dot} and ϵ . The gray color indicates superoutbursts with a stage B–C transition. The existence of stage B–C transitions is most strongly correlated with ϵ .

outbursts.

4.2. Relation between stage C Superhumps and Late Superhumps

During the final stage of a superoutburst and the subsequent post-superoutburst stages, some SU UMa-type dwarf nova have been reported to exhibit modulations having approximately the same period as P_{SH} , but having a maximum phase ~ 0.5 offset from those of usual superhumps. These modulations have been traditionally called “late superhumps” (Haefner et al. 1979; Vogt 1983; van der Woerd et al. 1988; Hessman et al. 1992). We, however, could not find very convincing evidence for this phenomenon in many well-sampled objects (see e.g. QZ Vir: Ohshima et al. 2009). Instead, there seems to be almost ubiquitous presence of a transition from the stage B to C associated with a period shortening (section 3.6) and the continuity of superhump phases in well-observed systems (see also Ohshima et al. 2009).

This might suggest that at least some of claimed “late superhumps” in the literature actually referred to superhumps during the stage C. The $P_{\text{SH}} (= P_2)$ being typically ~ 0.5 – 1.0 % shorter than in earlier stages (P_1), a observational gap in ~ 30 – 50 cycles (~ 2 – 3 d) can result a phase shift of 0.15 – 0.5 , and it may have been attributed to a ~ 0.5 phase offset. Although it would be already difficult to re-examine historical observations reporting late superhumps, we should pay attention to this possibility and avoid attributing the term “late superhumps” simply because a phase offset is detected. If this interpretation is indeed the case, the term “late superhumps” should better be attributed to superhumps during the stage C (P_2).⁷

There is some evidence of traditional late superhumps in DT Oct (subsection 6.90) and HS Vir (subsection 6.136).

⁷ Note, however, we used “late superhumps” for late-stage superhumps different from ordinary ones in WZ Sge-type dwarf novae (Kato et al. 2008).

It may be that this type of traditional late superhumps is only observed in systems with a high mass-transfer rate, enabling sufficient luminosity from the hot spot.

4.3. Implications of Period Transition in Interpreting Observations

One of the important consequences of the period transition between stages B and C in interpreting observations is that this appearance of a new, stable, period is sometimes confused with the orbital period (see likely examples, IX Dra: Olech et al. 2004b, OT J102146.4+234926: Uemura et al. 2008a). Photometrically claimed orbital periods during superoutbursts, especially those giving $\epsilon < 1$ % need to be carefully re-examined.

Furthermore, the presence of two distinct periods with fair stability might be problematic in identifying multiple periodicity by analyzing power spectra of the entire data (e.g. Patterson et al. 2003).

A typical difference of 0.5 – 1.0 % in P_{SH} between P_1 and P_2 corresponds to a difference of 0.03 – 0.05 in q (Patterson et al. 2005). This difference could result a systematic error in calibrating ϵ – q relation, or estimating q depending on the stage when P_{SH} is measured. The situation could be worse if the relation is applied to superhump periods obtained around the termination of the stage B (subsection 3.5, figure 14). This issue is further discussed in subsection 4.12.

4.4. Minimum Superhump Period and 3:1 Resonance

Among surveyed sets of parameters, we have noticed that the fractional period excess for minimum P_{SH} of a given superoutburst (either P_2 or P_{SH} at the start of the stage B for $P_{\text{dot}} > 0$ systems) of a given system is most smoothly and tightly correlated with other system parameters (figures 20, 21; for a comparison of other representative P_{SH} , see figure 22). In figure 21, we give ϵ expected for dynamical precession rate at the 3:1 resonance ($\epsilon_{3:1}$),

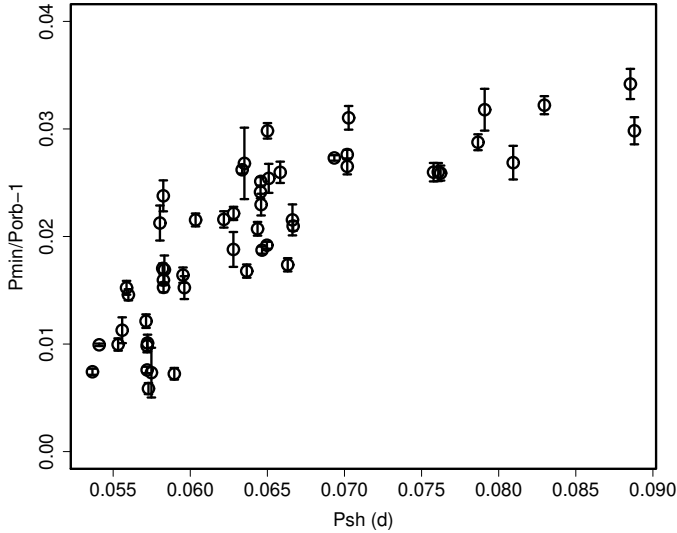


Fig. 20. Relation between the fractional period excess for the minimum P_{SH} and P_{SH} (P_1).

using the ϵ - q relation (Patterson et al. 2005, using the updated one discussed in subsection 4.12) and angular velocity of disk precession formulated by Osaki (1985). The ϵ for the minimum P_{SH} best parallels the expected ϵ for the 3:1 resonance. We therefore regard that the minimum P_{SH} represents the precession at the 3:1 resonance. This interpretation can naturally explain the ubiquitous presence of the stage C and the stability of the superhump period during the stage C. The systematic difference between $\epsilon_{3:1}$ and observed values is likely attributed to the scaling problem in interpreting hydrodynamical precession rate of a disk as a whole by single-particle dynamical precession (see Smith et al. 2007) rather than the real difference.

In systems lacking the stage C, such as many of extreme WZ Sge-type dwarf novae, the P_{SH} appears to always reflect the precession rate at the 3:1 resonance. The stability of the P_{SH} in such systems can then be naturally explained. In positive P_{dot} systems, P_{SH} at the start of the stage B is almost identical to P_2 (subsection 3.6). This can be understood as superhumps excited at the 3:1 resonance quickly dominates at the start of the stage B in these systems.

4.5. Maximum Superhump Period and Disk Radius

By assuming this interpretation and assuming the radial dependence of precession rate (Murray 2000), we can calculate the disk radius from ϵ at other epochs.⁸

⁸ In scaling the radius, we used the radius of single-particle dynamical 3:1 resonance for simplicity. This radius may be systematically too large (Smith et al. 2007). Other factors proposed to affect superhump periods include changes in temperature or pressure (Hirose, Osaki 1993; Murray 1998; Montgomery 2001; Pearson 2006). Since the disk temperature is expected to decrease during the decline phase, a slowing effect on the precession due to the pressure forces is expected to decrease Montgomery (2001). This expectation is contrary to the global period decrease generally observed, and we regard that the vari-

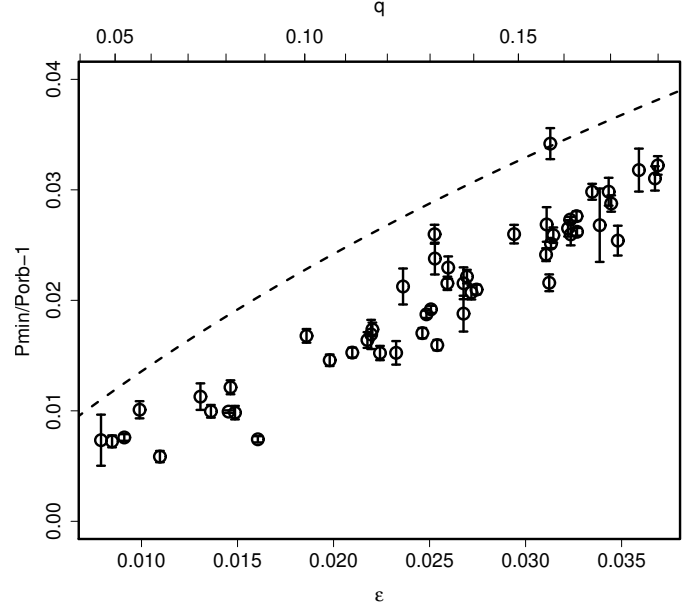


Fig. 21. Relation between the fractional period excess for the minimum P_{SH} and q , scaled from P_1 . The dashed line represents fractional excess expected for single particle dynamical precession rate at 1:3 resonance.

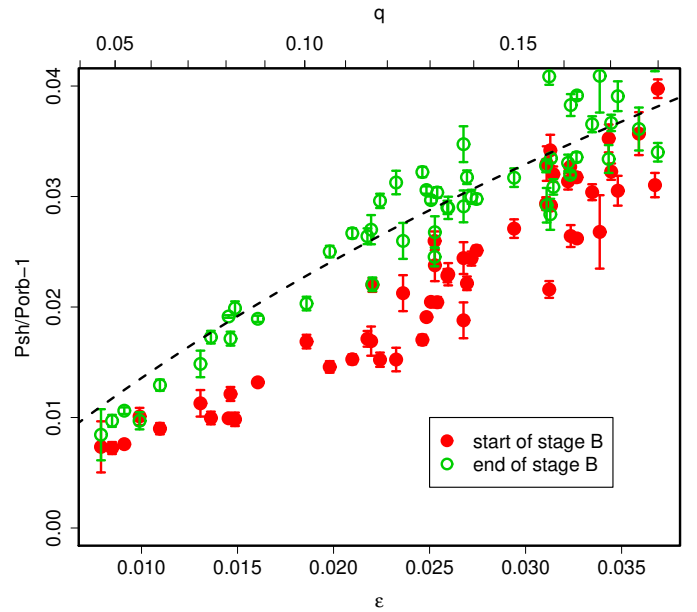


Fig. 22. Relation between the fractional period excess for the different epochs of stage B P_{SH} and q , scaled from P_1 . The dashed line is the same as in figure 21.

Table 3. Superhump Periods during Stage A

Object	Year	period (d)	err
V455 And	2007	0.05803	0.00008
V466 And	2008	0.05815	0.00008
DH Aql	2003	0.08079	0.00012
VY Aqr	2008	0.06558	0.00026
EG Aqr	2006	0.08128	0.00018
TT Boo	2004	0.07911	0.00009
UZ Boo	2003	0.06354	0.00024
AX Cap	2004	0.12279	0.00277
GX Cas	1996	0.09690	0.00055
V1040 Cen	2002	0.06243	0.00007
WX Cet	1989	0.06031	0.00003
WX Cet	1998	0.06027	0.00014
RX Cha	2009	0.08710	–
BZ Cir	2004	0.07692	0.00005
PU CMa	2008	0.05901	0.00022
AL Com	1995	0.05799	0.00014
AL Com	2001	0.05791	0.00022
GO Com	2003	0.06323	0.00010
V632 Cyg	2008	0.06628	0.00007
V1028 Cyg	1995	0.06269	0.00011
V1113 Cyg	1994	0.07963	0.00007
KV Dra	2009	0.06109	0.00026
XZ Eri	2008	0.06519	0.00021
UV Gem	2003	0.09635	0.00030
AW Gem	1995	0.08276	0.00053
AW Gem	2009	0.08185	0.00038
V844 Her	2006	0.05649	0.00005
MM Hya	2001	0.06032	0.00025
RZ Leo	2000	0.08046	0.00053
GW Lib	2007	0.05473	0.00007
V419 Lyr	2006	0.09131	0.00009
V585 Lyr	2003	0.06113	0.00008
AB Nor	2002	0.08174	0.00027
DT Oct	2003	0.07650	0.00017
V2527 Oph	2004	0.07226	0.00008
V368 Peg	2005	0.07130	–
UV Per	2003	0.06813	0.00009
UV Per	2007	0.06659	0.00002
QY Per	1999	0.08037	0.00032
WZ Sge	2001	0.05838	0.00006
SU UMa	1999	0.08054	0.00021
SW UMa	1991	0.05908	0.00014
SW UMa	2000	0.05877	0.00006
SW UMa	2006	0.05894	0.00005
BC UMa	2003	0.06512	0.00006
BZ UMa	2007	0.07113	0.00039
DV UMa	2005	0.08929	–
DV UMa	2007	0.08926	0.00018
IY UMa	2000	0.07666	0.00015
KS UMa	2003	0.07095	0.00009
HS Vir	1996	0.08118	0.00021

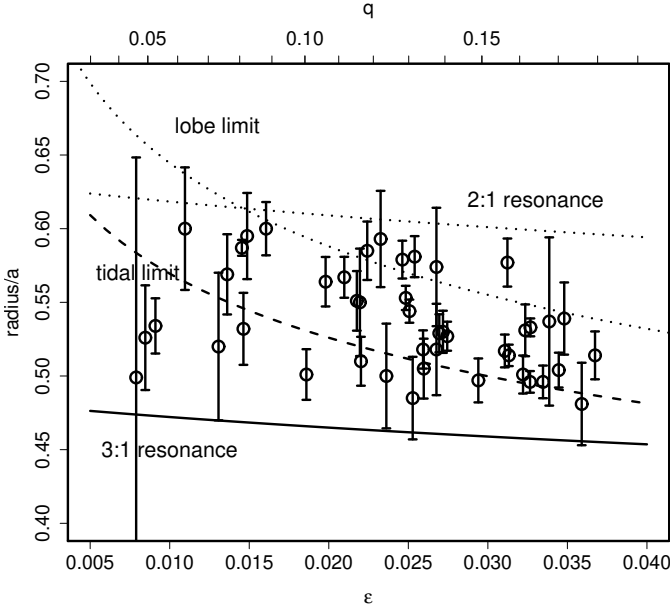


Fig. 23. Disk radius at the end of stage B scaled from ratios of ϵ (for P_1) between the end of stage B and the minimum P_{SH} . The locations of various resonances and limits are the same as in Kato et al. (2008).

The radii calculated for the end of stage B for systems with $P_{dot} > 0$, corresponding to the maximum radii, are given in table 4 and figure 23. The radii at the end of stage B for positive P_{dot} systems are reasonably situated, considering the errors and the simplified treatment, around the radii of tidal truncation or slightly beyond this. This result can lead to a picture that superhumps are initially excited at the 3:1 resonance, whose outward propagation (if there is sufficient matter outside the 3:1 resonance) is limited by tidal truncation. This probably determines the maximum attainable P_{SH} in positive P_{dot} systems. Since the superhumps usually quickly decay near the end of stage B, the large dissipation at large radius seems to quickly quench the eccentricity power.

This picture generally well applies to systems with $\epsilon > 0.02$ (corresponding to $q > 0.11$). Objects with smaller ϵ tend to deviate from this trend. These objects include extreme WZ Sge-type dwarf novae (WZ Sge, V455 And, AL Com) while some of (what are usually regarded as) WZ Sge-type dwarf novae (GW Lib, HV Vir) have a similar tendency to ordinary SU UMa-type dwarf novae. The small radii for V436 Cen, UV Per (2007) and others may have been a result of undersampling of superhump timings; the case for UV Per is particularly likely because other well-sampled superoutbursts of the same object generally gave larger radii.

The difference among WZ Sge-type dwarf novae can be attributed to the matter left beyond the 3:1 resonance (Kato et al. 2008): if the 2:1 resonance is strong enough

ation in the disk temperature is unlikely the primary cause of the period variation. We therefore focus on dynamical precession and did not consider other effects for simplicity.

Table 3. Superhump Periods during Stage A (continued)

Object	Year	period (d)	err
HV Vir	2002	0.05864	0.00002
1RXS J0423	2008	0.07970	0.00010
ASAS J0233	2006	0.05676	0.00007
ASAS J1025	2006	0.06407	0.00010
ASAS J1536	2004	0.06557	0.00014
ASAS J1600	2005	0.06653	0.00012
CTCV J0549	2006	0.08650	0.00026
SDSS J1556	2007	0.08395	0.00014
SDSS J1627	2008	0.11269	0.00067
OT J1443	2009	0.07461	0.00055

to accrete much of the matter beyond the radius of 3:1 resonance, the propagation of the eccentricity wave beyond the 3:1 resonance would not produce a strong superhump signal with a longer period. Further observations, however, are especially needed in these cases whether different types of superoutbursts (cf. Uemura et al. 2008b) in the same WZ Sge-type object lead to different behavior of P_{SH} .

4.6. Superhump Period at the Start of Stage B

The radii calculated for the start of stage B are given in table 5 and figure 24. In systems with positive P_{dot} , these radii match the supposed 3:1 resonance. The exceptions, AL Com in 1995 and OT J0238 in 2008, are likely a result of the poorly determined stage C superhumps. In negative P_{dot} systems (generally corresponding to $\epsilon > 0.025$), the decrease in the P_{SH} can be explained if superhumps are initially excited slightly outside the 3:1 resonance. In such systems, the large tidal torque caused by the large q might enable eccentricity wave originating even outside the 3:1 resonance.

4.7. Stage C Superhumps in Positive P_{dot} Systems

In our interpretation, the stage C superhumps in positive P_{dot} are regarded as superhumps stably originating from the radius of the 3:1 resonance. It looks as if superhumps are newly excited around the radius of 3:1 resonance after the original superhumps reached a larger radius (limiting radius as discussed in subsection 4.5) and their eccentric power is quenched. It may be that superhumps can be rejuvenized if the eccentricity of the original superhumps become sufficiently weak and there is still sufficient matter around the 3:1 resonance. Such a condition could be realized when the matter beyond the 3:1 resonance still remains after the termination of a superoutburst (cf. Kato et al. 2008) and if this matter is efficiently accreted inward. The brightening associated with the appearance (or regrowth) of superhumps at the start of the stage C can be naturally explained by this accretion and increased dissipation due to a renewed tidal instability.

4.8. Stage A Superhumps

We similarly calculated the radii for the start of the stage A (figure 25). In some systems, the fractional su-

Table 4. Estimated disk radius at the end of stage B.

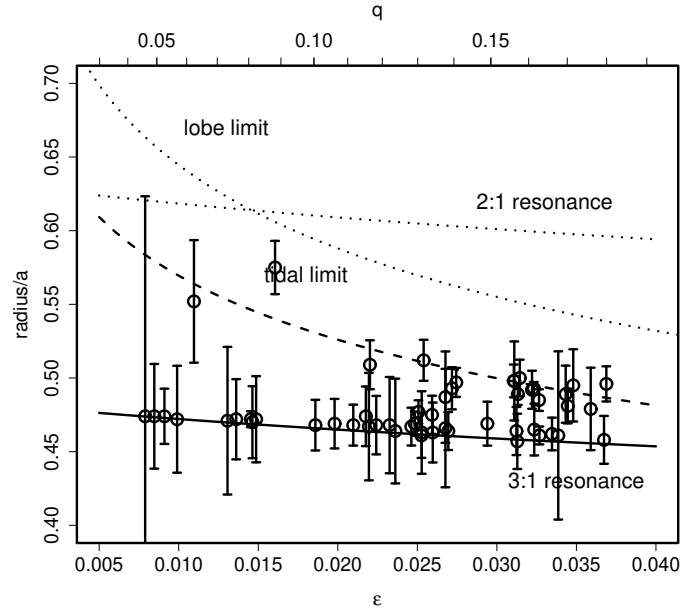
Object	Year	ϵ	r^a	err ^b
V1108 Her	2004	0.008	0.499	0.149
OT J1112	2007	0.008	0.526	0.036
WZ Sge	2001	0.009	0.534	0.019
AL Com	1995	0.011	0.600	0.042
TSS J0222	2005	0.013	0.520	0.050
DI UMa	2007a	0.014	0.569	0.027
GW Lib	2007	0.015	0.587	0.005
V455 And	2007	0.015	0.532	0.024
V466 And	2008	0.015	0.595	0.029
OT J0238	2008	0.016	0.600	0.018
V436 Cen	1978	0.019	0.501	0.017
ASAS J0233	2006	0.020	0.564	0.017
HV Vir	2002	0.021	0.567	0.014
WX Cet	1998	0.022	0.551	0.020
HV Vir	2008	0.022	0.550	0.036
UV Per	2007	0.022	0.510	0.017
V844 Her	2006	0.022	0.585	0.020
WX Cet	1989	0.023	0.593	0.033
PU CMa	2008	0.024	0.500	0.036
SW UMa	2006	0.025	0.579	0.013
VY Aqr	2008	0.025	0.553	0.008
ASAS J1600	2005	0.025	0.544	0.008
SW UMa	1991	0.025	0.485	0.028
SW UMa	2000	0.025	0.581	0.014
QZ Vir	1993	0.026	0.518	0.013
SDSS J1227	2007	0.026	0.505	0.020
XZ Eri	2008	0.027	0.574	0.040
UV Per	2000	0.027	0.518	0.031
XZ Eri	2007	0.027	0.529	0.013
HO Del	2008	0.027	0.530	0.014
UV Per	2003	0.027	0.527	0.010
IY UMa	2006	0.029	0.497	0.015
BC UMa	2000	0.031	0.517	0.011
V1040 Cen	2002	0.031	0.577	0.016
BC UMa	2003	0.031	0.514	0.007
BZ UMa	2007	0.032	0.501	0.013
V632 Cyg	2008	0.032	0.531	0.018
KS UMa	2003	0.033	0.496	0.007
ASAS J1025	2006	0.033	0.533	0.006
TV Crv	2001	0.033	0.496	0.011
V4140 Sgr	2004	0.034	0.537	0.057
RZ Leo	2000	0.034	0.504	0.012
TV Crv	2004	0.035	0.539	0.024
SU UMa	1999	0.036	0.481	0.028
SS UMi	2004	0.037	0.514	0.016

^a Estimated disk radius at the end of stage B.

^b Error in the radius.

Table 5. Estimated disk radius at the start of stage B.

Object	Year	ϵ	r^a	err ^b
V1108 Her	2004	0.008	0.474	0.149
OT J1112	2007	0.008	0.474	0.036
WZ Sge	2001	0.009	0.474	0.019
AL Com	2001	0.010	0.472	0.036
AL Com	1995	0.011	0.552	0.042
TSS J0222	2005	0.013	0.471	0.050
DI UMa	2007a	0.014	0.472	0.027
GW Lib	2007	0.015	0.472	0.005
V455 And	2007	0.015	0.470	0.024
V466 And	2008	0.015	0.472	0.029
OT J0238	2008	0.016	0.575	0.018
V436 Cen	1978	0.019	0.468	0.017
ASAS J0233	2006	0.020	0.469	0.017
HV Vir	2002	0.021	0.468	0.014
WX Cet	1998	0.022	0.474	0.020
HV Vir	2008	0.022	0.467	0.036
UV Per	2007	0.022	0.509	0.017
V844 Her	2006	0.022	0.468	0.020
WX Cet	1989	0.023	0.468	0.033
PU CMa	2008	0.024	0.464	0.036
SW UMa	2006	0.025	0.467	0.013
VY Aqr	2008	0.025	0.469	0.008
ASAS J1600	2005	0.025	0.477	0.008
IY UMa	2000	0.025	0.461	0.015
SW UMa	1991	0.025	0.463	0.028
SW UMa	2000	0.025	0.512	0.014
QZ Vir	1993	0.026	0.475	0.013
SDSS J1227	2007	0.026	0.463	0.020
XZ Eri	2008	0.027	0.466	0.040
UV Per	2000	0.027	0.487	0.031
XZ Eri	2007	0.027	0.464	0.013
HO Del	2008	0.027	0.493	0.014
UV Per	2003	0.027	0.497	0.010
IY UMa	2006	0.029	0.469	0.015
BC UMa	2000	0.031	0.498	0.011
CU Vel	2002	0.031	0.498	0.027
V1040 Cen	2002	0.031	0.464	0.016
DV UMa	2007	0.031	0.457	0.019
BC UMa	2003	0.031	0.489	0.007
IY UMa	2009	0.031	0.500	0.012
BZ UMa	2007	0.032	0.492	0.013
SX LMi	2002	0.032	0.493	0.004
V632 Cyg	2008	0.032	0.465	0.018
KS UMa	2003	0.033	0.485	0.007
ASAS J1025	2006	0.033	0.461	0.006
TV Crv	2001	0.033	0.462	0.011
V4140 Sgr	2004	0.034	0.461	0.057
DV UMa	1997	0.034	0.489	0.019
RZ Leo	2000	0.034	0.481	0.012
TV Crv	2004	0.035	0.495	0.024
SU UMa	1999	0.036	0.479	0.028
SS UMi	2004	0.037	0.458	0.016
SDSS J1556	2007	0.037	0.496	0.012

^a Estimated disk radius at the start of stage B.^b Error in the radius.**Fig. 24.** Disk radius at the start of stage B scaled from ratios of ϵ between the end of the stage B and the minimum P_{SH} .

perhump excesses exceed the range in Murray (2000), and they are shown in lower limits. The periods of stage A superhumps can be understood if they originate from the outermost disk. Since stage A and B superhumps show a smooth transition in phase, the eccentricity excited during the stage A in the outside the disk appears to efficiently excite the strong eccentricity at the radius of the 3:1 resonance. It may be that the eccentricity invoked during the stage A can efficiently work as a seed perturbation at the radius of the 3:1 resonance. The situation might be the same for the stage B–C transition.

Although many of very well observed superoutbursts show stage A, some superoutbursts showed different behavior. Among them, QZ Vir in 1993 and 1RXS J0532 in 2005 associated with precursor outbursts did not show long-period superhumps as in usual stage A. The initial period of superhumps during the 1993 superoutburst of QZ Vir was close to the orbital period (Kato 1997), an exceptional case in this study. The existence of a prominent precursor in these superoutburst can be understood as a result of a small disk-mass at the onset of superoutbursts (Osaki, Meyer 2003). In these superoutbursts, the disk mass may have been so small that virtually no mass was present beyond the 3:1 resonance.

Note, however, stage A with long-period superhumps was definitely recorded during superoutbursts of GO Com in 2003 (Imada et al. 2005) and PU CMa in 2008 (subsection 6.33). The condition whether stage A appears or not may depend on other factors.

With smoothed particle hydrodynamics (SPH), Murray (1998) reported a longer superhump period during the early stage of eccentricity growth. Although this might correspond to stage A superhumps, the exact identification should await further investigation.

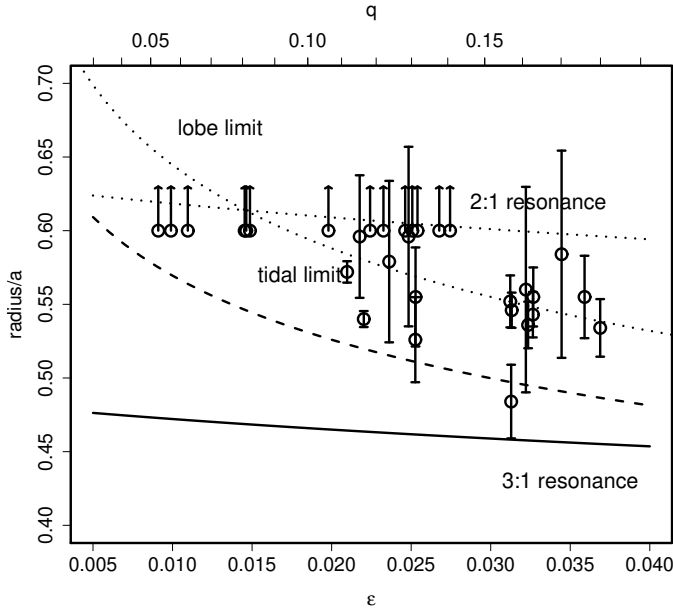


Fig. 25. Disk radius during the stage A scaled from ratios of ϵ between the end of stage B and the minimum P_{SH} . Upper arrow show lower limits.

4.9. ER UMa Stars

ER UMa stars are a subgroup of SU UMa-type dwarf novae characterized by the shortness (19–50 d) of their supercycles (Kato, Kunjaya 1995; Robertson et al. 1995; Misselt, Shafter 1995; Nogami et al. 1995c; Osaki 1995a). It has been demonstrated that at least some of ER UMa stars show large-amplitude superhumps at the onset of superoutbursts (Kato et al. 1996b) and a phase reversal of superhumps during the early plateau stage (Kato et al. 2003b). Osaki, Meyer (2003) interpreted large-amplitude superhumps in the early stage is a consequence of tidal heating at the outer edge by the continuous presence of tidal instability, resulting a superoutburst driven by the tidal instability. The origin of the phase reversal is not yet well understood. Kato et al. (2003b) suspected that a movement of the location of the strongest tidal dissipation to the opposite direction somehow happened, while Olech et al. (2004b) considered a beat between the superhump and orbital periods.⁹

Due to the complexity in the hump profile and limited availability of high-quality raw data, we do not discuss on these objects in detail. An $O-C$ analysis for ER UMa is presented here, and brief discussions on V1159 Ori and RZ LMi are given in Appendix section 6.

Upon examination of the data used in Kato et al. (2003b), we noticed that the early-stage superhumps can be tracked for a while even after the occurrence of the reported phase reversal (figure 26, open circles). These superhumps appear to comfortably follow a positive P_{dot} expected for this P_{SH} . In ER UMa, the stage C appeared to

⁹ As discussed in subsection 4.3 this “orbital period” likely referred to P_2 rather than the true P_{orb} .

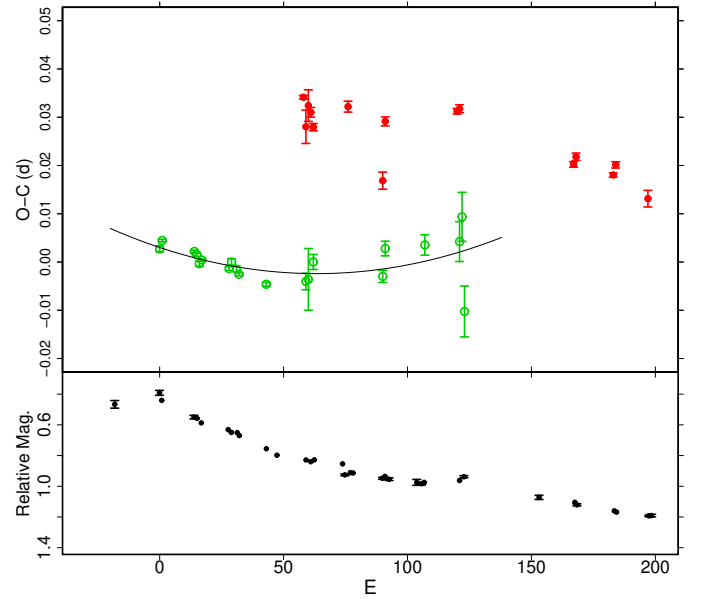


Fig. 26. $O-C$ variation in ER UMa (1995). (Upper) $O-C$. The open and filled circles represent early-stage and later-stage superhumps described in Kato et al. (2003b). (Lower) Light curve.

have started earlier than in ordinary SU UMa-type dwarf novae, and was observed as a regrowth of superhumps associated with a phase reversal (figure 26, filled circles). It may be that a combination of a large mass-transfer rate from the secondary, and the small amount of disk matter beyond the 3:1 resonance in ER UMa stars (Osaki, Meyer 2003) serves a condition enabling early rejuvenation of superhumps (cf. subsection 4.7). It is not known why only ER UMa stars show a ~ 0.5 phase shift at the onset of the stage C. Detailed observations of ER UMa stars might provide a clue to understanding the nature of the stage B–C transition.

The behavior of superhumps in RZ LMi is still poorly known. Olech et al. (2008) reported that its superhump periods were almost constant other than one well-observed, 2004 superoutburst. Olech et al. (2008) claimed that the phases of superhumps were even coherent between different superoutbursts. We should, however, note that many of observations by Olech et al. (2008) covered only a few days of individual superoutbursts, making it difficult to estimate P_{dot} for individual superoutbursts. Instead, reported superhump maxima in Olech et al. (2008) can be reasonably well expressed by a slightly positive P_{dot} , by the same overlaying method used in subsection 3.8 (figure 27). We consider that the P_{dot} observed during the 2004 superoutburst is typical for this object and the slight difference in P_{SH} between different superoutbursts (Olech et al. 2008) was a result of observation of different phase of superoutbursts. This interpretation needs to be tested by continuous observation throughout different superoutbursts. It would be intriguing to see whether or not the stage C is present in RZ LMi (see

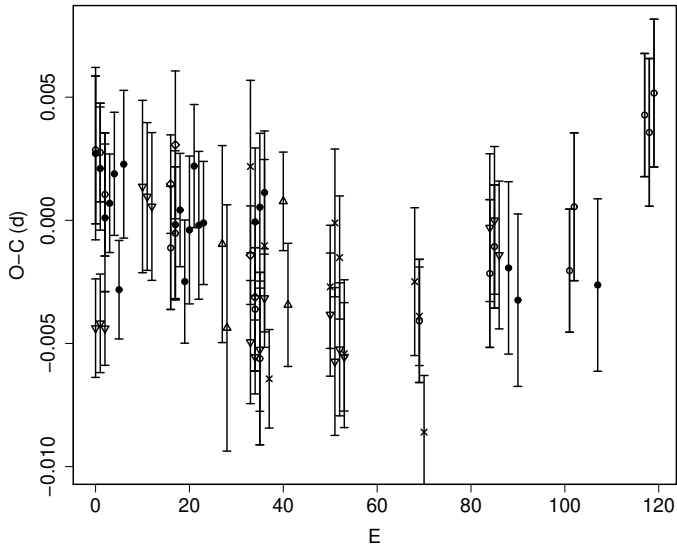


Fig. 27. $O - C$ variation in RZ LMi. The hump maxima are taken from Olech et al. (2008) and are shifted so that the start of individual superoutburst corresponds to $E = 0$.

subsection 6.77), which might provide a clue why superoutbursts in RZ LMi are quenched so early (cf. Osaki 1995b; Hellier 2001).

Most recently, Rutkowski et al. (2008) reported a positive, but a relatively small P_{dot} in another ultra-short P_{SH} ER UMa star, DI UMa. Rutkowski et al. (2008) also reported superhump-like variations during the rising stage but were shifted in phase by $\sim 0.5 P_{\text{SH}}$. These variations may have been stage A superhumps, and we obtained a period of 0.0569(2) d by assuming the phase continuity. The exact identification of their nature should await a further study. If the superhumps were evolving in period during the rising stage of DI UMa, as in the stage A in ordinary SU UMa-type dwarf novae, the onset of tidal instability likely coincides with the ignition of the outburst, on the contrary to the expectation in Osaki, Meyer (2003) that tidal instability triggers ER UMa-type superoutbursts.

4.10. Long-Period Systems

The period variation of superhumps in long-period (P_{SH}) systems appears to vary from system to system. Some systems, such as MN Dra and UV Gem, show smoothly decreasing P_{SH} (figure 28), while others, such as AX Cap and SDSS J1627, show stage transitions (accompanied by a break in the $O - C$ diagram and a well-defined stage C superhumps with a fairly constant period) as in short- P_{SH} systems (figure 29). Note, however, the degree of period variation is strongly different from system to system. Although the global pattern of period variation is similar between AX Cap and SDSS J1627, the amplitude of $O - C$'s are several times larger in the former system. There are apparently a class of systems with a much smaller period variation, such as TU Men, EF Peg, BF Ara and V725 Aql. Although further confirmation is necessary, SDSS J1702 (and possibly V725 Aql)

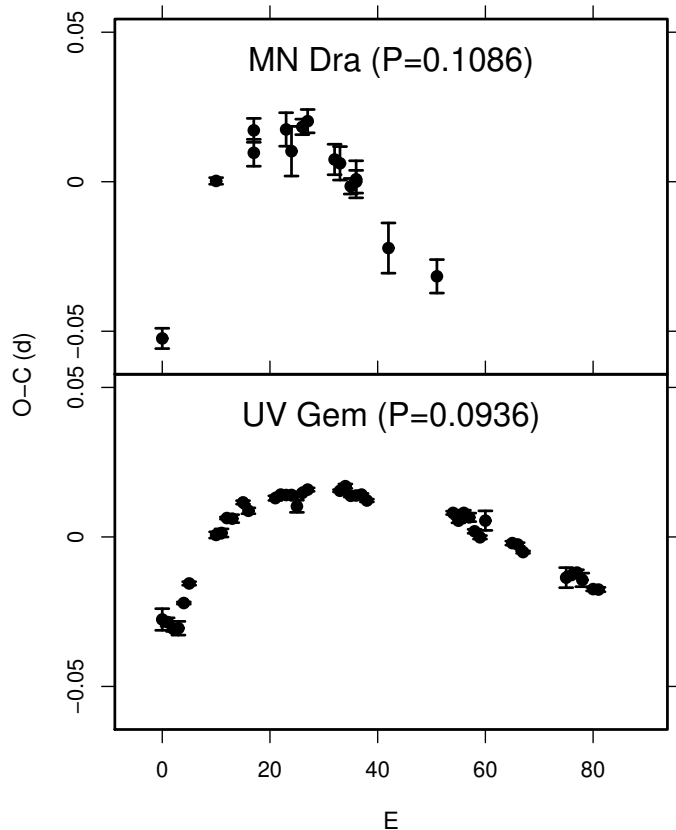


Fig. 28. $O - C$ variations of Long- P_{SH} systems with smooth period variations.

even appears to have a positive period derivative.

The systems with smoothly decreasing P_{SH} look like to have more frequent normal outbursts than in systems with stage transitions. The latter class of long- P_{SH} SU UMa-type dwarf novae seems to somehow mimic short- P_{SH} SU UMa-type dwarf novae with infrequent superoutbursts. Whether there is a difference in q or other system parameters, or whether suppression of normal outbursts somehow works in the latter class need to be tested by further observations.

4.11. Superhumps in Black-Hole X-Ray Transients

Black-hole X-ray transients (BHXTs) are known to show superhumps (cf. Bailyn 1992; Kato et al. 1995; O'Donoghue, Charles 1996; Haswell et al. 2001; Uemura et al. 2002c).

KV UMa (=XTE J1118+480) is the best studied superhumping system among BHXTs. The $O - C$ diagram (figure 30, see subsection 6.133 for the data) closely resemble those of SU UMa-type dwarf novae with intermediate P_{orb} . The similarity of the $O - C$ variation between SU UMa-type dwarf novae and a BHXT suggests that the evolution mechanism of superhumps is similar between these systems. The degree of period variation, such as $P_2/P_1 - 1 = 0.001$ and global $P_{\text{dot}} = -0.43(0.05) \times 10^{-5}$, is an order of magnitude smaller than those of typical SU UMa-type

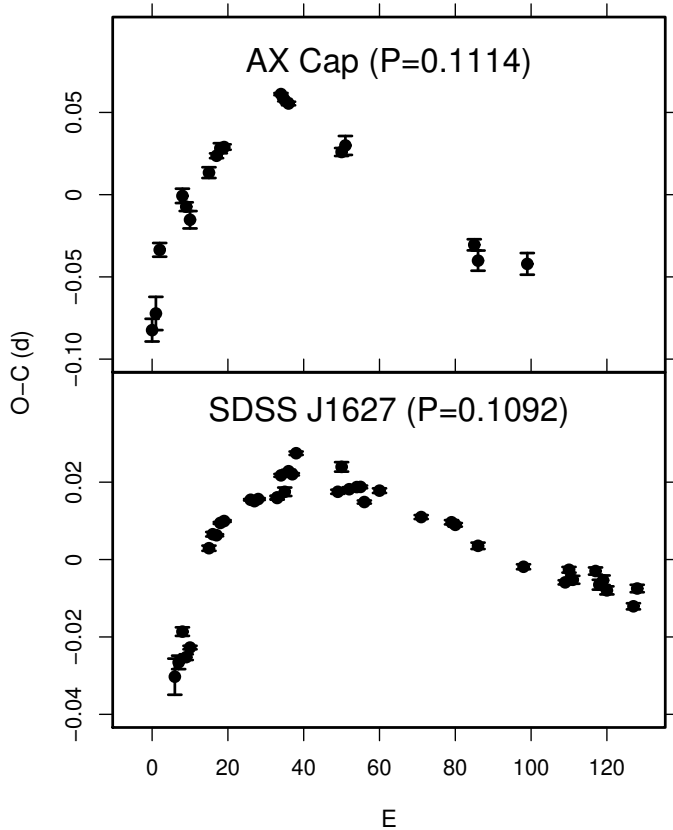


Fig. 29. $O - C$ variations of Long- P_{SH} systems with period breaks.

dwarf novae. This difference may be attributed to the difference in the emission mechanism of superhumps between CVs and BHXTs (Haswell et al. 2001). In BHXTs, the outer region of the accretion disk may be efficiently shadowed by the inner region and may not be sufficiently ionized for the eccentricity wave to propagate. A study of period variation of superhumps in BHXTs is expected to provide additional clue in understanding the origin of superhumps in these systems and might serve as a potential tool for studying the structure of the outer accretion disks in these systems.

An updated analysis for V518 Per is also presented in subsection 6.104.

4.12. ϵ - q Relation

Since it has become more evident that the shortest P_{SH} (in many cases, this agrees with P_2), rather than mean P_{SH} , represents the characteristic P_{SH} for SU UMa-type superoutbursts, we re-calibrated the ϵ - q relation using the shortest P_{SH} as in the way in Patterson et al. (2005). The data are given in table 6 (the q and ϵ for DW UMa and UU Aqr are from Patterson et al. 2005; ϵ for other objects are newly determined in this work). The updated ϵ - q is shown in equation 5 and figure 31.

$$\epsilon = 0.16(2)q + 0.25(7)q^2. \quad (5)$$

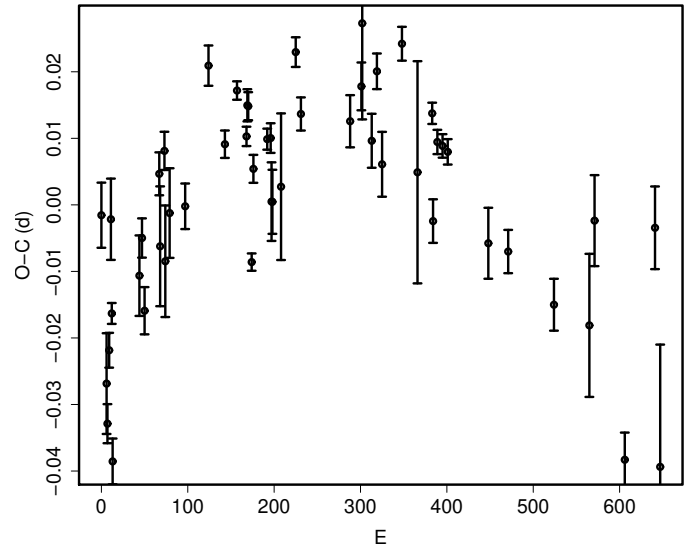


Fig. 30. $O - C$ diagram of KV UMa (=XTE J1118+480) during the 2000 outburst.

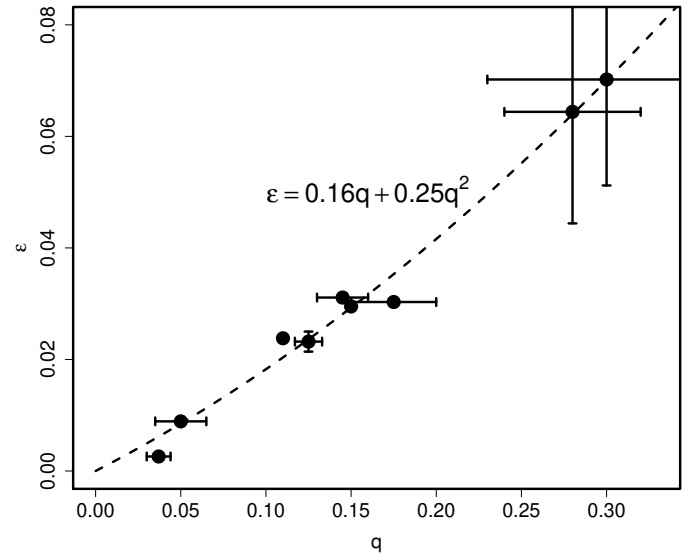


Fig. 31. Fractional superhump excess versus mass-ratio. ϵ denotes fractional superhump excess for the minimum P_{SH} .

Table 6. Fractional superhump excess versus mass-ratio

Object	ϵ	q
KV UMa	0.0026(2)	0.037(7)
WZ Sge	0.0089(1)	0.050(15)
XZ Eri	0.0238(4)	0.110(2)
IY UMa	0.0238(18)	0.125(8)
Z Cha	0.0311(8)	0.145(15)
DV UMa	0.0295(2)	0.150(1)
OU Vir	0.0303(2)	0.175(25)
DW UMa	0.0644(20)	0.28(4)
UU Aqr	0.0702(19)	0.30(7)

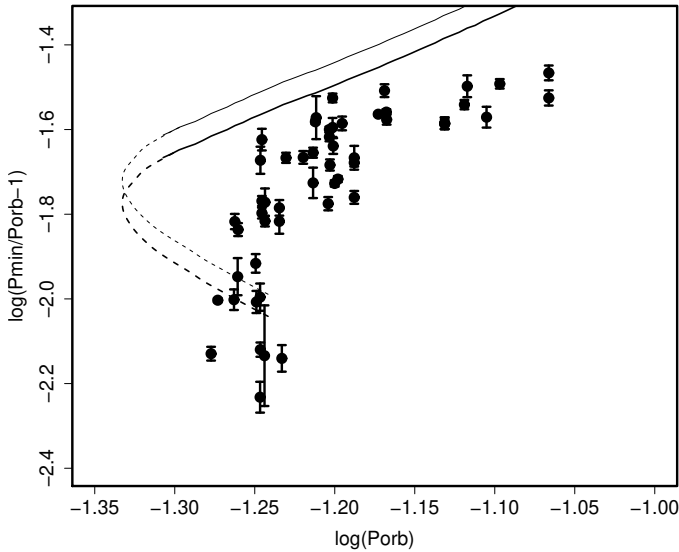


Fig. 32. Fractional superhump excess versus orbital period. ϵ denotes fractional superhump excess for the minimum P_{SH} . The two set of curves and dashed curves represent predicted ϵ for zero-age main-sequence following figure 20 of Patterson et al. (2003); the upper (thin) curve represents the relation in Patterson et al. (2003) and the lower (thick) curve represents the relation based on the improved ϵ - q relation.

4.13. ϵ - P_{orb} Relation

The improved relation between ϵ and P_{orb} is shown in figure 32. The predicted location of Roche-lobe filling zero-age main sequence is also shown following Patterson et al. (2003). Although the new calibration on the ϵ - q relation seems to slightly improve the deviation between observed and predicted ϵ , there still remains significant disagreement between them. The disagreement is the greatest where the period minimum appears to reside: $-1.27 < \log(P_{orb}) < -1.25$ ($0.053 < P_{orb} < 0.056$ d).

5. Period Variation of Superhumps in WZ Sge-Type Dwarf Novae

5.1. Late-Stage Superhumps in WZ Sge-Type Dwarf Novae: Case Studies

WZ Sge-type dwarf novae (see e.g. Bailey 1979; Downes 1990; Kato et al. 2001d) are a subgroup of SU UMa-type dwarf novae characterized by large-amplitude (typically ~ 8 mag) superoutbursts with very long (typically ~ 10 yr) recurrence times.

Some SU UMa-type dwarf novae with long recurrence times, most notably WZ Sge-type dwarf novae, are known to exhibit long-enduring superhumps during the late post-superoutburst stage. We will examine selected special cases (though the discussion may not be necessarily applicable to general cases) which provide new insight into the relation of late-stage superhumps and other periodicities.

The first case is GW Lib in 2007. During the late post-superoutburst stage, this object showed very stable superhumps whose period is $\sim 0.5\%$ longer than those of the

ordinary superhumps (Kato et al. 2008). These superhumps during the late post-superoutburst stage appear to be on a smooth extension of the $O-C$ diagram of the stage B (figure 33). This suggests that these superhumps are intrinsically of the same origin, and the transition to the stage C around the termination of the superoutburst looks like a disturbance in the $O-C$ diagram.

This temporary emergence of a new periodicity is in reality attributed to orbital humps (cf. subsection 6.76). Similar behavior was also recorded in well-observed WZ Sge-type systems V455 And (subsection 6.5) and WZ Sge (subsection 6.113). This phenomenon thus appears common to many WZ Sge-type dwarf novae, but apparently not very striking in usual SU UMa-type dwarf novae. Osaki, Meyer (2002) presented an interpretation that the orbital humps observed in WZ Sge-type superoutbursts can be well reproduced by a projection effect of the superhump source, rather than by an enhanced hot spot. Our observation in SDSS J080434.20+510349.2 (hereafter SDSS J0804) supports this interpretation (Kato et al. 2009). There appears to be a condition that this mechanism strongly works during the late stage of WZ Sge-type superoutbursts. There also remains a possibility that a mechanism similar to early superhumps works in this phase (see subsection 6.76).

Following Kato et al. (2008), late post-superoutburst superhumps are supposed to originate from the precessing eccentric disk near the tidal truncation. This leads to a picture that the eccentric disk continues to slowly expand after the end of stage B, and finally reaches the tidal truncation where the period stabilizes. This picture is a natural extension of the explanation of “late superhumps” in WZ Sge-type dwarf novae proposed by Kato et al. (2008). During the plateau stage when the disk is still bright enough, newly excited superhumps (stage C superhumps) can temporarily dominate over the superhump signal arising from the outer, relatively faint, disk, and behaves as a temporarily disturbance until the entire disk returns to the cool state. This interpretation, however, needs to be verified by more detailed study and by a comparison with numerical simulations of superhumps incorporating the thermal instability.

The second case is ASAS J002511+1217.2 (figure 34). Following a typical stage B-C evolution, the object showed double-humped superhumps with a shorter period between the end of the superoutburst plateau and the rebrightening. Outside this stage, superhumps during the late post-superoutburst stage are on a smooth extension of the stage C superhumps (see subsection 6.150 for details). Although the situation looks somewhat different from GW Lib, superhumps during the late post-superoutburst stage appears to have evolved from the stage C superhumps. The early post-superoutburst stage and the rebrightening acted like a disturbance as in GW Lib, although the emergence of orbital period was not yet confirmed in this case. It may be that $m=2$ waves were transiently excited in the inner disk, and the phenomenological difference from GW Lib may be associated with the presence of a rebrightening. It would be worth noting that both GW Lib and

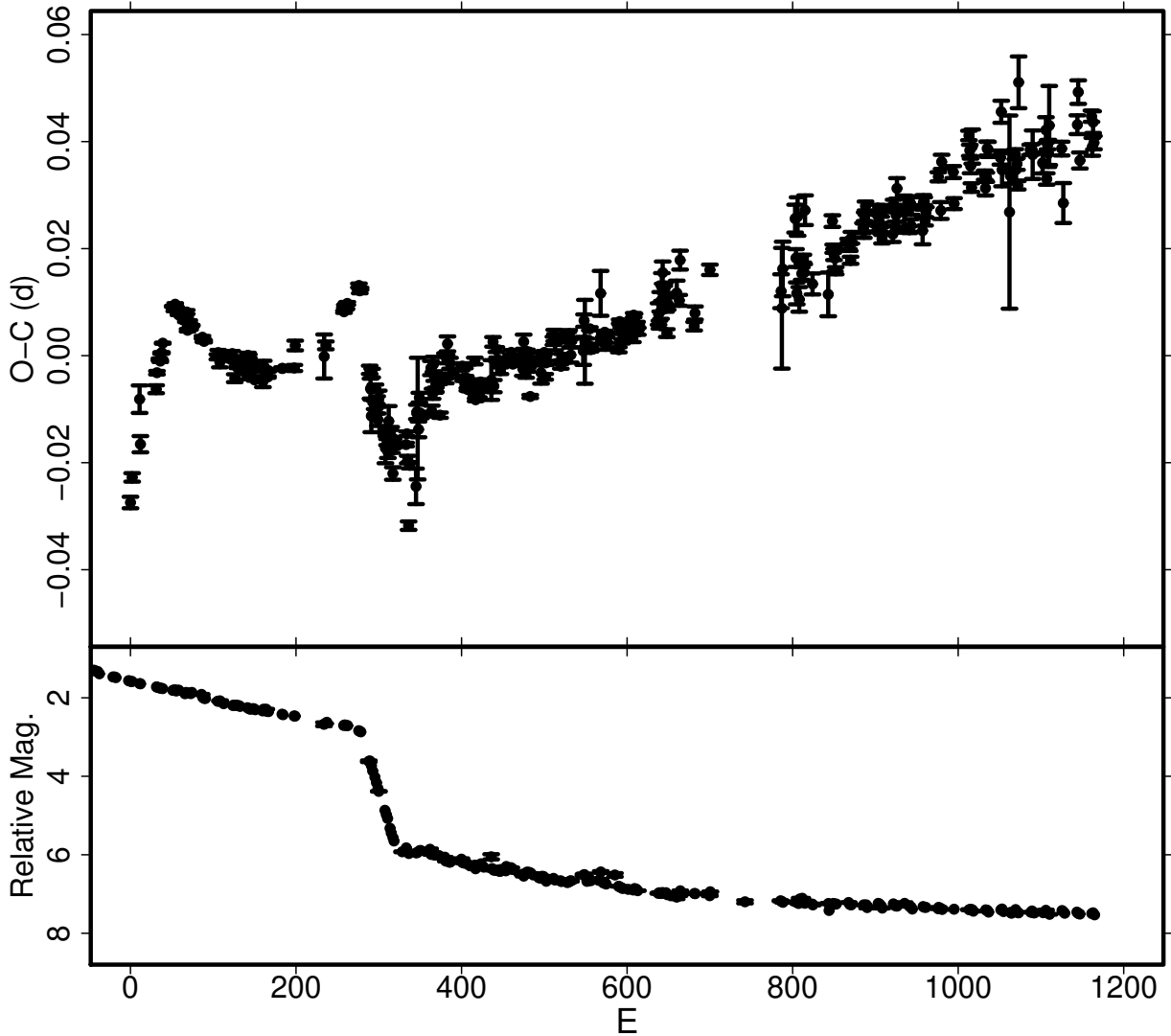


Fig. 33. $O - C$ variation in GW Lib (2007). (Upper) $O - C$; (Lower) Light curve. The early stage of the superoutburst, when ordinary superhump were not observed, is outside ($E < 0$) the figure.

ASAS J002511+1217.2 did not show a ~ 0.5 phase shift during the late stages.

We give a summary of late-stage superhumps in WZ Sge-type dwarf novae in table 7. The values of late-stage superhumps (P_{late}) listed in the table are representative periods. Since P_1 here represents a mean period of stage B, not one at its beginning, P_{late} can be shorter than P_1 in large P_{dot} systems (e.g. ASAS J0025), See subsections of individual objects for the details.

5.2. Period Variation in WZ Sge-Type Dwarf Novae

Although the borderline between WZ Sge-type dwarf novae and ordinary SU UMa-type dwarf novae is somewhat ambiguous, it has been proposed that a 2:1 orbital resonance in low- q systems is responsible for the phenomenon (Osaki, Meyer 2002). As already introduced in Kato et al. (2008), early superhumps (double-wave humps with a period close to P_{orb} seen during the earliest stages of WZ Sge-type superoutbursts; see also Kato

2002a) are considered to be a manifestation of the 2:1 resonance (Osaki, Meyer 2002). By the inferred mechanism, the existence of early superhumps might a best feature in discriminating WZ Sge-type dwarf novae from ordinary SU UMa-type dwarf novae (in low-inclination systems, though, the amplitudes of early superhumps can be too low to detect; e.g. GW Lib, Imada et al., in preparation). In this paper, we deal with objects with early superhumps or objects with very rare (less than once in several years) and large-amplitude superoutbursts as WZ Sge-type dwarf novae and analogs.

Kato et al. (2008) also listed nearly constant to positive P_{dot} as one of the common properties of WZ Sge-type dwarf novae. We examine this further in this subsection.

Table 8 summarizes properties of superoutbursts of WZ Sge-type dwarf novae. The quiescent magnitudes were mainly taken from the on-line version of Ritter, Kolb (2003), supplemented for V1251 Cyg (Henden, AAVSO-discussion 14842), V592 Her, HV Vir (SDSS g val-

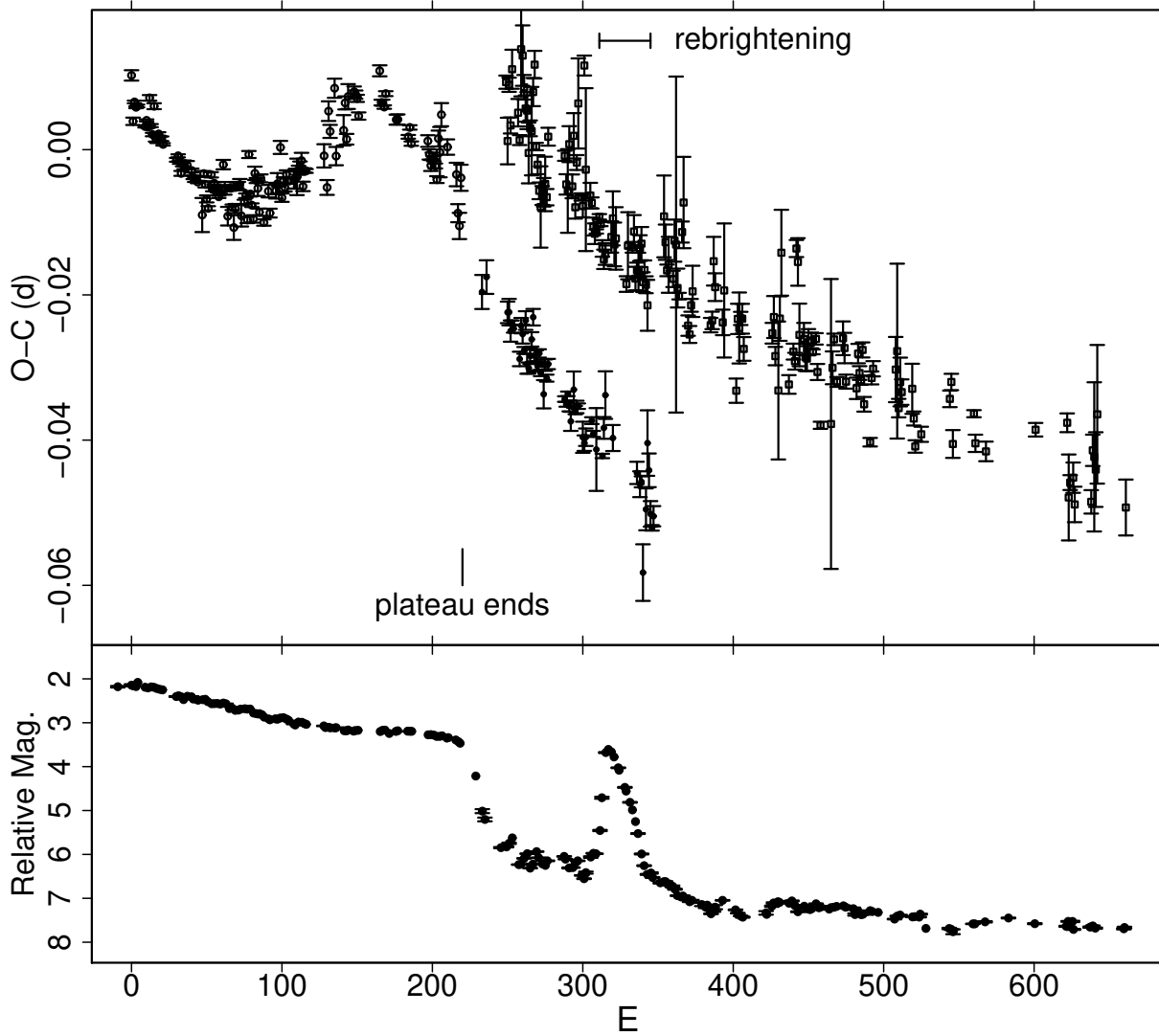


Fig. 34. $O - C$ variation in ASAS J0025 (2004). (Upper) $O - C$. Different symbols refer to humps of different categories (see subsection 6.150); (Lower) Light curve. The earliest stage of the superoutburst was not observed.

Table 7. Late-stage superhumps in WZ Sge-type dwarf novae.

Object	P_{orb} (d)	P_1 (d)	P_{late} (d)	source
V455 And	0.056309	0.057144(11)	0.057188(6)	this work
EG Cnc	0.05997	0.060337(6)	0.06051(2)	this work, Patterson et al. (1998)
GW Lib	0.05332	0.054095(10)	0.054156(1)	this work
WZ Sge	0.056688	0.057204(5)	0.057488(14)	this work
ASAS J0025	0.056540*	0.057093(12)	0.056995(3)	this work
ASAS J1536	–	0.064602(24)	0.064729(13)	this work
SDSS J0804	0.059005	0.059539(11)	0.059659(5)	Kato et al. (2009)
OT J0747	–	0.060750(7)	0.060771(3)	this work

*candidate P_{orb} .

ues), GW Lib (typical quiescent magnitudes reported to VSNET). The maximum magnitudes were mean magnitudes around maximum from reports to VSNET and other literature; V -band measurements are preferentially used whenever available. P_{SH} refers to P_1 .

Figure 36 shows the relation between P_{dot} versus ϵ for WZ Sge-type dwarf novae. For systems with $\epsilon < 0.026$, P_{dot} is a strong function of ϵ (equation 6). If ϵ indeed reflects q , the low q , rather than P_{orb} , is most responsible for smaller P_{dot} . Systems with nearly zero P_{dot} appear to represent a population with low-mass secondaries. Combined with figure 37, low- P_{dot} systems with $P_{\text{SH}} < 0.057$ d can be considered as a consequence of terminal evolution of CVs around the period minimum. Two long- P_{SH} objects (OT J1112 and EG Cnc¹⁰) are either good candidates for “period bouncers”, or the period minimum is broader than had been considered and these objects are presently reaching the period minimum at these P_{orb} . We should note, however, this empirical calibration implicitly assume that all superhumps in WZ Sge-type dwarf novae during the plateau stage B superhumps. If some systems show stage C superhump even in this phase, P_{dot} , and hence q might be underestimated (see a discussion in 1RXS J0232, subsection 6.146). Among our sample, 1RXS J0232 is a single candidate for a period bouncer having a longer superhump period than 0.0603 d (EG Cnc). The relative lack of promising candidates for period bouncers with long superhump periods, despite the greatly improved statistics, should be worth noting.

$$P_{\text{dot}} = -0.00002(1) + 0.0040(6)\epsilon. \quad (6)$$

Some object with WZ Sge-type characteristics (early superhumps and large outburst amplitudes) are present in a range of $\epsilon > 0.026$ (BC UMa, V1251 Cyg, RZ Leo). These objects do not follow the relation in equation 6 and appear to have higher q . These object may either consist “borderline” WZ Sge-type dwarf novae (cf. Patterson et al. 2003), or the existence of a large disk-mass at the onset of superoutbursts may enable the 2:1 resonance to appear in some high- q systems.

5.3. Period Variation versus Outburst Type

WZ Sge-type dwarf novae are known to exhibit a wide variety of outburst morphology, especially in post-outburst rebrightenings (Kato et al. 2004b; Imada et al. 2006c).

Figure 37 shows the relation between P_{dot} versus P_{SH} and outburst type, where the nomenclature of classification is after Imada et al. (2006c)¹¹ and type-D represents outbursts without a rebrightening (figure 35). The P_{dot} tends to decrease with decreasing P_{SH} . There appear to

¹⁰ The P_{orb} has been controversial (Kato et al. 2004b). The present analysis of $P_{\text{dot}}-\epsilon$ relation seems to support the period identification of Patterson et al. (1998). Accurate determination of the period of early superhumps, as well as independent estimates of P_{dot} in future superoutbursts is still wanted.

¹¹ Although the original classification Imada et al. (2006c) was for WZ Sge (SU UMa)-type dwarf novae, it should be worth noting that these types of rebrightenings sometimes appear in X-ray transients (Kuulkers et al. 1996).

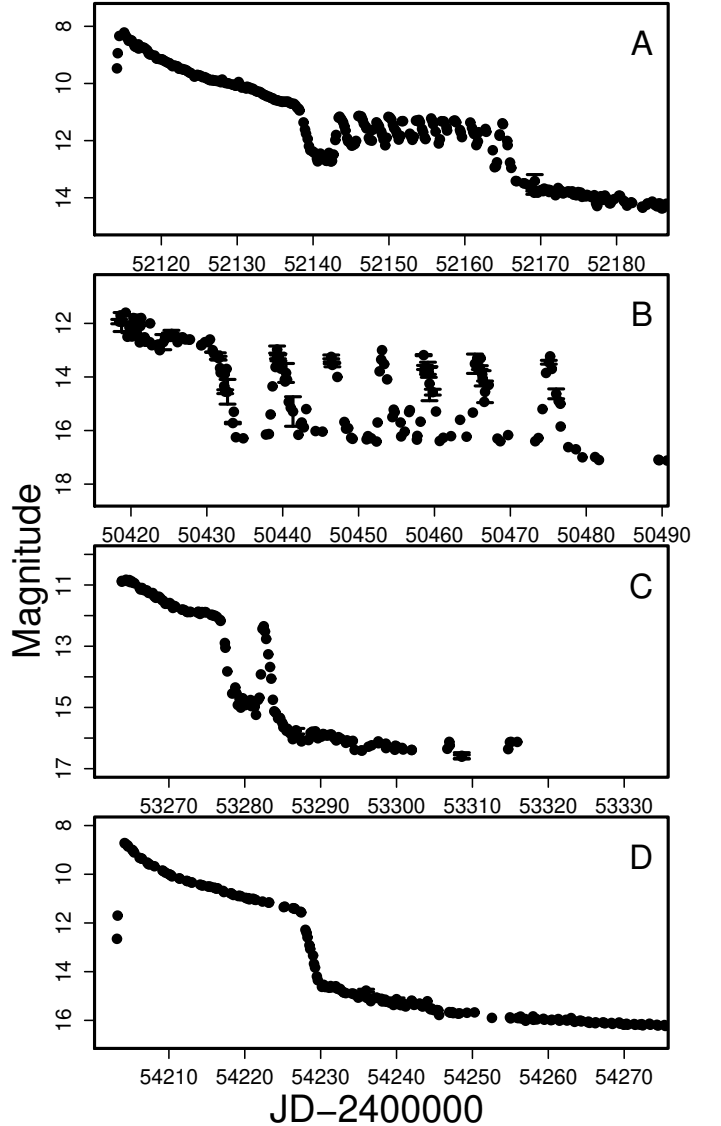


Fig. 35. Types of WZ Sge-type outbursts. A: WZ Sge (2001), B: EG Cnc (1996, data from Kato et al. 2004b), C: ASAS J0025 (2004), D: GW Lib (2007).

be two populations among WZ Sge-type dwarf novae: systems with P_{dot} nearly zero ($P_{\text{dot}} < +2 \times 10^{-5}$) and systems with larger P_{dot} .

Type-A outbursts (filled circles; long-duration rebrightening) are restricted to a region with short P_{SH} and small P_{dot} . Type-B outbursts (filled squares; multiple rebrightenings) tend to be located in a region with small P_{dot} but with larger P_{SH} than type-A. Type-C outbursts (open triangles; single rebrightening) are located in a region with middle-to-longer P_{SH} and larger P_{dot} . Type-D outbursts (open circles; no rebrightening) tend to have a small P_{SH} and a various P_{dot} . It should be noted that these classifications are not always the property unique for each objects, but can be different between superoutbursts of the same object (Uemura et al. 2008b).

The distinction between type-A and type-D outbursts

Table 8. Parameters of WZ Sge-type superoutbursts.

Object	Year	P_{SH}	P_{orb}	P_{dot}^*	err.*	ϵ	Type [†]	$N_{\text{reb}}^{\ddagger}$	delay [§]	Max	Min
LL And	1993	0.056900	0.055055	–	–	0.034	D?	0?	–	14.3	20.0
LL And	2004	0.056583	0.055055	1.0	0.6	0.028	D?	0?	–	12.6	20.0
V455 And	2007	0.057133	0.056309	4.7	1.2	0.015	D	0	10	8.7	16.1
V466 And	2008	0.057203	0.056365	5.7	0.7	0.015	D	0	>12	12.7	21.2
UZ Boo	1994	0.061743	–	–1.5	2.5	–	B	2:	1–5	11.7	20.4
UZ Boo	2003	0.061922	–	–1.9	6.3	–	B	4	3:	12.8	20.4
CG CMa	1999	–	0.063275	–	–	–	A/B	1/2	–	13.7	[22
EG Cnc	1996	0.060337	0.05997	0.8	0.5	0.006	B	6	>5	11.9	19.1
AL Com	1995	0.057289	0.056668	1.9	0.5	0.011	A	1	9	12.7	20.8
AL Com	2001	0.057229	0.056668	–0.2	0.8	0.010	A	1	10–14	12.8	20.8
AL Com	2008	0.057174	0.056668	–	–	0.009	B	≥ 4	–	13.2	20.8
V1251 Cyg	1991	0.076284	0.07433	–	–	0.026	D?	0?	3–9	12.4	20.6
V1251 Cyg	2008	0.075973	0.07433	6.0	2.7	0.022	C	1	5	12.6	20.6
V2176 Cyg	1997	0.056239	–	–	–	–	A	1	–]13.3	19.9
DV Dra	2005	–	0.05883	–	–	–	–	–	>6	15.0	21.0
V592 Her	1998	0.056498	–	2.1	0.8	–	D	0	7:	12.0	21.3
V1108 Her	2004	0.057480	0.05703	1.6	6.8	0.008	D	0	–	11.2	17.1
RZ Leo	2000	0.078658	0.076038	4.9	1.7	0.034	C	1	3:	12.1	18.5
RZ Leo	2006	0.078428	0.076038	–	–	0.031	C	1	–]12.5	18.5
GW Lib	2007	0.054095	0.05332	4.0	0.1	0.015	D	0	10	8.2	16.6
SS LMi	2006	–	0.056637	–	–	–	–	–	–]16.2	21.7
V358 Lyr	2008	0.055629	–	–	–	–	A	1	–]16.1	[23
WZ Sge	1978	0.057232	0.056688	0.4	0.8	0.010	A	1(>6)	11	7.8	15.0
WZ Sge	2001	0.057204	0.056688	2.0	0.4	0.009	A	1(12)	12	8.2	15.0
UW Tri	1995	–	0.05330	–	–	–	–	–	>8	14.7	22.6
UW Tri	2008	0.054194	0.05334	3.7	0.6	0.016	–	–	10	14.3	22.6
BC UMa	2000	0.064555	0.06261	4.0	1.4	0.031	C	1	4	11.6	18.6
BC UMa	2003	0.064571	0.06261	4.2	0.8	0.031	C	1	2	12.5	18.6
HV Vir	1992	0.058285	0.057069	5.7	0.6	0.021	D/C	1?	10	11.5	19.2
HV Vir	2002	0.058266	0.057069	7.4	0.6	0.021	D	0	2–5	13.0	19.2
HV Vir	2008	0.058322	0.057069	7.1	1.9	0.022	D?	0	6	12.3	19.2
1RXS J0232	2007	0.066166	–	–1.7	0.7	–	B	4	–	10.5	18.8
ASAS J0233	2006	0.055987	0.05490	4.9	0.5	0.020	D?	0?	8	12.0	18.2
ASAS J1025	2006	0.063365	0.06136	10.9	0.6	0.033	C	1	3	12.2	19.3
ASAS J1600	2005	0.064970	0.063381	11.1	0.8	0.025	C	1	2–7	12.7	17.9
SDSS J0804	2006	0.059537	0.059005	–	–	0.009	B	11	–]14	17.8
OT J0042	2008	0.056892	0.05550	4.0	1.8	0.025	C?	1?	10–12	14.5	22.8
OT J0238	2008	0.053658	0.05281	2.0	0.2	0.016	D	0	>9]14.1	21.7
OT J0747	2008	0.060736	–	4.0	0.8	–	B	6	<13	11.4	19.5
OT J0807	2007	0.061050	–	9.5	4.8	–	D?	0?	–]13.6	20.9
OT J0902	2008	–	0.05652	–	–	–	–	–	–]16.3	23.2
OT J1021	2006	0.056312	–	0.4	0.8	–	A	1	–]13.9	19.7
OT J1112	2007	0.058965	0.05847	0.9	0.4	0.008	D?	0?	21:	11.5	[20
OT J1959	2005	0.059919	–	–0.7	5.2	–	C	1	<6	14.7	22.5
TSS J0222	2005	0.055585	0.054868	2.2	1.5	0.013	A	1	6	15.5	19.5

*Unit 10^{-5} .

†A: long-lasting rebrightening; B: multiple rebrightenings; C: single rebrightening; D: no rebrightening.

‡Number of rebrightenings.

§Days before ordinary superhumps appeared.

in short P_{orb} systems may be understood in a scenario presented in Kato et al. (2008). That is, in most extreme WZ Sge-type systems, the 2:1 resonance can be strong enough to accrete much of the matter beyond the 3:1 resonance and leave no room for a positive P_{dot} . In less extreme systems, the remnant matter beyond the 3:1 resonance enables outward propagation of the eccentricity wave and resulting a positive P_{dot} .

If P_{dot} indeed reflects q , the location of type-B outbursts would indicate that these objects have small q , comparable to those with type-A outbursts, but longer P_{orb} . In these type-B superoutbursts, the intervals between superoutbursts tend to be shorter than in objects with type-A outbursts, and the delay in appearance of ordinary superhumps is generally shorter. It may be that type-B outbursts are a variety of type-A outbursts with a smaller disk mass at the onset of the outbursts. The presence of a type-B outburst in AL Com with a possibly fainter maximum (Uemura et al. 2008b) seems to support this interpretation. The presence of low-amplitude outbursts during the 1978 and 2001 superoutbursts of WZ Sge (Patterson et al. 1981; Patterson et al. 2002) would be a signature of a smooth transition between type-A and type-B outbursts (see also Osaki, Meyer 2002). The relatively long P_{orb} in type-B objects might suggest that the binary configuration in these systems is somehow responsible for an early ignition of a superoutburst than in objects with type-A outbursts. Another potential interpretation is that objects with type-B outbursts have a lower q (cf. Patterson et al. 1998) than in other systems. If this is the case, a smaller tidal torque in low- q systems might be insufficient to sustain a long-duration type-A rebrightening. The apparent presence of a higher ϵ system (SDSS J0804: Kato et al. 2009 and Zharikov et al. 2008) among objects with type-B outbursts, however, would indicate that not all type-B outbursts can be attributed to the low q .

Type-C outbursts are less featured than other types of outbursts; these outbursts resemble more usual superoutbursts with a rebrightening frequently seen in a broader spectrum of SU UMa-type dwarf novae. A further explanation would be needed why short- P_{orb} systems have little tendency to show type-C outbursts, despite the apparent presence of sufficient matter beyond the 3:1 resonance.

5.4. Delay of Appearance of Superhumps in WZ Sge-Type Dwarf Novae: Relation with Outburst Type

Kato et al. (2008) suggested that the long delays of appearance of ordinary superhumps in WZ Sge-type superoutburst can be attributed to the suppression of the 3:1 resonance by the 2:1 resonance, rather than these delays reflect the long growth time of the 3:1 resonance in low- q systems. The similarity of the duration of the stage A (~ 20 cycles), which can be considered as the growth time of superhumps, between SU UMa-type dwarf novae and WZ Sge-type dwarf novae would also support this interpretation. We also surveyed these delay times in WZ Sge-type outbursts for better statistics, and included them in table 8. In several cases, the delay times could not be well constrained due to the gap in observations, or due to

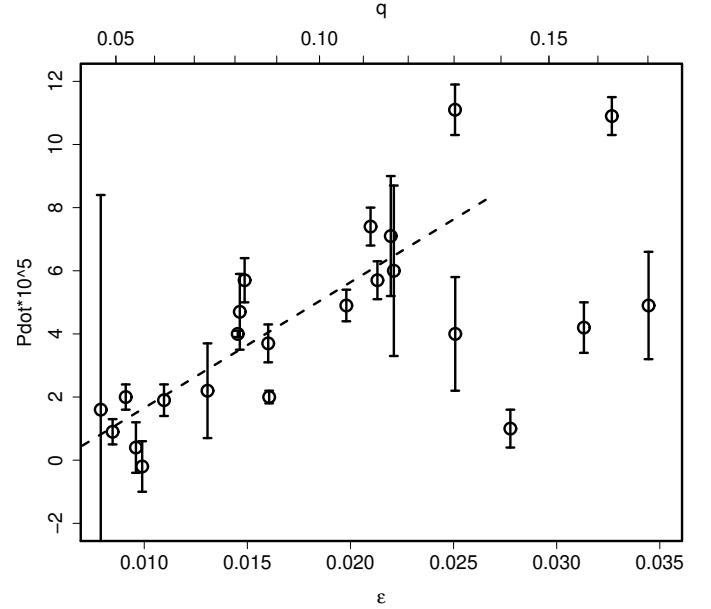


Fig. 36. P_{dot} versus ϵ for WZ Sge-type dwarf novae. ASAS J0025 was excluded from this figure due to the uncertain P_{orb} . The dashed line represents equation 6.

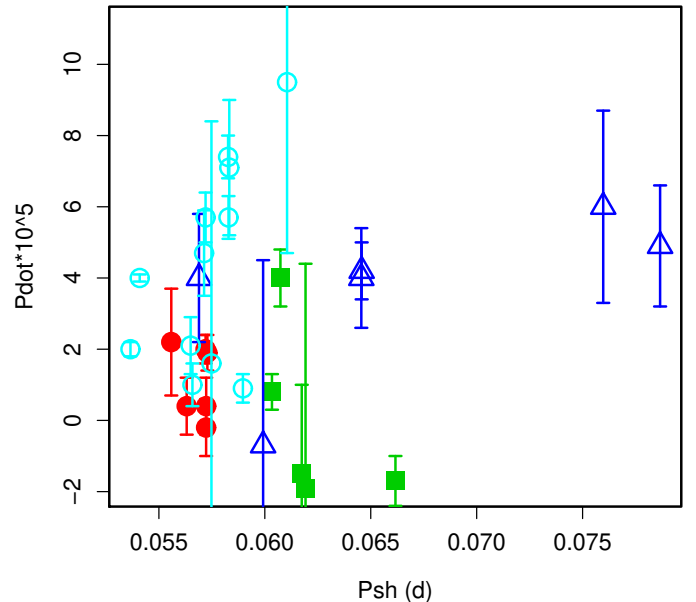


Fig. 37. P_{dot} versus P_{SH} for WZ Sge-type dwarf novae. Symbols represent the type of outburst: type-A (filled circles), type-B (filled squares), type-C (open triangles), type-D (open circles).

the apparent delay in detection of the outburst. In such cases, the possible ranges of the delay times are given. Since the development of superhumps usually takes ~ 1 d, the values have ~ 1 d uncertainty even in well-observed systems, and they may be different from values given in the different literature.

It is noteworthy that all well-observed type-A and type-D superoutbursts have longer (6–12 d, or even longer) delay times than in type-C superoutbursts (typically ~ 5 d). Many of type-B superoutburst were, unfortunately, not sampled very well, but they appear to have shorter (1–5 d) delay times. These results strengthen the similarity between type-A and type-D superoutbursts (subsection 5.3). Following Kato et al. (2008), the 2:1 resonance in these outbursts are strong enough to accrete most of the matter beyond the 3:1 resonance, and the the small P_{dot} and the lack of type-C rebrightening may be a natural consequence. Shorter delay times in type-C superoutbursts and the strongly positive P_{dot} can be interpreted as a result of a smaller mass and a smaller effect of the 2:1 resonance, leaving significant amount of matter beyond the 3:1 resonance (Kato et al. 2008).

Type-B superoutbursts appear to have intermediate delay times between type-A/D and ordinary SU UMa-type superoutbursts (1–3 d). This would suggest that the matter beyond the 3:1 resonance is smaller, and the 2:1 resonance is weaker than in type-A/D superoutbursts. The origin of type-B superoutbursts with low P_{dot} 's can then be understood as a consequence of small mass outside the 3:1 resonance (although the 2:1 resonance still works, the small mass in the outer disk does not allow sufficient outward propagation of the eccentricity wave), rather than a consequence of extremely low- q expected for period bouncers. Further detailed observations of type-B superoutbursts and determination of P_{orb} would discriminate these possibilities.

5.5. Delay of Appearance of Superhumps: Comparison between Different Superoutbursts

Kato et al. (2008) also suggested superoutbursts with a different extent are expected to show different delay times. In the present survey, HV Vir appears to perfectly fit this expectation. A fainter superoutburst in 2002 led to a shorter growth time compared to the 1992 one. In WX Cet, the delay time ($\geq 4d$) in the bright superoutburst in 1989 was longer than ~ 2 d in the 1998 superoutburst (Kato et al. 2001b; subsection 6.29). Different superoutbursts of SW UMa (subsection 6.124) also followed this tendency (see also Soejima et al. 2009). Ohshima et al. (in preparation) also suggested that the delay time in V844 Her during the bright superoutburst in 2008 appears to be longer than those in other superoutbursts of the same object (see also subsection 6.69). In BC UMa (subsection 6.125), the duration of the stage B was dependent on the extent of the superoutburst.

In summary, the present survey generally strengthened the expectations in Kato et al. (2008).

Table 9. Superhump maxima of FO And (1994).

E	\max^a	error	$O - C^b$	N^c
0	49578.1462	0.0008	-0.0033	23
13	49579.1158	0.0006	0.0022	49
14	49579.1896	0.0007	0.0018	31
26	49580.0778	0.0007	0.0001	34
27	49580.1520	0.0006	0.0001	48
68	49583.1917	0.0014	-0.0009	42

^a BJD-2400000.

^b Against $\max = 2449578.1495 + 0.074163E$.

^c Number of points used to determine the maximum.

Table 10. Superhump maxima of KV And (1994).

E	\max^a	error	$O - C^b$	N^c
0	49576.2102	0.0077	0.0012	16
1	49576.2723	0.0022	-0.0110	9
27	49578.2175	0.0011	-0.0002	45
28	49578.3010	0.0017	0.0089	21
41	49579.2609	0.0005	0.0016	49
55	49580.3074	0.0021	0.0065	48
95	49583.2699	0.0017	-0.0069	43

^a BJD-2400000.

^b Against $\max = 2449576.2090 + 0.074398E$.

^c Number of points used to determine the maximum.

6. Individual Objects

6.1. FO Andromedae

We reanalyzed the data in Kato (1995b). The times of superhump maxima are listed in table 9. This observation covered the late stage of the superoutburst and most likely caught the stage B–C transition. The mean periods were 0.07455(5) d for $E \leq 14$ (stage B) and 0.07402(1) d for $13 \leq E \leq 27$ (stage C).

6.2. KV Andromedae

KV And was originally reported as a large-amplitude dwarf nova (Kurochkin 1977). Kato et al. (1994) and Kato (1995a) reported the detection of superhumps, whose period suggested a more usual dwarf nova rather than a short-period, WZ Sge-like object.

We have analyzed two superoutbursts in 1994 (reanalysis of Kato 1995a) and 2002. The results are presented in tables 10 and 11. During both outbursts, the superhump period likely decreased. The global P_{dot} 's were $-12.8(6.0) \times 10^{-5}$ and $-8.2(2.9) \times 10^{-5}$, respectively. The period changes can be also interpreted as a result of transition from stage B to C (see table 2).

6.3. LL Andromedae

LL And is an eruptive object discovered in 1979 (Wild 1979). Little had been known until its first-ever outburst since the discovery in 1993, during which Kato (2004) established the SU UMa-type nature of this object, and

Table 11. Superhump maxima of KV And (2002).

E	\max^a	error	$O - C^b$	N^c
0	52584.1913	0.0005	-0.0030	337
1	52584.2647	0.0005	-0.0040	326
2	52584.3449	0.0014	0.0019	126
13	52585.1613	0.0007	0.0009	346
14	52585.2402	0.0028	0.0055	254
27	52586.1978	0.0033	-0.0030	72
40	52587.1639	0.0020	-0.0029	186
41	52587.2449	0.0041	0.0038	197
42	52587.3158	0.0015	0.0004	58
53	52588.1312	0.0032	-0.0016	135
54	52588.2100	0.0010	0.0028	145
55	52588.2863	0.0016	0.0049	114
67	52589.1712	0.0017	-0.0019	228
68	52589.2474	0.0018	-0.0000	115
69	52589.3196	0.0021	-0.0022	115
80	52590.1372	0.0019	-0.0019	62
81	52590.2109	0.0034	-0.0025	93
82	52590.2907	0.0062	0.0029	95

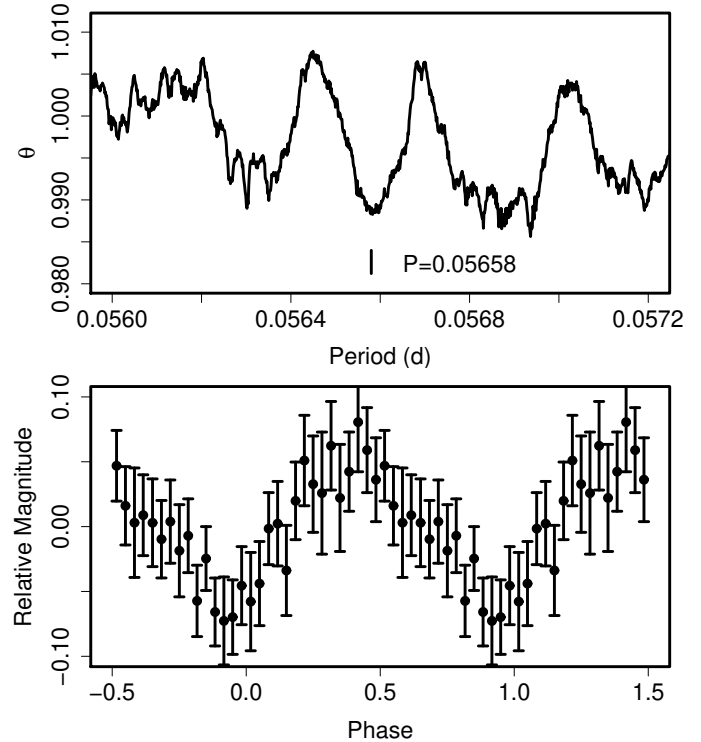
^a BJD-2400000.^b Against $\max = 2452584.1944 + 0.074310E$.^c Number of points used to determine the maximum.

reported a superhump period of 0.05697(3) d. The superhump maxima determined from these observations are listed in table 12. Excluding $E = 37$ with a large error and a significant deviation in $O - C$, the overall P_{dot} was $+19.7(17.3) \times 10^{-5}$.

The object underwent another superoutburst in 2004 May–June. The object was very unfavorably situated for long time-series photometry. The data were unavoidably taken at a large air-mass, $f(z)$. We subtracted the first-order atmospheric extinction term, $cf(z)$, where c was numerically determined for each observer by minimizing the deviation of the subtracted result from the general fading trend. With the help of the superhump period obtained in 1993, we selected the most likely mean superhump period of 0.05658(2) d with PDM analysis (figure 38). The times of superhump maxima determined using this period are given in table 13. The period and period derivative determined from $0 \leq E \leq 290$ were 0.05658(2) d and $P_{\text{dot}} = +1.0(0.6) \times 10^{-5}$, respectively. The resultant ϵ of 2.8 % is still large for this P_{orb} (see a discussion in Kato 2004).

6.4. V402 Andromedae

V402 And is a dwarf nova discovered by Antipin (1998). The SU UMa-type nature was confirmed during the 2000 superoutburst (vsnet-alert 5274). We analyzed the 2005, 2006 and 2008 superoutbursts (tables 14, 15, 16). The 2005 and 2006 superoutbursts were observed during their early stages and the 2008 one was observed during its middle stage. The resultant P_{dot} were $+12.7(2.1) \times 10^{-5}$ for the 2006 superoutburst and $+4.2(3.7) \times 10^{-5}$ for the 2008, respectively. A shorter mean P_{SH} for the 2005 superoutburst during its early stage is also consistent with

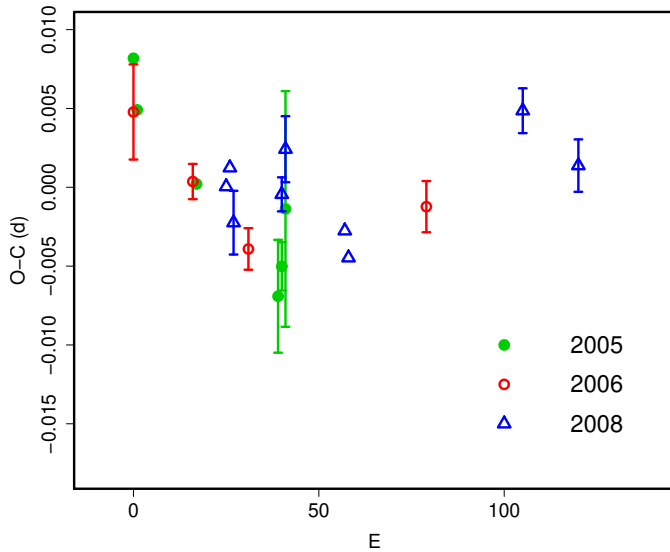
**Fig. 38.** Superhumps in LL And (2004). (Upper): PDM analysis. The selection of the period was based on the 1993 observation. (Lower): Phase-averaged profile.**Table 12.** Superhump maxima of LL And (1993).

E	\max^a	error	$O - C^b$	N^c
0	49330.9100	0.0142	0.0028	22
1	49330.9592	0.0058	-0.0048	22
36	49332.9513	0.0011	-0.0043	22
37	49333.0232	0.0056	0.0108	10
53	49333.9219	0.0016	-0.0009	21
54	49333.9759	0.0018	-0.0039	21
55	49334.0375	0.0014	0.0008	20
56	49334.0931	0.0019	-0.0005	20

^a BJD-2400000.^b Against $\max = 2449330.9072 + 0.056900E$.^c Number of points used to determine the maximum.

Table 13. Superhump maxima of LL And (2004).

E	\max^a	error	$O - C^b$	N^c
0	53152.8407	0.0049	0.0031	55
84	53157.5827	0.0030	-0.0045	51
95	53158.2028	0.0020	-0.0064	71
96	53158.2636	0.0011	-0.0022	115
131	53160.2482	0.0018	0.0034	207
149	53161.2683	0.0016	0.0058	80
172	53162.5636	0.0069	0.0005	47
290	53169.2458	0.0066	0.0107	84
308	53170.2472	0.0036	-0.0057	140
325	53171.2115	0.0043	-0.0026	103
326	53171.2684	0.0134	-0.0022	58

^a BJD-2400000.^b Against $\max = 2453152.8376 + 0.056543E$.^c Number of points used to determine the maximum.**Fig. 39.** Comparison of $O - C$ diagrams of V402 And between different superoutbursts. A period of 0.06350 d was used to draw this figure. Approximate cycle counts (E) after the start of the superoutburst were used.

the positive P_{dot} . A combined $O - C$ diagram is presented in figure 39.

6.5. *V455 Andromedae*

V455 And = HS 2331+3905 (Araujo-Betancor et al. 2005) underwent a spectacular superoutburst, the first time in its history, in 2007 (H. Maehara, vsnet-alert 9530; Templeton et al. 2007). Following a rapidly rising stage, the object developed early superhumps (vsnet-alert 9543) similar to those in WZ Sge. After about eleven days, ordinary superhumps appeared (vsnet-alert 9582, 9584). Representative mean periods of early and ordinary superhumps were 0.0562675(18) d (figure 40) and 0.0572038(14) d (figure 41), respectively.

The maxima times of ordinary superhumps (tables 17)

Table 14. Superhump maxima of V402 And (2005).

E	\max^a	error	$O - C^b$	N^c
0	53671.0724	0.0005	0.0020	107
1	53671.1326	0.0006	-0.0010	134
17	53672.1439	0.0010	-0.0014	117
39	53673.5338	0.0036	-0.0026	13
40	53673.5992	0.0015	-0.0004	22
41	53673.6663	0.0075	0.0035	19

^a BJD-2400000.^b Against $\max = 2453671.0704 + 0.063230E$.^c Number of points used to determine the maximum.**Table 15.** Superhump maxima of V402 And (2006).

E	\max^a	error	$O - C^b$	N^c
0	53952.2426	0.0030	0.0029	125
16	53953.2541	0.0011	-0.0006	130
31	53954.2024	0.0013	-0.0039	105
79	53957.2531	0.0016	0.0017	135

^a BJD-2400000.^b Against $\max = 2453952.2397 + 0.063439E$.^c Number of points used to determine the maximum.**Table 16.** Superhump maxima of V402 And (2008).

E	\max^a	error	$O - C^b$	N^c
0	54755.0811	0.0007	0.0010	103
1	54755.1458	0.0006	0.0022	136
2	54755.2058	0.0020	-0.0013	72
15	54756.0331	0.0011	0.0000	98
16	54756.0995	0.0021	0.0029	54
32	54757.1103	0.0006	-0.0028	113
33	54757.1721	0.0009	-0.0046	128
80	54760.1659	0.0014	0.0033	135
95	54761.1149	0.0017	-0.0007	100

^a BJD-2400000.^b Against $\max = 2454755.0801 + 0.063532E$.^c Number of points used to determine the maximum.

were obtained after subtracting phase-averaged orbital variations (mean orbital variations were determined from averages for 3–5 d during the main outburst and fading stage, 10 d for the post-superoutburst stage). During BJD 2454356–2454357.3, sporadic humps having a period close to superhumps were observed in addition to early superhumps. No apparent superhump signal was detected before this epoch. For the interval $E \leq 20$, clear stage A evolution was observed with a mean period of 0.05803(8) d (disregarding $E = 3$ and $E = 11$). We determined P_{dot} of $+4.7(1.2) \times 10^{-5}$ from maxima of $23 \leq E \leq 128$, after which the phases of maxima coincide with orbital humps and were disregarded (see a discussion in WZ Sge, subsection 6.113).

In contrast to WZ Sge, the orbital variations were so strong (figure 42) that it was practically impossible to directly extract the times of superhump maxima from the light curve during the post-superoutburst stage. We therefore measured the times of superhump maxima during the this stage after subtracting the orbital light curve (table 18). A relatively large scatter in the $O - C$'s was probably a result from the interfering orbital variation. There was an apparent change in the period around $E = 170$. The mean superhump periods (disregarding maxima coinciding orbital humps and discrepant ones deviating by more than 0.018 d from the mean trend) before and after the change were 0.057295(2) d and 0.057154(1) d, respectively. These periods were longer than the P_{SH} during the main superoutburst (cf. Kato et al. 2008). Figure 43 shows period analysis and mean superhump profiles during the post-superoutburst stage.

The overall evolution of $O - C$'s was remarkably similar to that of GW Lib (figure 44; only the first half of the post-superoutburst stage is shown for better visibility of the general feature).

A full analysis of the observation will be presented in Maehara et al., in preparation.

6.6. V466 Andromedae

The object was discovered by K. Itagaki (Yamaoka et al. 2008b). The object was soon recognized as a WZ Sge-type dwarf nova based on the presence of early superhumps with a period of 0.056365(7) d (vsnet-alert 10518; period refined in this paper, figure 45). The object later developed ordinary superhumps (mean period 0.057203(10) d with the PDM method; figure 46). We only deal with ordinary superhumps here (table 19). The $O - C$ diagram (figure 47) shows the clear presence of stages A–C. The P_{dot} during stage B was $+5.7(0.7) \times 10^{-5}$ ($20 \leq E \leq 194$). More detailed discussion will be presented in Ohshima et al., in preparation.

6.7. DH Aquilae

Nogami, Kato (1995) established the SU UMa-type nature of this object. We further observed the 2002, 2003 and 2008 superoutbursts (tables 20, 21, 23). The global P_{dot} during the 2002 superoutburst was $-8.4(0.8) \times 10^{-5}$, excluding $E = 0$ taken during the early evolutionary stage (cf. figure 4). A likely stage B–C transition was recorded

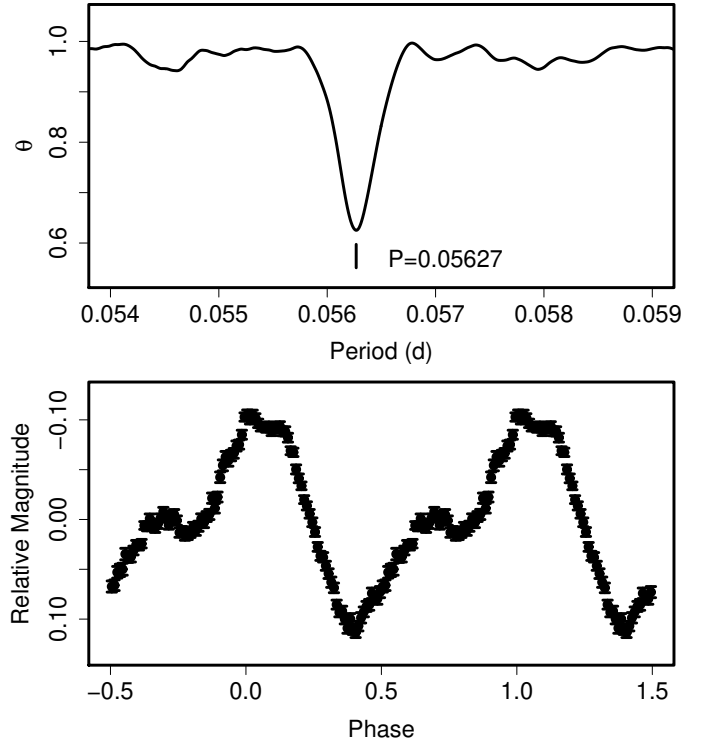


Fig. 40. Early superhumps in V455 And (2007) for BJD 2454349–2454356. (Upper): PDM analysis. (Lower): Phase-averaged profile.

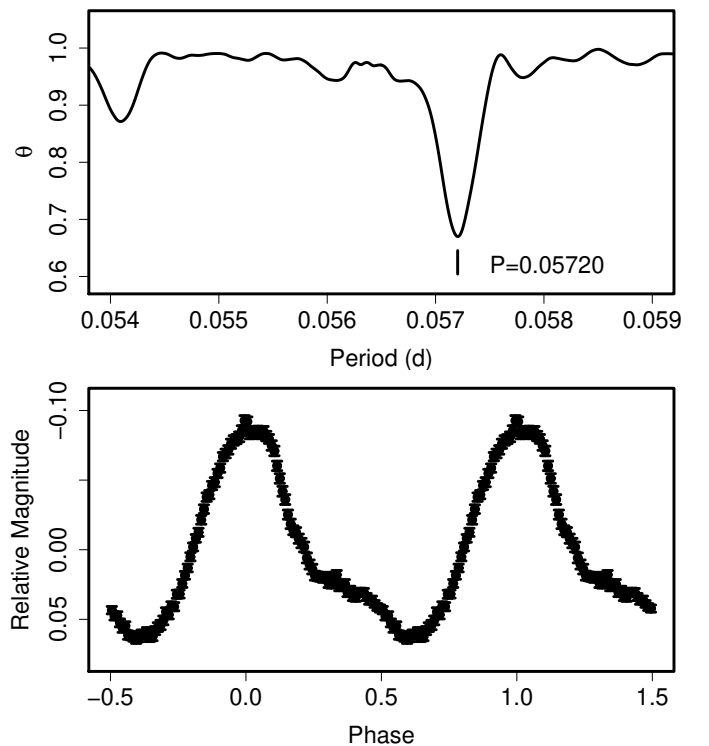


Fig. 41. Ordinary superhumps in V455 And (2007) for BJD 2454357.3–2454366. (Upper): PDM analysis. (Lower): Phase-averaged profile.

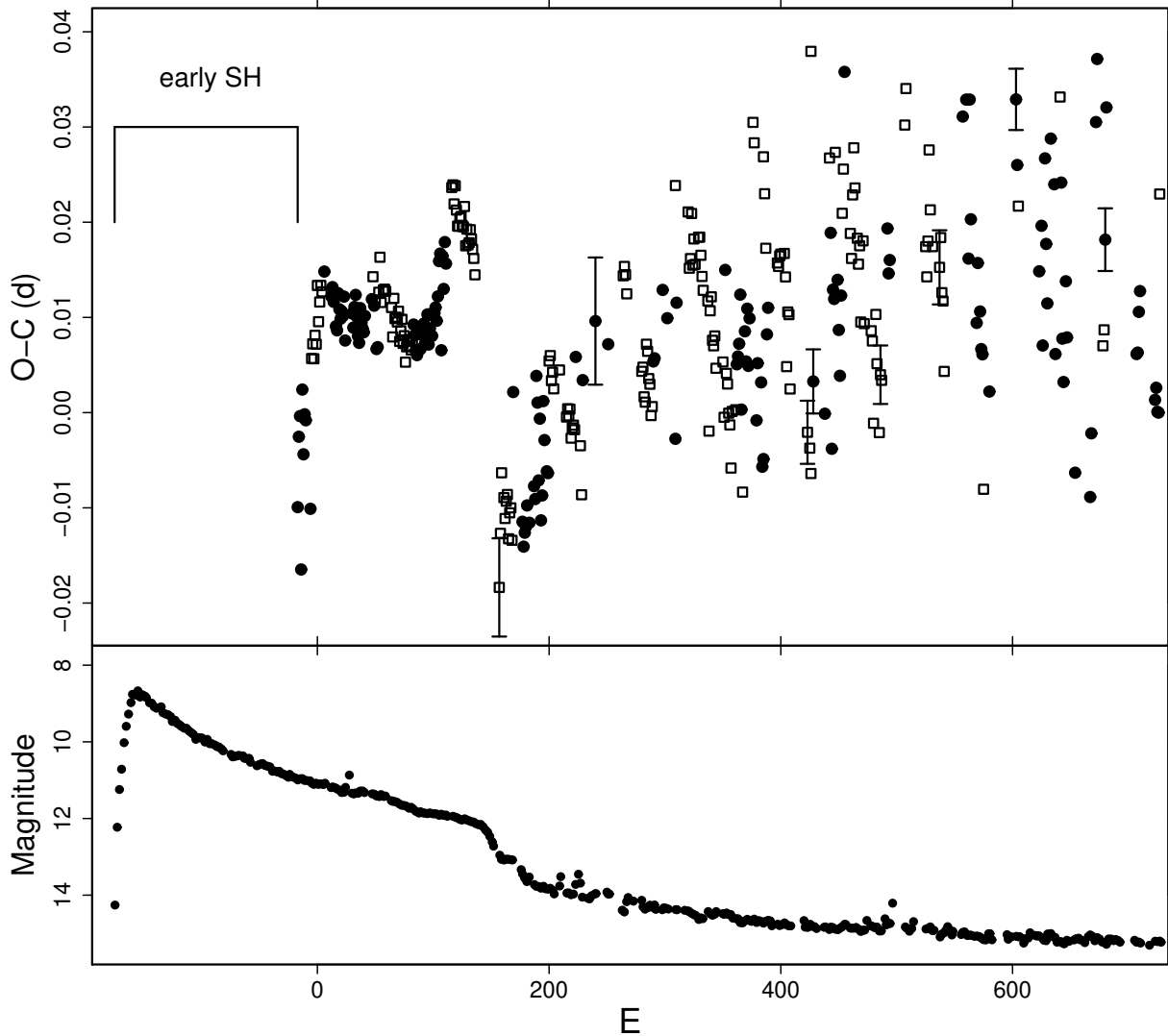


Fig. 44. $O - C$ variation in V455 And (2007). (Upper) $O - C$. Open squares indicate humps coinciding with the phase of orbital humps. Filled squares are humps outside the phase of orbital humps. We used a period of 0.05714 d for calculating the $O - C$'s. The global evolution of the $O - C$ diagram is remarkably similar to that of GW Lib (figure 33). (Lower) Light curve.

during the 2003 superoutburst. The 2007 and 2008 observations most likely recorded stage C superhumps. Mean periods 0.07952(4) d and 0.07949(4) d, respectively, determined with the PDM method were adopted in table 2.

A comparison of $O - C$ diagrams of DH Aql between different superoutbursts is shown in figure 48.

6.8. V725 Aquilae

We have reanalyzed the 1999 superoutburst (Uemura et al. 2001). The times of superhump maxima are listed in table 24. As shown in Uemura et al. (2001), superhumps were only sufficiently observed mainly after the brightening before termination of the plateau, presumably corresponding to the stage C. This would explain the apparently zero period derivative in Uemura et al. (2001). Although the present data nominally yielded an overall positive P_{dot} of $+34.9(15.4) \times 10^{-5}$, the times of

maxima for $E \geq 20$ are well-expressed by a constant period of 0.09977(13) d. There seems to have been a transition in the period of superhumps around $E = 20$, associated by a lengthening, rather than shortening in many SU UMA-type dwarf novae (see also SDSS J1702 for a possible lengthening of the superhump period in a long- P_{SH} system, subsection 6.171). A better coverage of the early stage of a next superoutburst is vital to test whether this object indeed has a nearly zero P_{dot} . The times of superhump maxima during the 2005 superoutburst are also listed in table 25. A combined $O - C$ diagram (figure 49) suggests a positive P_{dot} , which needs to be confirmed by further observations.

6.9. V1141 Aquilae

Olech (2003) reported the detection of superhumps during the 2002 superoutburst. The reported period was 0.05930(5) d. Although Olech (2003) attempted to make

Table 17. Superhump maxima of V455 And (2007).

E	\max^a	error	$O - C^b$	phase ^c	N^d
0	54357.3037	0.0005	-0.0134	0.23	466
1	54357.3682	0.0002	-0.0061	0.37	703
2	54357.4275	0.0002	-0.0041	0.43	832
3	54357.4686	0.0003	-0.0203	0.16	829
4	54357.5446	0.0002	-0.0014	0.51	659
5	54357.5949	0.0002	-0.0083	0.40	836
6	54357.6563	0.0001	-0.0042	0.49	859
7	54357.7128	0.0004	-0.0049	0.49	120
11	54357.9321	0.0005	-0.0146	0.39	243
12	54358.0050	0.0002	0.0011	0.68	410
13	54358.0637	0.0003	0.0026	0.72	506
14	54358.1192	0.0015	0.0009	0.71	569
15	54358.1788	0.0003	0.0033	0.77	538
16	54358.2351	0.0003	0.0023	0.77	291
17	54358.2984	0.0004	0.0083	0.89	463
18	54358.3517	0.0003	0.0044	0.84	300
19	54358.4109	0.0003	0.0064	0.89	341
20	54358.4698	0.0002	0.0081	0.94	94
21	54358.5262	0.0002	0.0073	0.94	42
23	54358.6427	0.0003	0.0093	0.01	93
29	54358.9829	0.0008	0.0061	0.05	324
30	54359.0410	0.0003	0.0070	0.08	583
31	54359.0966	0.0001	0.0054	0.07	550
32	54359.1547	0.0002	0.0063	0.10	1031
33	54359.2083	0.0001	0.0026	0.05	783
34	54359.2650	0.0002	0.0021	0.06	430
35	54359.3261	0.0002	0.0059	0.14	546
36	54359.3815	0.0002	0.0042	0.13	410
37	54359.4377	0.0002	0.0031	0.13	447
38	54359.4956	0.0002	0.0038	0.15	307
39	54359.5522	0.0004	0.0032	0.16	317
40	54359.6114	0.0003	0.0051	0.21	356
41	54359.6639	0.0004	0.0004	0.14	91
47	54360.0096	0.0004	0.0027	0.28	168
48	54360.0653	0.0002	0.0012	0.27	698
49	54360.1246	0.0001	0.0033	0.32	943
50	54360.1830	0.0003	0.0044	0.36	316
51	54360.2378	0.0003	0.0021	0.34	295
52	54360.2930	0.0002	-0.0001	0.31	646
53	54360.3494	0.0001	-0.0009	0.32	617
54	54360.4102	0.0004	0.0027	0.40	500
55	54360.4658	0.0004	0.0011	0.38	337
56	54360.5223	0.0002	0.0004	0.39	465
57	54360.5790	0.0003	-0.0001	0.40	435
58	54360.6379	0.0004	0.0015	0.44	194
64	54360.9825	0.0009	0.0027	0.56	92
65	54361.0420	0.0016	0.0050	0.62	80
66	54361.0961	0.0009	0.0019	0.58	111
67	54361.1538	0.0012	0.0024	0.60	94
68	54361.2058	0.0011	-0.0028	0.53	80
69	54361.2632	0.0009	-0.0027	0.54	62

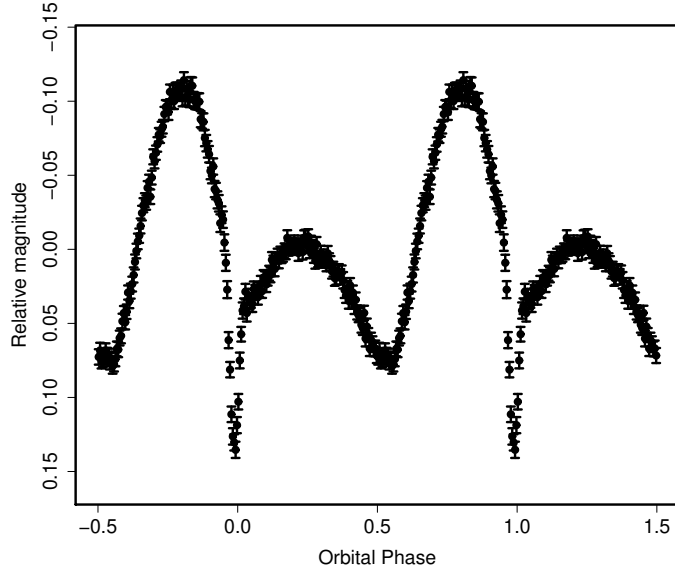
^a BJD-2400000.^b Against $\max = 2454357.3171 + 0.057228E$.^c Orbital phase.^d Number of points used to determine the maximum.

Fig. 42. Averaged orbital light curve of V455 And during the post-superoutburst stage.

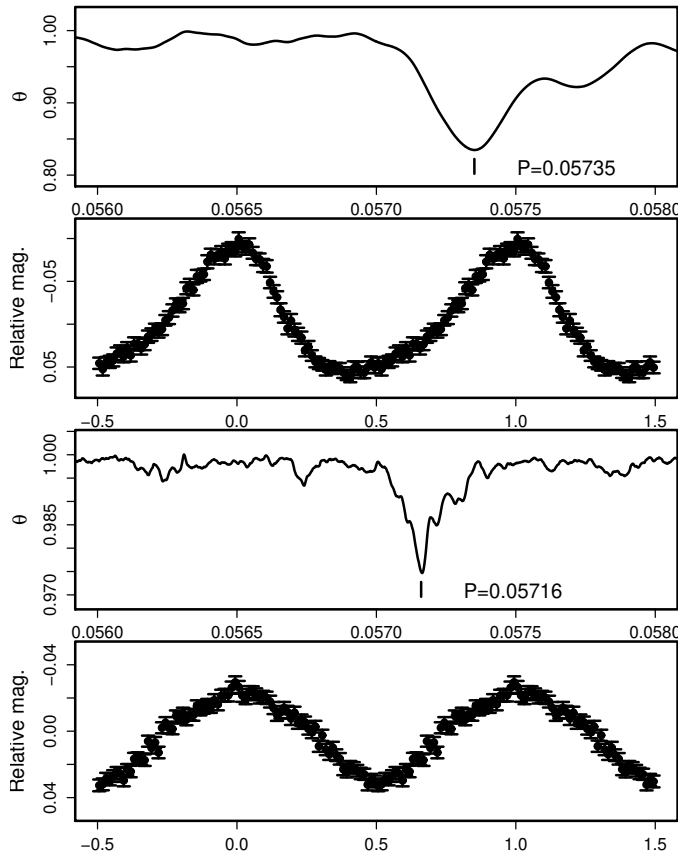


Fig. 43. Period analysis of V455 And (2007) during the post-superoutburst stage. Upper two figures represent the PDM analysis and mean superhump profile (after subtracting the orbital variation) before BJD 2454377, the epoch of the period change. Lower two figures represent the PDM analysis and mean superhump profile after BJD 2454377.

Table 17. Superhump maxima of V455 And (2007) (continued).

E	max	error	$O - C$	phase	N
70	54361.3261	0.0003	0.0030	0.66	542
71	54361.3869	0.0004	0.0065	0.74	500
72	54361.4393	0.0003	0.0017	0.67	408
74	54361.5549	0.0004	0.0028	0.72	288
75	54361.6121	0.0004	0.0028	0.74	440
76	54361.6690	0.0006	0.0025	0.75	236
81	54361.9530	0.0003	0.0004	0.80	534
82	54362.0070	0.0002	-0.0028	0.76	526
83	54362.0682	0.0002	0.0012	0.84	785
84	54362.1233	0.0001	-0.0011	0.82	788
85	54362.1805	0.0001	-0.0010	0.84	862
86	54362.2372	0.0001	-0.0016	0.84	824
87	54362.2954	0.0003	-0.0005	0.88	406
88	54362.3494	0.0002	-0.0038	0.84	207
89	54362.4077	0.0002	-0.0028	0.87	267
90	54362.4660	0.0003	-0.0017	0.91	166
91	54362.5206	0.0002	-0.0043	0.88	265
92	54362.5786	0.0002	-0.0036	0.91	310
93	54362.6329	0.0002	-0.0064	0.87	183
94	54362.6917	0.0002	-0.0049	0.91	150
95	54362.7495	0.0004	-0.0044	0.94	89
96	54362.8061	0.0002	-0.0050	0.95	171
97	54362.8639	0.0002	-0.0044	0.97	144
98	54362.9199	0.0004	-0.0056	0.97	119
99	54362.9780	0.0003	-0.0047	1.00	164
100	54363.0369	0.0002	-0.0031	0.04	98
101	54363.0929	0.0003	-0.0043	0.04	111
102	54363.1483	0.0008	-0.0061	0.02	104
103	54363.2051	0.0006	-0.0066	0.03	70
105	54363.3222	0.0002	-0.0039	0.11	614
106	54363.3771	0.0001	-0.0062	0.09	648
107	54363.4358	0.0002	-0.0048	0.13	464
108	54363.4939	0.0002	-0.0039	0.16	274
109	54363.5512	0.0002	-0.0038	0.18	793
110	54363.6063	0.0003	-0.0059	0.16	593
111	54363.6636	0.0002	-0.0058	0.17	320
112	54363.7236	0.0004	-0.0031	0.24	209
113	54363.7776	0.0004	-0.0063	0.20	142
114	54363.8364	0.0005	-0.0047	0.24	142
115	54363.8950	0.0006	-0.0034	0.28	132
116	54363.9499	0.0002	-0.0057	0.26	395
117	54364.0095	0.0003	-0.0033	0.32	419
118	54364.0666	0.0003	-0.0035	0.33	368
119	54364.1243	0.0004	-0.0030	0.36	304
120	54364.1801	0.0004	-0.0045	0.35	186
121	54364.2398	0.0006	-0.0020	0.41	216
122	54364.3006	0.0007	0.0016	0.49	489
123	54364.3585	0.0005	0.0023	0.52	391
124	54364.4055	0.0003	-0.0079	0.35	290
125	54364.4726	0.0010	0.0019	0.54	265
126	54364.5262	0.0004	-0.0016	0.49	359
127	54364.5883	0.0005	0.0032	0.60	505
128	54364.6432	0.0005	0.0008	0.57	556
133	54364.9369	0.0002	0.0084	0.79	172

Table 17. Superhump maxima of V455 And (2007) (continued).

E	max	error	$O - C$	phase	N
134	54364.9943	0.0003	0.0086	0.81	173
135	54365.0494	0.0002	0.0065	0.79	314
136	54365.1085	0.0003	0.0083	0.83	275
137	54365.1631	0.0003	0.0057	0.80	347
138	54365.2185	0.0003	0.0039	0.79	432
139	54365.2757	0.0006	0.0038	0.80	325
140	54365.3337	0.0003	0.0046	0.83	447
141	54365.3910	0.0003	0.0046	0.85	237
142	54365.4472	0.0003	0.0036	0.85	207
143	54365.5042	0.0005	0.0034	0.86	235
144	54365.5634	0.0007	0.0054	0.91	220
145	54365.6164	0.0003	0.0012	0.85	316
146	54365.6753	0.0004	0.0029	0.90	159
147	54365.7308	0.0003	0.0011	0.89	160
148	54365.7882	0.0003	0.0013	0.90	119
149	54365.8467	0.0005	0.0025	0.94	127
150	54365.9029	0.0007	0.0015	0.94	124
151	54365.9589	0.0002	0.0003	0.94	748
152	54366.0151	0.0013	-0.0007	0.93	480
153	54366.0705	0.0004	-0.0025	0.92	529

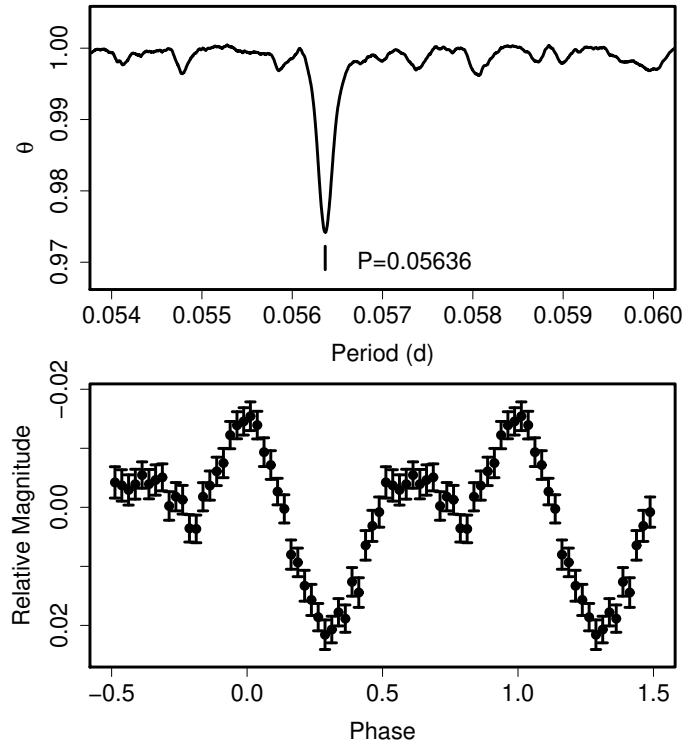
**Fig. 45.** Early superhumps in V466 And (2008). (Upper): PDM analysis. (Lower): Phase-averaged profile.

Table 18. Superhump maxima of V455 And during the Post-Superoutburst Stage (2007).

E	max ^a	error	$O - C^b$	phase ^c	N^d
0	54367.2376	0.0052	-0.0213	0.65	88
1	54367.3004	0.0010	-0.0157	0.76	240
2	54367.3639	0.0006	-0.0093	0.89	168
4	54367.4756	0.0004	-0.0119	0.87	85
5	54367.5306	0.0005	-0.0141	0.85	179
6	54367.5895	0.0004	-0.0123	0.89	323
7	54367.6474	0.0004	-0.0116	0.92	214
8	54367.6998	0.0003	-0.0163	0.85	244
9	54367.7597	0.0003	-0.0136	0.92	161
10	54367.8174	0.0003	-0.0131	0.94	165
11	54367.8711	0.0002	-0.0165	0.90	170
12	54367.9438	0.0029	-0.0009	0.19	40
20	54368.3873	0.0003	-0.0146	0.06	455
21	54368.4418	0.0005	-0.0172	0.03	374
22	54368.5004	0.0005	-0.0158	0.07	186
23	54368.5582	0.0006	-0.0152	0.10	196
24	54368.6176	0.0006	-0.0129	0.15	84
26	54368.7300	0.0005	-0.0148	0.15	71
30	54368.9625	0.0006	-0.0110	0.28	313
31	54369.0182	0.0006	-0.0123	0.27	343
32	54369.0883	0.0023	0.0006	0.51	273
33	54369.1426	0.0006	-0.0022	0.48	162
34	54369.1916	0.0007	-0.0104	0.35	119
35	54369.2552	0.0005	-0.0039	0.48	219
36	54369.3017	0.0003	-0.0146	0.30	300
37	54369.3615	0.0003	-0.0120	0.36	111
38	54369.4285	0.0016	-0.0021	0.55	77
39	54369.4816	0.0012	-0.0062	0.50	72
41	54369.5926	0.0015	-0.0095	0.47	63
42	54369.6495	0.0015	-0.0097	0.48	65
43	54369.7184	0.0007	0.0020	0.70	68
44	54369.7761	0.0004	0.0026	0.73	68
45	54369.8306	0.0005	-0.0000	0.70	69
46	54369.8887	0.0007	0.0008	0.73	69
47	54369.9441	0.0004	-0.0009	0.71	67
52	54370.2317	0.0007	0.0010	0.82	121
58	54370.5696	0.0004	-0.0040	0.82	87
59	54370.6276	0.0002	-0.0031	0.85	135
60	54370.6840	0.0003	-0.0039	0.85	119
61	54370.7419	0.0003	-0.0032	0.88	98
62	54370.7960	0.0005	-0.0062	0.84	66
63	54370.8542	0.0005	-0.0052	0.87	67
64	54370.9116	0.0003	-0.0049	0.89	66
65	54370.9683	0.0010	-0.0054	0.90	95
66	54371.0331	0.0008	0.0023	0.05	86
70	54371.2523	0.0005	-0.0071	0.94	137
71	54371.3043	0.0004	-0.0123	0.87	147
72	54371.3735	0.0013	-0.0002	0.09	35
83	54372.0082	0.0067	0.0059	0.37	87
94	54372.6343	0.0005	0.0033	0.49	167
107	54373.3843	0.0019	0.0104	0.81	30

^a BJD-2400000.^b Against $max = 2454367.5448 + 0.057162E$.^c Orbital phase.^d Number of points used to determine the maximum.**Table 18.** Superhump maxima of V455 And during the Post-Superoutburst Stage (2007) (continued).

E	max	error	$O - C$	phase	N
108	54373.4425	0.0009	0.0114	0.84	28
109	54373.4987	0.0016	0.0105	0.84	74
110	54373.5539	0.0006	0.0085	0.82	99
123	54374.2885	0.0011	0.0002	0.86	58
124	54374.3461	0.0009	0.0007	0.89	83
125	54374.4001	0.0006	-0.0025	0.85	86
126	54374.4567	0.0008	-0.0030	0.85	77
127	54374.5199	0.0010	0.0030	0.97	30
128	54374.5763	0.0017	0.0023	0.97	63
129	54374.6306	0.0016	-0.0006	0.94	91
130	54374.6872	0.0009	-0.0012	0.94	71
131	54374.7410	0.0006	-0.0045	0.90	70
132	54374.7991	0.0009	-0.0036	0.93	70
133	54374.8610	0.0011	0.0012	0.03	66
134	54374.9184	0.0008	0.0015	0.05	69
141	54375.3256	0.0016	0.0086	0.28	29
145	54375.5512	0.0011	0.0056	0.29	27
152	54375.9385	0.0003	-0.0071	0.17	248
152	54375.9651	0.0002	0.0195	0.64	363
153	54376.0099	0.0005	0.0072	0.43	366
163	54376.5909	0.0005	0.0166	0.75	66
164	54376.6421	0.0009	0.0107	0.66	70
165	54376.7003	0.0022	0.0117	0.69	70
166	54376.7621	0.0005	0.0164	0.79	70
167	54376.8138	0.0005	0.0110	0.71	69
168	54376.8737	0.0005	0.0137	0.77	68
169	54376.9282	0.0016	0.0110	0.74	70
172	54377.1025	0.0005	0.0139	0.84	121
173	54377.1596	0.0009	0.0139	0.85	133
174	54377.2149	0.0004	0.0120	0.83	132
175	54377.2698	0.0004	0.0097	0.81	132
176	54377.3255	0.0007	0.0083	0.80	65
180	54377.5529	0.0003	0.0071	0.84	196
181	54377.5964	0.0010	-0.0066	0.61	110
182	54377.6662	0.0005	0.0060	0.85	62
183	54377.7248	0.0006	0.0075	0.89	66
184	54377.7773	0.0005	0.0029	0.82	68
185	54377.8339	0.0005	0.0023	0.83	68
186	54377.8921	0.0004	0.0034	0.86	68
187	54377.9458	0.0005	-0.0000	0.81	64
193	54378.2893	0.0004	0.0006	0.91	82
194	54378.3407	0.0010	-0.0052	0.83	83
195	54378.4133	0.0020	0.0102	0.11	94
196	54378.4595	0.0008	-0.0007	0.94	161
197	54378.5156	0.0011	-0.0018	0.93	214
198	54378.5696	0.0004	-0.0049	0.89	112
199	54378.6255	0.0003	-0.0061	0.88	243
200	54378.6782	0.0011	-0.0106	0.82	140
201	54378.7412	0.0008	-0.0047	0.94	72
204	54378.9128	0.0007	-0.0045	0.99	201
205	54378.9748	0.0005	0.0002	0.09	460
206	54379.0327	0.0011	0.0010	0.12	441
207	54379.0912	0.0006	0.0024	0.15	459
208	54379.1535	0.0030	0.0075	0.26	207

Table 18. Superhump maxima of V455 And during the Post-Superoutburst Stage (2007) (continued).

E	max	error	$O - C$	phase	N
209	54379.1986	0.0005	-0.0046	0.06	435
210	54379.2470	0.0010	-0.0133	0.92	364
212	54379.3782	0.0005	0.0036	0.25	279
213	54379.4322	0.0006	0.0004	0.21	278
214	54379.4949	0.0012	0.0060	0.32	163
215	54379.5460	0.0004	-0.0000	0.23	399
216	54379.6081	0.0008	0.0049	0.33	529
220	54379.8001	0.0006	-0.0317	0.74	68
221	54379.8551	0.0007	-0.0338	0.72	68
222	54379.9402	0.0008	-0.0058	0.23	383
223	54380.0034	0.0003	0.0002	0.35	557
226	54380.1728	0.0011	-0.0019	0.36	364
227	54380.2211	0.0007	-0.0107	0.22	274
228	54380.2790	0.0012	-0.0099	0.25	293
228	54380.3108	0.0003	0.0218	0.81	279
229	54380.3640	0.0003	0.0179	0.76	278
230	54380.4154	0.0004	0.0122	0.67	270
231	54380.4635	0.0006	0.0031	0.53	275
232	54380.5235	0.0015	0.0059	0.59	251
240	54380.9853	0.0013	0.0105	0.79	96
241	54381.0421	0.0007	0.0102	0.80	93
242	54381.1003	0.0007	0.0113	0.83	72
243	54381.1577	0.0005	0.0114	0.85	84
246	54381.3291	0.0002	0.0115	0.90	303
247	54381.3838	0.0004	0.0090	0.87	298
248	54381.4315	0.0002	-0.0004	0.72	282
249	54381.4944	0.0004	0.0053	0.83	309
250	54381.5513	0.0005	0.0050	0.84	234
251	54381.6006	0.0008	-0.0028	0.72	96
266	54382.4532	0.0033	-0.0075	0.86	42
268	54382.5658	0.0009	-0.0092	0.86	206
269	54382.6202	0.0004	-0.0118	0.83	280
270	54382.6646	0.0006	-0.0247	0.61	88
271	54382.7442	0.0034	-0.0022	0.03	68
281	54383.3122	0.0009	-0.0057	0.12	241
285	54383.5676	0.0009	0.0211	0.65	232
286	54383.6169	0.0003	0.0133	0.53	212
287	54383.6514	0.0009	-0.0094	0.14	222
288	54383.7252	0.0011	0.0073	0.45	58
289	54383.7814	0.0017	0.0063	0.45	70
290	54383.8539	0.0009	0.0217	0.74	69
292	54383.9548	0.0006	0.0083	0.53	131
293	54384.0067	0.0004	0.0030	0.45	132
294	54384.0590	0.0014	-0.0018	0.38	225
295	54384.1246	0.0007	0.0066	0.54	206
296	54384.1904	0.0005	0.0152	0.71	136
297	54384.2521	0.0007	0.0199	0.81	182
299	54384.3195	0.0009	-0.0271	0.00	175
303	54384.5882	0.0007	0.0131	0.78	68
304	54384.6427	0.0005	0.0104	0.74	68
305	54384.7065	0.0011	0.0171	0.88	70
306	54384.7686	0.0010	0.0220	0.98	68
307	54384.8216	0.0007	0.0178	0.92	70

Table 18. Superhump maxima of V455 And during the Post-Superoutburst Stage (2007) (continued).

E	max	error	$O - C$	phase	N
309	54384.9306	0.0005	0.0125	0.86	160
310	54384.9850	0.0004	0.0098	0.82	355
311	54385.0440	0.0002	0.0117	0.87	377
312	54385.0932	0.0004	0.0037	0.74	326
314	54385.2160	0.0004	0.0122	0.92	376
315	54385.2644	0.0005	0.0035	0.79	223
321	54385.6065	0.0009	0.0027	0.86	67
322	54385.6626	0.0018	0.0016	0.86	68
323	54385.7111	0.0010	-0.0071	0.72	69
325	54385.8368	0.0008	0.0043	0.95	68
326	54385.8888	0.0009	-0.0008	0.87	69
328	54385.9958	0.0026	-0.0081	0.77	65
329	54386.0590	0.0031	-0.0020	0.90	67
330	54386.1156	0.0017	-0.0026	0.90	42
335	54386.4172	0.0009	0.0133	0.26	60
336	54386.4696	0.0007	0.0086	0.19	60
337	54386.5282	0.0009	0.0100	0.23	58
351	54387.2852	0.0008	-0.0331	0.67	99
352	54387.3462	0.0013	-0.0293	0.75	64
368	54388.3009	0.0008	0.0111	0.71	136
369	54388.3549	0.0003	0.0079	0.67	124
370	54388.4158	0.0004	0.0116	0.75	109
372	54388.4825	0.0005	-0.0359	0.94	181
372	54388.5334	0.0004	0.0149	0.84	182
374	54388.6438	0.0003	0.0110	0.80	172
380	54388.9844	0.0039	0.0088	0.85	151
381	54389.0447	0.0013	0.0119	0.92	377
382	54389.0961	0.0006	0.0061	0.83	308
383	54389.1523	0.0011	0.0052	0.83	377
384	54389.2021	0.0008	-0.0022	0.71	330
400	54390.1431	0.0028	0.0244	0.43	35
404	54390.3163	0.0007	-0.0310	0.50	84
405	54390.4139	0.0014	0.0095	0.23	84
407	54390.4877	0.0017	-0.0310	0.55	84
407	54390.5323	0.0017	0.0136	0.34	80
412	54390.8071	0.0015	0.0027	0.22	68
413	54390.8705	0.0006	0.0089	0.34	68
415	54390.9797	0.0011	0.0038	0.28	127
416	54391.0329	0.0016	-0.0001	0.23	144
417	54391.0895	0.0025	-0.0007	0.23	171
418	54391.1324	0.0019	-0.0149	1.00	140
423	54391.4284	0.0014	-0.0046	0.25	62
447	54392.7733	0.0032	-0.0313	0.14	67
447	54392.8236	0.0015	0.0189	0.03	59
448	54392.8764	0.0009	0.0146	0.97	65
466	54393.8981	0.0005	0.0076	0.11	64
468	54394.0171	0.0005	0.0123	0.22	184
469	54394.0617	0.0015	-0.0002	0.02	380
471	54394.1956	0.0015	0.0194	0.39	527
472	54394.2438	0.0021	0.0104	0.25	400
473	54394.2947	0.0008	0.0042	0.15	174
476	54394.4834	0.0009	0.0214	0.51	122
479	54394.6500	0.0005	0.0166	0.46	177
480	54394.6893	0.0007	-0.0012	0.16	174
485	54394.9449	0.0010	-0.0314	0.70	222

Table 18. Superhump maxima of V455 And during the Post-Superoutburst Stage (2007) (continued).

E	max	error	$O - C$	phase	N
485	54394.9930	0.0006	0.0167	0.56	232
486	54395.0338	0.0007	0.0003	0.28	197
487	54395.0864	0.0016	-0.0042	0.21	165
489	54395.2112	0.0018	0.0063	0.43	51
490	54395.2625	0.0023	0.0004	0.34	79
497	54395.6482	0.0010	-0.0139	0.19	68
509	54396.3290	0.0011	-0.0189	0.28	122
510	54396.3885	0.0006	-0.0165	0.34	122
511	54396.4523	0.0012	-0.0098	0.47	123
515	54396.7136	0.0016	0.0228	0.11	67
517	54396.7774	0.0008	-0.0277	0.24	69
520	54396.9561	0.0009	-0.0204	0.42	144
521	54397.0329	0.0008	-0.0007	0.78	223
522	54397.0918	0.0016	0.0009	0.83	176
523	54397.1584	0.0033	0.0104	0.01	128
524	54397.2294	0.0018	0.0243	0.27	154
550	54398.6891	0.0008	-0.0019	0.20	68
551	54398.7464	0.0008	-0.0017	0.21	70
552	54398.8078	0.0022	0.0025	0.30	69
553	54398.8672	0.0017	0.0047	0.36	69
566	54399.5986	0.0014	-0.0068	0.35	68
567	54399.6570	0.0012	-0.0056	0.38	70
568	54399.7116	0.0012	-0.0081	0.35	69
569	54399.7686	0.0008	-0.0082	0.37	68
570	54399.8487	0.0027	0.0147	0.79	68
618	54402.5771	0.0018	-0.0001	0.24	68
619	54402.6349	0.0009	0.0006	0.27	69
620	54402.7059	0.0012	0.0144	0.53	70
621	54402.7438	0.0011	-0.0048	0.20	70
622	54402.8160	0.0009	0.0102	0.48	70
623	54402.8862	0.0015	0.0233	0.73	54
626	54403.0402	0.0015	0.0059	0.47	90
627	54403.0972	0.0014	0.0057	0.48	79
660	54404.9795	0.0008	0.0021	0.91	126
661	54405.0351	0.0009	0.0006	0.89	87
662	54405.1088	0.0065	0.0171	0.20	59
670	54405.5667	0.0032	0.0178	0.34	68
671	54405.6199	0.0013	0.0138	0.28	51
672	54405.6729	0.0015	0.0097	0.22	67
673	54405.7252	0.0076	0.0048	0.15	68
674	54405.7827	0.0010	0.0052	0.17	60
675	54405.8333	0.0017	-0.0014	0.07	66
690	54406.6919	0.0007	0.0000	0.32	60
695	54406.9441	0.0016	-0.0336	0.80	69
696	54406.9976	0.0017	-0.0372	0.75	79
696	54407.0427	0.0010	0.0079	0.55	92
698	54407.1198	0.0012	-0.0293	0.92	92
699	54407.1793	0.0016	-0.0270	0.97	89
705	54407.5621	0.0006	0.0130	0.77	72
707	54407.6838	0.0009	0.0203	0.93	76
708	54407.7326	0.0010	0.0120	0.80	77
709	54407.7848	0.0035	0.0070	0.73	71
710	54407.8205	0.0012	-0.0144	0.36	77
711	54407.8711	0.0007	-0.0209	0.26	52
713	54408.0200	0.0011	0.0137	0.90	86

Table 18. Superhump maxima of V455 And during the Post-Superoutburst Stage (2007) (continued).

E	max	error	$O - C$	phase	N
715	54408.0882	0.0006	-0.0325	0.11	91
715	54408.1401	0.0015	0.0194	0.04	92
725	54408.7080	0.0011	0.0159	0.12	77
730	54408.9503	0.0025	-0.0276	0.42	79
742	54409.6787	0.0005	0.0150	0.36	77
744	54409.7458	0.0004	-0.0321	0.55	76
744	54409.7826	0.0016	0.0047	0.21	74
745	54409.8415	0.0011	0.0064	0.25	77
778	54411.7051	0.0007	-0.0160	0.35	21
779	54411.7451	0.0012	-0.0331	0.06	58
780	54411.8182	0.0008	-0.0171	0.36	99
782	54411.9668	0.0016	0.0172	1.00	221
787	54412.2265	0.0032	-0.0089	0.61	67
798	54412.8325	0.0013	-0.0315	0.37	74
814	54413.7843	0.0015	0.0059	0.27	79
815	54413.8399	0.0011	0.0043	0.26	73
884	54417.7831	0.0009	0.0042	0.29	79
885	54417.8362	0.0018	0.0002	0.23	78
887	54417.9551	0.0010	0.0048	0.34	81
888	54418.0135	0.0010	0.0061	0.38	100
889	54418.0621	0.0043	-0.0025	0.24	140
890	54418.1102	0.0026	-0.0115	0.10	116
904	54418.9231	0.0008	0.0012	0.53	70
905	54418.9700	0.0020	-0.0089	0.37	82
906	54419.0309	0.0014	-0.0052	0.45	105
907	54419.0968	0.0028	0.0035	0.62	112
908	54419.1505	0.0010	0.0001	0.57	109
909	54419.2033	0.0022	-0.0043	0.51	83
919	54419.7762	0.0018	-0.0028	0.68	74
920	54419.8253	0.0011	-0.0109	0.55	74
940	54420.9911	0.0010	0.0119	0.26	94
941	54421.0319	0.0009	-0.0045	0.98	78
944	54421.2073	0.0006	-0.0005	0.10	82
957	54421.9139	0.0011	-0.0368	0.65	77
957	54421.9613	0.0008	0.0106	0.49	80
994	54424.0840	0.0012	0.0187	0.18	92
1009	54424.9177	0.0026	-0.0048	0.99	79
1011	54425.0344	0.0017	-0.0024	0.06	81
1029	54426.0711	0.0023	0.0056	0.47	69
1030	54426.1341	0.0017	0.0115	0.59	75
1062	54427.9455	0.0011	-0.0059	0.76	147
1063	54428.0024	0.0032	-0.0061	0.77	172
1064	54428.0748	0.0089	0.0091	0.06	164
1080	54428.9456	0.0008	-0.0345	0.52	162
1081	54429.0459	0.0014	0.0087	0.30	92
1091	54429.6224	0.0017	0.0137	0.54	76
1092	54429.6651	0.0035	-0.0008	0.30	76
1093	54429.7452	0.0088	0.0221	0.72	77
1094	54429.7790	0.0236	-0.0011	0.32	77
1096	54429.8967	0.0009	0.0022	0.41	81
1097	54429.9560	0.0031	0.0044	0.47	81
1125	54431.5670	0.0019	0.0152	0.08	77
1126	54431.6214	0.0027	0.0124	0.04	78
1160	54433.5612	0.0008	0.0092	0.49	77

Table 18. Superhump maxima of V455 And during the Post-Superoutburst Stage (2007) (continued).

E	max	error	$O - C$	phase	N
1161	54433.6227	0.0011	0.0136	0.58	78
1201	54435.8936	0.0061	-0.0016	0.91	62
1202	54435.9601	0.0010	0.0078	0.09	81
1204	54436.0419	0.0009	-0.0246	0.55	165
1204	54436.0933	0.0027	0.0267	0.46	111
1239	54438.0607	0.0026	-0.0061	0.40	52
1272	54439.9187	0.0010	-0.0340	0.40	82
1272	54439.9763	0.0013	0.0236	0.42	81
1274	54440.0474	0.0024	-0.0196	0.68	102
1289	54440.9335	0.0010	0.0092	0.42	81
1290	54440.9862	0.0038	0.0048	0.35	34
1291	54441.0517	0.0012	0.0131	0.52	149
1292	54441.0985	0.0058	0.0027	0.35	84
1293	54441.1525	0.0009	-0.0004	0.31	55
1307	54441.9501	0.0011	-0.0029	0.47	65
1323	54442.8889	0.0008	0.0216	0.14	81
1324	54442.9489	0.0021	0.0244	0.21	76
1342	54443.9433	0.0041	-0.0099	0.87	182
1343	54443.9874	0.0016	-0.0229	0.65	260
1343	54444.0293	0.0006	0.0190	0.40	145
1344	54444.0791	0.0014	0.0116	0.28	74
1358	54444.8856	0.0009	0.0180	0.60	76
1359	54444.9252	0.0015	0.0005	0.31	81
1360	54444.9678	0.0021	-0.0141	0.06	81
1405	54447.5704	0.0006	0.0168	0.28	77
1406	54447.6291	0.0008	0.0184	0.33	74
1448	54449.9846	0.0020	-0.0264	0.16	125
1449	54450.0945	0.0022	0.0263	0.11	80
1458	54450.5688	0.0012	-0.0137	0.53	56
1464	54450.9005	0.0012	-0.0249	0.42	44
1465	54450.9585	0.0012	-0.0240	0.45	44
1475	54451.5628	0.0014	0.0088	0.18	75
1481	54451.9163	0.0010	0.0193	0.46	44
1482	54451.9780	0.0016	0.0240	0.56	45
1639	54460.9315	0.0033	0.0050	0.56	43
1640	54460.9821	0.0023	-0.0015	0.46	116
1641	54461.0252	0.0027	-0.0156	0.23	122
1691	54463.9164	0.0025	0.0181	0.57	43
1692	54463.9730	0.0012	0.0176	0.58	43
1780	54468.9547	0.0022	-0.0298	0.05	74
1781	54469.0230	0.0009	-0.0187	0.26	73
1797	54469.9389	0.0008	-0.0172	0.53	37
1837	54472.2254	0.0066	-0.0167	0.13	48
1838	54472.3032	0.0012	0.0040	0.51	49
1839	54472.3606	0.0026	0.0042	0.53	43
1902	54475.9420	0.0013	-0.0148	0.13	93
1954	54478.9490	0.0010	0.0205	0.54	83
2182	54491.9374	0.0009	-0.0211	0.20	77
2183	54491.9920	0.0026	-0.0237	0.17	75

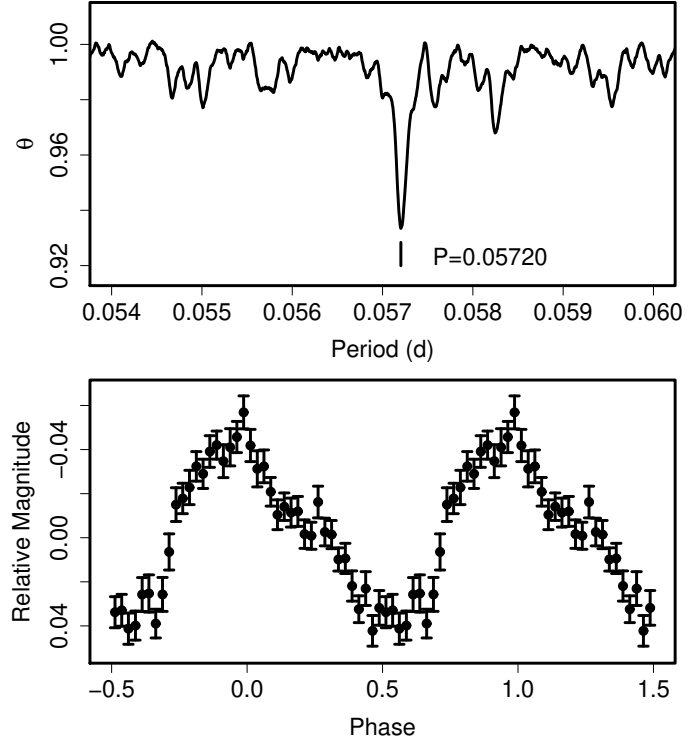
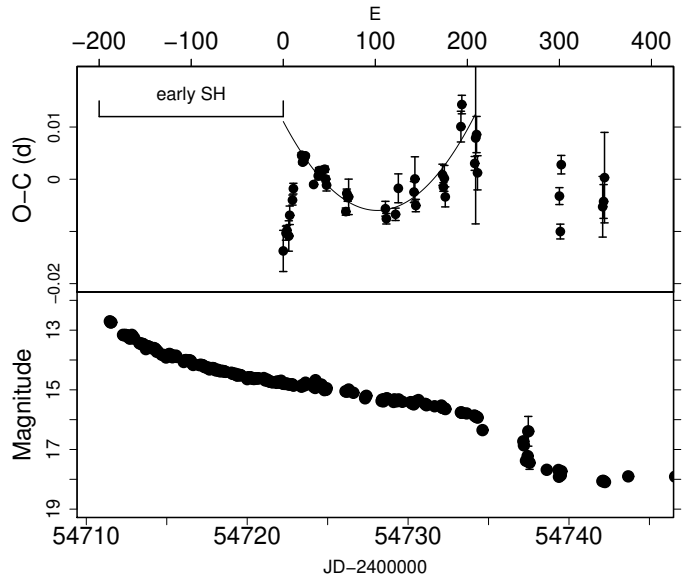
**Fig. 46.** Ordinary superhumps in V466 And (2008). (Upper): PDM analysis. (Lower): Phase-averaged profile.**Fig. 47.** $O - C$ of superhumps V466 And (2008). (Upper): $O - C$ diagram. The $O - C$ values were against the mean period for the stage B ($20 \leq E \leq 194$, thin curve). (Lower): Light curve.

Table 19. Superhump maxima of V466 And (2008).

E	max ^a	error	$O - C^b$	N^c
0	54722.2300	0.0039	-0.0115	207
3	54722.4050	0.0013	-0.0081	68
4	54722.4628	0.0010	-0.0076	33
6	54722.5761	0.0029	-0.0087	11
7	54722.6373	0.0018	-0.0048	21
10	54722.8118	0.0010	-0.0019	35
11	54722.8712	0.0010	0.0003	38
20	54723.3924	0.0005	0.0066	115
21	54723.4483	0.0004	0.0053	147
22	54723.5056	0.0004	0.0054	165
23	54723.5635	0.0004	0.0061	77
24	54723.6211	0.0004	0.0065	55
33	54724.1305	0.0003	0.0009	120
38	54724.4181	0.0008	0.0025	42
39	54724.4763	0.0006	0.0035	42
40	54724.5330	0.0005	0.0030	42
41	54724.5903	0.0005	0.0031	42
45	54724.8198	0.0006	0.0037	57
46	54724.8752	0.0006	0.0019	35
47	54724.9312	0.0011	0.0007	48
68	54726.1274	0.0007	-0.0046	282
69	54726.1881	0.0008	-0.0011	264
70	54726.2445	0.0007	-0.0019	273
71	54726.3018	0.0034	-0.0018	65
111	54728.5877	0.0014	-0.0044	91
112	54728.6430	0.0010	-0.0063	95
122	54729.2158	0.0012	-0.0056	222
125	54729.3924	0.0028	-0.0006	41
142	54730.3642	0.0020	-0.0015	61
143	54730.4239	0.0042	0.0010	48
144	54730.4760	0.0012	-0.0041	65
173	54732.1408	0.0020	0.0016	285
174	54732.1956	0.0008	-0.0008	270
175	54732.2545	0.0025	0.0009	257
176	54732.3082	0.0019	-0.0027	140
193	54733.2941	0.0029	0.0106	64
194	54733.3555	0.0018	0.0149	61
208	54734.1451	0.0013	0.0035	123
209	54734.2072	0.0165	0.0083	103
210	54734.2650	0.0035	0.0090	132
211	54734.3149	0.0033	0.0016	135
300	54739.4015	0.0016	-0.0036	24
301	54739.4519	0.0014	-0.0104	23
302	54739.5220	0.0018	0.0024	21
347	54742.0880	0.0058	-0.0060	109
348	54742.1463	0.0032	-0.0050	113
349	54742.2080	0.0087	-0.0005	110

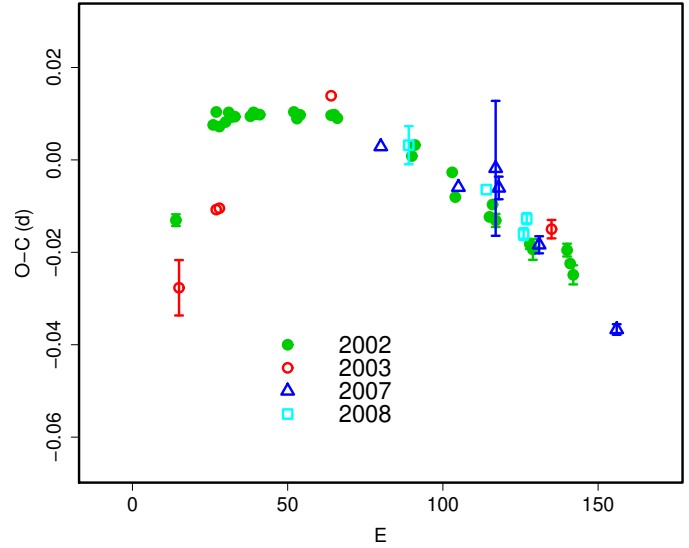
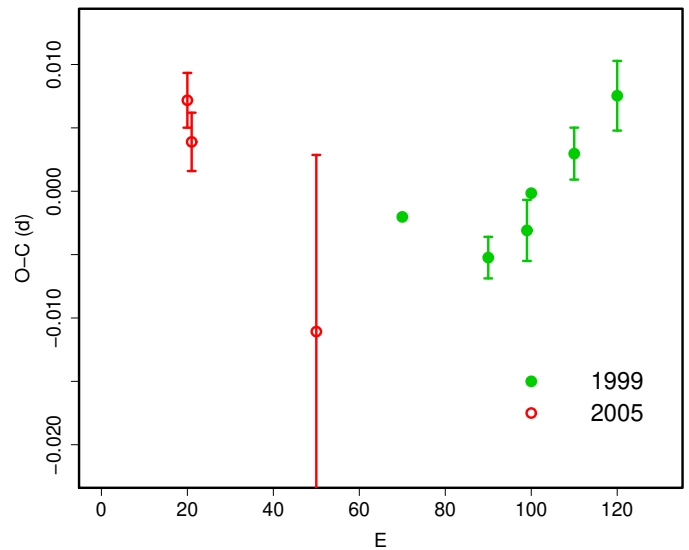
^a BJD-2400000.^b Against $max = 2454722.2415 + 0.057212E$.^c Number of points used to determine the maximum.**Fig. 48.** Comparison of $O - C$ diagrams of DH Aql between different superoutbursts. A period of 0.08000 d was used to draw this figure. Approximate cycle counts (E) after the start of the superoutburst were used. Since the start of the 2007 superoutburst was not well constrained, we shifted the $O - C$ diagrams to best fit the others.**Fig. 49.** Comparison of $O - C$ diagrams of V725 Aql between different superoutbursts. A period of 0.06350 d was used to draw this figure. Approximate cycle counts (E) after the start of the superoutburst were used.

Table 20. Superhumps Maxima of DH Aql (2002).

E	\max^a	error	$O - C^b$	N^c
0	52483.9809	0.0013	-0.0272	93
12	52484.9615	0.0001	-0.0037	267
13	52485.0443	0.0001	-0.0006	256
14	52485.1212	0.0002	-0.0035	250
16	52485.2822	0.0007	-0.0021	135
17	52485.3642	0.0001	0.0003	222
18	52485.4433	0.0001	-0.0005	223
19	52485.5233	0.0002	-0.0002	221
24	52485.9234	0.0001	0.0012	290
25	52486.0043	0.0001	0.0023	472
26	52486.0839	0.0002	0.0021	748
27	52486.1638	0.0003	0.0023	628
38	52487.0443	0.0004	0.0055	306
39	52487.1229	0.0003	0.0044	376
40	52487.2037	0.0002	0.0054	584
50	52488.0036	0.0004	0.0078	228
51	52488.0838	0.0003	0.0082	331
52	52488.1630	0.0003	0.0076	430
76	52490.0748	0.0004	0.0054	221
77	52490.1572	0.0004	0.0080	207
89	52491.1113	0.0009	0.0050	147
90	52491.1859	0.0005	-0.0001	281
101	52492.0616	0.0009	-0.0017	127
102	52492.1443	0.0006	0.0013	152
103	52492.2209	0.0014	-0.0019	120
114	52493.0958	0.0011	-0.0043	151
115	52493.1746	0.0022	-0.0053	136
126	52494.0544	0.0014	-0.0027	117
127	52494.1315	0.0010	-0.0053	325
128	52494.2091	0.0021	-0.0076	128

^a BJD-2400000.^b Against $\max = 2452484.0082 + 0.079754E$.^c Number of points used to determine the maximum.**Table 21.** Superhumps Maxima of DH Aql (2003).

E	\max^a	error	$O - C^b$	N^c
0	52886.0802	0.0060	-0.0154	81
12	52887.0571	0.0002	0.0008	124
13	52887.1374	0.0003	0.0010	150
49	52890.0418	0.0007	0.0233	76
120	52895.6929	0.0020	-0.0097	76

^a BJD-2400000.^b Against $\max = 2452886.0957 + 0.080058E$.^c Number of points used to determine the maximum.**Table 22.** Superhumps Maxima of DH Aql (2007).

E	\max^a	error	$O - C^b$	N^c
0	54232.2271	0.0005	-0.0058	121
25	54234.2183	0.0008	-0.0016	138
37	54235.1824	0.0146	0.0087	125
38	54235.2582	0.0024	0.0050	88
51	54236.2859	0.0018	-0.0005	80
76	54238.2676	0.0011	-0.0059	84

^a BJD-2400000.^b Against $\max = 2454232.2329 + 0.079481E$.^c Number of points used to determine the maximum.**Table 23.** Superhumps Maxima of DH Aql (2008).

E	\max^a	error	$O - C^b$	N^c
0	54628.1832	0.0041	-0.0005	60
25	54630.1736	0.0006	0.0016	142
37	54631.1240	0.0013	-0.0025	138
38	54631.2073	0.0012	0.0014	86

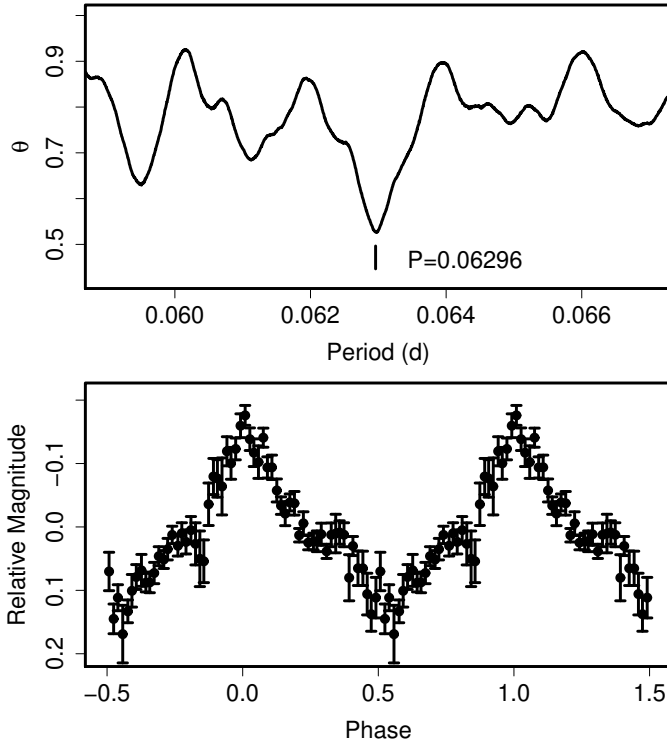
^a BJD-2400000.^b Against $\max = 2454628.1837 + 0.079534E$.^c Number of points used to determine the maximum.**Table 24.** Superhump maxima of V725 Aql (1999).

E	\max^a	error	$O - C^b$	N^c
0	51447.9596	0.0066	0.0008	116
1	51448.0635	0.0038	0.0055	137
2	51448.1632	0.0072	0.0062	85
4	51448.3580	0.0009	0.0026	56
10	51448.9388	0.0019	-0.0113	157
11	51449.0486	0.0077	-0.0006	185
12	51449.1689	0.0132	0.0205	147
20	51449.9295	0.0046	-0.0120	141
21	51450.0275	0.0091	-0.0131	181
24	51450.3365	0.0016	-0.0015	25
30	51450.9305	0.0040	-0.0023	143
31	51451.0263	0.0199	-0.0056	178
32	51451.1225	0.0087	-0.0086	160
33	51451.2305	0.0024	0.0003	30
34	51451.3325	0.0010	0.0032	53
44	51452.3266	0.0021	0.0059	33
54	51453.3220	0.0027	0.0100	36

^a BJD-2400000.^b Against $\max = 2451447.9588 + 0.099134E$.^c Number of points used to determine the maximum.

Table 25. Superhump maxima of V725 Aql (2005).

E	\max^a	error	$O - C^b$	N^c
0	53685.5353	0.0022	0.0013	120
1	53685.6311	0.0023	-0.0014	97
30	53688.4897	0.0139	0.0000	30

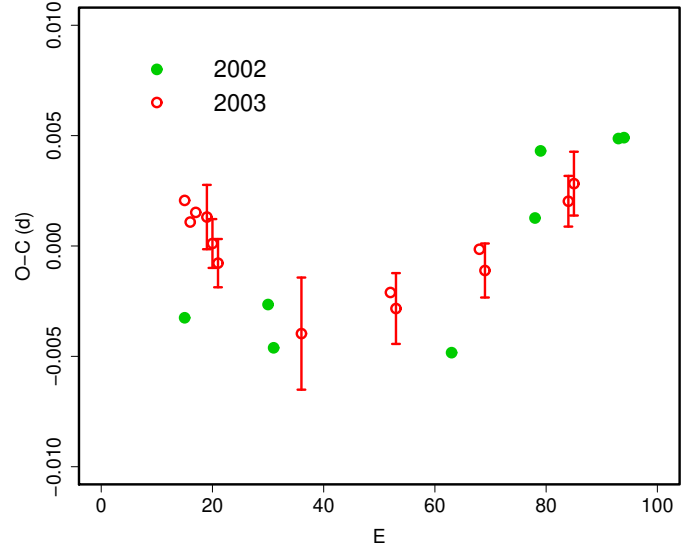
^a BJD-2400000.^b Against $\max = 2453685.5339 + 0.098525E$.^c Number of points used to determine the maximum.**Fig. 50.** Superhumps in V1141 Aql (2003). (Upper): PDM analysis. (Lower): Phase-averaged profile.

a comparison with the system SW UMa, which has similar outburst properties and superhump period, they failed to detect a positive period derivative.

During the 2003 superoutburst, we performed time-series photometry on consecutive five nights. The resultant timings of superhump maxima are presented in table 26. The period by Olech (2003) did not well fit our observations; instead, a period of 0.06296(2) d well expressed our observations (figure 50). The cycle numbers given in table 26 refer to this period. The observed times were well expressed by a $P_{\dot{\text{dot}}}$ of $+13.4(1.6) \times 10^{-5}$.

A comparison of $O - C$ diagrams of V1141 Aql between different superoutbursts is shown in figure 51.

By correctly identifying the cycle numbers based on this period, the reported times of maxima in Olech (2003) can also be well fit by a mean period of 0.06308(3) d and $P_{\dot{\text{dot}}}$ of $+9.3(4.3) \times 10^{-5}$. These period derivatives are indeed similar to that of SW UMa. The new period is also com-

**Fig. 51.** Comparison of $O - C$ diagrams of V1141 Aql between different superoutbursts. A period of 0.06296 d was used to draw this figure. Approximate cycle counts (E) after the start of the superoutburst were used.**Table 26.** Superhump maxima of V1141 Aql (2003).

E	\max^a	error	$O - C$	N^b
0	52823.0212	0.0005	0.0021	137
1	52823.0831	0.0005	0.0011	102
2	52823.1465	0.0007	0.0015	81
4	52823.2723	0.0015	0.0013	17
5	52823.3340	0.0011	0.0001	18
6	52823.3961	0.0011	-0.0008	18
21	52824.3373	0.0025	-0.0040	17
37	52825.3465	0.0010	-0.0021	17
38	52825.4087	0.0016	-0.0028	17
53	52826.3558	0.0008	-0.0002	17
54	52826.4178	0.0012	-0.0011	17
69	52827.3654	0.0011	0.0020	17
70	52827.4291	0.0014	0.0028	17

^a BJD-2400000.^b Number of points used to determine the maximum.

patible with the proposed orbital period of 0.0620 d from single-night quiescent photometry (Haefner 2004). By literally adopting this proposed orbital period, we obtain a fractional superhump excess of 1.5%. A comparison of $O - C$ diagrams between 2002 and 2003 superoutbursts is shown in figure 51.

6.10. VY Aquarii

VY Aqr had long been supposed to be a recurrent nova that erupted in 1907 and 1962 (Strohmeier 1962; Huth 1962). While the detection of the 1973 outburst (McNaught 1982) suggested a shorter recurrence time, the detection of additional outbursts (Richter 1983b; Richter 1983a; Liller 1983) led to a more likely classification as a WZ Sge-type dwarf nova. Further outbursts were recorded almost yearly (e.g. McAdam et al. 1983; Lubbock, McNaught 1986; Hurst et al. 1987), confirming the dwarf nova-type classification. Patterson et al. (1993) first established the SU UMA-type classification based on photoelectric observations during the 1986 outburst.

The only available timing observation of superhumps in the past (Patterson et al. 1993) reported a negative P_{dot} . The existence of a negative P_{dot} with this relatively short superhump period had been a mystery. The fresh outburst in 2008 has enabled us to finally establish P_{dot} of this object. The outburst was well-observed during the entire superoutburst plateau and subsequent decline, a rebrightening, and final fading. We only deal with superhumps during the plateau phase (table 27). The $O - C$ diagram shows all the distinct stages A–C (figure 52). The P_{dot} during stage B was $+8.5(0.5) \times 10^{-5}$ ($12 \leq E \leq 144$).

The times of superhump maxima of the 1986 superoutburst determined from the scanned figure are given in table 28. The negative P_{dot} in Patterson et al. (1993) was probably a result of the stage B–C transition around $E = 30 - 31$ (figure 53). For more details of this outburst, see Ohshima et al., in preparation.

6.11. EG Aquarii

The 2006 superoutburst of this object was extensively studied by Imada et al. (2008b). We further observed the 2008 superoutburst (table 29). Since the outburst detection was not noticed early enough, the observation only covered the middle part of the superoutburst. The resultant P_{dot} was similar to that obtained during the 2006 superoutburst. The supercycle of this object is likely ~ 750 d.

6.12. BF Arae

Kato et al. (2003a) studied the 2002 superoutburst of this object. A reanalysis of the same data has yielded improved determination of superhump maxima than those obtained by eye estimates (table 30). The resultant P_{dot} was $-2.8(1.6) \times 10^{-5}$, giving a slightly smaller value in Kato et al. (2003a). Olech et al. (2007) obtained photometry in quiescence and yielded a likely orbital period of 0.084176(21) d, giving a fractional superhump excess of 4.4 %.

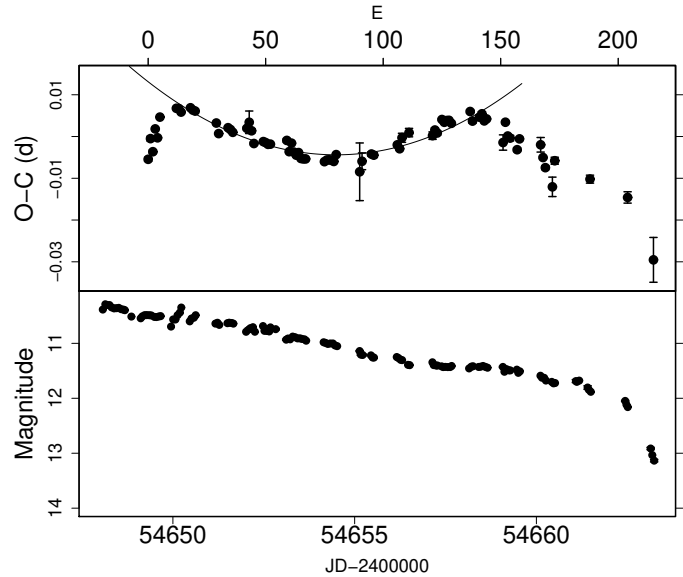


Fig. 52. $O - C$ of superhumps VY Aqr (2008). (Upper): $O - C$ diagram. The $O - C$ values were against the mean period for the stage B ($12 \leq E \leq 144$, thin curve) (Lower): Light curve. A brightening associated with the start of the stage C is clearly seen.

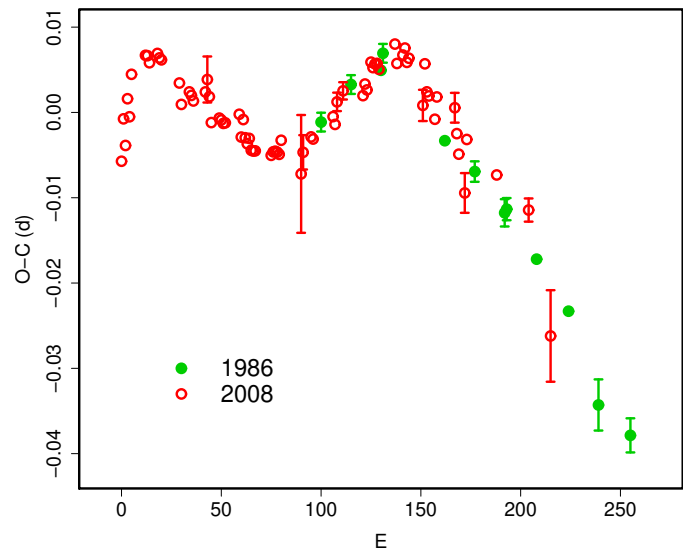


Fig. 53. Comparison of $O - C$ diagrams of VY Aqr between different superoutbursts. A period of 0.06464 d was used to draw this figure. Approximate cycle counts (E) after the estimated appearance of the superhumps were used.

Table 27. Superhump maxima of VY Aqr (2008).

E	max ^a	error	$O - C^b$	N^c
0	54649.3119	0.0005	-0.0075	122
1	54649.3815	0.0006	-0.0025	122
2	54649.4430	0.0004	-0.0056	41
3	54649.5132	0.0002	-0.0002	412
4	54649.5757	0.0001	-0.0022	378
5	54649.6453	0.0001	0.0028	286
12	54650.1000	0.0002	0.0051	109
13	54650.1646	0.0002	0.0051	115
14	54650.2284	0.0003	0.0043	70
18	54650.4881	0.0001	0.0055	658
19	54650.5522	0.0001	0.0050	388
20	54650.6166	0.0001	0.0048	267
29	54651.1956	0.0002	0.0022	304
30	54651.2578	0.0002	-0.0003	310
34	54651.5178	0.0002	0.0013	335
35	54651.5820	0.0001	0.0009	285
36	54651.6460	0.0001	0.0003	276
42	54652.0349	0.0004	0.0014	85
43	54652.1010	0.0027	0.0029	117
44	54652.1636	0.0005	0.0009	221
45	54652.2252	0.0004	-0.0021	285
49	54652.4843	0.0002	-0.0015	250
50	54652.5488	0.0001	-0.0017	299
51	54652.6130	0.0001	-0.0021	276
52	54652.6777	0.0002	-0.0020	171
59	54653.1312	0.0005	-0.0008	258
60	54653.1931	0.0002	-0.0035	535
61	54653.2598	0.0003	-0.0014	237
62	54653.3223	0.0002	-0.0035	105
63	54653.3863	0.0002	-0.0042	137
64	54653.4516	0.0001	-0.0035	357
65	54653.5148	0.0001	-0.0049	528
66	54653.5793	0.0001	-0.0050	283
67	54653.6440	0.0001	-0.0049	272
75	54654.1606	0.0002	-0.0053	398
76	54654.2257	0.0002	-0.0049	398
77	54654.2904	0.0003	-0.0048	238
78	54654.3549	0.0003	-0.0049	194
79	54654.4193	0.0002	-0.0051	487
80	54654.4856	0.0002	-0.0034	533
90	54655.1280	0.0069	-0.0072	85
91	54655.1952	0.0020	-0.0046	122
95	54655.4556	0.0005	-0.0027	48
96	54655.5200	0.0006	-0.0030	54
106	54656.1690	0.0002	-0.0001	241
107	54656.2327	0.0004	-0.0010	339
108	54656.3000	0.0011	0.0016	114
111	54656.4952	0.0010	0.0030	65
121	54657.1410	0.0009	0.0026	119
122	54657.2070	0.0005	0.0040	201
123	54657.2710	0.0005	0.0034	161
125	54657.4035	0.0003	0.0067	258
126	54657.4675	0.0002	0.0060	462
127	54657.5326	0.0002	0.0065	291
128	54657.5973	0.0002	0.0066	285

^a BJD-2400000.^b Against $max = 2454649.3195 + 0.064619E$.^c Number of points used to determine the maximum.**Table 27.** Superhump maxima of VY Aqr (2008). (continued)

E	max	error	$O - C$	N
129	54657.6612	0.0002	0.0059	218
137	54658.1813	0.0004	0.0090	158
138	54658.2437	0.0005	0.0068	157
141	54658.4386	0.0005	0.0078	406
142	54658.5041	0.0005	0.0087	320
143	54658.5670	0.0002	0.0070	278
144	54658.6321	0.0002	0.0075	272
151	54659.0791	0.0018	0.0021	136
152	54659.1486	0.0003	0.0070	506
153	54659.2100	0.0002	0.0037	358
154	54659.2741	0.0007	0.0033	130
157	54659.4653	0.0004	0.0006	145
158	54659.5326	0.0004	0.0032	195
167	54660.1131	0.0017	0.0022	93
168	54660.1747	0.0003	-0.0008	290
169	54660.2369	0.0005	-0.0032	221
172	54660.4263	0.0023	-0.0077	40
173	54660.4972	0.0008	-0.0014	57
188	54661.4626	0.0010	-0.0053	63
204	54662.4928	0.0014	-0.0091	64
215	54663.1890	0.0054	-0.0236	119

Table 28. Superhump maxima of VY Aqr (1986).

E	max ^a	error	$O - C^b$
0	46559.9687	0.0011	-0.0113
15	46560.9427	0.0011	-0.0028
30	46561.9140	0.0010	0.0030
31	46561.9806	0.0011	0.0053
62	46563.9742	0.0008	0.0035
77	46564.9402	0.0012	0.0040
92	46565.9050	0.0016	0.0033
93	46565.9700	0.0013	0.0040
108	46566.9338	0.0009	0.0023
124	46567.9619	0.0009	0.0006
139	46568.9205	0.0030	-0.0063
155	46569.9512	0.0020	-0.0055

^a BJD-2400000.^b Against $max = 2446559.9800 + 0.064365E$.^c Number of points used to determine the maximum.

Table 29. Superhump maxima of EG Aqr (2008).

E	\max^a	error	$O - C^b$	N^c
0	54802.9893	0.0003	-0.0014	216
3	54803.2277	0.0006	0.0007	46
12	54803.9365	0.0004	0.0006	262
13	54804.0154	0.0005	0.0007	173
38	54805.9831	0.0004	-0.0006	242
63	54807.9527	0.0006	0.0000	244

^a BJD-2400000.^b Against $\max = 2454802.9908 + 0.078760E$.^c Number of points used to determine the maximum.**Table 30.** Superhump maxima of BF Ara (2002).

E	\max^a	error	$O - C^b$	N^c
0	52504.9878	0.0005	-0.0031	143
1	52505.0774	0.0005	-0.0014	120
2	52505.1643	0.0005	-0.0023	114
12	52506.0456	0.0007	0.0001	87
13	52506.1311	0.0005	-0.0023	89
14	52506.2266	0.0024	0.0053	49
23	52507.0148	0.0008	0.0025	82
24	52507.1025	0.0007	0.0024	83
25	52507.1869	0.0008	-0.0012	89
35	52508.0672	0.0006	0.0003	88
36	52508.1565	0.0008	0.0017	88
60	52510.2640	0.0014	-0.0001	102
61	52510.3510	0.0014	-0.0010	100
80	52512.0207	0.0016	-0.0011	30
90	52512.9025	0.0023	0.0018	22
91	52512.9920	0.0017	0.0034	25
102	52513.9504	0.0021	-0.0050	27

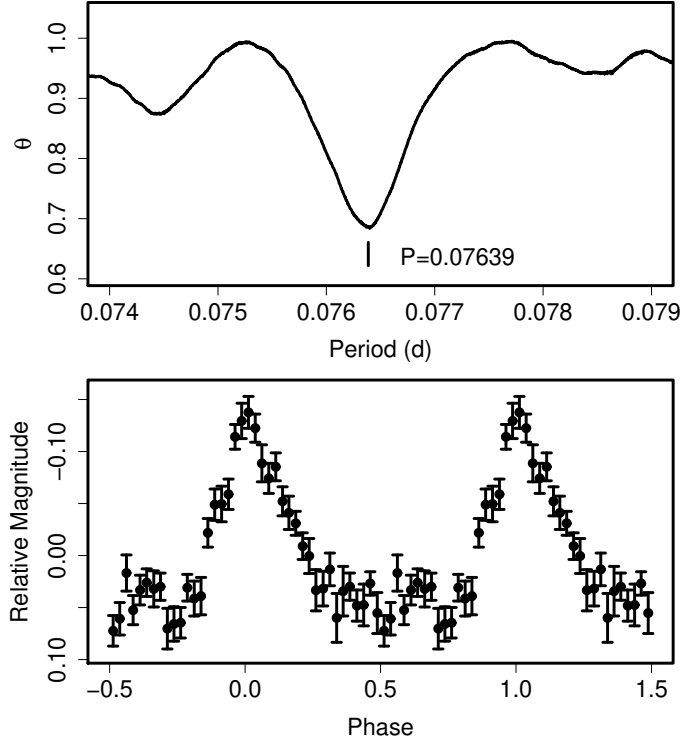
^a BJD-2400000.^b Against $\max = 2452504.9909 + 0.087887E$.^c Number of points used to determine the maximum.

6.13. V663 Arae

V663 Ara was discovered by Geßner (1974) as a long-period variable star. Downes et al. (2001) listed this object as a CV. The SU UMa-type nature of this object was established by B. Monard (vsnet-alert 8231, 8232). We obtained a mean superhump period of 0.07639(2) d from observations on four nights (figure 54). The times of superhump maxima are listed in table 31. The resultant P_{dot} was $-6.2(9.4) \times 10^{-5}$.

6.14. V877 Arae

Kato et al. (2003d) observed the 2002 superoutburst and reported a strongly negative period derivative. The variation of the superhump period occurred during the earliest stage of the superoutburst, and the originally reported P_{dot} more likely reflected the early stage of period shift from the stage A to B, as seen in the similar long-period system DT Oct (subsection 6.90). The refined superhump maxima are listed in table 32. By ne-

**Fig. 54.** Superhumps in V663 Ara (2004). (Upper): PDM analysis. (Lower): Phase-averaged profile.**Table 31.** Superhump maxima of V663 Ara (2004).

E	\max^a	error	$O - C^b$	N^c
0	53195.4364	0.0007	0.0001	82
11	53196.2782	0.0013	0.0020	63
12	53196.3546	0.0010	0.0020	83
13	53196.4265	0.0015	-0.0025	81
14	53196.5017	0.0018	-0.0037	81
37	53198.2603	0.0112	-0.0015	47
38	53198.3415	0.0016	0.0033	86
39	53198.4187	0.0020	0.0042	86
40	53198.4907	0.0016	-0.0002	84
50	53199.2517	0.0021	-0.0029	76
51	53199.3304	0.0015	-0.0005	81
52	53199.4068	0.0055	-0.0005	35

^a BJD-2400000.^b Against $\max = 2453195.4362 + 0.076366E$.^c Number of points used to determine the maximum.

Table 32. Superhump maxima of V877 Ara (2002).

E	\max^a	error	$O - C^b$	N^c
0	52434.9582	0.0011	-0.0123	61
1	52435.0470	0.0003	-0.0076	84
24	52436.9922	0.0011	0.0045	64
25	52437.0757	0.0007	0.0039	111
26	52437.1645	0.0005	0.0087	87
27	52437.2473	0.0007	0.0075	86
72	52441.0235	0.0015	0.0013	46
73	52441.1103	0.0008	0.0041	69
74	52441.1923	0.0007	0.0021	65
95	52442.9508	0.0013	-0.0044	23
96	52443.0389	0.0017	-0.0004	24
97	52443.1186	0.0012	-0.0047	51
98	52443.2047	0.0009	-0.0027	61

^a BJD-2400000.^b Against $\max = 2452434.9704 + 0.084050E$.^c Number of points used to determine the maximum.

glecting the early portion ($E < 24$), we obtained a P_{dot} of $-5.7(2.9) \times 10^{-5}$, typical for an usual SU UMa-type dwarf nova.

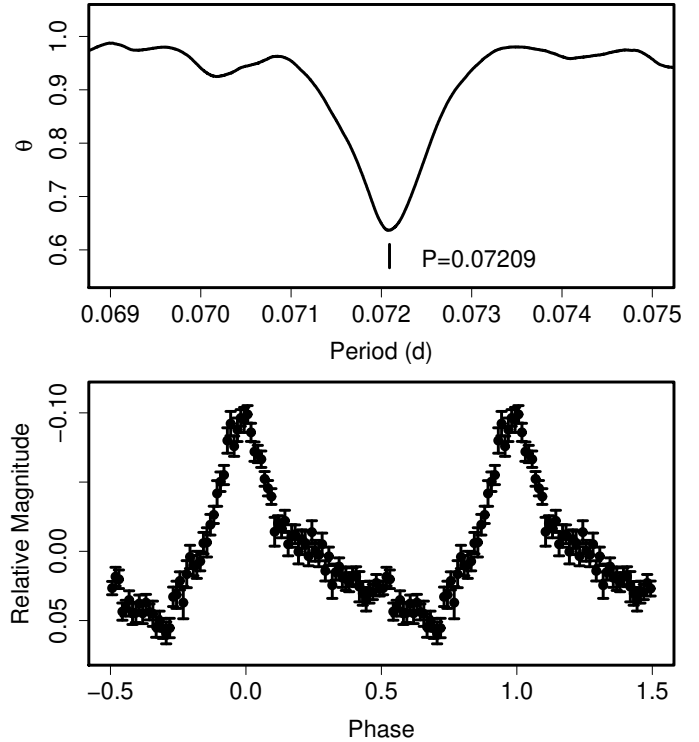
6.15. BB Arietis

This object was recognized during the identification project of the New Catalogue of Suspected Variable Stars (NSV, Kukarkin et al. 1982) objects against ROSAT X-ray source (Kato, vsnet-chat 3317). The proximity of a ROSAT source to the position of NSV 907, a large-amplitude variable star, suggested that the object may be a dwarf nova, as we have seen in DT Oct = NSV 10934 (Kato et al. 2002a).

The object has been monitored since, and the first outburst was detected by P. Schmeer on 2004 March 2 at an unfiltered CCD magnitude of 13.5. It is unclear how long this outburst lasted. On 2004 November 1, P. Schmeer detected another outburst at magnitude 13.7. Following this alert, we started time-resolved photometry and detected superhumps. A PDM analysis yielded a mean superhump period of 0.07209(1) d (figure 55). The times of superhump maxima are listed in table 33. We obtained $P_{\text{dot}} = +1.6(3.0) \times 10^{-5}$. Since the superoutburst was likely detected during its final stage, the superhump period and period derivative most likely reflect the behavior after transition to the stage C. Although the object has been well monitored since, only two normal outbursts was recorded in 2006 November in 2009 February. The outburst frequency may be as low as UV Per and VY Aqr, having similar superhump periods.

6.16. HV Aurigae

Nogami et al. (1995b) reported a superhump period of 0.0855(1) d. During the 2002 superoutburst, we undertook an observing campaign. The observation confirmed the periodicity in Nogami et al. (1995b). The measured superhump maxima are listed in table 34. The data did

**Fig. 55.** Superhumps in BB Ari (2004). (Upper): PDM analysis. (Lower): Phase-averaged profile.**Table 33.** Superhump maxima of BB Ari (2004).

E	\max^a	error	$O - C^b$	N^c
0	53311.4608	0.0004	-0.0005	77
1	53311.5325	0.0005	-0.0009	44
12	53312.3280	0.0011	0.0012	113
22	53313.0479	0.0012	-0.0001	166
23	53313.1210	0.0006	0.0009	183
24	53313.1933	0.0008	0.0011	305
25	53313.2648	0.0007	0.0005	366
35	53313.9865	0.0005	0.0009	131
36	53314.0586	0.0005	0.0010	260
37	53314.1318	0.0003	0.0020	320
38	53314.2018	0.0005	-0.0002	226
39	53314.2753	0.0003	0.0013	304
42	53314.4881	0.0007	-0.0023	71
43	53314.5592	0.0008	-0.0034	71
60	53315.7811	0.0020	-0.0075	16
61	53315.8605	0.0017	-0.0002	17
73	53316.7295	0.0028	0.0033	22
74	53316.8010	0.0014	0.0027	23
75	53316.8705	0.0021	0.0000	16

^a BJD-2400000.^b Against $\max = 2453311.4613 + 0.072122E$.^c Number of points used to determine the maximum.

Table 34. Superhump maxima of HV Aur (2002).

E	max ^a	error	$O - C^b$	N^c
0	52605.9359	0.0038	-0.0044	83
1	52606.0296	0.0049	0.0037	106
2	52606.1087	0.0022	-0.0028	148
13	52607.0547	0.0009	0.0020	477
14	52607.1391	0.0010	0.0009	316
15	52607.2239	0.0008	0.0001	579
16	52607.3117	0.0020	0.0023	437
17	52607.3956	0.0006	0.0007	71
18	52607.4795	0.0007	-0.0009	60
20	52607.6508	0.0006	-0.0008	58
24	52607.9912	0.0044	-0.0026	214
25	52608.0808	0.0010	0.0015	217
29	52608.4213	0.0005	-0.0003	140
30	52608.5063	0.0005	-0.0009	139
32	52608.6785	0.0006	0.0001	44
33	52608.7650	0.0008	0.0011	40
41	52609.4485	0.0003	0.0001	88
42	52609.5330	0.0003	-0.0009	68
47	52609.9713	0.0050	0.0095	134
48	52610.0441	0.0038	-0.0033	166
50	52610.2187	0.0009	0.0002	160
51	52610.2989	0.0041	-0.0052	223
59	52610.9945	0.0045	0.0060	161
60	52611.0745	0.0024	0.0004	119
62	52611.2385	0.0050	-0.0067	224

^a BJD-2400000.^b Against $max = 2452605.9403 + 0.085563E$.^c Number of points used to determine the maximum.

not show a clear tendency of period changes. A high-quality subset ($O - C$'s with errors less than 0.0015 d) of superhump times gives a virtually zero ($-3.5(5.0) \times 10^{-5}$) period change. The object looks similar to BF Ara, another long-period system with a relatively constant superhump period, although we can not exclude the possibility that we observed only the stage C superhumps since the start of the outburst was unknown.

6.17. *TT Bootis*

Olech et al. (2004a) reported on period variation during the 2004 superoutburst. We observed the same superoutburst and obtained superhump maxima with higher precision than those in Olech et al. (2004a). A combined list of superhump maxima and the $O - C$ diagram are given in table 35 and figure 4. We applied a systematic correction of +0.0031 d to the times of Olech et al. (2004a) and disregarded maxima measured using Cook's observations, which are included in our own data set and were analyzed with a higher precision. Although Olech et al. (2004a) proposed a different treatment in dividing the $O - C$ diagram, we derived $P_{\text{dot}} = +8.3(0.7) \times 10^{-5}$ from the segment $13 \leq E \leq 120$ (stage B) by analogy with other systems with similar $O - C$ behavior (subsection 3.2). The extreme values in Olech et al. (2004a) reflected a tran-

sition from the stage A to B with positive P_{dot} , and a transition to the stage C observed during the late course of the superoutburst.

6.18. *UZ Bootis*

UZ Boo had long been suspected to be a WZ Sge-type dwarf nova (Bailey 1979). Due to the lack of an outburst since 1978, it was only in 1994 when the SU UMa-type nature of this object was established (cf. Kato et al. 2001d).

The 2003–2004 superoutburst was detected by P. Dubovsky on 2003 December 5 (vsnet-alert 7937). The true superhump period was finally identified (vsnet-alert 7952). The object underwent four rebrightenings (vsnet-alert 7954, 7960, 7962, 7967) following the main superoutburst (figure 56).¹² Due to the poor seasonal location, the quality of the observation was not always very good. We selected the superhump period of 0.06191(2) d with the PDM method (figure 57) for the best sampled segment between BJD 2452983 and 2452991. The times of superhump maxima and cycle counts identified with this period are listed in table 37. Although the superhump period was almost constant for $E \geq 30$ (with mean P_{SH} and P_{dot} of 0.06192(3) d and $-1.9(6.3) \times 10^{-5}$, respectively), there was clear evidence of period evolution before $E = 30$. We identified this segment to be stage A with a mean P_{SH} of 0.0635(2) d, lasting for ~ 30 superhump cycles. The relatively long P_{SH} , the lack of period variation during the stage B and the presence of multiple rebrightenings make UZ Boo a system analogous to EG Cnc (Patterson et al. 1998; Kato et al. 2004b).

The times of superhump maxima during the 1994 superoutburst were analyzed using the P_{SH} identified during the 2003 superoutburst (table 36). Although the maximum at $E = 0$ was on a smooth extrapolation of later maxima, this could have been an early superhump. The resultant P_{SH} and P_{dot} were 0.06174(4) d and $-1.5(2.5) \times 10^{-5}$, respectively.

6.19. *NN Camelopardalis*

NN Cam = NSV 1485 is a recently identified SU UMa-type dwarf nova (Khruslov 2005; for more historical information, see vsnet-alert 9557), whose outburst was detected on 2007 September 11. Although this outburst rapidly faded, a genuine superoutburst followed after eight days (vsnet-alert 9598).

The times of superhump maxima obtained during this superoutburst are listed in table 38. A stage B–C transition was probably recorded. Using the orbital period of 0.0717 d determined photometrically (vsnet-alert 9557), we obtained a fractional superhump excess for P_2 of 3.0 %. During the precursor, low-amplitude modulations were observed (figure 58). Although the duration of the observation was not long enough, the period of the variations is consistent with the suggested orbital period. If this period is confirmed, the outburst makes the second example of a transition from the orbital period to the superhump

¹² The 1994 superoutburst possibly had two rebrightenings (Kuulkers et al. 1996).

Table 35. Superhump maxima of TT Boo (2004).

E	\max^a	error	$O - C^b$	N^c
0	53161.7568	0.0004	-0.0150	141
1	53161.8360	0.0003	-0.0138	213
2	53161.9152	0.0003	-0.0126	158
9	53162.4705	0.0004	-0.0029	80
13	53162.7845	0.0002	-0.0007	157
14	53162.8624	0.0002	-0.0008	138
15	53162.9406	0.0002	-0.0006	123
22	53163.4858	0.0003	-0.0010	64
22	53163.4841	0.0015	-0.0027	0
34	53164.4176	0.0005	-0.0047	53
35	53164.4986	0.0008	-0.0016	42
35	53164.4973	0.0025	-0.0029	0
47	53165.4303	0.0004	-0.0053	81
47	53165.4321	0.0020	-0.0036	0
48	53165.5111	0.0080	-0.0025	0
59	53166.3676	0.0015	-0.0035	0
60	53166.4451	0.0030	-0.0040	0
61	53166.5243	0.0017	-0.0027	0
73	53167.4573	0.0020	-0.0051	0
98	53169.4156	0.0025	0.0043	0
99	53169.4954	0.0020	0.0062	0
106	53170.0422	0.0014	0.0073	130
107	53170.1215	0.0010	0.0087	188
108	53170.1960	0.0017	0.0052	68
111	53170.4354	0.0008	0.0107	85
111	53170.4339	0.0015	0.0092	0
112	53170.5131	0.0025	0.0105	0
119	53171.0603	0.0004	0.0120	136
120	53171.1384	0.0003	0.0122	182
124	53171.4490	0.0005	0.0110	79
129	53171.8395	0.0004	0.0117	138
130	53171.9188	0.0013	0.0130	77
132	53172.0715	0.0004	0.0099	182
133	53172.1503	0.0004	0.0107	150
141	53172.7718	0.0003	0.0086	162
142	53172.8488	0.0004	0.0076	158
143	53172.9272	0.0007	0.0080	123
144	53173.0028	0.0020	0.0057	98
145	53173.0765	0.0010	0.0015	215
150	53173.4702	0.0005	0.0053	76
153	53173.7031	0.0008	0.0045	94
154	53173.7821	0.0005	0.0055	140
155	53173.8586	0.0004	0.0040	100
167	53174.7902	0.0005	0.0002	121
188	53176.4183	0.0010	-0.0087	60
189	53176.5000	0.0013	-0.0050	80
192	53176.7321	0.0010	-0.0067	77
205	53177.7458	0.0007	-0.0065	103
206	53177.8227	0.0009	-0.0075	107
207	53177.8939	0.0016	-0.0143	91
213	53178.3623	0.0040	-0.0136	0
214	53178.4416	0.0030	-0.0122	0
215	53178.5173	0.0030	-0.0145	0
218	53178.7474	0.0007	-0.0182	104

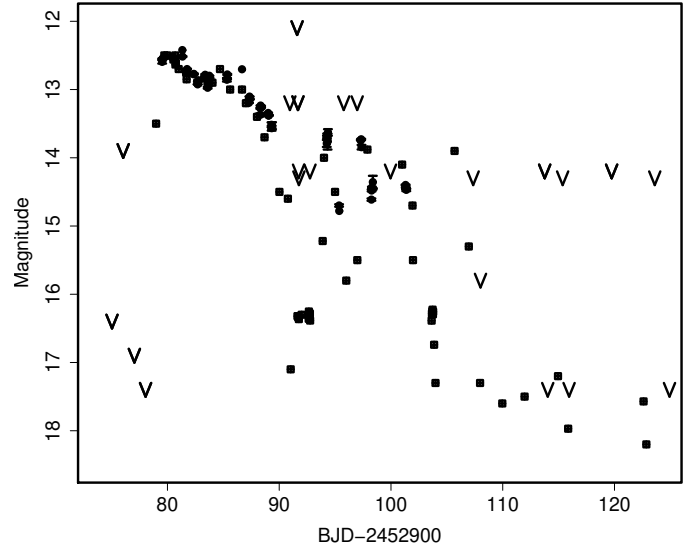
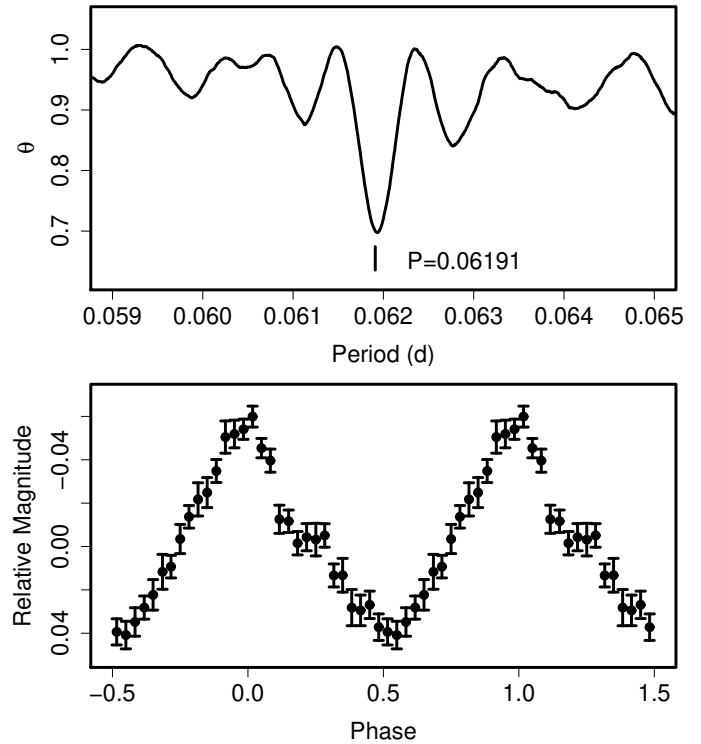
^a BJD-2400000.^b Against $\max = 2453161.7719 + 0.077953E$.^c Number of points used to determine the maximum.
 $N = 0$ refers to Olech et al. (2004a).**Fig. 56.** Superoutburst of UZ Boo in 2003-2004. The data are a combination of our observations (filled squares), and AAVSO and VSNET observations (filled squares; the “V”-marks indicate upper limits). Four post-superoutburst rebrightenings were recorded.**Fig. 57.** Superhumps in UZ Boo (2003). (Upper): PDM analysis between BJD 2452983 and 2452991. (Lower): Phase-averaged profile.

Table 36. Superhump maxima of UZ Boo (1994).

E	max ^a	error	$O - C^b$	N^c
0	49582.9956	0.0009	-0.0012	106
81	49587.9933	0.0019	-0.0047	40
97	49588.9930	0.0036	0.0071	41
161	49592.9429	0.0027	0.0055	63
177	49593.9195	0.0077	-0.0058	57
178	49593.9862	0.0019	-0.0009	48

^a BJD-2400000.^b Against $max = 2449582.9968 + 0.061743E$.^c Number of points used to determine the maximum.**Table 37.** Superhump maxima of UZ Boo (2003–2004).

E	max ^a	error	$O - C^b$	N^c
0	52981.7156	0.0009	-0.0263	79
10	52982.3523	0.0029	-0.0109	90
16	52982.7409	0.0007	0.0049	72
30	52983.6210	0.0007	0.0153	34
31	52983.6789	0.0005	0.0111	82
32	52983.7415	0.0005	0.0116	74
58	52985.3526	0.0020	0.0073	35
90	52987.3377	0.0009	0.0044	239
106	52988.3281	0.0016	0.0008	225
107	52988.3793	0.0033	-0.0101	92
117	52989.0067	0.0042	-0.0040	76
118	52989.0687	0.0006	-0.0042	87

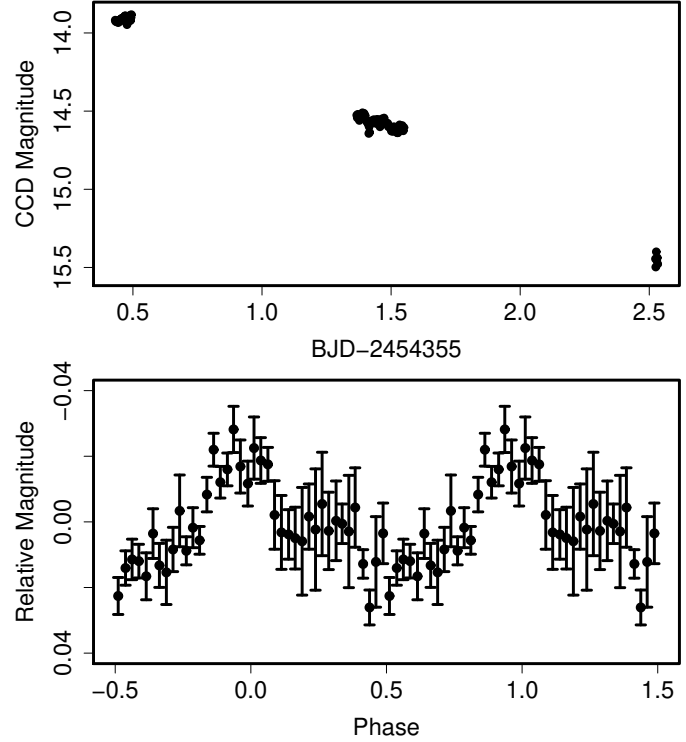
^a BJD-2400000.^b Against $max = 2452981.7419 + 0.062127E$.^c Number of points used to determine the maximum.

period after the case of the 1993 superoutburst of QZ Vir (Kato 1997).

The object underwent normal outbursts in 2008 March and October (vsnet-alert 10588). Photometric observations during the 2008 October outburst did not record modulations similar to those recorded during the precursor outburst in 2007 September. This suggests that some kind of (immature) superhumps were indeed excited during this precursor outburst in 2007.

6.20. SY Capricorni

SY Cap was originally classified as a long-period variable (Kholopov et al. 1985). The dwarf nova-type nature was pointed out by one of the authors (T. Kato, vsnet-alert 10025). Observations during the 2008 outburst established the SU UMa-type nature of this object (vsnet-alert 10453, figure 59). The times of superhump maxima are listed in table 39. The mean superhump period and global P_{dot} were 0.06376(2) d and $-11.4(9.0) \times 10^{-5}$, respectively. The negative value of P_{dot} is probably a result of transition between stages B and C. The object resembles CI UMa in its short supercycles, combined with relatively few normal outbursts and the short duration of superoutbursts (cf. Nogami, Kato 1997).

**Fig. 58.** Precursor outburst of NN Cam in 2007 (Upper): Light curve. (Lower): Phase-averaged profile referring to the orbital period.**Table 38.** Superhump maxima of NN Cam.

E	max ^a	error	$O - C^b$	N^c
0	54363.5492	0.0004	-0.0070	83
13	54364.5159	0.0002	-0.0014	260
14	54364.5891	0.0003	-0.0022	301
24	54365.3323	0.0005	0.0017	57
25	54365.4071	0.0006	0.0026	83
26	54365.4816	0.0005	0.0032	173
27	54365.5551	0.0003	0.0027	387
28	54365.6289	0.0006	0.0025	191
39	54366.4393	0.0003	-0.0003	87
40	54366.5162	0.0003	0.0027	324
41	54366.5879	0.0002	0.0005	402
54	54367.5477	0.0005	-0.0009	207
55	54367.6229	0.0003	0.0004	250
66	54368.4375	0.0006	0.0016	87
67	54368.5094	0.0005	-0.0004	86
81	54369.5403	0.0007	-0.0046	267
82	54369.6179	0.0007	-0.0009	218

^a BJD-2400000.^b Against $max = 2454363.5562 + 0.073935E$.^c Number of points used to determine the maximum.

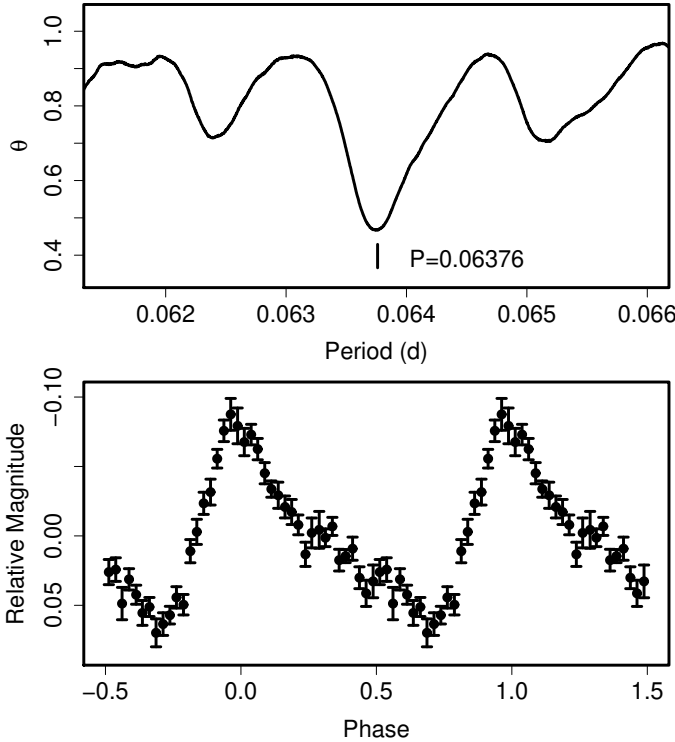


Fig. 59. Superhumps in SY Cap (2008). (Upper): PDM analysis. (Lower): Phase-averaged profile.

Table 39. Superhump maxima of SY Cap (2008).

E	\max^a	error	$O - C^b$	N^c
0	54700.0560	0.0006	-0.0009	121
1	54700.1206	0.0006	0.0000	120
2	54700.1844	0.0009	0.0000	81
14	54700.9505	0.0005	0.0011	78
47	54703.0539	0.0018	0.0004	70
48	54703.1186	0.0006	0.0013	92
49	54703.1790	0.0010	-0.0020	99

^a BJD-2400000.

^b Against $\max = 2454700.0568 + 0.063759E$.

^c Number of points used to determine the maximum.

Table 40. Superhump maxima of AX Cap (2004).

E	\max^a	error	$O - C^b$	N^c
0	53204.3758	0.0069	-0.0824	259
1	53204.4990	0.0101	-0.0722	265
2	53204.6508	0.0042	-0.0336	194
8	53205.3625	0.0044	-0.0007	176
9	53205.4690	0.0026	-0.0073	256
10	53205.5742	0.0053	-0.0153	258
15	53206.1685	0.0033	0.0134	62
17	53206.4050	0.0014	0.0237	260
18	53206.5227	0.0031	0.0282	373
19	53206.6365	0.0016	0.0290	239
34	53208.3657	0.0007	0.0612	257
35	53208.4751	0.0007	0.0575	258
36	53208.5862	0.0011	0.0554	213
50	53210.1405	0.0024	0.0259	200
51	53210.2576	0.0058	0.0299	119
85	53214.0435	0.0034	-0.0305	116
86	53214.1470	0.0061	-0.0401	317
99	53215.6157	0.0066	-0.0421	155

^a BJD-2400000.

^b Against $\max = 2453204.4582 + 0.113128E$.

^c Number of points used to determine the maximum.

6.21. AX Capricorni

AX Cap was serendipitously discovered as a dwarf nova during a search for asteroids (Howell et al. 1994). Howell et al. (1994) reported a spectrum during a faint outburst. An exceptionally bright (15.4 mag) outburst was reported on 2004 July 17 (R. Stubbings, vsnet-obs 50216). The confirmation of superhumps (vsnet-campaign-dn 4337) led to a classification as a long- P_{SH} SU UMa-type dwarf nova. Table 40 lists the observed superhump maxima. During $E \leq 2$, the superhumps were still evolving. The period smoothly decreased with a large negative P_{dot} until $E = 34$, then it apparently shifted to a shorter one (figure 29). The P_{dot} for the former interval ($8 \leq E \leq 34$) was $P_{\text{dot}} = -87(65) \times 10^{-5}$.

Among SU UMa-type dwarf novae, AX Cap has the second longest P_{SH} next to TU Men. Together with the large period variation similar to MN Dra, this object certainly deserves a further detailed study.

6.22. GX Cassiopeiae

The object has one of the longest superhump periods among known SU UMa-type dwarf novae. Nogami et al. (1998c) reported the detection of superhumps during the 1994 superoutburst.

We further observed the 1999 and 2006 superoutbursts from the start of the appearance of superhumps. We also analyzed the AAVSO data of the 1996 superoutburst. The determined times of superhump maxima are listed in tables 41, 42, 43 and 44.

The early and late stages were observed during the 1996 superoutburst. Based on the identification of the P_{SH} during other superoutbursts, we can unambiguously de-

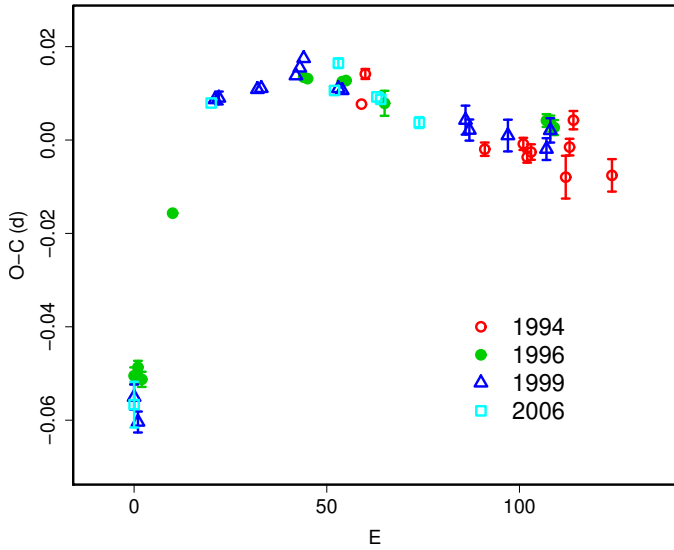


Fig. 60. Comparison of $O-C$ diagrams of GX Cas between different superoutbursts. A period of 0.09320 d was used to draw this figure. Approximate cycle counts (E) after the start of the superoutburst were used.

termine E for each superhumps. The results demonstrate the clear presence of stages A and C. The parameters are listed in table 2. It might be worth noting that a PDM analysis gave a false period (0.0862 d) due to the strong period variation, similar to the case in CTCV J0549–4921 (Imada et al. 2008a).

During the 1999 superoutburst, the object showed a significantly longer period ($P > 0.0964$ d) for $E < 21$, probably reflecting the stage A as in the 1996 superoutburst. The rest of the superoutburst showed a relatively regular decrease of the superhump period. The mean P_{dot} was $-7.6(2.5) \times 10^{-5}$. The present analysis confirmed the period identification in Nogami et al. (1998c).

The 2006 superoutburst showed a similar tendency of a large period change during the early stage. Such large variations of superhump periods appear to be common in long-period SU UMa-type dwarf novae (cf. subsection 4.10; Rutkowski et al. 2007).

A combined $O-C$ diagram (figure 60) now clearly illustrates the period variation of superhumps in this system. Having observed ~ 5 d after the outburst detection, the 1994 observation recorded the stage C superhumps.

6.23. HT Cassiopeiae

The only superoutburst observed for superhumps was in 1985 (Zhang et al. 1986), who reported P_{SH} of 0.076077 d without giving details. Although this observations were based on only two nights, we extracted the observations from the published light curves by referring to published times of eclipses and obtained times of superhump maxima (table 45). Since the determination of the maximum at $E=0$ was affected by the lack of observations before the maximum, we calculated the period by using two remaining maxima. The nominal P_{SH} was 0.07592(2) d, giving a

Table 41. Superhump maxima of GX Cas (1994).

E	\max^a	error	$O-C^b$	N^c
0	49585.1684	0.0003	-0.0021	48
1	49585.2681	0.0011	0.0046	20
32	49588.1412	0.0014	-0.0037	126
42	49589.0743	0.0013	-0.0000	49
43	49589.1647	0.0012	-0.0026	65
44	49589.2590	0.0017	-0.0013	67
53	49590.0924	0.0046	-0.0044	33
54	49590.1920	0.0018	0.0023	32
55	49590.2910	0.0020	0.0083	49
65	49591.2112	0.0035	-0.0010	39

^a BJD–2400000.

^b Against $\max = 2449585.1706 + 0.092947E$.

^c Number of points used to determine the maximum.

Table 42. Superhump maxima of GX Cas (1996).

E	\max^a	error	$O-C^b$	N^c
0	50358.5124	0.0018	-0.0199	28
1	50358.6074	0.0014	-0.0185	27
2	50358.6980	0.0016	-0.0216	11
10	50359.4792	0.0009	0.0104	38
44	50362.6771	0.0006	0.0242	26
45	50362.7700	0.0007	0.0234	26
54	50363.6082	0.0007	0.0187	22
55	50363.7016	0.0007	0.0185	21
65	50364.6287	0.0027	0.0091	11
107	50368.5394	0.0014	-0.0136	22
108	50368.6320	0.0017	-0.0147	20
109	50368.7243	0.0016	-0.0160	22

^a BJD–2400000.

^b Against $\max = 2450358.5323 + 0.093652E$.

^c Number of points used to determine the maximum.

slightly smaller ϵ of 3.0 % than in Zhang et al. (1986).

6.24. KP Cassiopeiae

Little had been known about KP Cas before the detection of a bright outburst by Y. Sano (vsnet-alert 10629). The outburst soon turned out to be a superoutburst. The mean superhump period with the PDM method was 0.085283(12) d (figure 61). The times of superhump maxima are listed in table 46. The outburst was apparently detected during the middle-to-late stage, and a clear transition of the superhump period (stage B to C) was detected around $E = 15$.

6.25. V452 Cassiopeiae

In addition to Shears et al. (2008d), we analyzed the 1999 superoutburst and the AAVSO data during the 2008 December superoutburst (tables 47, 48). The 1999 observation covered the middle-to-late stage of the superoutburst. A PDM analysis yielded a mean P_{SH} of 0.08856(6) d, which probably corresponds to the stage C super-

Table 43. Superhump maxima of GX Cas (1999).

E	\max^a	error	$O - C^b$	N^c
0	51472.1436	0.0027	-0.0416	140
1	51472.2314	0.0022	-0.0472	188
21	51474.1645	0.0005	0.0167	187
22	51474.2580	0.0014	0.0168	142
32	51475.1919	0.0006	0.0160	187
33	51475.2853	0.0008	0.0160	165
42	51476.1268	0.0009	0.0164	121
43	51476.2217	0.0005	0.0178	185
44	51476.3169	0.0008	0.0195	121
53	51477.1493	0.0005	0.0107	187
54	51477.2421	0.0005	0.0101	187
86	51480.2181	0.0031	-0.0046	181
87	51480.3092	0.0023	-0.0070	138
97	51481.2400	0.0034	-0.0108	143
107	51482.1691	0.0023	-0.0162	184
108	51482.2663	0.0026	-0.0125	188

^a BJD-2400000.^b Against $\max = 2451472.1852 + 0.093459E$.^c Number of points used to determine the maximum.**Table 44.** Superhump maxima of GX Cas (2006).

E	\max^a	error	$O - C^b$	N^c
0	54069.0790	0.0049	-0.0240	66
20	54071.0076	0.0006	0.0266	78
52	54073.9927	0.0004	0.0068	99
53	54074.0917	0.0010	0.0119	72
63	54075.0165	0.0009	-0.0023	130
64	54075.1092	0.0009	-0.0035	136
74	54076.0362	0.0012	-0.0155	129

^a BJD-2400000.^b Against $\max = 54069.1030 + 0.093902E$.^c Number of points used to determine the maximum.**Table 45.** Superhump maxima of HT Cas (1985).

E	\max^a	error	$O - C^b$
0	46084.5704	0.0004	-0.0069
1	46084.6612	0.0001	0.0074
14	46085.6482	0.0001	-0.0005

^a BJD-2400000.^b Against $\max = 2446084.5773 + 0.076529E$.**Table 46.** Superhump maxima of KP Cas (2008).

E	\max^a	error	$O - C^b$	N^c
0	54767.0256	0.0003	-0.0020	130
1	54767.1100	0.0004	-0.0029	133
3	54767.2827	0.0005	-0.0008	71
4	54767.3600	0.0014	-0.0087	139
5	54767.4551	0.0014	0.0011	183
6	54767.5440	0.0012	0.0047	136
8	54767.7096	0.0005	-0.0002	37
9	54767.7945	0.0005	-0.0006	41
10	54767.8798	0.0005	-0.0005	43
11	54767.9668	0.0006	0.0011	123
12	54768.0512	0.0006	0.0003	179
14	54768.2228	0.0011	0.0014	137
15	54768.3094	0.0004	0.0027	89
16	54768.3930	0.0005	0.0010	120
17	54768.4785	0.0002	0.0013	259
18	54768.5623	0.0003	-0.0003	184
19	54768.6481	0.0025	0.0003	24
23	54768.9903	0.0007	0.0014	85
24	54769.0774	0.0014	0.0032	54
27	54769.3304	0.0003	0.0004	174
31	54769.6712	0.0005	0.0001	41
32	54769.7581	0.0005	0.0018	42
33	54769.8435	0.0005	0.0019	41
34	54769.9293	0.0008	0.0024	153
35	54770.0107	0.0008	-0.0015	164
36	54770.0967	0.0006	-0.0008	165
37	54770.1849	0.0013	0.0022	109
39	54770.3527	0.0004	-0.0005	474
40	54770.4389	0.0004	0.0004	374
41	54770.5233	0.0002	-0.0005	271
42	54770.6073	0.0004	-0.0018	97
43	54770.6938	0.0004	-0.0006	37
44	54770.7784	0.0005	-0.0012	41
45	54770.8638	0.0005	-0.0011	42
46	54770.9488	0.0009	-0.0014	29
50	54771.2907	0.0004	-0.0005	223
51	54771.3755	0.0005	-0.0010	223
52	54771.4594	0.0004	-0.0024	259
53	54771.5484	0.0038	0.0013	265

^a BJD-2400000.^b Against $\max = 2454767.0276 + 0.085273E$.^c Number of points used to determine the maximum.

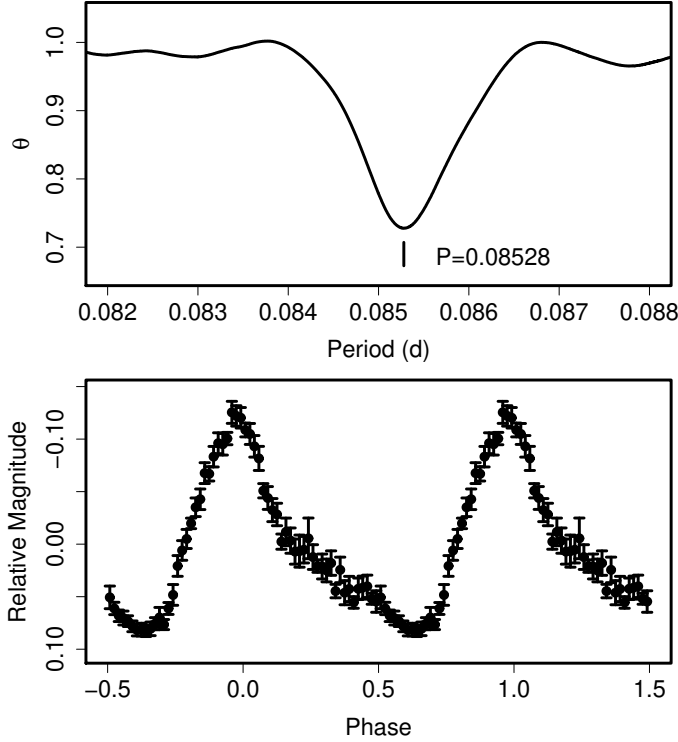


Fig. 61. Superhumps in KP Cas (2008). (Upper): PDM analysis. (Lower): Phase-averaged profile.

Table 47. Superhump maxima of V452 Cas (1999).

E	\max^a	error	$O - C^b$	N^c
0	51496.2273	0.0043	-0.0067	153
1	51496.3314	0.0072	0.0088	121
46	51500.2964	0.0026	-0.0100	17
57	51501.2882	0.0061	0.0079	54

^a BJD-2400000.

^b Against $\max = 2451496.2340 + 0.088532E$.

^c Number of points used to determine the maximum.

humps. The 2008 observations recorded the early part of this superoutburst and yielded a slightly shorter P_{SH} of 0.08932(3) d than in Shears et al. (2008d). A combined $O - C$ diagram is shown in figure 62.

Table 48. Superhump maxima of V452 Cas (2008).

E	\max^a	error	$O - C^b$	N^c
0	54805.3812	0.0005	0.0000	76
33	54808.3282	0.0009	-0.0005	100
34	54808.4186	0.0012	0.0005	74

^a BJD-2400000.

^b Against $\max = 2454805.3812 + 0.089319E$.

^c Number of points used to determine the maximum.

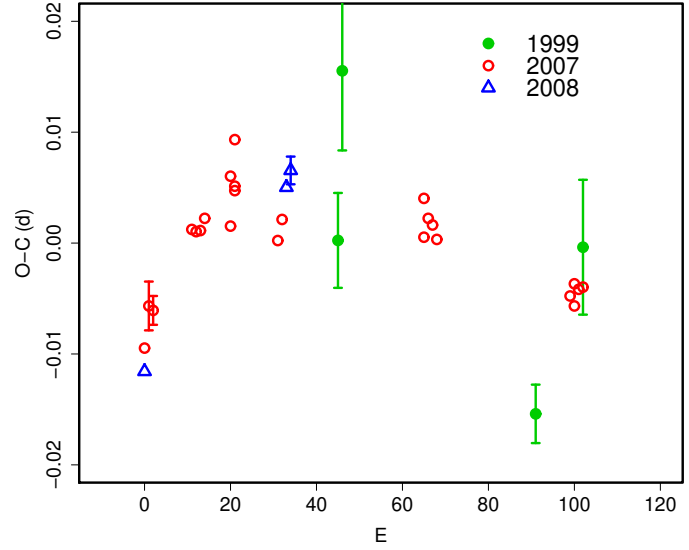


Fig. 62. Comparison of $O - C$ diagrams of V452 Cas between different superoutbursts. A period of 0.08880 d was used to draw this figure. Approximate cycle counts (E) after the start of the superoutburst were used.

Table 49. Superhump maxima of V359 Cen (2002).

E	\max^a	error	$O - C^b$	N^c
0	52423.9416	0.0004	-0.0137	106
1	52424.0235	0.0003	-0.0129	130
23	52425.8215	0.0004	0.0025	109
35	52426.7972	0.0007	0.0058	94
36	52426.8804	0.0006	0.0080	195
37	52426.9619	0.0009	0.0084	71
49	52427.9337	0.0004	0.0078	166
50	52428.0149	0.0009	0.0080	107
62	52428.9865	0.0004	0.0072	86
84	52430.7602	0.0007	-0.0018	47
85	52430.8391	0.0018	-0.0040	11
102	52432.2163	0.0008	-0.0043	91
103	52432.2971	0.0009	-0.0046	92
104	52432.3762	0.0012	-0.0065	92

^a BJD-2400000.

^b Against $\max = 2452423.9553 + 0.081033E$.

^c Number of points used to determine the maximum.

6.26. V359 Centauri

We reanalyzed the data of the 2002 superoutburst (Kato et al. 2002c). The result (table 49) generally confirmed the conclusion in Kato et al. (2002c): the global P_{dot} was $-16.3(1.7) \times 10^{-5}$ while P_{dot} for $E > 22$ was $-9.4(3.0) \times 10^{-5}$ (see discussion in Kato et al. 2002c for a selection of the interval). We adopted the latter as being the representative P_{dot} for this object.

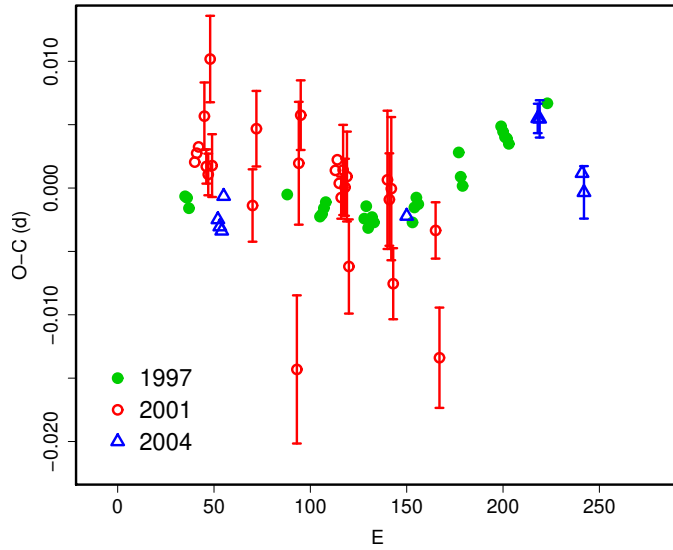


Fig. 63. Comparison of $O - C$ diagrams of V485 Cen between different superoutbursts. A period of 0.04212 d was used to draw this figure. Approximate cycle counts (E) after the start of the superoutburst were used.

6.27. V485 Centauri

The period evolution of this ultrashort- P_{orb} SU UMa-type dwarf nova was studied by Olech (1997), yielding a positive P_{dot} (the value has been corrected in this paper, see subsection 3.5).

We observed the 2001 superoutburst (table 50). Although the data were rather sparse, there was again no indication of an exceptionally large P_{dot} .

We also examined the 2004 superoutburst using the AAVSO data (table 51). The data clearly showed a stage B–C transition around $E = 166$. The P_{dot} during the stage B was $+3.1(0.9) \times 10^{-5}$, strengthening our interpretation that this object has an usual P_{dot} . The existence of the stage C has been demonstrated for this class of objects first time in this superoutburst.

A comparison of $O - C$ diagrams from different superoutbursts is presented in figure 63.

6.28. V1040 Centauri

V1040 Cen (=RX J1155.4–5641) is an ROSAT-selected CV (Motch et al. 1998). Patterson et al. (2003) reported a P_{SH} of 0.06215(10) d for the 2002 superoutburst. We analyzed the same superoutburst using the available data. The times of superhump maxima are listed in table 52. Except $50 \leq E \leq 54$, the overall $O - C$ diagram showed typical stage A–C transitions. The epochs of $50 \leq E \leq 54$ were affected by strong variation in the superhump profile (broad maxima), which may be due to overlapping orbital signals. Disregarding these epochs, we obtained a strongly positive P_{dot} of $+27.1(2.2) \times 10^{-5}$ ($17 \leq E \leq 86$). Other parameters are listed in table 2. The behavior is somewhat reminiscent to ER UMa stars (subsection 4.9). A further analysis and observations might shed light to further understanding period variations and the evolution

Table 50. Superhump maxima of V485 Cen (2001).

E	max ^a	error	$O - C^b$	N^c
0	51999.8526	0.0004	−0.0019	37
1	51999.8954	0.0004	−0.0012	39
2	51999.9380	0.0004	−0.0006	40
5	52000.0668	0.0027	0.0020	79
6	52000.1049	0.0014	−0.0019	82
7	52000.1464	0.0016	−0.0024	82
8	52000.1976	0.0034	0.0068	65
9	52000.2314	0.0025	−0.0016	53
30	52001.1127	0.0029	−0.0033	75
32	52001.2030	0.0030	0.0029	68
53	52002.0686	0.0058	−0.0146	60
54	52002.1269	0.0048	0.0018	76
55	52002.1729	0.0027	0.0056	71
73	52002.9267	0.0007	0.0025	38
74	52002.9696	0.0007	0.0034	39
75	52003.0099	0.0005	0.0017	40
76	52003.0509	0.0017	0.0006	21
77	52003.0952	0.0036	0.0029	76
78	52003.1359	0.0022	0.0016	71
79	52003.1789	0.0035	0.0025	44
80	52003.2139	0.0037	−0.0046	82
100	52004.0632	0.0055	0.0037	81
101	52004.1037	0.0036	0.0022	82
102	52004.1467	0.0056	0.0031	81
103	52004.1813	0.0028	−0.0043	81
125	52005.1122	0.0022	0.0014	78
127	52005.1864	0.0040	−0.0085	74

^a BJD−2400000.

^b Against $max = 2451999.8544 + 0.042050E$.

^c Number of points used to determine the maximum.

Table 51. Superhump maxima of V485 Cen (2004).

E	max ^a	error	$O - C^b$	N^c
0	53140.0437	0.0003	0.0000	74
1	53140.0853	0.0002	−0.0006	66
2	53140.1271	0.0003	−0.0009	74
3	53140.1719	0.0004	0.0018	39
98	53144.1718	0.0007	−0.0024	42
166	53147.0436	0.0012	0.0034	37
167	53147.0857	0.0015	0.0033	38
189	53148.0081	0.0008	−0.0016	33
190	53148.0487	0.0021	−0.0031	41

^a BJD−2400000.

^b Against $max = 2453140.0437 + 0.042148E$.

^c Number of points used to determine the maximum.

of stage C superhumps in this object and ER UMa stars.

We used BJD 2452383–2452402 (post-outburst re-brightening and subsequent phase) and obtained a refined photometric period of 0.060296(8) d, which has been attributed to P_{orb} (Patterson et al. 2003). No strong superhump signals were evident during this stage. This period, however, was not dominant during the quiescence in 2008 (BJD 2454547–2454574). The exact identification of P_{orb} should await a spectroscopic study.

6.29. *WX Ceti*

We reanalyzed the 1998 data in Kato et al. (2001b) combined with the AAVSO data and obtained refined times of maxima (table 53). Several newly determined maxima are also included. The new $O - C$ diagram basically confirms the finding in Kato et al. (2001b), but now clearly shows three stages of A–C. The timings of “late superhumps” in Kato et al. (2001b) were somewhat contaminated by the incorrect phase identification in the stage C. We obtained $P_{\text{dot}} = +6.4(1.0) \times 10^{-5}$ for the stage B ($15 \leq E \leq 157$).

We analyzed the 2001 superoutburst after combining our data and those in Sterken et al. (2007). The resultant times of maxima are listed in table 54. The observation well covered the middle part of the superoutburst and yielded $P_{\text{dot}} = +7.5(1.1) \times 10^{-5}$.

The 2004 observation (table 55) also covered the stages A–C. The P_{dot} of the stage B was $+5.5(1.8) \times 10^{-5}$ ($E \leq 137$).

We also analyzed the data for the 1989 superoutburst (O’Donoghue et al. 1991) after extracting the data from the scanned figure. Although systematic errors may be significantly larger than the errors given in the table, we could extract times of superhump maxima (table 56). The $O - C$ diagram clearly exhibits stages A–C. The P_{dot} of the stage B was $+10.3(1.4) \times 10^{-5}$ ($33 \leq E \leq 185$). The difficulty in determining the period in O’Donoghue et al. (1991) was probably a result from this strong period variation.

In summary, all observed superoutbursts of *WX Ceti* showed a similar pattern of $O - C$ and P_{dot} was always positive in the middle of the plateau phase (figure 64).

6.30. *RX Chameleontis*

Kato et al. (2001a) analyzed the 1998 outburst and reported a superhump period of 0.084 d. We observed the 2009 superoutburst during the early stage (table 57). The $O - C$ diagram showed a typical stage A–B transition. The mean superhump period during the stage B with the PDM method was 0.08492(2) d (figure 65), confirming the long- P_{SH} nature claimed in Kato et al. (2001a).

6.31. *BZ Circini*

BZ Cir is an X-ray selected CV (=1E 1449.7–6804; Grindlay et al. 1987; Hertz et al. 1990). The first recorded outburst was detected by B. Monard in 2004 June (vsnet-alert 8194). The outburst soon turned out to be a superoutburst (vsnet-alert 8201). We analyzed this superoutburst. The mean superhump period with the PDM method was 0.076422(5) d (figure 66). The times of su-

Table 52. Superhump maxima of V1040 Cen (2002).

E	max ^a	error	$O - C^b$	N^c
0	52366.2446	0.0002	0.0006	93
1	52366.3075	0.0001	0.0013	92
2	52366.3688	0.0003	0.0004	93
3	52366.4303	0.0003	−0.0002	93
4	52366.4925	0.0003	−0.0002	93
5	52366.5560	0.0003	0.0012	93
6	52366.6173	0.0003	0.0003	93
17	52367.3057	0.0005	0.0051	131
18	52367.3668	0.0003	0.0041	165
19	52367.4287	0.0003	0.0038	161
20	52367.4882	0.0004	0.0012	116
22	52367.6126	0.0004	0.0013	164
32	52368.2284	0.0002	−0.0045	160
33	52368.2919	0.0002	−0.0031	154
34	52368.3528	0.0002	−0.0044	163
47	52369.1609	0.0005	−0.0042	187
48	52369.2231	0.0003	−0.0041	338
49	52369.2840	0.0003	−0.0054	346
50	52369.3512	0.0005	−0.0003	351
51	52369.4163	0.0009	0.0026	164
52	52369.4793	0.0006	0.0034	165
53	52369.5359	0.0006	−0.0022	164
54	52369.6009	0.0009	0.0007	165
61	52370.0311	0.0004	−0.0041	154
62	52370.0948	0.0003	−0.0025	154
63	52370.1570	0.0004	−0.0025	153
64	52370.2191	0.0004	−0.0026	238
65	52370.2834	0.0004	−0.0005	246
66	52370.3437	0.0004	−0.0023	234
67	52370.4058	0.0006	−0.0024	93
68	52370.4657	0.0009	−0.0046	93
69	52370.5342	0.0009	0.0018	93
70	52370.5928	0.0007	−0.0018	92
78	52371.0964	0.0005	0.0046	112
79	52371.1568	0.0004	0.0028	104
83	52371.4064	0.0008	0.0039	46
84	52371.4716	0.0006	0.0069	93
85	52371.5304	0.0004	0.0036	89
86	52371.5957	0.0004	0.0067	47
101	52372.5226	0.0008	0.0013	93
102	52372.5812	0.0006	−0.0022	93
103	52372.6424	0.0014	−0.0032	67

^a BJD−2400000.

^b Against $max = 2452366.2440 + 0.062151E$.

^c Number of points used to determine the maximum.

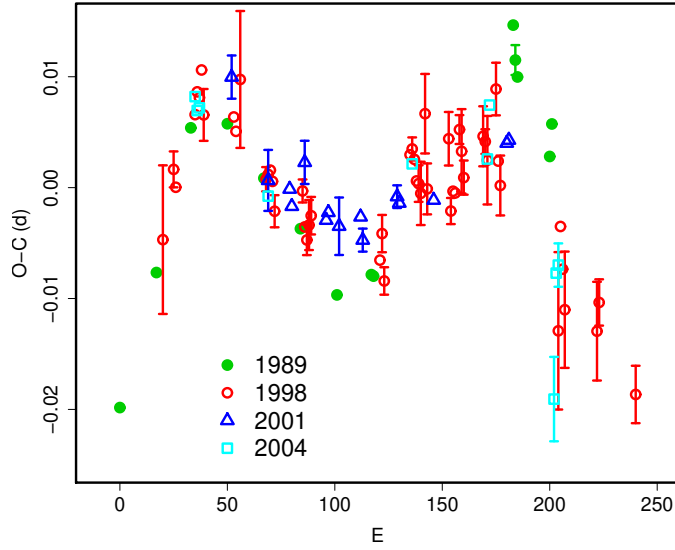


Fig. 64. Comparison of $O-C$ diagrams of WX Cet between different superoutbursts. A period of 0.05955 d was used to draw this figure. Estimated cycle counts (E) after the appearance of the superhumps were used.

Table 53. Superhump maxima of WX Cet (1998).

E	\max^a	error	$O - C^b$	N^c
0	51129.0492	0.0067	-0.0100	114
5	51129.3533	0.0016	-0.0034	35
6	51129.4112	0.0009	-0.0050	34
15	51129.9537	0.0005	0.0020	138
16	51130.0153	0.0005	0.0041	128
17	51130.0743	0.0006	0.0037	85
18	51130.1364	0.0006	0.0062	118
19	51130.1919	0.0023	0.0022	22
33	51131.0254	0.0005	0.0028	184
34	51131.0836	0.0006	0.0015	87
36	51131.2074	0.0062	0.0063	29
48	51131.9130	0.0011	-0.0021	73
49	51131.9730	0.0004	-0.0016	227
50	51132.0329	0.0004	-0.0011	181
51	51132.0915	0.0009	-0.0021	69
52	51132.1483	0.0014	-0.0047	80
65	51132.9243	0.0010	-0.0022	149
66	51132.9806	0.0005	-0.0054	259
67	51133.0390	0.0014	-0.0065	193
68	51133.0999	0.0023	-0.0051	63
69	51133.1603	0.0017	-0.0042	87
101	51135.0619	0.0008	-0.0066	112
102	51135.1238	0.0017	-0.0041	141
103	51135.1791	0.0012	-0.0083	115
115	51135.9051	0.0008	0.0037	116
116	51135.9652	0.0010	0.0042	110
117	51136.0238	0.0006	0.0034	112
118	51136.0814	0.0007	0.0015	142
119	51136.1407	0.0016	0.0013	140
120	51136.1994	0.0029	0.0004	91
122	51136.3256	0.0036	0.0077	34
123	51136.3784	0.0023	0.0010	24
133	51136.9784	0.0024	0.0061	40
134	51137.0315	0.0012	-0.0004	169
135	51137.0928	0.0008	0.0014	246
136	51137.1522	0.0009	0.0013	204
138	51137.2770	0.0013	0.0072	24
139	51137.3346	0.0038	0.0052	35
140	51137.3918	0.0015	0.0029	31
149	51137.9314	0.0027	0.0071	94
150	51137.9905	0.0011	0.0067	110
151	51138.0484	0.0040	0.0051	78
155	51138.2930	0.0024	0.0117	34
156	51138.3461	0.0009	0.0053	34
157	51138.4034	0.0027	0.0031	30
184	51139.9982	0.0071	-0.0086	50
185	51140.0671	0.0007	0.0009	117
186	51140.1228	0.0010	-0.0029	118
187	51140.1787	0.0052	-0.0065	88
202	51141.0700	0.0045	-0.0077	109
203	51141.1322	0.0021	-0.0050	82
220	51142.1362	0.0026	-0.0124	119

^a BJD-2400000.

^b Against $\max = 2451129.0592 + 0.059498E$.

^c Number of points used to determine the maximum.

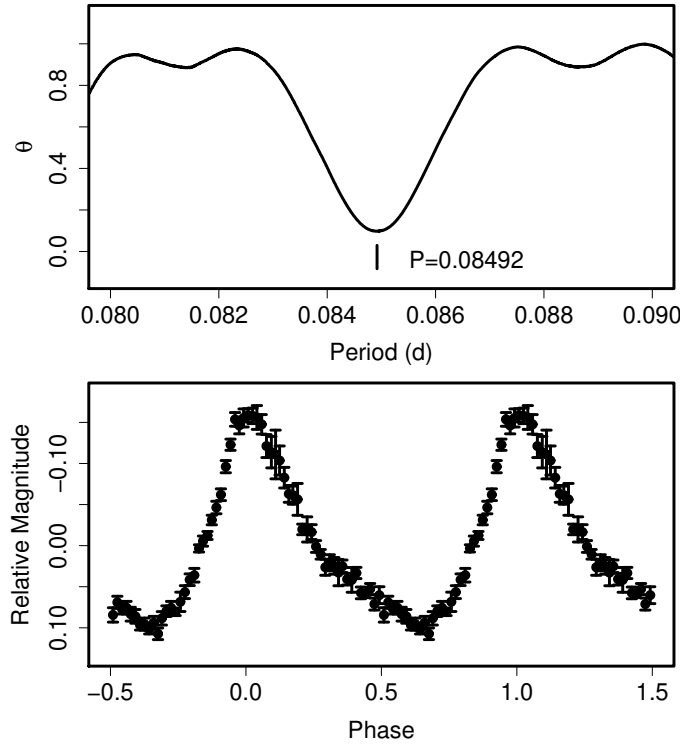


Fig. 65. Superhumps in RX Cha (2009). (Upper): PDM analysis excluding the early evolutionary stage before BJD 2454857.5). (Lower): Phase-averaged profile.

Table 54. Superhump maxima of WX Cet (2001).

E	\max^a	error	$O - C^b$	N^c
0	52092.2687	0.0019	0.0099	41
17	52093.2717	0.0027	0.0006	50
27	52093.8664	0.0002	-0.0002	73
28	52093.9244	0.0002	-0.0017	67
34	52094.2857	0.0019	0.0022	72
44	52094.8760	0.0002	-0.0030	72
45	52094.9362	0.0003	-0.0023	58
50	52095.2327	0.0026	-0.0035	54
60	52095.8291	0.0005	-0.0026	12
61	52095.8865	0.0010	-0.0047	15
77	52096.8433	0.0010	-0.0008	15
78	52096.9022	0.0004	-0.0014	67
94	52097.8553	0.0006	-0.0011	58
128	52099.8851	0.0004	0.0041	62
129	52099.9450	0.0004	0.0044	40

^a BJD-2400000.^b Against $\max = 2452092.2588 + 0.059549E$.^c Number of points used to determine the maximum.**Table 55.** Superhump maxima of WX Cet (2004).

E	\max^a	error	$O - C^b$	N^c
0	53347.9434	0.0001	0.0007	282
1	53348.0017	0.0002	-0.0005	279
2	53348.0614	0.0002	-0.0002	331
34	53349.9591	0.0002	-0.0055	322
101	53353.9518	0.0007	0.0029	213
136	53356.0365	0.0004	0.0062	213
137	53356.1009	0.0006	0.0112	108
167	53357.8609	0.0038	-0.0129	196
168	53357.9318	0.0008	-0.0014	304
169	53357.9921	0.0020	-0.0006	262

^a BJD-2400000.^b Against $\max = 2453347.9427 + 0.0594678E$.^c Number of points used to determine the maximum.

perhump maxima are listed in table 58. While the global P_{dot} corresponds to $-6.9(0.5) \times 10^{-5}$, there was an apparent transition of periods around $E = 68$. The P_{dot} of the middle segment ($13 \leq E \leq 68$) was $-0.5(3.8) \times 10^{-5}$ (cf. figure 4).

6.32. CG Canis Majoris

CG CMa was originally classified as a classical nova in 1934 (Duerbeck 1987). A new outburst in 1999 finally led to a classification as a WZ Sge-type dwarf nova (Duerbeck et al. 1999; Kato et al. 1999b). We reanalyzed photometric data reported in Kato et al. (1999b). The period around ~ 0.063 d reported in Kato et al. (1999b) appears viable, although the faintness of the object and the existence of a close companion made the uncertainty large. We determined $O - C$'s based on this period selection (table 59). If this period is the true period, the P_{dot} is almost zero at

Table 56. Superhump maxima of WX Cet (1989).

E	\max^a	error	$O - C^b$
0	47683.6324	0.0009	-0.0105
17	47684.6569	0.0024	0.0003
33	47685.6227	0.0006	0.0120
50	47686.6355	0.0006	0.0109
67	47687.6429	0.0003	0.0045
84	47688.6507	0.0003	-0.0015
101	47689.6571	0.0006	-0.0089
117	47690.6117	0.0003	-0.0084
118	47690.6711	0.0012	-0.0087
183	47694.5645	0.0015	0.0084
184	47694.6209	0.0039	0.0052
185	47694.6789	0.0009	0.0036
200	47695.5650	0.0021	-0.0049
201	47695.6275	0.0012	-0.0020

^a BJD-2400000.^b Against $\max = 2447683.6428 + 0.059635E$.^c Number of points used to determine the maximum.**Table 57.** Superhump maxima of RX Cha (2009).

E	\max^a	error	$O - C^b$	N^c
0	54857.1087	0.0007	-0.0077	106
10	54857.9797	0.0007	0.0087	76
22	54859.0007	0.0003	0.0043	140
34	54860.0165	0.0004	-0.0054	110

^a BJD-2400000.^b Against $\max = 2454857.1164 + 0.085455E$.^c Number of points used to determine the maximum.

$+0.5(1.6) \times 10^{-5}$. Since this variation was detected during the early stage of the outburst, this period likely refers to that of early superhumps, rather than superhumps suggested in Kato et al. (1999b). Other candidate periods could not express observations well.

6.33. PU Canis Majoris

The SU Uma-type nature of PU CMa was pointed out by Kato et al. (2003d), but they were unable to uniquely determine the superhump period. Thanks to three superoutbursts in 2003, 2005 and 2008, we have been able to firmly establish the superhump period. The times of superhump maxima are summarized in tables 60, 61 and 62.

The 2003 superoutburst was observed during its later course and a clear transition from the stage B to C was observed. We also included some of post-outburst hump maxima having the same phase as in stage C superhumps. No clear phase shift, expected for traditional ‘‘late superhumps’’, was observed during and soon after the rapidly fading stage.

The 2005 and 2008 superoutbursts were observed during their earlier stages and the superhump period showed an increase during the superoutburst plateau. The P_{dot} 's

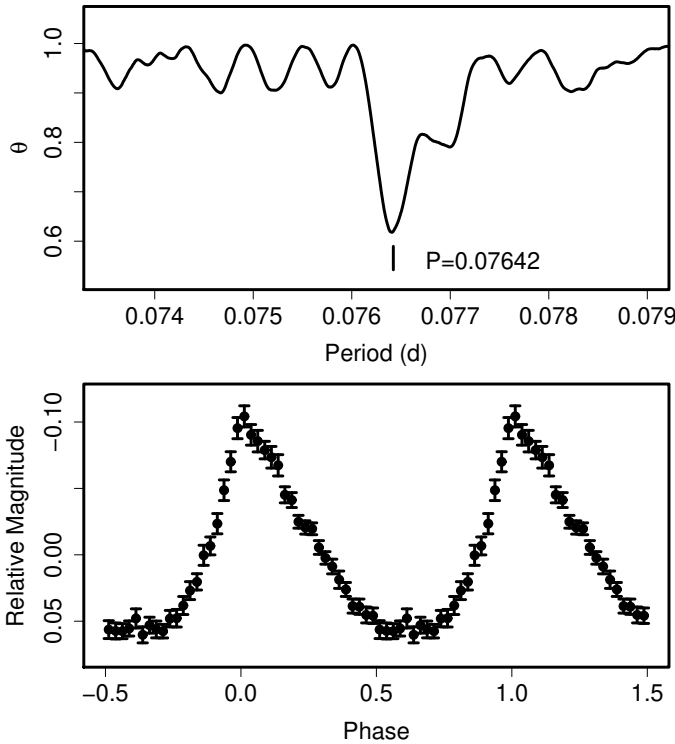


Fig. 66. Superhumps in BZ Cir (2004). (Upper): PDM analysis. (Lower): Phase-averaged profile.

Table 58. Superhump maxima of BZ Cir (2004).

E	\max^a	error	$O - C^b$	N^c
0	53183.2842	0.0004	-0.0102	86
13	53184.2835	0.0002	-0.0044	142
14	53184.3612	0.0002	-0.0031	172
15	53184.4375	0.0002	-0.0033	163
16	53184.5156	0.0004	-0.0016	114
26	53185.2797	0.0003	-0.0017	173
27	53185.3597	0.0006	0.0019	83
42	53186.5081	0.0009	0.0040	92
43	53186.5809	0.0019	0.0003	75
53	53187.3473	0.0004	0.0025	155
54	53187.4272	0.0007	0.0060	137
66	53188.3453	0.0005	0.0070	155
67	53188.4219	0.0004	0.0072	171
68	53188.4986	0.0007	0.0075	108
94	53190.4820	0.0005	0.0039	172
132	53193.3791	0.0011	-0.0030	145
145	53194.3683	0.0006	-0.0074	166
146	53194.4465	0.0004	-0.0056	167

^a BJD-2400000.

^b Against $\max = 2453183.2944 + 0.076422E$.

^c Number of points used to determine the maximum.

Table 59. Maxima of (Early) Superhumps in CG CMA (1999).

E	\max^a	error	$O - C^b$	N^c
0	51232.1013	0.0077	0.0005	101
45	51234.9526	0.0036	0.0045	127
47	51235.0719	0.0042	-0.0027	121
78	51237.0438	0.0048	0.0076	56
79	51237.0974	0.0036	-0.0020	62
92	51237.9213	0.0130	-0.0007	59
94	51238.0369	0.0066	-0.0117	127
95	51238.1084	0.0058	-0.0034	78
108	51238.9387	0.0054	0.0044	127
110	51239.0654	0.0036	0.0044	102
141	51241.0137	0.0039	-0.0088	118
171	51242.9313	0.0123	0.0107	62
173	51243.0503	0.0036	0.0031	36
187	51243.9274	0.0049	-0.0057	81
189	51244.0595	0.0053	-0.0002	85

^a BJD-2400000.

^b Against $\max = 2451232.1007 + 0.063275E$.

^c Number of points used to determine the maximum.

Table 60. Superhump maxima of PU CMA (2003).

E	\max^a	error	$O - C^b$	N^c
0	52784.8969	0.0007	-0.0104	248
23	52786.2337	0.0007	-0.0005	187
40	52787.2190	0.0003	0.0041	116
49	52787.7365	0.0005	0.0024	127
51	52787.8539	0.0006	0.0045	215
57	52788.1995	0.0005	0.0040	131
69	52788.8885	0.0004	0.0007	356
74	52789.1770	0.0009	0.0007	92
86	52789.8705	0.0004	0.0020	232
92	52790.2129	0.0005	-0.0017	132
109	52791.1955	0.0021	0.0002	59
144	52793.2083	0.0008	-0.0060	34

^a BJD-2400000.

^b Against $\max = 2452784.9074 + 0.057688E$.

^c Number of points used to determine the maximum.

were $+11.4(1.8) \times 10^{-5}$ and $+4.4(3.1) \times 10^{-5}$, respectively. The 2005 superoutburst showed a clear transition to the stage C (figure 67; $P_2 = 0.05768(2)$ d, disregarding $E = 196$ and $E = 215$).

The 2008 superoutburst was preceded by a distinct precursor (corresponding to $E \leq 17$), during which a longer P_{SH} was observed (figure 68). The fractional superhump excess was 2.3 % (mean period) against the orbital period by Thorstensen, Fenton (2003).

6.34. YZ Cancri

YZ Cnc is one of the oldest known SU UMa-type dwarf nova. The superhump period of 0.09204 d (Patterson 1979) has long been widely used. We, however, noticed

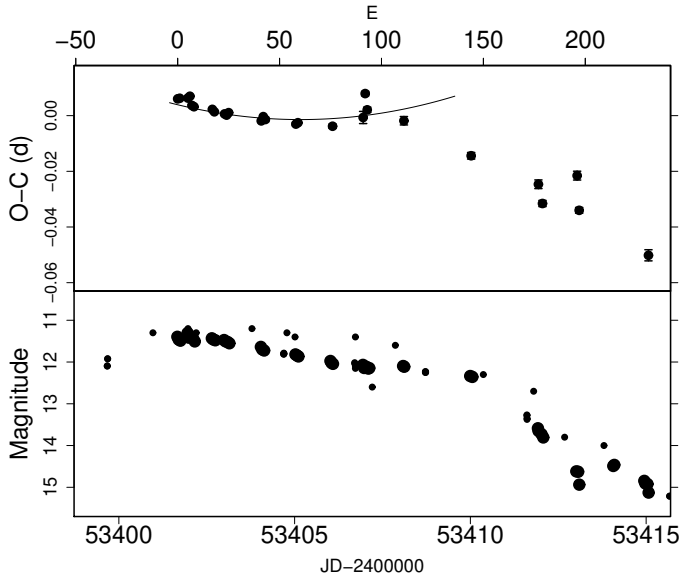


Fig. 67. $O - C$ of superhumps PU CMa (2005). (Upper): $O - C$ diagram. The $O - C$ values were against the mean period for the stage B ($E \leq 93$, thin curve) (Lower): Light curve. Large dots are our CCD observations and small dots are visual observation from the VSNET database.

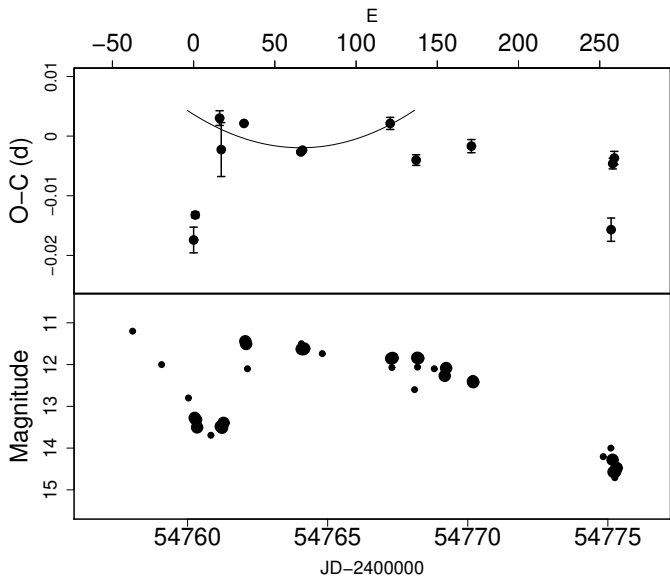


Fig. 68. $O - C$ of superhumps PU CMa (2008). (Upper): $O - C$ diagram. The $O - C$ values were against the mean period for the stage B ($16 \leq E \leq 121$, thin curve) (Lower): Light curve. Large dots are our CCD observations and small dots are visual observation from the VSNET database.

Table 61. Superhump maxima of PU CMa (2005).

E	\max^a	error	$O - C^b$	N^c
0	53401.6702	0.0002	-0.0033	45
1	53401.7285	0.0002	-0.0029	57
5	53401.9608	0.0004	-0.0019	60
6	53402.0195	0.0006	-0.0011	37
7	53402.0742	0.0004	-0.0042	90
8	53402.1319	0.0003	-0.0044	106
17	53402.6534	0.0003	-0.0034	56
18	53402.7106	0.0003	-0.0041	56
23	53403.0002	0.0004	-0.0037	167
24	53403.0578	0.0004	-0.0040	261
25	53403.1167	0.0004	-0.0029	226
41	53404.0427	0.0003	-0.0023	161
42	53404.1023	0.0003	-0.0006	251
43	53404.1593	0.0008	-0.0014	122
58	53405.0286	0.0006	0.0002	201
59	53405.0871	0.0004	0.0009	266
76	53406.0729	0.0008	0.0033	180
91	53406.9469	0.0022	0.0097	58
92	53407.0135	0.0008	0.0185	85
93	53407.0657	0.0010	0.0129	84
111	53408.1069	0.0015	0.0129	82
144	53410.0103	0.0012	0.0074	57
177	53411.9160	0.0016	0.0043	59
179	53412.0252	0.0011	-0.0021	80
196	53413.0222	0.0016	0.0116	74
197	53413.0678	0.0010	-0.0007	80
215	53414.0804	0.0012	-0.0292	85
231	53415.0256	0.0020	-0.0095	81

^a BJD-2400000.

^b Against $\max = 2453401.6735 + 0.057842E$.

^c Number of points used to determine the maximum.

Table 62. Superhump maxima of PU CMa (2008).

E	\max^a	error	$O - C^b$	N^c
0	54760.2505	0.0022	-0.0132	154
1	54760.3128	0.0005	-0.0090	255
16	54761.1995	0.0012	0.0073	86
17	54761.2523	0.0045	0.0020	58
31	54762.0691	0.0002	0.0064	214
66	54764.0955	0.0003	0.0018	177
67	54764.1538	0.0002	0.0021	166
121	54767.2920	0.0010	0.0068	110
137	54768.2144	0.0009	0.0007	56
171	54770.1899	0.0011	0.0032	37
257	54775.1667	0.0020	-0.0104	38
258	54775.2358	0.0009	0.0007	59
259	54775.2948	0.0011	0.0016	59

^a BJD-2400000.

^b Against $\max = 2454760.2158 + 0.057977E$.

^c Number of points used to determine the maximum.

Table 63. Superhump maxima of YZ Cnc (2007).

E	\max^a	error	$O - C^b$	N^c
0	54144.0639	0.0006	-0.0017	112
1	54144.1553	0.0008	-0.0006	110
22	54146.0535	0.0010	0.0012	104
23	54146.1421	0.0007	-0.0005	110
34	54147.1341	0.0022	-0.0019	81
35	54147.2321	0.0025	0.0058	49
65	54149.9319	0.0031	-0.0036	77
66	54150.0270	0.0014	0.0012	113

^a BJD-2400000.^b Against $\max = 2454144.0656 + 0.090307E$.^c Number of points used to determine the maximum.

that this period was incorrect. We obtained the times of superhump maxima from the observations of the 2007 February superoutburst (table 63). The period 0.09204 d could not fit the observation. A PDM analysis and superhump timing analysis yielded mean periods of 0.09042(4) d and 0.09031(5) d, respectively. The corresponding fractional superhump excess was 4.0 %. The P_{dot} was $-5.1(4.7) \times 10^{-5}$.

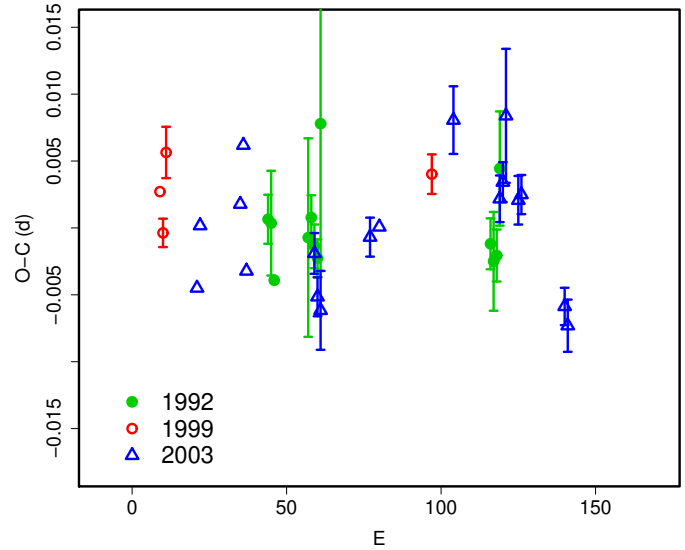
6.35. AK Cancri

Kato (1994) first detected superhumps in this object, and reported a period of 0.06735(5) d. We measured times of superhump maxima from these observations (table 64). The first two nights of the observation were likely taken during stage B, while the last night was likely during stage C. Mennickent et al. (1996) further observed the 1995 superoutburst and yielded a mean period of 0.06749(1) d.

We analyzed the 1999 superoutburst using the AAVSO data and the 2003 superoutburst using the data by VSNET Collaboration. The superhump maxima are given in table 65 and 66. The 1999 superoutburst was preceded by a precursor outburst 9 d before. The $O - C$ diagram during the 2003 superoutburst (figure 7) showed a feature characteristic to a short- P_{orb} SU UMa-type dwarf nova: following the stage B with a positive P_{dot} , the period switched to a shorter one (stage C) before the termination of the plateau phase. The P_{dot} for the first interval ($E < 101$) was $+4.8(3.2) \times 10^{-5}$.

6.36. CC Cancri

Kato, Nogami (1997b) first reported the detection of superhumps in this object. Kato et al. (2002e) further reported the result of a more extensive campaign in 2001, yielding a strongly negative $P_{\text{dot}} = -10.2(1.3) \times 10^{-5}$. Based on our new knowledge, this period derivative can be better understood to represent the rapid period decrease (stage A to B) during the early stage of a superoutburst. We thereby reexamined the 2001 data and obtained the times of maxima (table 67). The $O - C$ diagram can be interpreted as a combination of stage A evolution with a long superhump period ($E < 20$), and the stage B with a more stabilized superhump period. The P_{dot} of the latter

**Fig. 69.** Comparison of $O - C$ diagrams of AK Cnc between different superoutbursts. A period of 0.06736 d was used to draw this figure. Approximate cycle counts (E) after the start of the superoutburst were used.**Table 64.** Superhump maxima of AK Cnc (1992).

E	\max^a	error	$O - C^b$	N^c
0	48639.1631	0.0018	0.0006	34
1	48639.2302	0.0039	0.0003	29
2	48639.2933	0.0010	-0.0040	45
13	48640.0374	0.0074	-0.0008	59
14	48640.1063	0.0017	0.0007	101
15	48640.1715	0.0016	-0.0014	89
16	48640.2380	0.0014	-0.0023	86
17	48640.3154	0.0110	0.0078	89
72	48644.0112	0.0019	-0.0011	54
73	48644.0772	0.0037	-0.0024	58
74	48644.1450	0.0019	-0.0020	64
75	48644.2189	0.0043	0.0045	56

^a BJD-2400000.^b Against $\max = 2448639.1625 + 0.067358E$.^c Number of points used to determine the maximum.**Table 65.** Superhump maxima of AK Cnc (1999).

E	\max^a	error	$O - C^b$	N^c
0	51261.4195	0.0009	0.0001	30
1	51261.4838	0.0011	-0.0030	36
2	51261.5572	0.0019	0.0030	21
88	51267.3485	0.0015	-0.0000	36

^a BJD-2400000.^b Against $\max = 2451261.4195 + 0.067376E$.^c Number of points used to determine the maximum.

Table 66. Superhump maxima of AK Cnc (2003).

E	max ^a	error	$O - C^b$	N^c
0	52722.3924	0.0004	-0.0035	65
1	52722.4644	0.0005	0.0011	52
14	52723.3417	0.0008	0.0025	31
15	52723.4135	0.0008	0.0069	66
16	52723.4714	0.0007	-0.0025	70
38	52724.9547	0.0015	-0.0015	118
39	52725.0188	0.0015	-0.0048	108
40	52725.0851	0.0029	-0.0058	115
56	52726.1683	0.0015	-0.0006	144
59	52726.3712	0.0004	0.0001	67
83	52727.9958	0.0025	0.0077	70
98	52729.0003	0.0017	0.0016	71
99	52729.0689	0.0015	0.0028	90
100	52729.1413	0.0050	0.0078	74
104	52729.4044	0.0018	0.0014	32
105	52729.4722	0.0015	0.0018	57
119	52730.4068	0.0014	-0.0068	45
120	52730.4728	0.0020	-0.0082	34

^a BJD-2400000.^b Against $max = 2452722.3959 + 0.067375E$.^c Number of points used to determine the maximum.

interval was $-7.3(2.5) \times 10^{-5}$.

6.37. AL Comae Berenices

We have reanalyzed the data in Nogami et al. (1997a) of this well-known WZ Sge-type dwarf nova. The combined list of superhump maxima from Howell et al. (1996), Pych, Olech (1995) and Patterson et al. (1996) is presented in table 68. The $O - C$ diagram clearly showed the same characteristics to that of another WZ Sge-type dwarf nova, HV Vir. The P_{dot} of the middle segment (stage B) was $+1.9(0.5) \times 10^{-5}$ ($24 \leq E \leq 229$). This value supersedes the published period derivative in Nogami et al. (1997a).

The refined times of superhump maxima during the 2001 superoutburst (Ishioaka et al. 2002) are listed in table 69. The P_{dot} during the stage B was $-0.2(0.8) \times 10^{-5}$ ($28 \leq E \leq 222$). A comparison of the $O - C$ diagrams is shown in figure 70.

The object underwent another superoutburst in 2007 (Uemura et al. 2008b). This behavior of this superoutburst was different from those in 1995 and 2001 in that the object showed separate rebrightenings (type-B). Although the observations were incomplete due to the poor seasonal location, a weak periodicity of 0.05717(1) d was detected during this rebrightening stage. Since the object showed P_{SH} during the type-A superoutburst in 1995, we adopted this period as the P_{SH} of the 2007 superoutburst in table 2.

6.38. GO Comae Berenices

We reanalyzed the data used in Imada et al. (2005), combined with Crimea (Pav) data, and new data for the 2005 and 2006 superoutbursts (tables 70, 71, 72). The val-

Table 67. Superhump maxima of CC Cnc (2001).

E	max ^a	error	$O - C^b$	N^c
0	52226.3217	0.0039	-0.0107	70
11	52227.1401	0.0029	-0.0232	79
12	52227.2344	0.0015	-0.0044	93
13	52227.3099	0.0030	-0.0044	75
24	52228.1482	0.0008	0.0031	145
25	52228.2212	0.0011	0.0006	147
26	52228.3014	0.0013	0.0053	147
27	52228.3780	0.0012	0.0064	77
37	52229.1273	0.0030	0.0003	55
38	52229.2072	0.0007	0.0047	147
39	52229.2823	0.0009	0.0043	146
40	52229.3592	0.0020	0.0057	19
50	52230.1126	0.0034	0.0038	53
51	52230.1918	0.0010	0.0074	100
52	52230.2637	0.0013	0.0038	103
53	52230.3439	0.0020	0.0085	82
64	52231.1685	0.0017	0.0023	89
65	52231.2473	0.0028	0.0055	20
79	52232.3036	0.0014	0.0044	120
80	52232.3756	0.0013	0.0009	89
90	52233.1340	0.0015	0.0041	145
91	52233.2064	0.0017	0.0009	146
92	52233.2818	0.0020	0.0008	146
93	52233.3532	0.0010	-0.0033	82
104	52234.1860	0.0025	-0.0013	147
105	52234.2532	0.0013	-0.0097	147
106	52234.3374	0.0016	-0.0010	124
116	52235.0789	0.0069	-0.0147	115
119	52235.3201	0.0017	-0.0001	146

^a BJD-2400000.^b Against $max = 2452226.3324 + 0.075528E$.^c Number of points used to determine the maximum.

ues of P_{dot} were $+15.5(2.3) \times 10^{-5}$ (2003, $16 \leq E \leq 115$), $+6.9(1.5) \times 10^{-5}$ (2005, $13 \leq E \leq 142$). $+4.6(3.4) \times 10^{-5}$ (2006, excluding $E = 64$ and $E = 136$). The 2008 superoutburst was also observed (table 73). A marginally significant $P_{\text{dot}} = +16(11) \times 10^{-5}$ was recorded. The new observations in 2003 indicated that the stage C superhumps persisted even during the post-superoutburst stage ($E \geq 230$). The $O - C$ diagrams did not drastically vary between different superoutbursts (figure 71).

6.39. V728 Coronae Australis

This object was selected during the identification project of NSV objects against ROSAT X-ray source (Kato, vsnet-id-rosat 11). The proximity of the ROSAT position to the position of NSV 9923 suggested that the object may be a dwarf nova, as we have seen in BB Ari (subsection 6.15) and DT Oct (Kato et al. 2002a). Following this suggestion, the object was monitored for outbursts. An outburst detection was announced on 2003 June 28 (R. Stubbings, vsnet-alert 7787). The mean superhump period with the PDM method was 0.082200(13)

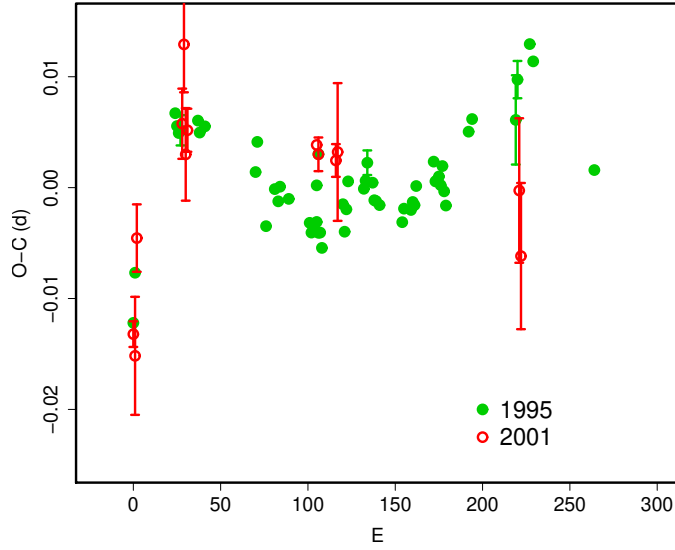


Fig. 70. Comparison of $O-C$ diagrams of AL Com Cnc between different superoutbursts. A period of 0.05728 d was used to draw this figure. Approximate cycle counts (E) after the appearance of the ordinary superhumps were used.

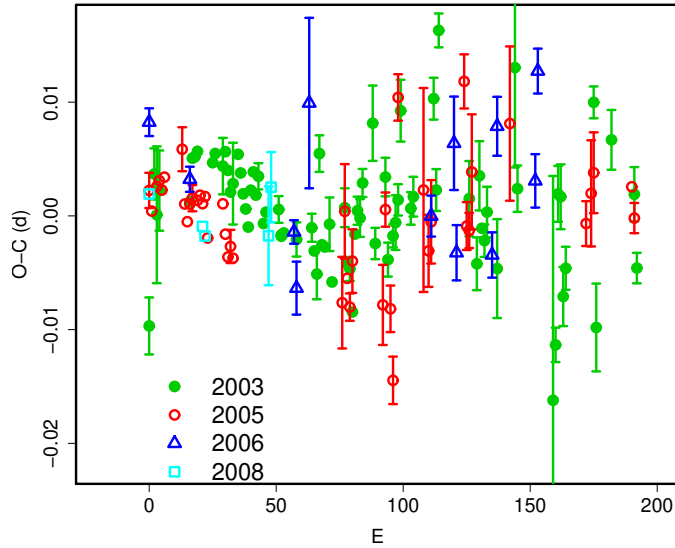


Fig. 71. Comparison of $O-C$ diagrams of GO Com between different superoutbursts. A period of 0.063059 d was used to draw this figure. Approximate cycle counts (E) after the start of the superoutburst were used.

Table 68. Superhump maxima of AL Com (1995).

E	\max^a	error	$O-C^b$	N^c
0	49823.5693	–	–0.0139	R3
1	49823.6311	–	–0.0094	R5
24	49824.9629	0.0007	0.0053	25
25	49825.0190	0.0007	0.0042	29
26	49825.0757	0.0008	0.0035	29
27	49825.1332	0.0014	0.0038	29
37	49825.7069	–	0.0048	R5
38	49825.7631	–	0.0037	R5
41	49825.9355	–	0.0043	R5
70	49827.5925	–	0.0006	R3
71	49827.6525	–	0.0033	R3
76	49827.9313	–	–0.0042	R5
81	49828.2210	0.0005	–0.0008	38
83	49828.3345	–	–0.0019	R4
84	49828.3931	–	–0.0005	R4
89	49828.6784	–	–0.0016	R5
101	49829.3636	–	–0.0036	R4
102	49829.4200	–	–0.0044	R4
103	49829.4778	–	–0.0039	R4
105	49829.5928	–	–0.0034	R5
105	49829.5961	–	–0.0001	R3
106	49829.6491	–	–0.0044	R5
106	49829.6562	–	0.0027	R3
107	49829.7064	–	–0.0044	R5
108	49829.7623	–	–0.0057	R5
120	49830.4536	–	–0.0016	R4
121	49830.5084	–	–0.0041	R4
122	49830.5677	–	–0.0021	R4
123	49830.6275	–	0.0005	R5
132	49831.1424	0.0004	–0.0001	34
133	49831.2004	0.0009	0.0006	38
134	49831.2593	0.0011	0.0023	25
137	49831.4293	–	0.0005	R4
138	49831.4850	–	–0.0011	R4
139	49831.5422	–	–0.0011	R4
141	49831.6564	–	–0.0015	R5
154	49832.3995	–	–0.0028	R4
155	49832.4580	–	–0.0016	R4
159	49832.6870	–	–0.0017	R5
160	49832.7450	–	–0.0009	R5
161	49832.8020	–	–0.0012	R5
162	49832.8610	–	0.0005	R5
172	49833.4360	–	0.0029	R4
173	49833.4915	–	0.0011	R4
174	49833.5489	–	0.0012	R4
175	49833.6065	–	0.0016	R3
176	49833.6630	–	0.0008	R5
177	49833.7220	–	0.0025	R5
178	49833.7770	–	0.0003	R5

^a BJD–2400000.

^b Against $\max = 2449823.5832 + 0.057267E$.

^c Number of points used to determine the maximum.

$N = Rn(n = 3 - 4)$ are references

as in Nogami et al. (1997a)

$N = R5$ refers to Patterson et al. (1996)

Table 68. Superhump maxima of AL Com (1995) (continued).

E	max	error	$O - C$	N
179	49833.8330	–	–0.0010	R5
192	49834.5843	–	0.0058	R3
194	49834.7000	–	0.0070	R5
219	49836.1319	0.0040	0.0073	24
220	49836.1928	0.0017	0.0109	22
227	49836.5970	–	0.0142	R3
229	49836.7100	–	0.0127	R5
264	49838.7050	–	0.0033	R5
349	49843.5732	–	0.0038	R3
360	49844.1662	0.0089	–0.0331	21

Table 69. Superhump maxima of AL Com (2001).

E	max ^a	error	$O - C^b$	N^c
0	52056.3598	0.0012	–0.0124	142
1	52056.4151	0.0053	–0.0144	142
2	52056.4830	0.0030	–0.0038	85
28	52057.9826	0.0032	0.0062	67
29	52058.0470	0.0043	0.0134	89
30	52058.0944	0.0042	0.0035	78
31	52058.1538	0.0019	0.0056	77
105	52062.3912	0.0007	0.0036	51
106	52062.4477	0.0015	0.0027	42
116	52063.0199	0.0015	0.0021	104
117	52063.0779	0.0062	0.0028	101
221	52069.0316	0.0065	–0.0017	55
222	52069.0830	0.0066	–0.0076	69

^a BJD–2400000.^b Against $max = 2452056.3722 + 0.057290E$.^c Number of points used to determine the maximum.

d (figure 72). The times of superhump maxima are listed in table 74. Although the original observations included later stage at $E > 50$, the superhump signal became weaker and irregular, sometimes with multiple peaks. We therefore restricted our $O - C$ analysis to $E \leq 50$. The situation may be similar to another long-period system SS UMi (Olech et al. 2006). The resultant P_{dot} was $-2.3(3.4) \times 10^{-5}$. Upon announcement of this observation, the variable has been given a General Catalogue of Variable Stars (GCVS) designation V728 CrA (Kazarovets et al. 2006).

6.40. VW Coronae Borealis

Nogami et al. (2004b) presented an analysis of 2003 superoutburst and other recorded superoutbursts. We re-analyzed the 2003 data and yielded refined times of superhump maxima (table 75). The resultant $O - C$ diagram basically confirmed the finding in Nogami et al. (2004b), giving $P_{\text{dot}} = +7.7(0.8) \times 10^{-5}$ for $E \leq 142$.

As discussed in Nogami et al. (2004b), positive period derivatives are rare in systems with long superhump periods ($P_{\text{SH}} > 0.07$ d). This phenomenon may be analo-

Table 70. Superhump maxima of GO Com (2003).

E	max ^a	error	$O - C^b$	N^c
0	52794.1340	0.0025	–0.0141	225
2	52794.2734	0.0022	–0.0007	65
3	52794.3329	0.0060	–0.0042	72
4	52794.3981	0.0035	–0.0020	39
16	52795.1538	0.0008	–0.0024	109
17	52795.2207	0.0003	0.0015	36
18	52795.2839	0.0003	0.0016	37
19	52795.3474	0.0004	0.0022	60
25	52795.7248	0.0004	0.0015	89
26	52795.7887	0.0004	0.0023	88
29	52795.9767	0.0025	0.0013	107
30	52796.0411	0.0004	0.0027	767
31	52796.1025	0.0004	0.0011	455
32	52796.1636	0.0006	–0.0008	364
33	52796.2274	0.0036	0.0000	96
35	52796.3561	0.0009	0.0027	32
36	52796.4175	0.0004	0.0011	90
37	52796.4788	0.0005	–0.0007	82
38	52796.5405	0.0009	–0.0020	50
39	52796.6020	0.0009	–0.0035	26
40	52796.6683	0.0004	–0.0002	37
41	52796.7329	0.0005	0.0014	97
42	52796.7939	0.0005	–0.0006	85
43	52796.8587	0.0012	0.0011	49
45	52796.9806	0.0010	–0.0029	39
46	52797.0447	0.0004	–0.0019	342
52	52797.4209	0.0007	–0.0037	103
51	52797.3602	0.0012	–0.0014	30
52	52797.4210	0.0007	–0.0036	105
53	52797.4843	0.0006	–0.0033	116
58	52797.7990	0.0015	–0.0037	29
64	52798.1784	0.0012	–0.0023	21
65	52798.2394	0.0006	–0.0043	30
66	52798.3004	0.0022	–0.0063	49
67	52798.3741	0.0016	0.0043	70
68	52798.4291	0.0005	–0.0036	151
69	52798.4920	0.0008	–0.0038	131
71	52798.6201	0.0024	–0.0017	25
72	52798.6781	0.0008	–0.0067	50
77	52798.9999	0.0017	0.0001	306
78	52799.0580	0.0010	–0.0048	453
79	52799.1206	0.0011	–0.0052	333
80	52799.1799	0.0010	–0.0089	254
81	52799.2498	0.0008	–0.0020	34
82	52799.3149	0.0012	0.0001	53
83	52799.3773	0.0017	–0.0005	39
84	52799.4435	0.0012	0.0026	81
88	52799.7010	0.0033	0.0080	66
89	52799.7535	0.0014	–0.0025	61
93	52800.0115	0.0017	0.0036	175
94	52800.0673	0.0015	–0.0036	127

^a BJD–2400000.^b Against $max = 2452794.1481 + 0.063009E$.^c Number of points used to determine the maximum.

Table 70. Superhump maxima of GO Com (2003) (continued).

E	max	error	$O - C$	N
96	52800.1955	0.0010	-0.0015	35
97	52800.2598	0.0024	-0.0002	35
98	52800.3248	0.0014	0.0018	60
99	52800.3957	0.0027	0.0097	67
103	52800.6394	0.0014	0.0013	41
104	52800.7035	0.0017	0.0024	28
112	52801.2166	0.0018	0.0114	34
113	52801.2716	0.0018	0.0034	24
114	52801.3487	0.0015	0.0175	36
115	52801.4228	0.0035	0.0286	33
126	52802.0906	0.0033	0.0033	71
129	52802.2740	0.0023	-0.0023	16
130	52802.3448	0.0030	0.0055	35
131	52802.4033	0.0007	0.0009	132
132	52802.4652	0.0014	-0.0001	120
133	52802.5308	0.0022	0.0025	40
137	52802.7781	0.0043	-0.0023	29
144	52803.2372	0.0088	0.0157	34
145	52803.2896	0.0020	0.0051	35
159	52804.1538	0.0197	-0.0128	24
160	52804.2217	0.0015	-0.0079	34
161	52804.2981	0.0025	0.0055	59
162	52804.3609	0.0028	0.0053	38
163	52804.4152	0.0026	-0.0035	77
164	52804.4807	0.0019	-0.0009	70
175	52805.1889	0.0014	0.0142	34
176	52805.2322	0.0039	-0.0055	33
182	52805.6271	0.0026	0.0112	41
191	52806.1898	0.0024	0.0069	24
192	52806.2464	0.0013	0.0005	34
230	52808.6277	0.0072	-0.0126	26
231	52808.6935	0.0036	-0.0098	40
241	52809.3289	0.0016	-0.0044	13
262	52810.6366	0.0017	-0.0200	24

gous to the one observed in TT Boo (Olech et al. 2004a), another SU UMa-type dwarf nova with a relatively long superhump period and long superoutbursts (see also FQ Mon, subsection 6.88). For objects with positive P_{dot} , also see subsections RU Hor (6.71) and QY Per (6.103).

We also included times of superhump maxima during the 2001 and 2006 superoutbursts (tables 76, 77). Although the superhump signal was present, we did not use the 2001 superoutburst to determine P_{dot} because of the lower quality of the data. This outburst was only observed for its late stage, and the observed superhumps were likely stage C superhumps. The 2006 superoutburst was observed for its early part. The derived $P_{\text{SH}} = 0.07268(6)$ d, shorter than the mean P_1 for the 2003 superoutburst, also supports that the P_{SH} was shorter (i.e. with a probable positive P_{dot}) near the start of this superoutburst.

A combined $O - C$ diagram is presented in figure 73. The stage C behavior may have been different between

Table 71. Superhump maxima of GO Com (2005).

E	max ^a	error	$O - C^b$	N^c
0	53482.1748	0.0015	0.0023	144
1	53482.2360	0.0009	0.0005	277
3	53482.3643	0.0002	0.0027	57
4	53482.4279	0.0003	0.0032	69
5	53482.4901	0.0002	0.0024	68
6	53482.5543	0.0002	0.0035	70
13	53482.9982	0.0019	0.0059	232
14	53483.0564	0.0009	0.0011	417
15	53483.1179	0.0007	-0.0004	381
16	53483.1825	0.0010	0.0011	411
17	53483.2461	0.0012	0.0016	386
19	53483.3720	0.0008	0.0014	64
20	53483.4356	0.0006	0.0019	66
21	53483.4979	0.0008	0.0011	66
22	53483.5615	0.0007	0.0018	68
23	53483.6210	0.0007	-0.0019	63
29	53484.0023	0.0010	0.0011	306
30	53484.0627	0.0009	-0.0016	464
31	53484.1238	0.0007	-0.0036	442
32	53484.1878	0.0015	-0.0026	399
33	53484.2498	0.0004	-0.0037	191
76	53486.9574	0.0040	-0.0076	22
77	53487.0285	0.0042	0.0004	105
78	53487.0857	0.0008	-0.0055	367
79	53487.1462	0.0012	-0.0080	371
80	53487.2133	0.0028	-0.0040	215
92	53487.9662	0.0035	-0.0079	226
93	53488.0376	0.0015	0.0005	209
95	53488.1550	0.0020	-0.0082	344
96	53488.2118	0.0021	-0.0145	348
98	53488.3628	0.0020	0.0104	26
108	53488.9852	0.0090	0.0022	155
110	53489.1060	0.0032	-0.0031	249
111	53489.1716	0.0037	-0.0006	121
124	53490.0037	0.0024	0.0118	259
125	53490.0540	0.0021	-0.0010	297
126	53490.1167	0.0015	-0.0014	266
127	53490.1849	0.0051	0.0038	191
142	53491.1351	0.0068	0.0080	198
172	53493.0180	0.0020	-0.0008	161
174	53493.1468	0.0047	0.0018	139
175	53493.2117	0.0036	0.0036	118
190	53494.1563	0.0006	0.0024	312
191	53494.2166	0.0013	-0.0004	221

^a BJD-2400000.

^b Against $max = 2453482.1725 + 0.063060E$.

^c Number of points used to determine the maximum.

Table 72. Superhump maxima of GO Com (2006).

E	max ^a	error	$O - C^b$	N^c
0	54084.6993	0.0012	0.0097	13
16	54085.7033	0.0011	0.0044	18
57	54088.2841	0.0010	-0.0008	93
58	54088.3422	0.0023	-0.0058	90
63	54088.6737	0.0075	0.0104	7
64	54088.7004	0.0021	-0.0260	9
111	54091.6906	0.0018	-0.0002	12
120	54092.2646	0.0041	0.0060	129
121	54092.3180	0.0024	-0.0036	89
135	54093.2006	0.0020	-0.0040	111
136	54093.2359	0.0023	-0.0318	84
136	54093.2880	0.0014	0.0203	123
137	54093.3381	0.0026	0.0073	214
152	54094.2792	0.0023	0.0023	72
153	54094.3519	0.0020	0.0119	87

^a BJD-2400000.^b Against $max = 2454084.6897 + 0.063074E$.^c Number of points used to determine the maximum.**Table 73.** Superhump maxima of GO Com (2008).

E	max ^a	error	$O - C^b$	N^c
0	54631.0857	0.0006	0.0016	195
21	54632.4071	0.0005	-0.0010	94
22	54632.4693	0.0009	-0.0018	88
47	54634.0458	0.0043	-0.0015	195
48	54634.1132	0.0031	0.0028	118

^a BJD-2400000.^b Against $max = 2454631.0842 + 0.063047E$.^c Number of points used to determine the maximum.

the 2001 and 2003 superoutbursts.

6.41. TU Crateris

TU Crt had long been suspected to be an SU UMA-type candidate since the discovery (cf. Maza et al. 1992; Hazen 1993; Wenzel 1993). It was only in 1998 when its SU UMA-type nature was confirmed (Mennickent et al. 1998). Mennickent et al. (1998) reported an superhump period of 0.08535(5) d and P_{dot} of $-7.2(0.9) \times 10^{-5}$ (the reference apparently had an error in conversion from coefficients to P_{dot}).

We observed the 2001 and 2009 superoutbursts. The times of superhump maxima are listed in tables 78 and 79. The mean superhump period of the 2001 superoutburst determined with PDM method was 0.08532(8) d. The P_{dot} was $-12.3(9.2) \times 10^{-5}$.

A combined $O - C$ diagram is presented in figure 74. The early part of the 2001 superoutburst was likely missed and we shifted the $O - C$ diagram to best fit the 1998 superoutburst. None of observations yet recorded the epoch of stage A evolution.

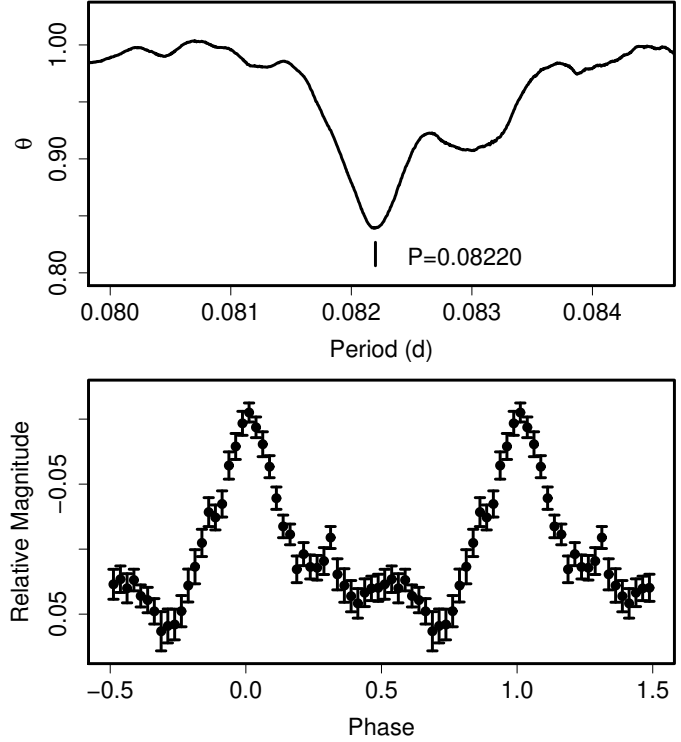
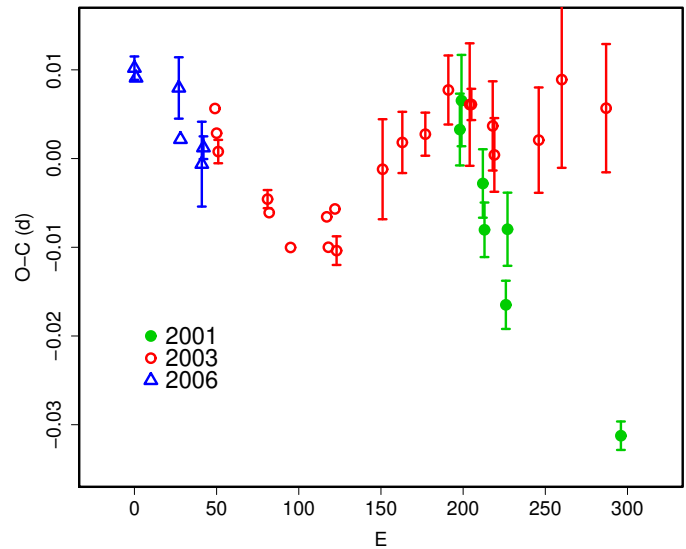
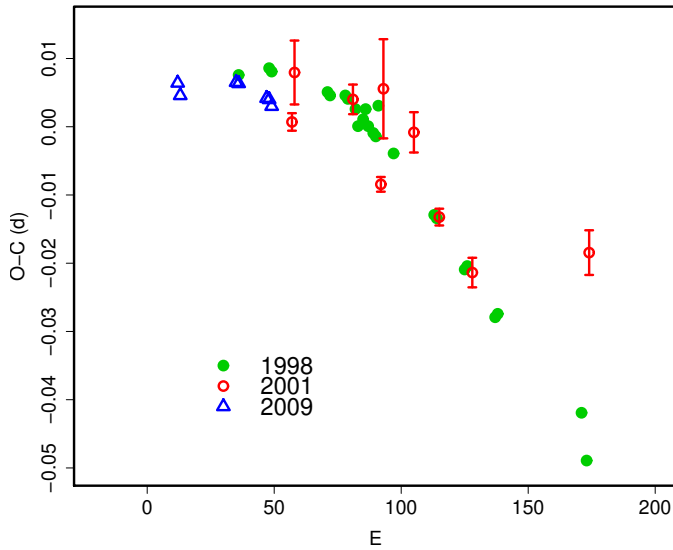
**Fig. 72.** Superhumps in V728 CrA (2003). (Upper): PDM analysis. (Lower): Phase-averaged profile.**Fig. 73.** Comparison of $O - C$ diagrams of VW CrB between different superoutbursts. A period of 0.07290 d was used to draw this figure. Approximate cycle counts (E) after the start of the superoutburst were used.

Table 74. Superhump maxima of V728 CrA (2003).

E	\max^a	error	$O - C^b$	N^c
0	52820.3295	0.0006	0.0006	36
1	52820.4098	0.0003	-0.0014	47
2	52820.4925	0.0003	-0.0011	47
12	52821.3170	0.0010	-0.0004	24
13	52821.4015	0.0010	0.0017	41
14	52821.4828	0.0006	0.0007	37
15	52821.5651	0.0004	0.0005	43
23	52822.2260	0.0005	0.0024	48
24	52822.3031	0.0005	-0.0028	41
25	52822.3891	0.0007	0.0008	47
26	52822.4706	0.0004	-0.0001	46
27	52822.5525	0.0005	-0.0005	43
35	52823.2133	0.0010	0.0012	41
36	52823.2926	0.0005	-0.0018	44
37	52823.3784	0.0005	0.0016	48
38	52823.4586	0.0006	-0.0006	48
39	52823.5405	0.0014	-0.0012	44
44	52823.9541	0.0005	0.0006	87
45	52824.0362	0.0005	0.0003	93
46	52824.1181	0.0007	-0.0001	60
48	52824.2860	0.0009	0.0030	46
49	52824.3637	0.0007	-0.0017	45
50	52824.4460	0.0008	-0.0017	45

^a BJD-2400000.^b Against $\max = 2452820.3288 + 0.082378E$.^c Number of points used to determine the maximum.**Table 75.** Superhump maxima of VW CrB (2003).

E	\max^a	error	$O - C^b$	N^c
0	52847.0644	0.0005	0.0103	134
1	52847.1345	0.0006	0.0075	135
2	52847.2053	0.0013	0.0053	122
32	52849.3870	0.0010	-0.0014	51
33	52849.4583	0.0009	-0.0029	52
46	52850.4021	0.0009	-0.0074	48
68	52852.0094	0.0008	-0.0050	260
69	52852.0788	0.0009	-0.0084	168
73	52852.3747	0.0008	-0.0043	47
74	52852.4429	0.0016	-0.0090	51
102	52854.4933	0.0056	-0.0011	51
114	52855.3711	0.0035	0.0014	32
c128	52856.3927	0.0024	0.0017	26
142	52857.4183	0.0039	0.0060	32
155	52858.3643	0.0069	0.0038	24
156	52858.4372	0.0018	0.0038	40
169	52859.3825	0.0050	0.0008	30
170	52859.4521	0.0042	-0.0025	27
197	52861.4221	0.0059	-0.0021	34
211	52862.4495	0.0099	0.0041	29
238	52864.4146	0.0072	-0.0003	40

^a BJD-2400000.^b Against $\max = 2452847.0541 + 0.072945E$.^c Number of points used to determine the maximum.**Fig. 74.** Comparison of $O - C$ diagrams of TU CrA between different superoutbursts. A period of 0.08550 d was used to draw this figure. Approximate cycle counts (E) after the start of the superoutburst were used.**Table 76.** Superhump maxima of VW CrB (2001).

E	\max^a	error	$O - C^b$	N^c
0	52087.1633	0.0034	-0.0025	89
69	52092.1822	0.0047	0.0136	112
82	52093.1104	0.0040	-0.0007	158
83	52093.1866	0.0051	0.0030	189
96	52094.1249	0.0039	-0.0012	199
97	52094.1926	0.0031	-0.0060	147
110	52095.1318	0.0027	-0.0094	142
111	52095.2133	0.0041	-0.0004	127
180	52100.2201	0.0016	0.0036	64

^a BJD-2400000.^b Against $\max = 2452087.1658 + 0.072504E$.^c Number of points used to determine the maximum.

Table 77. Superhump maxima of VW CrB (2006).

E	\max^a	error	$O - C^b$	N^c
0	53842.7528	0.0013	0.0001	10
1	53842.8246	0.0009	-0.0008	27
27	53844.7189	0.0035	0.0038	11
28	53844.7860	0.0009	-0.0018	27
41	53845.7309	0.0048	-0.0017	19
42	53845.8056	0.0013	0.0004	27

^a BJD-2400000.^b Against $\max = 2453842.7527 + 0.072679E$.^c Number of points used to determine the maximum.**Table 78.** Superhump maxima of TU Crt (2001).

E	\max^a	error	$O - C^b$	N^c
0	52010.0402	0.0013	-0.0070	101
1	52010.1329	0.0047	0.0005	69
24	52012.0955	0.0022	0.0040	109
35	52013.0235	0.0011	-0.0050	57
36	52013.1230	0.0073	0.0094	59
48	52014.1427	0.0030	0.0068	18
58	52014.9852	0.0012	-0.0024	158
71	52016.0886	0.0022	-0.0063	141

^a BJD-2400000.^b Against $\max = 2452010.0460 + 0.085175E$.^c Number of points used to determine the maximum.**Table 79.** Superhump maxima of TU Crt (2009).

E	\max^a	error	$O - C^b$	N^c
0	54881.1051	0.0001	0.0003	287
1	54881.1888	0.0002	-0.0014	173
23	54883.0717	0.0005	0.0015	205
24	54883.1570	0.0003	0.0014	261
35	54884.0954	0.0004	-0.0002	80
36	54884.1807	0.0005	-0.0003	86
37	54884.2652	0.0008	-0.0013	88

^a BJD-2400000.^b Against $\max = 2454881.1048 + 0.085452E$.^c Number of points used to determine the maximum.**Table 80.** Superhump maxima of TV Crv (2001).

E	\max^a	error	$O - C^b$	N^c
0	51960.2263	0.0019	-0.0148	55
1	51960.2923	0.0015	-0.0138	157
13	51961.0918	0.0010	0.0055	40
14	51961.1568	0.0002	0.0054	105
15	51961.2211	0.0003	0.0047	103
16	51961.2854	0.0003	0.0041	109
17	51961.3505	0.0005	0.0041	74
32	51962.3235	0.0010	0.0018	67
46	51963.2321	0.0004	0.0002	145
47	51963.2971	0.0008	0.0002	107
90	51966.0944	0.0012	0.0018	26
91	51966.1609	0.0010	0.0032	33
108	51967.2694	0.0008	0.0064	140
109	51967.3295	0.0016	0.0015	71
168	51971.1537	0.0025	-0.0103	88

^a BJD-2400000.^b Against $\max = 2451960.2411 + 0.065017E$.^c Number of points used to determine the maximum.**Table 81.** Superhump maxima of TV Crv (2003).

E	\max^a	error	$O - C^b$	N^c
0	52770.0238	0.0003	-0.0007	66
1	52770.0885	0.0003	-0.0009	66
2	52770.1534	0.0003	-0.0009	66
3	52770.2204	0.0007	0.0011	34
93	52776.0758	0.0024	0.0111	19
107	52776.9741	0.0032	0.0002	69
121	52777.8773	0.0010	-0.0059	152
122	52777.9413	0.0048	-0.0068	56
170	52781.0686	0.0017	0.0029	58

^a BJD-2400000.^b Against $\max = 2452770.0245 + 0.064948E$.^c Number of points used to determine the maximum.

6.4.2. TV Corvi

We reanalyzed the 2001, 2003 and 2004 data published in Uemura et al. (2005) (tables 80, 81 and 82). Regarding the 2001 superoutburst, we obtained a result similar to that in Uemura et al. (2005). The P_{dot} was $+6.2(1.5) \times 10^{-5}$ ($1 \leq E \leq 109$). We, however, obtained a different result for the 2004 superoutburst. The $O - C$ diagram was similar to that of 2001 one, contrary to the analysis in Uemura et al. (2005) (subsection 3.8; figure 18). We obtained $P_{\text{dot}} = +9.5(3.1) \times 10^{-5}$ ($16 \leq E \leq 103$), excluding the initial stage of early evolution (stage A) and last segment (stage C) after a period decrease.

6.4.3. V337 Cygni

Although V337 Cyg had long been registered as a dwarf nova, the identification of the true object was made only recently by J. Manek based on archival Sonneberg plate

Table 82. Superhump maxima of TV Crv (2004).

E	max ^a	error	$O - C^b$	N^c
0	53161.0000	0.0023	0.0153	118
1	53161.0532	0.0034	0.0036	120
16	53162.0201	0.0010	-0.0045	81
23	53162.4772	0.0010	-0.0023	40
25	53162.6056	0.0007	-0.0039	59
26	53162.6715	0.0007	-0.0030	67
40	53163.5796	0.0013	-0.0048	71
41	53163.6465	0.0011	-0.0029	59
42	53163.7117	0.0011	-0.0026	44
62	53165.0089	0.0008	-0.0053	34
86	53166.5737	0.0009	-0.0003	73
87	53166.6360	0.0094	-0.0030	39
88	53166.7068	0.0022	0.0028	36
102	53167.6177	0.0016	0.0038	70
103	53167.6882	0.0015	0.0094	63
117	53168.5850	0.0085	-0.0037	48
118	53168.6551	0.0009	0.0013	80

^a BJD-2400000.^b Against $max = 2453160.9847 + 0.064992E$.^c Number of points used to determine the maximum.**Table 83.** Superhump maxima of V337 Cyg (2006).

E	max ^a	error	$O - C^b$	N^c
0	53886.4495	0.0010	-0.0021	69
1	53886.5209	0.0014	-0.0008	61
4	53886.7305	0.0009	-0.0011	72
5	53886.8052	0.0010	0.0035	71
6	53886.8741	0.0009	0.0024	71
7	53886.9404	0.0012	-0.0012	72
28	53888.4064	0.0081	-0.0053	40
29	53888.4885	0.0014	0.0068	117
30	53888.5495	0.0009	-0.0023	119

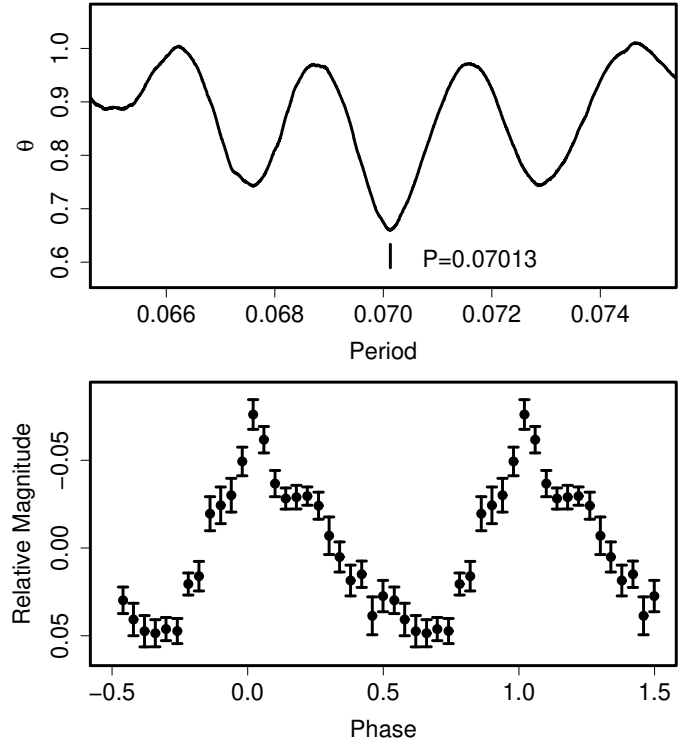
^a BJD-2400000.^b Against $max = 2453886.4516 + 0.070003E$.^c Number of points used to determine the maximum.

(vsnet 775, 780¹³; see also Boyd et al. 2007).

We analyzed the AAVSO data of the 2006 superoutburst, the same outburst reported in Boyd et al. (2007). These observations were performed during the late stage of the superoutburst, and the superhumps were most likely stage C superhumps. The times of maxima are given in table 83. The mean P_{SH} was determined with the PDM method to be 0.07013(3) d (figure 75). This outburst was followed by a rebrightening according to the AAVSO data. We might expect a positive P_{dot} if observations covered the earlier stage of this superoutburst.

6.44. V503 Cygni

Harvey et al. (1995) established the SU UMa-type nature of this object and reported a mean P_{SH} of 0.08101(4)

**Fig. 75.** Superhumps in V337 Cyg (2006). (Upper): PDM analysis. (Lower): Phase-averaged profile.

d.

We observed the 2002 July superoutburst. The times of superhump maxima are listed in table 84. Although the coverage of the observation was not sufficient, a likely stage B-C transition was recorded. The parameters are listed in table 2. The observation of the 2008 December superoutburst is given in table 85. There was an apparent break in the $O - C$ around $E = 49$. Due to the limited phase coverage, we determined superhump periods for the first (before BJD 2454824) and the second (after BJD 2454823) intervals with the PDM method. The periods were 0.081767(45) d and 0.081022(18) d, respectively. These periods were adopted in table 2.

This object is of particular interest since its supercycle is one of the next shortest to ER UMa stars and MN Dra (Harvey et al. 1995; Kato et al. 2002b) and there appears to be a hint of superhump evolution similar to ER UMa stars (Harvey et al. 1995, figure 7). It would be worth studying whether a phase reversal, or early emergence of stage C superhumps (cf. subsection 4.9), also takes place in this system.

6.45. V550 Cygni

Although V550 Cyg had long been known as a dwarf nova, the supposed identification became available only in 1999 (Skiff 1999). Two outbursts were detected in 2000 (vsnet-alert 3993, 5191). Superhumps were detected during the August outburst (vsnet-alert 5196). H. Yamaoka provided astrometry from outburst images (vsnet-alert

¹³ <<http://www.kusastro.kyoto-u.ac.jp/vsnet/DNe/v337cyg.html>>

Table 84. Superhump maxima of V503 Cyg (2002).

E	max ^a	error	$O - C^b$	N^c
0	52478.2155	0.0004	-0.0110	312
13	52479.2861	0.0014	0.0047	196
17	52479.5975	0.0047	-0.0085	28
18	52479.7013	0.0036	0.0142	28
25	52480.2501	0.0008	-0.0051	309
30	52480.6656	0.0008	0.0047	44
31	52480.7429	0.0006	0.0009	55
37	52481.2303	0.0009	0.0014	324
38	52481.3145	0.0008	0.0044	180
49	52482.2026	0.0007	-0.0000	238
76	52484.3913	0.0008	-0.0023	50
77	52484.4713	0.0014	-0.0034	65

^a BJD-2400000.^b Against $max = 2452478.2265 + 0.081145E$.^c Number of points used to determine the maximum.**Table 85.** Superhump maxima of V503 Cyg (2008).

E	max ^a	error	$O - C^b$	N^c
0	54819.9455	0.0012	-0.0035	81
36	54822.8735	0.0017	0.0029	78
49	54823.9288	0.0010	0.0033	100
98	54827.8995	0.0017	-0.0027	64

^a BJD-2400000.^b Against $max = 2454819.9490 + 0.081155E$.^c Number of points used to determine the maximum.

5210), which slightly differed from the position in Skiff (1999), making the full amplitude of outbursts larger than five magnitudes.

The mean superhump period with the PDM method was 0.06871(6) d (figure 76). The times of superhump maxima are listed in table 86. The outburst was apparently observed during its middle-to-late course, and a stage B-C transition was recorded. The mean P_{SH} for stages B and C were 0.06917(26) d and 0.06848(6) d, respectively.

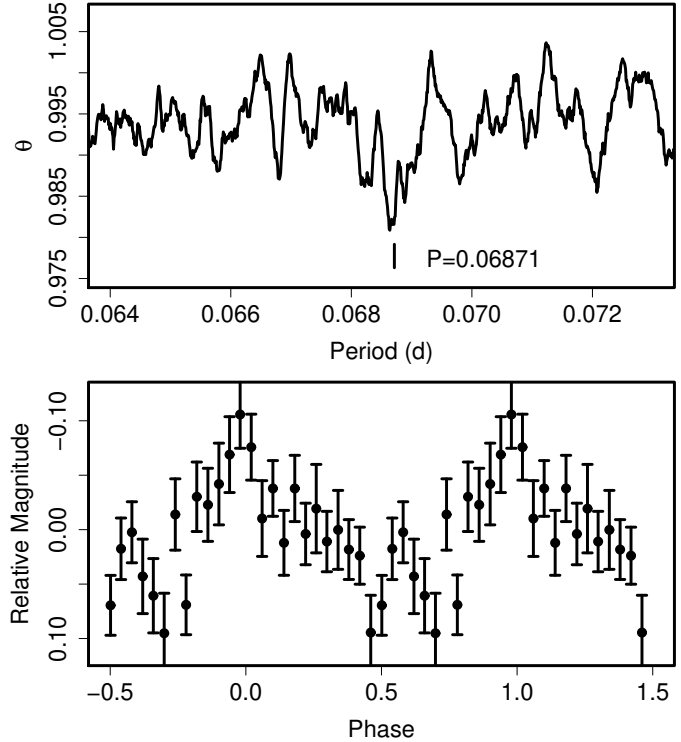
6.46. V630 Cygni

The SU UMa-type nature of this dwarf nova was established by Nogami et al. (2001a). The times of superhump maxima during the 1996 superoutburst measured from these data are listed in table 87.

We further observed the 2008 superoutburst (table 88). The $O - C$'s apparently showed a stage B-C transition. The mean P_{SH} and P_{dot} for the stage B were 0.07918(7) d and $+27.4(7.7) \times 10^{-5}$, respectively. Since the value was derived from a limited sample, the large positive P_{dot} needs to be confirmed by further observations.

6.47. V632 Cygni

The SU UMa-type nature of this dwarf nova had long been suggested (cf. Wenzel 1989 for a historical record of

**Fig. 76.** Superhumps in V550 Cyg (2000). (Upper): PDM analysis. (Lower): Phase-averaged profile.**Table 86.** Superhump maxima of V550 Cyg (2000).

E	max ^a	error	$O - C^b$	N^c
0	51777.0086	0.0018	-0.0003	129
14	51777.9680	0.0011	-0.0031	148
15	51778.0417	0.0016	0.0018	149
16	51778.0926	0.0011	-0.0161	147
17	51778.1784	0.0040	0.0010	147
18	51778.2396	0.0018	-0.0066	265
32	51779.2210	0.0088	0.0126	87
33	51779.2910	0.0094	0.0138	116
35	51779.4164	0.0011	0.0017	34
50	51780.4497	0.0009	0.0040	41
61	51781.2028	0.0015	0.0009	104
62	51781.2697	0.0044	-0.0009	124
64	51781.4099	0.0016	0.0018	11
65	51781.4741	0.0014	-0.0027	26
76	51782.2311	0.0088	-0.0019	106
79	51782.4381	0.0012	-0.0010	35
91	51783.2589	0.0143	-0.0051	130

^a BJD-2400000.^b Against $max = 2451777.0088 + 0.068738E$.^c Number of points used to determine the maximum.

Table 87. Superhump maxima of V630 Cyg (1996).

E	max ^a	error	$O - C^b$	N^c
0	50313.9866	0.0012	0.0007	52
1	50314.0667	0.0012	0.0014	45
16	50315.2506	0.0014	-0.0045	55
29	50316.2887	0.0063	0.0024	34

^a BJD-2400000.^b Against $max = 2450313.9860 + 0.079320E$.^c Number of points used to determine the maximum.**Table 88.** Superhump maxima of V630 Cyg (2008).

E	max ^a	error	$O - C^b$	N^c
0	54690.0683	0.0007	-0.0053	129
12	54691.0151	0.0006	-0.0040	81
25	54692.0444	0.0007	0.0010	112
26	54692.1213	0.0004	-0.0009	167
39	54693.1564	0.0261	0.0099	10
40	54693.2342	0.0052	0.0088	70
51	54694.0912	0.0055	-0.0009	51
76	54696.0586	0.0007	-0.0034	165
77	54696.1350	0.0009	-0.0057	118
103	54698.1900	0.0113	0.0005	115

^a BJD-2400000.^b Against $max = 2454690.0736 + 0.078795E$.^c Number of points used to determine the maximum.

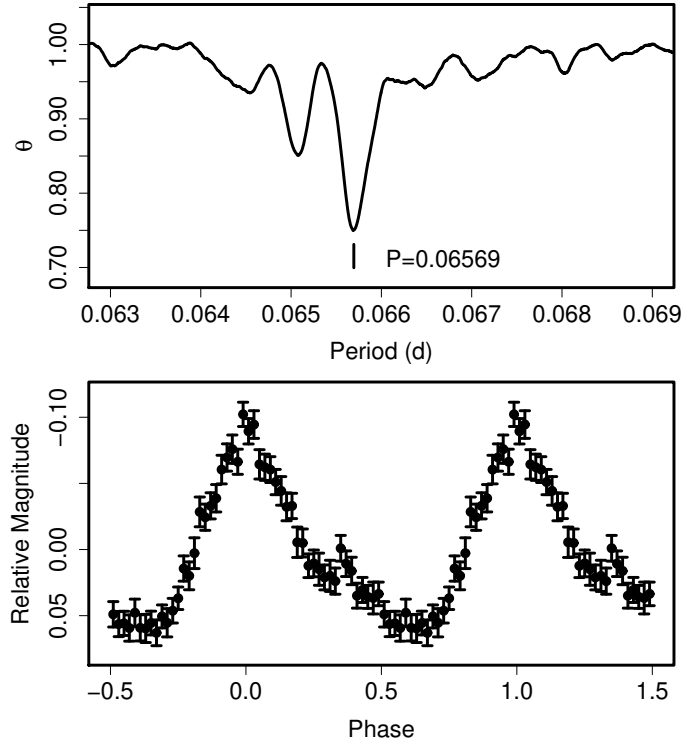
bright outbursts). Sheets et al. (2007) determined its orbital period to be 0.06377(8) d. The SU UMa-type nature was finally established during the 2008 superoutburst.

The global mean superhump period during the 2008 superoutburst was 0.065695(6) d (PDM method, figure 77). The times of superhump maxima are listed in table 89. Although the stage A-B and B-C transitions were observed, a gap in the middle of the stage B makes determination of P_{dot} rather uncertain. The value for $16 \leq E \leq 82$ was $+17.4(3.0) \times 10^{-5}$.

6.48. V1028 Cygni

Baba et al. (2000) reported the detection of positive period derivative during the 1995 superoutburst. This outburst was indeed one of the earliest with significantly positive P_{dot} 's. We reanalyzed the data, combined with the AAVSO observations, for an improvement of the parameters. The results generally confirmed the conclusion by Baba et al. (2000) (table 90). The P_{dot} for the interval $15 \leq E \leq 148$ (stage B) was $+8.2(1.2) \times 10^{-5}$.

We further analyzed the 1996, 1999, 2001, 2002, 2004 and 2008 superoutbursts (tables 91, 92, 93, 94, 95, 96). The observation in 2001 and 2002 covered the middle-to-late portion of the superoutburst, and the $O - C$ diagram commonly showed a transition to a shorter period (stage C). For the 1999 and 2002 superoutbursts, we obtained P_{dot} before this transition as follows: $P_{\text{dot}} = +12.2(3.1) \times 10^{-5}$ (1999, $E \leq 148$) and $P_{\text{dot}} = +14.7(5.5) \times 10^{-5}$ (2002,

**Fig. 77.** Superhumps in V632 Cyg (2008). (Upper): PDM analysis. (Lower): Phase-averaged profile.

$E \leq 55$). Although the 1996 and 2004 superoutbursts were preceded by a distinct precursor, only the late stage of the superoutburst was meaningfully observed.

A comparison of $O - C$ diagrams is shown in figure 78. There appears to be a slight variation in the $O - C$ behavior during the late stage (stage B-C). This may have been caused by the difference in the extent between superoutbursts.

6.49. V1113 Cygni

We have reanalyzed the observation in Kato et al. (1996c) and obtained new observations during the 2008 superoutburst. Both observations covered the relatively early stages of the superoutbursts. The times of superhump maxima are listed in tables 97 and 98, respectively. The resultant global P_{dot} 's were $-19.2(6.8) \times 10^{-5}$ and $-5.2(4.7) \times 10^{-5}$, respectively. The former strongly negative value can be interpreted as a result of a possible stage A-B transition.

6.50. V1251 Cygni

The history of V1251 Cyg was summarized in Kato (1995c). Only five outbursts (1963, 1991, 1994-1995, 1997 and 2008) have been recorded. All of these outbursts were superoutbursts, and were associated with a rebrightening (1997, 2008). Despite the long P_{SH} , Kato et al. (2001d) included this object as a candidate WZ Sge-type dwarf nova based on the long recurrence time, the large outburst amplitude and the lack of normal outbursts.

Table 89. Superhump maxima of V632 Cyg (2008).

E	max ^a	error	$O - C^b$	N^c
0	54782.3640	0.0079	-0.0094	112
1	54782.4310	0.0048	-0.0081	69
9	54782.9596	0.0014	-0.0052	35
13	54783.2258	0.0003	-0.0018	125
14	54783.2922	0.0005	-0.0010	102
15	54783.3567	0.0007	-0.0023	96
16	54783.4264	0.0018	0.0017	39
23	54783.8856	0.0003	0.0010	106
24	54783.9505	0.0003	0.0002	129
30	54784.3441	0.0005	-0.0004	63
31	54784.4103	0.0005	0.0001	155
32	54784.4755	0.0008	-0.0004	81
65	54786.6457	0.0008	0.0016	46
66	54786.7131	0.0008	0.0033	64
67	54786.7801	0.0007	0.0047	55
80	54787.6374	0.0005	0.0078	55
81	54787.7034	0.0006	0.0081	66
82	54787.7729	0.0016	0.0119	31
104	54789.2107	0.0004	0.0042	105
105	54789.2759	0.0008	0.0037	115
106	54789.3450	0.0020	0.0071	46
110	54789.6027	0.0006	0.0020	45
111	54789.6694	0.0006	0.0031	68
112	54789.7352	0.0007	0.0031	69
115	54789.9278	0.0011	-0.0014	36
116	54789.9920	0.0009	-0.0029	49
130	54790.9178	0.0013	0.0031	123
131	54790.9802	0.0013	-0.0002	128
145	54791.8925	0.0013	-0.0077	63
156	54792.6065	0.0014	-0.0165	48
157	54792.6792	0.0020	-0.0095	32

^a BJD-2400000.^b Against $max = 2454782.3734 + 0.065702E$.^c Number of points used to determine the maximum.**Table 90.** Superhump maxima of V1028 Cyg (1995).

E	max ^a	error	$O - C^b$	N^c
0	49929.0867	0.0014	-0.0077	48
1	49929.1451	0.0023	-0.0111	77
2	49929.2117	0.0007	-0.0063	124
3	49929.2781	0.0010	-0.0016	125
15	49930.0276	0.0004	0.0067	35
16	49930.0905	0.0002	0.0078	95
17	49930.1525	0.0002	0.0081	30
19	49930.2751	0.0011	0.0072	46
33	49931.1344	0.0006	0.0017	32
34	49931.1978	0.0004	0.0034	75
67	49933.2288	0.0006	-0.0040	80
68	49933.2906	0.0008	-0.0039	49
83	49934.2176	0.0006	-0.0034	76
84	49934.2760	0.0009	-0.0068	81
98	49935.1431	0.0009	-0.0045	136
100	49935.2663	0.0009	-0.0047	124
114	49936.1419	0.0016	0.0061	75
115	49936.1957	0.0026	-0.0019	62
116	49936.2584	0.0034	-0.0009	63
130	49937.1227	0.0053	-0.0013	16
132	49937.2489	0.0023	0.0014	31
139	49937.6846	0.0030	0.0047	15
140	49937.7445	0.0024	0.0028	17
141	49937.8140	0.0032	0.0105	13
147	49938.1770	0.0025	0.0029	32
148	49938.2405	0.0017	0.0047	31
154	49938.6106	0.0016	0.0041	17
155	49938.6717	0.0031	0.0035	18
156	49938.7341	0.0030	0.0042	17
162	49939.1010	0.0014	0.0005	24
163	49939.1637	0.0016	0.0014	32
164	49939.2272	0.0051	0.0032	29
188	49940.6966	0.0041	-0.0099	30
189	49940.7534	0.0132	-0.0148	12
194	49941.0751	0.0021	-0.0019	20
195	49941.1389	0.0080	0.0000	22

^a BJD-2400000.^b Against $max = 2449929.0944 + 0.061766E$.^c Number of points used to determine the maximum.

We observed the 1991 (Kato 1995c), 1994–1995, and 2008 superoutbursts. The 1995 observation was performed on single night, only confirming the presence of a superhump. The times of superhump maxima (refined times for the 1991 superoutburst) are listed in tables 99 and 100.

The 2008 superoutburst was clearly composed of stages B and C. The mean P_{SH} and P_{dot} for the stage B were 0.07597(2) d and $+6.0(2.7) \times 10^{-5}$, respectively. ($0 \leq E \leq 62$). The last part of the stage C includes superhumps during the rapid fading stage ($E = 141$) and the post-superoutburst stage ($E = 153, 154$). A phase shift expected for traditional late superhumps was not recorded. It took five days ordinary superhumps (figure 79) to appear after the onset of the outburst, which is unusually long for an SU UMa-type dwarf nova with this P_{SH} (this anomaly was already addressed in Kato 1991b). During this stage, double-wave modulations similar to early superhumps in WZ Sge-type dwarf novae were observed (figure 80). The

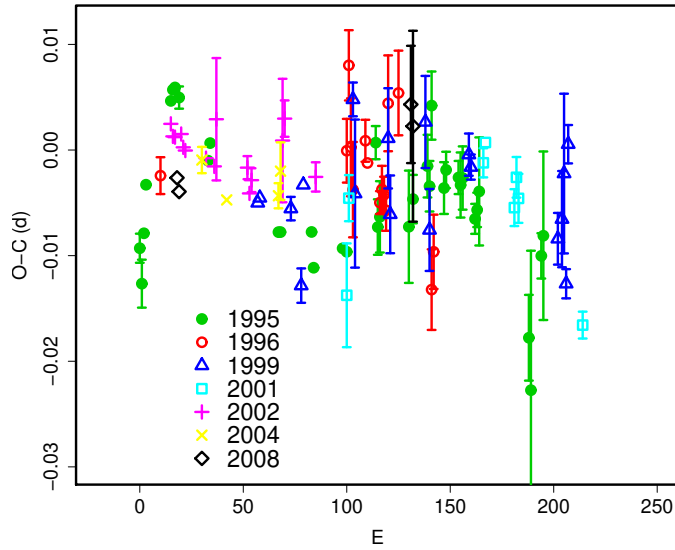


Fig. 78. Comparison of $O - C$ diagrams of V1028 Cyg between different superoutbursts. A period of 0.06180 d was used to draw this figure. Approximate cycle counts (E) after the start of the superoutburst (the start of the main superoutburst when preceded by a precursor) were used. The E for the 2008 superoutburst was somewhat uncertain due to the lack of observations at the early stage.

Table 92. Superhump maxima of V1028 Cyg (1999).

E	\max^a	error	$O - C^b$	N^c
0	51427.4199	0.0011	0.0277	110
45	51430.1621	0.0006	-0.0079	121
46	51430.2243	0.0008	-0.0074	122
61	51431.1503	0.0011	-0.0074	120
66	51431.4520	0.0016	-0.0143	109
67	51431.5234	0.0007	-0.0047	83
91	51433.0147	0.0016	0.0051	61
92	51433.0675	0.0070	-0.0038	79
108	51434.0616	0.0047	0.0026	99
109	51434.1162	0.0037	-0.0046	122
126	51435.1755	0.0044	0.0054	121
128	51435.2889	0.0039	-0.0047	94
147	51436.4702	0.0020	0.0038	82
148	51436.5309	0.0012	0.0026	94
190	51439.1197	0.0024	-0.0012	98
192	51439.2451	0.0046	0.0008	38
193	51439.3112	0.0076	0.0052	32
194	51439.3626	0.0014	-0.0052	61
195	51439.4376	0.0018	0.0081	85

^a BJD-2400000.

^b Against $\max = 2451427.3922 + 0.061730E$.

^c Number of points used to determine the maximum.

Table 91. Superhump maxima of V1028 Cyg (1996).

E	\max^a	error	$O - C^b$	N^c
0	50308.0425	0.0017	-0.0049	33
90	50313.6069	0.0030	0.0015	17
91	50313.6768	0.0033	0.0097	19
92	50313.7308	0.0046	0.0019	16
93	50313.7886	0.0045	-0.0020	14
99	50314.1640	0.0020	0.0029	59
100	50314.2237	0.0008	0.0008	59
106	50314.5908	0.0011	-0.0027	19
107	50314.6538	0.0022	-0.0014	19
108	50314.7151	0.0017	-0.0018	15
109	50314.7754	0.0019	-0.0033	19
110	50314.8474	0.0045	0.0069	18
115	50315.1574	0.0040	0.0081	49
131	50316.1275	0.0038	-0.0098	42
132	50316.1929	0.0035	-0.0062	47

^a BJD-2400000.

^b Against $\max = 2450308.0473 + 0.061755E$.

^c Number of points used to determine the maximum.

Table 93. Superhump maxima of V1028 Cyg (2001).

E	\max^a	error	$O - C^b$	N^c
0	52261.5987	0.0049	-0.0077	17
1	52261.6697	0.0022	0.0015	11
66	52265.6900	0.0014	0.0048	15
67	52265.7537	0.0007	0.0067	14
81	52266.6128	0.0017	0.0005	15
82	52266.6774	0.0019	0.0034	16
83	52266.7372	0.0023	0.0014	13
114	52268.6410	0.0013	-0.0106	14

^a BJD-2400000.

^b Against $\max = 2452261.6064 + 0.061800E$.

^c Number of points used to determine the maximum.

Table 94. Superhump maxima of V1028 Cyg (2002).

E	\max^a	error	$O - C^b$	N^c
0	52618.5958	0.0004	0.0016	27
1	52618.6564	0.0005	0.0004	31
2	52618.7181	0.0007	0.0004	22
5	52618.9038	0.0009	0.0008	159
6	52618.9644	0.0005	-0.0004	233
7	52619.0259	0.0007	-0.0007	116
17	52619.6431	0.0009	-0.0011	25
21	52619.8896	0.0008	-0.0017	112
22	52619.9558	0.0058	0.0028	86
37	52620.8782	0.0011	-0.0012	116
38	52620.9376	0.0009	-0.0036	218
39	52621.0007	0.0011	-0.0023	105
54	52621.9314	0.0058	0.0020	153
55	52621.9953	0.0017	0.0041	107
70	52622.9168	0.0014	-0.0009	121

^a BJD-2400000.^b Against $\max = 2452618.5942 + 0.061763E$.^c Number of points used to determine the maximum.**Table 95.** Superhump maxima of V1028 Cyg (2004).

E	\max^a	error	$O - C^b$	N^c
0	53321.9325	0.0012	0.0014	87
12	53322.6703	0.0009	-0.0020	60
37	53324.2157	0.0012	-0.0009	39
38	53324.2798	0.0027	0.0015	48

^a BJD-2400000.^b Against $\max = 2453321.9311 + 0.061770E$.^c Number of points used to determine the maximum.**Table 96.** Superhump maxima of V1028 Cyg (2008).

E	\max^a	error	$O - C^b$	N^c
0	54828.3145	0.0003	0.0007	127
1	54828.3750	0.0002	-0.0007	99
113	54835.3049	0.0056	0.0011	68
114	54835.3646	0.0090	-0.0011	38

^a BJD-2400000.^b Against $\max = 2454828.3138 + 0.061858E$.^c Number of points used to determine the maximum.**Table 97.** Superhump maxima of V1113 Cyg (1994).

E	\max^a	error	$O - C^b$	N^c
0	49598.0086	0.0022	-0.0046	24
14	49599.1249	0.0007	0.0022	29
26	49600.0790	0.0005	0.0052	47
51	49602.0541	0.0005	-0.0009	35
64	49603.0835	0.0005	-0.0018	25

^a BJD-2400000.^b Against $\max = 2449598.0132 + 0.079253E$.^c Number of points used to determine the maximum.**Table 98.** Superhump maxima of V1113 Cyg (2008).

E	\max^a	error	$O - C^b$	N^c
0	54757.2763	0.0003	-0.0012	109
1	54757.3568	0.0004	0.0002	139
2	54757.4356	0.0004	-0.0001	135
8	54757.9108	0.0005	0.0009	143
9	54757.9866	0.0008	-0.0024	81
13	54758.3069	0.0003	0.0017	156
14	54758.3849	0.0004	0.0007	159
21	54758.9386	0.0009	0.0010	118
34	54759.9650	0.0009	-0.0002	155
46	54760.9125	0.0013	-0.0014	73
47	54760.9936	0.0009	0.0007	68

^a BJD-2400000.^b Against $\max = 2454757.2775 + 0.079051E$.^c Number of points used to determine the maximum.

period (0.07433(6) d, vsnet-alert 10612; refined in this paper) is 2.2 % shorter than the above P_{SH} and can be good candidate for P_{orb} . Despite its long P_{SH} , V1251 Cyg is extremely analogous to WZ Sge-type dwarf novae. The implication for the presence of such a long- P_{SH} WZ Sge-like objects was discussed in Ishioka et al. (2001), Kato (2002a). Compared to the 2008 superoutburst, only later half of the stage B was likely recorded during the 1991 superoutburst (figure 81).

6.51. V1316 Cygni

Although V1316 Cyg was listed as an SU UMa-type dwarf nova in the GCVS (Kholopov et al. 1985), the misidentification on the original discovery paper (Romano 1969) led to a long-lasting confusion. Henden, Honeycutt (1997) suggested a nearby faint blue star to be the genuine V1316 Cyg, whose variability in quiescence was confirmed in 2000 (B. Sumner, AAVSO discussion message). This suggestion was confirmed by the later detection of an outburst in 2002 (M. Moriyama, vsnet-campaign-dn 2910). Subsequent observations starting in 2003 recorded a number of outbursts. It has now been established that the object a short cycle length of outbursts (Shears et al. 2006) as originally reported by Romano (1969).

Boyd et al. (2008a) observed the 2006 superoutburst of this object and reported a phase shift around $E = 90$,

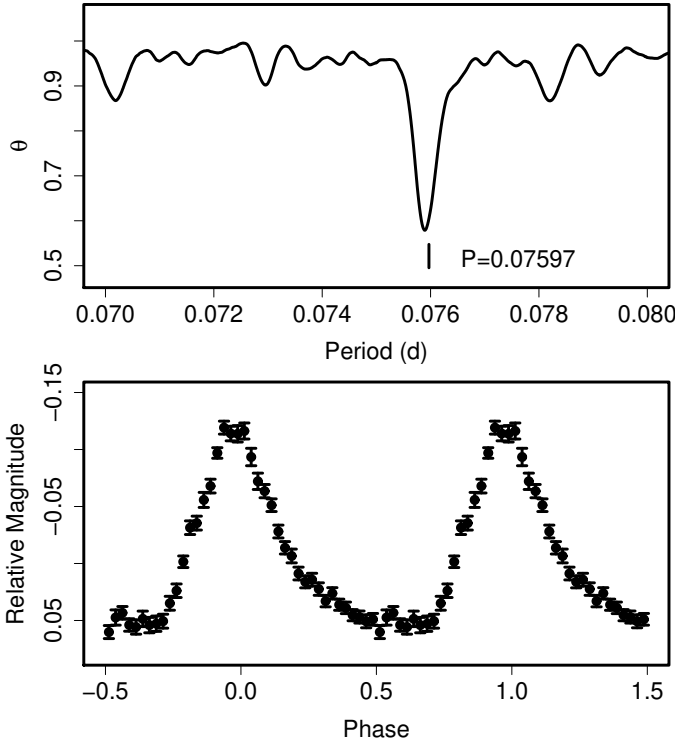


Fig. 79. Ordinary superhumps in V1251 Cyg (2008). (Upper): PDM analysis. (Lower): Phase-averaged profile.

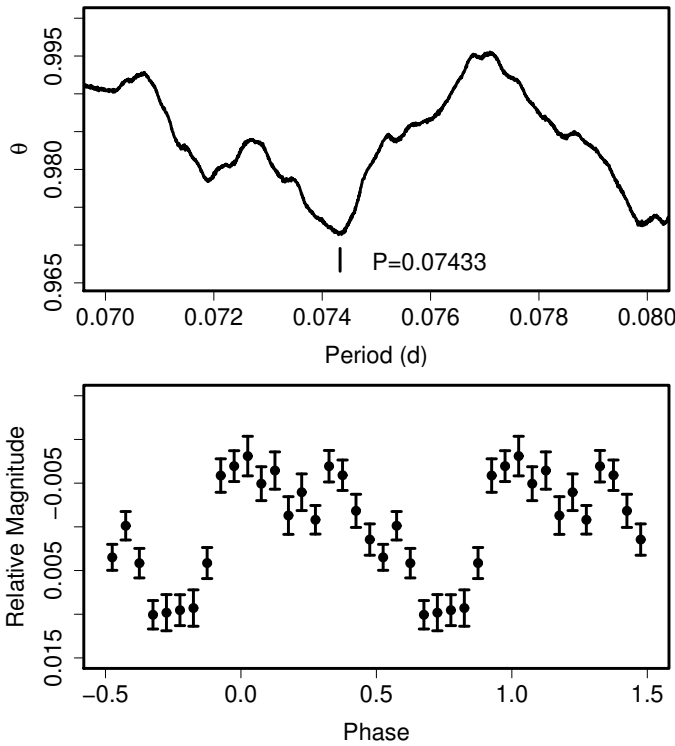


Fig. 80. Early superhumps in V1251 Cyg (2008). (Upper): PDM analysis. (Lower): Phase-averaged profile.

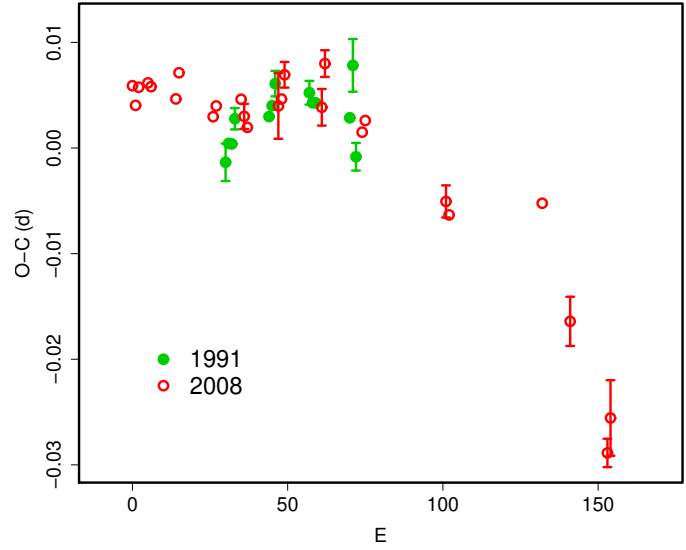


Fig. 81. Comparison of $O - C$ diagrams of V1251 Cyg between different superoutbursts. A period of 0.06180 d was used to draw this figure. Approximate cycle counts (E , estimated ones for the 1991 superoutbursts) after the appearance of superhumps were used.

Table 99. Superhump maxima of V1251 Cyg (1991).

E	\max^a	error	$O - C^b$	N^c
0	48563.8754	0.0018	-0.0029	33
1	48563.9532	0.0005	-0.0012	75
2	48564.0291	0.0009	-0.0013	68
3	48564.1075	0.0010	0.0010	65
14	48564.9435	0.0008	0.0004	71
15	48565.0205	0.0007	0.0014	75
16	48565.0986	0.0012	0.0034	72
27	48565.9335	0.0011	0.0017	67
28	48566.0085	0.0008	0.0007	74
29	48566.0845	0.0009	0.0006	54
40	48566.9188	0.0009	-0.0016	50
41	48566.9998	0.0025	0.0032	46
42	48567.0671	0.0013	-0.0055	43

^a BJD-2400000.

^b Against $\max = 2448563.8783 + 0.076054E$.

^c Number of points used to determine the maximum.

Table 100. Superhump maxima of V1251 Cyg (2008).

E	\max^a	error	$O - C^b$	N^c
0	54764.3130	0.0003	-0.0038	264
1	54764.3871	0.0004	-0.0055	295
2	54764.4648	0.0002	-0.0036	312
5	54764.6931	0.0002	-0.0027	139
6	54764.7688	0.0002	-0.0028	151
14	54765.3755	0.0004	-0.0026	106
15	54765.4539	0.0003	0.0000	131
26	54766.2855	0.0004	-0.0022	80
27	54766.3625	0.0005	-0.0010	74
35	54766.9710	0.0009	0.0010	131
36	54767.0454	0.0012	-0.0005	138
37	54767.1203	0.0007	-0.0013	179
47	54767.8821	0.0031	0.0024	141
48	54767.9588	0.0009	0.0032	418
49	54768.0370	0.0012	0.0057	41
61	54768.9457	0.0017	0.0047	83
62	54769.0258	0.0013	0.0090	51
74	54769.9311	0.0007	0.0046	275
75	54770.0082	0.0006	0.0059	362
101	54771.9760	0.0015	0.0027	274
102	54772.0507	0.0003	0.0016	156
132	54774.3312	0.0008	0.0079	135
141	54775.0039	0.0023	-0.0018	87
153	54775.9032	0.0013	-0.0122	118
154	54775.9824	0.0036	-0.0087	143

^a BJD-2400000.^b Against $\max = 2454764.3168 + 0.075807E$.^c Number of points used to determine the maximum.

which they interpreted as the appearance of (traditional) late superhumps. The phase shift was so large that it is difficult to attribute it to the stage B period increase. The relatively early appearance of late superhumps, or the occurrence of a phase reversal, is somewhat reminiscent to ER UMa (section 4.9). Judging from the short (~ 10 d) outburst (Shears et al. 2006), this object appears to have a high mass-transfer rate that could enable ER UMa-like evolution of superhumps. The other parameters, such as the duration of the superoutburst and P_{SH} are, however, unlike those of ER UMa and resemble those of a long P_{SH} -system BF Ara (Kato et al. 2003a). Since Boyd et al. (2008a) used a different method in extracting maxima times, a reanalysis of their data and tracking maxima of the original superhumps as in ER UMa (section 4.9) might be helpful in better understanding this system and its relation to ER UMa. We identified the period for $E \geq 94$ as the stage C superhumps and listed in table 2.

6.52. V1454 Cygni

V1454 Cyg is a poorly-known dwarf nova. Although discovery observations suggested the existence of long and short outbursts resembling an SU UMa-type dwarf nova (Pinto, Romano 1972; Loser 1979), spectroscopic observation could not confirm the CV nature of the suggested

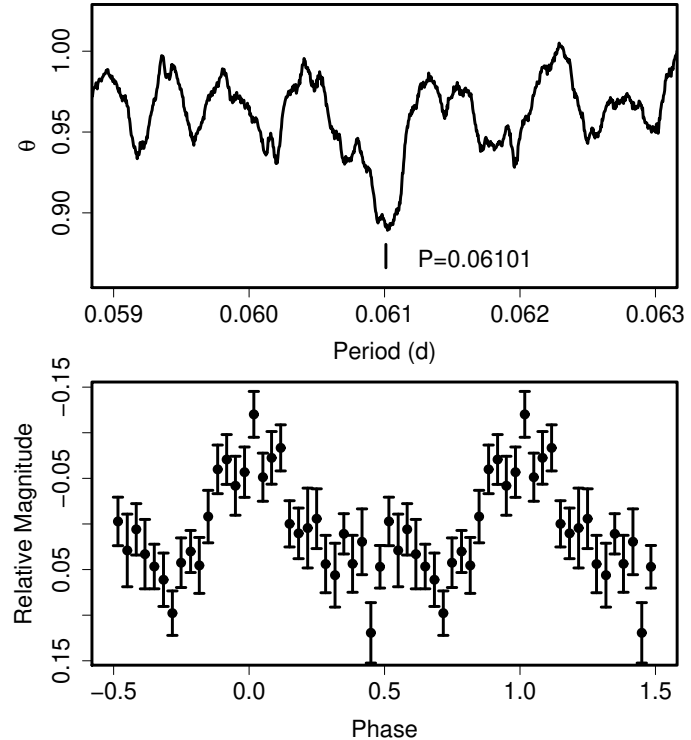


Fig. 82. Superhumps in V1454 Cyg (2006) for BJD 2454070.5–2454076.5. (Upper): PDM analysis. (Lower): Phase-averaged profile.

quiescent counterpart (Liu et al. 1999; this later turned out to be a false identification).

The object underwent a long, bright outburst in 1996 (vsnet-obs 4039). During the 2006 outburst, announced by J. Shears (November 23), one of the authors (Njh) undertook time-resolved CCD photometry, and detected superhumps. During the first seven days, the superhump signal was very weak. The superhumps showed a remarkable growth on December 1 and were followed until December 6. On December 11, the object showed a trend of rebrightening around the termination of the plateau stage (cf. Kato et al. 2003c). We used the data for December 1–6 to determine the superhump period and its variation. A PDM analysis yielded a mean period of 0.06101(2) d (figure 82). One-day aliases appear to be excluded from the December 1 data. The times of maxima identified with this P_{SH} are listed in table 101, likely composed of a stage B–C transition and a possible stage A observation at $E = 0$. The P_{dot} for $113 \leq E \leq 196$ (stage B) was $+15.0(4.3) \times 10^{-5}$.

6.53. V1504 Cygni

Rajkov, Yushchenko (1987) suggested that this object is an SU UMa-type dwarf nova based on the presence of two types of outbursts. Nogami, Masuda (1997) indeed confirmed the presence of superhumps during the 1994 outburst. Thorstensen, Taylor (1997) reported spectroscopic orbital period. Since the alias selection was incorrect in

Table 101. Superhump maxima of V1454 Cyg (2006).

E	\max^a	error	$O - C^b$	N^c
0	54063.9562	0.0019	-0.0274	83
113	54070.8827	0.0008	0.0113	88
114	54070.9395	0.0012	0.0071	87
135	54072.2185	0.0007	0.0061	23
163	54073.9221	0.0048	0.0029	84
179	54074.9054	0.0017	0.0110	88
195	54075.8850	0.0020	0.0153	66
196	54075.9445	0.0031	0.0138	66
234	54078.2569	0.0024	0.0100	34
261	54079.8787	0.0221	-0.0140	49
262	54079.9336	0.0047	-0.0201	73
278	54080.9128	0.0027	-0.0161	89

^a BJD-2400000.^b Against $\max = 2454063.9836 + 0.060955E$.^c Number of points used to determine the maximum.**Table 102.** Superhump maxima of V1504 Cyg (2008).

E	\max^a	error	$O - C^b$	N^c
0	54710.1735	0.0004	-0.0001	143
13	54711.1116	0.0009	0.0016	189
14	54711.1805	0.0011	-0.0015	134

^a BJD-2400000.^b Against $\max = 2454710.1736 + 0.072028E$.^c Number of points used to determine the maximum.

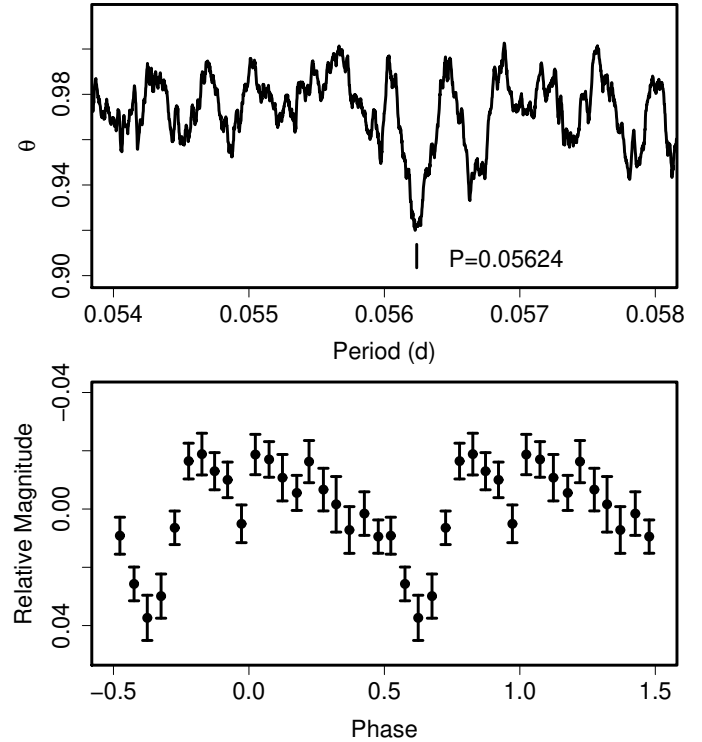
Nogami, Masuda (1997), we (re)analyzed the 1994, 2008 and 2009 superoutbursts (tables 102, 103) to determine the superhump period. The results are summarized in table 2. The 1994 and 2008 superoutbursts were probably observed during the stage B, and the 2009 was probably observed during the stage C. Pavlenko et al. (2002) also reported correct period identification.

6.54. V2176 Cygni

V2176 Cyg was discovered by Hu et al. (1997). Vanmunster, Sarneczky (1997) reported the detection of superhumps with a period of 0.0561(4) d. The object soon entered a 2-mag “dip” characteristic to a WZ Sge-type outburst (type-A outburst) and exhibited a long-lasting second plateau stage following a short precursor-like maxi-

Table 103. Superhump maxima of V1504 Cyg (2009).

E	\max^a	error	$O - C^b$	N^c
0	54950.2615	0.0011	0.0000	142
41	54953.2040	0.0019	-0.0005	97
42	54953.2768	0.0015	0.0005	132

^a BJD-2400000.^b Against $\max = 2454950.2615 + 0.071782E$.^c Number of points used to determine the maximum.**Fig. 83.** Superhumps in V2176 Cyg after the dip (1997). (Upper): PDM analysis. (Lower): Phase-averaged profile.

mum (Novák et al. 2001). Since only insufficient data were available before the dip, we analyzed the second plateau stage. The data used for analysis were from AAVSO database and ones extracted from electronic figures in Novák et al. (2001) (the data for their figure 3 were not included for analysis). A PDM analysis after removing the overall trend yielded a strong periodicity of 0.056239(12) d. The period agrees with that by Vanmunster, Sarneczky (1997) within their errors, and we regard it as a refined value of P_{SH} . The times of superhump maxima are listed in table 104.

We also determined times of maxima during the initial superoutburst plateau using the data in Kwast, Semeniuk (1998) (table 105). These maxima could not be directly linked by the above period. By assuming phase continuity, we obtained a mean period of 0.05607(5) d between BJD 2450696 and 2450703. Since early observations by Vanmunster, Sarneczky (1997) are unavailable, the possibility remains open whether the P_{SH} increased after the dip, or whether there was a phase discontinuity. By allowing a 0.5 phase shift, the period from the combined data is 0.05630(4) d.

6.55. HO Delphini

Kato et al. (2003c) reported on three superoutbursts in 1994, 1996 and 2001. Kato et al. (2003c) did not attempt to determine P_{dot} because of the decaying signal of the superhumps. We present times of superhump maxima for the 1994 and 2001 superoutbursts (tables 106, 107).

Table 104. Superhump maxima of V2176 Cyg after the dip (1997).

E	\max^a	error	$O - C^b$	N^c
0	50702.4013	0.0063	0.0121	–
1	50702.4365	0.0018	–0.0089	–
3	50702.5537	0.0013	–0.0043	–
4	50702.5991	0.0020	–0.0151	–
19	50703.4775	0.0046	0.0197	–
20	50703.5277	0.0031	0.0137	–
52	50705.3081	0.0020	–0.0055	21
53	50705.3589	0.0022	–0.0110	22
123	50709.3007	0.0255	–0.0058	34
124	50709.3531	0.0028	–0.0097	34
125	50709.4246	0.0055	0.0056	30
141	50710.3297	0.0201	0.0109	29
142	50710.3605	0.0046	–0.0145	28
143	50710.4327	0.0035	0.0015	22
152	50710.9360	0.0015	–0.0014	53
153	50710.9964	0.0016	0.0028	54
154	50711.0464	0.0200	–0.0035	33
159	50711.3335	0.0033	0.0025	30
160	50711.3982	0.0042	0.0109	25

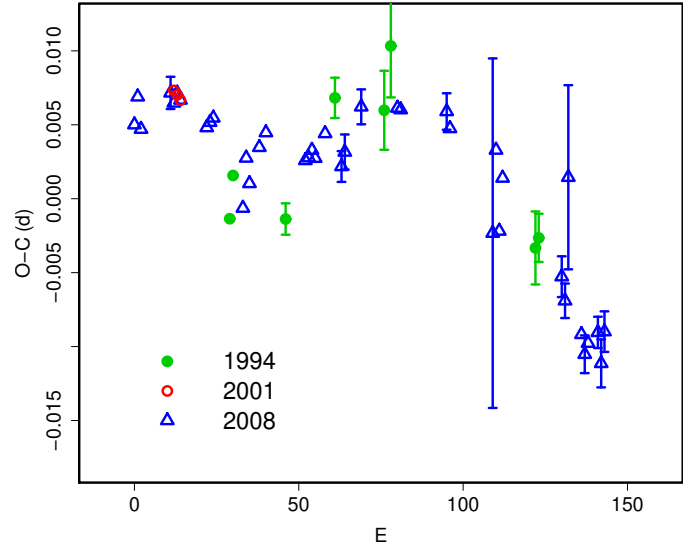
^a BJD–2400000.^b Against $\max = 2450702.3893 + 0.056238E$.^c Number of points used to determine the maximum.**Table 105.** Superhump maxima of V2176 Cyg before the dip (1997).

E	\max^a	error	$O - C^b$	N^c
0	50696.3318	0.0008	0.0005	26
1	50696.3893	0.0011	0.0008	26
2	50696.4425	0.0013	–0.0030	27
3	50696.5041	0.0012	0.0015	27
4	50696.5597	0.0017	0.0001	19

^a BJD–2400000.^b Against $\max = 2450696.3314 + 0.057048E$.^c Number of points used to determine the maximum.

The 2008 superoutburst was well-observed. This outburst was preceded by a precursor outburst and followed by a rebrightening. The times of superhump maxima are listed in table 108. The $O - C$ diagram (figure 7) was clearly composed of the stage A ($E \leq 2$), the stage B with a positive P_{dot} , and a transition to the stage C with a shorter period, associated with the brightening near the termination of the superoutburst (cf. Kato et al. 2003c). The P_{dot} for the stage B was $+6.4(1.5) \times 10^{-5}$.

A comparison of $O - C$ diagrams between different superoutbursts (figure 84) now clearly indicate that the 1994 observation recorded the stage B–C transition, in good agreement with the presence of a terminal brightening, and the short P_{SH} during the 2001 superoutburst reflects the short P_{SH} at the start of the stage B.

**Fig. 84.** Comparison of $O - C$ diagrams of HO Del between different superoutbursts. A period of 0.06437 d was used to draw this figure. Approximate cycle counts (E) after the start of the superoutburst (the start of the main superoutburst when preceded by a precursor) were used.**Table 106.** Superhump maxima of HO Del (1994).

E	\max^a	error	$O - C^b$	N^c
0	49591.0526	0.0008	–0.0044	59
1	49591.1199	0.0008	–0.0015	44
17	49592.1469	0.0011	–0.0040	43
32	49593.1206	0.0014	0.0046	43
47	49594.0854	0.0027	0.0041	43
49	49594.2185	0.0035	0.0085	43
93	49597.0371	0.0025	–0.0040	24
94	49597.1021	0.0016	–0.0033	29

^a BJD–2400000.^b Against $\max = 2449591.0570 + 0.064345E$.^c Number of points used to determine the maximum.**Table 107.** Superhump maxima of HO Del (2001).

E	\max^a	error	N^c
0	52150.3235	0.0002	221
1	52150.3875	0.0001	220
2	52150.4516	0.0002	150

^a BJD–2400000.^c Number of points used to determine the maximum.

Table 108. Superhump maxima of HO Del (2008).

E	max ^a	error	$O - C^b$	N^c
0	54682.9928	0.0009	-0.0043	175
1	54683.0590	0.0004	-0.0022	271
2	54683.1212	0.0008	-0.0043	153
11	54683.7030	0.0011	-0.0007	52
12	54683.7667	0.0005	-0.0013	23
13	54683.8317	0.0005	-0.0005	16
14	54683.8956	0.0006	-0.0008	17
22	54684.4087	0.0003	-0.0017	243
23	54684.4734	0.0004	-0.0012	177
24	54684.5381	0.0004	-0.0008	124
33	54685.1113	0.0003	-0.0058	128
34	54685.1791	0.0005	-0.0023	256
35	54685.2417	0.0005	-0.0039	201
38	54685.4373	0.0005	-0.0011	118
40	54685.5670	0.0008	0.0002	112
52	54686.3376	0.0004	-0.0002	132
53	54686.4022	0.0007	0.0001	166
54	54686.4670	0.0006	0.0008	157
55	54686.5309	0.0010	0.0003	134
58	54686.7256	0.0007	0.0024	87
63	54687.0453	0.0010	0.0008	79
64	54687.1106	0.0012	0.0019	84
69	54687.4355	0.0012	0.0055	27
80	54688.1435	0.0008	0.0068	220
81	54688.2078	0.0007	0.0069	201
95	54689.1088	0.0012	0.0085	118
96	54689.1720	0.0005	0.0074	217
109	54690.0018	0.0118	0.0020	37
110	54690.0718	0.0007	0.0077	63
111	54690.1306	0.0005	0.0024	208
112	54690.1986	0.0007	0.0061	79
130	54691.3506	0.0014	0.0017	62
131	54691.4133	0.0012	0.0001	61
132	54691.4861	0.0062	0.0086	25
136	54691.7329	0.0005	-0.0015	23
137	54691.7959	0.0013	-0.0027	22
138	54691.8611	0.0008	-0.0018	18
141	54692.0549	0.0011	-0.0007	93
142	54692.1172	0.0016	-0.0027	87
143	54692.1837	0.0014	-0.0004	122
164	54693.5166	0.0010	-0.0167	37
165	54693.5851	0.0016	-0.0124	37

^a BJD-2400000.^b Against $max = 2454682.9970 + 0.064245E$.^c Number of points used to determine the maximum.

Table 109. Superhump maxima of BC Dor (2003).

E	max ^a	error	$O - C^b$	N^c
0	52958.0575	0.0005	-0.0118	226
45	52961.1395	0.0005	0.0021	34
59	52962.0985	0.0006	0.0066	35
60	52962.1658	0.0005	0.0057	32
61	52962.2336	0.0006	0.0053	24
146	52968.0157	0.0012	-0.0078	100

^a BJD-2400000.^b Against $max = 2452958.0693 + 0.068180E$.^c Number of points used to determine the maximum.

6.56. BC Doradus

Kato et al. (2004a) suggested the SU UMa-type classification of BC Dor = CAL 86. This suggestion was confirmed by the detection of superhumps during the 2003 November superoutburst. The times of superhump maxima are listed in table 109. Since the superhumps were still growing on the first night and since the object was already fading on the last night, we used the middle two nights and determined the mean superhump period of 0.06850(12) d. The $O - C$'s were strongly negative on the first and last night, suggesting that early (stage A to B) and late (stage B to C) evolution took place. Although the global P_{dot} of $-8.9(0.5) \times 10^{-5}$ was obtained, this value should be treated with caution since it was determined from presumably segments of different types of behavior.

6.57. CP Draconis

CP Dra was initially discovered as a suspect supernova in NGC 3147. Subsequent observations established the dwarf nova-type nature of the object (Kholopov 1972; Kolotovkina 1979). The object has been regularly monitored by visual observers. During the 2001 outburst, T. Vanmunster detected superhumps with a period of 0.0687(7) d (vsnet-alert 5709). The period, however, did not agree with later observations.

During the 2003 superoutburst, we succeeded in identifying the superhump period from the high-quality observations on first two nights. The best period determined from the entire outburst was 0.08348(10) d. The times of superhump maxima are shown in table 110. The period decreased at $P_{\text{dot}} = -22.6(4.6) \times 10^{-5}$, probably reflecting the stage B-C transition.

The 2009 superoutburst was well-observed during its middle-to-late stage (table 111). A clear stage B-C transition was recorded. The mean P_{SH} during the stage C was 0.083323(11) d (PDM method). The other parameters are listed in table 2.

6.58. DM Draconis

DM Dra was discovered as a dwarf nova by Stepanian (1982). Kato et al. (2002d) studied the 2001 outburst and reported superhumps with a period of 0.07561(3) d. The coverage of this outburst was insufficient to determine P_{dot} . We undertook a more extensive campaign during

Table 110. Superhump maxima of CP Dra (2003).

E	max ^a	error	$O - C^b$	N^c
0	52648.1234	0.0005	-0.0022	156
1	52648.2076	0.0005	-0.0015	158
14	52649.2950	0.0016	0.0015	134
15	52649.3794	0.0017	0.0024	101
36	52651.1326	0.0028	0.0036	82
48	52652.1296	0.0036	-0.0005	146
49	52652.2103	0.0022	-0.0033	149

^a BJD-2400000.^b Against $max = 2452648.1256 + 0.083427E$.^c Number of points used to determine the maximum.**Table 111.** Superhump maxima of CP Dra (2009).

E	max ^a	error	$O - C^b$	N^c
0	54915.4402	0.0002	-0.0044	79
1	54915.5231	0.0003	-0.0049	109
2	54915.6080	0.0006	-0.0035	87
24	54917.4506	0.0003	0.0036	374
25	54917.5330	0.0003	0.0025	386
26	54917.6226	0.0007	0.0087	154
34	54918.2832	0.0010	0.0018	155
45	54919.1955	0.0015	-0.0036	133
46	54919.2869	0.0022	0.0044	118
48	54919.4502	0.0004	0.0007	94
49	54919.5330	0.0008	0.0002	256
50	54919.6164	0.0004	0.0002	168
59	54920.3640	0.0010	-0.0032	144
60	54920.4507	0.0006	0.0001	149
61	54920.5339	0.0009	-0.0002	61
68	54921.1155	0.0013	-0.0026	180
69	54921.2052	0.0034	0.0037	62
72	54921.4542	0.0018	0.0024	37
83	54922.3702	0.0024	0.0006	76
84	54922.4540	0.0008	0.0010	76
95	54923.3656	0.0023	-0.0052	131
96	54923.4515	0.0027	-0.0028	97
97	54923.5383	0.0023	0.0006	14

^a BJD-2400000.^b Against $max = 2454915.4446 + 0.083434E$.^c Number of points used to determine the maximum.**Table 112.** Superhump maxima of DM Dra (2003).

E	max ^a	error	$O - C^b$	N^c
0	52706.2096	0.0005	-0.0086	182
1	52706.2893	0.0005	-0.0045	245
12	52707.1236	0.0045	-0.0008	80
13	52707.1984	0.0014	-0.0015	80
14	52707.2737	0.0021	-0.0017	79
15	52707.3546	0.0039	0.0037	49
25	52708.1070	0.0011	0.0010	176
26	52708.1834	0.0011	0.0018	185
27	52708.2588	0.0007	0.0017	185
28	52708.3360	0.0014	0.0035	163
38	52709.0884	0.0013	0.0007	81
39	52709.1661	0.0006	0.0029	176
40	52709.2405	0.0006	0.0018	236
41	52709.3206	0.0006	0.0064	239
51	52710.0709	0.0011	0.0016	79
52	52710.1467	0.0012	0.0019	81
53	52710.2205	0.0011	0.0001	81
54	52710.2987	0.0073	0.0028	77
80	52712.2539	0.0006	-0.0052	96
81	52712.3270	0.0016	-0.0076	73

^a BJD-2400000.^b Against $max = 2452706.2183 + 0.075510E$.^c Number of points used to determine the maximum.

the 2003 superoutburst. The times of superhump maxima are listed in table 112. We obtained a global $P_{\text{dot}} = -15.3(1.8) \times 10^{-5}$. Excluding the first two maxima, which may have been recorded during the stage A, we obtained $P_{\text{dot}} = -13.6(2.3) \times 10^{-5}$ (cf. figure 7).

6.59. DV Draconis

DV Dra is a dwarf nova discovered by Pavlov, Shugarov (1985). The object had long been suspected to be a WZ Sge-type dwarf nova (Wenzel 1991). Iida et al. (1995a) claimed a detection of a new outburst, but was later confirmed to be a false recognition of a field star (vsnet-id 182, 183). In 2005 November, P. Schmeer detected an outburst at an unfiltered CCD magnitude of 15.0 (vsnet-alert 8749). T. Vanmunster reported the detection of double-wave early superhumps (cvnet-outburst 790). We observed the outburst between November 22 (just preceding Vanmunster's observation) and December 6. Early superhumps with a mean period of 0.05883(2) d were detected at least until November 27 (figure 85). Due to the short visibility, we could not convincingly detect the appearance of ordinary superhumps. We include this object for improving the statistics of WZ Sge-type dwarf novae.

6.60. KV Draconis

The 2000 superoutburst was observed by two teams, Nogami et al. (2000) and Vanmunster et al. (2000a). Although Vanmunster et al. (2000a) reported a slight increase of the superhump period from 0.0601 d to 0.0603 d, we could not calculate P_{dot} because they did not publish

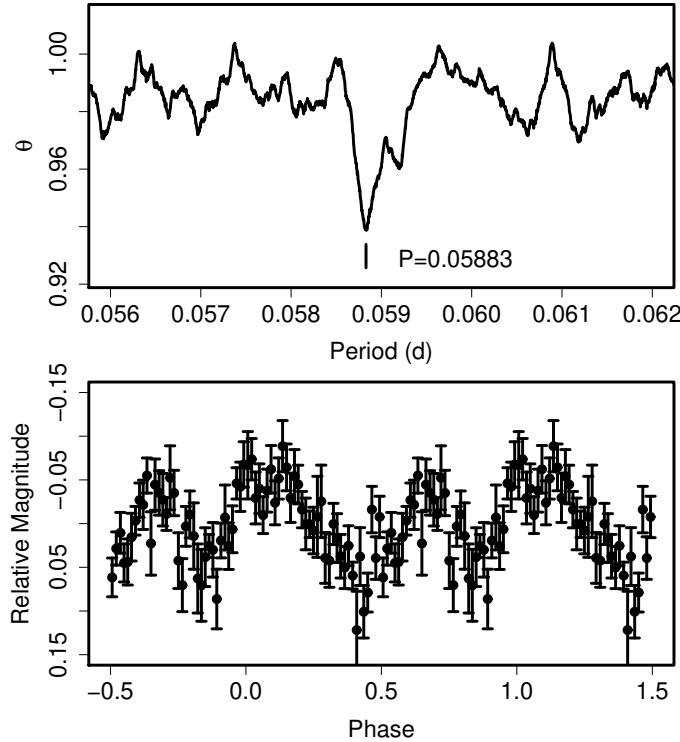


Fig. 85. Early superhumps in DV Dra (2005). (Upper): PDM analysis. (Lower): Phase-averaged profile.

the times of maxima. Nogami et al. (2000) reported a candidate period of 0.06019(2) d based on observations separated by seven days. The period by Nogami et al. (2000) was severely suffered from an aliasing problem, particularly when the period was changing, due to the large gap in observation. Although the SU UMa-type nature was well-established upon this superoutburst, we still needed a better coverage to determine the superhump period and its derivative.

The 2002 superoutburst was relatively well-observed during the most of the course of the outburst (table 113). Although we obtained $P_{\text{dot}} = +11.4(3.9) \times 10^{-5}$ for $E \leq 108$, the period variation appeared rather abrupt, giving a relatively constant period of 0.06002(3) d for $E \leq 59$. The similar pattern of period variation was also observed during the 2008 superoutburst of AQ Eri (subsection 6.63). A stage B–C transition was also recorded.

The 2004 superoutburst was well-observed for the early stage (table 114). The $P_{\text{dot}} = +43.4(8.5) \times 10^{-5}$ for $E \leq 96$ appears too large. There might have been a phase shift between $E = 70$ and $E = 79$. The period for $E \leq 24$ was relatively constant at 0.06001(8) d, a period very close to the 2002 one. The rather anomalous $O - C$ behavior during the late course of the superoutburst in this system requires further investigation.

We also observed the 2005 superoutburst, covering the middle-to-later portion of the plateau phase. The estimated times of superhump maxima are listed in table 115. The data gave a significantly longer mean period

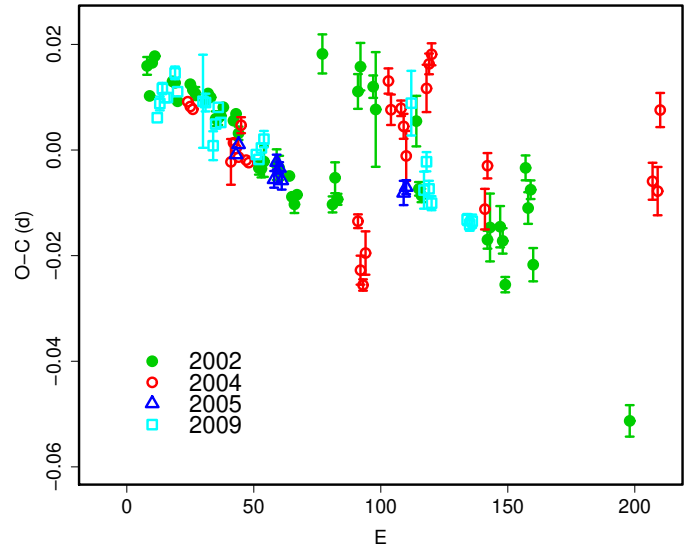


Fig. 86. Comparison of $O - C$ diagrams of KV Dra between different superoutbursts. A period of 0.06044 d was used to draw this figure. Approximate cycle counts (E) after the start of the superoutburst were used.

of 0.06034(3) d, which is in better agreement with the longer value in Vanmunster et al. (2000a). The P_{dot} from these data was $+11.2(4.2) \times 10^{-5}$.

The 2009 superoutburst was observed during the stage A–B transition and a later stage (table 116). The P_1 in table 2 refers to the mean period of the early part of the stage B, shorter than P_1 's of other superoutbursts. The maximum of $E = 100$ was not included in calculating the P_2 . This maximum may have been a final part of the stage B.

A comparison of $O - C$ diagrams between different superoutbursts is given in figure 86. The stage B in this system appears to be composed of two linear segments rather than a continuous period change. The behavior of the late stage B was different between 2002 and 2004 superoutbursts. The difference may be a result of early appearance of stage C superhumps during the 2002 superoutburst.

6.61. MN Draconis

This object was discovered by Antipin, Pavlenko (2002). Nogami et al. (2003b) presented an extensive study of this object and established its unusual properties: long P_{SH} of 0.104–0.106 d and unusually short (~ 60 d) supercycle length. The difference of periods between two superoutbursts can be attributed to different stages observed: stage C in 2002 October and stage B–C transition in 2002 December (figure 28). We present periods based on this interpretation in table 2.

Since the photometric orbital period (0.10424 d) mentioned in (Nogami et al. 2003b) is extremely close to the P_2 in the present identification, we analyzed the corresponding segment in our data and obtained a period a periodicity around 0.1042–0.1047 d. We suspect that this

Table 113. Superhump maxima of KV Dra (2002).

E	\max^a	error	$O - C^b$	N^c
0	52517.9567	0.0017	0.0024	116
1	52518.0114	0.0009	-0.0031	196
2	52518.0781	0.0005	0.0034	246
3	52518.1398	0.0008	0.0048	135
10	52518.5581	0.0007	0.0015	25
11	52518.6183	0.0005	0.0014	40
12	52518.6753	0.0009	-0.0019	64
17	52518.9807	0.0005	0.0024	117
18	52519.0400	0.0006	0.0015	117
19	52519.0998	0.0012	0.0010	110
23	52519.3403	0.0005	0.0006	74
24	52519.4020	0.0005	0.0021	149
25	52519.4617	0.0005	0.0016	175
27	52519.5785	0.0014	-0.0021	41
28	52519.6391	0.0013	-0.0018	42
29	52519.7000	0.0007	-0.0011	132
30	52519.7620	0.0009	0.0007	31
34	52520.0013	0.0006	-0.0010	180
35	52520.0630	0.0006	0.0005	175
36	52520.1197	0.0013	-0.0030	112
44	52520.5967	0.0012	-0.0079	41
45	52520.6570	0.0016	-0.0078	89
46	52520.7188	0.0029	-0.0063	57
51	52521.0204	0.0029	-0.0058	221
52	52521.0802	0.0023	-0.0062	138
56	52521.3205	0.0007	-0.0069	38
57	52521.3770	0.0009	-0.0107	25
58	52521.4360	0.0016	-0.0119	38
59	52521.4982	0.0005	-0.0099	28
69	52522.1293	0.0037	0.0189	96
73	52522.3426	0.0015	-0.0088	42
74	52522.4080	0.0029	-0.0036	48
75	52522.4644	0.0010	-0.0074	27
83	52522.9683	0.0033	0.0146	112
84	52523.0335	0.0045	0.0195	115
89	52523.3319	0.0021	0.0168	40
90	52523.3880	0.0109	0.0127	42
106	52524.3529	0.0048	0.0138	54
107	52524.4005	0.0013	0.0011	72
108	52524.4597	0.0013	0.0001	48
134	52526.0227	0.0017	-0.0029	117
135	52526.0855	0.0064	-0.0004	114
139	52526.3274	0.0039	0.0006	43
140	52526.3851	0.0024	-0.0019	43
141	52526.4373	0.0015	-0.0100	31
149	52526.9429	0.0024	0.0138	78
150	52526.9958	0.0030	0.0064	117
151	52527.0597	0.0018	0.0100	117
152	52527.1059	0.0032	-0.0040	100
190	52529.3730	0.0030	-0.0257	55

^a BJD-2400000.^b Against $\max = 2452517.9543 + 0.060234E$.^c Number of points used to determine the maximum.**Table 114.** Superhump maxima of KV Dra (2004).

E	\max^a	error	$O - C^b$	N^c
0	53120.0483	0.0005	0.0079	84
1	53120.1078	0.0004	0.0070	85
2	53120.1677	0.0004	0.0065	67
17	53121.0644	0.0043	-0.0032	43
18	53121.1284	0.0009	0.0004	83
19	53121.1878	0.0006	-0.0006	185
20	53121.2466	0.0008	-0.0022	192
21	53121.3131	0.0015	0.0038	56
23	53121.4273	0.0009	-0.0028	57
24	53121.4873	0.0009	-0.0032	62
67	53124.0751	0.0013	-0.0135	113
68	53124.1263	0.0027	-0.0228	109
69	53124.1839	0.0011	-0.0256	107
70	53124.2504	0.0041	-0.0195	110
79	53124.8270	0.0024	0.0132	44
80	53124.8820	0.0029	0.0078	40
84	53125.1240	0.0015	0.0081	114
85	53125.1810	0.0024	0.0047	216
86	53125.2359	0.0047	-0.0008	117
94	53125.7322	0.0045	0.0121	32
95	53125.7972	0.0020	0.0167	48
96	53125.8595	0.0021	0.0186	38
117	53127.0994	0.0038	-0.0104	69
118	53127.1681	0.0024	-0.0021	102
183	53131.0937	0.0035	-0.0039	83
185	53131.2127	0.0046	-0.0058	66
186	53131.2885	0.0032	0.0096	63

^a BJD-2400000.^b Against $\max = 2453120.0404 + 0.060422E$.^c Number of points used to determine the maximum.**Table 115.** Superhump maxima of KV Dra (2005).

E	\max^a	error	$O - C^b$	N^c
0	53465.1897	0.0005	0.0007	185
1	53465.2521	0.0005	0.0027	180
15	53466.0916	0.0016	-0.0025	105
16	53466.1553	0.0014	0.0008	130
17	53466.2147	0.0011	-0.0002	124
18	53466.2727	0.0017	-0.0025	103
66	53469.1715	0.0023	-0.0001	114
67	53469.2330	0.0013	0.0011	115

^a BJD-2400000.^b Against $\max = 2453465.1890 + 0.060341E$.^c Number of points used to determine the maximum.

Table 116. Superhump maxima of KV Dra (2009).

E	\max^a	error	$O - C^b$	N^c
0	54971.0059	0.0010	-0.0038	164
1	54971.0690	0.0013	-0.0009	157
2	54971.1323	0.0011	0.0021	176
3	54971.1910	0.0005	0.0005	291
4	54971.2515	0.0005	0.0007	261
7	54971.4375	0.0012	0.0059	24
8	54971.4943	0.0004	0.0025	31
18	54972.0969	0.0088	0.0023	81
19	54972.1571	0.0017	0.0022	119
22	54972.3303	0.0027	-0.0055	60
23	54972.3948	0.0003	-0.0012	116
24	54972.4584	0.0004	0.0021	111
25	54972.5160	0.0004	-0.0006	116
39	54973.3561	0.0006	-0.0044	118
40	54973.4156	0.0005	-0.0052	118
41	54973.4782	0.0006	-0.0028	113
42	54973.5403	0.0016	-0.0010	74
100	54977.0527	0.0061	0.0152	65
105	54977.3384	0.0035	-0.0004	72
106	54977.4042	0.0018	0.0051	108
107	54977.4595	0.0015	0.0002	109
108	54977.5172	0.0013	-0.0024	98
122	54978.3603	0.0011	-0.0032	63
123	54978.4198	0.0012	-0.0040	63
124	54978.4809	0.0013	-0.0032	60

^a BJD-2400000.^b Against $\max = 2454971.0097 + 0.060277E$.^c Number of points used to determine the maximum.

period was not the true orbital period, but persisting (or permanent) superhumps having a period close to P_2 . The presence of permanent superhumps, if confirmed, would strengthen the resemblance of MN Dra to ER UMa stars (e.g. Gao et al. 1999; Olech et al. 2008). If the true orbital period is shorter, the problem of an exceptionally small fractional superhump excess Nogami et al. (2003b) will be solved.

We further point out that the 2003 April outburst was a superoutburst (table 117). The derived superhump period of 0.10480(5) d with the PDM method is in good agreement with the mean period of the 2002 October superoutburst. This superoutburst occurred ~ 65 d after the 2003 February superoutburst mentioned in Nogami et al. (2003b), confirming the relatively stable, short supercycle. A PDM analysis of the 2008 July superoutburst yielded a mean period of 0.10514(14) d (table 118).

6.62. XZ Eridani

XZ Eri is an eclipsing SU UMa-type dwarf nova with a short orbital period (Uemura et al. 2004; Woudt, Warner 2001). We reanalyzed the observations presented in Uemura et al. (2004) and determined the times of superhump maxima (table 119). Although the scatter was rather large, we can see an earlier segment with a posi-

Table 117. Superhump maxima of MN Dra (2003 April).

E	\max^a	error	$O - C^b$	N^c
0	52750.4325	0.0008	-0.0017	91
9	52751.3812	0.0013	0.0039	51
10	52751.4814	0.0011	-0.0007	43
19	52752.4238	0.0021	-0.0015	43

^a BJD-2400000.^b Against $\max = 2452750.4342 + 0.10479E$.^c Number of points used to determine the maximum.**Table 118.** Superhump maxima of MN Dra (2008 July).

E	\max^a	error	$O - C^b$	N^c
0	54677.5447	0.0014	-0.0001	60
9	54678.4928	0.0015	0.0009	60
10	54678.5963	0.0016	-0.0008	41

^a BJD-2400000.^b Against $\max = 2454677.5448 + 0.10524E$.^c Number of points used to determine the maximum.

tive P_{dot} (stage B) followed by a transition to a shorter period (stage C). The P_{dot} for the stage B ($E \leq 77$) was $+15.3(5.6) \times 10^{-5}$, strengthening the suggestion in Uemura et al. (2004).

We also observed two superoutbursts in 2003 December (table 120), in 2007 (table 121) and in 2008 (table 122, combined data with the AAVSO observations). We only recorded the transition to a shorter period during the first superoutburst, while we managed to mainly record the stages of early evolution (stage A to B) and a positive P_{dot} . The P_{dot} for the 2007 superoutburst was $+7.6(1.0) \times 10^{-5}$ ($15 \leq E \leq 138$). The 2008 superoutburst showed all stages of A-C. The P_{dot} during the stage B was $+22.5(4.7) \times 10^{-5}$ ($23 \leq E \leq 92$).

A comparison of $O - C$ diagrams between different superoutbursts is presented in figure 87.

6.63. AQ Eridani

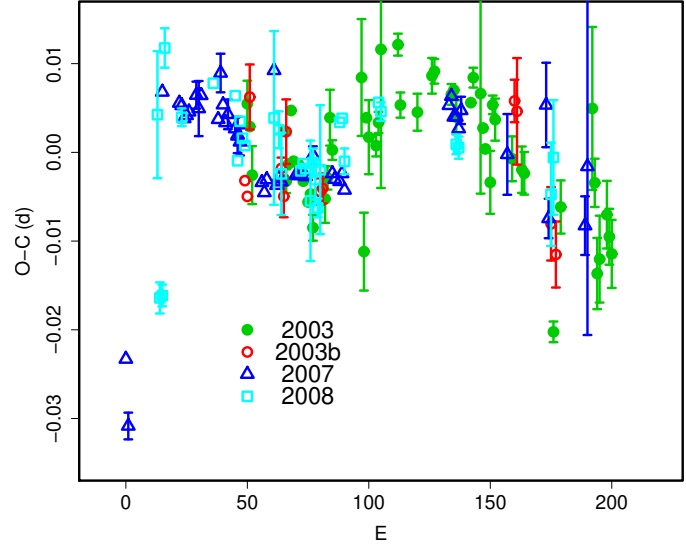
Kato (1991a) observed the 1991 superoutburst and reported a period of 0.06225 d. Kato (2001b) reported a single-night observation of the 1992 superoutburst, and found an anomalously long (0.0642(4) d) superhump period.

Although the original data for the 1991 superoutburst is already unavailable, we reanalyzed the 1992 data together with unpublished observations (table 123). The anomalously long P_{SH} has been confirmed (0.0638(7) d for $0 \leq E \leq 3$). The period, however, of the entire observation is 0.0616(2). The observation likely caught the transition from the stage B to C.

We further observed the 2006 superoutburst during its late plateau stage (table 124). Because the observation was performed when the superhumps had small amplitudes and relatively irregular profiles, the quality of the $O - C$ analysis was not satisfactory. The mean period

Table 119. Superhump maxima of XZ Eri (2003a).

E	\max^a	error	$O - C^b$	N^c
0	52667.9769	0.0026	0.0027	41
1	52668.0372	0.0009	0.0002	135
2	52668.0946	0.0033	-0.0052	132
15	52668.9163	0.0006	0.0002	240
16	52668.9735	0.0013	-0.0054	247
17	52669.0383	0.0007	-0.0034	343
18	52669.1071	0.0009	0.0027	161
19	52669.1642	0.0004	-0.0030	28
21	52669.2896	0.0005	-0.0033	59
22	52669.3520	0.0006	-0.0036	62
23	52669.4133	0.0007	-0.0051	57
25	52669.5366	0.0007	-0.0074	54
26	52669.6004	0.0006	-0.0064	56
27	52669.6594	0.0015	-0.0102	38
32	52669.9768	0.0027	-0.0067	105
33	52670.0420	0.0013	-0.0043	282
34	52670.1116	0.0031	0.0025	125
35	52670.1708	0.0011	-0.0011	28
47	52670.9329	0.0066	0.0075	62
48	52670.9761	0.0044	-0.0121	188
49	52671.0540	0.0008	0.0031	36
50	52671.1147	0.0042	0.0009	37
53	52671.3022	0.0012	0.0001	31
54	52671.3676	0.0012	0.0027	63
55	52671.4387	0.0156	0.0110	28
62	52671.8791	0.0012	0.0118	56
63	52671.9351	0.0014	0.0050	79
70	52672.3741	0.0021	0.0045	44
76	52672.7552	0.0020	0.0089	80
77	52672.8185	0.0014	0.0094	85
84	52673.2557	0.0012	0.0071	51
85	52673.3190	0.0008	0.0076	54
86	52673.3788	0.0019	0.0046	31
92	52673.7574	0.0009	0.0065	86
93	52673.8231	0.0011	0.0093	61
96	52674.0098	0.0113	0.0076	46
97	52674.0687	0.0010	0.0038	26
98	52674.1292	0.0010	0.0015	35
100	52674.2511	0.0035	-0.0022	34
101	52674.3226	0.0010	0.0066	42
102	52674.3838	0.0024	0.0049	33
109	52674.8192	0.0025	0.0008	83
113	52675.0693	0.0026	-0.0003	53
114	52675.1317	0.0024	-0.0006	53
126	52675.8678	0.0012	-0.0180	84
129	52676.0704	0.0030	-0.0038	46
142	52676.8983	0.0092	0.0078	33
143	52676.9527	0.0027	-0.0006	169
144	52677.0053	0.0040	-0.0108	191
145	52677.0698	0.0049	-0.0091	142
148	52677.2633	0.0038	-0.0040	59
149	52677.3236	0.0031	-0.0064	59
150	52677.3845	0.0038	-0.0083	60

^a BJD-2400000.^b Against $\max = 2452667.9742 + 0.062791E$.^c Number of points used to determine the maximum.**Fig. 87.** Comparison of $O - C$ diagrams of XZ Eri between different superoutbursts. A period of 0.06283 d was used to draw this figure. Approximate cycle counts (E) after the start of the superoutburst were used.**Table 120.** Superhump maxima of XZ Eri (2003b).

E	\max^a	error	$O - C^b$	N^c
0	52988.1179	0.0007	-0.0019	114
1	52988.1790	0.0010	-0.0037	116
2	52988.2530	0.0037	0.0075	48
15	52989.0617	0.0012	-0.0003	47
16	52989.1214	0.0024	-0.0035	86
17	52989.1915	0.0036	0.0038	63
31	52990.0644	0.0015	-0.0027	109
32	52990.1276	0.0017	-0.0023	60
111	52995.1010	0.0024	0.0087	49
112	52995.1627	0.0060	0.0076	49
126	52996.0296	0.0041	-0.0049	62
128	52996.1518	0.0037	-0.0083	91

^a BJD-2400000.^b Against $\max = 2452988.1199 + 0.062815E$.^c Number of points used to determine the maximum.

Table 121. Superhump maxima of XZ Eri (2007).

E	max ^a	error	$O - C^b$	N^c
0	54440.1704	0.0004	-0.0228	84
1	54440.2257	0.0015	-0.0303	145
15	54441.1429	0.0004	0.0072	31
22	54441.5815	0.0001	0.0059	120
23	54441.6440	0.0001	0.0056	116
24	54441.7054	0.0001	0.0042	116
25	54441.7686	0.0001	0.0045	110
26	54441.8318	0.0002	0.0049	104
29	54442.0222	0.0015	0.0068	65
30	54442.0835	0.0031	0.0053	68
31	54442.1478	0.0010	0.0067	67
38	54442.5849	0.0004	0.0040	93
39	54442.6530	0.0022	0.0092	71
40	54442.7122	0.0004	0.0056	93
41	54442.7731	0.0004	0.0036	93
42	54442.8368	0.0017	0.0045	48
45	54443.0237	0.0012	0.0029	61
46	54443.0858	0.0020	0.0022	123
47	54443.1479	0.0015	0.0014	98
56	54443.7088	0.0002	-0.0033	86
57	54443.7705	0.0003	-0.0044	84
58	54443.8347	0.0003	-0.0030	102
61	54444.0355	0.0009	0.0093	45
62	54444.0854	0.0004	-0.0036	185
63	54444.1491	0.0007	-0.0027	160
64	54444.2115	0.0007	-0.0032	113
70	54444.5892	0.0003	-0.0025	76
71	54444.6520	0.0005	-0.0026	81
72	54444.7149	0.0005	-0.0025	92
73	54444.7778	0.0004	-0.0025	92
74	54444.8404	0.0005	-0.0027	89
77	54445.0312	0.0010	-0.0004	35
85	54445.5318	0.0005	-0.0025	85
86	54445.5940	0.0005	-0.0031	91
88	54445.7194	0.0003	-0.0034	100
89	54445.7831	0.0003	-0.0025	108
90	54445.8441	0.0003	-0.0044	88
133	54448.5554	0.0006	0.0049	57
134	54448.6192	0.0008	0.0059	52
135	54448.6797	0.0004	0.0036	56
136	54448.7425	0.0005	0.0035	53
137	54448.8041	0.0004	0.0022	51
138	54448.8689	0.0015	0.0043	34
157	54450.0577	0.0046	-0.0008	37
173	54451.0686	0.0048	0.0046	41
174	54451.1186	0.0022	-0.0082	48
189	54452.0603	0.0033	-0.0091	38
190	54452.1298	0.0190	-0.0024	38

^a BJD-2400000.^b Against $max = 2454440.1931 + 0.062837E$.^c Number of points used to determine the maximum.**Table 122.** Superhump maxima of XZ Eri (2008).

E	max ^a	error	$O - C^b$	N^c
0	54796.9957	0.0072	0.0043	47
1	54797.0379	0.0017	-0.0164	79
2	54797.1010	0.0012	-0.0161	65
3	54797.1917	0.0022	0.0118	12
10	54797.6237	0.0010	0.0040	48
23	54798.4443	0.0007	0.0078	40
32	54799.0084	0.0010	0.0064	51
33	54799.0639	0.0004	-0.0009	124
34	54799.1312	0.0008	0.0035	101
35	54799.1921	0.0006	0.0016	38
36	54799.2541	0.0006	0.0008	38
48	54800.0112	0.0098	0.0039	5
50	54800.1355	0.0021	0.0026	37
51	54800.1934	0.0046	-0.0024	65
59	54800.6963	0.0009	-0.0021	35
60	54800.7600	0.0007	-0.0013	50
61	54800.8223	0.0007	-0.0018	44
63	54800.9443	0.0068	-0.0055	18
64	54801.0114	0.0016	-0.0012	15
65	54801.0723	0.0022	-0.0031	40
66	54801.1320	0.0011	-0.0063	50
67	54801.1991	0.0073	-0.0020	33
75	54801.7071	0.0010	0.0034	33
76	54801.7704	0.0008	0.0038	37
77	54801.8283	0.0015	-0.0010	38
91	54802.7146	0.0009	0.0056	41
92	54802.7764	0.0010	0.0046	45
123	54804.7204	0.0011	0.0009	38
124	54804.7829	0.0013	0.0005	37
162	54807.1652	0.0058	-0.0048	74
163	54807.2322	0.0065	-0.0006	67

^a BJD-2400000.^b Against $max = 2454796.9914 + 0.062830E$.^c Number of points used to determine the maximum.

(likely P_2) was 0.0617(1) d.

The 2008 superoutburst was well observed (table 125), first clearly establishing the positive P_{dot} of $+4.4(0.8) \times 10^{-5}$ (figure 88). This superoutburst was preceded by a distinct precursor, strengthening that the overall behavior of period derivatives are not strongly affected by the presence of a precursor outburst.

6.64. UV Geminorum

UV Gem has long been known as a dwarf nova (Kholopov et al. 1985). Kato, Uemura (2001a) suggested the SU UMa-type classification based on the long-term light curve consisting of a likely superoutburst and short outbursts with a short cycle length. T. Vanmunster (vsnet-alert 3821) first reported the detection of superhumps with a period of 0.0902(6) d. During the 2003 superoutburst, we conducted an extensive campaign and obtained a high-quality set of superhump times (table 126). The large variation in the $O - C$ diagram indicates

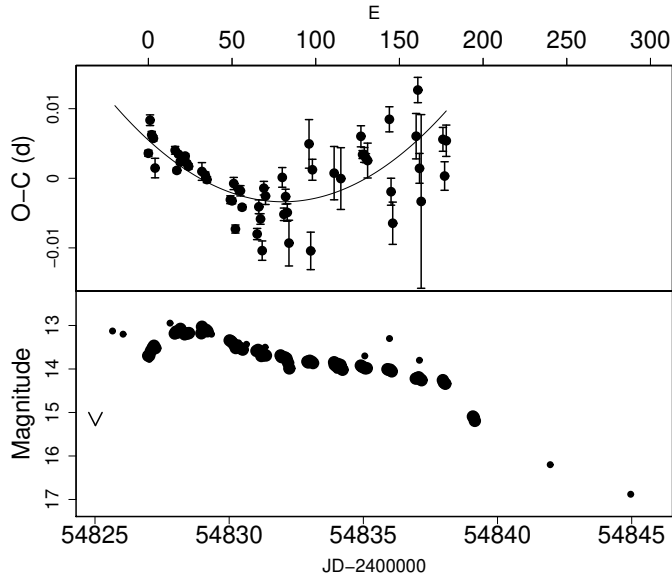


Fig. 88. $O - C$ of superhumps AQ Eri (2008). (Upper): $O - C$ diagram. The $O - C$ values were against the mean period for the stage B ($E \leq 163$, thin curve) (Lower): Light curve. Large dots are our CCD observations and small dots are visual and V observation from the VSOLJ database and ASAS-3 observations.

Table 123. Superhump maxima of AQ Eri (1992).

E	\max^a	error	$O - C^b$	N^c
0	48626.0215	0.0006	-0.0036	65
1	48626.0857	0.0002	-0.0011	111
2	48626.1516	0.0003	0.0032	110
3	48626.2123	0.0006	0.0022	56
18	48627.1339	0.0012	-0.0007	59

^a BJD-2400000.

^b Against $\max = 2448626.0252 + 0.061634E$.

^c Number of points used to determine the maximum.

Table 124. Superhump maxima of AQ Eri (2006).

E	\max^a	error	$O - C^b$	N^c
0	54070.1471	0.0046	0.0026	61
49	54073.1713	0.0037	0.0045	69
50	54073.2291	0.0011	0.0006	67
65	54074.1520	0.0043	-0.0017	55
67	54074.2623	0.0012	-0.0148	58
97	54076.1363	0.0021	0.0088	30

^a BJD-2400000.

^b Against $\max = 2454070.1445 + 0.061681E$.

^c Number of points used to determine the maximum.

Table 125. Superhump maxima of AQ Eri (2008).

E	\max^a	error	$O - C^b$	N^c
0	54826.9930	0.0004	0.0040	208
1	54827.0601	0.0008	0.0087	233
2	54827.1204	0.0005	0.0066	233
3	54827.1822	0.0004	0.0061	271
4	54827.2403	0.0014	0.0018	50
16	54827.9912	0.0006	0.0043	183
17	54828.0507	0.0003	0.0014	316
18	54828.1153	0.0002	0.0037	300
19	54828.1766	0.0003	0.0026	173
22	54828.3645	0.0003	0.0034	75
23	54828.4258	0.0003	0.0023	87
24	54828.4877	0.0004	0.0019	77
32	54828.9859	0.0013	0.0011	44
34	54829.1101	0.0004	0.0006	93
35	54829.1718	0.0004	-0.0001	87
49	54830.0419	0.0006	-0.0031	88
50	54830.1041	0.0004	-0.0032	92
51	54830.1690	0.0009	-0.0008	126
52	54830.2248	0.0006	-0.0073	82
54	54830.3552	0.0006	-0.0016	81
55	54830.4174	0.0007	-0.0018	78
56	54830.4773	0.0004	-0.0042	83
65	54831.0347	0.0008	-0.0081	123
66	54831.1010	0.0010	-0.0042	174
67	54831.1616	0.0008	-0.0060	90
68	54831.2194	0.0014	-0.0105	82
69	54831.2907	0.0010	-0.0016	61
70	54831.3520	0.0012	-0.0027	77
80	54831.9782	0.0014	-0.0001	91
81	54832.0353	0.0009	-0.0054	92
82	54832.1002	0.0011	-0.0029	105
83	54832.1603	0.0012	-0.0052	85
84	54832.2182	0.0033	-0.0096	90
96	54832.9808	0.0035	0.0046	109
97	54833.0278	0.0027	-0.0108	47
98	54833.1018	0.0015	0.0009	83
111	54833.9120	0.0038	0.0003	38
115	54834.1606	0.0044	-0.0005	88
127	54834.9150	0.0015	0.0055	76
128	54834.9747	0.0006	0.0028	205
129	54835.0370	0.0011	0.0028	74
130	54835.0989	0.0006	0.0023	44
131	54835.1609	0.0025	0.0020	24
144	54835.9775	0.0018	0.0078	124
145	54836.0295	0.0019	-0.0026	92
146	54836.0873	0.0030	-0.0072	26
160	54836.9728	0.0033	0.0052	89
161	54837.0418	0.0018	0.0119	93
162	54837.0929	0.0021	0.0006	60
163	54837.1505	0.0125	-0.0042	47
176	54837.9701	0.0017	0.0047	31
177	54838.0272	0.0020	-0.0006	81
178	54838.0946	0.0023	0.0045	34

^a BJD-2400000.

^b Against $\max = 2454826.9891 + 0.062366E$.

^c Number of points used to determine the maximum.

a strong period decrease (figure 28). Using all the data, the P_{dot} was $-53.4(3.6) \times 10^{-5}$. Even if we exclude the early part ($E \leq 5$), the P_{dot} was $-33.5(2.0) \times 10^{-5}$, still extreme. The situation is particularly similar to a long- P_{orb} system MN Dra (Nogami et al. 2003b), who reported a global P_{dot} of $-170(20) \times 10^{-5}$. The present data of UV Gem neither has cycle ambiguity nor a large gap in observation, thereby firmly demonstrating the existence of an exceptionally strong decrease in the superhump period. Long- P_{orb} systems appear to share this tendency of period variation.

The times of superhump maxima for the 2008 superoutburst are also given (table 127). This superoutburst was probably observed during its late stage.

6.65. AW Geminorum

Kato (1996b) observed the 1995 superoutburst during its early stage. The refined times of superhump maxima are listed in table 128. The $O-C$ diagram shows a similar trend to those of V877 Ara and DT Oct (a period shift from a longer period during the earliest stage). Excluding the early part (stage A, $E \leq 1$), we obtained the mean $P_{\text{SH}} = 0.07935(9)$ d and $P_{\text{dot}} = -3.2(1.5) \times 10^{-5}$. We also observed the 2008 superoutburst (table 129) during its early stage and the 2009 superoutburst (table 130). A strong period variation, as recorded in the 1995 superoutburst, was recorded during the latter superoutburst.

6.66. CI Geminorum

Wenzel (1990) suggested the SU UMa-type classification of this object based on the existence of long and short outbursts. The large rate of decline of a short outburst in 1999 was consistent with that of a normal outburst of an SU UMa-type dwarf nova (Kato, Schmeer 1999), although Schmeer, Duerbeck (1999) favored the SS Cyg-type classification. The object underwent a long outburst in 2005 April, consisting of a precursor and a long plateau (figure 89).

Although the presence of superhumps with a period about ~ 0.1 d is apparent in the sparse raw data, a PDM analysis of the entire set of data did not yield a significant period. The situation appears similar to CTCV J0549 with a long P_{SH} and large period variation. We therefore analyzed the data in separate segments, measured superhump maxima (table 131) and searched for a likely period. The period of ~ 0.117 d with a significant period decrease only can naturally express the available observations (figure 90). Although the exact identification of the period should await further observations, the present analysis suggests that CI Gem is an excellent candidate for a dwarf nova in the period gap.

6.67. IR Geminorum

We measured times of superhump maxima (table 132) from observations reported in Kato (2001a). We also observed the 2009 superoutburst (table 133). Although the data were limited, we can see a likely stage B–C transition (the presence of a phase shift between $E = 27$ and $E = 86$ is not completely excluded). Because the profile of the su-

Table 126. Superhump maxima of UV Gem (2003).

E	max ^a	error	$O - C^b$	N^c
0	52645.9759	0.0036	-0.0276	106
1	52646.0681	0.0014	-0.0285	179
2	52646.1590	0.0009	-0.0307	238
3	52646.2522	0.0023	-0.0305	202
4	52646.3538	0.0004	-0.0221	48
5	52646.4534	0.0006	-0.0156	57
10	52646.9352	0.0010	0.0007	178
11	52647.0290	0.0014	0.0013	177
12	52647.1271	0.0004	0.0063	292
13	52647.2200	0.0013	0.0061	264
15	52647.4116	0.0006	0.0116	49
16	52647.5019	0.0010	0.0087	56
21	52647.9717	0.0008	0.0130	178
22	52648.0660	0.0005	0.0142	180
23	52648.1589	0.0004	0.0140	178
24	52648.2520	0.0009	0.0140	178
25	52648.3414	0.0020	0.0102	170
26	52648.4389	0.0004	0.0147	127
27	52648.5332	0.0006	0.0158	90
33	52649.0914	0.0004	0.0154	165
34	52649.1860	0.0007	0.0170	98
35	52649.2759	0.0004	0.0137	163
36	52649.3691	0.0006	0.0139	114
37	52649.4626	0.0004	0.0142	168
38	52649.5537	0.0005	0.0122	75
54	52651.0392	0.0006	0.0080	160
55	52651.1297	0.0007	0.0054	146
56	52651.2254	0.0009	0.0080	122
57	52651.3171	0.0014	0.0065	72
58	52651.4055	0.0007	0.0019	130
59	52651.4966	0.0006	-0.0001	124
60	52651.5953	0.0033	0.0055	37
65	52652.0533	0.0007	-0.0021	189
66	52652.1459	0.0006	-0.0025	185
67	52652.2365	0.0004	-0.0051	188
75	52652.9728	0.0034	-0.0136	105
76	52653.0668	0.0009	-0.0127	187
77	52653.1607	0.0009	-0.0119	163
78	52653.2514	0.0023	-0.0144	74
80	52653.4345	0.0006	-0.0174	76
81	52653.5275	0.0007	-0.0176	74

^a BJD-2400000.

^b Against $max = 2452646.0035 + 0.093106E$.

^c Number of points used to determine the maximum.

Table 127. Superhump maxima of UV Gem (2008).

E	max ^a	error	$O - C^b$	N^c
0	54806.1048	0.0108	-0.0059	44
1	54806.2067	0.0014	0.0032	126
2	54806.2995	0.0036	0.0033	34
11	54807.1312	0.0019	0.0002	97
12	54807.2253	0.0016	0.0015	191
13	54807.3149	0.0007	-0.0016	208
22	54808.1435	0.0048	-0.0078	98
23	54808.2512	0.0021	0.0071	97

^a BJD-2400000.^b Against $max = 2454806.1107 + 0.092758E$.^c Number of points used to determine the maximum.**Table 128.** Superhump maxima of AW Gem (1995).

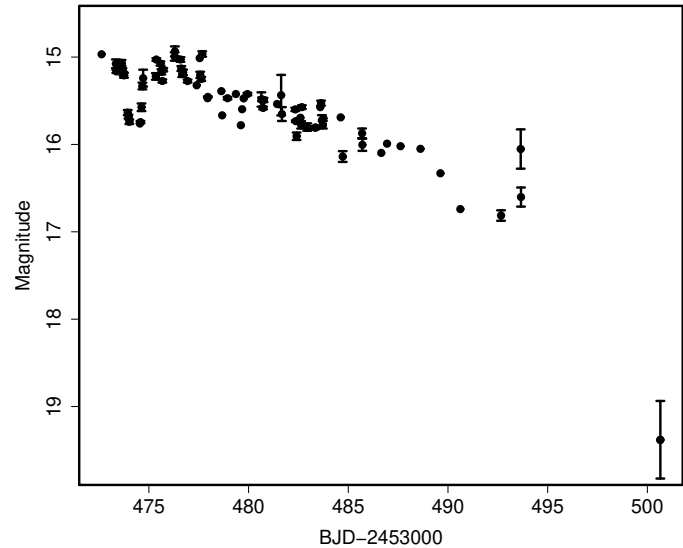
E	max ^a	error	$O - C^b$	N^c
0	50001.2611	0.0017	-0.0133	74
1	50001.3368	0.0027	-0.0176	43
12	50002.2511	0.0003	0.0155	75
13	50002.3325	0.0006	0.0169	61
25	50003.2896	0.0004	0.0126	58
38	50004.3172	0.0004	-0.0011	75
51	50005.3468	0.0009	-0.0129	54

^a BJD-2400000.^b Against $max = 2450001.2743 + 0.080106E$.^c Number of points used to determine the maximum.**Table 129.** Superhump maxima of AW Gem (2008).

E	max ^a	error	$O - C^b$	N^c
0	54567.9600	0.0009	0.0024	180
1	54568.0420	0.0009	0.0054	235
2	54568.1064	0.0150	-0.0091	190
38	54570.9630	0.0017	0.0038	135
52	54572.0625	0.0014	-0.0025	191

^a BJD-2400000.^b Against $max = 2454567.9576 + 0.078990E$.^c Number of points used to determine the maximum.**Table 130.** Superhump maxima of AW Gem (2009).

E	max ^a	error	$O - C^b$	N^c
0	54922.9682	0.0032	-0.0156	95
1	54923.0417	0.0074	-0.0215	147
12	54923.9486	0.0012	0.0132	137
13	54924.0267	0.0022	0.0121	119
63	54927.9950	0.0007	0.0156	144
64	54928.0751	0.0017	0.0164	95
88	54929.9653	0.0008	0.0035	82
89	54930.0420	0.0015	0.0009	81
101	54930.9870	0.0010	-0.0056	81
102	54931.0698	0.0025	-0.0021	53
114	54932.0064	0.0016	-0.0170	81

^a BJD-2400000.^b Against $max = 2454922.9838 + 0.079295E$.^c Number of points used to determine the maximum.**Fig. 89.** Superoutburst of CI Gem in 2005. The data are a combination of the AAVSO data and our observations. The fading around BJD 2453473-2453474 is a precursor outburst.**Table 131.** Superhump maxima of CI Gem (2005).

E	max ^a	error	$O - C^b$	N^c
0	53474.6646	0.0077	-0.0206	55
6	53475.3707	0.0017	-0.0072	16
9	53475.7219	0.0048	-0.0023	91
16	53476.5655	0.0144	0.0333	21
17	53476.6938	0.0011	0.0461	25
25	53477.5421	0.0059	-0.0290	7
26	53477.6663	0.0023	-0.0203	19

^a BJD-2400000.^b Against $max = 2453474.6853 + 0.115433E$.^c Number of points used to determine the maximum.

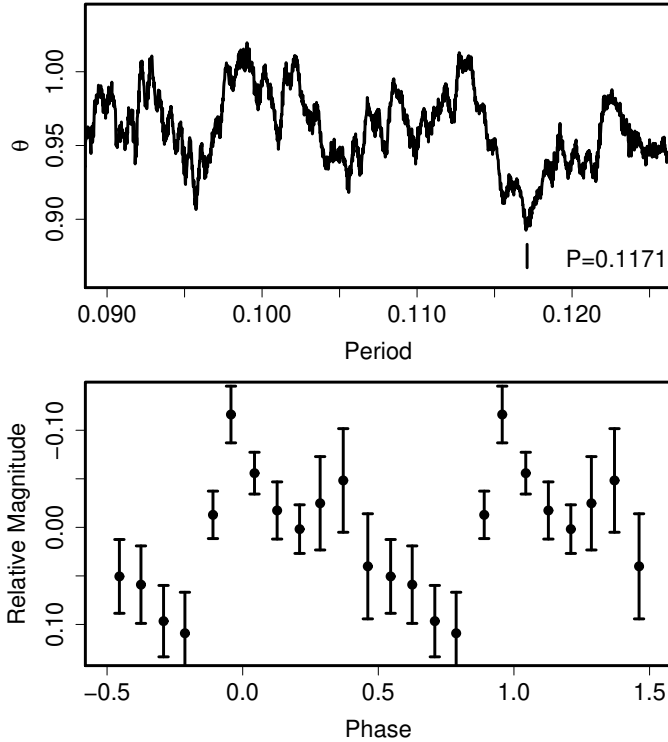


Fig. 90. Superhumps in CI Gem for the early stage the plateau (BJD 2453474.5 – 2453476). (Upper): PDM analysis. (Lower): Phase-averaged profile.

Table 132. Superhump maxima of IR Gem (1991).

E	\max^a	error	$O - C^b$	N^c
0	48333.9835	0.0006	0.0018	268
1	48334.0507	0.0006	-0.0019	260
14	48334.9742	0.0009	0.0009	269
15	48335.0434	0.0010	-0.0007	261

^a BJD-2400000.

^b Against $\max = 2448333.9818 + 0.070821E$.

^c Number of points used to determine the maximum.

perhumps was rather irregular, we determined the mean period for stage B with the PDM method as 0.07093(3) d.

6.68. CI Gruis

CI Gru was discovered as an outbursting CV (Hawkins 1983). Haefner (1995) reported semi-periodic variations with a period of 0.056 d during the possible fading stage of an outburst. B. Monard detected an outburst on 2004 June 4 at a CCD magnitude of 16.2. The outburst lasted at least for five days, accompanied by a rapid fading. The overall behavior suggests that the object underwent a superoutburst. Based on a single-night observation covering for 7.7 hours, likely superhumps were detected (figure 91, table 134). The best period was 0.05402(14) d. Although this value needs to be confirmed by future observations,

Table 133. Superhump maxima of IR Gem (2009).

E	\max^a	error	$O - C^b$	N^c
0	54838.0172	0.0003	-0.0048	196
2	54838.1611	0.0007	-0.0018	73
3	54838.2338	0.0006	0.0005	74
4	54838.3022	0.0008	-0.0016	63
27	54839.9357	0.0007	0.0117	63
86	54844.0724	0.0019	-0.0080	61
87	54844.1521	0.0036	0.0013	24
100	54845.0674	0.0010	0.0007	193
101	54845.1414	0.0009	0.0043	185
102	54845.2089	0.0015	0.0014	145
103	54845.2744	0.0019	-0.0036	53

^a BJD-2400000.

^b Against $\max = 2454838.0220 + 0.070447E$.

^c Number of points used to determine the maximum.

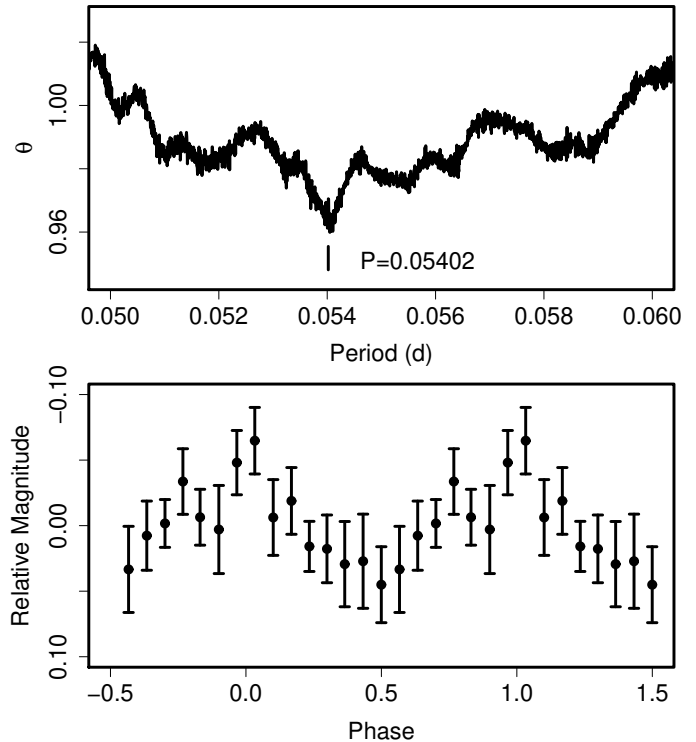


Fig. 91. Superhumps in CI Gru (2004). (Upper): PDM analysis. (Lower): Phase-average profile.

this object would be a candidate for a very short- P_{orb} SU UMa-type dwarf nova. The object underwent another outburst (possibly a superoutburst) in 2006 September at a visual magnitude of 15.4 (Stubbings, vsnet-alert 9023).

6.69. V844 Hercules

Oizumi et al. (2007) summarized the analysis of past outbursts. We present observation of the 2008 superoutburst, an analysis the AAVSO data for the 1997 superoutburst and a reanalysis of the 1999 superoutburst

Table 134. Superhump maxima of CI Gru (2004).

E	\max^a	error	$O - C^b$	N^c
0	53162.3545	0.0036	0.0008	35
1	53162.3994	0.0050	-0.0078	62
2	53162.4689	0.0199	0.0081	62
3	53162.5175	0.0091	0.0032	62
4	53162.5642	0.0083	-0.0037	62
5	53162.6208	0.0030	-0.0007	59

^a BJD-2400000.

^b Against $\max = 2453162.3537 + 0.053553E$.

^c Number of points used to determine the maximum.

(Kato, Uemura 2000). The times of superhumps maxima are listed in tables 135, 136, 137.

During the 1999 superoutburst, we obtained $P_{\text{dot}} = +4.5(2.8) \times 10^{-5}$. No significant period variation was recorded during the 1997 superoutburst. This was probably due to the limited sampling near the end of the stage B.

A comparison of $O - C$ diagrams between different superoutbursts is given in figure 92. While P_{dot} 's were relatively similar, the start of the stage B was different between different superoutbursts: the stage B started earlier during a faint (maximum 12.4 mag) superoutburst in 2002 and later during a bright (12.1 mag) superoutburst in 2006. This result further supports the earlier claim (Kato et al. 2008) that the duration before the start of the stage B (or the appearance of superhumps) depends on the extent of the superoutburst (see also Soejima et al. 2009).

During the 2008 superoutburst we obtained $P_{\text{dot}} = +7.1(0.4) \times 10^{-5}$ for $E \leq 149$ (stage B). There was, however, a phase reversal (associated with secondary maxima) on BJD 2454584. These maxima were omitted for calculating the P_{dot} . This phenomenon may have been similar to the one observed in OT J055718+683226 (Uemura et al. 2009).

A full description of the outburst will be discussed in Ohshima et al., in preparation.

6.70. V1108 Herculis

V1108 Her was discovered by Y. Nakamura on 2004 June 16 (Nakano et al. 2004). The earliest positive detection of the outburst was on 2004 Jun 12 (unfiltered CCD magnitude of 12.0) by A. Takao (vsnet-alert 8190). Due to the delayed announcement of the discovery, only the late part of the superoutburst (11 d after the initial detection) was observed. We used a combined data set of ours and from the AAVSO data, which were used in Price et al. (2004a). The times of superhump maxima are listed in table 138. As in WZ Sge, a strong hump feature appeared and surpassed in amplitude in the late stage of the outburst. For the interval $E \geq 79$, we used a fit to a smaller width $\pm 0.1 P_{\text{SH}}$ around the peaks whose phases can be smoothly linked to earlier peaks, as in V455 And and WZ Sge. The resultant data clearly showed a transition from

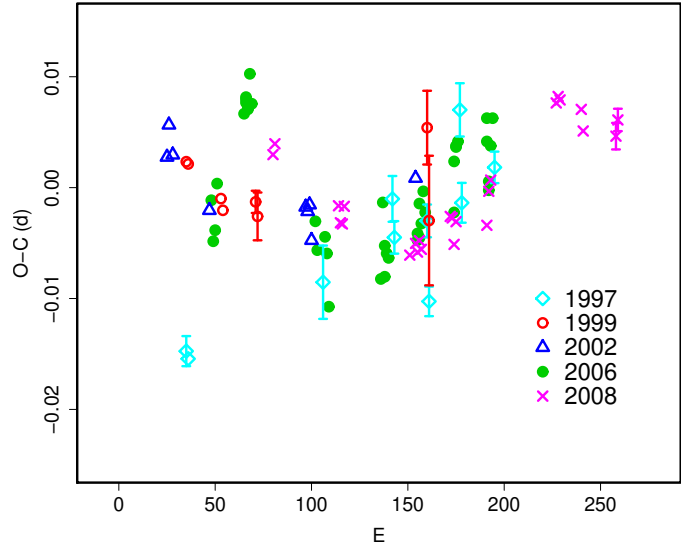


Fig. 92. Comparison of $O - C$ diagrams of V844 Her between different superoutbursts. A period of 0.05590 d was used to draw this figure. Approximate cycle counts (E) after the start of the superoutburst were used. The evolution of superhumps apparently started earlier during a faint (maximum 12.4 mag) superoutburst in 2002 and later during a bright (12.1 mag) superoutburst in 2006.

Table 135. Superhump maxima of V844 Her (1997).

E	\max^a	error	$O - C^b$	N^c
0	50593.4682	0.0014	0.0008	30
1	50593.5235	0.0010	-0.0000	33
71	50597.4434	0.0033	-0.0006	17
107	50599.4633	0.0021	0.0031	26
108	50599.5157	0.0015	-0.0005	20
125	50600.4675	0.0015	-0.0009	32
126	50600.5161	0.0013	-0.0082	22
142	50601.4278	0.0024	0.0073	20
143	50601.4753	0.0018	-0.0011	32
160	50602.4288	0.0014	0.0002	18

^a BJD-2400000.

^b Against $\max = 2450593.4675 + 0.056007E$.

^c Number of points used to determine the maximum.

Table 136. Superhump maxima of V844 Her (1999).

E	max ^a	error	$O - C^b$	N^c
0	51454.9147	0.0006	0.0026	91
1	51454.9704	0.0007	0.0024	100
18	51455.9176	0.0004	-0.0008	111
19	51455.9724	0.0007	-0.0019	107
36	51456.9235	0.0010	-0.0012	91
37	51456.9781	0.0022	-0.0025	67
125	51461.9053	0.0033	0.0050	64
126	51461.9528	0.0058	-0.0034	48

^a BJD-2400000.^b Against $max = 2451454.9121 + 0.055906E$.^c Number of points used to determine the maximum.**Table 137.** Superhump maxima of V844 Her (2008).

E	max ^a	error	$O - C^b$	N^c
0	54577.1964	0.0003	0.0078	104
1	54577.2533	0.0003	0.0088	78
34	54579.0924	0.0007	0.0015	73
35	54579.1468	0.0004	-0.0001	102
36	54579.2026	0.0004	-0.0003	99
37	54579.2601	0.0007	0.0013	74
71	54581.1563	0.0003	-0.0049	171
74	54581.3250	0.0005	-0.0040	67
75	54581.3801	0.0002	-0.0048	116
76	54581.4371	0.0003	-0.0039	108
77	54581.4922	0.0002	-0.0047	113
92	54582.3337	0.0003	-0.0025	113
93	54582.3894	0.0005	-0.0027	91
94	54582.4429	0.0005	-0.0051	50
95	54582.5009	0.0003	-0.0031	113
111	54583.3950	0.0006	-0.0043	112
112	54583.4539	0.0005	-0.0013	116
113	54583.5108	0.0006	-0.0003	99
147	54585.4184	0.0003	0.0049	115
148	54585.4749	0.0005	0.0054	114
149	54585.5305	0.0004	0.0051	91
160	54586.1445	0.0004	0.0036	171
161	54586.1985	0.0005	0.0016	172
178	54587.1483	0.0012	0.0003	173
179	54587.2057	0.0010	0.0017	163

^a BJD-2400000.^b Against $max = 2454577.1886 + 0.055952E$.^c Number of points used to determine the maximum.

a longer period to a shorter one around $E = 29$. The mean period for $E \leq 29$ was 0.05880(18) d, while the period for $E \geq 29$ was 0.05748(3) d. The maxima of secondary (but stronger in the final fading stage) peaks are listed in table 139. For the interval $81 \leq E \leq 108$, they had a relatively stable periodicity of 0.05703(8) d. By analogy with WZ Sge, this periodicity might be considered to be the orbital period.¹⁴ Using this period, we obtained the fractional superhump excesses for the two segments ($E \leq 29$ and $E \geq 29$) of 3.1(3) % and 0.8(1) %, respectively. These period excesses might be attributed to stage B and C superhumps. The unusually large fractional superhump excess (3.1 %) might be a result of lengthening in the P_{SH} during the stage B (see an example of AQ Eri, subsection 6.63). This value might not be used to derive system parameters such as q . This object, with relatively frequent historical outbursts (Price et al. 2004a), appears more analogous to positive- P_{dot} systems such as HV Vir and AL Com rather than extreme WZ Sge-type dwarf novae with little variation in the superhump period (e.g. WZ Sge and V455 And).

6.71. RU Horologii

The times of superhump maxima obtained during the 2003 superoutburst are listed in table 140. The object clearly showed brightening near the termination of a superoutburst (cf. Kato et al. 2003c and discussion in subsection 6.3), after which ($E > 80$) the superhump period remarkably decreased (cf. figure 7). Using the timings for the interval $0 \leq E \leq 76$, we obtained $P_{dot} = +7.5(1.1) \times 10^{-5}$ and a mean superhump period of 0.07095(2) d.

The 2008 superoutburst (table 141) was observed during the middle-to-late stage of the plateau phase. There is a clear signature of a transition to a shorter period (stage B to C). The P_{dot} before this transition, disregarding the slightly discrepant point $E = 0$, was $+6.5(3.2) \times 10^{-5}$ ($1 \leq E \leq 44$).

A comparison of $O - C$ diagrams of RU Hor between different superoutbursts is given in figure 93. Although the actual start of the outburst was not well constrained, the $O - C$ diagram of the 2008 superoutburst almost perfectly fits the 2003 one by assuming a 50-cycle difference in E .

6.72. CT Hydrae

Superhumps during two superoutbursts (1995 and 1999) were reported in the past literature (Nogami et al. 1996; Kato et al. 1999a). We reanalyzed the 1999 observations in view of the modern knowledge. The times of superhump maxima are listed in table 142. The Brno data were removed before the analysis because of the yet unsolved phase problem (cf. Kato et al. 1999a). Although Kato et al. (1999a) stated that the change in

¹⁴ This period, though, might refer to a variety of superhumps. Price et al. (2004a) reported another candidate periodicity of 0.05686(7) d marginally detected in post-superoutburst stage. The exact identification of the periodicities should await future observations.

Table 138. Superhump maxima of V1108 Her (2004).

E	\max^a	error	$O - C^b$	N^c
0	53179.8955	0.0006	-0.0106	107
1	53179.9527	0.0010	-0.0112	89
4	53180.1292	0.0063	-0.0079	63
5	53180.1739	0.0011	-0.0210	82
12	53180.5920	0.0011	-0.0072	94
13	53180.6493	0.0027	-0.0077	37
14	53180.7084	0.0012	-0.0063	55
15	53180.7684	0.0010	-0.0041	62
16	53180.8246	0.0014	-0.0056	44
26	53181.4212	0.0006	0.0134	53
27	53181.4733	0.0015	0.0078	70
29	53181.6027	0.0030	0.0216	49
30	53181.6487	0.0013	0.0098	14
31	53181.7095	0.0019	0.0129	23
32	53181.7693	0.0014	0.0149	92
33	53181.8174	0.0008	0.0053	136
34	53181.8762	0.0012	0.0063	106
35	53181.9293	0.0018	0.0017	168
36	53181.9847	0.0009	-0.0007	26
44	53182.4512	0.0007	0.0038	52
45	53182.5083	0.0005	0.0031	66
46	53182.5654	0.0005	0.0025	67
47	53182.6209	0.0011	0.0002	41
48	53182.6816	0.0005	0.0032	143
49	53182.7392	0.0003	0.0029	143
50	53182.7979	0.0004	0.0039	163
51	53182.8555	0.0003	0.0037	65
52	53182.9132	0.0007	0.0037	34
54	53183.0264	0.0010	0.0014	159
64	53183.6029	0.0004	0.0003	148
65	53183.6631	0.0003	0.0028	233
66	53183.7192	0.0002	0.0011	264
67	53183.7757	0.0003	-0.0001	219
68	53183.8349	0.0006	0.0013	67
71	53184.0055	0.0009	-0.0013	129
72	53184.0635	0.0007	-0.0011	107
73	53184.1268	0.0045	0.0045	82
79	53184.4642	0.0002	-0.0047	33
80	53184.5229	0.0006	-0.0037	62
83	53184.6956	0.0019	-0.0044	47
84	53184.7495	0.0007	-0.0082	47
85	53184.8085	0.0008	-0.0070	53
87	53184.9224	0.0013	-0.0085	7
97	53185.4979	0.0004	-0.0106	17

^a BJD-2400000.^b Against $\max = 2453179.9061 + 0.057757E$.^c Number of points used to determine the maximum.**Table 139.** Secondary Superhump of V1108 Her (2004).

E	\max^a	error	$O - C^b$	N^c
81	53184.5950	0.0011	0.0250	72
82	53184.6526	0.0020	0.0251	32
83	53184.7130	0.0010	0.0281	46
84	53184.7696	0.0004	0.0272	50
85	53184.8292	0.0019	0.0292	54
87	53184.9434	0.0026	0.0285	7
89	53185.0577	0.0007	0.0277	39
90	53185.1140	0.0004	0.0266	53
96	53185.4575	0.0006	0.0252	18
97	53185.5162	0.0005	0.0264	17
98	53185.5715	0.0005	0.0242	17
100	53185.6789	0.0010	0.0166	30
101	53185.7386	0.0027	0.0188	26
102	53185.7916	0.0044	0.0143	31
103	53185.8525	0.0009	0.0178	43
107	53186.0817	0.0025	0.0170	18
108	53186.1389	0.0011	0.0167	23
116	53186.5952	0.0014	0.0131	38
117	53186.6528	0.0030	0.0132	49
118	53186.7174	0.0015	0.0203	45
119	53186.7712	0.0027	0.0166	33
120	53186.8319	0.0025	0.0198	37
121	53186.8899	0.0033	0.0203	11

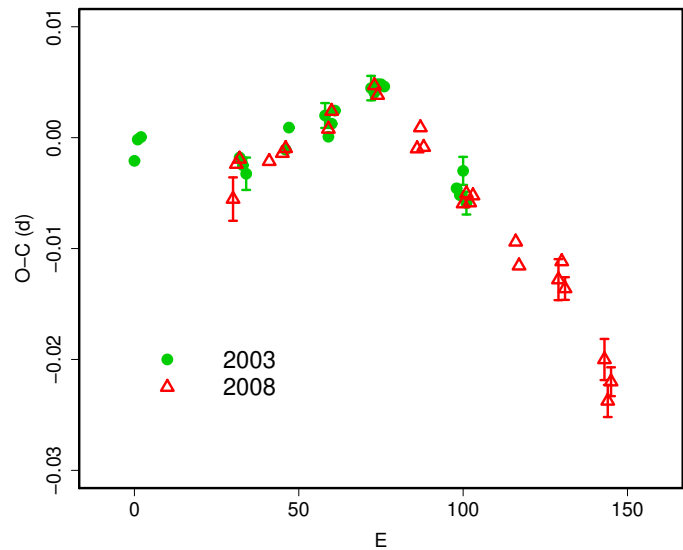
^a BJD-2400000.^b Against the same ephemeris in table 138.^c Number of points used to determine the maximum.**Fig. 93.** Comparison of $O - C$ diagrams of RU Hor between different superoutbursts. A period of 0.07087 d was used to draw this figure. Although the actual start of the outburst was not well constrained, the $O - C$ diagram of the 2008 superoutburst almost perfectly fits the 2003 one by assuming a 50-cycle difference in E .

Table 140. Superhump maxima of RU Hor (2003).

E	max ^a	error	$O - C^b$	N^c
0	52910.1929	0.0003	-0.0023	123
1	52910.2657	0.0003	-0.0004	132
2	52910.3368	0.0003	-0.0002	124
32	52912.4611	0.0006	-0.0019	71
33	52912.5312	0.0004	-0.0026	75
34	52912.6013	0.0015	-0.0033	42
46	52913.4539	0.0008	-0.0011	81
47	52913.5268	0.0006	0.0009	81
58	52914.3075	0.0011	0.0020	110
59	52914.3764	0.0008	0.0001	102
60	52914.4485	0.0009	0.0013	107
61	52914.5205	0.0006	0.0025	110
72	52915.3021	0.0011	0.0045	82
73	52915.3726	0.0008	0.0041	82
74	52915.4442	0.0007	0.0049	74
75	52915.5151	0.0006	0.0049	81
76	52915.5857	0.0010	0.0047	62
98	52917.1357	0.0008	-0.0044	132
99	52917.2060	0.0008	-0.0050	134
100	52917.2790	0.0013	-0.0028	134
101	52917.3470	0.0010	-0.0057	129

^a BJD-2400000.^b Against $max = 2452910.1952 + 0.070866E$.^c Number of points used to determine the maximum.

the superhump period was negligible, the present analysis seems to show a tendency of a period increase. The negative $O - C$ of the last ($E = 105$) being likely a result of the period decrease associated with a stage B-C transition, we excluded this point and obtained $P_{\text{dot}} = +7.0(4.3) \times 10^{-5}$. If we include this point, the resultant P_{dot} is almost zero ($-1.0(8.7) \times 10^{-5}$), confirming the analysis in Kato et al. (1999a). We further present the superoutbursts in 2000, 2002 February, 2002 November and 2009 January. (tables 143, 144, 145, 146). The resultant values of P_{dot} for the stage B were $+9.6(5.2) \times 10^{-5}$ (2000, $E \leq 78$), $+11.6(3.8) \times 10^{-5}$ (2002 February, $E \geq 14$) and $+13.2(3.1) \times 10^{-5}$ (2002 November, $E \leq 90$), respectively.

A comparison of $O - C$ diagrams between different superoutbursts is given in figure 94. The relatively large error in $O - C$'s in this system makes a comparison rather difficult. The behavior (and diversity) of the late stage B is somewhat reminiscent to KV Dra.

6.73. MM Hydrae

MM Hya, selected by the Palomer-Green survey (Green et al. 1982), had long been suspected to be a WZ Sge-like object based on the short orbital period (Misselt, Shafter 1995). The object was soon confirmed to undergo long outbursts approximately once per year, indicating a more usual SU UMa-type dwarf nova rather than a WZ Wge-like object. Patterson et al. (2003) reported a mean P_{SH} of 0.05868 d during the 1998 superoutburst without giving the details. We analyzed the AAVSO observations of

Table 141. Superhump maxima of RU Hor (2008).

E	max ^a	error	$O - C^b$	N^c
0	54686.4831	0.0020	-0.0089	82
1	54686.5571	0.0003	-0.0056	164
2	54686.6285	0.0003	-0.0049	164
11	54687.2661	0.0006	-0.0037	133
15	54687.5503	0.0005	-0.0023	164
16	54687.6216	0.0004	-0.0017	163
29	54688.5447	0.0005	0.0021	162
30	54688.6172	0.0005	0.0038	162
43	54689.5408	0.0004	0.0082	163
44	54689.6108	0.0003	0.0075	163
56	54690.4564	0.0004	0.0046	146
57	54690.5292	0.0004	0.0067	164
58	54690.5983	0.0004	0.0051	164
70	54691.4436	0.0007	0.0019	146
71	54691.5154	0.0007	0.0029	164
72	54691.5854	0.0006	0.0023	164
73	54691.6569	0.0009	0.0031	96
86	54692.5741	0.0008	0.0010	163
87	54692.6428	0.0005	-0.0010	138
99	54693.4920	0.0018	-0.0004	164
100	54693.5645	0.0010	0.0014	164
101	54693.6329	0.0010	-0.0008	163
113	54694.4770	0.0019	-0.0053	164
114	54694.5441	0.0014	-0.0089	163
115	54694.6167	0.0013	-0.0070	164

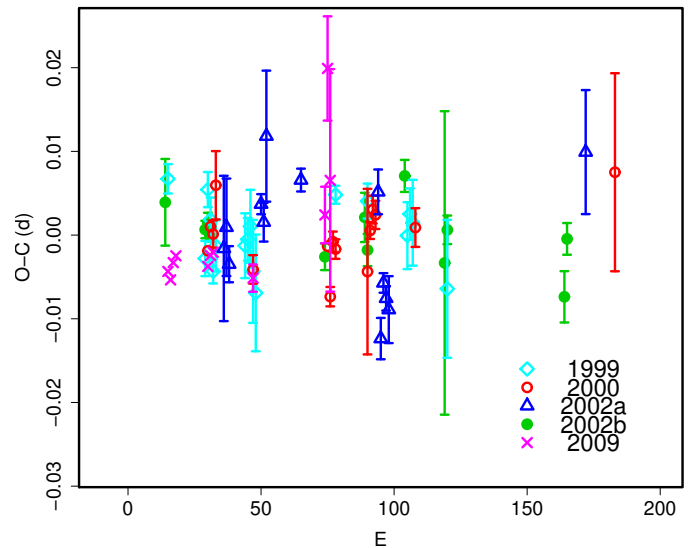
^a BJD-2400000.^b Against $max = 2454686.4920 + 0.070711E$.^c Number of points used to determine the maximum.

Fig. 94. Comparison of $O - C$ diagrams of CT Hya between different superoutbursts. A period of 0.06640 d was used to draw this figure. Approximate cycle counts (E) after the start of the superoutburst were used.

Table 142. Superhump maxima of CT Hya (1999).

E	\max^a	error	$O - C^b$	N^c
0	51225.0000	0.0018	0.0064	79
14	51225.9200	0.0021	-0.0030	91
15	51225.9947	0.0021	0.0052	110
16	51226.0575	0.0026	0.0017	28
17	51226.1177	0.0014	-0.0045	68
18	51226.1872	0.0031	-0.0015	71
29	51226.9176	0.0039	-0.0014	92
30	51226.9847	0.0026	-0.0006	130
31	51227.0527	0.0044	0.0010	73
32	51227.1137	0.0062	-0.0044	61
33	51227.1775	0.0070	-0.0070	23
63	51229.1813	0.0011	0.0049	115
75	51229.9773	0.0021	0.0043	96
90	51230.9692	0.0040	0.0002	68
91	51231.0382	0.0031	0.0028	17
92	51231.1035	0.0051	0.0018	23
105	51231.9588	0.0082	-0.0060	71

^a BJD-2400000.^b Against $\max = 2451224.9935 + 0.066394E$.^c Number of points used to determine the maximum.**Table 143.** Superhump maxima of CT Hya (2000).

E	\max^a	error	$O - C^b$	N^c
0	51880.1597	0.0005	-0.0003	57
1	51880.2290	0.0006	0.0025	148
2	51880.2945	0.0016	0.0016	184
3	51880.3667	0.0041	0.0074	82
17	51881.2863	0.0017	-0.0031	93
45	51883.1482	0.0010	-0.0013	51
46	51883.2086	0.0012	-0.0074	63
47	51883.2816	0.0012	-0.0008	131
48	51883.3471	0.0012	-0.0018	140
60	51884.1412	0.0099	-0.0049	32
61	51884.2125	0.0010	0.0000	63
62	51884.2814	0.0017	0.0025	131
63	51884.3472	0.0017	0.0018	97
78	51885.3417	0.0023	-0.0002	99
153	51890.3283	0.0118	0.0038	10

^a BJD-2400000.^b Against $\max = 2451880.1600 + 0.066434E$.^c Number of points used to determine the maximum.**Table 144.** Superhump maxima of CT Hya (2002a).

E	\max^a	error	$O - C^b$	N^c
0	52317.1711	0.0087	-0.0016	81
1	52317.2400	0.0058	0.0010	81
2	52317.3020	0.0022	-0.0035	94
14	52318.1060	0.0012	0.0037	126
15	52318.1702	0.0023	0.0016	129
16	52318.2469	0.0078	0.0118	117
29	52319.1048	0.0014	0.0066	128
58	52321.0290	0.0027	0.0052	63
59	52321.0779	0.0025	-0.0124	124
60	52321.1509	0.0012	-0.0057	129
61	52321.2155	0.0015	-0.0076	127
62	52321.2806	0.0040	-0.0089	81
136	52326.2130	0.0074	0.0099	17

^a BJD-2400000.^b Against $\max = 2452317.1726 + 0.066401E$.^c Number of points used to determine the maximum.**Table 145.** Superhump maxima of CT Hya (2002b).

E	\max^a	error	$O - C^b$	N^c
0	52591.1998	0.0052	0.0017	26
15	52592.1926	0.0010	-0.0011	126
16	52592.2597	0.0013	-0.0003	213
17	52592.3244	0.0003	-0.0020	221
60	52595.1773	0.0016	-0.0030	126
75	52596.1780	0.0029	0.0022	114
76	52596.2405	0.0019	-0.0017	122
90	52597.1790	0.0019	0.0076	89
105	52598.1646	0.0181	-0.0023	92
106	52598.2349	0.0017	0.0017	126
150	52601.1485	0.0031	-0.0049	125
151	52601.2219	0.0019	0.0020	200

^a BJD-2400000.^b Against $\max = 2452591.1981 + 0.066369E$.^c Number of points used to determine the maximum.

the 1998 superoutburst and obtained times of superhump maxima (table 147). The mean P_{SH} determined with the PDM method was 0.05894(3) d. This period is significantly longer than that by Patterson et al. (2003). The present observation was probably obtained near the end of the stage B. A possible decrease in $O - C$, although the uncertainty is large, in $E = 65 - 66$ may be a result of a transition to the stage C.

We also observed the 2001 superoutburst during its earliest stage (table 148). The observations corresponded to the stage A-B transition. The mean periods during the stage A was 0.0603(3) d. The observed length of the stage B was too short to determine the period. On the first night of the observation (2001 May 15), double-wave modulations similar to early superhumps in WZ Sge-type dwarf novae were observed (figure 95). Although the length of observations was insufficient to discriminate between P_{SH}

Table 146. Superhump maxima of CT Hya (2009).

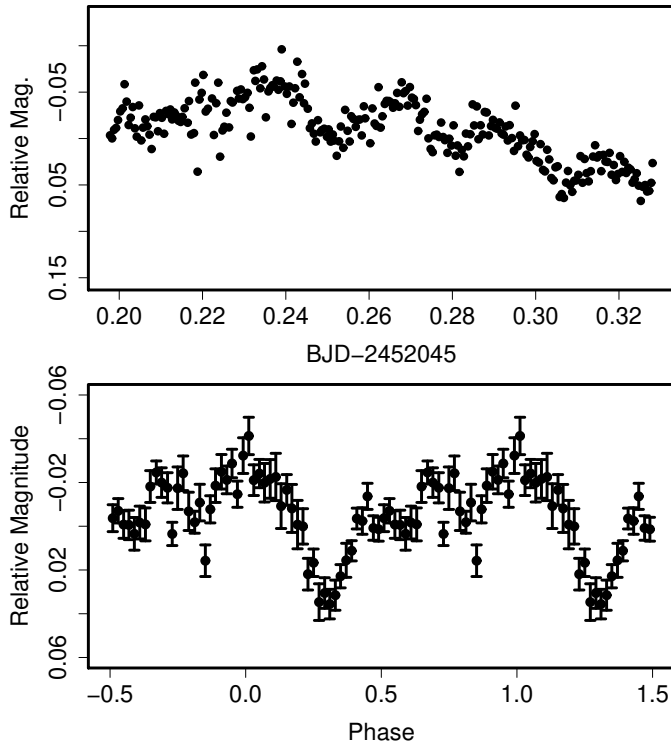
E	max ^a	error	$O - C^b$	N^c
0	54847.0839	0.0004	0.0012	72
1	54847.1493	0.0007	-0.0000	54
2	54847.2178	0.0005	0.0018	83
3	54847.2850	0.0006	0.0024	48
15	54848.0805	0.0004	-0.0016	132
16	54848.1482	0.0008	-0.0006	100
17	54848.2150	0.0008	-0.0004	117
32	54849.2079	0.0016	-0.0069	76
59	54851.0083	0.0034	-0.0056	63
60	54851.0922	0.0062	0.0117	138
61	54851.1452	0.0133	-0.0019	73

^a BJD-2400000.^b Against $max = 2454847.0827 + 0.066630E$.^c Number of points used to determine the maximum.**Table 147.** Superhump maxima of MM Hya (1998).

E	max ^a	error	$O - C^b$	N^c
0	50882.2853	0.0076	-0.0050	17
1	50882.3503	0.0023	0.0011	33
2	50882.4123	0.0021	0.0042	34
3	50882.4671	0.0012	0.0001	29
15	50883.1732	0.0026	-0.0011	58
51	50885.3016	0.0030	0.0058	23
52	50885.3517	0.0016	-0.0031	34
65	50886.1191	0.0058	-0.0018	48
66	50886.1796	0.0029	-0.0002	48

^a BJD-2400000.^b Against $max = 2450882.2903 + 0.058931E$.^c Number of points used to determine the maximum.**Table 148.** Superhump maxima of MM Hya (2001).

E	max ^a	error	$O - C^b$	N^c
0	52045.9826	0.0025	-0.0000	89
4	52046.2195	0.0007	-0.0022	615
17	52047.0068	0.0021	0.0082	71
21	52047.2359	0.0003	-0.0017	707
22	52047.2931	0.0001	-0.0043	703

^a BJD-2400000.^b Against $max = 2452045.9826 + 0.059762E$.^c Number of points used to determine the maximum.**Fig. 95.** Double-wave humps in MM Hya (2001) (Upper): Light curve. (Lower): Phase-averaged profile referring to the orbital period.

and P_{orb} , the profile strongly suggests the presence of early superhumps. The object is similar to BC UMa (Patterson et al. 2003; Maehara et al. 2007) and RZ Leo (Ishioaka et al. 2001; Patterson et al. 2003) that showed early superhumps during the earliest stage of their superoutbursts.

6.74. VW Hydri

We analyzed the 2000 May superoutburst (table 149). The observation covered the early stage of the superout-

burst and we obtained a mean P_{SH} of 0.07699(6) d. The observations were slightly insufficient to estimate a P_{dot} . The $O - C$ variation in Vogt (1974) confirmed the presence of the stage B-C transition. Liller (1996) reported little evidence for period variation of superhumps during the 1995 November superoutburst. We did not, however, include this observation because the periods were not based on an $O - C$ analysis nor times of superhumps were given. The reported period of 0.076646(3) d with the Fourier analysis was between P_1 and P_2 of the 2000 superoutburst.

Table 149. Superhump maxima of VW Hyi (2000).

E	max ^a	error	$O - C^b$	N^c
0	51680.9054	0.0022	-0.0014	6
8	51681.5219	0.0020	-0.0007	7
13	51681.9050	0.0074	-0.0026	7
33	51683.4515	0.0032	0.0042	6
34	51683.5298	0.0059	0.0056	7
46	51684.4467	0.0045	-0.0014	5
47	51684.5265	0.0024	0.0014	7
52	51684.9081	0.0099	-0.0019	7
60	51685.5228	0.0022	-0.0031	9

^a BJD-2400000.^b Against $max = 2451680.9067 + 0.076986E$.^c Number of points used to determine the maximum.

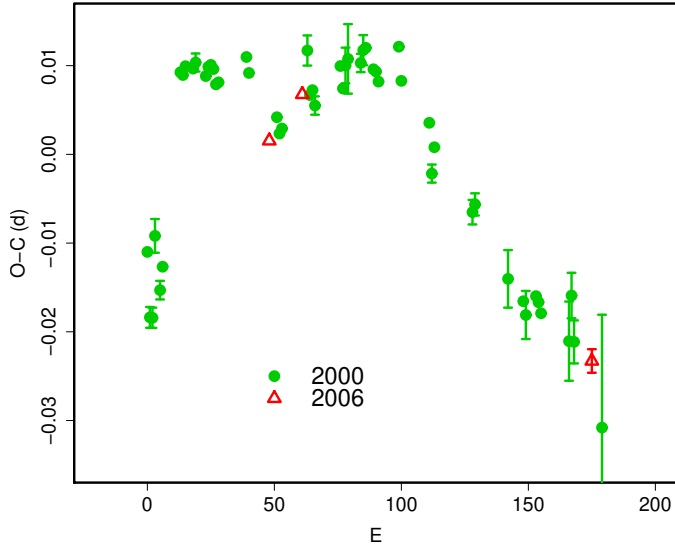


Fig. 96. Comparison of $O - C$ diagrams of RZ Leo between different superoutbursts. A period of 0.07865 d was used to draw this figure. Approximate cycle counts (E) after the start of the superoutburst were used.

6.75. *RZ Leonis*

We reanalyzed a combination of Ishioka et al. (2001) and the AAVSO data. The times of superhump maxima are given in table 150. Although Ishioka et al. (2001) identified earlier maxima ($E \leq 6$) as being early superhumps, we examined whether these maxima can be tracked back as in the stage A of other SU UMa-type dwarf novae. Although we could track back the maxima with a slightly longer period for ~ 1 d, as in the stage A of other SU UMa-type dwarf novae, this attempt failed to express earlier ($E < 0$) epochs. This analysis also supports the identification of these humps as being early superhumps, rather than a smooth extension of ordinary superhumps. The $O - C$ diagram showed a transition to the stage C after $E = 100$. For the interval $13 \leq E \leq 100$ (stage B), we obtained $P_{\text{dot}} = +4.9(1.7) \times 10^{-5}$. The value is in good agreement with Ishioka et al. (2001).

The object underwent another superoutburst in 2006. Although the seasonal condition was poor, we obtained several superhump maxima (table 151). The $O - C$'s against the mean period of 2000 suggest that the observation caught the increasing period during the first two nights, and last observation with a strongly negative $O - C$ should have caught the late transition from the stage B to C (see figure 96). We did not attempt to derive a global P_{dot} .

6.76. *GW Librae*

GW Lib, originally reported as a nova in 1983 (Maza, Gonzalez 1983), and long suspected to be a WZ Sge-type dwarf nova, underwent a spectacular outburst in 2007 (R. Stubbings, vsnet-alert 9279; Waagen et al. 2007). The object initially showed only very low-amplitude modulations similar to early superhumps, whose period was not

Table 150. Superhump maxima of RZ Leo (2000–2001).

E	max ^a	error	$O - C^b$	N^c
0	51901.1571	0.0009	-0.0189	106
1	51901.2283	0.0012	-0.0262	145
2	51901.3069	0.0011	-0.0261	146
3	51901.3948	0.0019	-0.0168	76
5	51901.5460	0.0010	-0.0227	173
6	51901.6273	0.0009	-0.0199	183
13	51902.1998	0.0004	0.0027	214
14	51902.2781	0.0004	0.0025	203
15	51902.3578	0.0004	0.0036	165
18	51902.5934	0.0006	0.0037	134
19	51902.6728	0.0010	0.0045	46
23	51902.9858	0.0005	0.0034	42
24	51903.0655	0.0004	0.0045	41
25	51903.1444	0.0007	0.0048	114
26	51903.2226	0.0003	0.0045	174
27	51903.2995	0.0003	0.0029	207
28	51903.3784	0.0008	0.0032	105
39	51904.2464	0.0007	0.0072	83
40	51904.3232	0.0004	0.0055	114
51	51905.1834	0.0004	0.0017	181
52	51905.2602	0.0003	-0.0000	176
53	51905.3394	0.0005	0.0006	146
63	51906.1347	0.0017	0.0105	102
64	51906.2083	0.0006	0.0056	150
65	51906.2875	0.0004	0.0062	218
66	51906.3645	0.0010	0.0046	118
76	51907.1554	0.0005	0.0101	147
77	51907.2315	0.0007	0.0077	105
78	51907.3128	0.0020	0.0104	39
79	51907.3922	0.0039	0.0112	29
84	51907.7850	0.0010	0.0113	35
85	51907.8651	0.0017	0.0129	17
86	51907.9440	0.0009	0.0132	17
89	51908.1775	0.0005	0.0111	149
90	51908.2559	0.0005	0.0110	289
91	51908.3334	0.0004	0.0099	260
99	51908.9665	0.0006	0.0147	40
100	51909.0413	0.0006	0.0110	40
111	51909.9018	0.0010	0.0074	33
112	51909.9747	0.0010	0.0018	40
113	51910.0563	0.0006	0.0049	41
128	51911.2287	0.0014	-0.0008	224
129	51911.3083	0.0013	0.0001	220
142	51912.3223	0.0032	-0.0069	27
148	51912.7917	0.0009	-0.0088	36
149	51912.8688	0.0027	-0.0102	20
153	51913.1855	0.0009	-0.0077	206
154	51913.2635	0.0007	-0.0082	222
155	51913.3409	0.0008	-0.0094	226
166	51914.2029	0.0045	-0.0114	74
167	51914.2867	0.0026	-0.0061	63
168	51914.3601	0.0024	-0.0112	91
179	51915.2156	0.0127	-0.0197	26

^a BJD-2400000.

^b Against $max = 2451901.1760 + 0.078544E$.

^c Number of points used to determine the maximum.

Table 151. Superhump maxima of RZ Leo (2006).

E	max ^a	error	$O - C^b$	N^c
0	53886.0103	0.0002	-0.0038	195
13	53887.0380	0.0006	0.0043	314
127	53895.9741	0.0013	-0.0004	81

^a BJD-2400000.^b Against $max = 2453886.0142 + 0.078428E$.^c Number of points used to determine the maximum.

well determined. After ~ 11 days, ordinary superhumps emerged (vsnet-alert 9315, 9316).

The maxima times of ordinary superhumps are listed in table 152. The $O - C$ diagram (figure 33) very clearly consisted of the stage A with a long superhump period ($E \leq 39$), the stage B with a definitely positive P_{dot} , and later stage ($E \geq 289$) with noticeably negative $O - C$'s. For the stage B ($51 \leq E \leq 278$), we obtained $P_{\text{dot}} = +4.0(0.1) \times 10^{-5}$. It seems that the phase was discontinuous between the middle and the last segments. This may be attributed to the appearance of the orbital humps (figure 97). At an estimated orbital inclination of 11° (Thorstensen et al. 2002), the appearance of orbital humps is surprising. The orbital inclination is either higher or there is a special mechanism for manifesting orbital humps during the late stage of the plateau phase of WZ Sge-type dwarf novae (see also V455 And and WZ Sge, subsections 6.5 and 6.113. The double-wave profile in GW Lib might suggest that a sort of the 2:1 resonance, as in early superhumps, is somehow excited, or persists, during the last stage of the superoutburst plateau of WZ Sge-type dwarf novae.

More detailed analysis of the outburst will be presented by Imada et al., in preparation.

6.77. RZ Leonis Minoris

We analyzed the 2005 April superoutburst of RZ LMi (table 153). This superoutburst had a marginally positive P_{dot} of $+2.3(1.1) \times 10^{-5}$, as in the 2004 superoutburst Olech et al. (2008). The maxima for $E \geq 118$ (during the rapid fading stage) were either phase 0.5 offset (traditional late superhumps), stage C superhumps with a period of 0.05875(8) d ($E \geq 84$), or even a candidate for orbital humps. Since none of these kinds of phenomena have not yet been reported in RZ LMi (Olech et al. 2008), further detailed observations during the rapid fading stage might provide crucial information.

6.78. SS Leonis Minoris

SS LMi was discovered as an extragalactic nova or an unusual dwarf nova (Alksnis, Zacs 1981). Although Harrison (1991) reported a "red" outburst in 1991, the nature of this outburst remained unclear.¹⁵ Shears et al. (2008a) reported the 2006 superoutburst. Based on their times of superhump maxima, we obtained $P_{\text{dot}} =$

¹⁵ See also Howell, Kreidl (1991); the unusual color in these observations could have been a combination with a nearby field star Shears et al. (2008a).

Table 152. Superhump maxima of GW Lib (2007).

E	max ^a	error	$O - C^b$	N^c
0	54212.3805	0.0011	-0.0274	249
2	54212.4933	0.0008	-0.0227	206
11	54212.9948	0.0026	-0.0081	148
12	54213.0405	0.0015	-0.0165	168
31	54214.0785	0.0007	-0.0063	416
32	54214.1357	0.0003	-0.0032	1040
35	54214.3004	0.0002	-0.0007	249
36	54214.3542	0.0002	-0.0010	249
37	54214.4098	0.0001	0.0005	249
38	54214.4639	0.0001	0.0005	245
39	54214.5198	0.0001	0.0023	249
51	54215.1758	0.0001	0.0092	171
53	54215.2834	0.0003	0.0086	112
54	54215.3385	0.0002	0.0096	97
55	54215.3920	0.0001	0.0090	209
56	54215.4457	0.0001	0.0086	250
57	54215.4996	0.0001	0.0085	250
58	54215.5529	0.0001	0.0076	248
66	54215.9851	0.0002	0.0071	158
67	54216.0385	0.0001	0.0064	158
68	54216.0943	0.0004	0.0082	341
69	54216.1450	0.0002	0.0047	1099
70	54216.2006	0.0001	0.0062	1245
71	54216.2548	0.0002	0.0064	689
72	54216.3075	0.0002	0.0050	499
73	54216.3621	0.0001	0.0055	250
74	54216.4164	0.0001	0.0057	213
87	54217.1173	0.0002	0.0034	1105
88	54217.1708	0.0002	0.0028	1433
89	54217.2248	0.0002	0.0027	1250
105	54218.0873	0.0005	-0.0002	356
106	54218.1422	0.0005	0.0006	386
107	54218.1956	0.0003	-0.0001	293
108	54218.2486	0.0009	-0.0012	117
123	54219.0616	0.0005	0.0004	137
124	54219.1147	0.0002	-0.0006	468
125	54219.1687	0.0004	-0.0007	729
126	54219.2193	0.0007	-0.0042	341
128	54219.3305	0.0001	-0.0012	246
129	54219.3836	0.0001	-0.0022	250
130	54219.4389	0.0001	-0.0010	246
131	54219.4920	0.0001	-0.0019	250
132	54219.5464	0.0001	-0.0016	250
141	54220.0311	0.0007	-0.0037	238
142	54220.0890	0.0005	0.0001	379
143	54220.1430	0.0003	-0.0001	720
144	54220.1959	0.0003	-0.0013	782
145	54220.2491	0.0008	-0.0022	404
146	54220.3034	0.0002	-0.0020	260
147	54220.3567	0.0002	-0.0028	249
148	54220.4114	0.0001	-0.0021	249

^a BJD-2400000.^b Against $max = 2454212.4079 + 0.054092E$.^c Number of points used to determine the maximum.

Table 152. Superhump maxima of GW Lib (2007) (continued).

E	max	error	$O - C$	N
149	54220.4655	0.0002	-0.0022	249
150	54220.5172	0.0002	-0.0045	249
151	54220.5735	0.0001	-0.0023	249
160	54221.0578	0.0010	-0.0048	175
161	54221.1148	0.0010	-0.0019	192
165	54221.3302	0.0002	-0.0028	249
166	54221.3832	0.0002	-0.0040	250
167	54221.4385	0.0001	-0.0028	249
183	54222.3044	0.0002	-0.0024	250
184	54222.3584	0.0002	-0.0024	250
198	54223.1158	0.0006	-0.0023	263
199	54223.1741	0.0009	0.0019	358
234	54225.0653	0.0041	-0.0002	31
236	54225.1755	0.0007	0.0019	87
258	54226.3718	0.0002	0.0082	247
259	54226.4270	0.0003	0.0093	241
260	54226.4808	0.0003	0.0089	197
261	54226.5352	0.0006	0.0093	217
262	54226.5898	0.0003	0.0098	237
276	54227.3504	0.0004	0.0131	249
277	54227.4035	0.0005	0.0121	190
278	54227.4580	0.0002	0.0125	249
289	54228.0378	0.0008	-0.0026	383
290	54228.0884	0.0019	-0.0062	859
291	54228.1374	0.0030	-0.0113	1258
292	54228.1995	0.0008	-0.0033	1160
295	54228.3558	0.0008	-0.0092	191
296	54228.4130	0.0007	-0.0061	249
297	54228.4633	0.0009	-0.0099	249
298	54228.5190	0.0008	-0.0084	249
299	54228.5694	0.0012	-0.0120	248
300	54228.6274	0.0015	-0.0081	228
308	54229.0510	0.0028	-0.0173	261
309	54229.1079	0.0006	-0.0144	703
310	54229.1603	0.0006	-0.0162	719
311	54229.2126	0.0012	-0.0180	619
312	54229.2724	0.0028	-0.0122	154
314	54229.3783	0.0006	-0.0145	181
315	54229.4318	0.0018	-0.0151	187
316	54229.4832	0.0004	-0.0177	187
317	54229.5330	0.0012	-0.0220	188
318	54229.5928	0.0008	-0.0164	187
333	54230.4039	0.0003	-0.0166	186
334	54230.4600	0.0004	-0.0146	187
335	54230.5093	0.0007	-0.0194	188
336	54230.5510	0.0008	-0.0318	187
337	54230.6164	0.0006	-0.0205	134
345	54231.0452	0.0033	-0.0244	44
346	54231.1132	0.0013	-0.0105	79
347	54231.1661	0.0114	-0.0118	46
348	54231.2181	0.0015	-0.0138	63
349	54231.2782	0.0009	-0.0078	179
350	54231.3294	0.0002	-0.0107	188
351	54231.3828	0.0003	-0.0114	179
363	54232.0410	0.0013	-0.0023	175

Table 152. Superhump maxima of GW Lib (2007) (continued).

E	max	error	$O - C$	N
364	54232.0870	0.0010	-0.0104	211
365	54232.1444	0.0009	-0.0071	308
366	54232.2039	0.0014	-0.0016	82
367	54232.2558	0.0009	-0.0038	172
368	54232.3072	0.0004	-0.0065	186
369	54232.3615	0.0004	-0.0064	188
373	54232.5795	0.0006	-0.0047	188
374	54232.6272	0.0005	-0.0111	140
380	54232.9630	0.0003	0.0001	67
381	54233.0126	0.0008	-0.0044	111
382	54233.0704	0.0008	-0.0006	60
383	54233.1273	0.0014	0.0022	27
386	54233.2860	0.0010	-0.0014	188
387	54233.3378	0.0004	-0.0037	188
400	54234.0426	0.0007	-0.0021	120
401	54234.0968	0.0004	-0.0020	245
402	54234.1487	0.0005	-0.0042	194
404	54234.2590	0.0003	-0.0021	249
405	54234.3111	0.0003	-0.0041	249
406	54234.3647	0.0003	-0.0046	248
407	54234.4171	0.0002	-0.0063	249
408	54234.4719	0.0003	-0.0056	249
409	54234.5251	0.0003	-0.0064	234
416	54234.9092	0.0006	-0.0010	33
417	54234.9560	0.0003	-0.0082	50
418	54235.0106	0.0003	-0.0077	46
419	54235.0664	0.0008	-0.0060	206
420	54235.1207	0.0007	-0.0059	244
421	54235.1740	0.0011	-0.0066	144
423	54235.2839	0.0005	-0.0049	173
424	54235.3367	0.0003	-0.0062	248
425	54235.3907	0.0003	-0.0063	249
426	54235.4449	0.0003	-0.0062	241
427	54235.4996	0.0003	-0.0056	235
436	54235.9875	0.0037	-0.0046	95
438	54236.1028	0.0009	0.0026	142
439	54236.1486	0.0011	-0.0057	171
442	54236.3177	0.0005	0.0011	249
443	54236.3699	0.0004	-0.0007	250
444	54236.4239	0.0003	-0.0008	250
445	54236.4778	0.0004	-0.0010	250
446	54236.5319	0.0005	-0.0011	236
447	54236.5842	0.0006	-0.0028	222
454	54236.9644	0.0005	-0.0013	27
460	54237.2908	0.0004	0.0006	189
461	54237.3439	0.0003	-0.0005	249
462	54237.3968	0.0003	-0.0016	250
463	54237.4520	0.0006	-0.0005	249
474	54238.0450	0.0013	-0.0025	179
475	54238.1042	0.0013	0.0026	200
476	54238.1554	0.0004	-0.0003	355
477	54238.2095	0.0013	-0.0003	205
478	54238.2610	0.0013	-0.0029	187
479	54238.3187	0.0003	0.0008	125
480	54238.3694	0.0004	-0.0027	124

Table 152. Superhump maxima of GW Lib (2007) (continued).

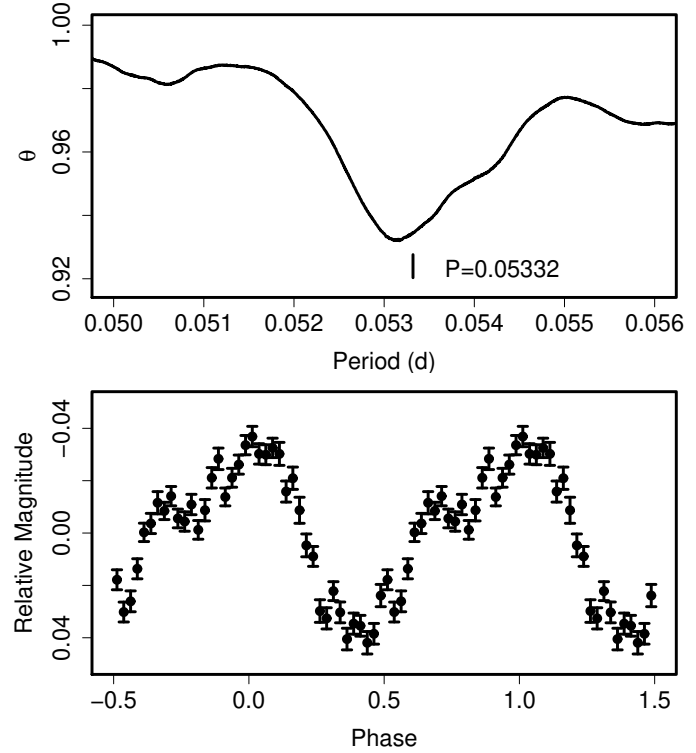
E	max	error	$O - C$	N
481	54238.4256	0.0003	-0.0006	125
482	54238.4791	0.0004	-0.0011	125
483	54238.5267	0.0003	-0.0076	125
484	54238.5870	0.0004	-0.0014	124
496	54239.2343	0.0020	-0.0032	63
498	54239.3458	0.0006	0.0001	101
499	54239.3992	0.0005	-0.0006	124
500	54239.4545	0.0003	0.0006	125
501	54239.5040	0.0005	-0.0040	125
502	54239.5607	0.0004	-0.0013	123
511	54240.0517	0.0008	0.0028	78
512	54240.1068	0.0011	0.0038	131
513	54240.1596	0.0015	0.0025	111
520	54240.5337	0.0004	-0.0020	116
521	54240.5896	0.0006	-0.0003	85
528	54240.9714	0.0005	0.0030	110
529	54241.0260	0.0009	0.0034	164
530	54241.0807	0.0007	0.0041	338
531	54241.1330	0.0007	0.0023	324
532	54241.1850	0.0014	0.0001	255
547	54241.9971	0.0026	0.0009	54
548	54242.0569	0.0011	0.0066	58
549	54242.1070	0.0078	0.0026	17
551	54242.2148	0.0010	0.0022	82
552	54242.2678	0.0005	0.0012	123
553	54242.3221	0.0005	0.0014	124
554	54242.3767	0.0003	0.0019	125
555	54242.4340	0.0003	0.0050	124
556	54242.4842	0.0003	0.0011	125
568	54243.1438	0.0042	0.0116	43
571	54243.2970	0.0005	0.0026	117
572	54243.3516	0.0004	0.0031	125
573	54243.4070	0.0003	0.0044	125
574	54243.4585	0.0007	0.0018	125
575	54243.5147	0.0005	0.0039	108
590	54244.3233	0.0005	0.0011	122
591	54244.3826	0.0004	0.0064	121
592	54244.4364	0.0003	0.0061	125
593	54244.4891	0.0006	0.0046	124
594	54244.5412	0.0004	0.0027	124
595	54244.5964	0.0010	0.0037	89
601	54244.9234	0.0005	0.0062	26
607	54245.2449	0.0007	0.0032	93
608	54245.3034	0.0004	0.0076	125
609	54245.3567	0.0010	0.0068	123
610	54245.4091	0.0005	0.0051	125
611	54245.4635	0.0005	0.0054	125
612	54245.5180	0.0005	0.0058	124
613	54245.5708	0.0006	0.0045	123
638	54246.9264	0.0020	0.0078	26
639	54246.9785	0.0007	0.0058	26
640	54247.0368	0.0018	0.0101	66
641	54247.0893	0.0015	0.0084	29
642	54247.1478	0.0026	0.0128	44
643	54247.2046	0.0021	0.0155	22

Table 152. Superhump maxima of GW Lib (2007) (continued).

E	max	error	$O - C$	N
645	54247.3087	0.0016	0.0114	77
646	54247.3640	0.0010	0.0127	125
647	54247.4150	0.0013	0.0095	124
648	54247.4637	0.0007	0.0042	125
649	54247.5234	0.0012	0.0098	105
660	54248.1203	0.0023	0.0117	87
663	54248.2812	0.0010	0.0103	125
664	54248.3428	0.0018	0.0178	98
681	54249.2501	0.0008	0.0055	125
682	54249.3066	0.0012	0.0080	125
700	54250.2883	0.0010	0.0160	124
786	54254.9363	0.0032	0.0120	23
787	54254.9872	0.0113	0.0089	29
788	54255.0486	0.0051	0.0162	27
803	54255.8694	0.0026	0.0256	18
804	54255.9161	0.0017	0.0182	27
805	54255.9636	0.0020	0.0116	21
806	54256.0321	0.0036	0.0260	149
808	54256.1247	0.0023	0.0105	162
811	54256.2919	0.0012	0.0153	78
812	54256.3486	0.0008	0.0180	124
813	54256.4028	0.0007	0.0181	125
814	54256.4543	0.0016	0.0155	124
815	54256.5201	0.0028	0.0272	65
824	54256.9931	0.0020	0.0134	25
843	54258.0189	0.0041	0.0114	47
848	54258.3031	0.0011	0.0251	80
849	54258.3520	0.0008	0.0200	125
850	54258.4050	0.0010	0.0189	124
851	54258.4584	0.0024	0.0182	125
852	54258.5101	0.0007	0.0159	125
867	54259.3271	0.0004	0.0214	92
868	54259.3804	0.0007	0.0206	125
869	54259.4341	0.0006	0.0202	114
870	54259.4858	0.0007	0.0178	125
871	54259.5441	0.0011	0.0220	97
885	54260.3031	0.0010	0.0238	74
886	54260.3568	0.0013	0.0233	124
887	54260.4135	0.0008	0.0260	125
888	54260.4696	0.0008	0.0280	125
889	54260.5205	0.0016	0.0248	125
903	54261.2805	0.0006	0.0276	124
904	54261.3323	0.0011	0.0252	125
905	54261.3852	0.0008	0.0240	125
906	54261.4387	0.0006	0.0234	125
907	54261.4962	0.0009	0.0268	125
908	54261.5452	0.0008	0.0218	87
921	54262.2493	0.0015	0.0227	82
922	54262.3090	0.0009	0.0283	125
923	54262.3623	0.0007	0.0275	125
924	54262.4129	0.0010	0.0240	125
925	54262.4693	0.0013	0.0263	125
926	54262.5283	0.0019	0.0313	78
935	54263.0107	0.0031	0.0268	154
941	54263.3320	0.0006	0.0235	125

Table 152. Superhump maxima of GW Lib (2007) (continued).

E	max	error	$O - C$	N
942	54263.3911	0.0012	0.0286	125
943	54263.4410	0.0012	0.0243	125
944	54263.4987	0.0016	0.0280	124
957	54264.1973	0.0025	0.0233	101
958	54264.2567	0.0014	0.0286	125
959	54264.3110	0.0007	0.0289	125
960	54264.3613	0.0008	0.0251	125
961	54264.4171	0.0010	0.0268	125
976	54265.2351	0.0009	0.0334	94
979	54265.3911	0.0016	0.0271	115
980	54265.4543	0.0013	0.0362	30
994	54266.2096	0.0011	0.0343	124
995	54266.2578	0.0010	0.0284	125
1013	54267.2442	0.0009	0.0411	123
1014	54267.2956	0.0010	0.0384	125
1015	54267.3467	0.0014	0.0355	125
1016	54267.3968	0.0008	0.0314	124
1017	54267.4585	0.0032	0.0391	124
1032	54268.2646	0.0009	0.0337	89
1033	54268.3162	0.0014	0.0313	125
1034	54268.3724	0.0009	0.0333	125
1035	54268.4318	0.0013	0.0387	124
1036	54268.4857	0.0014	0.0385	125
1051	54269.2956	0.0013	0.0370	124
1052	54269.3583	0.0021	0.0456	124
1053	54269.4015	0.0031	0.0347	125
1062	54269.8804	0.0180	0.0268	15
1063	54269.9413	0.0015	0.0336	25
1069	54270.2699	0.0009	0.0376	125
1070	54270.3211	0.0021	0.0348	125
1071	54270.3763	0.0011	0.0358	125
1072	54270.4264	0.0008	0.0318	125
1073	54270.4997	0.0048	0.0511	68
1087	54271.2444	0.0009	0.0385	112
1089	54271.3526	0.0010	0.0385	124
1090	54271.4057	0.0045	0.0376	125
1102	54272.0533	0.0020	0.0360	44
1106	54272.2758	0.0024	0.0422	125
1107	54272.3208	0.0011	0.0330	125
1108	54272.3812	0.0008	0.0394	125
1109	54272.4337	0.0025	0.0378	125
1110	54272.4930	0.0074	0.0430	66
1125	54273.3001	0.0013	0.0387	124
1127	54273.3981	0.0037	0.0285	125
1144	54274.3323	0.0018	0.0432	124
1145	54274.3925	0.0022	0.0492	125
1147	54274.4879	0.0015	0.0365	105
1161	54275.2535	0.0011	0.0447	125
1162	54275.3018	0.0017	0.0390	125
1163	54275.3605	0.0020	0.0436	125
1164	54275.4108	0.0012	0.0398	124

**Fig. 97.** Orbital humps in GW Lib (2007) during the late stage (BJD 2454227–2454230) of the superoutburst plateau. (Upper): PDM analysis. The tick mark is given at the orbital period. (Lower): Phase-averaged profile.**Table 153.** Superhump maxima of RZ LMi (2005).

E	max ^a	error	$O - C^b$	N^c
0	53473.7101	0.0004	-0.0054	40
1	53473.7688	0.0004	-0.0058	36
2	53473.8282	0.0003	-0.0057	36
33	53475.6684	0.0005	-0.0003	45
34	53475.7284	0.0006	0.0005	36
35	53475.7862	0.0006	-0.0009	35
36	53475.8467	0.0009	0.0004	30
50	53476.6803	0.0008	0.0053	37
51	53476.7379	0.0006	0.0037	40
52	53476.7962	0.0005	0.0028	38
53	53476.8563	0.0006	0.0037	37
84	53478.7001	0.0008	0.0126	40
86	53478.8169	0.0017	0.0111	41
118	53480.7007	0.0079	0.0007	20
119	53480.7497	0.0025	-0.0094	20
120	53480.8145	0.0017	-0.0038	20
136	53481.7560	0.0069	-0.0094	20

^a BJD-2400000.^b Against $max = 2453473.7154 + 0.059191E$.^c Number of points used to determine the maximum.

Table 154. Superhump maxima of SX LMi (1994).

E	max ^a	error	$O - C^b$	N^c
0	49702.1736	0.0010	-0.0031	14
1	49702.2438	0.0006	-0.0022	27
2	49702.3122	0.0003	-0.0030	36
16	49703.2854	0.0005	0.0007	66
17	49703.3543	0.0004	0.0004	63
29	49704.1875	0.0009	0.0026	30
45	49705.3009	0.0007	0.0081	42
89	49708.3412	0.0007	0.0015	46
103	49709.3076	0.0007	-0.0016	46
104	49709.3794	0.0008	0.0010	29
118	49710.3435	0.0011	-0.0044	44

^a BJD-2400000.^b Against $max = 2449702.1767 + 0.069248E$.^c Number of points used to determine the maximum.

+0.3(0.4) × 10⁻⁵ ($E \leq 128$). Since these superhumps were detected during the initial stage of a likely WZ Sge-type outburst, they can be interpreted as early superhumps rather than ordinary superhumps. The lack of period variation and a hint of double-wave modulations (Shears et al. 2008a) may support this interpretation. We listed the period in table 2 based on this identification.

6.79. *SX Leonis Minoris*

Nogami et al. (1997b) reported on the 1994 superoutburst. We reanalyzed the data during this superoutburst. The resultant times of superhump maxima are listed in table 154. The overall P_{dot} was $-8.2(1.1) \times 10^{-5}$, in good agreement with Nogami et al. (1997b).

We also observed the 2001 and 2002 superoutbursts (tables 155, 156). The resultant values of P_{dot} were $-3.3(3.0) \times 10^{-5}$ and $-4.1(1.5) \times 10^{-5}$ (excluding $E = 0$), respectively. The 2002 result might be interpreted as a sudden shift to a shorter superhump period (stage B to C) between $E = 116$ and $E = 130$. Using the interval of $14 \leq E \leq 115$, the resultant period change was almost zero, $P_{\text{dot}} = -0.7(0.5) \times 10^{-5}$.

6.80. *BR Lupi*

We observed the 2003 and 2004 superoutbursts. The times of superhump maxima are listed in tables 157 and 158. The both observations covered the relatively late stages of the superoutbursts (figure 98). A stage B-C transition was probably caught during the 2003 superoutburst and the only the stage C was likely recorded during the 2004 superoutburst. We give parameters in table 2 based on this interpretation.

6.81. *AY Lyrae*

Although AY Lyr has long been known a representative SU UMa-type dwarf nova, little is known about the variation of the superhump period except for the classical study by Udalski, Szymanski (1988). We observed the 2008 and 2009 superoutbursts (tables 159, 160). Although

Table 155. Superhump maxima of SX LMi (2001).

E	max ^a	error	$O - C^b$	N^c
0	51938.3604	0.0111	0.0013	70
12	51939.1870	0.0011	-0.0017	121
13	51939.2539	0.0014	-0.0039	119
14	51939.3245	0.0016	-0.0023	133
26	51940.1626	0.0019	0.0063	113
70	51943.1962	0.0008	-0.0014	120
71	51943.2680	0.0010	0.0012	132
72	51943.3358	0.0022	-0.0001	68
84	51944.1640	0.0036	-0.0014	112
85	51944.2400	0.0057	0.0055	105
113	51946.1665	0.0021	-0.0034	56

^a BJD-2400000.^b Against $max = 2451938.3592 + 0.069122E$.^c Number of points used to determine the maximum.**Table 156.** Superhump maxima of SX LMi (2002).

E	max ^a	error	$O - C^b$	N^c
0	52297.3399	0.0036	-0.0077	110
14	52298.3214	0.0003	0.0029	100
29	52299.3616	0.0010	0.0029	115
43	52300.3326	0.0009	0.0030	101
101	52304.3547	0.0020	0.0029	77
115	52305.3246	0.0011	0.0020	130
129	52306.2904	0.0021	-0.0031	101
130	52306.3599	0.0010	-0.0029	97

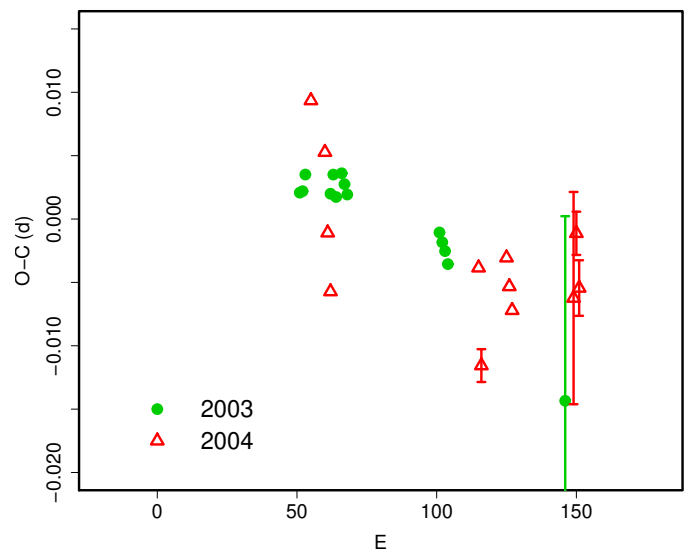
^a BJD-2400000.^b Against $max = 2452297.3477 + 0.069347E$.^c Number of points used to determine the maximum.**Fig. 98.** Comparison of $O - C$ diagrams of BR Lup between different superoutbursts. A period of 0.08228 d was used to draw this figure. Approximate cycle counts (E) after the start of the superoutburst were used.

Table 157. Superhump maxima of BR Lup (2003).

E	\max^a	error	$O - C^b$	N^c
0	52737.2349	0.0005	-0.0023	83
1	52737.3172	0.0004	-0.0020	83
2	52737.4008	0.0006	-0.0006	59
11	52738.1398	0.0005	-0.0007	66
12	52738.2236	0.0004	0.0010	83
13	52738.3041	0.0005	-0.0006	82
15	52738.4706	0.0006	0.0016	89
16	52738.5520	0.0005	0.0009	94
17	52738.6335	0.0006	0.0002	78
50	52741.3457	0.0008	0.0025	69
51	52741.4272	0.0006	0.0019	88
52	52741.5088	0.0008	0.0013	79
53	52741.5901	0.0009	0.0005	58
95	52745.0350	0.0146	-0.0037	18

^a BJD-2400000.^b Against $\max = 2452737.2372 + 0.082121E$.^c Number of points used to determine the maximum.**Table 158.** Superhump maxima of BR Lup (2004).

E	\max^a	error	$O - C^b$	N^c
0	53139.6291	0.0003	0.0077	176
5	53140.0364	0.0006	0.0041	44
6	53140.1124	0.0008	-0.0022	40
7	53140.1900	0.0006	-0.0067	38
60	53144.5527	0.0005	-0.0002	186
61	53144.6273	0.0013	-0.0079	186
70	53145.3763	0.0006	0.0014	186
71	53145.4563	0.0005	-0.0008	186
72	53145.5367	0.0006	-0.0026	186
94	53147.3479	0.0084	0.0003	167
95	53147.4352	0.0017	0.0055	181
96	53147.5132	0.0022	0.0013	141

^a BJD-2400000.^b Against $\max = 2453139.6214 + 0.082193E$.^c Number of points used to determine the maximum.

we only observed five consecutive nights during the 2008 superoutburst, a transition from stage B to C was apparently recorded. The early stage of the 2009 superoutburst was likely missed. The period variation probably reflects a stage B-C transition. A comparison of $O - C$ diagrams of between different superoutbursts is given in figure 99.

6.82. DM Lyræ

Nogami et al. (2003a) studied the 1996 and 1997 outbursts and confirmed the SU UMa-type nature of this object (the times of superhump maxima measured from the 1997 data are listed in table 161). We further observed the 2002 superoutburst (table 162). As in 1996 and 1997 ones, the 2002 superoutburst was observed during its later stage. Although we could not determine P_{dot} for the stage B, other parameters are given in table 2.

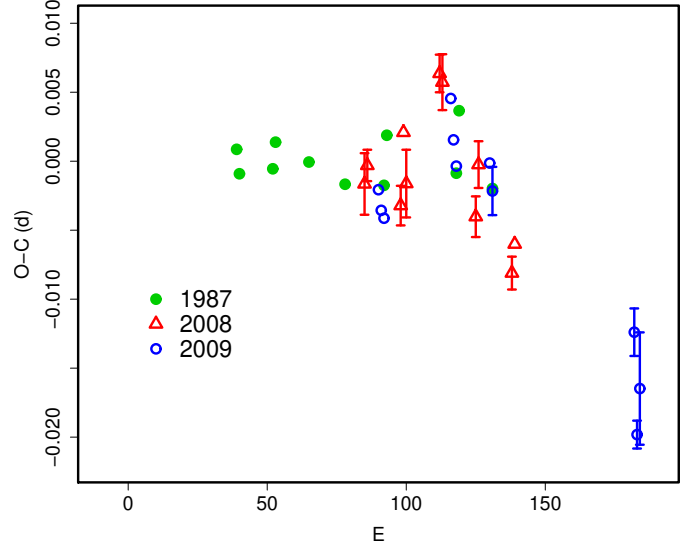


Fig. 99. Comparison of $O - C$ diagrams of AY Lyr between different superoutbursts. A period of 0.07597 d was used to draw this figure. Approximate cycle counts (E) after the start of the superoutburst were used. Since the start of the 2009 superoutburst was not well constrained, we shifted the $O - C$ diagrams to best fit the others.

Table 159. Superhump maxima of AY Lyr (2008).

E	\max^a	error	$O - C^b$	N^c
0	54754.9197	0.0022	-0.0031	87
1	54754.9970	0.0011	-0.0016	140
13	54755.9057	0.0014	-0.0034	77
14	54755.9870	0.0009	0.0020	243
15	54756.0593	0.0025	-0.0017	119
27	54756.9789	0.0014	0.0075	82
28	54757.0542	0.0020	0.0069	67
40	54757.9561	0.0015	-0.0017	58
41	54758.0359	0.0017	0.0022	75
53	54758.9396	0.0012	-0.0046	141
54	54759.0177	0.0008	-0.0024	105

^a BJD-2400000.^b Against $\max = 2454754.9228 + 0.075876E$.^c Number of points used to determine the maximum.

Table 160. Superhump maxima of AY Lyr (2009).

E	\max^a	error	$O - C^b$	N^c
0	54963.1200	0.0006	-0.0038	151
1	54963.1944	0.0005	-0.0052	269
2	54963.2698	0.0008	-0.0056	139
26	54965.1018	0.0005	0.0071	190
27	54965.1748	0.0004	0.0043	256
28	54965.2488	0.0004	0.0026	266
40	54966.1607	0.0004	0.0048	125
41	54966.2346	0.0017	0.0029	75
92	54970.0989	0.0017	0.0013	99
93	54970.1674	0.0010	-0.0060	114
94	54970.2467	0.0041	-0.0025	99

^a BJD-2400000.^b Against $\max = 2454963.1238 + 0.075802E$.^c Number of points used to determine the maximum.**Table 161.** Superhump maxima of DM Lyr (1997).

E	\max^a	error	$O - C^b$	N^c
0	50509.2862	0.0015	-0.0001	61
45	50512.3171	0.0011	0.0066	63
46	50512.3713	0.0014	-0.0065	33

^a BJD-2400000.^b Against $\max = 2450509.2863 + 0.067205E$.^c Number of points used to determine the maximum.**Table 162.** Superhump maxima of DM Lyr (2002).

E	\max^a	error	$O - C^b$	N^c
0	52580.0178	0.0073	-0.0019	100
58	52583.9153	0.0027	-0.0001	101
59	52583.9862	0.0010	0.0037	103
104	52587.0065	0.0097	0.0015	41
119	52588.0084	0.0108	-0.0041	58
134	52589.0209	0.0068	0.0009	60

^a BJD-2400000.^b Against $\max = 2452580.0197 + 0.067166E$.^c Number of points used to determine the maximum.**Table 163.** Superhump maxima of V344 Lyr (1993).

E	\max^a	error	$O - C^b$	N^c
0	49133.1065	0.0014	-0.0042	49
1	49133.2004	0.0011	-0.0015	48
2	49133.2949	0.0019	0.0016	29
12	49134.2104	0.0024	0.0035	34
34	49136.2187	0.0016	0.0020	47
78	49140.2348	0.0046	-0.0014	23

^a BJD-2400000.^b Against $\max = 2449133.1106 + 0.091354E$.^c Number of points used to determine the maximum.

6.83. V344 Lyrae

Kato (1993) reported on the 1993 superoutburst. We determined superhump maxima from these observations (table 163). The resultant P_{dot} was $-7.1(4.3) \times 10^{-5}$. Since this object has one of the longest P_{orb} , more complicated period variation may be expected as in MN Dra and UV Gem. Future better observations are needed to test this possibility.

6.84. V358 Lyrae

Although the object was originally discovered as a nova (Hoffmeister 1967b), Richter (1986) suggested that it is a WZ Sge-type dwarf nova based on its faintness and the similarity in the light curve with that of WZ Sge. Antipin et al. (2004) pointed out that the reported maximum in Richter (1986) referred to a plate defect and presented the correct identification. The maximum recorded photographic magnitude was 16.42.

J. Shears detected a new outburst on 2008 November 22 at an unfiltered CCD magnitude of 16.26 (vsnet-outburst 9714). The object experienced a “dip”-like fading characteristic to (type-A) WZ Sge-type superoutbursts and exhibited a long-lasting second plateau stage.

Due to the low amplitudes of variations and faintness of the object, we mainly focus on the variation before the dip. Using the best segments of observations, we obtained a P_{SH} of 0.05563(3) with the PDM method (figure 100). The profile of variation appeared doubly humped. Although the profile resembles those of early superhumps, we identified these variations as ordinary superhumps because these variations were observed ~ 10 d before the dip, at an epoch when all well-observed WZ Sge-type dwarf novae exhibited ordinary superhumps. The low-amplitude, double-wave modulations may have been a result of temporary reduction of amplitudes of superhumps frequently seen in many systems in the middle-to-late stage of a superoutburst plateau (see e.g. Kato et al. 2003c). Although we measured times of superhump maxima (table 164), the quality was not sufficient because of this complexity in the profile. Shears et al. (2009a) reported possible detection of small-scale periodic signals including a candidate period of 0.05556(32) d.

The overall light curve of the superoutburst bears strong similarity to that of AL Com in 1995 (figure 101).

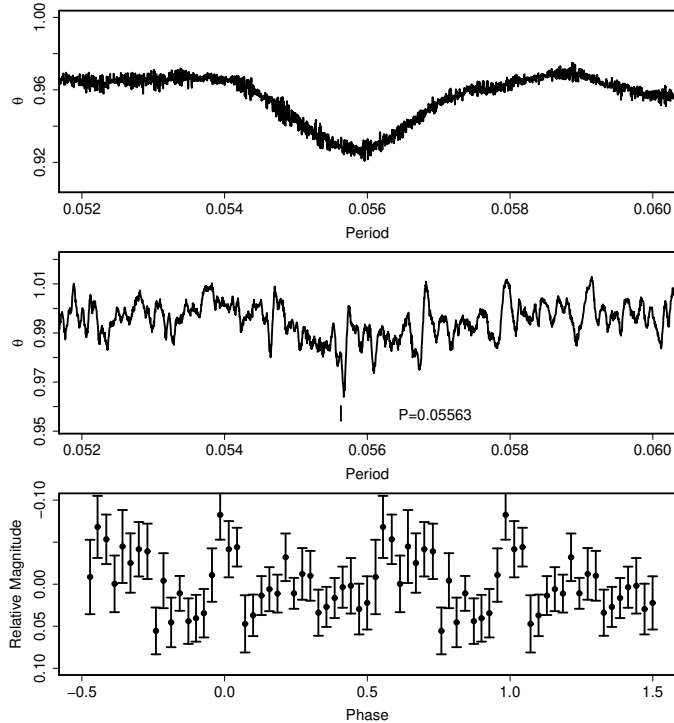


Fig. 100. Superhumps in V358 Lyr (2008). (Upper): PDM analysis of the interval BJD 2454793.8–2454794.3. (Middle): PDM analysis of the interval BJD 2454793.8–2454797.0. (Lower): Phase-averaged profile.

Table 164. Superhump maxima of V358 Lyr (2008).

E	\max^a	error	$O - C^b$	N^c
0	54793.8615	0.0049	0.0039	55
1	54793.9053	0.0226	-0.0080	130
13	54794.5960	0.0030	0.0133	13
26	54795.3027	0.0036	-0.0051	48
27	54795.3578	0.0030	-0.0057	47
48	54796.5339	0.0014	-0.0010	14
55	54796.9275	0.0043	0.0022	44
109	54799.9377	0.0043	0.0004	30

^a BJD-2400000.

^b Against $\max = 2454793.8576 + 0.055777E$.

^c Number of points used to determine the maximum.

The earlier stage of the outburst, potentially with early superhumps, may have been unfortunately missed below the detection limit of visual observations.

6.85. V419 Lyrae

Nogami et al. (1998c) reported the detection of superhumps in this object and proposed candidate periods. Although their observations were not long enough to discriminate the possibilities, the long superhump period already made V419 Lyr an outstanding object. We observed the 1999 superoutburst, and obtained the following superhump maxima and first identified the correct superhump

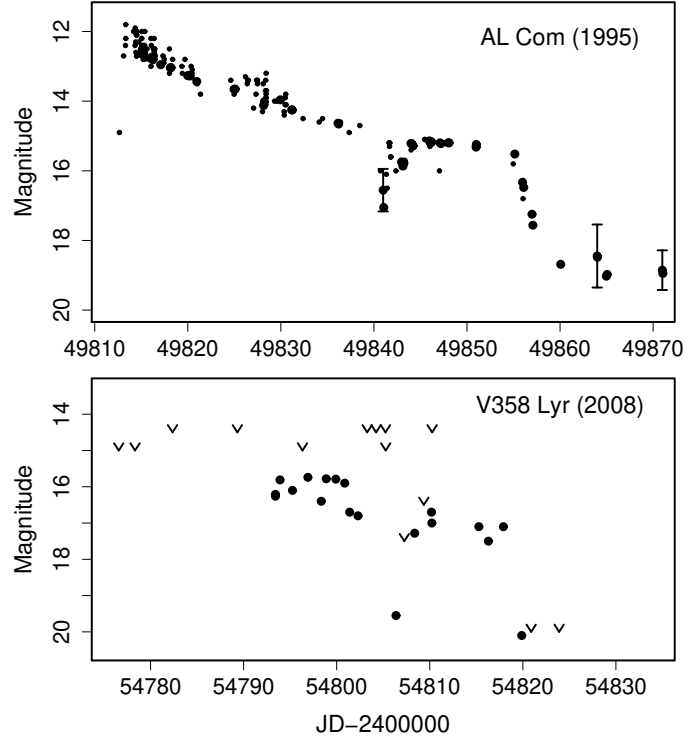


Fig. 101. Comparison of light curves of AL Com and V358 Lyr. (Upper) AL Com in 1995. The data are from Kato et al. (1996a). (Lower) V358 Lyr. The “v” marks indicate upper limits.

period (table 165). The superhump period apparently largely varied between $E = 0$ and $E = 3$. Excluding the point of $E = 11$ (observation of the maximum somewhat affected by thin clouds), and $E \leq 3$ epochs, we obtained $P_{\text{dot}} = -32.4(2.4) \times 10^{-5}$.

Rutkowski et al. (2007) obtained $P_{\text{dot}} = -24.8(2.2) \times 10^{-5}$ during the 2006 superoutburst. We analyzed the available data (from the AAVSO database and Dubovsky’s data) and combined with Rutkowski et al. (2007) after adding a systematic correction of 0.0026 d to Rutkowski et al. (2007) and removing maxima of Boyd’s observations, which were included in our own analysis (table 166)

A comparison of $O - C$ diagrams between different superoutbursts is given in figure 102.

This long-period system resembles UV Gem, MN Dra and NY Ser in its strongly negative superhump derivative. It would be notable that V419 Lyr shows frequent normal outbursts (intervals 9–12 d), which is also reminiscent of the behavior in UV Gem (Kato, Uemura 2001a) and NY Ser (Iida et al. 1995b). Very long- P_{SH} systems with frequent normal outbursts may be associated with strongly negative P_{dot} (see subsection 4.10).

6.86. V585 Lyrae

V585 Lyr was discovered by Kryachko (2001). An extensive photometric campaign was undertaken during the 2003 superoutburst. The times of superhump maxima

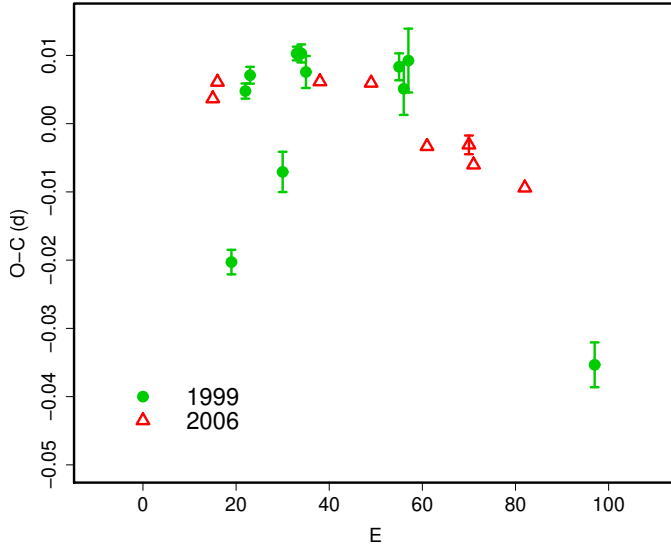


Fig. 102. Comparison of $O - C$ diagrams of V419 Lyr between different superoutbursts. A period of 0.09005 d was used to draw this figure. Approximate cycle counts (E) after the start of the superoutburst were used.

Table 165. Superhump maxima of V419 Lyr (1999).

E	\max^a	error	$O - C^b$	N^c
0	51415.0770	0.0018	-0.0270	96
3	51415.3722	0.0011	-0.0010	89
4	51415.4646	0.0012	0.0016	90
11	51416.0808	0.0029	-0.0106	66
14	51416.3683	0.0010	0.0077	89
15	51416.4583	0.0013	0.0080	82
16	51416.5456	0.0023	0.0056	56
36	51418.3474	0.0020	0.0122	82
37	51418.4342	0.0038	0.0092	86
38	51418.5284	0.0047	0.0137	38
78	51422.0858	0.0033	-0.0192	71

^a BJD-2400000.

^b Against $\max = 2451415.1040 + 0.089758E$.

^c Number of points used to determine the maximum.

Table 166. Superhump maxima of V419 Lyr (2006).

E	\max^a	error	$O - C^b$	N^c
0	53934.4226	0.0015	-0.0179	0
11	53935.4264	0.0004	-0.0026	64
12	53935.5188	0.0004	-0.0000	77
22	53936.4226	0.0016	0.0051	0
33	53937.4106	0.0014	0.0046	0
34	53937.5000	0.0005	0.0042	114
45	53938.4903	0.0005	0.0060	100
47	53938.6716	0.0022	0.0076	0
48	53938.7596	0.0025	0.0057	0
55	53939.3856	0.0044	0.0027	0
57	53939.5617	0.0006	-0.0010	85
58	53939.6526	0.0034	0.0001	0
59	53939.7436	0.0029	0.0012	0
60	53939.8336	0.0033	0.0014	0
61	53939.9226	0.0033	0.0005	0
66	53940.3723	0.0014	0.0009	62
67	53940.4595	0.0004	-0.0018	202
78	53941.4466	0.0007	-0.0031	118
79	53941.5356	0.0030	-0.0040	0
88	53942.3466	0.0015	-0.0018	0
89	53942.4346	0.0033	-0.0037	0
103	53943.6986	0.0047	0.0023	0
104	53943.7856	0.0044	-0.0006	0
111	53944.4096	0.0022	-0.0056	0

^a BJD-2400000.

^b Against $\max = 2453934.4405 + 0.089862E$.

^c Number of points used to determine the maximum.
 $N = 0$ refers to Rutkowski et al. (2007).

during this superoutburst are listed in table 167. The interval $32 \leq E \leq 150$ (stage B) showed a positive P_{dot} of $+10.7(1.2) \times 10^{-5}$, then followed by the emergence of a shorter period (stage C) and a regrowth of superhumps, typical behavior for a short-period system (cf. figure 4).

6.87. AD Mensae

AD Men was discovered as a variable star in the region of the Large Magellanic Cloud. The GCVS (Kholopov et al. 1985) listed the object as an SS Cyg-type dwarf nova with an outburst cycle length of ~ 30 d.

The object underwent a bright outburst in 2003 March at a visual magnitude of 14.0. The existence of superhumps was inconclusive during this outburst.¹⁶

The object underwent another bright outburst in 2004 March. The existence of superhumps was confirmed during this outburst, establishing the SU UMa-type nature of this object. Although a single superhump maximum of BJD 2453090.3137(7) was obtained, a PDM analysis and the examination of the single-night observation yielded the most likely period of 0.0966(2) d (figure 103). The object is an SU UMa-type dwarf nova likely in the period gap. The present P_{SH} is consistent with a photometric measurement of $P_{\text{orb}} = 0.0917(10)$ d (Schmidtobreick,

¹⁶ <<http://vsnet.kusastro.kyoto-u.ac.jp/vsnet/DNe/admen.html>>.

Table 167. Superhump maxima of V585 Lyr (2003).

E	max ^a	error	$O - C^b$	N^c
0	52898.3727	0.0027	-0.0155	67
9	52898.9215	0.0085	-0.0106	68
12	52899.1050	0.0024	-0.0085	149
13	52899.1703	0.0033	-0.0036	28
18	52899.4708	0.0129	-0.0053	52
19	52899.5337	0.0031	-0.0028	58
28	52900.0831	0.0018	0.0027	74
29	52900.1338	0.0083	-0.0072	44
32	52900.3316	0.0005	0.0094	54
33	52900.3949	0.0004	0.0122	61
34	52900.4514	0.0007	0.0083	63
35	52900.5124	0.0016	0.0088	62
36	52900.5742	0.0010	0.0102	40
37	52900.6346	0.0002	0.0102	58
43	52900.9988	0.0016	0.0118	80
44	52901.0575	0.0020	0.0100	60
45	52901.1120	0.0018	0.0040	38
49	52901.3559	0.0007	0.0062	63
50	52901.4149	0.0006	0.0048	63
51	52901.4759	0.0008	0.0053	61
52	52901.5340	0.0008	0.0030	57
62	52902.1375	0.0004	0.0021	33
63	52902.1968	0.0006	0.0010	33
64	52902.2578	0.0006	0.0014	33
65	52902.3176	0.0008	0.0008	71
66	52902.3843	0.0011	0.0071	43
67	52902.4358	0.0007	-0.0018	54
68	52902.4959	0.0008	-0.0022	59
69	52902.5576	0.0024	-0.0009	26
72	52902.7388	0.0011	-0.0010	74
73	52902.8007	0.0007	0.0004	99
81	52903.2806	0.0014	-0.0032	21
82	52903.3423	0.0019	-0.0019	272
83	52903.4017	0.0010	-0.0030	291
84	52903.4641	0.0015	-0.0010	273
85	52903.5191	0.0025	-0.0065	123
88	52903.7031	0.0009	-0.0038	118
90	52903.8223	0.0008	-0.0054	118
96	52904.1860	0.0011	-0.0044	29
97	52904.2454	0.0012	-0.0054	28
98	52904.3065	0.0010	-0.0048	91
99	52904.3683	0.0011	-0.0034	99
100	52904.4262	0.0014	-0.0059	125
101	52904.4913	0.0017	-0.0013	105
104	52904.6723	0.0010	-0.0016	111
105	52904.7299	0.0008	-0.0045	104
106	52904.7915	0.0007	-0.0032	112
107	52904.8530	0.0020	-0.0023	77
110	52905.0369	0.0012	0.0004	113
111	52905.0860	0.0020	-0.0110	115
114	52905.2735	0.0018	-0.0048	53
115	52905.3363	0.0017	-0.0025	59
116	52905.3994	0.0012	0.0002	61
117	52905.4517	0.0017	-0.0080	61
118	52905.5241	0.0049	0.0040	60

^a BJD-2400000.^b Against $max = 2452898.3882 + 0.060440E$.^c Number of points used to determine the maximum.**Table 167.** Superhump maxima of V585 Lyr (2003) (continued).

E	max	error	$O - C$	N
120	52905.6324	0.0045	-0.0085	16
122	52905.7636	0.0012	0.0018	22
123	52905.8222	0.0021	-0.0001	18
128	52906.1229	0.0021	-0.0016	33
129	52906.1848	0.0028	-0.0001	32
130	52906.2455	0.0020	0.0002	33
137	52906.6630	0.0046	-0.0055	22
138	52906.7280	0.0020	-0.0009	25
139	52906.7790	0.0074	-0.0103	21
145	52907.1628	0.0047	0.0108	17
149	52907.3974	0.0008	0.0038	102
148	52907.3366	0.0009	0.0033	109
149	52907.3971	0.0008	0.0034	100
150	52907.4603	0.0014	0.0062	47
164	52908.3061	0.0018	0.0058	38
166	52908.4220	0.0017	0.0008	33
166	52908.4220	0.0019	0.0009	37
167	52908.4865	0.0030	0.0049	17
178	52909.1489	0.0014	0.0025	17
179	52909.2107	0.0006	0.0038	17
180	52909.2680	0.0017	0.0007	17
181	52909.3286	0.0029	0.0009	32

Tappert 2006). The fractional superhump excess is $\sim 5\%$.

6.88. FQ Monocerotis

FQ Mon, originally classified as a possible Mira-type variable (Kholopov et al. 1985), was suspected to be a CV (vsnet-chat 3063,3066). The first known outburst since the discovery was recorded in 2004 (vsnet-alert 8048). We observed the 2004, 2006, 2007–2008 superoutbursts.

The 2004 superoutburst was relatively well observed (table 168). The $O - C$ diagram was composed of a typical stage B–C transition. The P_{dot} for the stage B was $+9.2(2.4) \times 10^{-5}$ ($E \leq 111$).

The later part of the 2006 superoutburst was observed (table 169). Compared to other superoutbursts, the fairly constant period after $E = 51$ likely corresponds to P_2 .

A photometric campaign was undertaken during the 2007–2008 superoutburst. The times of superhump maxima are listed in table 170. The object reached the maximum light around $E = 40$. Although superhumps were still prominent before this epoch, the period was significantly shorter than in the later epoch. The combined $O - C$ diagram (figure 104) suggests that stages B and C were recorded during this superoutburst. The P_{dot} for the stage B was $+5.4(1.3) \times 10^{-5}$ ($E \leq 124$).

The overall behavior resembles the $O - C$ variation in TT Boo (Olech et al. 2004a). These two objects have common properties of a relatively long superhump period (0.07–0.08 d), unusually long superoutburst (≥ 15 d) and relatively few normal outbursts.

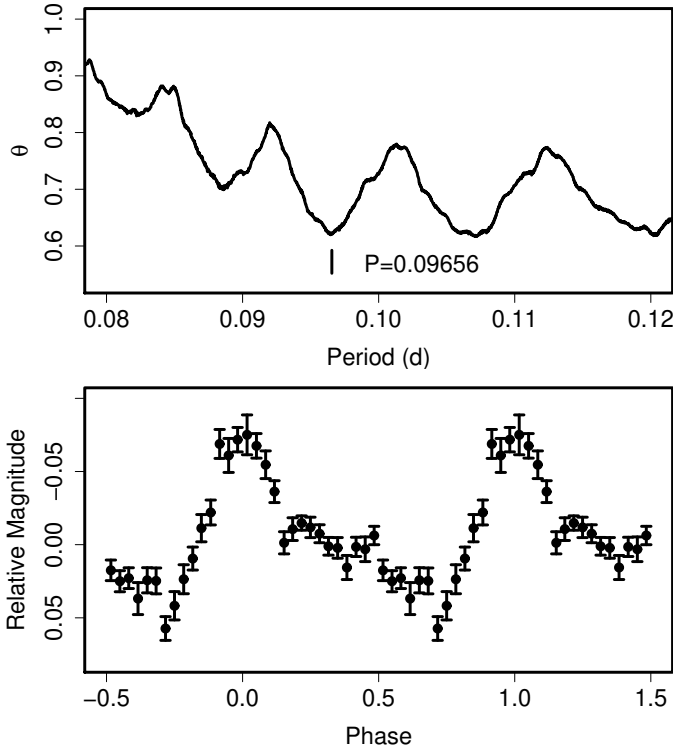


Fig. 103. Superhumps in AD Men (2004). (Upper): PDM analysis. (Lower): Phase-averaged profile.

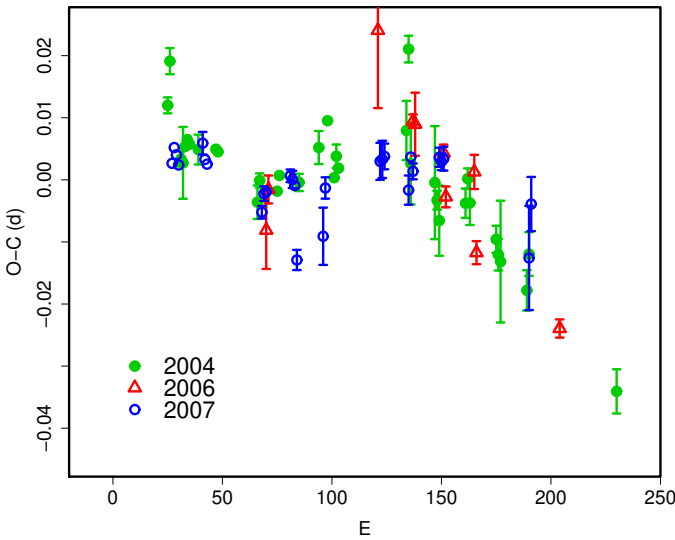


Fig. 104. Comparison of $O - C$ diagrams of FQ Mon between different superoutbursts. A period of 0.07335 d was used to draw this figure. Approximate cycle counts (E) after the start of the superoutburst were used.

Table 168. Superhump maxima of FQ Mon (2004).

E	max ^a	error	$O - C$ ^b	N ^c
0	53068.9790	0.0013	0.0023	107
1	53069.0595	0.0021	0.0096	84
6	53069.4104	0.0012	-0.0056	78
7	53069.4832	0.0058	-0.0061	25
8	53069.5592	0.0002	-0.0033	53
9	53069.6336	0.0003	-0.0021	55
10	53069.7062	0.0003	-0.0027	55
14	53069.9988	0.0024	-0.0031	184
22	53070.5856	0.0003	-0.0021	60
23	53070.6586	0.0005	-0.0024	41
41	53071.9707	0.0027	-0.0083	113
42	53072.0476	0.0011	-0.0047	209
50	53072.6327	0.0006	-0.0055	60
51	53072.7086	0.0007	-0.0028	57
60	53073.3676	0.0014	-0.0029	57
69	53074.0333	0.0027	0.0038	133
73	53074.3311	0.0009	0.0086	101
76	53074.5419	0.0008	-0.0002	33
77	53074.6187	0.0019	0.0034	44
78	53074.6902	0.0010	0.0016	28
109	53076.9701	0.0048	0.0114	95
110	53077.0566	0.0022	0.0246	136
111	53077.1115	0.0066	0.0063	129
122	53077.9152	0.0091	0.0045	130
123	53077.9858	0.0015	0.0018	188
124	53078.0558	0.0057	-0.0013	178
136	53078.9388	0.0024	0.0029	171
137	53079.0161	0.0016	0.0070	243
138	53079.0856	0.0036	0.0032	86
150	53079.9599	0.0022	-0.0012	216
151	53080.0308	0.0026	-0.0036	188
152	53080.1030	0.0098	-0.0046	68
164	53080.9786	0.0032	-0.0078	94
165	53081.0578	0.0035	-0.0018	37
205	53083.9697	0.0036	-0.0191	31

^a BJD-2400000.

^b Against $max = 2453068.9766 + 0.073230E$.

^c Number of points used to determine the maximum.

Table 169. Superhump maxima of FQ Mon (2006).

E	\max^a	error	$O - C^b$	N^c
0	53754.1730	0.0062	-0.0151	256
1	53754.2529	0.0022	-0.0084	134
51	53757.9460	0.0125	0.0224	78
67	53759.1050	0.0011	0.0094	214
68	53759.1778	0.0051	0.0090	194
81	53760.1268	0.0013	0.0057	132
82	53760.1930	0.0017	-0.0012	131
95	53761.1506	0.0028	0.0041	132
96	53761.2109	0.0019	-0.0088	132
134	53763.9860	0.0015	-0.0171	100

^a BJD-2400000.^b Against $\max = 2453754.1881 + 0.073246E$.^c Number of points used to determine the maximum.**Table 170.** Superhump maxima of FQ Mon (2007–2008).

E	\max^a	error	$O - C^b$	N^c
0	54463.1149	0.0005	0.0007	53
1	54463.1908	0.0004	0.0033	76
2	54463.2629	0.0003	0.0022	76
3	54463.3347	0.0003	0.0005	55
14	54464.1450	0.0018	0.0044	41
15	54464.2158	0.0004	0.0018	76
16	54464.2883	0.0004	0.0010	77
41	54466.1144	0.0010	-0.0060	77
42	54466.1907	0.0012	-0.0030	125
43	54466.2643	0.0010	-0.0027	83
54	54467.0738	0.0010	0.0002	97
55	54467.1465	0.0014	-0.0003	138
56	54467.2189	0.0009	-0.0013	136
57	54467.2803	0.0016	-0.0132	114
69	54468.1643	0.0046	-0.0091	81
70	54468.2454	0.0017	-0.0013	138
95	54470.0834	0.0030	0.0037	152
96	54470.1571	0.0030	0.0041	152
97	54470.2309	0.0021	0.0046	64
108	54471.0324	0.0024	-0.0005	123
109	54471.1110	0.0009	0.0048	221
110	54471.1821	0.0013	0.0025	157
122	54472.0645	0.0015	0.0051	158
123	54472.1372	0.0014	0.0045	211
124	54472.2110	0.0019	0.0050	138
163	54475.0557	0.0084	-0.0099	141
164	54475.1377	0.0044	-0.0012	198

^a BJD-2400000.^b Against $\max = 2454463.1142 + 0.073322E$.^c Number of points used to determine the maximum.**Table 171.** Superhump maxima of AB Nor (2002).

E	\max^a	error	$O - C^b$	N^c
0	52518.9807	0.0013	-0.0189	36
4	52519.3045	0.0020	-0.0141	86
15	52520.2092	0.0007	0.0134	41
16	52520.2844	0.0015	0.0089	31
37	52521.9670	0.0003	0.0167	40
124	52528.8911	0.0022	0.0027	18
141	52530.2420	0.0019	-0.0022	87
142	52530.3175	0.0061	-0.0065	49

^a BJD-2400000.^b Against $\max = 2452518.9996 + 0.079749E$.^c Number of points used to determine the maximum.

6.89. AB Normae

Kato et al. (2004a) reported the detection of superhumps in AB Nor during its 2002 superoutburst. Due to the observational gap and apparent period variation, the identification of the correct P_{SH} was rather ambiguous. Based on the improved knowledge of period variations in long- P_{SH} systems, we succeeded in identifying a more likely P_{SH} (table 171). For $E \leq 16$, the system showed the stage A period evolution associated with the growth of superhumps. The mean period and P_{dot} 's were 0.07962(3) d and $-8.1(2.7) \times 10^{-5}$, respectively ($15 \leq E \leq 142$) or 0.07955(3) d and $-6.1(5.2) \times 10^{-5}$, respectively ($37 \leq E \leq 142$).

6.90. DT Octantis

Kato et al. (2004a) reported the detection of superhumps in DT Oct = NSV 10934 during its 2003 January superoutburst. Table 172 gives an upgraded list of superhump maxima. The epochs $156 \leq E \leq 158$ correspond to the post-superoutburst stage. There was a hint of double-wave modulation at this stage and was possibly from classical “late superhumps”. Disregarding this stage and the stage A ($E \leq 9$), the global P_{dot} corresponds to $-9.0(1.1) \times 10^{-5}$. The times of superhump maxima during the 2003 November superoutburst and the 2008 superoutburst are also given for a supplementary purpose (tables 173, 174). The latter superoutburst probably recorded the stage C superhumps (see figure 105).

6.91. V699 Ophiuchi

Until very recently, the nature of V699 Oph remained controversial. The object was originally discovered as a possible dwarf nova. Walker, Olmsted (1958) presented a finding chart, but later spectroscopic studies have shown that the marked object is a normal star (Zwitter, Munari 1996; Liu et al. 1999; Kato et al., unpublished).

On 1999 April 16, A. Pearce discovered an outburst of this object (vsnet-alert 2877). Astrometry and photometry of the outbursting object indicated that the true V699 Oph is an unresolved companion to a 16-th magnitude star (vsnet-alert 2878, vsnet-chat 1810, 1868).

The 2003 superoutburst was noteworthy in that it was

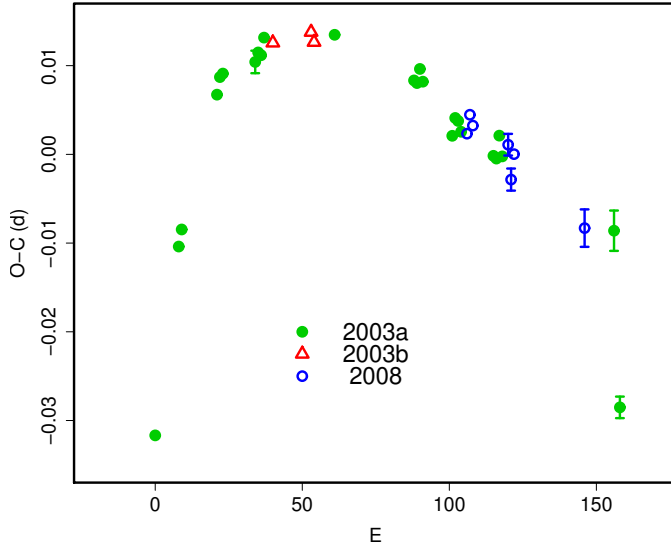


Fig. 105. Comparison of $O-C$ diagrams of DT Oct between different superoutbursts. A period of 0.07485 d was used to draw this figure. Approximate cycle counts (E) after the start of the superoutburst were used.

Table 172. Superhump maxima of DT Oct (2003a).

E	\max^a	error	$O - C^b$	N^c
0	52643.3689	0.0010	-0.0387	195
8	52643.9890	0.0003	-0.0167	82
9	52644.0657	0.0005	-0.0146	104
21	52644.9791	0.0002	0.0017	197
22	52645.0560	0.0002	0.0037	254
23	52645.1312	0.0004	0.0042	60
34	52645.9559	0.0013	0.0065	90
35	52646.0318	0.0002	0.0077	392
36	52646.1063	0.0002	0.0075	383
37	52646.1832	0.0003	0.0095	211
61	52647.9799	0.0002	0.0121	128
88	52649.9957	0.0002	0.0094	319
89	52650.0702	0.0003	0.0092	347
90	52650.1467	0.0004	0.0109	269
91	52650.2201	0.0004	0.0095	191
101	52650.9625	0.0008	0.0043	85
102	52651.0394	0.0006	0.0064	199
103	52651.1139	0.0004	0.0062	130
104	52651.1875	0.0005	0.0051	108
115	52652.0081	0.0005	0.0033	270
116	52652.0827	0.0004	0.0031	329
117	52652.1601	0.0007	0.0058	237
118	52652.2326	0.0006	0.0036	149
156	52655.0686	0.0023	-0.0013	26
157	52655.1075	0.0010	-0.0372	25
158	52655.1983	0.0012	-0.0211	20

^a BJD-2400000.

^b Against $\max = 2452643.4076 + 0.074759E$.

^c Number of points used to determine the maximum.

Table 173. Superhump maxima of DT Oct (2003b).

E	\max^a	error	$O - C^b$	N^c
0	52970.0252	0.0004	-0.0000	282
13	52970.9995	0.0004	0.0006	243
14	52971.0732	0.0006	-0.0006	152

^a BJD-2400000.

^b Against $\max = 2452970.0253 + 0.074893E$.

^c Number of points used to determine the maximum.

Table 174. Superhump maxima of DT Oct (2008).

E	\max^a	error	$O - C^b$	N^c
0	54526.0354	0.0008	-0.0014	34
1	54526.1124	0.0008	0.0010	33
2	54526.1860	0.0007	0.0001	34
14	54527.0821	0.0012	0.0015	16
15	54527.1530	0.0012	-0.0021	17
16	54527.2307	0.0009	0.0010	17
40	54529.0188	0.0021	-0.0002	34

^a BJD-2400000.

^b Against $\max = 2454526.0368 + 0.074554E$.

^c Number of points used to determine the maximum.

preceded by a precursor outburst (vsnet-alert 7768, 7795) 11 d before the onset of the superoutburst and followed by a rebrightening (figure 106). The mean superhump period with the PDM method was 0.070242(12) d (figure 107). The superhump maxima during the plateau stage are listed in table 175. There was likely a stage B-C transition around $E = 43$. The P_{dot} during the stage B was $+14.2(7.7) \times 10^{-5}$. There was marginal evidence for ~ 0.02 mag modulation with a period of 0.0689(2) d during the first two days of the precursor, which might be related to orbital modulations.

The 2008 superoutburst (table 176) lacked good coverage in the middle of the superoutburst. The maxima with $E \geq 87$ were obtained during the late-stage decline of the superoutburst and most likely correspond to the stage C. Using all the superhump maxima, we obtained a global P_{dot} of $-6.9(1.4) \times 10^{-5}$. The P_{dot} before the supposed stage B-C transition should have been closer to zero than this global value.

6.92. V2051 Ophiuchi

V2051 Oph is an eclipsing dwarf nova whose SU UMa-type nature was established by Kiyota, Kato (1998). Patterson et al. (2003) observed the 1999 superoutburst and reported a representative superhump period.

We observed the 1999, 2003 and 2009 superoutburst. The times of superhump maxima (tables 177, 178, 179) were obtained after removing observations within 0.07 P_{orb} of eclipses. The 1999 observation covered the later part of a superoutburst and 2003 mostly covered the earlier part. We could not reliably determine superhump maxima during the later course of the 2003 superout-

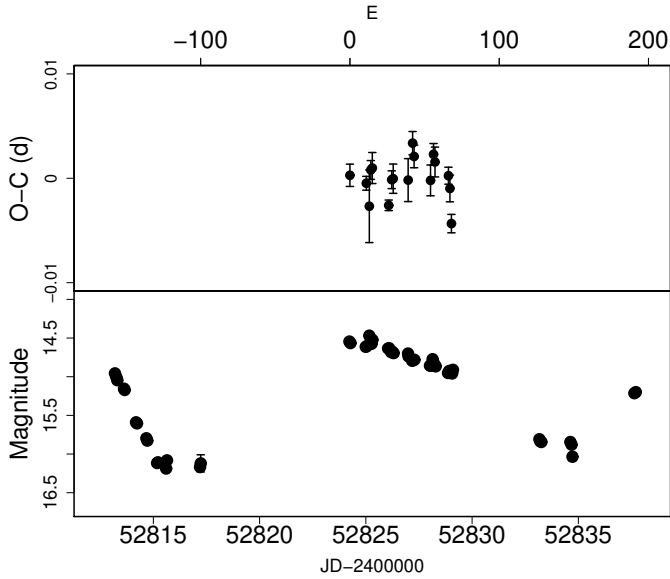


Fig. 106. $O - C$ of superhumps V699 Oph (2003). (Upper): $O - C$ diagram. (Lower): Light curve. The superoutburst was preceded by a precursor and followed by a rebrightening. The flat bottom at magnitude ~ 16.1 was a result of an unresolved companion.

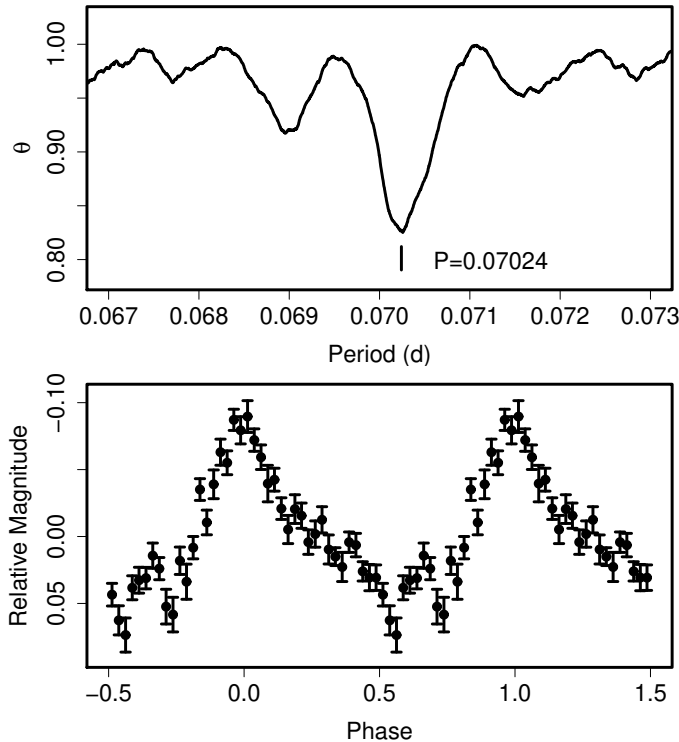


Fig. 107. Superhumps in V699 Oph (2003). (Upper): PDM analysis. (Lower): Phase-averaged profile.

Table 175. Superhump maxima of V699 Oph (2003).

E	\max^a	error	$O - C^b$	N^c
0	52824.2510	0.0011	0.0003	38
11	52825.0233	0.0007	-0.0005	389
13	52825.1616	0.0035	-0.0027	20
14	52825.2354	0.0009	0.0008	39
15	52825.3058	0.0015	0.0010	27
26	52826.0753	0.0005	-0.0026	121
28	52826.2183	0.0009	-0.0001	39
29	52826.2887	0.0014	-0.0000	39
39	52826.9913	0.0021	-0.0002	93
42	52827.2056	0.0011	0.0034	39
43	52827.2746	0.0011	0.0021	38
54	52828.0453	0.0015	-0.0002	220
56	52828.1884	0.0010	0.0023	37
57	52828.2579	0.0014	0.0016	38
66	52828.8891	0.0008	0.0002	150
67	52828.9581	0.0013	-0.0010	192
68	52829.0250	0.0009	-0.0043	291

^a BJD-2400000.

^b Against $\max = 2452824.2508 + 0.070274E$.

^c Number of points used to determine the maximum.

Table 176. Superhump maxima of V699 Oph (2008).

E	\max^a	error	$O - C^b$	N^c
0	54618.1103	0.0026	-0.0063	72
1	54618.1851	0.0006	-0.0017	141
14	54619.1009	0.0007	0.0030	131
15	54619.1697	0.0008	0.0017	121
16	54619.2392	0.0007	0.0011	115
17	54619.3097	0.0010	0.0015	128
87	54624.2193	0.0019	0.0047	100
128	54627.0849	0.0039	-0.0034	144
129	54627.1577	0.0063	-0.0007	61

^a BJD-2400000.

^b Against $\max = 2454618.1166 + 0.070091E$.

^c Number of points used to determine the maximum.

burst because of the complex superhump profile and the presence of eclipses and the orbital signature. The 1999 $O - C$ diagram clearly showed a shift to a shorter superhump period (stage B to C) associated with a regrowth of superhumps. Using the $0 \leq E \leq 113$ segment, we obtained $P_{\text{dot}} = +2.9(2.9) \times 10^{-5}$. Using the entire data ($0 \leq E \leq 48$) of the 2003 superoutburst, we obtained $P_{\text{dot}} = -44.8(15.1) \times 10^{-5}$. Such a large decrease in the period was most likely due to the early development of the superhump period from a longer period (stage A to B). Using the interval of $E \leq 16$, we obtained a mean superhump period of 0.06380(8) d and P_{dot} of $+14.0(26.8) \times 10^{-5}$. Patterson et al. (2003) reported a possible period decrease from 0.0641 d to 0.0637 d during the 1998 superoutburst, which may have been a similar phenomenon as seen in the 2003 superoutburst. Combining the 1999 and 2003 results,

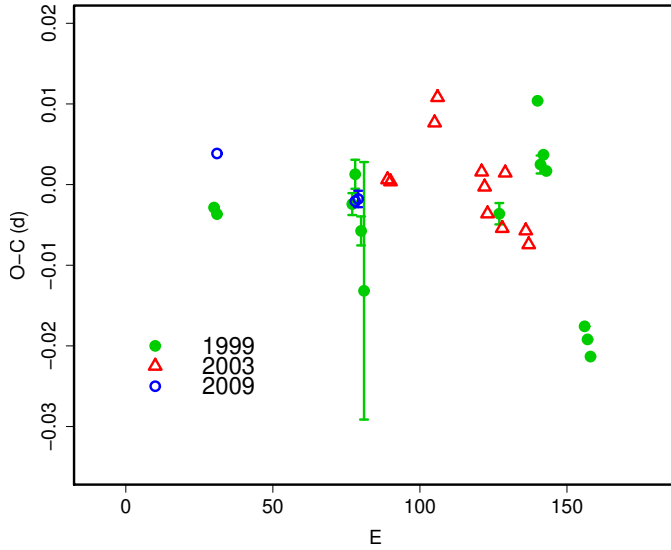


Fig. 108. Comparison of $O - C$ diagrams of V2051 Oph between different superoutbursts. A period of 0.06430 d was used to draw this figure. Approximate cycle counts (E) after the start of the superoutburst were used.

Table 177. Superhump maxima of V2051 Oph (1999).

E	\max^a	error	$O - C^b$	N^c
0	51387.8383	0.0008	-0.0027	80
1	51387.9018	0.0006	-0.0035	83
47	51390.8609	0.0014	0.0001	94
48	51390.9289	0.0018	0.0039	102
50	51391.0504	0.0018	-0.0030	108
97	51394.0747	0.0013	0.0015	82
110	51394.9246	0.0010	0.0162	85
111	51394.9810	0.0011	0.0084	78
112	51395.0465	0.0007	0.0096	80
113	51395.1088	0.0007	0.0076	83
126	51395.9254	0.0004	-0.0109	83
127	51395.9881	0.0005	-0.0125	84
128	51396.0503	0.0008	-0.0146	80

^a BJD-2400000.

^b Against $\max = 2451387.8411 + 0.064248E$.

^c Number of points used to determine the maximum.

the behavior of the period change was not dramatically different from those of other SU UMa-type dwarf novae with similar superhump periods. More comprehensive observations covering the entire superoutburst are needed to clearly identify the superhump period and its evolution.

A comparison of $O - C$ diagrams of V2051 Oph between different superoutbursts is shown in figure 108.

6.93. V2527 Ophiuchi

V2527 Oph was an X-ray selected CV, 1E1719.1-1946 (Hertz et al. 1990). The low absolute magnitude in quiescence inferred from spectroscopy was already suggestive of a short-period SU UMa-type dwarf nova. The first de-

Table 178. Superhump maxima of V2051 Oph (2003).

E	\max^a	error	$O - C^b$	N^c
0	52749.0260	0.0006	-0.0048	69
1	52749.0901	0.0003	-0.0048	312
16	52750.0619	0.0004	0.0054	260
17	52750.1293	0.0003	0.0087	268
32	52751.0846	0.0004	0.0024	171
33	52751.1470	0.0009	0.0007	395
34	52751.2080	0.0007	-0.0024	352
39	52751.5277	0.0004	-0.0033	280
40	52751.5989	0.0003	0.0038	239
47	52752.0418	0.0003	-0.0020	244
48	52752.1044	0.0003	-0.0036	384

^a BJD-2400000.

^b Against $\max = 2452749.0308 + 0.064108E$.

^c Number of points used to determine the maximum.

Table 179. Superhump maxima of V2051 Oph (2009).

E	\max^a	error	$O - C^b$	N^c
0	54974.0782	0.0006	0.0000	66
47	54977.0944	0.0006	-0.0002	167
48	54977.1590	0.0010	0.0002	115

^a BJD-2400000.

^b Against $\max = 2454974.0782 + 0.064178E$.

^c Number of points used to determine the maximum.

tection of an outburst was reported in 1999 October (P. Schmeer).

The 2004 superoutburst was very well observed. The mean superhump period during the entire outburst was 0.071919(5) d (PDM method, figure 109). This superoutburst had a distinct precursor outburst, during which superhumps already started emerging. The times of superhump maxima are listed in table 180. The portion $E \leq 7$ corresponds to the precursor, and $20 \leq E \leq 22$ rising stage from the minimum following the precursor. The superhump period showed stage A ($E \leq 29$), stage B with a positive period derivative, and a transition to the stage C with a shorter period ($E \geq 103$). Using the stage B, we obtained $P_{\text{dot}} = +6.0(1.7) \times 10^{-5}$ ($29 \leq E \leq 103$). The times of superhump maxima and period analyses of two other superoutbursts in 2006 and 2008 are also given (tables 181 and 182). A comparison of $O - C$ diagrams between different superoutbursts is given in figure 111.

6.94. V1159 Orionis

V1159 Ori is a member of ER UMa stars (Nogami et al. 1995a; Robertson et al. 1995; Patterson et al. 1995), having outburst characteristics similar to those of the prototype ER UMa itself. We analyzed the 2002 November-December superoutburst (table 183). Since the waveform of superhumps in ER UMa stars are relatively complex and sometimes show double peaks (cf. Kato et al. 2003b; Patterson et al. 1995), we only deal with prominent max-

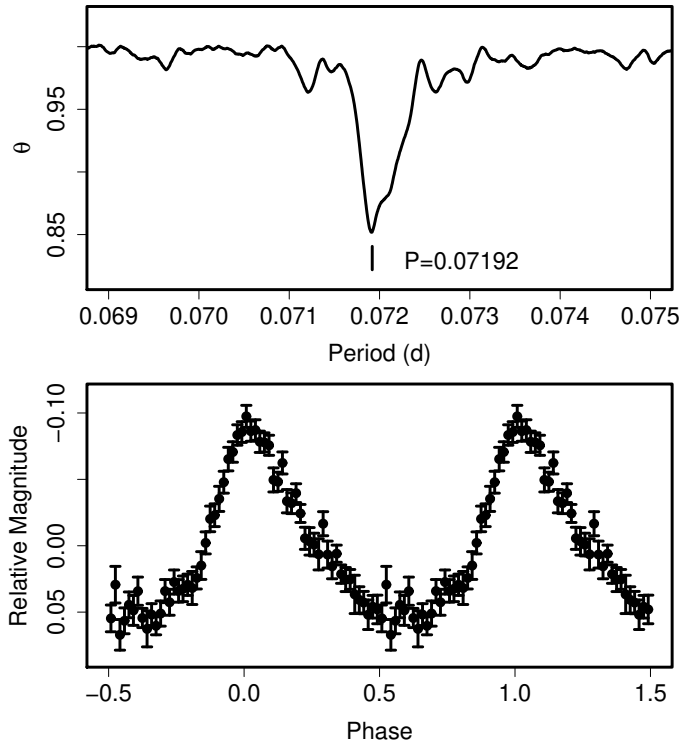


Fig. 109. Superhumps in V2527 Oph (2004). (Upper): PDM analysis. (Lower): Phase-averaged profile.

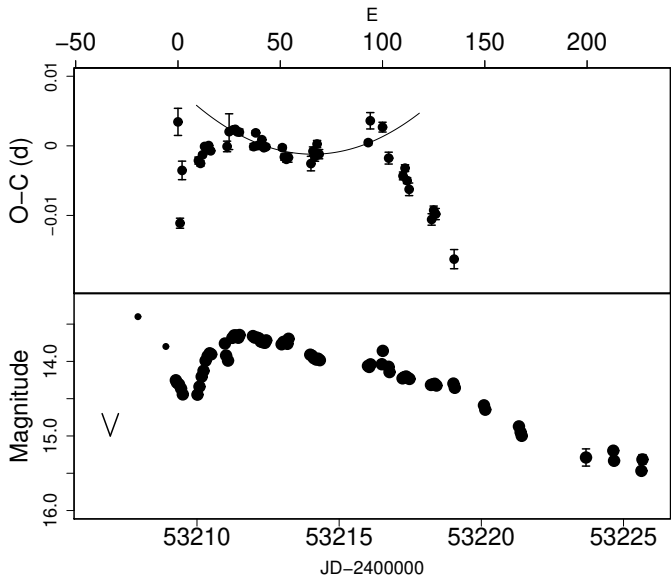


Fig. 110. $O-C$ of superhumps V2527 Oph (2004). (Upper): $O-C$ diagram. The curve represents a quadratic fit to $29 \leq E \leq 103$. (Lower): Light curve. The superoutburst was preceded by a precursor. Large dots represent CCD observations. Small dots and a “V” mark represent visual observations and an upper limit, respectively.

Table 180. Superhump maxima of V2527 Oph (2004).

E	max ^a	error	$O - C^b$	N^c
0	53209.3317	0.0019	-0.0003	163
1	53209.3892	0.0007	-0.0148	163
2	53209.4688	0.0013	-0.0071	163
10	53210.0466	0.0005	-0.0047	73
11	53210.1183	0.0004	-0.0050	74
12	53210.1915	0.0003	-0.0037	164
13	53210.2648	0.0002	-0.0023	188
14	53210.3364	0.0001	-0.0027	163
15	53210.4090	0.0002	-0.0020	163
16	53210.4803	0.0002	-0.0026	162
24	53211.0574	0.0008	-0.0011	130
25	53211.1315	0.0026	0.0012	66
27	53211.2759	0.0002	0.0017	163
28	53211.3480	0.0002	0.0018	162
29	53211.4197	0.0002	0.0016	163
30	53211.4917	0.0004	0.0017	113
37	53211.9940	0.0004	0.0004	68
38	53212.0680	0.0003	0.0025	70
39	53212.1383	0.0004	0.0008	74
40	53212.2103	0.0003	0.0009	182
41	53212.2832	0.0003	0.0019	162
42	53212.3541	0.0003	0.0008	160
43	53212.4263	0.0003	0.0011	132
51	53213.0025	0.0003	0.0019	70
52	53213.0732	0.0004	0.0006	87
53	53213.1450	0.0004	0.0004	75
54	53213.2173	0.0007	0.0008	47
65	53214.0090	0.0010	0.0012	155
66	53214.0828	0.0006	0.0031	250
67	53214.1541	0.0007	0.0025	77
68	53214.2279	0.0005	0.0043	183
69	53214.2985	0.0007	0.0030	157
93	53216.0294	0.0003	0.0074	157
94	53216.1046	0.0012	0.0107	115
100	53216.5360	0.0007	0.0105	98
103	53216.7477	0.0009	0.0064	108
110	53217.2495	0.0006	0.0046	160
111	53217.3226	0.0005	0.0058	159
112	53217.3929	0.0004	0.0042	158
113	53217.4637	0.0009	0.0030	116
124	53218.2519	0.0008	-0.0000	153
125	53218.3253	0.0006	0.0014	152
126	53218.3968	0.0008	0.0010	150
135	53219.0388	0.0014	-0.0045	122
167	53221.3264	0.0011	-0.0187	161
168	53221.3975	0.0014	-0.0196	140

^a BJD-2400000.

^b Against $max = 2453209.3320 + 0.071935E$.

^c Number of points used to determine the maximum.

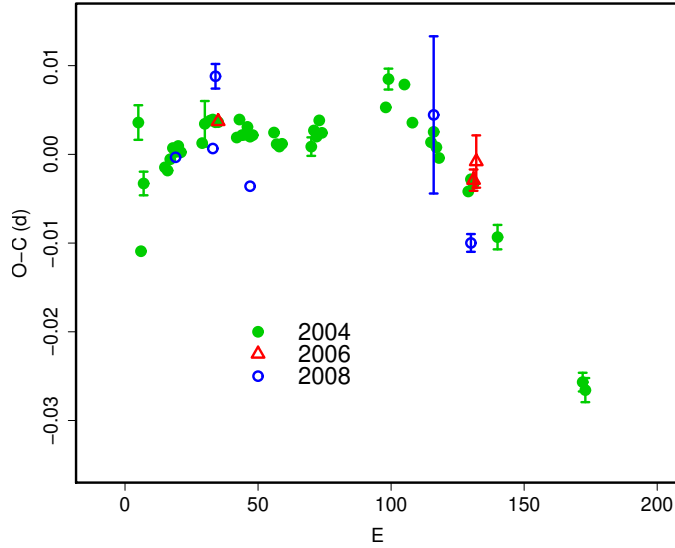


Fig. 111. Comparison of $O - C$ diagrams of V2527 Oph between different superoutbursts. A period of 0.07200 d was used to draw this figure. Approximate cycle counts (E) after the start of the superoutburst were used.

Table 181. Superhump maxima of V2527 Oph (2006).

E	\max^a	error	$O - C^b$	N^c
0	53938.0839	0.0003	0.0000	190
96	53944.9892	0.0012	-0.0011	99
97	53945.0633	0.0029	0.0011	97

^a BJD-2400000.

^b Against $\max = 2453938.0838 + 0.071942E$.

^c Number of points used to determine the maximum.

Table 182. Superhump maxima of V2527 Oph (2008).

E	\max^a	error	$O - C^b$	N^c
0	54709.9750	0.0006	-0.0028	115
14	54710.9839	0.0007	-0.0011	175
15	54711.0641	0.0014	0.0072	124
28	54711.9877	0.0007	-0.0045	139
97	54716.9637	0.0089	0.0074	86
111	54717.9573	0.0010	-0.0062	174

^a BJD-2400000.

^b Against $\max = 2454709.9778 + 0.071943E$.

^c Number of points used to determine the maximum.

Table 183. Superhump maxima of V1159 Ori (2002).

E	\max^a	error	$O - C^b$	N^c
0	52604.1949	0.0006	0.0004	67
16	52605.2186	0.0008	-0.0035	86
30	52606.1185	0.0012	-0.0027	98
31	52606.1800	0.0026	-0.0055	81
32	52606.2399	0.0011	-0.0098	118
45	52607.0753	0.0009	-0.0093	85
46	52607.1406	0.0010	-0.0082	64
48	52607.2707	0.0009	-0.0066	190
62	52608.1717	0.0024	-0.0047	88
63	52608.2363	0.0023	-0.0043	284
93	52610.1934	0.0015	0.0262	97
94	52610.2460	0.0011	0.0145	130
109	52611.2102	0.0046	0.0153	148
110	52611.2447	0.0028	-0.0143	196
110	52611.2762	0.0028	0.0171	187
138	52613.0700	0.0056	0.0127	85
139	52613.1316	0.0057	0.0101	74
233	52619.1500	0.0034	-0.0084	53
234	52619.2248	0.0023	0.0022	82
235	52619.2805	0.0009	-0.0064	85
248	52620.1199	0.0023	-0.0019	58
249	52620.1730	0.0008	-0.0130	70

^a BJD-2400000.

^b Against $\max = 2452604.1946 + 0.064222E$.

^c Number of points used to determine the maximum.

ima and do not discuss on secondary maxima.¹⁷ There appears to be a ~ 0.5 phase shift before $E = 93$ as reported in ER UMa (Kato et al. 2003b). The nominal P_{dot} for the segment $E \leq 63$ was $+14.9(5.4) \times 10^{-5}$. After $E = 93$, the object showed a fairly constant P_{SH} of 0.06409(5) d, which likely corresponds to P_2 in ordinary SU UMa-type dwarf novae. The overall feature is similar to that reported by Patterson et al. (1995). The times of superhump minima listed in Patterson et al. (1995) can be expressed by a segment with a positive P_{dot} , followed by a transition (without a phase shift) to a shorter period which was very close to ours. Note, however, the difference may have been caused by different methods (Patterson et al. 1995 used superhump minima rather than maxima) in determining period variation.

6.95. V344 Pavonis

We analyzed the data in Uemura et al. (2004) and obtained the times of superhump maxima (table 184). Since the observation started during the late stage of the superoutburst, we did not attempt to determine a P_{dot} . It would be noteworthy that no phase reversal, expected for traditional late superhumps, was recorded even after the rapid fading.

¹⁷ In table 183, two maxima are given for $E = 110$. These maxima, with nearly equal amplitudes, were probably a result of manifestation of the secondary maximum. We only used the latter maximum, which fits the trend of the rest of superhump

Table 184. Superhump maxima of V344 Pav (2004).

E	max ^a	error	$O - C^b$	N^c
0	53235.5965	0.0009	0.0029	158
13	53236.6301	0.0009	0.0007	168
14	53236.7121	0.0014	0.0031	169
15	53236.7940	0.0022	0.0053	169
25	53237.5816	0.0014	-0.0037	166
26	53237.6655	0.0045	0.0005	170
27	53237.7345	0.0077	-0.0102	169
37	53238.5451	0.0083	0.0038	120
38	53238.6052	0.0154	-0.0158	165
50	53239.5808	0.0046	0.0038	153
51	53239.6663	0.0066	0.0097	111

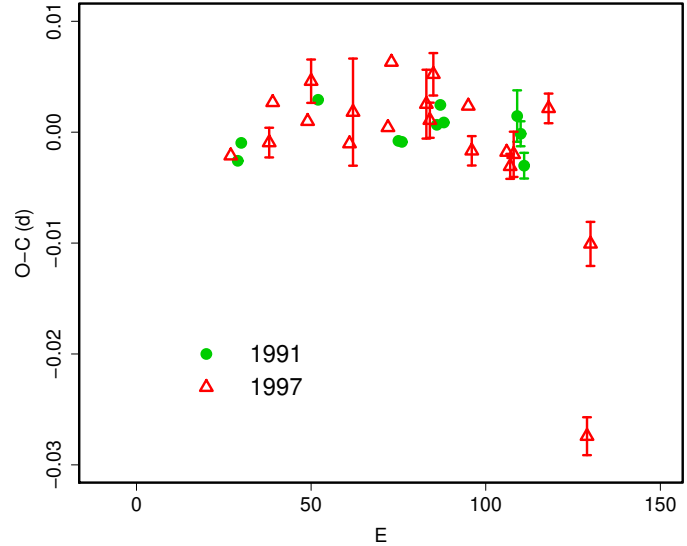
^a BJD-2400000.^b Against $max = 2453235.5937 + 0.079667E$.^c Number of points used to determine the maximum.

6.96. EF Pegasi

Howell et al. (1993) and Kato (2002b) reported on the 1991 superoutburst. Kato (2002b) reported a period decrease at $P_{\text{dot}} = -5.1(0.7) \times 10^{-5}$ after combination with the times of maxima in Howell et al. (1993). We further observed this object during the 1997 superoutburst. The times of superhump maxima are listed in table 185. The P_{dot} determined from these data, excluding the last two maxima, corresponds to $-4.2(2.1) \times 10^{-5}$, similar to the one in 1991. There was an indication that the earliest superhump maxima of the 1991 were obtained during the evolutionary stage of superhumps. An exclusion of these maxima has only yielded an insignificant P_{dot} due to the fragmentary observational coverage. We thus regard the 1997 result more reliable based on homogeneous set of observations. This result supersedes the preliminary argument on period changes in Kato (2002b). A comparison of 1991 and 1997 $O - C$ variations is presented in figure 112.

6.97. V364 Pegasi

V364 Peg is a dwarf nova discovered during the super-nova survey (Qiu et al. 1997a). Kato, Matsumoto (1999a) reported, based on time-resolved photometry during the 1997 November outburst, that this object is a likely SU UMa-type dwarf nova with a long superhump period. This suggestion has been confirmed during the 2004 outburst (T. Vanmunster, aavso-photometry message), reporting a superhump period of 0.0882(70) d. We have refined the period to 0.08556(5) d with the PDM method (figure 113). The times of superhump maxima are listed in table 186. If there was a stage B-C transition as in many SU UMa-type dwarf novae, this period likely represents P_2 . The inferred orbital period lies close to the lower edge of the period gap. The object appears to show rather frequent outbursts (cf. Qiu et al. 1997b).

**Fig. 112.** Comparison of $O - C$ diagrams of EF Peg between different superoutbursts. A period of 0.08705 d was used to draw this figure. Approximate cycle counts (E) after the start of the superoutburst were used.**Table 185.** Superhump maxima of EF Peg (1997).

E	max ^a	error	$O - C^b$	N^c
0	50757.0034	0.0005	-0.0073	152
11	50757.9621	0.0013	-0.0049	117
12	50758.0528	0.0006	-0.0011	126
22	50758.9216	0.0003	-0.0017	193
23	50759.0123	0.0020	0.0021	145
34	50759.9642	0.0008	-0.0023	162
35	50760.0541	0.0048	0.0007	56
45	50760.9232	0.0004	0.0004	165
46	50761.0162	0.0007	0.0064	126
56	50761.8829	0.0031	0.0038	100
57	50761.9685	0.0016	0.0025	160
58	50762.0597	0.0019	0.0067	143
68	50762.9273	0.0009	0.0050	186
69	50763.0103	0.0013	0.0011	163
79	50763.8807	0.0008	0.0021	115
80	50763.9665	0.0011	0.0010	151
81	50764.0546	0.0020	0.0022	62
91	50764.9292	0.0013	0.0075	23
102	50765.8572	0.0017	-0.0208	44
103	50765.9616	0.0020	-0.0034	132

^a BJD-2400000.^b Against $max = 2450757.0107 + 0.086934E$.^c Number of points used to determine the maximum.

maxima, in the analysis.

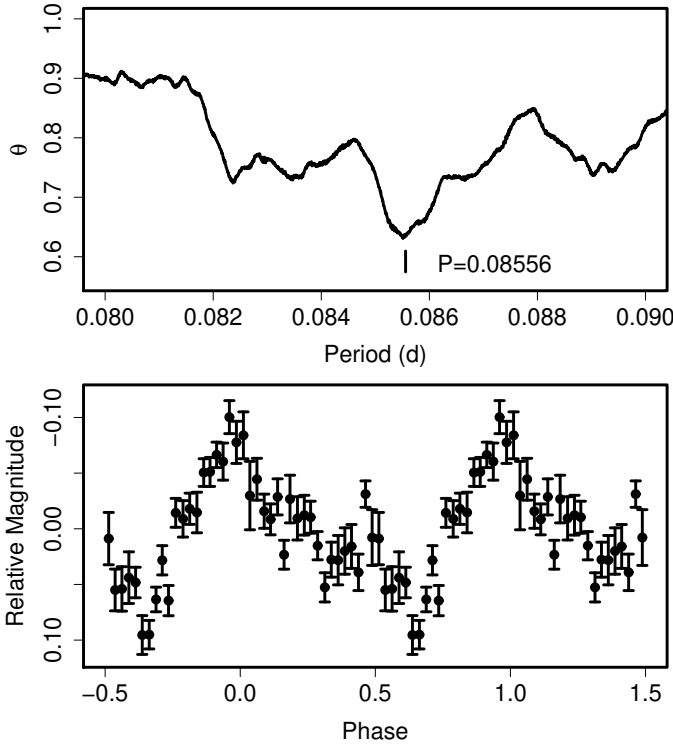


Fig. 113. Superhumps in V364 Peg (2004). (Upper): PDM analysis. (Lower): Phase-averaged profile.

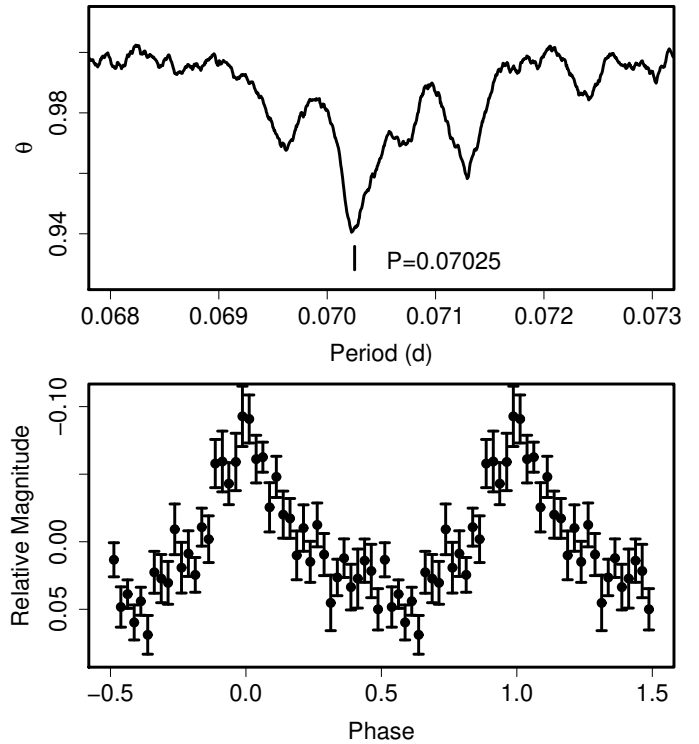


Fig. 114. Superhumps in V368 Peg (2000). (Upper): PDM analysis. (Lower): Phase-averaged profile.

Table 186. Superhump maxima of V364 Peg (2004).

E	max ^a	error	$O - C^b$	N^c
0	53329.2263	0.0007	0.0008	57
1	53329.3101	0.0007	-0.0007	70
2	53329.3967	0.0024	0.0006	30
4	53329.5654	0.0024	-0.0015	48
5	53329.6529	0.0012	0.0008	60
27	53331.5302	0.0364	0.0006	29
28	53331.6144	0.0032	-0.0005	46

^a BJD-2400000.

^b Against $max = 2453329.2255 + 0.085338E$.

^c Number of points used to determine the maximum.

6.98. V368 Pegasi

V368 Peg is a dwarf nova discovered by Antipin (1999). The SU UMa-type nature of this object was established by J. Pietz during the 1999 superoutburst (vsnet-alert 3317). We observed the 2000 superoutburst. The mean superhump period with the PDM method was 0.070253(17) d (figure 114). The times of superhump maxima are listed in table 187. There was a clear transition in the superhump period around $E = 86$. The mean P_{SH} and P_{dot} for $E \leq 86$ were 0.070380(8) d and $+0.5(1.2) \times 10^{-5}$, respectively. We also observed the 2005 superoutburst (table 188) during the growing stage of superhumps. A likely stage A–B transition was recorded ($E \leq 14$). Combined with the AAVSO observations, we obtained $P_{SH} = 0.07038(3)$ d for $70 \leq E \leq 97$. The 2006 superoutburst was observed during its late stage (table 189), yielding $P_2 = 0.069945(18)$ d with the PDM method. A comparison of $O - C$ diagrams between different superoutbursts is shown in figure 115.

6.99. V369 Pegasi

The SU UMa-type nature of V369 Peg (=KUV 23012+1702) was established during the 1999 superoutburst (Kato, Uemura 2001b). We reanalyzed the data in Kato, Uemura (2001b) and AAVSO observations. The times of superhump maxima are listed in table 190. The $O - C$ diagram shows a stage B–C transition.

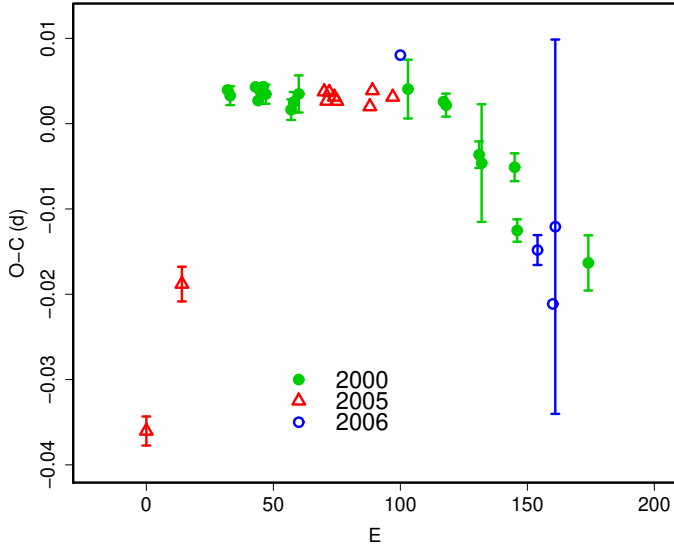


Fig. 115. Comparison of $O - C$ diagrams of V368 Peg between different superoutbursts. A period of 0.07039 d was used to draw this figure. Approximate cycle counts (E) after the start of the superoutburst were used.

Table 187. Superhump maxima of V368 Peg (2000).

E	\max^a	error	$O - C^b$	N^c
0	51785.2531	0.0005	-0.0017	145
1	51785.3229	0.0011	-0.0023	95
11	51786.0278	0.0006	-0.0002	51
12	51786.0966	0.0007	-0.0017	50
13	51786.1680	0.0009	-0.0005	42
14	51786.2390	0.0004	0.0002	144
15	51786.3085	0.0011	-0.0006	102
25	51787.0106	0.0012	-0.0013	45
26	51787.0819	0.0012	-0.0003	42
28	51787.2236	0.0022	0.0008	59
71	51790.2509	0.0034	0.0060	19
85	51791.2349	0.0006	0.0060	140
86	51791.3049	0.0013	0.0057	96
99	51792.2142	0.0016	0.0012	142
100	51792.2836	0.0069	0.0004	118
113	51793.1981	0.0016	0.0013	126
114	51793.2611	0.0013	-0.0060	136
142	51795.2282	0.0032	-0.0069	125

^a BJD-2400000.

^b Against $\max = 2451785.2548 + 0.070284E$.

^c Number of points used to determine the maximum.

Table 188. Superhump maxima of V368 Peg (2005).

E	\max^a	error	$O - C^b$	N^c
0	53621.1701	0.0017	-0.0073	191
14	53622.1728	0.0020	0.0044	163
70	53626.1372	0.0003	0.0048	201
71	53626.2065	0.0003	0.0033	212
72	53626.2779	0.0008	0.0039	139
74	53626.4181	0.0003	0.0026	49
75	53626.4880	0.0004	0.0017	71
88	53627.4024	0.0004	-0.0041	53
89	53627.4747	0.0009	-0.0026	57
97	53628.0371	0.0009	-0.0065	96

^a BJD-2400000.

^b Against $\max = 2453621.1774 + 0.070785E$.

^c Number of points used to determine the maximum.

Table 189. Superhump maxima of V368 Peg (2006).

E	\max^a	error	$O - C^b$	N^c
0	53993.2190	0.0006	0.0001	78
54	53996.9972	0.0017	-0.0006	75
60	53997.4132	0.0009	-0.0045	103
61	53997.4927	0.0219	0.0050	52

^a BJD-2400000.

^b Against $\max = 2453993.2189 + 0.069981E$.

^c Number of points used to determine the maximum.

Table 190. Superhump maxima of V369 Peg (1999).

E	\max^a	error	$O - C^b$	N^c
0	51490.0631	0.0057	-0.0153	53
12	51491.1040	0.0040	0.0055	90
24	51492.1264	0.0042	0.0079	166
26	51492.2963	0.0025	0.0078	56
27	51492.3757	0.0012	0.0022	92
35	51493.0500	0.0035	-0.0035	155
36	51493.1412	0.0047	0.0027	168
71	51496.1034	0.0180	-0.0101	170
82	51497.0513	0.0031	0.0027	111

^a BJD-2400000.

^b Against $\max = 2451490.0785 + 0.085001E$.

^c Number of points used to determine the maximum.

Table 191. Superhump maxima of UV Per (1991–1992).

E	\max^a	error	$O - C^b$	N^c
0	48615.0640	0.0021	-0.0118	63
58	48618.9295	0.0006	0.0044	107
73	48619.9247	0.0007	0.0042	62
88	48620.9195	0.0019	0.0035	45
91	48621.1213	0.0016	0.0062	68
92	48621.1855	0.0008	0.0040	128
103	48621.9170	0.0007	0.0055	143
104	48621.9773	0.0006	-0.0005	7
105	48622.0463	0.0062	0.0021	70
106	48622.1199	0.0030	0.0093	51
120	48623.0287	0.0024	-0.0110	80
121	48623.1109	0.0017	0.0048	154
134	48623.9528	0.0017	-0.0161	117
135	48624.0368	0.0012	0.0016	116
136	48624.0954	0.0019	-0.0062	116

^a BJD-2400000.^b Against $\max = 2448615.0758 + 0.066366E$.^c Number of points used to determine the maximum.

6.100. UV Persei

UV Per is a well-known SU UMa-type dwarf nova with a relatively long recurrence time and a large outburst amplitude. Udalski, Pych (1992) detected superhumps during the 1989 superoutburst. Udalski, Pych (1992) reported that they did not detect a significant quadratic term (P_{dot}), probably due to the short (~ 3 d) coverage.

We observed four superoutbursts in 1991–1992, 2000, 2003 and 2007 (tables 191, 192, 193, 194). The 2000 observation covered the entire superoutburst, including the growing stage of superhumps and the rapid fading stage, but with lower signal statistics. The 2003 observation covered the superoutburst with higher statistics. The $O - C$ diagrams of these outbursts can be interpreted as a well-demonstrated sequence of stages A–C. The P_{dot} 's of the stage B corresponded to $+9.5(6.0) \times 10^{-5}$ ($14 \leq E \leq 62$) for the 2000 superoutburst, and $+5.1(1.0) \times 10^{-5}$ ($20 \leq E \leq 109$) for the 2003 superoutburst, respectively. The 1991–1992 and 2007 superoutbursts were observed during the (middle-to-)final stage of the plateau and clearly showed a transition to a shorter period (stage B to C). Although the P_{dot} of the entire 2007 data was $-7.0(0.9) \times 10^{-5}$, this value should be used carefully since the measured segment of the $O - C$ diagram was different from those in the 2000 and 2003 superoutburst.

6.101. PU Persei

PU Per was discovered as a dwarf nova by Hoffmeister (1967a). The object has a relatively long outburst recurrence time and a large outburst amplitude (cf. Romano, Minello 1976; Busch et al. 1979; Kato, Nogami 1995). Although the detection of superhumps in this object was reported in Kato, Matsumoto (1999b), the identification of the period had awaited further observation. We observed the object during the 2009 superoutburst and iden-

Table 192. Superhump maxima of UV Per (2000).

E	\max^a	error	$O - C^b$	N^c
0	51904.0426	0.0006	-0.0098	129
1	51904.1035	0.0037	-0.0154	73
2	51904.1784	0.0018	-0.0070	85
14	51904.9789	0.0011	-0.0046	77
15	51905.0530	0.0023	0.0030	51
16	51905.1145	0.0026	-0.0020	30
19	51905.3151	0.0002	-0.0010	130
20	51905.3821	0.0004	-0.0004	76
29	51905.9802	0.0005	-0.0009	79
31	51906.1163	0.0006	0.0022	69
44	51906.9772	0.0003	-0.0015	106
45	51907.0468	0.0005	0.0017	84
51	51907.4439	0.0006	-0.0003	56
53	51907.5815	0.0006	0.0043	32
54	51907.6477	0.0006	0.0040	32
55	51907.7161	0.0006	0.0059	31
58	51907.9119	0.0006	0.0022	91
59	51907.9784	0.0004	0.0022	212
60	51908.0444	0.0004	0.0017	246
61	51908.1145	0.0004	0.0052	167
62	51908.1849	0.0008	0.0091	88
75	51909.0494	0.0021	0.0091	113
105	51911.0415	0.0007	0.0061	105
119	51911.9732	0.0005	0.0067	111
120	51912.0354	0.0008	0.0024	123
121	51912.1057	0.0009	0.0062	86
134	51912.9633	0.0008	-0.0008	82
135	51913.0334	0.0007	0.0029	129
136	51913.0953	0.0030	-0.0018	91
164	51914.9453	0.0033	-0.0139	91
185	51916.3404	0.0029	-0.0154	72

^a BJD-2400000.^b Against $\max = 2451904.0524 + 0.066505E$.^c Number of points used to determine the maximum.

tified the superhump period as 0.06811(3) d (figure 116), a one-day alias to Kato, Matsumoto (1999b).

The times of superhump maxima are listed in table 195. Since the object faded shortly after the last observation, it was most likely that we observed the later part of the superoutburst, corresponding to the stage B–C transition. We presented the measured periods based on this interpretation in table 2.

6.102. PV Persei

In contrast to PU Per, discovered at the same time (Hoffmeister 1967a), PV Per shows frequent outbursts (Romano, Minello 1976; Busch et al. 1979). The SU UMa-type nature of PV Per was established by Vanmunster (1997), who reported a period of 0.0805(1) d. We further observed the 2008 superoutburst. The mean superhump period with the PDM method was 0.08031(4) d (figure 117). The times of superhump maxima during the 2008 superoutburst are listed in table 196. The

Table 193. Superhump maxima of UV Per (2003).

E	max ^a	error	$O - C^b$	N^c
0	52950.0550	0.0007	-0.0130	77
2	52950.1920	0.0006	-0.0091	103
3	52950.2599	0.0010	-0.0077	127
4	52950.3278	0.0012	-0.0063	185
5	52950.3964	0.0005	-0.0043	192
6	52950.4647	0.0004	-0.0024	101
7	52950.5315	0.0009	-0.0022	38
20	52951.3978	0.0003	-0.0008	329
21	52951.4634	0.0004	-0.0018	264
22	52951.5311	0.0004	-0.0005	182
23	52951.5976	0.0006	-0.0006	16
24	52951.6646	0.0003	-0.0001	98
25	52951.7286	0.0002	-0.0027	216
26	52951.7941	0.0002	-0.0037	207
27	52951.8612	0.0005	-0.0031	222
28	52951.9292	0.0005	-0.0016	172
29	52951.9944	0.0006	-0.0030	76
34	52952.3283	0.0002	-0.0017	226
35	52952.3948	0.0003	-0.0017	149
37	52952.5287	0.0011	-0.0009	71
38	52952.5936	0.0002	-0.0026	184
39	52952.6606	0.0002	-0.0021	193
42	52952.8608	0.0005	-0.0015	15
43	52952.9263	0.0008	-0.0025	18
44	52952.9930	0.0011	-0.0023	18
45	52953.0573	0.0006	-0.0045	16
48	52953.2590	0.0005	-0.0024	64
49	52953.3266	0.0006	-0.0014	70
50	52953.3921	0.0006	-0.0024	64
51	52953.4559	0.0004	-0.0051	121
52	52953.5254	0.0003	-0.0021	190
53	52953.5921	0.0002	-0.0019	157
54	52953.6584	0.0003	-0.0022	175
55	52953.7251	0.0003	-0.0020	169
56	52953.7919	0.0004	-0.0017	163
57	52953.8597	0.0004	-0.0005	170
58	52953.9250	0.0003	-0.0017	159
64	52954.3231	0.0007	-0.0027	118
65	52954.3926	0.0005	0.0002	283
66	52954.4596	0.0004	0.0006	340
67	52954.5264	0.0004	0.0009	455
68	52954.5937	0.0005	0.0017	343
69	52954.6597	0.0003	0.0012	498
70	52954.7265	0.0002	0.0014	622
71	52954.7927	0.0002	0.0011	550
72	52954.8618	0.0002	0.0037	274
73	52954.9228	0.0014	-0.0018	154
78	52955.2640	0.0004	0.0067	160
79	52955.3286	0.0005	0.0048	172
80	52955.3939	0.0004	0.0036	172
81	52955.4611	0.0004	0.0042	152
82	52955.5280	0.0004	0.0046	192
82	52955.5280	0.0004	0.0046	192

^a BJD-2400000.^b Against $max = 2452950.0680 + 0.066529E$.^c Number of points used to determine the maximum.**Table 193.** Superhump maxima of UV Per (2003). (continued)

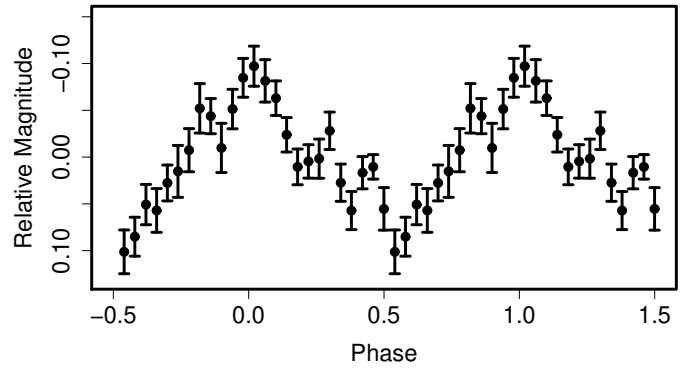
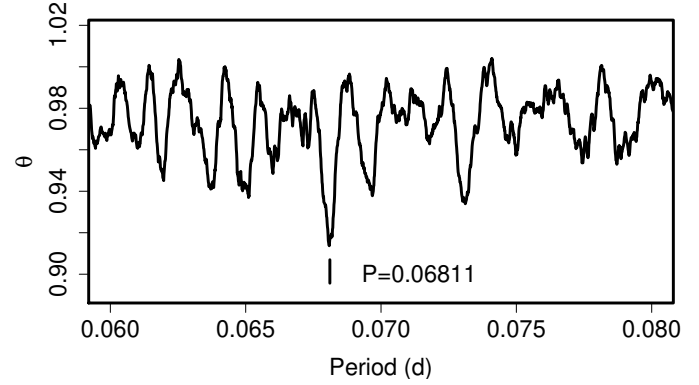
E	max	error	$O - C$	N
83	52955.5956	0.0004	0.0056	246
84	52955.6634	0.0002	0.0069	562
85	52955.7302	0.0003	0.0073	510
86	52955.7967	0.0003	0.0072	382
87	52955.8631	0.0003	0.0070	286
95	52956.3966	0.0005	0.0083	116
96	52956.4639	0.0004	0.0090	111
99	52956.6633	0.0002	0.0089	382
100	52956.7295	0.0002	0.0086	380
101	52956.7965	0.0002	0.0090	375
102	52956.8630	0.0002	0.0090	360
103	52956.9256	0.0004	0.0051	234
104	52956.9959	0.0002	0.0088	365
105	52957.0619	0.0002	0.0083	361
106	52957.1274	0.0003	0.0073	271
107	52957.1934	0.0003	0.0067	355
108	52957.2601	0.0002	0.0069	354
109	52957.3271	0.0002	0.0074	406
112	52957.5248	0.0010	0.0055	16
113	52957.5921	0.0008	0.0063	41
114	52957.6581	0.0009	0.0057	41
115	52957.7237	0.0012	0.0048	33
116	52957.7910	0.0009	0.0056	16
117	52957.8570	0.0006	0.0050	18
118	52957.9229	0.0007	0.0044	17
119	52957.9894	0.0004	0.0044	110
120	52958.0600	0.0003	0.0084	91
124	52958.3199	0.0004	0.0023	86
125	52958.3864	0.0004	0.0022	87
126	52958.4529	0.0004	0.0022	85
127	52958.5193	0.0004	0.0021	82
128	52958.5862	0.0003	0.0024	90
131	52958.7848	0.0016	0.0014	12
132	52958.8508	0.0007	0.0009	18
133	52958.9182	0.0007	0.0018	18
140	52959.3808	0.0005	-0.0013	62
141	52959.4451	0.0014	-0.0036	50
142	52959.5085	0.0019	-0.0067	156
143	52959.5820	0.0005	0.0003	164
144	52959.6470	0.0004	-0.0012	177
145	52959.7134	0.0003	-0.0014	152
146	52959.7794	0.0003	-0.0019	152
147	52959.8464	0.0004	-0.0015	152
148	52959.9128	0.0003	-0.0015	421
149	52959.9769	0.0004	-0.0039	385
150	52960.0445	0.0003	-0.0029	360
151	52960.1105	0.0004	-0.0034	285
152	52960.1774	0.0003	-0.0031	359
153	52960.2430	0.0004	-0.0040	354
154	52960.3119	0.0006	-0.0016	408
155	52960.3791	0.0007	-0.0009	208
156	52960.4431	0.0007	-0.0034	120
159	52960.6431	0.0010	-0.0031	30
164	52960.9715	0.0004	-0.0073	361
165	52961.0392	0.0004	-0.0062	360

Table 193. Superhump maxima of UV Per (2003). (continued)

E	max	error	$O - C$	N
166	52961.1021	0.0004	-0.0097	318
167	52961.1677	0.0005	-0.0107	357
168	52961.2337	0.0006	-0.0112	307
169	52961.2962	0.0009	-0.0153	337
175	52961.6975	0.0007	-0.0132	341
176	52961.7642	0.0005	-0.0130	360

Table 194. Superhump maxima of UV Per (2007).

E	max ^a	error	$O - C^b$	N^c
0	54379.0219	0.0003	-0.0039	366
1	54379.0890	0.0004	-0.0031	359
2	54379.1550	0.0003	-0.0035	358
9	54379.6212	0.0006	-0.0015	103
20	54380.3538	0.0005	0.0014	66
21	54380.4187	0.0009	0.0001	76
22	54380.4869	0.0005	0.0019	75
23	54380.5522	0.0007	0.0008	67
24	54380.6204	0.0004	0.0027	76
25	54380.6851	0.0027	0.0011	72
36	54381.4147	0.0003	0.0011	136
37	54381.4817	0.0002	0.0018	134
38	54381.5484	0.0003	0.0021	141
39	54381.6143	0.0003	0.0016	101
67	54383.4704	0.0003	0.0006	138
68	54383.5371	0.0003	0.0010	124
69	54383.6032	0.0003	0.0007	138
75	54384.0013	0.0005	0.0009	296
76	54384.0666	0.0009	-0.0002	178
82	54384.4653	0.0003	0.0005	110
83	54384.5320	0.0005	0.0009	136
84	54384.5973	0.0004	-0.0000	137
85	54384.6670	0.0011	0.0033	82
97	54385.4584	0.0006	-0.0012	140
98	54385.5215	0.0010	-0.0045	123
99	54385.5877	0.0008	-0.0046	58

^a BJD-2400000.^b Against $max = 2454379.0258 + 0.066328E$.^c Number of points used to determine the maximum.**Fig. 116.** Superhumps in PU Per (2009). (Upper): PDM analysis. (Lower): Phase-averaged profile.**Table 195.** Superhump maxima of PU Per (2009).

E	max ^a	error	$O - C^b$	N^c
0	54837.8888	0.0021	0.0026	42
1	54837.9477	0.0025	-0.0067	70
2	54838.0191	0.0038	-0.0034	69
3	54838.0902	0.0050	-0.0004	38
18	54839.1206	0.0031	0.0082	139
60	54841.9793	0.0014	0.0060	132
61	54842.0340	0.0021	-0.0073	133
75	54843.0002	0.0039	0.0053	58
76	54843.0678	0.0086	0.0048	72
89	54843.9468	0.0013	-0.0018	142
90	54844.0095	0.0018	-0.0072	125

^a BJD-2400000.^b Against $max = 2454837.8863 + 0.068116E$.^c Number of points used to determine the maximum.

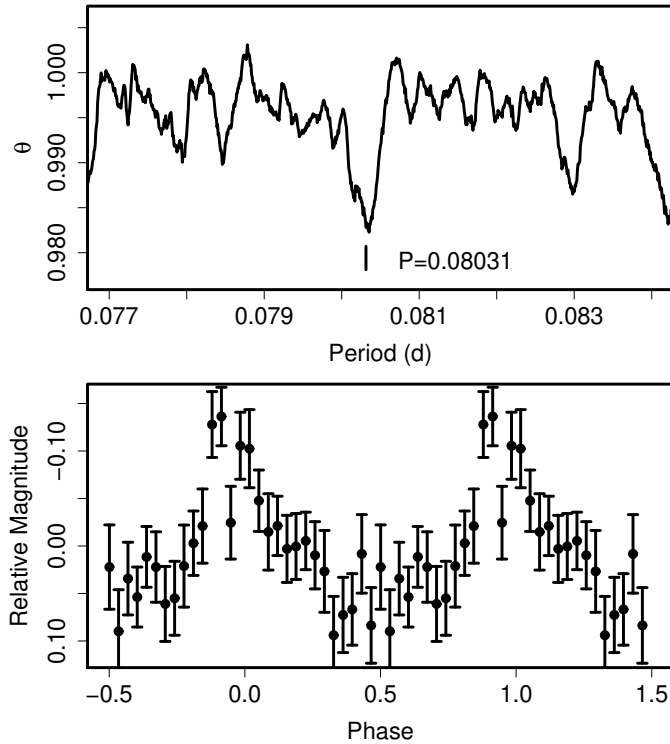


Fig. 117. Superhumps in PV Per (2008). (Upper): PDM analysis. (Lower): Phase-averaged profile.

Table 196. Superhump maxima of PV Per (2008).

E	\max^a	error	$O - C^b$	N^c
0	54745.3856	0.0006	-0.0074	60
1	54745.4668	0.0008	-0.0066	86
35	54748.2132	0.0007	0.0057	150
36	54748.2952	0.0011	0.0073	136
73	54751.2686	0.0005	0.0054	170
74	54751.3372	0.0036	-0.0064	89
121	54755.1253	0.0011	0.0022	151
122	54755.2073	0.0033	0.0038	132
123	54755.2909	0.0048	0.0070	127
135	54756.2568	0.0068	0.0079	153
146	54757.1335	0.0027	0.0000	149
147	54757.2170	0.0046	0.0032	151
159	54758.1612	0.0033	-0.0177	168
160	54758.2475	0.0055	-0.0118	149
161	54758.3471	0.0075	0.0074	78

^a BJD-2400000.

^b Against $\max = 2454745.3930 + 0.080414E$.

^c Number of points used to determine the maximum.

observation mainly covered the later stage of the superoutburst. Although the global P_{dot} was $-4.4(2.1) \times 10^{-5}$, this change can be interpreted as a result of a stage B-C transition (see also table 2).

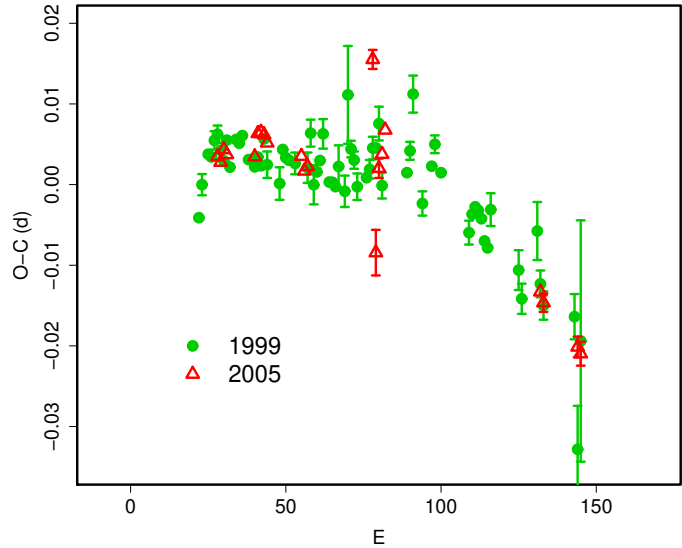


Fig. 118. Comparison of $O-C$ diagrams of QY Per between different superoutbursts. A period of 0.07862 d was used to draw this figure. Approximate cycle counts (E) after the start of the superoutburst were used.

6.103. QY Persei

QY Per is a dwarf nova discovered by Hoffmeister (1966). The object had long been suspected to be an excellent candidate for a WZ Sge-like object based on the large outburst amplitude and long recurrence time.

We observed two superoutbursts in 1999 (Mattei et al. 1999; Kato et al. 2000) and 2005. The 1999 superoutburst (table 197) was one of the the best sampled superoutbursts among all SU UMa-type dwarf novae. The $O-C$ diagram consisted of all stages A-C (cf. figure 4). The P_{dot} during the stage B corresponds to $+7.8(3.1) \times 10^{-5}$ ($5 \leq E \leq 69$). This example demonstrates that a positive P_{dot} system is present among systems with longer superhump periods. A stage B-C transition was recorded during the 2005 superoutburst (table 198). A comparison of $O-C$ diagrams between different superoutbursts is shown in figure 118.

6.104. V518 Persei

This object (=GRO J0422+32) is a BHXT (see subsection 4.11). We present reanalysis of observations in Kato et al. (1995). A new analysis has yielded a slightly longer superhump period of 0.2159(3) d. (table 199). The fractional superhump excess is 1.8(1) %. Using the relation in subsection 199), we can expect $q = 0.096(7)$, reasonably consistent with the determination from radial-velocity studies ($q = 0.116(8)$, Harlaftis et al. 1999).

6.105. TY Piscis Austrini

Although TY PsA is among the SU UMa-type dwarf novae earliest discovered (Barwig et al. 1982), the only published P_{SH} was 0.08765 d, determined from the relatively limited data taken during the 1984 superoutburst (Warner et al. 1989).

We observed the 2008 superoutburst starting 2 d after

Table 197. Superhump maxima of QY Per (1999).

E	max ^a	error	$O - C^b$	N^c
0	51542.3954	0.0007	-0.0115	204
1	51542.4781	0.0013	-0.0073	108
3	51542.6392	0.0006	-0.0032	231
4	51542.7174	0.0007	-0.0034	194
5	51542.7981	0.0011	-0.0012	106
6	51542.8775	0.0011	-0.0003	120
7	51542.9541	0.0006	-0.0022	143
8	51543.0314	0.0006	-0.0033	150
9	51543.1126	0.0005	-0.0006	159
10	51543.1879	0.0008	-0.0038	150
12	51543.3486	0.0007	-0.0001	74
13	51543.4267	0.0004	-0.0004	92
14	51543.5063	0.0005	0.0007	114
16	51543.6605	0.0006	-0.0020	233
17	51543.7392	0.0007	-0.0018	200
18	51543.8169	0.0008	-0.0026	148
19	51543.8967	0.0006	-0.0012	157
20	51543.9743	0.0008	-0.0022	114
21	51544.0562	0.0009	0.0013	153
22	51544.1316	0.0016	-0.0017	138
26	51544.4438	0.0020	-0.0035	17
27	51544.5266	0.0008	0.0009	20
28	51544.6042	0.0009	0.0000	21
29	51544.6825	0.0007	-0.0001	19
31	51544.8394	0.0013	-0.0002	15
35	51545.1533	0.0019	-0.0002	144
36	51545.2362	0.0017	0.0042	161
37	51545.3084	0.0024	-0.0020	36
38	51545.3887	0.0005	-0.0003	144
39	51545.4687	0.0007	0.0013	101
40	51545.5506	0.0018	0.0047	37
42	51545.7019	0.0007	-0.0009	166
43	51545.7805	0.0007	-0.0008	213
44	51545.8586	0.0009	-0.0012	204
45	51545.9397	0.0026	0.0014	64
47	51546.0938	0.0019	-0.0013	110
48	51546.1844	0.0061	0.0108	39
49	51546.2563	0.0010	0.0042	111
50	51546.3336	0.0011	0.0030	109
51	51546.4089	0.0016	-0.0002	24
54	51546.6459	0.0009	0.0014	227
55	51546.7255	0.0012	0.0026	207
56	51546.8068	0.0014	0.0053	183
57	51546.8854	0.0009	0.0055	248
58	51546.9671	0.0021	0.0087	113
59	51547.0380	0.0016	0.0011	155
67	51547.6685	0.0009	0.0039	158
68	51547.7499	0.0011	0.0068	113
69	51547.8355	0.0023	0.0140	33

^a BJD-2400000.^b Against $max = 2451542.4070 + 0.078473E$.^c Number of points used to determine the maximum.**Table 197.** Superhump maxima of QY Per (1999) (continued).

E	max	error	$O - C$	N
72	51548.0578	0.0015	0.0008	80
75	51548.2983	0.0009	0.0059	128
76	51548.3796	0.0011	0.0088	87
78	51548.5334	0.0007	0.0055	55
87	51549.2335	0.0015	-0.0006	62
88	51549.3144	0.0005	0.0019	102
89	51549.3939	0.0005	0.0029	99
90	51549.4721	0.0005	0.0026	97
91	51549.5497	0.0005	0.0018	91
92	51549.6256	0.0009	-0.0009	201
93	51549.7033	0.0009	-0.0016	157
94	51549.7867	0.0020	0.0033	82
103	51550.4868	0.0025	-0.0029	39
104	51550.5619	0.0019	-0.0063	40
109	51550.9634	0.0036	0.0029	35
110	51551.0354	0.0017	-0.0035	145
111	51551.1114	0.0018	-0.0061	157
121	51551.8962	0.0028	-0.0060	152
122	51551.9583	0.0054	-0.0223	123
123	51552.0504	0.0150	-0.0087	158

Table 198. Superhump maxima of QY Per (2005).

E	max ^a	error	$O - C^b$	N^c
0	53667.0498	0.0003	-0.0047	306
1	53667.1278	0.0005	-0.0052	361
2	53667.2079	0.0005	-0.0034	315
3	53667.2860	0.0003	-0.0039	362
12	53667.9933	0.0005	-0.0023	134
13	53668.0748	0.0003	0.0007	212
14	53668.1536	0.0003	0.0011	281
15	53668.2318	0.0003	0.0010	409
16	53668.3095	0.0004	0.0002	309
27	53669.1726	0.0005	0.0007	159
28	53669.2494	0.0005	-0.0009	158
29	53669.3286	0.0008	-0.0002	126
50	53670.9929	0.0012	0.0173	138
51	53671.0476	0.0028	-0.0065	131
52	53671.1366	0.0012	0.0042	280
53	53671.2170	0.0005	0.0061	226
54	53671.2986	0.0005	0.0093	224
104	53675.2095	0.0007	-0.0008	154
105	53675.2868	0.0011	-0.0019	109
116	53676.1462	0.0013	-0.0052	151
117	53676.2239	0.0015	-0.0058	164

^a BJD-2400000.^b Against $max = 2453667.0545 + 0.078421E$.^c Number of points used to determine the maximum.

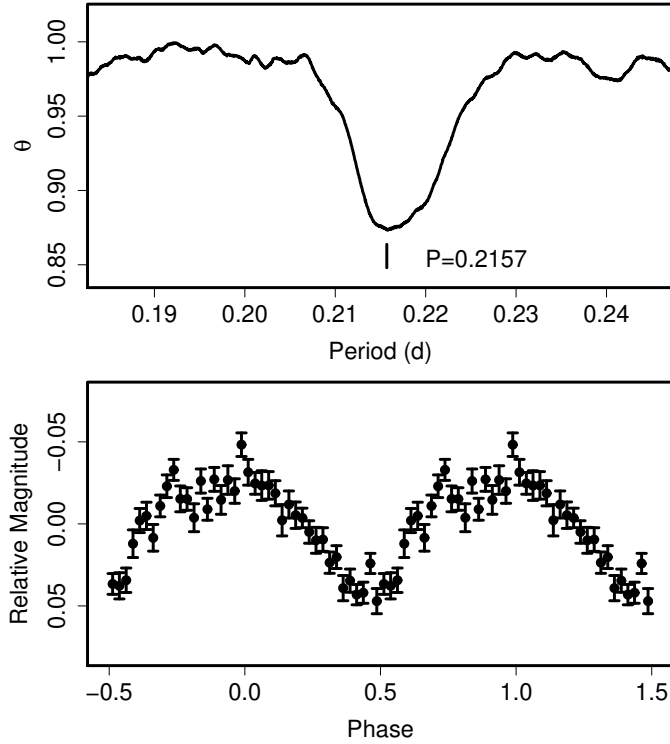


Fig. 119. Superhumps in V518 Per (1992). (Upper): PDM analysis. (Lower): Phase-averaged profile.

Table 199. Superhump maxima of V518 Per (1992).

E	\max^a	error	$O - C^b$	N^c
0	48948.0905	0.0061	-0.0064	249
1	48948.3060	0.0051	-0.0099	228
4	48948.9895	0.0052	0.0168	247
5	48949.1934	0.0033	0.0017	254
9	48950.0745	0.0027	0.0069	265
13	48950.9336	0.0195	-0.0099	174
14	48951.1657	0.0029	0.0033	293
18	48952.0357	0.0023	-0.0026	260

^a BJD-2400000.

^b Against $\max = 2448948.0969 + 0.21897E$.

^c Number of points used to determine the maximum.

Table 200. Superhump maxima of TY PsA (2008).

E	\max^a	error	$O - C^b$	N^c
0	54798.9021	0.0003	-0.0043	148
11	54799.8674	0.0019	-0.0044	89
12	54799.9677	0.0005	0.0081	99
23	54800.9228	0.0004	-0.0021	156
34	54801.8976	0.0007	0.0074	74
x46	54802.9482	0.0010	0.0048	86
57	54803.9093	0.0006	0.0006	163
68	54804.8764	0.0012	0.0024	128
69	54804.9378	0.0028	-0.0240	98
80	54805.9325	0.0020	0.0053	75
91	54806.8987	0.0009	0.0062	197

^a BJD-2400000.

^b Against $\max = 2454798.9064 + 0.087759E$.

^c Number of points used to determine the maximum.

the initial detection of the outburst. The times of superhump maxima are listed in table 200. Although a stage B–C transition was likely present around $E = 40$, the times of maxima were not very well determined because the durations of each observations were comparable to the superhump period and the maxima often fell close to start or end of the observation. We therefore determined periods for the stage B ($E \leq 34$) and the stage C ($E \geq 46$) using the PDM method. The values were 0.087790(17) d and 0.087730(30) d, respectively, and these values are adopted in table 2. The latter period is close to one reported by Warner et al. (1989), suggesting that Warner et al. (1989) recorded the stage C superhumps.

6.106. TY Piscium

TY Psc has long been known as an SU UMa-type dwarf nova (cf. Szkody, Feinswog 1988), though accurate determination of the superhump period has not yet been published. Although Kunjaya et al. (2001) reported observations of the 2000 superoutburst, the resultant period had a large uncertainty.

We observed the 2005 and 2008 superoutbursts (tables 201, 202). The global P_{dot} during the 2005 superoutburst was $+1.5(3.0) \times 10^{-5}$. A stage B–C transition was observed during the 2008 superoutburst, although this outburst may have had a prolonged state with stage A superhumps (figure 120). The nominal global superhump period and derivative were 0.07045(2) d and $P_{\text{dot}} = -9.2(0.8) \times 10^{-5}$, respectively.

6.107. EI Piscium

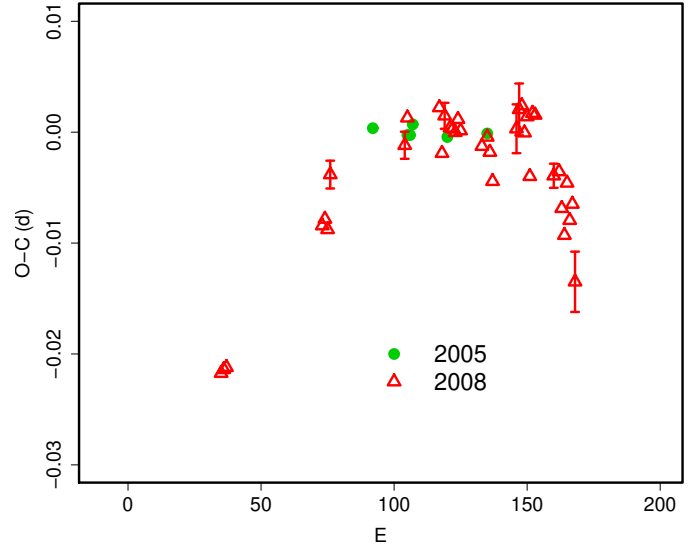
EI Psc (=1RXS J232953.9+062814) is one of two (the other being V485 Cen) unusually short- P_{SH} SU UMa-type dwarf novae with evolved secondaries (Uemura et al. 2002b; Skillman et al. 2002). Since the orbital variation, arising from the ellipsoidal variation of the secondary star, is strong, we subtracted the mean orbital variation from the raw data in Uemura et al. (2002a). The resultant times of superhump maxima are listed in table 203. A combi-

Table 201. Superhump maxima of TY Psc (2005).

E	\max^a	error	$O - C^b$	N^c
0	53614.2326	0.0004	0.0001	129
13	53615.1465	0.0006	-0.0003	100
14	53615.2168	0.0005	-0.0003	104
15	53615.2882	0.0004	0.0007	97
28	53616.2016	0.0003	-0.0003	145
43	53617.2571	0.0002	0.0002	205

^a BJD-2400000.^b Against $\max = 2453614.2324 + 0.070338E$.^c Number of points used to determine the maximum.**Table 202.** Superhump maxima of TY Psc (2008).

E	\max^a	error	$O - C^b$	N^c
0	54752.2907	0.0008	-0.0092	67
1	54752.3614	0.0005	-0.0089	114
2	54752.4319	0.0004	-0.0088	115
38	54754.9773	0.0005	0.0005	138
39	54755.0482	0.0004	0.0010	137
40	54755.1176	0.0007	-0.0000	222
41	54755.1929	0.0013	0.0049	152
69	54757.1654	0.0012	0.0048	79
70	54757.2382	0.0010	0.0072	74
82	54758.0833	0.0009	0.0070	101
83	54758.1495	0.0008	0.0028	115
84	54758.2233	0.0012	0.0061	64
86	54758.3629	0.0003	0.0048	127
87	54758.4332	0.0003	0.0046	128
88	54758.5032	0.0003	0.0042	128
89	54758.5747	0.0008	0.0053	90
90	54758.6440	0.0009	0.0042	68
98	54759.2054	0.0008	0.0020	124
100	54759.3470	0.0005	0.0026	145
101	54759.4159	0.0006	0.0012	138
102	54759.4837	0.0005	-0.0015	139
111	54760.1216	0.0022	0.0023	93
112	54760.1937	0.0023	0.0040	222
113	54760.2643	0.0006	0.0042	353
114	54760.3322	0.0005	0.0017	225
115	54760.4040	0.0006	0.0031	223
116	54760.4690	0.0007	-0.0024	214
117	54760.5451	0.0009	0.0032	84
118	54760.6152	0.0008	0.0029	86
125	54761.1022	0.0011	-0.0032	83
127	54761.2433	0.0009	-0.0030	96
128	54761.3103	0.0005	-0.0064	248
129	54761.3783	0.0008	-0.0090	235
130	54761.4533	0.0005	-0.0043	128
131	54761.5203	0.0008	-0.0078	125
132	54761.5921	0.0010	-0.0064	125
133	54761.6555	0.0027	-0.0135	118

^a BJD-2400000.^b Against $\max = 2454752.2998 + 0.070445E$.^c Number of points used to determine the maximum.**Fig. 120.** Comparison of $O - C$ diagrams of TY Psc between different superoutbursts. A period of 0.07035 d was used to draw this figure. Approximate cycle counts (E) after the start of the superoutburst were used.

nation of the times of reported superhumps in Skillman et al. (2002) yielded a slightly discontinuous $O - C$ variation, although the transition to a shorter period was recorded in both sets of observations (figure 121). The discrepancy between these analyses was largest between the fading stage of the main superoutburst and the rebrightening, suggesting that the times of maxima in Skillman et al. (2002) were more affected by orbital variations. We therefore used times in Uemura et al. (2002a), updated here, and obtained $P_{\text{dot}} = +0.3(0.8) \times 10^{-5}$ ($E \leq 141$). The period then experienced a transition to a shorter one 0.046090(12) d. We regard this transition as a stage B-C transition based on the $O - C$ characteristics. Since this transition is usually observed during the superoutburst plateau in most SU UMa-type dwarf novae, the existence of a transition around the rebrightening looks peculiar to EI Psc.

We also analyzed the 2005 superoutburst and obtained the times of superhump maxima (table 204). The global P_{dot} was $-2.8(2.0) \times 10^{-5}$, although there may have been a break in the $O - C$ diagram around $E = 9$. This possible break may be a stage A-B transition (cf. figure 122). This superoutburst exhibited a rebrightening in a similar way as in the 2001 one.

6.108. VZ Pyxidis

VZ Pyx was identified as an SU UMa-type dwarf nova by Kato, Nogami (1997a). We observed the 2008 superoutburst (table 208). Since multiple maxima apparently appeared around and after the rapid fading stage ($E \geq 120$), we restricted our analysis to $E < 120$. Although a global $P_{\text{dot}} = -16.3(1.3) \times 10^{-5}$ ($E \leq 80$) was obtained, there was apparently a break in the period between $E = 27$ and $E = 54$. In table 2, we presented the periods based in

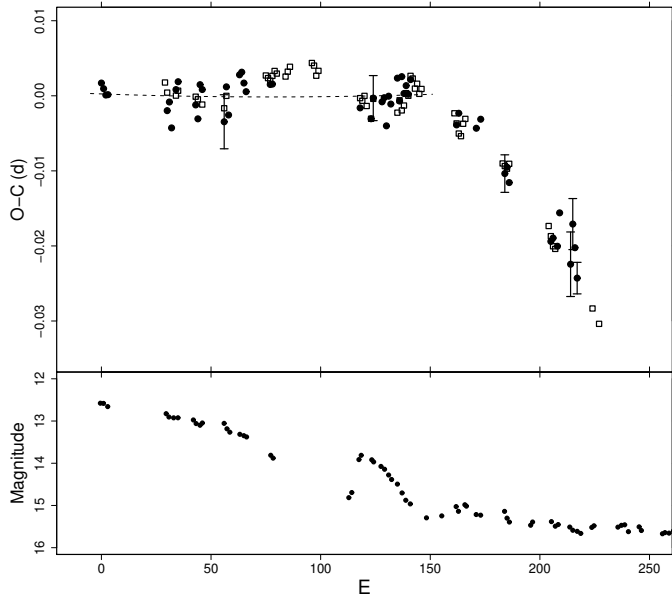


Fig. 121. $O - C$ diagram of EI Psc during the superoutburst in 2001. (Upper) $O - C$ diagram. The filled circles and open squares represent maxima presented here and maxima reported in Skillman et al. (2002). We used only the former set of maxima in order to avoid a systematic error potentially caused by superimposed orbital modulations. The dashed curve corresponds to $P_{\text{dot}} = +0.3 \times 10^{-5}$. (Lower) light curve.

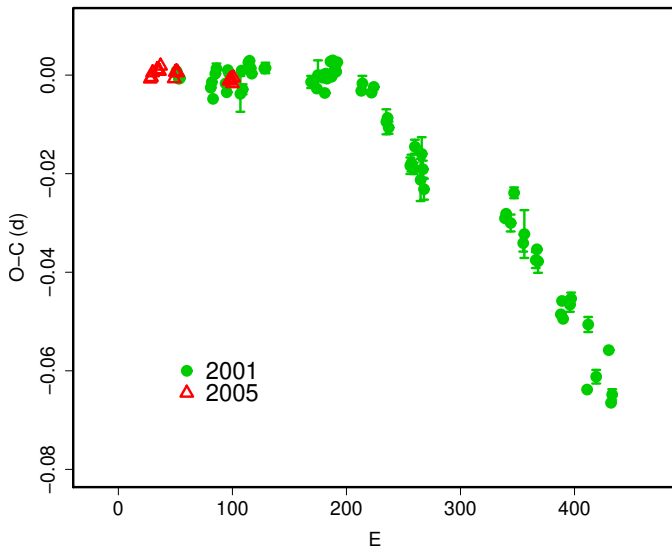


Fig. 122. Comparison of $O - C$ diagrams of EI Psc between different superoutbursts. A period of 0.04634 d was used to draw this figure. Approximate cycle counts (E) after the start of the superoutburst were used. Since the start of the 2001 superoutburst was unknown, the E was shifted assuming that the two superoutbursts have the same duration of the plateau phase.

Table 203. Superhump maxima of EI Psc (2001).

E	max ^a	error	$O - C$ ^b	N ^c
0	52218.0208	0.0003	-0.0120	84
1	52218.0664	0.0004	-0.0126	76
2	52218.1119	0.0002	-0.0133	80
3	52218.1583	0.0002	-0.0130	84
30	52219.4076	0.0005	-0.0106	94
31	52219.4551	0.0007	-0.0093	64
32	52219.4980	0.0005	-0.0125	45
34	52219.5958	0.0010	-0.0071	35
35	52219.6432	0.0010	-0.0059	36
43	52220.0109	0.0008	-0.0077	47
44	52220.0554	0.0007	-0.0093	51
45	52220.1063	0.0006	-0.0046	66
46	52220.1520	0.0008	-0.0051	28
56	52220.6112	0.0036	-0.0077	30
57	52220.6622	0.0009	-0.0028	53
58	52220.7048	0.0010	-0.0064	108
63	52220.9419	0.0005	-0.0002	124
64	52220.9886	0.0005	0.0003	132
65	52221.0335	0.0004	-0.0010	132
66	52221.0787	0.0010	-0.0020	101
77	52221.5895	0.0007	0.0008	38
78	52221.6359	0.0011	0.0011	37
118	52223.4867	0.0012	0.0047	82
123	52223.7170	0.0008	0.0042	200
124	52223.7661	0.0030	0.0071	170
128	52223.9510	0.0004	0.0072	148
129	52223.9979	0.0005	0.0080	148
130	52224.0405	0.0003	0.0044	314
131	52224.0908	0.0004	0.0085	316
132	52224.1361	0.0005	0.0076	238
135	52224.2786	0.0009	0.0116	88
136	52224.3219	0.0006	0.0087	88
137	52224.3715	0.0006	0.0121	150
138	52224.4156	0.0006	0.0100	160
139	52224.4630	0.0006	0.0112	148
140	52224.5082	0.0007	0.0103	56
141	52224.5565	0.0005	0.0124	68
162	52225.5238	0.0008	0.0100	22
163	52225.5717	0.0015	0.0117	25
171	52225.9405	0.0007	0.0111	106
173	52226.0344	0.0003	0.0125	93
184	52226.5370	0.0025	0.0072	16
185	52226.5842	0.0010	0.0082	25
186	52226.6285	0.0012	0.0064	24
205	52227.5013	0.0017	0.0017	17
206	52227.5481	0.0017	0.0024	25
208	52227.6397	0.0011	0.0016	25
209	52227.6905	0.0014	0.0062	17
214	52227.9154	0.0043	0.0003	80

^a BJD-2400000.

^b Against $\text{max} = 2452218.0328 + 0.046179E$.

^c Number of points used to determine the maximum.

Table 203. Superhump maxima of EI Psc (2001). (continued)

E	max	error	$O - C$	N
215	52227.9671	0.0034	0.0057	76
216	52228.0103	0.0017	0.0028	85
217	52228.0526	0.0021	-0.0011	85
288	52231.3368	0.0005	0.0044	76
289	52231.3841	0.0008	0.0055	94
293	52231.5676	0.0017	0.0042	52
296	52231.7127	0.0011	0.0108	48
304	52232.0732	0.0017	0.0019	180
305	52232.1214	0.0049	0.0039	146
315	52232.5795	0.0016	0.0002	52
316	52232.6280	0.0008	0.0026	50
317	52232.6719	0.0023	0.0003	50
337	52233.5880	0.0009	-0.0072	80
338	52233.6371	0.0006	-0.0044	104
339	52233.6798	0.0009	-0.0078	78
345	52233.9607	0.0014	-0.0040	170
346	52234.0082	0.0012	-0.0026	172
360	52234.6386	0.0009	-0.0188	52
361	52234.6981	0.0015	-0.0054	50
368	52235.0119	0.0014	-0.0149	254
379	52235.5270	0.0006	-0.0078	54
381	52235.6090	0.0009	-0.0181	76
382	52235.6570	0.0011	-0.0163	52

Table 204. Superhump maxima of EI Psc (2005).

E	max ^a	error	$O - C^b$	N^c
0	53592.8642	0.0001	-0.0014	112
1	53592.9108	0.0002	-0.0011	104
2	53592.9581	0.0002	-0.0001	60
6	53593.1441	0.0003	0.0006	68
7	53593.1903	0.0003	0.0005	68
8	53593.2364	0.0002	0.0003	143
9	53593.2838	0.0003	0.0014	165
21	53593.8374	0.0003	-0.0009	98
22	53593.8850	0.0001	0.0004	147
23	53593.9315	0.0001	0.0006	146
24	53593.9776	0.0001	0.0004	65
69	53596.0612	0.0008	-0.0003	68
70	53596.1078	0.0005	0.0000	68
71	53596.1543	0.0006	0.0002	68
72	53596.1997	0.0005	-0.0008	67
73	53596.2472	0.0005	0.0004	68

^a BJD-2400000.^b Against $max = 2453592.8656 + 0.046317E$.^c Number of points used to determine the maximum.**Table 205.** Superhump maxima of VZ Pyx (1996).

E	max ^a	error	$O - C^b$	N^c
0	50161.0287	0.0005	-0.0002	119
1	50161.1048	0.0007	0.0002	57
27	50163.0742	0.0005	-0.0000	107

^a BJD-2400000.^b Against $max = 2450161.0289 + 0.075754E$.^c Number of points used to determine the maximum.**Table 206.** Superhump maxima of VZ Pyx (2000).

E	max ^a	error	$O - C^b$	N^c
0	51888.2125	0.0014	-0.0006	48
27	51890.2523	0.0006	0.0009	38
94	51895.3091	0.0018	-0.0002	40

^a BJD-2400000.^b Against $max = 2451888.2132 + 0.075492E$.^c Number of points used to determine the maximum.

this interpretation. We also included a reanalysis of Kato, Nogami (1997a) (table 205) and the times of superhump maxima during the 2002 and 2004 superoutbursts (tables 206, 207). The 2000 superoutburst was observed during the terminal stage and the 2004 superoutburst was observed between 5 and 9 d from the onset of the outburst. The period for the 2000 superoutburst could be considered as a typical period for stage C superhumps in this object.

6.109. DV *Scorpii*

DV Sco was recently reclassified as a likely dwarf nova (Pastukhova, Samus 2003). The SU UMA-type nature of this dwarf nova was established by B. Monard (cf. vsnet-alert 8321, 8322) during its 2004 outburst. This object is a dwarf nova in the period gap (vsnet-alert 8325). We analyzed this superoutburst (table 209) and another in 2008 (table 210). The mean superhump period with the PDM method was 0.09970(7) d for the 2004 superoutburst (figure 123). The resultant global P_{dot} for the 2004 superoutburst was $-15.1(5.5) \times 10^{-5}$. The 2008 superoutburst was observed during its late course to its final decline. Due to relatively large error in maxima times and the short coverage, we did not attempt to determine P_{dot} .

Table 207. Superhump maxima of VZ Pyx (2004).

E	max ^a	error	$O - C^b$	N^c
0	53047.1835	0.0012	0.0000	133
51	53051.0513	0.0004	-0.0018	134
52	53051.1308	0.0011	0.0018	120

^a BJD-2400000.^b Against $max = 2453047.1835 + 0.075875E$.^c Number of points used to determine the maximum.

Table 208. Superhump maxima of VZ Pyx (2008).

E	max ^a	error	$O - C^b$	N^c
0	54790.2587	0.0004	-0.0087	253
1	54790.3343	0.0005	-0.0086	181
13	54791.2463	0.0006	-0.0026	147
14	54791.3223	0.0004	-0.0022	210
26	54792.2360	0.0007	0.0056	213
27	54792.3113	0.0004	0.0054	265
54	54794.3546	0.0008	0.0100	88
79	54796.2390	0.0005	0.0068	147
80	54796.3145	0.0007	0.0069	148
120	54799.3427	0.0011	0.0149	97
132	54800.2288	0.0008	-0.0050	224
133	54800.2869	0.0015	-0.0224	255

^a BJD-2400000.^b Against $max = 2454790.2674 + 0.075503E$.^c Number of points used to determine the maximum.**Table 209.** Superhump maxima of DV Sco (2004).

E	max ^a	error	$O - C^b$	N^c
0	53274.2954	0.0011	-0.0027	211
7	53274.9935	0.0007	-0.0004	84
10	53275.2893	0.0012	-0.0028	225
17	53275.9922	0.0010	0.0044	61
20	53276.2884	0.0013	0.0024	214
30	53277.2821	0.0025	0.0021	220
50	53279.2655	0.0068	-0.0023	103
53	53279.5652	0.0037	-0.0008	149

^a BJD-2400000.^b Against $max = 2453274.2982 + 0.099393E$.^c Number of points used to determine the maximum.**Table 210.** Superhump maxima of DV Sco (2008).

E	max ^a	error	$O - C^b$	N^c
0	54713.2375	0.0010	-0.0058	240
1	54713.3385	0.0022	-0.0040	278
20	54715.2247	0.0021	-0.0054	127
21	54715.3316	0.0009	0.0021	140
28	54716.0314	0.0013	0.0065	186
50	54718.2417	0.0066	0.0313	181
51	54718.3210	0.0351	0.0112	213
61	54719.2735	0.0032	-0.0297	212
70	54720.1956	0.0107	-0.0017	119
71	54720.2922	0.0132	-0.0044	142

^a BJD-2400000.^b Against $max = 2454713.2432 + 0.099344E$.^c Number of points used to determine the maximum.6.110. *MM Scorpii*

The updated times of superhump maxima from the 2002 data (Kato et al. 2004a) are listed in table 211. The observation was likely performed in the middle of the stage B, after 5 d of the visual maximum (Kato et al. 2004a).

Table 211. Superhump maxima of MM Sco (2002).

E	max ^a	error	$O - C^b$	N^c
0	52528.2351	0.0008	-0.0002	51
1	52528.2954	0.0011	-0.0012	66
2	52528.3599	0.0013	0.0020	61
16	52529.2160	0.0010	-0.0005	59
17	52529.2793	0.0009	0.0015	67
18	52529.3379	0.0009	-0.0013	68
19	52529.3990	0.0016	-0.0015	65
25	52529.7697	0.0008	0.0013	143

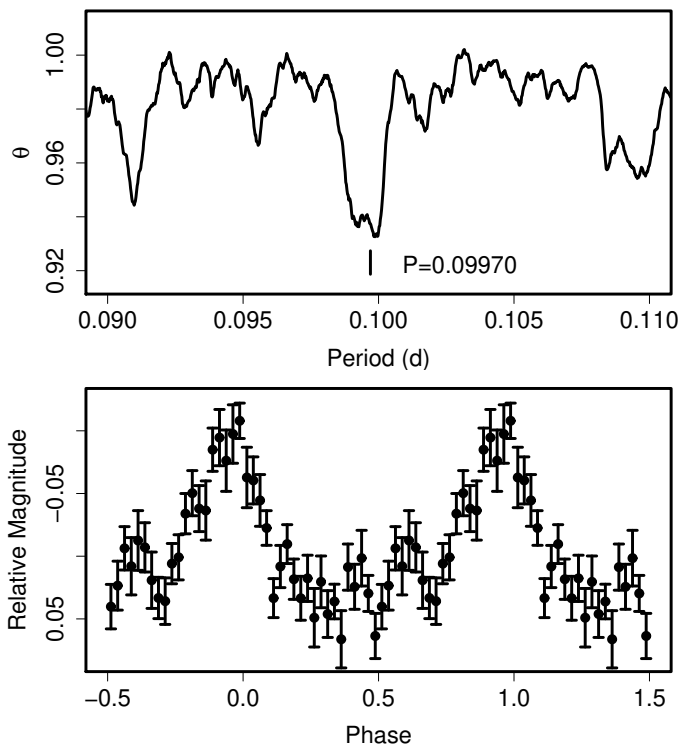
^a BJD-2400000.^b Against $max = 2452528.2353 + 0.061323E$.^c Number of points used to determine the maximum.**Fig. 123.** Superhumps in DV Sco (2004). (Upper): PDM analysis. (Lower): Phase-averaged profile.

Table 212. Superhump maxima of NY Ser (1996).

E	max ^a	error	$O - C^b$	N^c
0	50195.2477	0.0029	-0.0103	69
18	50197.2027	0.0006	0.0145	71
27	50198.1604	0.0007	0.0071	75
28	50198.2642	0.0008	0.0037	59
37	50199.2107	0.0014	-0.0150	31

^a BJD-2400000.^b Against $max = 2450195.2580 + 0.107235E$.^c Number of points used to determine the maximum.

6.111. NY Serpentis

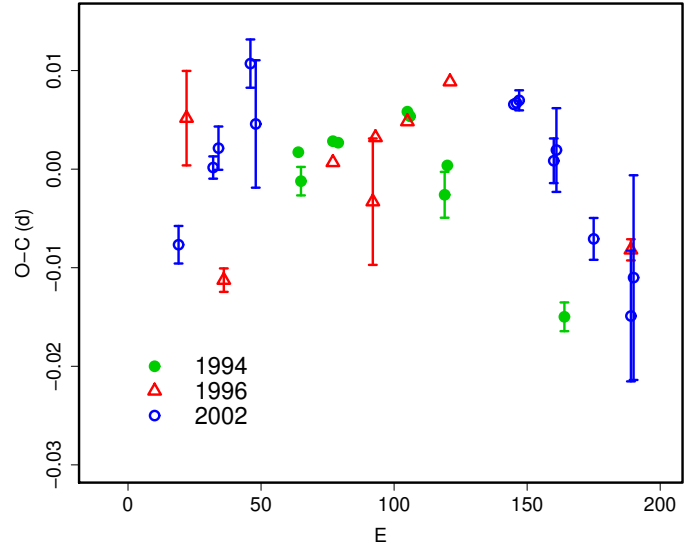
We used the data in Nogami et al. (1998b) to determine the refined times of superhump maxima (table 212). Although the initial maximum was recorded during the developmental stage of superhumps, we adopted $P_{\text{dot}} = -144(8) \times 10^{-5}$ using all maxima times because the effect of the evolutionary stage is relatively small in systems with strongly negative P_{dot} 's (cf. UV Gem: subsection 6.64). Excluding the initial maximum, the P_{dot} amounted to $-117(27) \times 10^{-5}$. More observations are needed to see if such an extreme period variation is indeed present during the entire superoutburst.

6.112. RZ Sagittae

Kato (1996a) reported on the 1994 superoutburst, giving $P_{\text{dot}} = -10(2) \times 10^{-5}$. Table 213 gives refined and newly measured times of superhump maxima from the data used in Kato (1996a). The refined global P_{dot} corresponds to $-11.0(2.2) \times 10^{-5}$. The 1996 superoutburst was observed by us and by Semeniuk et al. (1997a). A combined list of superhump maxima is given in table 214. The global P_{dot} corresponds to $-6.9(1.6) \times 10^{-5}$. The difference in P_{dot} from Semeniuk et al. (1997a) was probably because they only observed the late stage of the superoutburst. There is an indication of a transition from a longer to a shorter period (already somewhat evident on the figure 4 in Semeniuk et al. 1997a), corresponding to a stage B-C transition. If we restrict the fit to $E < 100$, we obtain $P_{\text{dot}} = +0.6(5.1) \times 10^{-5}$ indicating a relatively constant superhump period. This phenomenon may be analogous to the one observed in TT Boo (Olech et al. 2004a), another SU UMa-type dwarf nova with a relatively long superhump period and long superoutbursts (see also FQ Mon, subsection 6.88). We also observed the 2002 superoutburst (table 215). Although the coverage was not sufficient (our observation covered the early to middle stage of the superoutburst), we obtained the global $P_{\text{dot}} = -4.9(3.0) \times 10^{-5}$. A comparison of $O - C$ diagrams between different superoutbursts is shown in figure 124. The 1994 superoutburst may have had a shorter stage B than in other superoutbursts.

6.113. WZ Sagittae

Several authors reported on the 2001 superoutburst of WZ Sge (Patterson et al. 2002; Ishioka et al. 2002). We

**Fig. 124.** Comparison of $O - C$ diagrams of RZ Sge between different superoutbursts. A period of 0.07045 d was used to draw this figure. Approximate cycle counts (E) after the start of the superoutburst were used. The 1994 superoutburst probably had a shorter stage B.**Table 213.** Superhump maxima of RZ Sge (1994).

E	max ^a	error	$O - C^b$	N^c
0	49576.0726	0.0008	-0.0029	42
1	49576.1401	0.0014	-0.0057	30
13	49576.9896	0.0008	-0.0001	58
15	49577.1303	0.0008	-0.0000	50
41	49578.9652	0.0005	0.0065	91
42	49579.0351	0.0004	0.0061	90
55	49579.9430	0.0023	-0.0001	52
56	49580.0165	0.0005	0.0030	77
100	49583.1009	0.0015	-0.0067	29

^a BJD-2400000.^b Against $max = 2449576.0755 + 0.070322E$.^c Number of points used to determine the maximum.

Table 214. Superhump maxima of RZ Sge (1996).

E	max ^a	error	$O - C^b$	N^c
0	50302.2160	0.0012	-0.0158	143
41	50305.1164	0.0004	-0.0012	102
45	50305.3974	-	-0.0018	S
46	50305.4671	-	-0.0025	S
47	50305.5375	-	-0.0024	S
56	50306.1692	0.0064	-0.0042	37
57	50306.2462	0.0008	0.0024	53
59	50306.3829	-	-0.0017	S
69	50307.0932	0.0005	0.0047	102
74	50307.4413	-	0.0009	S
85	50308.2244	0.0009	0.0098	109
87	50308.3618	-	0.0064	S
88	50308.4345	-	0.0087	S
103	50309.4890	-	0.0074	S
116	50310.4030	-	0.0064	S
117	50310.4726	-	0.0056	S
118	50310.5431	-	0.0058	S
130	50311.3829	-	0.0009	S
132	50311.5233	-	0.0006	S
153	50312.9980	0.0011	-0.0029	101
160	50313.4833	-	-0.0103	S
173	50314.3914	-	-0.0172	S

^a BJD-2400000.^b Against $max = 2450302.2318 + 0.070386E$.^c Number of points used to determine the maximum.
S refers to Semeniuk et al. (1997a).**Table 215.** Superhump maxima of RZ Sge (2002).

E	max ^a	error	$O - C^b$	N^c
0	52549.0368	0.0019	-0.0114	48
13	52549.9604	0.0011	-0.0031	131
15	52550.1033	0.0022	-0.0010	110
27	52550.9573	0.0024	0.0080	65
29	52551.0921	0.0065	0.0020	107
126	52557.9277	0.0007	0.0077	111
127	52557.9983	0.0008	0.0079	125
128	52558.0690	0.0010	0.0082	96
141	52558.9787	0.0023	0.0026	106
142	52559.0503	0.0042	0.0037	84
156	52560.0275	0.0021	-0.0047	133
170	52561.0060	0.0066	-0.0120	28
171	52561.0804	0.0104	-0.0081	11

^a BJD-2400000.^b Against $max = 2452549.0482 + 0.070411E$.^c Number of points used to determine the maximum.

used the data used in Ishioka et al. (2002) to determine superhump maxima. We deal with ordinary superhumps and give only a representative figure of early superhumps (figure 125).

We extracted times of superhump maxima after subtracting the general trend of the outburst and subtracting averaged orbital variation as in V455 And. The interval for averaging the orbital variation was 4–6 d during the superoutburst plateau and 1 d for the final stage of early superhumps and the final stage of the superoutburst plateau.

The tables of maxima are separately given for the earlier half before double humps became apparent (table 216) and the final stage when newly arising humps became apparent (table 217) because different base periods were used for calculating the $O - C$'s. The humps having orbital phases $0.6 < \text{phase} < 1.0$ in the latter table can be attributed to orbital humps. The situation can be clearly seen on the combined $O - C$ diagram during this stage and the early part the subsequent rebrightening phase (figure 127). It is evident from the $O - C$ diagram that our method is less affected by the orbital (eclipse) feature than in Patterson et al. (2002), enabling a firmer estimate of the period variation. The interval $E \leq 27$ showed an early-stage transition with a longer period (stage A). Since the orbital phases of these humps do not coincide either of two maxima of early superhumps, we regard them as genuine superhumps. The mean period was 0.05839(6) d.

The mean P_{SH} and P_{dot} for $27 \leq E \leq 177$ ¹⁸ (stage B) was 0.057204(5) d and $P_{\text{dot}} = +2.0(0.4) \times 10^{-5}$. During the last stage of the superoutburst plateau, rapid fading and the dip, the orbital humps dominated (see figure 127). A new series of superhumps with a longer period emerged (filled circles in figure 127 for $E > 200$) during the rapid fading and smoothly evolved into superhumps during the rebrightening phase. The mean period and period derivative of these superhumps for $200 \leq E \leq 400$ were 0.057488(14) d and $P_{\text{dot}} = +5.0(0.7) \times 10^{-5}$.

We also analyzed the rebrightening phase. The analysis follows the similar manner as in SDSS J0804 (Kato et al. 2009). The phase-averaged light curve (figure 128) closely resembles that of SDSS J0804 and is in good agreement with the analysis by Patterson et al. (2002). After subtracting orbital light curves averaged over three days, we extracted the times of measured maxima (table 219). The P_{SH} was 0.057501(12) d for $E \leq 199$ and was 0.057305(11) d for $E \geq 200$ (see figure 129). These periods are 0.52(2) % and 0.18(2) % longer than the mean P_{SH} during the main superoutburst, respectively. These long-period superhumps correspond to long-period late(-stage) superhumps reported in Kato et al. (2008).

During the post-superoutburst stage, although eclipses and orbital humps were prominent (figure 130), overlapping superhumps persisted at least for ~ 600 cycles (~ 30 d). The times of maxima, determined after subtracting the orbital modulations, during the post-superoutburst

¹⁸ The epochs $E > 165$ in this paragraph denotes maxima in table 217. The epoch $E = 0$ in table 217 corresponds to $E = 169$.

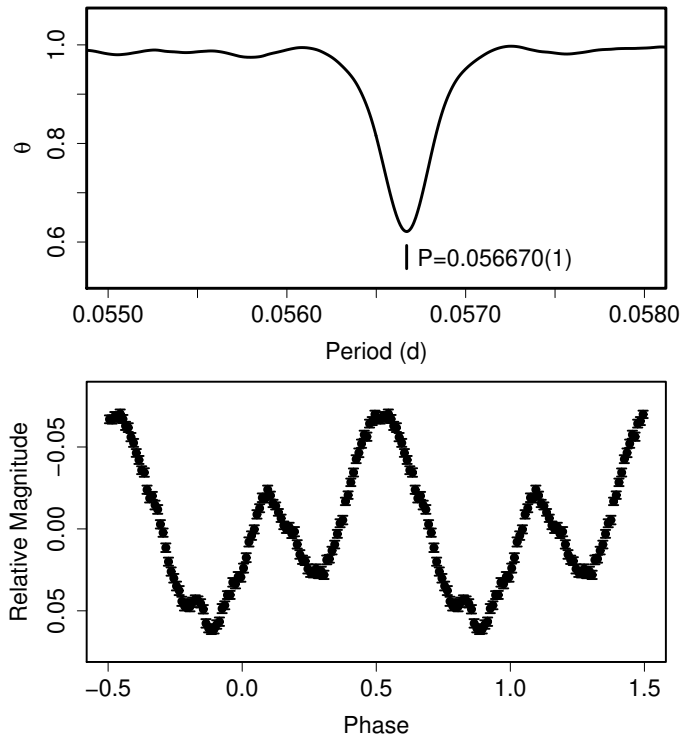


Fig. 125. Early superhumps in WZ Sge (2001). (Upper): PDM analysis. (Lower): Phase-averaged profile. The phase zero corresponds to eclipses in quiescence.

stage are listed in table 220. The interval for averaging the orbital variation was 10 d. For $E \leq 598$, the mean P_{SH} and P_{dot} were 0.057351(3) d and $+0.5(0.1) \times 10^{-5}$. This period is 0.25(1) % longer than the mean P_{SH} during the main superoutburst. There was some indication of the persisting superhumps after $E = 848$ with a different period before $E = 598$.

The overall $O - C$ behavior during the entire course of the superoutburst is shown in figure 131. The behavior is remarkably similar to GW Lib (subsection 5.1). In WZ Sge, a disturbance in the $O - C$ diagram also appeared during the rapid fading stage and subsequent “dip” phase. During the rebrightening and post-superoutburst stages, the superhump period lengthened in a similar way to GW Lib. The $O - C$ diagram showed a slightly positive deviation from this overall trend during the rebrightening phase. The $O - C$ behavior after the rebrightening phase appears to be a natural extension of the stage B superhumps, as in GW Lib.

The times of superhump maxima during the 1978 superoutburst are listed in table 221. The times were taken from literature except for Heiser, Henry (1979), for which we measured the maxima from individual observations. We obtained $P_{dot} = +0.4(0.8) \times 10^{-5}$.

6.114. *AW Sagittae*

This dwarf nova has long been known since its early discovery (Wolf, Wolf 1906). The SU UMA-type nature was established during the 2000 superoutburst (vsnet-

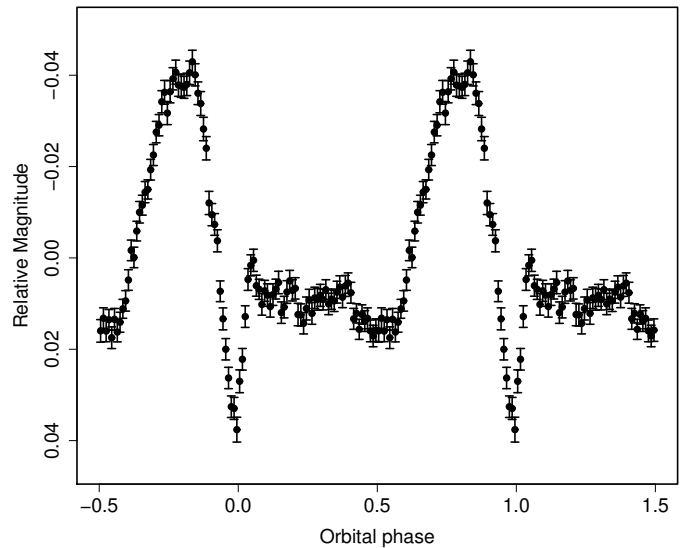


Fig. 128. Orbital light curve of WZ Sge during the rebrightening phase of the 2001 superoutburst (BJD 2452141–2452167)

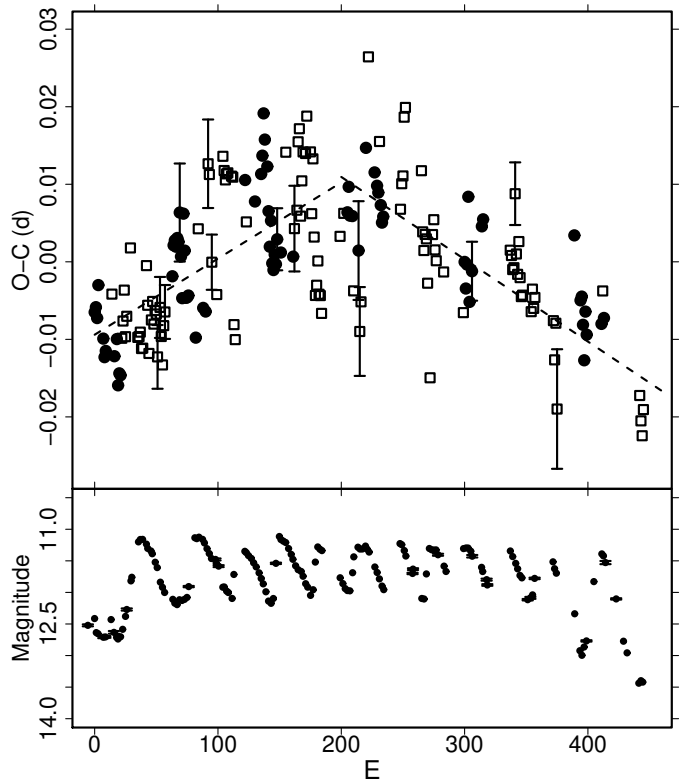


Fig. 129. $O - C$ of humps during the rebrightening phase of WZ Sge (2001). (Upper): $O - C$ diagram. Filled squares and open squares represent superhumps and humps coinciding with orbital humps, respectively. Two dashes represent the superhump periods of 0.057501(12) d and 0.057305(11) d. (Lower): Light curve.

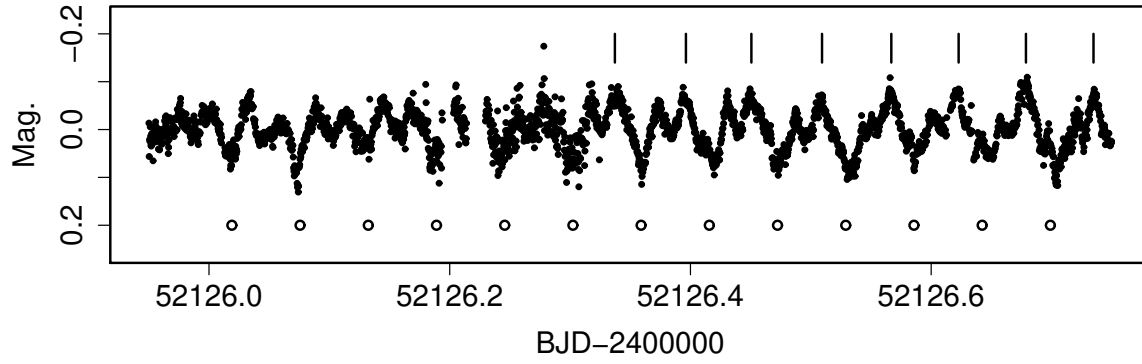


Fig. 126. Transition from early superhumps to ordinary superhumps in WZ Sge (2001). The open circles represent minima of early superhumps. The stage A superhumps (ticks) smoothly developed from one of two peaks of early superhumps.

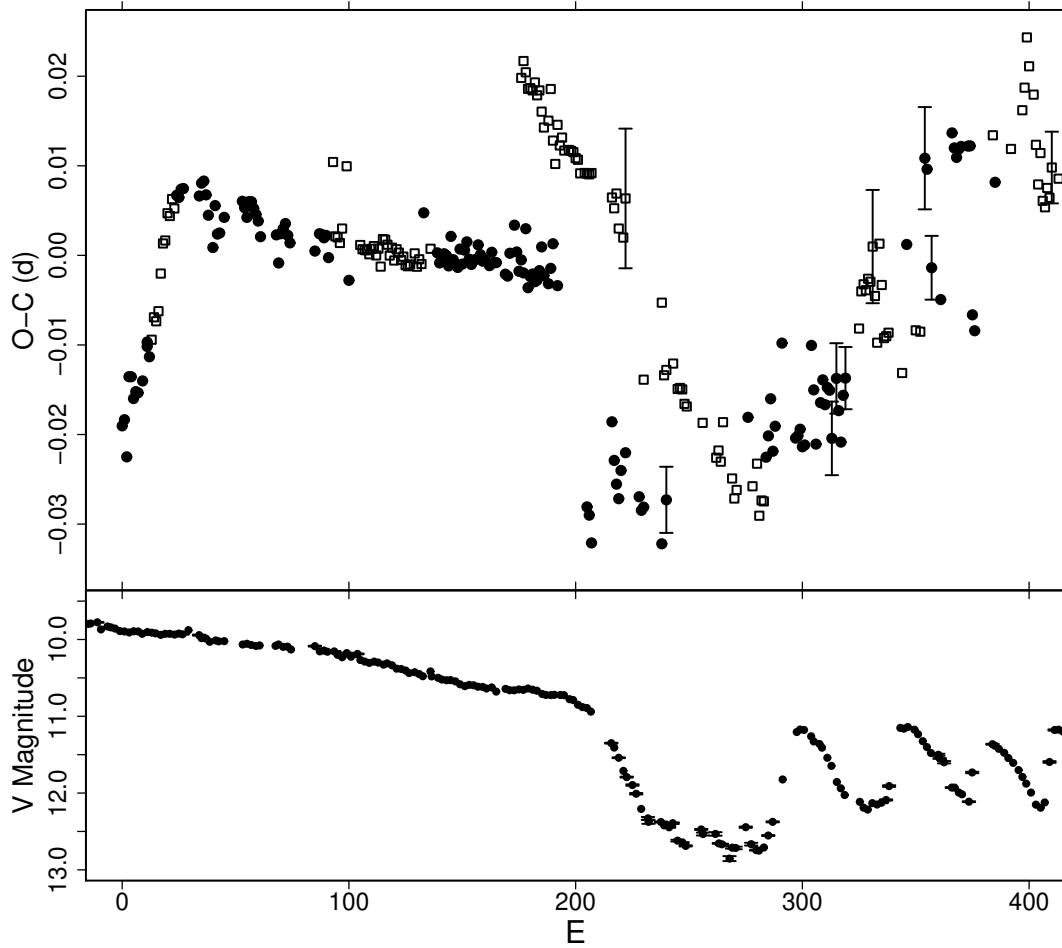


Fig. 127. $O - C$ variation in WZ Sge (2001). (Upper) $O - C$. Open squares indicate humps coinciding with the phase of orbital humps. Filled circles are humps outside the phase of orbital humps. We used a period of 0.057244 d for calculating the $O - C$'s. The evolution of the $O - C$ diagram is remarkably similar to that of GW Lib (figure 33). (Lower) Light curve.

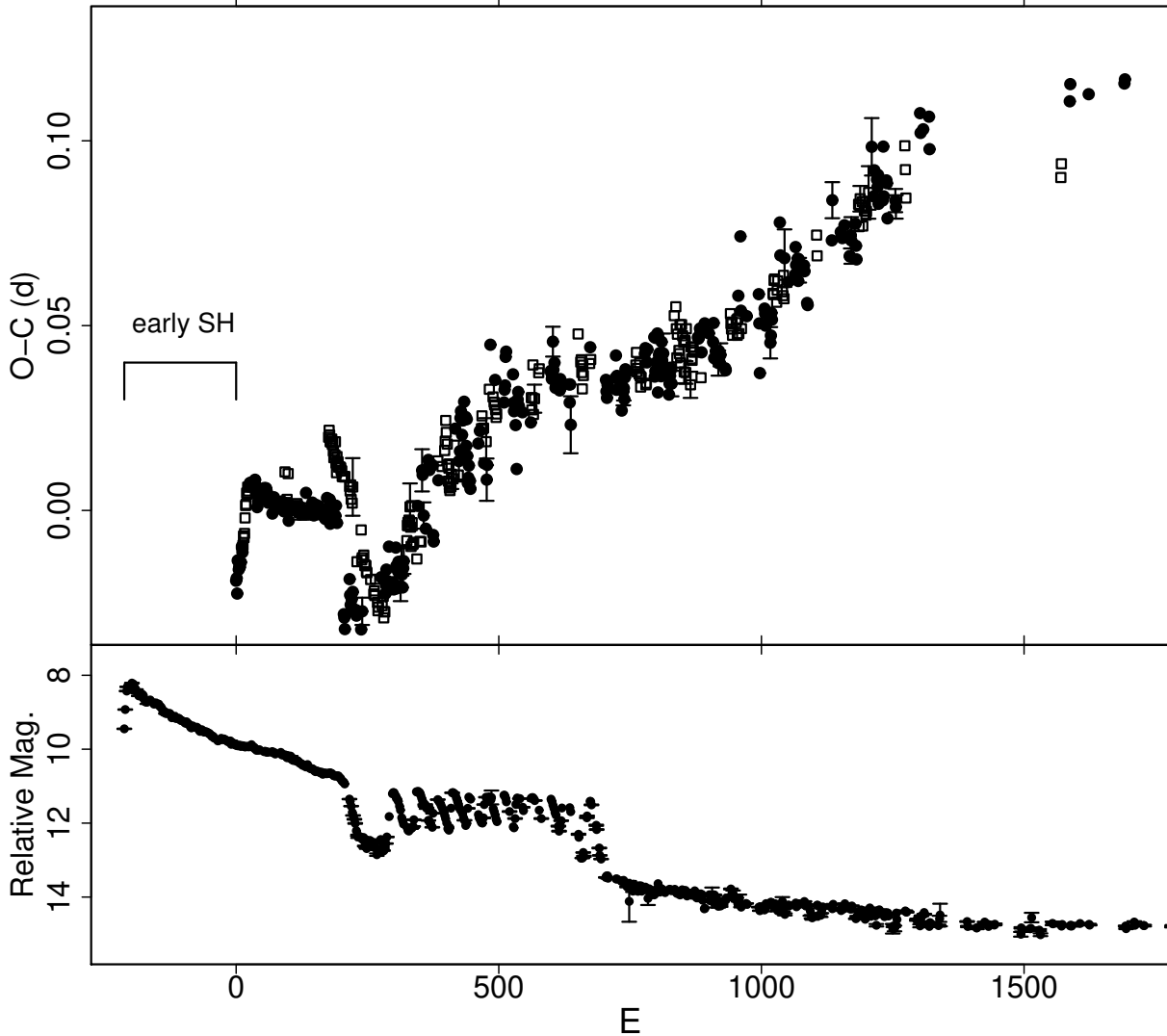


Fig. 131. $O - C$ variation in WZ Sge (2001). (Upper) $O - C$. Open squares and filled circles represent superhumps and humps coinciding with orbital humps, respectively. We used a period of 0.057244 d for calculating the $O - C$'s. The global evolution of the $O - C$ diagram is remarkably similar to that of GW Lib (figure 33). (Lower) Light curve.

alert 5111, 5112, 5114). Lloyd (2007) summarized the history of outbursts of this object and Lloyd, Pickard (2008) presented observations during the 2007 normal outburst. We analyzed the available AAVSO observation of the 2006 superoutburst, a part of the data reported in Shears et al. (2008e). The observation apparently covered the middle-to-late stage of the superoutburst. The times of superhump maxima are listed in table 223. The mean P_{SH} with the PDM method was 0.07449(2) d (figure 132) and $P_{dot} = -7.9(6.4) \times 10^{-5}$, which may be a result of combination of stage B and C superhumps. We also give times of superhump maxima during the 2000 superoutburst (table 222). The mean mean P_{SH} with the PDM method was 0.07473(8) d.

6.115. V551 Sagittarii

V551 Sgr has long been suspected to be a candidate WZ Sge-type dwarf nova (cf. Downes 1990). During the

2003 superoutburst, we managed to obtain excellent time-series photometry. A PDM analysis has yielded a mean period of 0.06757(1) d (figure 133). The times of superhump maxima are listed in table 224. The $O - C$ diagram clearly shows a positive period derivative except for the earliest part (figure 134). Excluding $E = 0$ (stage A), we obtained $P_{dot} = +6.0(1.5) \times 10^{-5}$. There were no indication of early superhumps. Together with the relatively long superhump period, and a likely supercycle of ~ 1 yr, the object is likely an SU UMa-type dwarf nova similar to UV Per (subsection 6.100) and QY Per (subsection 6.103), rather than a genuine WZ Sge-type object.

The 2004 superoutburst was less sufficiently observed (table 225). The P_{dot} was likely positive and apparently recorded during the stage B (figure 135), but we did not attempt to measure the P_{dot} because of the short baseline.

Table 216. Superhump maxima of WZ Sge (2001).

E	\max^a	error	$O - C^b$	phase ^c	N^d
0	52126.3302	0.0013	-0.0163	0.32	361
1	52126.3881	0.0009	-0.0157	0.34	245
2	52126.4412	0.0011	-0.0199	0.27	245
3	52126.5074	0.0009	-0.0109	0.44	245
4	52126.5646	0.0004	-0.0110	0.45	300
5	52126.6194	0.0007	-0.0134	0.42	109
6	52126.6775	0.0005	-0.0127	0.44	164
7	52126.7346	0.0005	-0.0128	0.45	315
9	52126.8504	0.0003	-0.0116	0.49	337
11	52126.9692	0.0003	-0.0073	0.59	523
11	52126.9687	0.0002	-0.0078	0.58	536
12	52127.0248	0.0002	-0.0090	0.57	460
13	52127.0840	0.0003	-0.0071	0.61	463
14	52127.1437	0.0002	-0.0046	0.67	465
15	52127.2005	0.0003	-0.0051	0.67	361
16	52127.2589	0.0010	-0.0040	0.70	208
17	52127.3203	0.0005	0.0002	0.78	304
18	52127.3809	0.0003	0.0035	0.85	311
19	52127.4385	0.0002	0.0038	0.87	312
20	52127.4988	0.0002	0.0068	0.93	261
21	52127.5557	0.0003	0.0065	0.94	298
22	52127.6149	0.0004	0.0083	0.98	185
23	52127.6710	0.0004	0.0072	0.97	214
24	52127.7298	0.0002	0.0087	0.01	273
25	52127.7868	0.0002	0.0084	0.01	262
26	52127.8449	0.0003	0.0093	0.04	256
27	52127.9022	0.0009	0.0093	0.05	71
34	52128.3021	0.0002	0.0083	0.10	183
35	52128.3608	0.0002	0.0097	0.14	237
36	52128.4183	0.0003	0.0099	0.15	236
37	52128.4740	0.0003	0.0083	0.13	236
38	52128.5290	0.0005	0.0060	0.10	237
40	52128.6398	0.0010	0.0024	0.06	59
41	52128.7018	0.0004	0.0070	0.15	298
42	52128.7558	0.0004	0.0038	0.11	257
43	52128.8132	0.0007	0.0039	0.12	116
45	52128.9294	0.0003	0.0056	0.17	153
53	52129.3892	0.0002	0.0071	0.28	224
54	52129.4457	0.0002	0.0064	0.28	224
55	52129.5019	0.0003	0.0053	0.27	224
56	52129.5609	0.0002	0.0070	0.31	292
57	52129.6181	0.0005	0.0070	0.32	106
58	52129.6746	0.0003	0.0062	0.31	219
59	52129.7312	0.0002	0.0055	0.31	222
60	52129.7877	0.0003	0.0047	0.31	213
61	52129.8432	0.0003	0.0029	0.29	138
68	52130.2441	0.0002	0.0029	0.36	377
69	52130.2982	0.0005	-0.0002	0.31	187
70	52130.3587	0.0002	0.0030	0.38	238
71	52130.4165	0.0003	0.0035	0.40	238
72	52130.4743	0.0002	0.0041	0.42	238

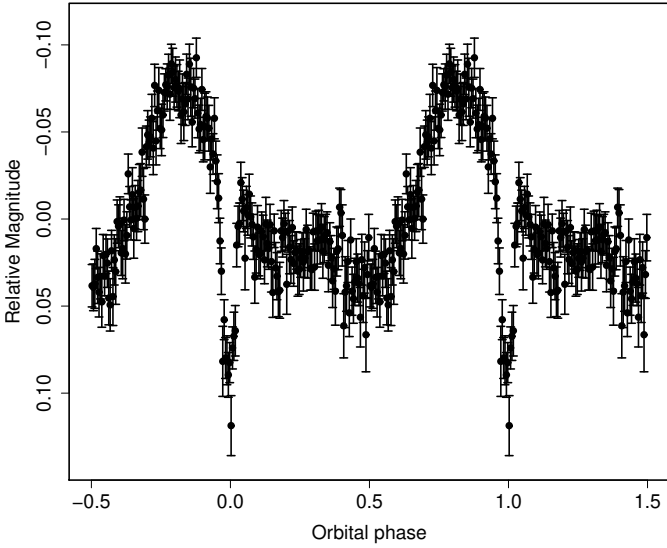
^a BJD-2400000.^b Against $\max = 2452126.3465 + 0.057274E$.^c Orbital phase.^d Number of points used to determine the maximum.

Fig. 130. Orbital light curve of WZ Sge during the post-superoutburst stage (BJD 2452167–2452267)

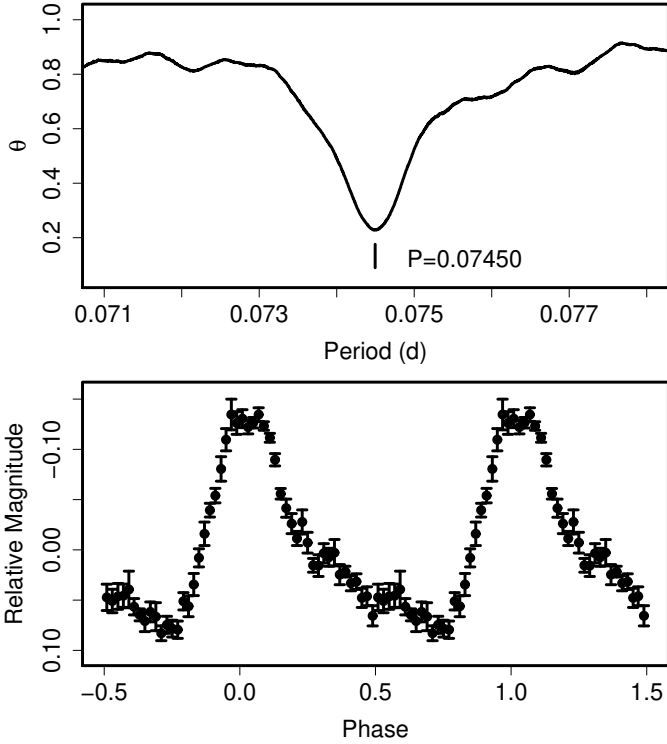


Fig. 132. Superhumps in AW Sge (2006). (Upper): PDM analysis. (Lower): Phase-averaged profile.

Table 216. Superhump maxima of WZ Sge (2001) (continued).

E	max	error	$O - C$	phase	N
73	52130.5303	0.0002	0.0027	0.41	238
74	52130.5866	0.0004	0.0019	0.40	180
85	52131.2154	0.0005	0.0006	0.49	209
87	52131.3318	0.0004	0.0025	0.55	230
88	52131.3890	0.0004	0.0024	0.56	245
89	52131.4459	0.0004	0.0020	0.56	361
90	52131.5034	0.0004	0.0022	0.57	320
91	52131.5582	0.0003	-0.0003	0.54	174
93	52131.6833	0.0004	0.0103	0.75	99
94	52131.7323	0.0007	0.0020	0.61	153
95	52131.7894	0.0005	0.0018	0.62	154
96	52131.8460	0.0004	0.0012	0.62	152
97	52131.9049	0.0005	0.0028	0.66	153
99	52132.0263	0.0005	0.0097	0.80	184
100	52132.0708	0.0010	-0.0031	0.58	100
105	52132.3610	0.0003	0.0007	0.70	241
106	52132.4177	0.0002	0.0002	0.70	332
107	52132.4749	0.0003	0.0001	0.71	296
108	52132.5321	0.0002	0.0000	0.72	344
109	52132.5889	0.0002	-0.0005	0.72	520
110	52132.6468	0.0003	0.0001	0.74	268
111	52132.7043	0.0002	0.0004	0.76	345
112	52132.7605	0.0002	-0.0007	0.75	378
113	52132.8185	0.0003	0.0000	0.77	355
114	52132.8738	0.0004	-0.0020	0.75	197
115	52132.9341	0.0005	0.0010	0.81	248
116	52132.9913	0.0002	0.0009	0.82	505
117	52133.0479	0.0002	0.0004	0.82	496
118	52133.1040	0.0006	-0.0009	0.81	303
119	52133.1621	0.0002	-0.0000	0.83	510
120	52133.2179	0.0002	-0.0015	0.82	516
121	52133.2764	0.0005	-0.0003	0.85	576
122	52133.3333	0.0005	-0.0007	0.85	465
123	52133.3897	0.0003	-0.0015	0.85	369
124	52133.4473	0.0002	-0.0012	0.87	370
125	52133.5036	0.0003	-0.0022	0.86	171
126	52133.5607	0.0002	-0.0023	0.87	327
127	52133.6182	0.0003	-0.0022	0.88	209
129	52133.7339	0.0003	-0.0010	0.92	150
130	52133.7897	0.0003	-0.0025	0.91	151
131	52133.8477	0.0003	-0.0017	0.93	152
132	52133.9044	0.0003	-0.0023	0.93	152
133	52133.9674	0.0008	0.0034	0.04	90
136	52134.1351	0.0004	-0.0007	1.00	306
139	52134.3064	0.0008	-0.0012	0.02	253
140	52134.3625	0.0003	-0.0024	0.01	242
141	52134.4203	0.0002	-0.0019	0.03	242
142	52134.4780	0.0002	-0.0014	0.05	242
143	52134.5351	0.0001	-0.0017	0.05	226
144	52134.5912	0.0003	-0.0028	0.04	317
145	52134.6517	0.0008	0.0004	0.11	127
146	52134.7063	0.0004	-0.0022	0.08	205
147	52134.7631	0.0005	-0.0028	0.08	229
148	52134.8200	0.0005	-0.0031	0.08	172

Table 216. Superhump maxima of WZ Sge (2001) (continued).

E	max	error	$O - C$	phase	N
149	52134.8793	0.0006	-0.0011	0.13	111
150	52134.9348	0.0004	-0.0028	0.11	143
151	52134.9936	0.0008	-0.0013	0.14	373
152	52135.0518	0.0005	-0.0004	0.17	397
153	52135.1071	0.0004	-0.0024	0.15	372
154	52135.1638	0.0003	-0.0030	0.15	407
155	52135.2215	0.0003	-0.0025	0.16	386
156	52135.2788	0.0005	-0.0025	0.17	427
157	52135.3377	0.0005	-0.0009	0.21	392
158	52135.3938	0.0003	-0.0020	0.20	321
159	52135.4504	0.0003	-0.0028	0.20	300
160	52135.5078	0.0003	-0.0026	0.21	278
162	52135.6216	0.0011	-0.0034	0.22	76
163	52135.6803	0.0008	-0.0019	0.26	69
164	52135.7364	0.0007	-0.0031	0.25	76
165	52135.7937	0.0007	-0.0031	0.26	75

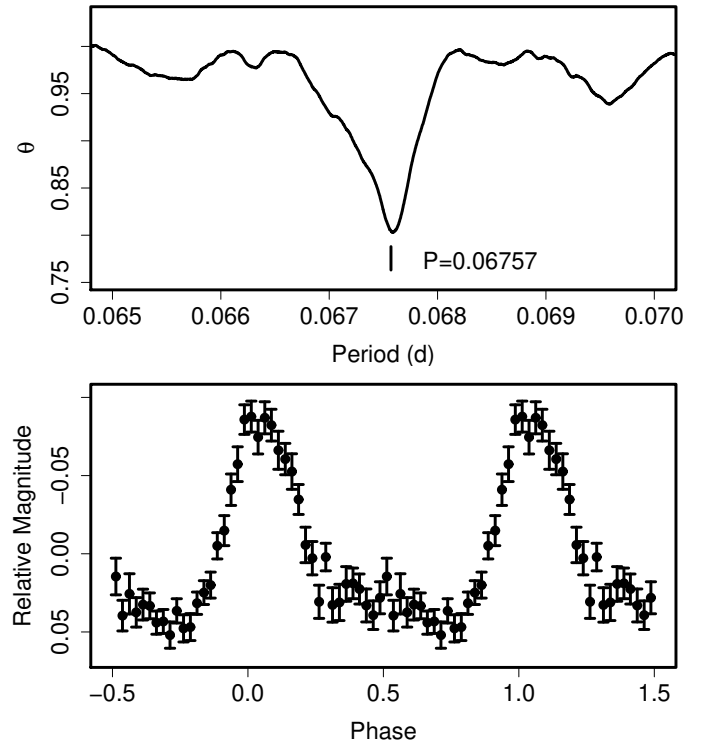
**Fig. 133.** Superhumps in V551 Sgr (2003). (Upper): PDM analysis. (Lower): Phase-averaged profile.

Table 217. Hump Maxima of WZ Sge during the end stage of the superoutburst plateau (2001).

E	\max^a	error	$O - C^b$	phase ^c	N^d
0	52136.0213	0.0002	-0.0144	0.27	235
1	52136.0784	0.0002	-0.0142	0.28	241
2	52136.1382	0.0010	-0.0113	0.33	203
4	52136.2558	0.0017	-0.0073	0.41	48
5	52136.3100	0.0009	-0.0099	0.37	230
6	52136.3651	0.0005	-0.0116	0.34	164
7	52136.4236	0.0003	-0.0100	0.37	176
7	52136.4440	0.0003	0.0104	0.73	174
8	52136.4794	0.0003	-0.0110	0.35	178
8	52136.5031	0.0002	0.0126	0.77	170
9	52136.5416	0.0006	-0.0057	0.45	100
9	52136.5591	0.0004	0.0118	0.76	120
10	52136.5923	0.0011	-0.0119	0.34	245
10	52136.6145	0.0004	0.0103	0.74	153
11	52136.6507	0.0006	-0.0102	0.38	122
11	52136.6718	0.0004	0.0108	0.75	137
12	52136.7083	0.0007	-0.0095	0.39	126
12	52136.7288	0.0004	0.0110	0.75	174
13	52136.7647	0.0005	-0.0100	0.39	165
13	52136.7869	0.0004	0.0123	0.78	154
14	52136.8221	0.0002	-0.0094	0.40	195
14	52136.8427	0.0003	0.0112	0.76	158
15	52136.8804	0.0006	-0.0079	0.43	72
15	52136.9005	0.0004	0.0122	0.78	76
16	52136.9403	0.0016	-0.0049	0.48	90
16	52136.9554	0.0004	0.0102	0.75	277
17	52136.9943	0.0006	-0.0077	0.44	201
17	52137.0109	0.0008	0.0089	0.73	147
19	52137.1079	0.0007	-0.0078	0.44	167
19	52137.1261	0.0002	0.0104	0.76	199
20	52137.1669	0.0005	-0.0056	0.48	197
20	52137.1869	0.0013	0.0144	0.83	198
21	52137.2269	0.0008	-0.0025	0.54	202
21	52137.2384	0.0004	0.0090	0.74	204
22	52137.2930	0.0015	0.0068	0.71	89
23	52137.3367	0.0005	-0.0064	0.48	35
23	52137.3546	0.0002	0.0116	0.79	41
24	52137.4096	0.0004	0.0097	0.76	46
25	52137.4677	0.0001	0.0110	0.79	170
26	52137.5235	0.0001	0.0099	0.77	235
28	52137.6380	0.0003	0.0108	0.79	98
29	52137.6952	0.0002	0.0111	0.80	133
30	52137.7523	0.0003	0.0114	0.81	70
31	52137.8089	0.0004	0.0111	0.81	74
32	52137.8659	0.0004	0.0113	0.81	80
33	52137.9216	0.0003	0.0102	0.80	83
35	52138.0362	0.0002	0.0111	0.82	335
36	52138.0561	0.0003	-0.0258	0.17	388
36	52138.0934	0.0002	0.0114	0.82	309
37	52138.1125	0.0010	-0.0263	0.16	311
37	52138.1505	0.0001	0.0117	0.83	390

^a BJD-2400000.

^b Against $\max = 2452136.0357 + 0.056839E$.

^c Orbital phase.

^d Number of points used to determine the maximum.

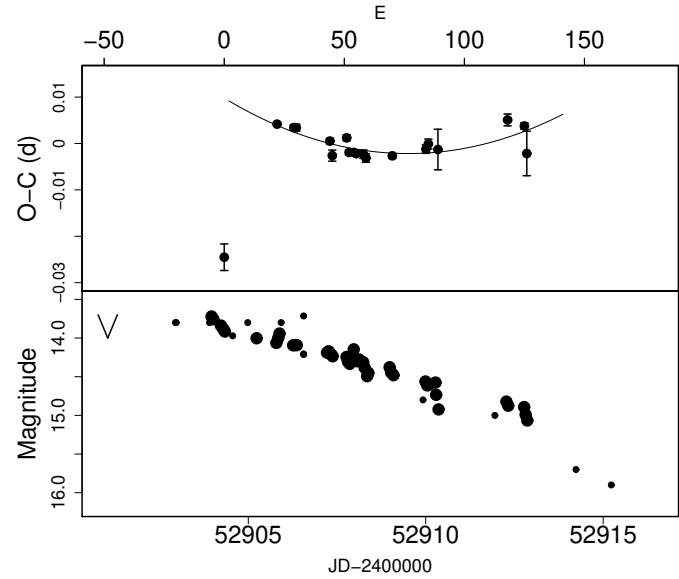


Fig. 134. $O - C$ of superhumps V551 Sgr (2003). (Upper): $O - C$ diagram. The curve represents a quadratic fit to $E \geq 22$. (Lower): Light curve. Large dots represent CCD observations. Small dots and a “V” mark represent visual observations and a upper limit, respectively.

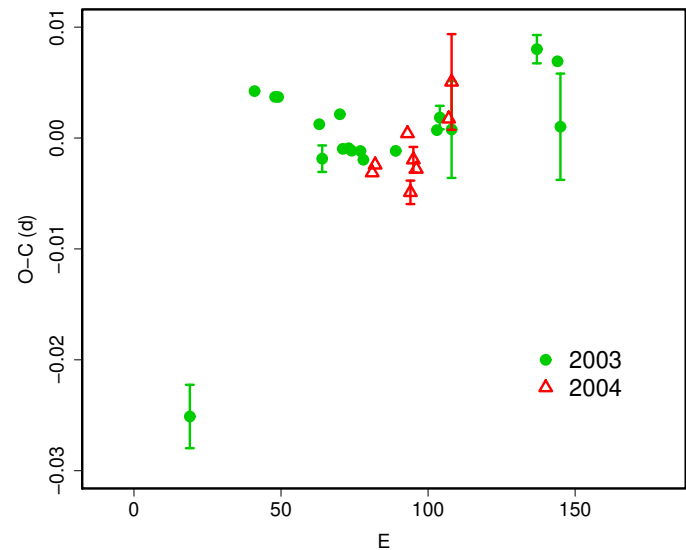


Fig. 135. Comparison of $O - C$ diagrams of V551 Sgr between different superoutbursts. A period of 0.06757 d was used to draw this figure. Approximate cycle counts (E) after the start of the superoutburst were used.

Table 218. Hump Maxima of WZ Sge during the end stage of the superoutburst plateau (2001).

E	max	error	$O - C$	phase	N
38	52138.1666	0.0020	-0.0290	0.12	349
38	52138.2079	0.0003	0.0123	0.85	257
47	52138.6953	0.0004	-0.0118	0.44	34
47	52138.7204	0.0021	0.0132	0.89	35
48	52138.7483	0.0005	-0.0157	0.38	35
48	52138.7764	0.0011	0.0124	0.87	35
49	52138.8029	0.0011	-0.0180	0.34	35
49	52138.8353	0.0007	0.0145	0.91	35
50	52138.8585	0.0014	-0.0192	0.32	35
50	52138.8886	0.0008	0.0110	0.85	36
51	52138.9189	0.0021	-0.0156	0.39	35
52	52139.0021	0.0029	0.0108	0.86	211
53	52139.0353	0.0005	-0.0129	0.44	202
53	52139.0637	0.0078	0.0155	0.94	193
59	52139.3739	0.0015	-0.0153	0.41	29
60	52139.4296	0.0003	-0.0164	0.40	83
61	52139.4872	0.0008	-0.0157	0.41	57
61	52139.5014	0.0004	-0.0015	0.66	48
69	52139.9411	0.0008	-0.0165	0.42	130
69	52139.9680	0.0028	0.0104	0.89	137
70	52140.0171	0.0007	0.0027	0.76	129
71	52140.0605	0.0037	-0.0108	0.53	105
71	52140.0750	0.0012	0.0037	0.78	96
74	52140.2474	0.0005	0.0056	0.82	94
76	52140.3591	0.0003	0.0036	0.79	27
77	52140.4164	0.0007	0.0041	0.80	20
78	52140.4735	0.0004	0.0044	0.81	58
79	52140.5291	0.0003	0.0031	0.79	60
80	52140.5861	0.0004	0.0033	0.80	36
87	52140.9850	0.0005	0.0043	0.83	181

6.116. *V4140 Sagittarii*

V4140 Sgr has long been known as an eclipsing CV below the period gap (Jablonski, Steiner 1987). The dwarf nova-type nature was confirmed only very recently (Borges, Baptista 2005), who interpreted short outbursts of this object as being normal outbursts of an SU UMa-type dwarf nova. In 2004, B. Monard detected a long outburst and reported the existence of superhumps (vsnet-alert 8313). We analyzed the data obtained during this superoutburst. We used out-of-eclipse observations as was done for V2051 Oph, using the ephemeris by Baptista et al. (2003). The times of superhump maxima are listed in table 226 (the identification of maxima was slightly uncertain for $E \geq 149$ due to the faintness of the object and shortness of the observing runs). Disregarding the first night, when superhumps were likely still evolving, the $O - C$ diagram seems to be composed of the stage B with a positive P_{dot} ($16 \leq E \leq 70$), followed by a transition to the stage C with a shorter period. The P_{dot} for the stage B was $+25.3(12.3) \times 10^{-5}$. The mean superhump period from the first five nights (with better statistics) was 0.06324(3) d, yielding a fractional superhump excess of 2.9(1) %.

Table 219. Superhump maxima of WZ Sge during the re-brightening phase (2001).

E	max ^a	error	$O - C^b$	phase ^c	N^d
0	52141.3245	0.0006	-0.0065	0.82	34
1	52141.3826	0.0002	-0.0059	0.85	120
2	52141.4386	0.0003	-0.0073	0.84	167
3	52141.5002	0.0006	-0.0030	0.92	150
7	52141.7229	0.0005	-0.0099	0.85	44
8	52141.7779	0.0009	-0.0123	0.82	45
9	52141.8361	0.0006	-0.0115	0.85	44
14	52142.1305	0.0011	-0.0042	0.04	65
16	52142.2373	0.0015	-0.0122	0.92	25
18	52142.3543	0.0008	-0.0100	0.99	164
19	52142.4057	0.0011	-0.0159	0.90	229
20	52142.4646	0.0008	-0.0144	0.94	154
21	52142.5218	0.0008	-0.0146	0.94	152
22	52142.5840	0.0019	-0.0099	0.04	145
23	52142.6436	0.0011	-0.0076	0.09	59
24	52142.7050	0.0016	-0.0037	0.18	40
25	52142.7564	0.0009	-0.0097	0.08	59
26	52142.8164	0.0023	-0.0070	0.14	42
29	52142.9974	0.0014	0.0018	0.33	176
35	52143.3303	0.0009	-0.0097	0.21	42
36	52143.3878	0.0007	-0.0096	0.22	204
37	52143.4457	0.0009	-0.0091	0.24	454
38	52143.5010	0.0006	-0.0112	0.22	430
39	52143.5585	0.0008	-0.0111	0.23	518
42	52143.7413	0.0009	-0.0005	0.46	72
43	52143.7936	0.0007	-0.0056	0.38	105
44	52143.8448	0.0011	-0.0118	0.28	104
46	52143.9639	0.0004	-0.0075	0.38	868
47	52144.0237	0.0011	-0.0051	0.44	855
48	52144.0782	0.0014	-0.0080	0.40	158
49	52144.1373	0.0002	-0.0063	0.44	1393
50	52144.1943	0.0003	-0.0067	0.45	1065
51	52144.2461	0.0041	-0.0123	0.36	235
53	52144.3673	0.0039	-0.0059	0.50	51
54	52144.4210	0.0016	-0.0096	0.45	117
55	52144.4747	0.0012	-0.0133	0.39	134
56	52144.5372	0.0022	-0.0082	0.50	86
57	52144.5963	0.0035	-0.0065	0.54	88
63	52144.9453	0.0007	-0.0019	0.70	851
64	52145.0067	0.0002	0.0021	0.78	1155
65	52145.0648	0.0002	0.0028	0.80	1191
66	52145.1213	0.0002	0.0019	0.80	1177
67	52145.1799	0.0002	0.0031	0.83	1225
68	52145.2368	0.0006	0.0026	0.84	256
69	52145.2979	0.0063	0.0064	0.92	87
70	52145.3497	0.0005	0.0007	0.83	150
71	52145.4017	0.0015	-0.0047	0.75	43
72	52145.4700	0.0013	0.0062	0.95	104
73	52145.5226	0.0005	0.0014	0.88	89
74	52145.5739	0.0009	-0.0046	0.79	64
75	52145.6314	0.0013	-0.0046	0.80	35

^a BJD-2400000.^b Against $max = 2452141.3310 + 0.057399E$.^c Orbital phase.^d Number of points used to determine the maximum.

Table 219. Superhump maxima of WZ Sge during the re-brightening phase (2001) (continued).

E	max	error	$O - C$	phase	N
76	52145.6890	0.0016	-0.0043	0.82	56
82	52146.0280	0.0011	-0.0098	0.80	736
84	52146.1568	0.0026	0.0043	0.07	319
88	52146.3762	0.0017	-0.0059	0.94	182
90	52146.4906	0.0005	-0.0064	0.96	179
92	52146.6244	0.0057	0.0126	0.32	210
93	52146.6804	0.0030	0.0113	0.30	145
95	52146.7839	0.0036	-0.0000	0.13	103
99	52147.0093	0.0019	-0.0042	0.11	133
104	52147.3142	0.0005	0.0136	0.48	288
105	52147.3697	0.0003	0.0118	0.46	331
106	52147.4259	0.0003	0.0106	0.46	427
107	52147.4841	0.0003	0.0113	0.48	450
108	52147.5416	0.0004	0.0115	0.50	325
111	52147.7134	0.0006	0.0110	0.53	64
112	52147.7707	0.0008	0.0109	0.54	64
113	52147.8091	0.0017	-0.0081	0.21	59
114	52147.8645	0.0017	-0.0100	0.19	39
122	52148.3443	0.0005	0.0105	0.66	58
123	52148.3963	0.0006	0.0051	0.57	58
130	52148.8007	0.0017	0.0078	0.71	45
135	52149.0913	0.0003	0.0113	0.83	1456
136	52149.1510	0.0008	0.0137	0.89	1339
137	52149.2139	0.0007	0.0191	1.00	489
138	52149.2679	0.0013	0.0158	0.95	261
140	52149.3792	0.0007	0.0123	0.91	146
141	52149.4309	0.0004	0.0065	0.82	138
142	52149.4837	0.0005	0.0019	0.76	141
143	52149.5444	0.0004	0.0053	0.83	163
144	52149.5963	0.0003	-0.0002	0.74	187
145	52149.6529	0.0004	-0.0011	0.74	91
146	52149.7123	0.0003	0.0009	0.79	97
147	52149.7684	0.0004	-0.0003	0.78	96
148	52149.8290	0.0040	0.0029	0.85	54
151	52149.9995	0.0023	0.0012	0.86	178
155	52150.2421	0.0018	0.0141	0.13	236
161	52150.5730	0.0011	0.0007	0.97	461
162	52150.6340	0.0055	0.0043	0.05	180
164	52150.7512	0.0013	0.0067	0.11	79
165	52150.8174	0.0009	0.0155	0.28	45
166	52150.8765	0.0028	0.0172	0.32	45
167	52150.9226	0.0014	0.0059	0.14	46
168	52150.9846	0.0016	0.0104	0.23	357
169	52151.0457	0.0012	0.0142	0.31	375
171	52151.1603	0.0019	0.0140	0.33	178
172	52151.2225	0.0020	0.0188	0.43	121
175	52151.3901	0.0016	0.0142	0.39	91
176	52151.4395	0.0010	0.0062	0.26	78
177	52151.5040	0.0012	0.0133	0.39	88
178	52151.5513	0.0005	0.0032	0.23	190
179	52151.6012	0.0010	-0.0043	0.11	208
180	52151.6599	0.0008	-0.0030	0.14	172
181	52151.7204	0.0018	0.0001	0.21	164
182	52151.7735	0.0008	-0.0042	0.15	143

Table 219. Superhump maxima of WZ Sge during the re-brightening phase (2001) (continued).

E	max	error	$O - C$	phase	N
183	52151.8308	0.0007	-0.0044	0.16	62
184	52151.8859	0.0019	-0.0067	0.13	46
199	52152.7568	0.0012	0.0033	0.49	54
202	52152.9320	0.0009	0.0062	0.58	324
205	52153.1043	0.0006	0.0064	0.62	436
206	52153.1650	0.0007	0.0097	0.69	294
207	52153.2187	0.0007	0.0060	0.64	270
209	52153.3334	0.0004	0.0059	0.67	79
210	52153.3812	0.0004	-0.0037	0.51	83
214	52153.6159	0.0064	0.0014	0.65	47
215	52153.6629	0.0057	-0.0090	0.48	94
216	52153.7241	0.0027	-0.0052	0.56	93
220	52153.9736	0.0023	0.0147	0.96	315
222	52154.1001	0.0012	0.0264	0.19	231
227	52154.3722	0.0014	0.0115	0.99	97
229	52154.4853	0.0015	0.0098	0.99	145
230	52154.5418	0.0008	0.0089	0.98	189
231	52154.6058	0.0026	0.0155	0.11	130
232	52154.6550	0.0011	0.0073	0.98	97
233	52154.7101	0.0012	0.0051	0.95	93
234	52154.7683	0.0008	0.0058	0.98	96
248	52155.5728	0.0006	0.0068	0.17	207
249	52155.6335	0.0010	0.0101	0.24	199
250	52155.6919	0.0006	0.0111	0.27	213
251	52155.7569	0.0006	0.0186	0.42	208
252	52155.8156	0.0023	0.0199	0.45	145
265	52156.5536	0.0007	0.0118	0.47	101
266	52156.6031	0.0005	0.0039	0.35	114
267	52156.6581	0.0009	0.0015	0.32	88
268	52156.7176	0.0008	0.0035	0.36	134
269	52156.7744	0.0004	0.0030	0.37	144
270	52156.8261	0.0009	-0.0028	0.28	134
272	52156.9287	0.0003	-0.0150	0.09	572
274	52157.0620	0.0002	0.0035	0.44	961
275	52157.1213	0.0002	0.0054	0.49	1003
276	52157.1748	0.0005	0.0015	0.43	815
277	52157.2308	0.0013	0.0001	0.42	275
283	52157.5737	0.0017	-0.0013	0.47	42
299	52158.4869	0.0012	-0.0066	0.58	51
300	52158.5508	0.0005	-0.0000	0.70	55
301	52158.6048	0.0017	-0.0034	0.66	51
302	52158.6653	0.0016	-0.0004	0.72	94
303	52158.7314	0.0018	0.0084	0.89	41
304	52158.7753	0.0008	-0.0052	0.66	44
306	52158.8940	0.0038	-0.0012	0.76	30
314	52159.3590	0.0017	0.0046	0.96	182
315	52159.4173	0.0007	0.0055	0.99	92
337	52160.6761	0.0019	0.0015	0.19	42
338	52160.7328	0.0005	0.0008	0.20	45
339	52160.7884	0.0003	-0.0010	0.18	42
340	52160.8461	0.0010	-0.0008	0.19	45
341	52160.9130	0.0040	0.0088	0.37	54
342	52160.9626	0.0009	0.0010	0.25	280
343	52161.0174	0.0010	-0.0016	0.22	237

Table 219. Superhump maxima of WZ Sge during the re-brightening phase (2001) (continued).

E	max	error	$O - C$	phase	N
344	52161.0790	0.0007	0.0026	0.30	300
345	52161.1318	0.0008	-0.0020	0.23	271
346	52161.1867	0.0017	-0.0045	0.20	175
347	52161.2443	0.0018	-0.0043	0.22	170
354	52161.6440	0.0009	-0.0064	0.27	48
355	52161.7043	0.0006	-0.0035	0.33	75
356	52161.7592	0.0010	-0.0060	0.30	101
357	52161.8180	0.0006	-0.0046	0.34	70
372	52162.6760	0.0006	-0.0076	0.47	75
373	52162.7283	0.0005	-0.0126	0.40	59
374	52162.7905	0.0008	-0.0079	0.49	55
375	52162.8368	0.0077	-0.0190	0.31	46
389	52163.6628	0.0007	0.0034	0.88	38
394	52163.9414	0.0010	-0.0050	0.80	254
395	52163.9993	0.0012	-0.0045	0.82	143
396	52164.0530	0.0006	-0.0081	0.77	108
397	52164.1059	0.0003	-0.0127	0.70	279
398	52164.1695	0.0006	-0.0064	0.82	124
399	52164.2240	0.0007	-0.0094	0.78	182
411	52164.9142	0.0011	-0.0080	0.96	237
412	52164.9758	0.0013	-0.0038	0.04	297
413	52165.0297	0.0014	-0.0072	0.99	243
442	52166.6843	0.0005	-0.0172	0.18	46
443	52166.7384	0.0009	-0.0205	0.14	45
444	52166.7939	0.0008	-0.0224	0.12	45
445	52166.8547	0.0008	-0.0191	0.19	45

6.117. V701 Tauri

V701 Tau was discovered by Erastova (1973) as an eruptive object. The SU UMa-type nature was first reported by us during the 1995–1996 outburst (vsnet-alert 303). Shears, Boyd (2007) further reported the 2005 superoutburst and obtained a superhump period of 0.0690(2) d, or its one-day alias, 0.0663(2) d. Based on our 1995–1996 observations, we obtained a mean period of 0.06898(3) d. The times of superhump maxima are listed in table 227. During the interval $0 \leq E \leq 3$, the superhumps were still in the growing stage (stage A) and the mean period (0.073(1) d) significantly differed from the later observations. The P_{dot} estimated from the segment of $31 \leq E \leq 159$ was $-2.6(0.8) \times 10^{-5}$.

We also analyzed the 2005 superoutburst (table 228). The mean superhump period with the PDM method was 0.069037(12) d (figure 136). The P_{SH} showed a clear increase (stage B) at $P_{\text{dot}} = +11.0(3.5) \times 10^{-5}$.

6.118. V1208 Tauri

V1208 Tau was originally identified as a CV during the course of identification of ROSAT sources (Motch et al. 1996). P. Schmeer detected the first-ever recorded outburst in 2000 (vsnet-alert 4118). Time-resolved photometry during this superoutburst established the SU UMa-type dwarf novae (vsnet-alert 4122).

We observed two superoutbursts in 2000 and 2002–

Table 220. Superhump maxima of WZ Sge during the post-superoutburst stage (2001).

E	max ^a	error	$O - C^b$	phase ^c	N^d
0	52167.7152	0.0004	0.0046	0.37	38
1	52167.7785	0.0009	0.0106	0.48	44
2	52167.8265	0.0006	0.0012	0.33	45
3	52167.8875	0.0014	0.0048	0.41	34
10	52168.2867	0.0004	0.0026	0.45	169
11	52168.3431	0.0003	0.0017	0.44	173
12	52168.3933	0.0009	-0.0054	0.33	113
15	52168.5702	0.0037	-0.0006	0.45	41
16	52168.6284	0.0034	0.0003	0.48	53
17	52168.6826	0.0007	-0.0029	0.43	45
18	52168.7457	0.0006	0.0029	0.55	44
19	52168.8052	0.0004	0.0051	0.60	45
20	52168.8616	0.0009	0.0041	0.59	45
39	52169.9512	0.0006	0.0042	0.81	240
40	52170.0119	0.0003	0.0075	0.88	255
41	52170.0639	0.0004	0.0022	0.80	216
42	52170.1220	0.0007	0.0030	0.83	186
45	52170.2923	0.0005	0.0012	0.83	220
46	52170.3525	0.0003	0.0041	0.89	159
47	52170.4062	0.0003	0.0005	0.84	225
48	52170.4605	0.0007	-0.0026	0.80	135
49	52170.5203	0.0014	-0.0001	0.85	44
56	52170.9274	0.0007	0.0056	0.03	278
57	52170.9862	0.0005	0.0070	0.07	275
58	52171.0335	0.0005	-0.0030	0.90	279
59	52171.0912	0.0009	-0.0027	0.92	280
60	52171.1541	0.0005	0.0029	0.03	276
61	52171.2148	0.0019	0.0063	0.10	243
74	52171.9623	0.0022	0.0084	0.29	180
75	52172.0089	0.0004	-0.0024	0.11	340
76	52172.0676	0.0003	-0.0011	0.15	340
77	52172.1338	0.0020	0.0078	0.31	280
78	52172.1844	0.0011	0.0011	0.21	274
80	52172.3068	0.0005	0.0088	0.36	133
81	52172.3481	0.0009	-0.0073	0.09	133
83	52172.4726	0.0006	0.0026	0.29	108
84	52172.5304	0.0019	0.0030	0.31	59
86	52172.6444	0.0018	0.0023	0.32	37
87	52172.6959	0.0006	-0.0035	0.23	44
88	52172.7624	0.0012	0.0057	0.40	45
89	52172.8147	0.0007	0.0006	0.33	45
90	52172.8683	0.0012	-0.0032	0.27	26
91	52172.9311	0.0054	0.0023	0.38	321
92	52172.9850	0.0007	-0.0011	0.33	340
93	52173.0414	0.0007	-0.0021	0.32	340
102	52173.5496	0.0013	-0.0099	0.29	75
103	52173.6098	0.0006	-0.0071	0.35	26
104	52173.6692	0.0005	-0.0050	0.40	45
105	52173.7286	0.0007	-0.0030	0.45	45
106	52173.7854	0.0011	-0.0035	0.45	42
107	52173.8388	0.0034	-0.0075	0.39	37

^a BJD-2400000.

^b Against $max = 2452167.7106 + 0.057342E$.

^c Orbital phase.

^d Number of points used to determine the maximum.

Table 220. Superhump maxima of WZ Sge during the post-superoutburst stage (2001) (continued).

E	max	error	$O - C$	phase	N
112	52174.1434	0.0015	0.0104	0.76	266
115	52174.3175	0.0009	0.0125	0.84	94
116	52174.3688	0.0015	0.0065	0.74	50
117	52174.4182	0.0008	-0.0014	0.61	107
118	52174.4818	0.0018	0.0048	0.73	44
121	52174.6492	0.0015	0.0001	0.69	80
122	52174.7055	0.0011	-0.0008	0.68	75
123	52174.7706	0.0027	0.0069	0.83	45
124	52174.8175	0.0004	-0.0036	0.66	45
126	52174.9424	0.0007	0.0066	0.86	338
128	52175.0539	0.0004	0.0034	0.83	338
130	52175.1666	0.0005	0.0014	0.81	281
131	52175.2158	0.0031	-0.0067	0.68	206
132	52175.2816	0.0006	0.0018	0.84	34
133	52175.3385	0.0006	0.0014	0.85	40
134	52175.3874	0.0031	-0.0071	0.71	39
135	52175.4565	0.0014	0.0046	0.93	43
143	52175.8992	0.0035	-0.0113	0.74	164
144	52175.9668	0.0004	-0.0011	0.93	341
145	52176.0207	0.0008	-0.0045	0.88	341
146	52176.0776	0.0011	-0.0050	0.88	344
147	52176.1383	0.0005	-0.0016	0.96	297
148	52176.1949	0.0012	-0.0024	0.95	251
150	52176.3088	0.0008	-0.0032	0.96	45
157	52176.7135	0.0009	0.0002	0.10	43
158	52176.7704	0.0013	-0.0003	0.11	46
159	52176.8280	0.0011	-0.0001	0.12	45
161	52176.9449	0.0003	0.0021	0.18	1274
162	52177.0015	0.0002	0.0014	0.18	1273
163	52177.0460	0.0007	-0.0114	0.97	1202
164	52177.1102	0.0006	-0.0046	0.10	873
168	52177.3449	0.0003	0.0008	0.24	81
169	52177.4020	0.0007	0.0006	0.25	88
170	52177.4615	0.0012	0.0027	0.30	55
178	52177.9167	0.0005	-0.0008	0.33	889
186	52178.3723	0.0008	-0.0040	0.36	60
187	52178.4347	0.0010	0.0011	0.46	100
188	52178.4824	0.0020	-0.0085	0.31	90
191	52178.6561	0.0004	-0.0069	0.37	44
192	52178.7115	0.0006	-0.0088	0.35	44
196	52178.9391	0.0034	-0.0106	0.36	572
197	52178.9996	0.0007	-0.0074	0.43	1028
198	52179.0539	0.0005	-0.0105	0.39	1229
200	52179.1703	0.0031	-0.0088	0.44	108
209	52179.6818	0.0013	-0.0133	0.46	43
210	52179.7385	0.0009	-0.0140	0.46	20
219	52180.2690	0.0019	0.0005	0.82	28
220	52180.3236	0.0010	-0.0023	0.79	41
221	52180.3794	0.0023	-0.0039	0.77	29
222	52180.4385	0.0014	-0.0021	0.81	44
223	52180.4922	0.0009	-0.0058	0.76	34
230	52180.8963	0.0012	-0.0030	0.89	700
231	52180.9542	0.0002	-0.0024	0.91	1053
232	52181.0074	0.0003	-0.0067	0.85	1084

Table 220. Superhump maxima of WZ Sge during the post-superoutburst stage (2001) (continued).

E	max	error	$O - C$	phase	N
233	52181.0690	0.0004	-0.0023	0.94	1296
234	52181.1325	0.0011	0.0039	0.06	341
235	52181.1795	0.0024	-0.0065	0.88	252
238	52181.3776	0.0028	0.0195	0.38	136
239	52181.4147	0.0014	-0.0007	0.03	159
240	52181.4671	0.0019	-0.0056	0.96	106
250	52182.0429	0.0005	-0.0032	0.12	747
273	52183.3655	0.0004	0.0004	0.45	82
274	52183.4148	0.0006	-0.0076	0.32	87
275	52183.4586	0.0006	-0.0211	0.09	55
284	52183.9913	0.0007	-0.0045	0.49	279
285	52184.0472	0.0013	-0.0060	0.47	276
286	52184.1011	0.0016	-0.0094	0.42	253
295	52184.6117	0.0042	-0.0149	0.43	49
296	52184.6709	0.0005	-0.0130	0.47	37
297	52184.7343	0.0008	-0.0070	0.59	38
298	52184.7897	0.0010	-0.0089	0.57	34
300	52184.9113	0.0007	-0.0020	0.71	190
301	52184.9682	0.0004	-0.0024	0.72	330
302	52185.0293	0.0010	0.0013	0.80	280
303	52185.0869	0.0014	0.0016	0.81	222
307	52185.3096	0.0019	-0.0051	0.74	36
308	52185.3701	0.0008	-0.0019	0.81	44
309	52185.4299	0.0020	0.0005	0.86	29
313	52185.6746	0.0029	0.0159	0.18	38
314	52185.7230	0.0007	0.0069	0.03	38
318	52185.9421	0.0020	-0.0033	0.90	318
319	52185.9983	0.0015	-0.0045	0.89	276
320	52186.0610	0.0015	0.0009	1.00	279
321	52186.1120	0.0008	-0.0055	0.90	276
322	52186.1802	0.0078	0.0054	0.10	170
329	52186.5745	0.0015	-0.0017	0.05	54
342	52187.3206	0.0010	-0.0010	0.22	67
343	52187.3853	0.0014	0.0063	0.36	82
344	52187.4377	0.0016	0.0014	0.28	52
347	52187.6112	0.0009	0.0028	0.34	38
348	52187.6624	0.0016	-0.0033	0.24	38
349	52187.7255	0.0011	0.0024	0.36	37
350	52187.7797	0.0033	-0.0006	0.32	31
359	52188.2963	0.0014	-0.0002	0.43	37
360	52188.3519	0.0018	-0.0019	0.41	22
365	52188.6296	0.0016	-0.0110	0.31	40
366	52188.6862	0.0029	-0.0116	0.31	41
383	52189.6783	0.0007	0.0056	0.81	30
384	52189.7299	0.0015	-0.0001	0.72	29
412	52191.3370	0.0012	0.0014	0.07	43
413	52191.4051	0.0049	0.0121	0.27	45
429	52192.3124	0.0014	0.0020	0.27	54
431	52192.4257	0.0012	0.0006	0.27	20
432	52192.4824	0.0009	0.0000	0.27	30
435	52192.6544	0.0015	-0.0001	0.31	36
436	52192.7149	0.0022	0.0031	0.37	34
446	52193.2790	0.0018	-0.0062	0.33	25
447	52193.3361	0.0016	-0.0064	0.33	72

Table 220. Superhump maxima of WZ Sge during the post–superoutburst stage (2001) (continued).

E	max	error	$O - C$	phase	N
448	52193.3991	0.0036	-0.0008	0.44	84
449	52193.4550	0.0063	-0.0023	0.43	51
457	52193.9174	0.0008	0.0014	0.59	944
458	52193.9687	0.0009	-0.0046	0.49	833
459	52194.0223	0.0009	-0.0084	0.44	641
463	52194.2662	0.0012	0.0061	0.74	40
464	52194.3174	0.0024	-0.0000	0.64	79
465	52194.3804	0.0006	0.0056	0.75	77
466	52194.4394	0.0035	0.0073	0.79	81
470	52194.6676	0.0009	0.0062	0.82	40
471	52194.7182	0.0010	-0.0006	0.71	33
474	52194.8941	0.0006	0.0033	0.82	263
475	52194.9520	0.0006	0.0038	0.84	333
476	52195.0111	0.0013	0.0056	0.88	315
477	52195.0646	0.0014	0.0018	0.82	336
478	52195.1229	0.0014	0.0027	0.85	290
482	52195.3570	0.0071	0.0075	0.98	85
487	52195.6398	0.0015	0.0035	0.97	34
488	52195.7128	0.0078	0.0192	0.26	35
492	52195.9284	0.0004	0.0054	0.06	633
493	52195.9927	0.0013	0.0124	0.20	514
498	52196.2764	0.0018	0.0094	0.20	43
499	52196.3317	0.0012	0.0073	0.18	68
500	52196.3921	0.0012	0.0104	0.24	61
501	52196.4416	0.0021	0.0025	0.11	31
509	52196.9004	0.0005	0.0027	0.21	713
510	52196.9722	0.0012	0.0171	0.48	504
511	52197.0160	0.0005	0.0035	0.25	390
516	52197.3066	0.0003	0.0074	0.37	69
517	52197.3630	0.0007	0.0065	0.37	93
518	52197.4108	0.0020	-0.0031	0.21	35
533	52198.2742	0.0031	0.0002	0.44	41
534	52198.3298	0.0032	-0.0016	0.42	23
551	52199.3195	0.0012	0.0133	0.88	37
552	52199.3703	0.0019	0.0068	0.78	43
553	52199.4198	0.0010	-0.0010	0.65	42
580	52200.9884	0.0018	0.0193	0.32	281
581	52201.0403	0.0011	0.0138	0.24	273
586	52201.3275	0.0011	0.0143	0.30	69
597	52201.9606	0.0017	0.0167	0.47	355
598	52202.0090	0.0016	0.0078	0.33	331
848	52216.3123	0.0011	-0.0244	0.64	30
849	52216.3733	0.0015	-0.0208	0.72	36
865	52217.3061	0.0012	-0.0055	0.17	31
866	52217.3680	0.0025	-0.0009	0.27	33
901	52219.3688	0.0009	-0.0071	0.56	35
969	52223.2643	0.0012	-0.0109	0.28	16
970	52223.3227	0.0012	-0.0098	0.31	25

Table 221. Superhump maxima of WZ Sge (1978).

E	max ^a	$O - C^b$	Ref. ^c
0	43857.4731	-0.0053	3
0	43857.4767	-0.0017	4
1	43857.5365	0.0008	2
1	43857.5394	0.0037	3
2	43857.5934	0.0005	1
17	43858.4496	-0.0018	4
71	43861.5563	0.0144	1
83	43862.2360	0.0073	2
87	43862.4575	-0.0001	4
117	43864.1710	-0.0036	2
118	43864.2280	-0.0039	2
119	43864.2850	-0.0041	2
124	43864.5694	-0.0058	1
135	43865.2010	-0.0038	2
140	43865.4899	-0.0011	3
141	43865.5488	0.0006	3
159	43866.5709	-0.0075	1
176	43867.5505	-0.0008	1
193	43868.5263	0.0020	3
193	43868.5299	0.0056	1
194	43868.5859	0.0044	1
210	43869.4950	-0.0022	1
228	43870.5299	0.0025	1

^a HJD-2400000.^b Against $max = 2443857.4782 + 0.057232E$.^c 1: Patterson et al. (1981), 2: Bohusz, Udalski (1979), 3: Heiser, Henry (1979), 4: Targan (1979)**Table 222.** Superhump maxima of AW Sge (2000).

E	max ^a	error	$O - C^b$	N^c
0	51741.5174	0.0010	-0.0001	61
12	51742.4131	0.0025	0.0014	40
13	51742.4849	0.0012	-0.0013	52

^a BJD-2400000.^b Against $max = 2451741.5175 + 0.074519E$.^c Number of points used to determine the maximum.**Table 223.** Superhump maxima of AW Sge (2006).

E	max ^a	error	$O - C^b$	N^c
0	54056.3222	0.0007	-0.0004	53
30	54058.5593	0.0004	0.0009	139
31	54058.6336	0.0003	0.0006	139
43	54059.5258	0.0009	-0.0015	47
44	54059.6022	0.0004	0.0004	115

^a BJD-2400000.^b Against $max = 2454056.3226 + 0.074528E$.^c Number of points used to determine the maximum.

Table 224. Superhump maxima of V551 Sgr (2003).

E	max ^a	error	$O - C^b$	N^c
0	52904.3030	0.0029	-0.0187	68
22	52905.8189	0.0003	0.0084	165
29	52906.2914	0.0006	0.0072	68
30	52906.3589	0.0008	0.0070	49
44	52907.3025	0.0006	0.0032	74
45	52907.3669	0.0012	-0.0000	62
51	52907.7764	0.0006	0.0034	123
52	52907.8408	0.0006	0.0001	167
54	52907.9760	0.0006	-0.0000	32
55	52908.0433	0.0004	-0.0003	46
58	52908.2460	0.0009	-0.0007	61
59	52908.3128	0.0009	-0.0016	61
70	52909.0569	0.0006	-0.0019	45
84	52910.0047	0.0009	-0.0014	153
85	52910.0734	0.0011	-0.0004	177
89	52910.3426	0.0044	-0.0019	37
118	52912.3094	0.0013	0.0024	63
125	52912.7813	0.0007	0.0006	145
126	52912.8430	0.0048	-0.0054	154

^a BJD-2400000.^b Against $max = 2452904.3217 + 0.067672E$.^c Number of points used to determine the maximum.**Table 226.** Superhump maxima of V4140 Sgr (2004).

E	max ^a	error	$O - C^b$	N^c
0	53269.2561	0.0025	0.0047	176
1	53269.3193	0.0013	0.0045	238
2	53269.3858	0.0013	0.0079	240
16	53270.2604	0.0021	-0.0035	118
17	53270.3227	0.0021	-0.0045	116
18	53270.3850	0.0019	-0.0054	107
19	53270.4474	0.0032	-0.0063	113
53	53272.6051	0.0043	-0.0002	97
69	53273.6226	0.0021	0.0049	113
70	53273.6919	0.0026	0.0109	111
133	53277.6735	0.0023	0.0059	93
140	53278.1180	0.0030	0.0075	26
155	53279.0477	0.0023	-0.0120	26
156	53279.1107	0.0050	-0.0123	27
165	53279.6901	0.0098	-0.0024	106
181	53280.6891	0.0131	-0.0159	87
275	53286.6694	0.0025	0.0162	121

^a BJD-2400000.^b Against $max = 2453269.2514 + 0.063279E$.^c Number of points used to determine the maximum.**Table 225.** Superhump maxima of V551 Sgr (2004).

E	max ^a	error	$O - C^b$	N^c
0	53153.5658	0.0008	0.0010	150
1	53153.6341	0.0007	0.0015	153
12	53154.3802	0.0008	0.0018	151
13	53154.4424	0.0011	-0.0038	153
14	53154.5129	0.0012	-0.0011	153
15	53154.5797	0.0008	-0.0021	153
26	53155.3275	0.0008	-0.0002	131
27	53155.3984	0.0043	0.0029	16

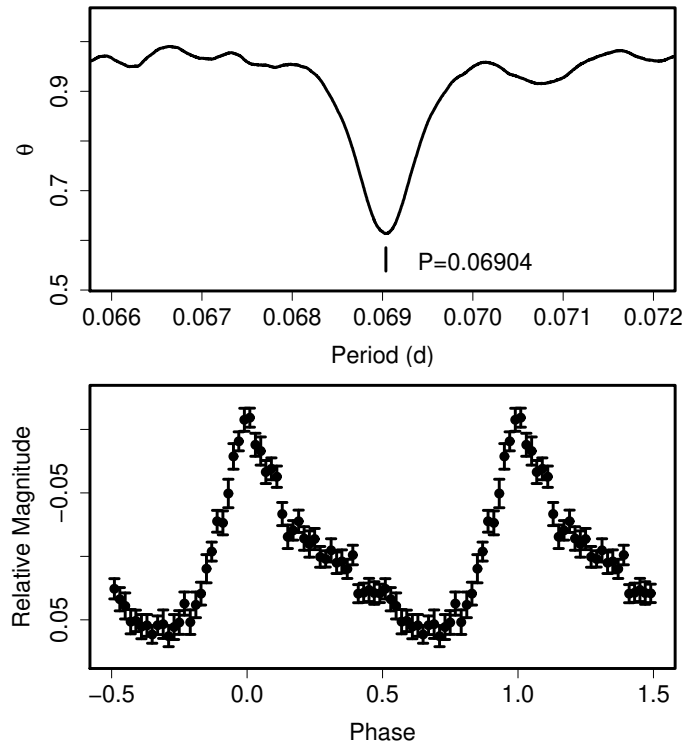
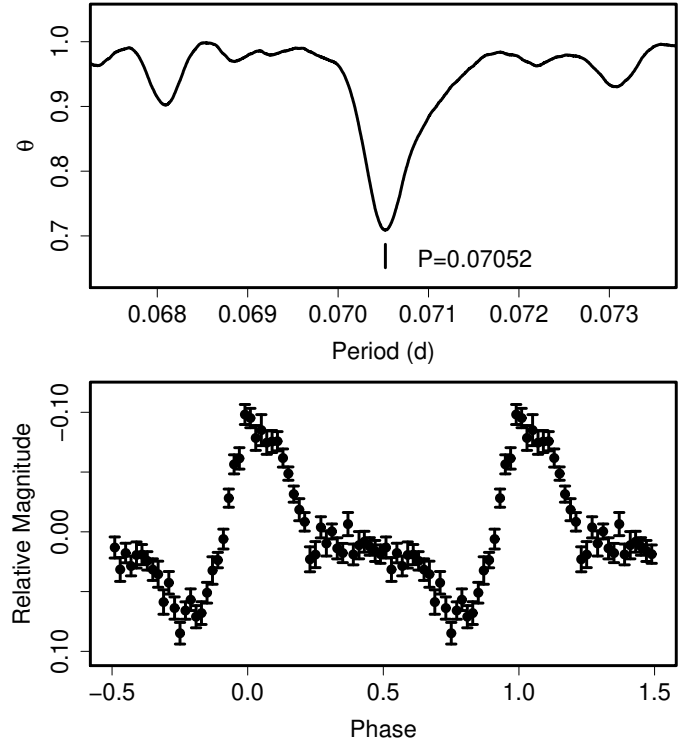
^a BJD-2400000.^b Against $max = 2453153.5648 + 0.067803E$.^c Number of points used to determine the maximum.**Fig. 136.** Superhumps in V701 Tau (2005). (Upper): PDM analysis. (Lower): Phase-averaged profile.

Table 227. Superhump maxima of V701 Tau (1995–1996).

E	max ^a	error	$O - C^b$	N^c
0	50078.9780	0.0016	-0.0077	61
1	50079.0485	0.0020	-0.0061	65
2	50079.1260	0.0035	0.0024	64
3	50079.1946	0.0013	0.0021	55
31	50081.1266	0.0005	0.0029	65
58	50082.9901	0.0016	0.0042	46
59	50083.0577	0.0116	0.0028	46
60	50083.1280	0.0021	0.0042	44
159	50089.9471	0.0059	-0.0047	37

^a BJD-2400000.^b Against $max = 2450078.9857 + 0.068970E$.^c Number of points used to determine the maximum.**Table 228.** Superhump maxima of V701 Tau (2005).

E	max ^a	error	$O - C^b$	N^c
0	53711.4936	0.0007	0.0033	67
1	53711.5650	0.0013	0.0056	34
14	53712.4576	0.0005	0.0008	57
23	53713.0767	0.0007	-0.0015	137
24	53713.1447	0.0007	-0.0025	146
25	53713.2144	0.0009	-0.0019	127
27	53713.3536	0.0007	-0.0007	68
28	53713.4233	0.0020	-0.0000	42
36	53713.9687	0.0095	-0.0070	86
37	53714.0437	0.0009	-0.0010	145
38	53714.1135	0.0009	-0.0002	145
39	53714.1764	0.0047	-0.0063	83
40	53714.2561	0.0012	0.0043	71
41	53714.3195	0.0008	-0.0013	60
54	53715.2204	0.0046	0.0021	121
69	53716.2549	0.0021	0.0010	34
70	53716.3218	0.0016	-0.0011	36
71	53716.3959	0.0007	0.0040	33
73	53716.5323	0.0009	0.0023	88

^a BJD-2400000.^b Against $max = 2453711.4903 + 0.069036E$.^c Number of points used to determine the maximum.**Fig. 137.** Superhumps in V1208 Tau (2002–2003). (Upper): PDM analysis. (Lower): Phase-averaged profile.**Table 229.** Superhump maxima of V1208 Tau (2000).

E	max ^a	error	$O - C^b$	N^c
0	51580.3069	0.0008	0.0013	67
1	51580.3761	0.0012	-0.0001	65
9	51580.9383	0.0007	-0.0019	55
10	51581.0109	0.0006	0.0002	77
12	51581.1505	0.0150	-0.0012	88
23	51581.9230	0.0023	-0.0042	178
24	51581.9997	0.0016	0.0020	140
38	51582.9904	0.0012	0.0057	82
39	51583.0557	0.0015	0.0005	65
66	51584.9573	0.0045	-0.0015	139
80	51585.9450	0.0072	-0.0008	139

^a BJD-2400000.^b Against $max = 2451580.3057 + 0.070501E$.^c Number of points used to determine the maximum.

2003. The superhump profile for the 2002–2003 super-outburst is shown in figure 137. The times of superhump maxima are listed in tables 229 and 230, respectively. The values of P_{dot} were $-2.8(4.0) \times 10^{-5}$ and $-6.3(3.8) \times 10^{-5}$, respectively. These negative values appear to have resulted from stage B–C transitions (figure 138).

6.119. *KK Telescopii*

Kato et al. (2003d) reported the detection of superhumps and derived an exceptionally large rate of pe-

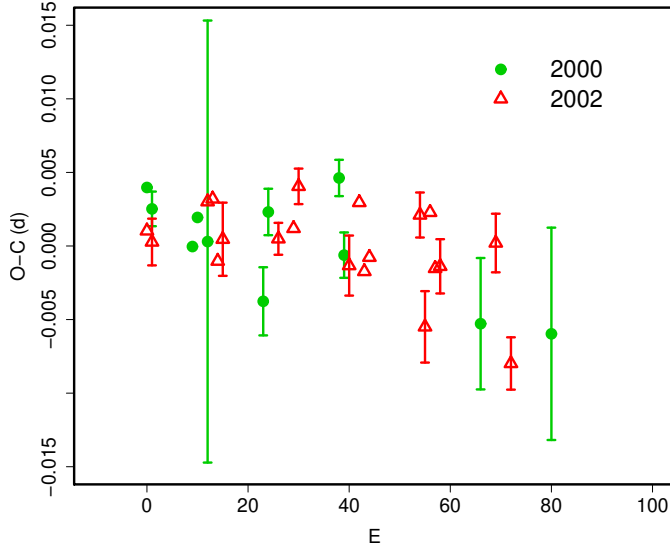


Fig. 138. Comparison of $O-C$ diagrams of V1208 Tau between different superoutbursts. A period of 0.07060 d was used to draw this figure. Since the start of the outburst was unknown, the start of time-resolved photometry was chosen as $E = 0$.

Table 230. Superhump maxima of V1208 Tau (2002–2003).

E	\max^a	error	$O-C^b$	N^c
0	52635.1220	0.0008	-0.0013	85
1	52635.1918	0.0016	-0.0020	57
12	52635.9711	0.0009	0.0015	162
13	52636.0419	0.0006	0.0017	186
14	52636.1083	0.0007	-0.0024	215
15	52636.1804	0.0025	-0.0009	38
26	52636.9570	0.0011	-0.0002	102
29	52637.1695	0.0008	0.0007	134
30	52637.2430	0.0012	0.0036	72
40	52637.9436	0.0020	-0.0011	81
42	52638.0891	0.0008	0.0033	136
43	52638.1550	0.0008	-0.0013	136
44	52638.2266	0.0009	-0.0003	137
54	52638.9354	0.0015	0.0032	129
55	52638.9984	0.0024	-0.0043	107
56	52639.0768	0.0008	0.0035	136
57	52639.1436	0.0008	-0.0002	136
58	52639.2144	0.0018	-0.0000	96
69	52639.9925	0.0020	0.0023	50
72	52640.1962	0.0018	-0.0057	37

^a BJD-2400000.

^b Against $\max = 2452635.1232 + 0.070537E$.

^c Number of points used to determine the maximum.

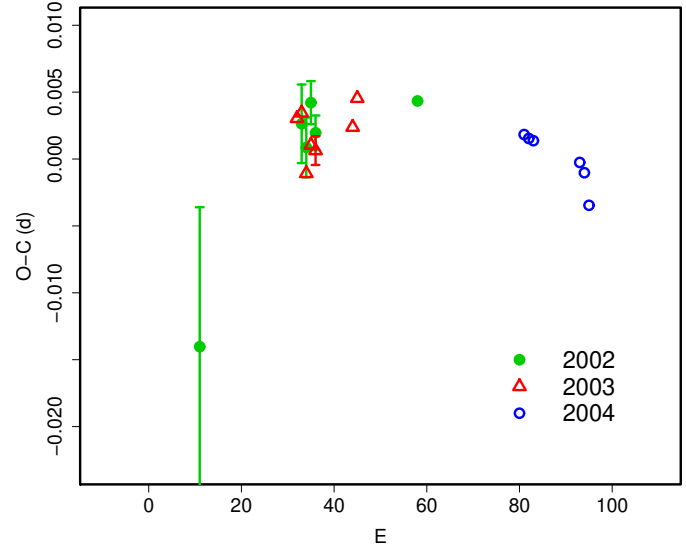


Fig. 139. Comparison of $O-C$ diagrams of KK Tel between different superoutbursts. A period of 0.08761 d was used to draw this figure. Approximate cycle counts (E) after the start of the superoutburst were used.

Table 231. Superhump maxima of KK Tel (2002).

E	\max^a	error	$O-C^b$	N^c
0	52444.0061	0.0104	-0.0139	185
22	52445.9501	0.0029	0.0028	20
23	52446.0360	0.0022	0.0010	30
24	52446.1269	0.0016	0.0043	48
25	52446.2123	0.0013	0.0021	37
47	52448.1421	0.0006	0.0045	90

^a BJD-2400000.

^b Against $\max = 2452444.2000 + 0.08761E$.

^c Number of points used to determine the maximum.

riod decrease. We also observed the 2003 superoutburst, and identified an unambiguous superhump period of 0.08753(5) d, which is in good agreement with Patterson et al. (2003), who observed the 2000 superoutburst. Based on this identification of the period, we give refined $O-C$'s for the 2002 superoutburst (table 231). It is now evident the times of superhumps for $22 \leq E \leq 47$ are well expressed by this improved superhump period. The maximum at $E = 0$ has a strongly negative $O-C$, indicating that this maximum was observed during the stage A evolution. The period derivative shown in Kato et al. (2003d) was thus a result of a stage A–B transition, and should not be used as a global P_{dot} . The times of superhump maxima during the 2003 superoutburst are listed in table 232. The mean period of 0.08734(6) d determined from the late stage of the 2004 superoutburst (table 233) suggests that a shortening of the period (stage C) near the termination of the superoutburst also occurred in this system (see also the combined $O-C$ diagram in figure 139).

Table 232. Superhump maxima of KK Tel (2003).

E	max ^a	error	$O - C^b$	N^c
0	52816.0225	0.0004	0.0018	91
1	52816.1105	0.0003	0.0020	90
2	52816.1936	0.0005	-0.0026	83
3	52816.2833	0.0004	-0.0007	91
4	52816.3705	0.0011	-0.0012	52
12	52817.0732	0.0008	-0.0006	64
13	52817.1629	0.0009	0.0014	25

^a BJD-2400000.^b Against $max = 2452816.0207 + 0.087756E$.^c Number of points used to determine the maximum.**Table 233.** Superhump maxima of KK Tel (2004).

E	max ^a	error	$O - C^b$	N^c
0	53151.4369	0.0003	-0.0001	157
1	53151.5242	0.0003	-0.0001	199
2	53151.6116	0.0003	-0.0000	198
12	53152.4861	0.0003	0.0011	198
13	53152.5730	0.0003	0.0006	199
14	53152.6581	0.0006	-0.0015	120

^a BJD-2400000.^b Against $max = 2453151.4370 + 0.087335E$.^c Number of points used to determine the maximum.

6.120. EK Trianguli Australis

Although EK TrA had long been known as an SU UMa-type dwarf nova (Vogt, Semeniuk 1980), the precise superhump period was not reported. We observed the 2007 superoutburst and obtained a mean superhump period of 0.064309(6) with the PDM method (figure 140). The times of superhump maxima are listed in table 234. The $O - C$'s were almost zero, and the P_{dot} for the entire observation was $-0.5(0.5) \times 10^{-5}$. There was no noticeable structure in the $O - C$ diagram. Individual superhumps, however, showed strongly variable profiles: double-humped around $0 \leq E \leq 1$ (maxima matching the ephemeris were given in the table), and around $E = 63$, a complex, double wave-like profile emerged with reduced superhump amplitudes (maxima not determined). The latter feature somewhat resembled the behavior observed in OT J055718+683226 (Uemura et al. 2009).

6.121. UW Trianguli

This object was originally reported as a nova (Kurochkin 1984; Argyle 1983). The detection of a second outburst in 1995 by T. Vanmunster led to an identification as a large-amplitude dwarf nova (Kato et al. 2001c). Kato et al. (2001c) reported a candidate superhump period 0.0569 d, whose selection was based on the period distribution of known CVs. Other one-day aliases were not excluded due to the shortness of observations.

The object underwent a new outburst in 2008 (vsnet-alert 10635). The data taken during this superout-

Table 234. Superhump maxima of EK TrA (2007).

E	max ^a	error	$O - C^b$	N^c
0	54294.2815	0.0015	-0.0060	148
1	54294.3559	0.0016	0.0041	91
16	54295.3112	0.0008	-0.0056	148
31	54296.2840	0.0008	0.0021	148
32	54296.3473	0.0011	0.0011	148
33	54296.4101	0.0007	-0.0004	149
46	54297.2488	0.0005	0.0020	148
47	54297.3105	0.0015	-0.0007	148
48	54297.3760	0.0004	0.0005	148
49	54297.4317	0.0016	-0.0081	148
77	54299.2400	0.0008	-0.0012	149
78	54299.3099	0.0011	0.0043	148
79	54299.3763	0.0009	0.0064	148
80	54299.4360	0.0008	0.0017	148
93	54300.2697	0.0010	-0.0009	149
94	54300.3375	0.0012	0.0026	148
95	54300.4075	0.0013	0.0082	149
108	54301.2350	0.0014	-0.0005	148
109	54301.2989	0.0010	-0.0011	148
110	54301.3618	0.0007	-0.0024	149
124	54302.2590	0.0007	-0.0059	148
125	54302.3328	0.0007	0.0035	148
126	54302.3889	0.0007	-0.0047	148
127	54302.4575	0.0007	-0.0005	141
155	54304.2554	0.0009	-0.0039	149
156	54304.3223	0.0012	-0.0013	148
157	54304.3915	0.0010	0.0035	149
158	54304.4523	0.0010	-0.0001	140
172	54305.3570	0.0010	0.0040	149
173	54305.4195	0.0014	0.0021	141
186	54306.2550	0.0018	0.0013	121
187	54306.3107	0.0018	-0.0073	149
188	54306.3916	0.0029	0.0093	150
249	54310.2996	0.0007	-0.0072	142
250	54310.3722	0.0014	0.0011	122

^a BJD-2400000.^b Against $max = 2454294.2875 + 0.064335E$.^c Number of points used to determine the maximum.

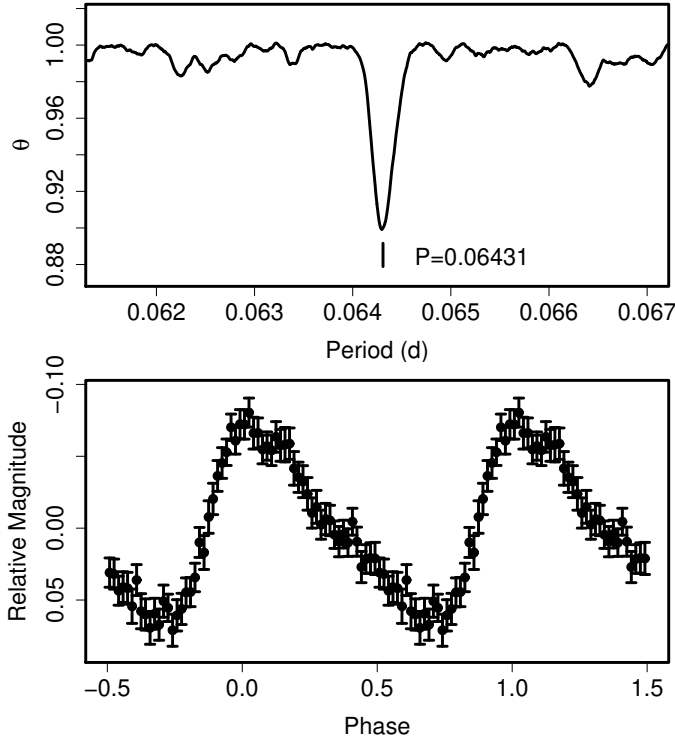


Fig. 140. Superhumps in EK TrA (2007). (Upper): PDM analysis. (Lower): Phase-averaged profile.

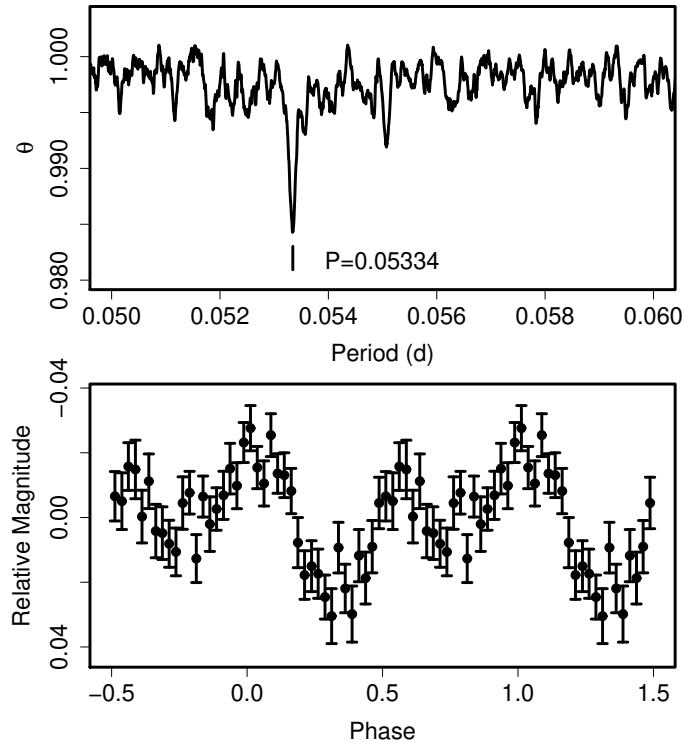


Fig. 141. Early superhumps in UW Tri (2008). (Upper): PDM analysis. (Lower): Phase-averaged profile.

burst now strongly favor a shorter period of 0.05334(2) d for early superhumps and 0.05427(2) for ordinary superhumps (figures 141, 142). We adopted these values as the basic periods for the following analysis. We also reanalyzed the data in Kato et al. (2001c) and yielded a period of 0.05330(2) d based on the present alias selection. The light curve of the 1995 observation averaged with this period now exhibits double-wave modulations characteristic to early superhumps (figure 143).

The maxima of ordinary superhump in 2008 are listed in table 235. The resultant P_{dot} was $+3.7(0.6) \times 10^{-5}$, although there remained some uncertainty in the constancy of the P_{dot} due to long gaps between observations. If the P_{dot} is confirmed, the parameters of superhumps and outbursts resemble those of another short P_{SH} WZ Sge-type dwarf nova OT J0238 (subsection 6.178).

The details will be presented in Ohshima et al., in preparation.

6.122. WY Trianguli

WY Tri is a dwarf nova discovered by Meinunger (1986). The SU UMa-type nature was established during its 2000 superoutburst (Vanmunster 2001). Since the original data in Vanmunster (2001) were not available, we extracted the data from a scanned figure. The quality of the extracted data were sufficient for the following analysis. The times of maxima determined from the combined data set with Vanmunster (2001) are listed in table 236. Although the global P_{dot} was $-18.3(5.9) \times 10^{-5}$, this variation can be

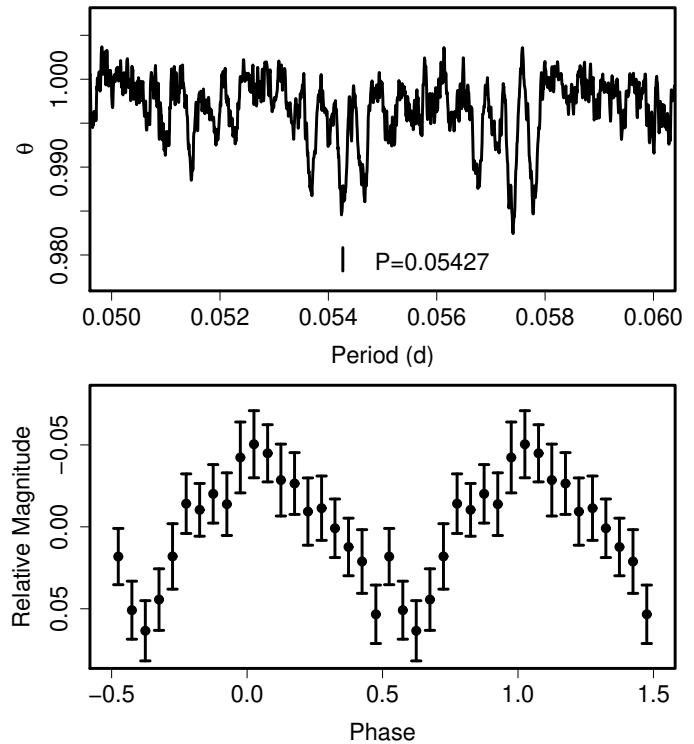


Fig. 142. Ordinary superhumps in UW Tri (2008). (Upper): PDM analysis. (Lower): Phase-averaged profile.

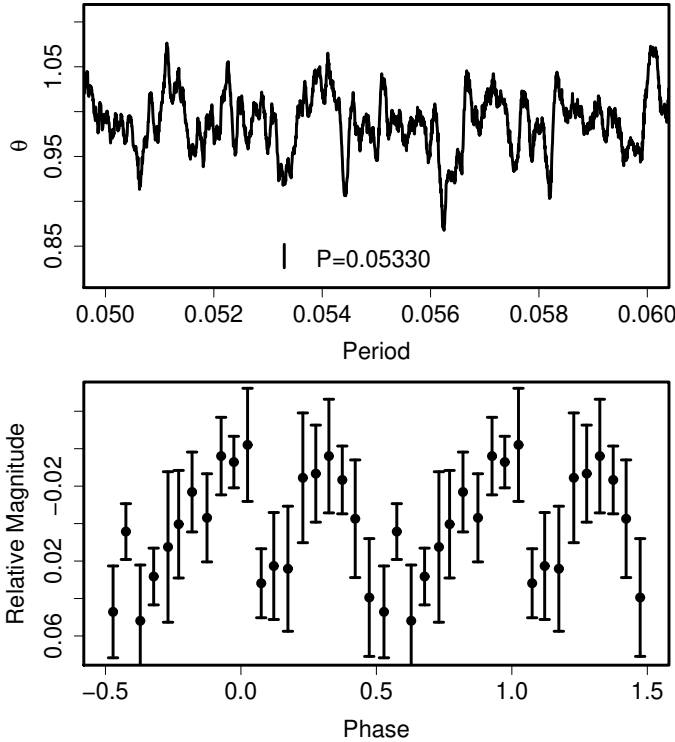


Fig. 143. Early superhumps in UW Tri (1995). (Upper): PDM analysis. (Lower): Phase-averaged profile.

Table 235. Superhump maxima of UW Tri (2008).

E	\max^a	error	$O - C^b$	N^c
0	54777.4487	0.0007	0.0144	40
1	54777.5041	0.0007	0.0156	40
101	54782.9032	0.0023	-0.0047	86
102	54782.9616	0.0024	-0.0005	110
104	54783.0654	0.0017	-0.0051	109
105	54783.1148	0.0009	-0.0100	113
106	54783.1829	0.0017	0.0040	111
107	54783.2300	0.0014	-0.0031	107
108	54783.2810	0.0024	-0.0063	87
123	54784.0994	0.0015	-0.0008	104
124	54784.1527	0.0052	-0.0017	85
125	54784.1944	0.0017	-0.0142	95
126	54784.2621	0.0054	-0.0007	110
217	54789.1923	0.0023	-0.0022	100
233	54790.0511	0.0146	-0.0105	65
234	54790.1127	0.0012	-0.0031	117
235	54790.1698	0.0012	-0.0002	115
236	54790.2187	0.0039	-0.0055	96
271	54792.1292	0.0059	0.0082	30
272	54792.1780	0.0070	0.0028	44
288	54793.0662	0.0133	0.0239	44

^a BJD-2400000.

^b Against $\max = 2454777.4343 + 0.054194E$.

^c Number of points used to determine the maximum.

Table 236. Superhump maxima of WY Tri(2000).

E	\max^a	error	$O - C^b$	N^c
0	51899.3738	0.0015	-0.0038	-
1	51899.4552	0.0027	-0.0007	-
2	51899.5306	0.0027	-0.0036	-
12	51900.3197	0.0015	0.0026	-
13	51900.3951	0.0024	-0.0002	-
14	51900.4758	0.0033	0.0022	-
15	51900.5547	0.0030	0.0028	-
20	51900.9382	0.0047	-0.0052	82
21	51901.0216	0.0019	-0.0000	113
22	51901.0999	0.0038	-0.0001	62
24	51901.2571	0.0024	0.0006	-
25	51901.3355	0.0021	0.0007	-
26	51901.4140	0.0015	0.0009	-
27	51901.4923	0.0021	0.0009	-
37	51902.2808	0.0030	0.0066	-
38	51902.3551	0.0015	0.0025	-
39	51902.4357	0.0024	0.0049	-
40	51902.5101	0.0033	0.0009	-
46	51902.9736	0.0046	-0.0053	82
47	51903.0572	0.0035	0.0001	83
58	51903.9114	0.0129	-0.0069	113

^a BJD-2400000.

^b Against $\max = 2451899.3776 + 0.078287E$.

^c Number of points used to determine the maximum.

attributed to a stage B-C transition. The parameters are given in table 2. A PDM analysis of the stage B superhumps yielded a period of 0.07838(5) d.

6.123. *SU Ursae Majoris*

We observed the 1999 January superoutburst. This outburst had a precursor outburst, and the observation covered the precursor phase. The times of superhump maxima are listed in table 237. The segment of $0 \leq E \leq 2$ corresponds to the precursor phase, when the superhump period rapidly evolved. Since there were multiple hump maxima within one cycle after $E > 170$ (post-superoutburst stage), we restricted our analysis to $E \leq 165$. Although the global P_{dot} was $-10.2(1.9) \times 10^{-5}$ ($13 \leq E \leq 165$), the $O - C$ diagram can be better interpreted as a combination of A-C stages. The P_{dot} for the stage B was $-0.2(3.9) \times 10^{-5}$ ($34 \leq E \leq 92$, disregarding $E = 78$ and $E = 79$). Other parameters are presented in table 2. A comparison between the 1989 and 1999 superoutbursts is shown in figure 144.

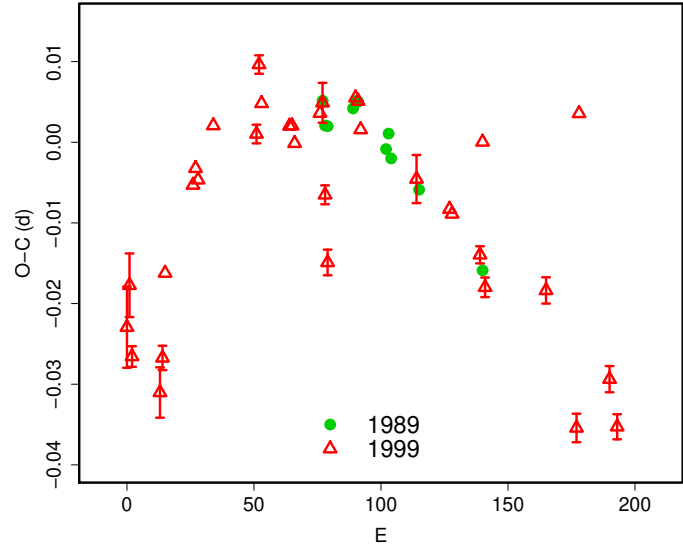
6.124. *SW Ursae Majoris*

We present observations of the 1991, 1997, 2000, 2002, and 2006 superoutbursts (tables 238, 239, 240, 241, 242), a part of which are a reanalysis of the data in Soejima et al. (2009).

The 1991 superoutburst was a faint superoutburst reaching a visual magnitude of ~ 11.0 . The superoutburst was associated with a precursor outburst (figure

Table 237. Superhump maxima of SU UMa (1999).

E	max ^a	error	$O - C$ ^b	N ^c
0	51185.9020	0.0050	-0.0152	80
1	51185.9863	0.0039	-0.0100	98
2	51186.0566	0.0013	-0.0188	87
13	51186.9220	0.0031	-0.0233	120
14	51187.0053	0.0015	-0.0190	124
15	51187.0949	0.0008	-0.0085	122
26	51187.9757	0.0004	0.0025	134
27	51188.0569	0.0003	0.0046	146
28	51188.1345	0.0002	0.0031	152
34	51188.6157	0.0002	0.0099	51
51	51189.9591	0.0012	0.0089	77
52	51190.0468	0.0011	0.0175	44
53	51190.1210	0.0005	0.0127	50
64	51190.9881	0.0009	0.0099	96
65	51191.0672	0.0010	0.0100	34
66	51191.1441	0.0010	0.0078	68
76	51191.9386	0.0004	0.0116	115
77	51192.0190	0.0025	0.0129	40
78	51192.0867	0.0012	0.0015	67
79	51192.1574	0.0016	-0.0069	21
90	51193.0477	0.0006	0.0135	152
91	51193.1263	0.0007	0.0131	68
92	51193.2019	0.0007	0.0096	91
114	51194.9355	0.0030	0.0035	41
127	51195.9598	0.0009	-0.0001	117
128	51196.0383	0.0004	-0.0008	118
139	51196.9031	0.0011	-0.0058	138
140	51196.9962	0.0009	0.0082	156
141	51197.0573	0.0012	-0.0098	98
165	51198.9548	0.0016	-0.0101	107
177	51199.8867	0.0018	-0.0271	62
178	51200.0048	0.0007	0.0119	143
190	51200.9208	0.0016	-0.0210	109
191	51201.0514	0.0005	0.0306	126
193	51201.1521	0.0016	-0.0269	91

^a BJD-2400000.^b Against $max = 2451185.9172 + 0.079077E$.^c Number of points used to determine the maximum.**Fig. 144.** Comparison of $O - C$ diagrams of SU UMa between different superoutbursts. A period of 0.07908 d was used to draw this figure. Approximate cycle counts (E) after the start of the superoutburst were used.

145). The identification of E in table 238¹⁹ is based on the present knowledge, assuming that the object experienced stage A during the precursor phase and the presence of the stage C during the post-superoutburst stage. The segment $52 \leq E \leq 88$ seems to be the early phase of the stage B. The shortness of the mean $P_{SH} = 0.05825(2)$ d probably reflects a short P_{SH} at the beginning of the stage B.

The 1997 superoutburst showed $P_{dot} = +8.6(0.5) \times 10^{-5}$.

The $O - C$ diagram of the 2000 superoutburst was clearly composed of the three distinct stages A-C. We obtained $P_{dot} = +5.1(0.5) \times 10^{-5}$ (stage B, $27 \leq E \leq 217$).

During the 2002 superoutburst, we obtained $P_{dot} = +9.9(0.9) \times 10^{-5}$ for the interval $E \leq 142$ (stage B). After $E = 142$, the $O - C$ diagram showed a clear transition to a shorter superhump period (stage C).

During the 2006 superoutburst, we obtained $P_{dot} = +9.5(0.6) \times 10^{-5}$ during the stage B ($33 \leq E \leq 189$). Although this superoutburst was one of the brightest (reaching a visual magnitude of 10.2) in the last decade, the behavior in the $O - C$ diagram during the stage B was similar to the ones in other superoutbursts. The start of the stage B was ~ 8.5 d after the initial detection of the outburst. The corresponding delay time for the 2000 superoutburst was ~ 7 d, and the delay time for the 1991 superoutburst was less than 3 d. The duration before the start of the stage B (or the appearance of superhumps) depends on the extent of the superoutburst, as pointed out by Kato et al. (2008). A comparison of the $O - C$ diagrams further indicates that the stage B evolution was

¹⁹ Since original data have become unavailable, we extracted observations from printed light curves. The errors of maxima times may be larger than the listed values.

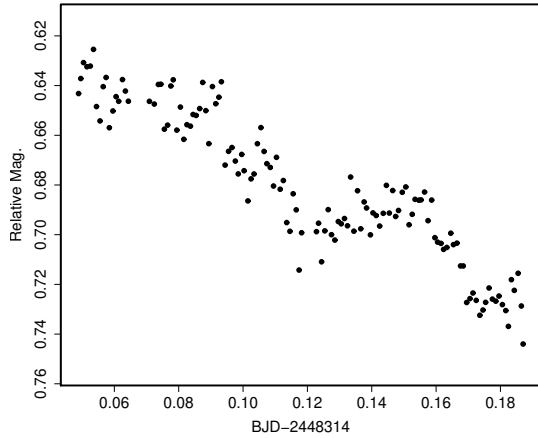


Fig. 145. Precursor outburst of SW UMa on 1991 February 26.

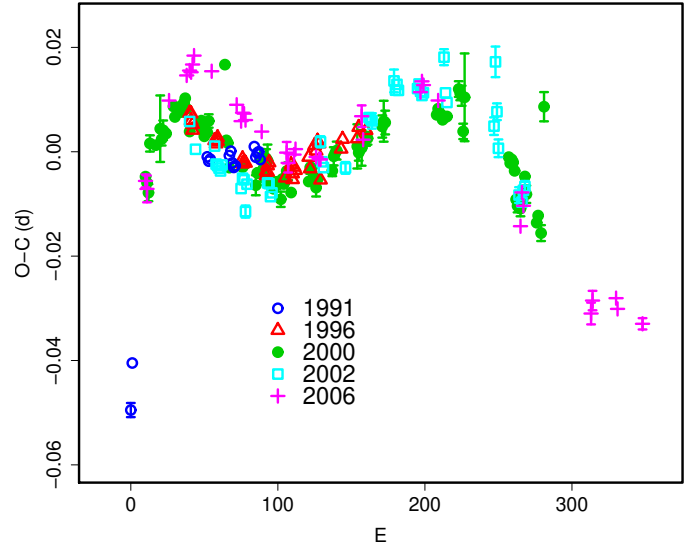


Fig. 147. Comparison of $O - C$ diagrams of SW UMa between different superoutbursts. A period of 0.05822 d was used to draw this figure. Since the delay in the appearance of superhumps is known to vary in SW UMa, we shifted individual $O - C$ diagrams to get a best match (approximately corresponds to a definition of the appearance of superhumps to be $E = 0$). The evolution of the bright 2008 superoutburst was apparently different from the other superoutbursts.

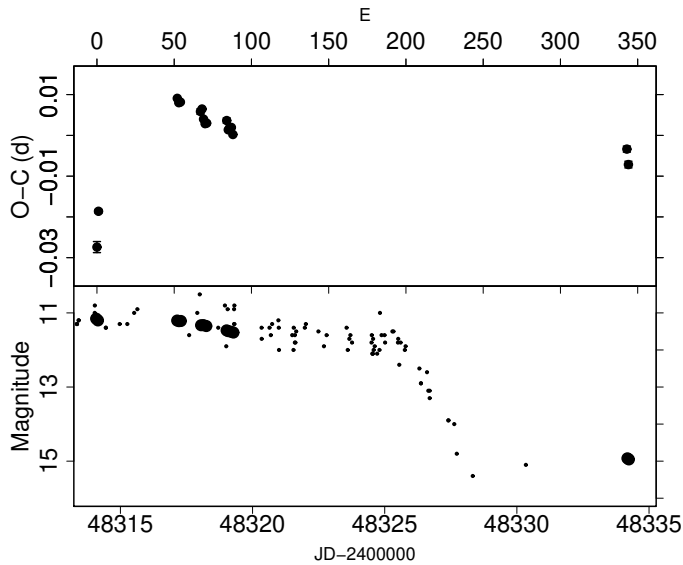


Fig. 146. $O - C$ of superhumps SW UMa (1991). (Upper): $O - C$ diagram. (Lower): Light curve. Large dots are our CCD observations and small dots are visual observation from the VSOLJ and AAVSO databases.

also different in this superoutburst (figure 147).

During the rapid fading stage of this superoutburst, large-amplitude quasi-periodic oscillations (QPOs) were recorded (figure 148). The appearance of large-amplitude QPOs during the rapid fading stage was recorded during the 2000 and 2002 superoutbursts (Soejima et al. 2009). The present period of the QPOs is close to theirs (i.e. about the double of “super-QPOs” observed during the 1992 superoutburst, Kato et al. 1992). There must be a common mechanism to excite these QPOs during the terminal stage of superoutbursts.

In summary, although the behavior of period variation is generally similar between different superoutbursts of SW UMa, there was a subtle dependence on the extent of superoutbursts.

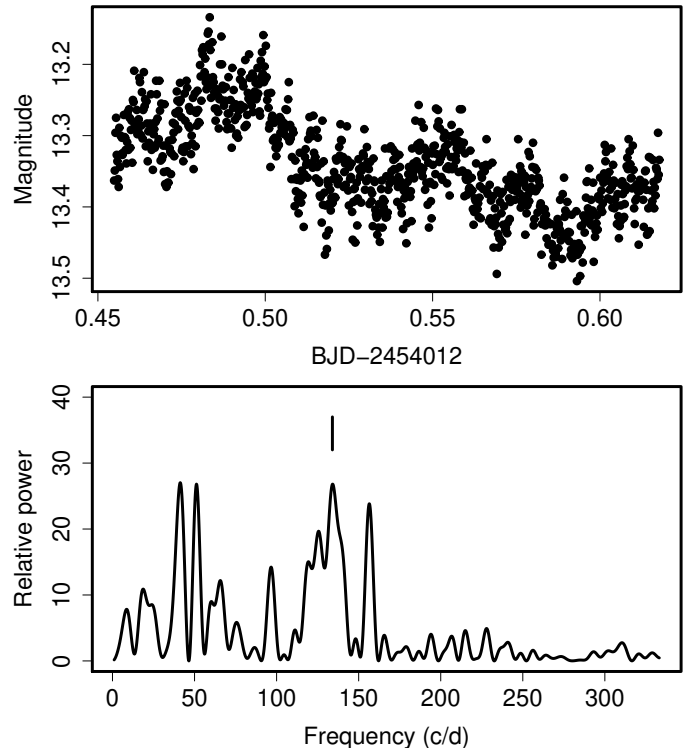


Fig. 148. Quasi-periodic oscillations (QPOs) on 2006 October 4. (Upper): Light curve. (Lower): Power spectrum after subtracting superhumps. The signal around a frequency 134 cycle/d (11 m) corresponds to the QPOs.

Table 238. Superhump maxima of SW UMa (1991).

E	max ^a	error	$O - C^b$
0	48314.0851	0.0028	-0.0274
1	48314.1524	0.0010	-0.0186
52	48317.1611	0.0004	0.0091
53	48317.2185	0.0004	0.0080
54	48317.2771	0.0004	0.0082
67	48318.0346	0.0014	0.0059
68	48318.0937	0.0004	0.0065
69	48318.1497	0.0004	0.0040
70	48318.2070	0.0004	0.0029
71	48318.2656	0.0008	0.0030
84	48319.0261	0.0012	0.0036
85	48319.0823	0.0004	0.0014
86	48319.1413	0.0004	0.0019
87	48319.1998	0.0004	0.0019
88	48319.2565	0.0008	0.0002
343	48334.1581	0.0014	-0.0034
344	48334.2127	0.0016	-0.0072

^a BJD-2400000.^b Against $max = 2448314.1125 + 0.058452E$.**Table 239.** Superhump maxima of SW UMa (1997).

E	max ^a	error	$O - C^b$	N^c
0	50744.5437	0.0005	0.0113	27
69	50748.5497	0.0023	-0.0043	17
70	50748.6075	0.0006	-0.0048	33
71	50748.6648	0.0006	-0.0058	28
85	50749.4834	0.0006	-0.0032	25
86	50749.5422	0.0009	-0.0026	33
87	50749.5986	0.0010	-0.0045	28
138	50752.5794	0.0009	0.0038	31
139	50752.6382	0.0009	0.0043	33
140	50752.6980	0.0016	0.0058	20

^a BJD-2400000.^b Against $max = 2450744.5324 + 0.058284E$.^c Number of points used to determine the maximum.**Table 240.** Superhump maxima of SW UMa (2000).

E	max ^a	error	$O - C^b$	N^c
0	51590.5432	0.0008	-0.0071	17
1	51590.6002	0.0009	-0.0083	16
2	51590.6565	0.0016	-0.0101	16
3	51590.7242	0.0016	-0.0007	18
7	51590.9567	0.0008	-0.0009	241
10	51591.1346	0.0064	0.0023	137
11	51591.1908	0.0012	0.0003	176
12	51591.2507	0.0019	0.0020	131
13	51591.3085	0.0004	0.0016	285
14	51591.3665	0.0006	0.0014	257
19	51591.6628	0.0002	0.0067	36
20	51591.7190	0.0003	0.0047	36
21	51591.7791	0.0002	0.0066	37
22	51591.8369	0.0002	0.0062	36
23	51591.8946	0.0004	0.0057	127
24	51591.9528	0.0004	0.0057	233
25	51592.0123	0.0002	0.0070	301
26	51592.0710	0.0002	0.0075	284
27	51592.1301	0.0003	0.0085	207
28	51592.1864	0.0005	0.0065	176
30	51592.2984	0.0010	0.0021	37
37	51592.7077	0.0003	0.0040	37
38	51592.7663	0.0003	0.0044	35
39	51592.8227	0.0002	0.0026	37
40	51592.8797	0.0008	0.0014	51
41	51592.9404	0.0004	0.0040	273
42	51592.9969	0.0002	0.0022	279
43	51593.0573	0.0013	0.0044	174
54	51593.7085	0.0002	0.0154	114
55	51593.7522	0.0002	0.0009	140
56	51593.8099	0.0003	0.0004	132
57	51593.8634	0.0006	-0.0043	110
66	51594.3875	0.0004	-0.0040	87
67	51594.4462	0.0004	-0.0035	91
75	51594.9080	0.0019	-0.0073	99
76	51594.9686	0.0009	-0.0049	190
77	51595.0268	0.0005	-0.0049	242
78	51595.0878	0.0018	-0.0021	160
80	51595.2022	0.0011	-0.0041	228
81	51595.2587	0.0006	-0.0058	244
82	51595.3207	0.0017	-0.0020	108
83	51595.3785	0.0031	-0.0024	81
84	51595.4329	0.0004	-0.0062	32
85	51595.4901	0.0006	-0.0072	33
86	51595.5490	0.0006	-0.0065	33
87	51595.6060	0.0005	-0.0077	33
88	51595.6651	0.0005	-0.0068	33
89	51595.7235	0.0011	-0.0066	18
92	51595.8951	0.0015	-0.0096	145
93	51595.9572	0.0007	-0.0057	221

^a BJD-2400000.^b Against $max = 2451590.5503 + 0.058200E$.^c Number of points used to determine the maximum.

6.125. *BC Ursae Majoris*

BC UMa was one of the classically known objects displaying a diversity in the extent of (super)outbursts (Romano 1964). Although the SU UMa-type nature had long been suspected, the definite detection of superhumps awaited the 1994 detection by M. Iida and confirmation by C. Kunjaya (unpublished; vsnet-alert 154).²⁰

Maehara et al. (2007) observed the 2003 superoutburst and obtained $P_{\text{dot}} = +3.2(0.8) \times 10^{-5}$. Maehara et al. (2007) also detected double-wave “early superhumps” before ordinary superhumps appeared.

We observed the 2000 and 2003 superoutbursts, the latter also including the data used in Maehara et al. (2007). The times of superhump maxima are listed in

²⁰ <<http://www.kusastro.kyoto-u.ac.jp/vsnet/DNe/bcuma.html>>.

Table 240. Superhump maxima of SW UMa (2000) (continued).

E	max	error	$O - C$	N
94	51596.0145	0.0006	-0.0067	262
95	51596.0739	0.0010	-0.0054	238
96	51596.1334	0.0005	-0.0041	233
97	51596.1916	0.0017	-0.0042	151
99	51596.3039	0.0005	-0.0082	258
111	51597.0047	0.0006	-0.0058	273
112	51597.0656	0.0012	-0.0031	136
113	51597.1237	0.0007	-0.0032	176
114	51597.1800	0.0005	-0.0051	284
115	51597.2382	0.0005	-0.0051	258
116	51597.2946	0.0017	-0.0069	155
117	51597.3544	0.0008	-0.0053	281
127	51597.9382	0.0010	-0.0035	220
128	51597.9992	0.0017	-0.0007	227
129	51598.0581	0.0011	-0.0000	251
130	51598.1168	0.0017	0.0005	215
144	51598.9327	0.0042	0.0015	111
145	51598.9897	0.0015	0.0003	266
147	51599.1070	0.0034	0.0013	123
150	51599.2834	0.0013	0.0030	29
151	51599.3418	0.0012	0.0032	45
161	51599.9262	0.0021	0.0057	294
162	51599.9854	0.0039	0.0067	198
163	51600.0434	0.0023	0.0065	155
198	51602.0826	0.0004	0.0087	284
199	51602.1420	0.0003	0.0098	294
200	51602.1993	0.0005	0.0090	277
201	51602.2573	0.0004	0.0088	365
202	51602.3145	0.0005	0.0078	349
204	51602.4315	0.0004	0.0083	82
205	51602.4898	0.0006	0.0085	89
213	51602.9608	0.0015	0.0139	157
214	51603.0182	0.0013	0.0131	192
215	51603.0760	0.0019	0.0126	109
216	51603.1274	0.0015	0.0058	203
217	51603.1921	0.0084	0.0124	60
247	51604.9273	0.0006	0.0015	294
248	51604.9843	0.0006	0.0004	286
249	51605.0433	0.0004	0.0011	284
250	51605.1009	0.0005	0.0006	280
251	51605.1575	0.0006	-0.0010	276
252	51605.2103	0.0007	-0.0065	293
253	51605.2672	0.0012	-0.0077	227
254	51605.3258	0.0013	-0.0073	30
255	51605.3832	0.0015	-0.0082	25
256	51605.4440	0.0014	-0.0056	33
257	51605.5025	0.0013	-0.0053	34
258	51605.5640	0.0010	-0.0020	31
259	51605.6188	0.0017	-0.0054	22
266	51606.0209	0.0007	-0.0107	120
267	51606.0805	0.0008	-0.0093	116
269	51606.1935	0.0015	-0.0126	120
271	51606.3342	0.0028	0.0117	125

Table 241. Superhump maxima of SW UMa (2002).

E	max ^a	error	$O - C$ ^b	N ^c
0	52575.0555	0.0010	0.0090	66
4	52575.2830	0.0005	0.0035	88
17	52576.0405	0.0005	0.0035	90
18	52576.0953	0.0004	-0.0000	90
19	52576.1532	0.0004	-0.0004	126
20	52576.2109	0.0002	-0.0009	467
21	52576.2686	0.0002	-0.0015	479
22	52576.3280	0.0002	-0.0004	404
35	52577.0803	0.0008	-0.0055	53
36	52577.1405	0.0002	-0.0036	90
37	52577.1984	0.0005	-0.0039	261
38	52577.2506	0.0012	-0.0100	335
39	52577.3140	0.0004	-0.0049	377
53	52578.1293	0.0004	-0.0053	90
54	52578.1874	0.0005	-0.0054	87
55	52578.2432	0.0004	-0.0080	90
56	52578.3021	0.0005	-0.0073	85
89	52580.2331	0.0011	0.0009	90
90	52580.2875	0.0007	-0.0030	90
91	52580.3446	0.0009	-0.0041	49
106	52581.2179	0.0011	-0.0049	131
122	52582.1591	0.0009	0.0040	88
123	52582.2170	0.0010	0.0037	88
124	52582.2748	0.0015	0.0033	88
139	52583.1558	0.0022	0.0103	102
140	52583.2123	0.0008	0.0084	103
141	52583.2716	0.0009	0.0095	274
142	52583.3287	0.0005	0.0083	287
155	52584.0859	0.0006	0.0080	89
156	52584.1450	0.0005	0.0089	102
157	52584.2018	0.0005	0.0074	102
158	52584.2592	0.0004	0.0066	102
159	52584.3179	0.0004	0.0070	310
173	52585.1398	0.0015	0.0132	85
174	52585.1912	0.0007	0.0063	101
175	52585.2476	0.0008	0.0044	86
207	52587.1061	0.0017	-0.0016	101
208	52587.1767	0.0029	0.0107	102
209	52587.2253	0.0016	0.0011	101
210	52587.2765	0.0017	-0.0060	46
224	52588.0826	0.0015	-0.0156	204
226	52588.1977	0.0008	-0.0170	345
227	52588.2582	0.0006	-0.0148	455
228	52588.3172	0.0011	-0.0141	325

^a BJD-2400000.^b Against $max = 2452575.0465 + 0.058267E$.^c Number of points used to determine the maximum.

Table 242. Superhump maxima of SW UMa (2006).

E	max ^a	error	$O - C$ ^b	N ^c
0	53997.6540	0.0012	-0.0201	113
1	53997.7107	0.0026	-0.0216	59
16	53998.6010	0.0006	-0.0030	87
28	53999.3044	0.0004	0.0031	65
30	53999.4218	0.0002	0.0043	56
31	53999.4797	0.0002	0.0041	56
32	53999.5394	0.0002	0.0057	57
33	53999.5993	0.0004	0.0075	31
45	54000.2950	0.0005	0.0058	206
62	54001.2783	0.0006	0.0012	157
65	54001.4498	0.0004	-0.0016	119
66	54001.5096	0.0002	0.0001	237
67	54001.5677	0.0002	0.0001	272
68	54001.6247	0.0003	-0.0010	80
79	54002.2629	0.0002	-0.0020	257
96	54003.2486	0.0020	-0.0042	37
97	54003.3048	0.0018	-0.0061	48
101	54003.5393	0.0004	-0.0040	96
102	54003.5986	0.0003	-0.0029	99
116	54004.4121	0.0003	-0.0029	74
118	54004.5282	0.0004	-0.0030	92
119	54004.5863	0.0002	-0.0030	87
147	54006.2248	0.0021	0.0084	78
148	54006.2785	0.0004	0.0040	174
187	54008.5582	0.0006	0.0173	152
188	54008.6185	0.0003	0.0195	236
189	54008.6760	0.0003	0.0189	206
199	54009.2552	0.0006	0.0171	126
255	54012.4915	0.0006	-0.0009	241
256	54012.5562	0.0008	0.0057	241
257	54012.6118	0.0008	0.0032	135
303	54015.2693	0.0021	-0.0124	25
304	54015.3300	0.0019	-0.0098	36
320	54016.2620	0.0010	-0.0076	149
321	54016.3181	0.0007	-0.0095	159
338	54017.3050	0.0011	-0.0105	118

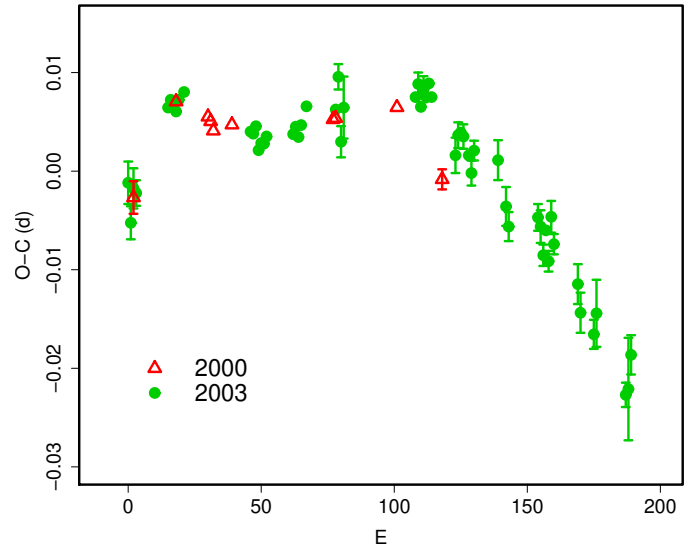
^a BJD-2400000.^b Against $max = 2453997.6742 + 0.058110E$.^c Number of points used to determine the maximum.

Fig. 149. Comparison of $O - C$ diagrams of BC UMa between different superoutbursts. A period of 0.06455 d was used to draw this figure. Approximate cycle counts (E) after the appearance of the superhumps were used.

tables 243 and 244. These epochs do not include maxima of early superhumps. The times of maxima for the 2003 superoutburst systematically differ from those in Maehara et al. (2007), probably reflecting the difference in the template superhump light curve. This difference was almost constant during the outburst and did not affect the determination of the P_{dot} . The both sets of $O - C$'s showed all stages A-C. We measured P_{dot} for the stage B: $+4.0(1.4) \times 10^{-5}$ (2000, $16 \leq E \leq 99$) and $+4.2(0.8) \times 10^{-5}$ (2003, $15 \leq E \leq 114$). The 2003 data also include the times of superhump maxima during the rapidly fading stage. The maxima times for $123 \leq E \leq 189$ were very well expressed by a constant period of 0.06418(2) d, 0.5 % shorter than the mean superhump period. No apparent phase shift, corresponding to traditional late superhumps, was detected during the rapid fading.

A comparison of $O - C$ diagrams between different superoutbursts is shown in figure 149. The duration of the stage B was shorter in the 2003 superoutburst, corresponding to the maximum brightness of the outbursts (11.1 mag for 2000 and 12.2 mag for 2003).

6.126. BZ Ursae Majoris

Although BZ UMa had long been suspected to be an SU UMa-type dwarf nova, no definite superoutbursts were recorded before 2007 (Jurcevic et al. 1994; Ringwald, Thorstensen 1990). The first-ever recorded superoutburst occurred in 2007. The times of superhump maxima during this superoutburst are listed in table 245. We included hump maxima during the post-superoutburst stage, which will be discussed later. During the first night of the observation ($E \leq 4$), we observed the growing stage of superhumps. The superhump period was almost constant for $19 \leq E \leq 64$ with $P_{\text{dot}} = +3.6(3.3) \times 10^{-5}$. We regard this

Table 243. Superhump maxima of BC UMa (2000).

E	max ^a	error	$O - C^b$	N^c
0	51639.5559	0.0017	-0.0066	21
16	51640.5985	0.0003	0.0031	54
28	51641.3715	0.0004	0.0016	140
29	51641.4356	0.0004	0.0011	157
30	51641.4992	0.0002	0.0001	71
37	51641.9517	0.0009	0.0007	125
75	51644.4051	0.0005	0.0012	89
76	51644.4698	0.0007	0.0013	54
99	51645.9555	0.0006	0.0023	121
116	51647.0456	0.0010	-0.0050	124

^a BJD-2400000.^b Against $max = 2451639.5625 + 0.064553E$.^c Number of points used to determine the maximum.

as the stage B. An discontinuous transition to a shorter period (stage C, $72 \leq E \leq 138$) occurred. The mean periods for the stages B and C were 0.07018(1) d and 0.06979(1) d, 3.3 % and 2.6 % longer than the orbital period, respectively. The superhump period further experienced a discontinuous shortening after $E = 138$ to 0.06968(5) d, 2.4 % longer than the orbital period. BZ UMa is a rare SU UMa-type object around $P_{SH} = 0.07$ d without a distinct segment having a positive P_{dot} . This feature may be related to the extreme rarity of its superoutbursts. Furthermore, the present superoutburst was accompanied by a slow rise before superhumps grew, suggesting that the outburst was an “inside-out” type (vsnet-alert 9300), rarely met in SU UMa-type dwarf novae. There was also a suggestion of the presence of a precursor-type outburst (figure 150). These features possibly suggest that the 3:1 resonance is difficult to achieve in this system, and the superhumps were critically excited during this superoutburst, likely leaving little mass beyond the 3:1 resonance.

After $E = 167$ (around the start of the post-superoutburst stage), secondary hump maxima were sometimes present, which later became stronger than the original hump maxima. The times of these secondary humps are listed in table 246, giving $O - C$'s using the same ephemeris as in the earlier maxima. These data indicated that post-superoutburst superhumps persisted at least for ~ 150 cycles, or ~ 10 d.

6.127. *CI Ursae Majoris*

CI UMa was discovered as a dwarf nova by Goranskij (1972). Nogami, Kato (1997) observed the 1995 superoutburst and reported the superhump period. This observation was not long enough to determine the period derivative. Although Nogami, Kato (1997) suggested a supercycle of ~ 140 d based on the shortest interval between apparent superoutbursts (Kolotovkina 1979), recent observations suggest that superoutbursts occur less regularly.

We further observed the 2001, 2003 and 2006 superoutburst (tables 247, 248, 249). The 2001 observation prob-

Table 244. Superhump maxima of BC UMa (2003).

E	max ^a	error	$O - C^b$	N^c
0	52673.1330	0.0022	-0.0100	46
1	52673.1935	0.0017	-0.0139	49
2	52673.2615	0.0020	-0.0104	50
3	52673.3256	0.0013	-0.0107	48
15	52674.1088	0.0006	-0.0010	55
16	52674.1742	0.0003	-0.0001	71
17	52674.2381	0.0003	-0.0007	118
18	52674.3021	0.0003	-0.0011	73
19	52674.3678	0.0003	0.0002	155
21	52674.4977	0.0002	0.0011	66
46	52676.1075	0.0007	-0.0006	56
47	52676.1718	0.0006	-0.0007	68
48	52676.2371	0.0006	0.0001	151
49	52676.2992	0.0008	-0.0022	51
50	52676.3645	0.0004	-0.0014	116
51	52676.4290	0.0004	-0.0014	67
52	52676.4943	0.0004	-0.0006	61
62	52677.1400	0.0005	0.0006	171
63	52677.2053	0.0005	0.0014	180
64	52677.2688	0.0005	0.0005	197
65	52677.3346	0.0005	0.0018	135
67	52677.4656	0.0010	0.0039	42
78	52678.1753	0.0009	0.0045	107
79	52678.2432	0.0013	0.0079	56
80	52678.3011	0.0016	0.0014	91
81	52678.3691	0.0031	0.0050	88
108	52680.1131	0.0006	0.0085	178
109	52680.1789	0.0012	0.0099	73
110	52680.2412	0.0010	0.0077	145
111	52680.3075	0.0013	0.0096	66
112	52680.3713	0.0008	0.0089	80
113	52680.4372	0.0006	0.0103	132
114	52680.5004	0.0010	0.0090	81
123	52681.0754	0.0018	0.0040	81
124	52681.1420	0.0013	0.0061	75
125	52681.2068	0.0002	0.0064	300
126	52681.2710	0.0012	0.0061	167
128	52681.3981	0.0006	0.0044	67
129	52681.4609	0.0013	0.0027	51
130	52681.5277	0.0010	0.0051	48
139	52682.1077	0.0020	0.0049	102
142	52682.2967	0.0020	0.0005	63
143	52682.3592	0.0015	-0.0015	84
154	52683.0702	0.0014	0.0005	113
155	52683.1338	0.0017	-0.0004	173
156	52683.1954	0.0011	-0.0032	326
157	52683.2625	0.0006	-0.0006	265
158	52683.3239	0.0010	-0.0036	150
159	52683.3930	0.0016	0.0010	85

^a BJD-2400000.^b Against $max = 2452673.1429 + 0.064459E$.^c Number of points used to determine the maximum.

Table 244. Superhump maxima of BC UMa (2003). (continued)

E	max	error	$O - C$	N
160	52683.4547	0.0010	-0.0017	55
169	52684.0316	0.0020	-0.0049	102
170	52684.0933	0.0020	-0.0078	74
175	52684.4138	0.0015	-0.0095	45
176	52684.4805	0.0034	-0.0073	44
187	52685.1823	0.0012	-0.0145	123
188	52685.2474	0.0052	-0.0139	129
189	52685.3155	0.0020	-0.0103	130

Table 245. Superhump maxima of BZ UMa (2007).

E	max ^a	error	$O - C$ ^b	N ^c
0	54204.3391	0.0010	-0.0185	41
1	54204.4092	0.0009	-0.0182	111
2	54204.4748	0.0013	-0.0224	82
3	54204.5525	0.0006	-0.0145	43
4	54204.6245	0.0006	-0.0124	60
5	54204.6943	0.0003	-0.0124	26
6	54204.7647	0.0002	-0.0118	27
7	54204.8343	0.0002	-0.0121	26
15	54205.3965	0.0002	-0.0085	491
16	54205.4671	0.0002	-0.0077	512
17	54205.5368	0.0002	-0.0078	452
18	54205.6073	0.0001	-0.0072	340
19	54205.6786	0.0002	-0.0058	163
20	54205.7483	0.0002	-0.0058	156
21	54205.8185	0.0005	-0.0055	37
23	54205.9590	0.0002	-0.0046	101
24	54206.0295	0.0002	-0.0040	102
29	54206.3789	0.0003	-0.0037	502
30	54206.4492	0.0003	-0.0032	422
31	54206.5231	0.0005	0.0008	220
32	54206.5906	0.0005	-0.0016	396
33	54206.6610	0.0003	-0.0010	483
34	54206.7317	0.0004	-0.0001	278
35	54206.8012	0.0003	-0.0005	139
43	54207.3620	0.0003	0.0017	250
44	54207.4336	0.0004	0.0035	275
45	54207.5022	0.0006	0.0023	150
46	54207.5729	0.0006	0.0031	249
47	54207.6417	0.0007	0.0021	272
48	54207.7126	0.0007	0.0032	197
49	54207.7822	0.0010	0.0029	49
52	54207.9923	0.0005	0.0035	57
57	54208.3454	0.0003	0.0074	207
58	54208.4159	0.0004	0.0082	438
59	54208.4864	0.0003	0.0088	428
60	54208.5581	0.0015	0.0107	92
61	54208.6262	0.0005	0.0090	72
62	54208.6954	0.0005	0.0083	89
63	54208.7655	0.0006	0.0086	55
64	54208.8365	0.0006	0.0097	53
72	54209.3952	0.0003	0.0098	611
73	54209.4659	0.0003	0.0106	416
81	54210.0235	0.0002	0.0096	252
86	54210.3711	0.0002	0.0081	266
87	54210.4425	0.0004	0.0096	210
88	54210.5127	0.0003	0.0100	142
89	54210.5803	0.0004	0.0078	43
90	54210.6500	0.0003	0.0077	50
91	54210.7220	0.0003	0.0098	131
100	54211.3510	0.0006	0.0103	134

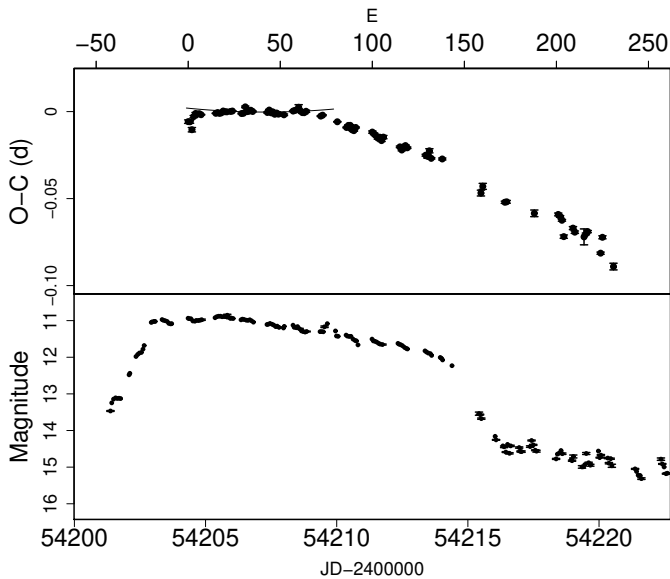
^a BJD-2400000.^b Against $max = 2454204.3575 + 0.069831E$.^c Number of points used to determine the maximum.**Fig. 150.** $O - C$ of superhumps BZ UMa (2007). (Upper): $O - C$ diagram. The values of $O - C$'s are different from those listed in table 313 and were calculated from a linear fit for the times of superhumps for $19 \leq E \leq 64$. The curve represents a quadratic fit with $P_{\text{dot}} = +3.2 \times 10^{-5}$. (Lower): Light curve. The rise of the superoutburst was very slow, apparently accompanied by a stagnation phase (BJD 2454201.5-2454201.8). There was a relatively rapid fading probably corresponding to a precursor outburst (BJD 2454203.3-2454203.7)

Table 245. Superhump maxima of BZ UMa (2007). (continued)

E	max	error	$O - C$	N
101	54211.4202	0.0005	0.0096	276
102	54211.4893	0.0005	0.0089	323
103	54211.5581	0.0006	0.0079	229
104	54211.6288	0.0004	0.0088	136
105	54211.6970	0.0005	0.0072	12
106	54211.7692	0.0010	0.0095	7
115	54212.3952	0.0005	0.0070	496
116	54212.4636	0.0005	0.0056	403
117	54212.5356	0.0009	0.0078	113
118	54212.6065	0.0004	0.0088	154
119	54212.6754	0.0004	0.0079	77
129	54213.3729	0.0005	0.0071	389
130	54213.4424	0.0011	0.0068	285
131	54213.5158	0.0012	0.0103	109
132	54213.5816	0.0004	0.0064	103
138	54214.0024	0.0006	0.0081	196
159	54215.4565	0.0017	-0.0042	109
160	54215.5306	0.0017	0.0000	33
172	54216.3636	0.0006	-0.0049	38
173	54216.4340	0.0008	-0.0043	127
188	54217.4801	0.0019	-0.0057	83
201	54218.3918	0.0008	-0.0019	76
202	54218.4608	0.0005	-0.0027	84
203	54218.5288	0.0005	-0.0045	88
204	54218.5896	0.0010	-0.0136	70
209	54218.9454	0.0009	-0.0069	53
210	54219.0132	0.0007	-0.0089	73
215	54219.3614	0.0046	-0.0099	58
216	54219.4333	0.0005	-0.0078	205
217	54219.5048	0.0006	-0.0062	40
224	54219.9837	0.0006	-0.0161	162
225	54220.0630	0.0009	-0.0066	128
231	54220.4672	0.0019	-0.0214	52

ably covered only the later part of the superoutburst and likely recorded a stage B–C transition. The 2003 $O - C$ diagram showed a clear stage B–C transition (cf. figure 7). We determined $P_{\text{dot}} = +6.4(1.2) \times 10^{-5}$ for $E \leq 93$. The 2006 observation recorded the terminal stage of the superoutburst (stage C superhumps). A combined $O - C$ diagram is presented in figure 151.

6.128. *CY Ursae Majoris*

Harvey, Patterson (1995) observed the 1995 superoutburst and reported a global P_{dot} of -5.8×10^{-5} . Their $O - C$ diagram, however, also can be interpreted as a transition from a longer to a shorter period (stage B–C transition) during the late stage of the superoutburst. Using the earlier part ($E \leq 73$) of their table of superhump maxima, we obtained $P_{\text{dot}} = +2.7(1.0) \times 10^{-5}$.

We analyzed the 1998 AAVSO data and found a clear stage B–C transition (table 250). The parameters are given in table 2. Our 1999 observation (Kato, Matsumoto 1999c) did not show a clear tendency of a period decrease,

Table 246. Secondary Maxima of BZ UMa (2007).

E	max ^a	error	$O - C$ ^b	N ^c
167	54216.0487	0.0004	0.0291	193
181	54217.0363	0.0024	0.0391	64
187	54217.4455	0.0009	0.0294	84
188	54217.5202	0.0015	0.0342	54
189	54217.5908	0.0018	0.0350	46
201	54218.4225	0.0014	0.0287	88
202	54218.4932	0.0018	0.0295	87
224	54220.0259	0.0007	0.0259	131
229	54220.3687	0.0032	0.0196	56
230	54220.4371	0.0059	0.0181	50
244	54221.4154	0.0006	0.0188	287
245	54221.4962	0.0011	0.0297	244
246	54221.5601	0.0013	0.0238	88
259	54222.4642	0.0050	0.0201	88
260	54222.5345	0.0053	0.0205	46
272	54223.3672	0.0016	0.0153	108
287	54224.4043	0.0049	0.0049	21
315	54226.3639	0.0020	0.0092	80
316	54226.4287	0.0014	0.0042	144
317	54226.4951	0.0021	0.0007	88
318	54226.5706	0.0053	0.0064	47

^a BJD–2400000.

^b Against $\text{max} = 2454204.3576 + 0.069832E$.

^c Number of points used to determine the maximum.

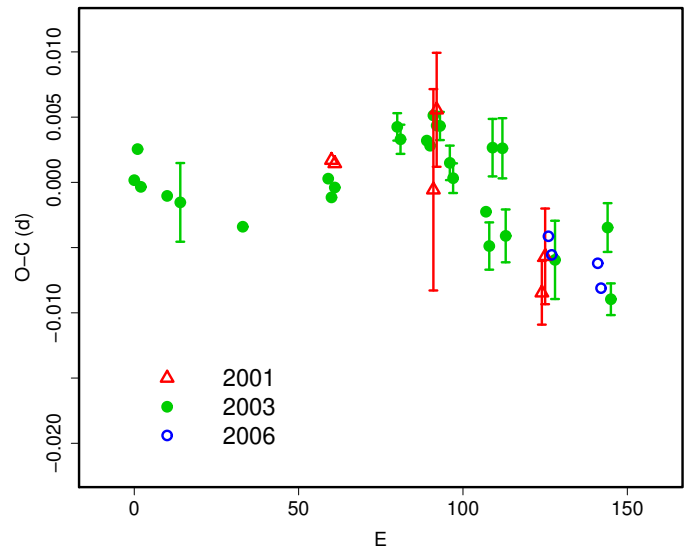


Fig. 151. Comparison of $O - C$ diagrams of CI UMa between different superoutbursts. A period of 0.06264 d was used to draw this figure. Since the start of the outbursts were not clearly defined, the $O - C$ diagrams were shifted to best match the 2003 one.

Table 247. Superhump maxima of CI UMa (2001).

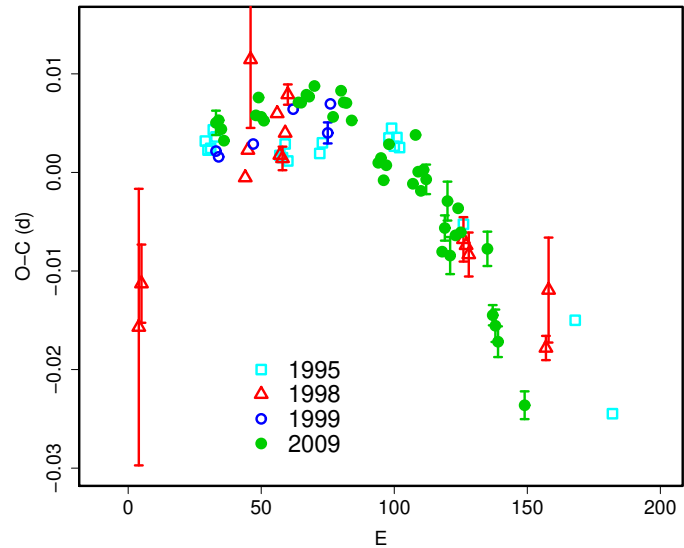
E	\max^a	error	$O - C^b$	N^c
0	52214.2376	0.0010	0.0026	115
1	52214.3000	0.0008	0.0023	118
31	52216.1772	0.0077	-0.0011	31
32	52216.2460	0.0044	0.0050	32
64	52218.2364	0.0024	-0.0105	71
65	52218.3018	0.0037	-0.0077	113
112	52221.2651	0.0096	0.0093	31

^a BJD-2400000.^b Against $\max = 2452214.2350 + 0.062686E$.^c Number of points used to determine the maximum.**Table 248.** Superhump maxima of CI UMa (2003).

E	\max^a	error	$O - C^b$	N^c
0	52739.3819	0.0006	-0.0012	64
1	52739.4469	0.0006	0.0012	64
2	52739.5067	0.0006	-0.0017	57
10	52740.0071	0.0008	-0.0022	84
14	52740.2572	0.0030	-0.0027	70
33	52741.4455	0.0005	-0.0042	58
59	52743.0778	0.0005	-0.0000	144
60	52743.1390	0.0005	-0.0015	145
61	52743.2024	0.0009	-0.0007	99
80	52744.3972	0.0010	0.0043	43
81	52744.4589	0.0011	0.0034	45
89	52744.9599	0.0005	0.0034	133
90	52745.0222	0.0004	0.0030	105
91	52745.0871	0.0006	0.0054	204
92	52745.1490	0.0008	0.0046	264
93	52745.2116	0.0011	0.0046	205
96	52745.3967	0.0013	0.0018	44
97	52745.4582	0.0011	0.0007	41
107	52746.0820	0.0009	-0.0017	156
108	52746.1420	0.0018	-0.0043	228
109	52746.2122	0.0022	0.0032	216
112	52746.4000	0.0023	0.0032	43
113	52746.4560	0.0020	-0.0035	45
128	52747.3937	0.0030	-0.0051	45
144	52748.3985	0.0019	-0.0023	42
145	52748.4556	0.0012	-0.0078	66

^a BJD-2400000.^b Against $\max = 2452739.3831 + 0.062622E$.^c Number of points used to determine the maximum.**Table 249.** Superhump maxima of CI UMa (2006).

E	\max^a	error	$O - C^b$	N^c
0	53936.4310	0.0003	0.0006	90
1	53936.4922	0.0003	-0.0007	89
15	53937.3686	0.0008	0.0009	54
16	53937.4293	0.0006	-0.0008	65

^a BJD-2400000.^b Against $\max = 2453936.4304 + 0.062479E$.^c Number of points used to determine the maximum.**Fig. 152.** Comparison of $O - C$ diagrams of CY UMa between different superoutbursts. A period of 0.07212 d was used to draw this figure. Approximate cycle counts (E) after the start of the superoutburst were used.

probably because of the insufficient data coverage (table 251). The 2009 superoutburst was well-observed during the middle-to-late stage (table 252). A clear stage B-C transition was recorded. A comparison of $O - C$ diagrams between different superoutbursts is shown in figure 152. There was a possible slight difference in behavior during the stage B between different superoutbursts. Observations at early epochs of superoutbursts are wanted.

6.129. DV Ursae Majoris

This eclipsing SU UMa-type dwarf nova has been well documented (Patterson et al. 2000b, Nogami et al. 2001b). Relatively large negative period derivatives have been reported. We summarize our observations of five superoutbursts (1997, 1999, 2002, 2005 and 2007). The maxima were determined from observations outside the eclipses, as described in V2051 Oph.

The times of superhump maxima for the 1997 superoutburst (table 253) were determined by using a combination of the AAVSO and data in Nogami et al. (2001b). We also incorporated times of superhump maxima reported

Table 250. Superhump maxima of CY UMa (1998).

E	\max^a	error	$O - C^b$	N^c
0	50882.5614	0.0140	-0.0176	42
1	50882.6379	0.0040	-0.0131	41
40	50885.4614	0.0009	0.0003	28
41	50885.5363	0.0008	0.0032	28
42	50885.6176	0.0069	0.0125	15
52	50886.3333	0.0009	0.0077	28
53	50886.4012	0.0009	0.0035	28
54	50886.4730	0.0012	0.0032	28
55	50886.5477	0.0009	0.0059	28
56	50886.6237	0.0010	0.0099	28
122	50891.3689	0.0023	-0.0003	28
123	50891.4404	0.0009	-0.0009	28
124	50891.5116	0.0022	-0.0017	28
153	50893.5936	0.0012	-0.0093	20
154	50893.6716	0.0053	-0.0033	20

^a BJD-2400000.^b Against $\max = 2450882.5789 + 0.072052E$.^c Number of points used to determine the maximum.**Table 251.** Superhump maxima of CY UMa (1999).

E	\max^a	error	$O - C^b$	N^c
0	51222.9702	0.0003	0.0002	140
1	51223.0417	0.0004	-0.0005	102
14	51223.9806	0.0005	-0.0004	124
29	51225.0659	0.0008	0.0017	90
42	51226.0010	0.0011	-0.0019	105
43	51226.0761	0.0007	0.0009	85

^a BJD-2400000.^b Against $\max = 2451222.9699 + 0.072216E$.^c Number of points used to determine the maximum.

in Patterson et al. (2000b). Although the AAVSO data we analyzed were included in Patterson et al. (2000b), we presented our new determinations because Patterson et al. (2000b) gave epochs only to 0.001 d. Since the mean difference between our measurements and those by Patterson et al. (2000b) was negligible (0.0010(9) d), we did not make a systematic correction between them. The combined result showed negative $O - C$'s for the earliest stage (stage A, $E \leq 5$), followed by a segment of relatively constant period (stage B, $7 \leq E \leq 79$), then by a transition to a shorter period (stage C, $104 \leq E \leq 184$). The mean superhump periods of the stages B and C were 0.08878(4) d and 0.08840(3) d, respectively. The P_{dot} for the stage B was $-0.9(4.0) \times 10^{-5}$.

During The 1999 superoutburst (table 254), there was a discontinuous shortening (stage B to C) of the period after $E = 80$ as in the 1997 superoutburst. The mean periods before and after this transitions were 0.08893(3) d and 0.08836(8) d, respectively. The P_{dot} before the transition was $-4.7(3.4) \times 10^{-5}$. The 2002 superoutburst showed a similar pattern of $O - C$ variation (table 255), although

Table 252. Superhump maxima of CY UMa (2009).

E	\max^a	error	$O - C^b$	N^c
0	54917.9589	0.0012	-0.0063	95
1	54918.0313	0.0006	-0.0058	137
2	54918.1025	0.0004	-0.0065	102
3	54918.1735	0.0006	-0.0075	121
15	54919.0415	0.0005	-0.0026	131
16	54919.1154	0.0009	-0.0006	139
17	54919.1855	0.0003	-0.0024	141
18	54919.2573	0.0004	-0.0026	150
31	54920.1967	0.0006	0.0018	136
32	54920.2688	0.0009	0.0019	104
34	54920.4138	0.0004	0.0031	527
35	54920.4858	0.0004	0.0031	528
37	54920.6311	0.0005	0.0046	67
44	54921.1328	0.0005	0.0028	123
47	54921.3518	0.0005	0.0060	67
48	54921.4227	0.0004	0.0051	456
49	54921.4948	0.0004	0.0052	522
51	54921.6373	0.0004	0.0038	47
61	54922.3542	0.0004	0.0014	378
62	54922.4268	0.0005	0.0021	423
63	54922.4966	0.0009	0.0000	474
64	54922.5703	0.0006	0.0018	183
65	54922.6445	0.0008	0.0041	47
74	54923.2896	0.0004	0.0018	120
75	54923.3667	0.0005	0.0069	244
76	54923.4351	0.0007	0.0034	208
77	54923.5052	0.0010	0.0017	196
78	54923.5795	0.0006	0.0040	191
79	54923.6506	0.0015	0.0032	65
85	54924.0760	0.0007	-0.0030	131
86	54924.1506	0.0013	-0.0004	174
87	54924.2254	0.0020	0.0025	113
88	54924.2920	0.0019	-0.0028	72
90	54924.4383	0.0010	-0.0004	133
91	54924.5132	0.0008	0.0026	128
92	54924.5828	0.0009	0.0003	85
102	54925.3024	0.0017	0.0006	88
104	54925.4399	0.0010	-0.0058	136
105	54925.5109	0.0016	-0.0066	137
106	54925.5814	0.0016	-0.0081	134
116	54926.2962	0.0014	-0.0126	85

^a BJD-2400000.^b Against $\max = 2454917.9652 + 0.071927E$.^c Number of points used to determine the maximum.

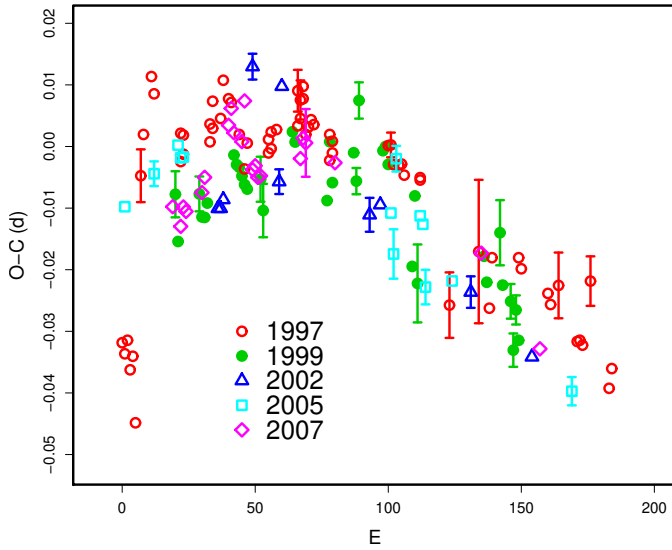


Fig. 153. Comparison of $O - C$ diagrams of DV UMa between different superoutbursts. The $O - C$'s were calculated against a period of 0.0888 d. Approximate cycle counts (E) after the start of the superoutburst were used.

the observations were rather sparse.

The 2005 and 2007 observations well covered the growing stage of superhumps (tables 256 and 257). As in other systems and as in 1997 superoutburst, the $O - C$'s of this evolutionary stage were negative. Regarding the 2007 superoutburst, we can determine $P_{\text{dot}} = -1.7(1.8) \times 10^{-5}$ after this evolutionary stage, corresponding to the stage B of the 1997 superoutburst. In summary, we did not find strong difference in the behavior of period variation between different superoutbursts (figure 153).

6.130. *ER Ursae Majoris*

The times of superhump maxima used to draw figure 26 are listed in tables 258 and 259.

6.131. *IY Ursae Majoris*

This eclipsing SU UMa-type dwarf nova has been well documented (Uemura et al. 2000; Patterson et al. 2000a). The superhump maxima were determined from observations outside the eclipses, as described in V2051 Oph.

Patterson et al. (2000a) reported a “normal” negative period derivative. We combined the reported times of superhump maxima with ours, by adding a systematic difference of 0.0028 d (presumably due to the difference in the procedure of determination of maxima) to the times of Patterson et al. (2000a). The resultant times are listed in table 260. We restricted the analysis to the interval before the rapid fading started, i.e. excluding times of late superhumps. The $O - C$ diagram was complex and was different from the one in Patterson et al. (2000a), in that the present diagram clearly showed a transition from a longer period to a stable period around $E = 23$ (stage A–B transition). The main difference in appearance between Patterson et al. (2000a) and ours was thus caused by the

Table 253. Superhump maxima of DV UMa (1997).

E	max ^a	error	$O - C$ ^b	N ^c
0	50548.4270	–	–0.0395	0
1	50548.5140	–	–0.0411	0
2	50548.6050	–	–0.0386	0
3	50548.6890	–	–0.0432	0
4	50548.7800	–	–0.0408	0
5	50548.8580	–	–0.0513	0
7	50549.0757	0.0043	–0.0107	80
8	50549.1712	0.0015	–0.0038	92
11	50549.4470	–	0.0063	0
12	50549.5330	–	0.0037	0
22	50550.4146	0.0007	–0.0003	47
22	50550.4100	–	–0.0049	0
23	50550.5031	0.0007	–0.0004	41
23	50550.5000	–	–0.0035	0
33	50551.3900	–	0.0009	0
33	50551.3929	0.0020	0.0038	41
34	50551.4810	–	0.0034	0
34	50551.4854	0.0017	0.0078	41
37	50551.7490	–	0.0057	0
38	50551.8440	–	0.0121	0
40	50552.0186	0.0005	0.0096	74
41	50552.1068	0.0005	0.0092	74
44	50552.3680	–	0.0047	0
46	50552.5400	–	–0.0004	0
47	50552.6330	–	0.0040	0
55	50553.3418	0.0007	0.0043	40
55	50553.3440	–	0.0065	0
56	50553.4313	0.0008	0.0053	43
56	50553.4340	–	0.0080	0
58	50553.6120	–	0.0089	0
66	50554.3230	–	0.0114	0
66	50554.3287	0.0034	0.0171	32
67	50554.4130	–	0.0128	0
67	50554.4160	0.0032	0.0158	41
68	50554.5070	–	0.0182	0
68	50554.5050	0.0013	0.0162	41
69	50554.5880	–	0.0107	0
70	50554.6780	–	0.0121	0
71	50554.7680	–	0.0135	0
72	50554.8560	–	0.0130	0
78	50555.3872	0.0012	0.0128	47
78	50555.3830	–	0.0086	0
79	50555.4749	0.0018	0.0119	47
79	50555.4730	–	0.0100	0
100	50557.3390	0.0014	0.0162	37
101	50557.4279	0.0020	0.0166	43
102	50557.5135	0.0015	0.0136	20
104	50557.6910	–	0.0140	0

^a BJD–2400000.

^b Against $max = 2450548.4665 + 0.088563E$.

^c Number of points used to determine the maximum.

^c $N = 0$ refers to Patterson et al. (2000b).

Table 253. Superhump maxima of DV UMa (1997). (continued)

E	max	error	$O - C$	N
105	50557.7800	–	0.0144	0
106	50557.8670	–	0.0128	0
112	50558.3994	0.0014	0.0139	43
112	50558.3990	–	0.0135	0
123	50559.3555	0.0053	–0.0042	34
134	50560.3410	0.0116	0.0071	29
138	50560.6870	–	–0.0012	0
139	50560.7840	–	0.0073	0
149	50561.6720	–	0.0097	0
150	50561.7590	–	0.0081	0
160	50562.6430	–	0.0065	0
161	50562.7300	–	0.0049	0
164	50562.9995	0.0053	0.0087	38
171	50563.6120	–	0.0013	0
172	50563.7010	–	0.0017	0
173	50563.7890	–	0.0011	0
176	50564.0658	0.0040	0.0123	76
183	50564.6700	–	–0.0035	0
184	50564.7620	–	–0.0000	0
194	50565.6190	–	–0.0287	0
206	50566.6600	–	–0.0504	0
207	50566.7490	–	–0.0500	0
208	50566.8320	–	–0.0555	0

lack of early-stage superhumps in Patterson et al. (2000a).

The P_{dot} during the later interval was much closer to zero than the global P_{dot} reported in Patterson et al. (2000a). The behavior after $E = 106$ was slightly different between ours and Patterson et al. (2000a). Our data suggested a shortening of the period while Patterson et al. (2000a) showed a steady increase. This may have been caused by the increasing signal of late superhumps, which predominated in later epochs, during the observation of Patterson et al. (2000a). Excluding $E < 23$ and $E \geq 106$, we obtained $P_{\text{dot}} = -1.8(2.2) \times 10^{-5}$.

We also analyzed the 2002, 2004 and 2006 superoutbursts (table 261, 262 and 263). The 2002 observation covered the middle-to-late part of the outburst. There was an apparent discontinuous transition to a shorter period around $E = 137$. Due to the gap in the observation, we could not significantly determine the P_{dot} before this transition. This 2004 observation covered the middle part to the latter half of the outburst. Although the initial stage of the 2006 superoutburst was observed, the superhump maxima incidentally fell amid the eclipses. We excluded most of the first two nights for calculating times of superhump maxima. The superhump profile at this stage was probably double-peaked. Such a feature may have reflected the growing stage of the superhumps and needs to be investigated in future superoutbursts. The $O - C$'s after $E > 221$ apparently showed a phase shift attributable to traditional late superhumps, as in the 2000 superoutburst. The periods given in table 2 were determined by excluding the maximum $E = 176$.

Table 254. Superhump maxima of DV UMa (1999).

E	max ^a	error	$O - C$ ^b	N ^c
0	51521.2279	0.0037	–0.0063	80
1	51521.3090	0.0010	–0.0138	121
9	51522.0272	0.0028	–0.0050	85
10	51522.1122	0.0011	–0.0086	140
11	51522.2010	0.0009	–0.0085	132
12	51522.2921	0.0010	–0.0061	142
22	51523.1879	0.0007	0.0031	149
23	51523.2751	0.0005	0.0017	138
24	51523.3635	0.0007	0.0014	130
25	51523.4509	0.0006	0.0001	47
26	51523.5383	0.0007	–0.0011	40
27	51523.6263	0.0009	–0.0017	26
32	51524.0720	0.0037	0.0006	42
33	51524.1557	0.0043	–0.0044	48
44	51525.1453	0.0014	0.0099	146
45	51525.2324	0.0015	0.0084	146
57	51526.2885	0.0017	0.0006	69
58	51526.3868	0.0015	0.0103	85
59	51526.4690	0.0010	0.0038	44
67	51527.1843	0.0010	0.0097	121
68	51527.2684	0.0021	0.0053	140
69	51527.3703	0.0029	0.0185	61
78	51528.1614	0.0011	0.0116	138
79	51528.2509	0.0007	0.0124	146
80	51528.3368	0.0007	0.0097	146
89	51529.1194	0.0018	–0.0057	137
90	51529.2196	0.0015	0.0059	143
91	51529.2942	0.0063	–0.0081	51
116	51531.5186	0.0014	–0.0003	38
117	51531.6032	0.0019	–0.0043	41
122	51532.0553	0.0053	0.0044	74
123	51532.1356	0.0017	–0.0040	161
126	51532.3993	0.0028	–0.0062	72
127	51532.4802	0.0027	–0.0140	28
128	51532.5755	0.0024	–0.0073	43
129	51532.6594	0.0019	–0.0121	41

^a BJD–2400000.

^b Against $max = 2451521.2342 + 0.088661E$.

^c Number of points used to determine the maximum.

Table 255. Superhump maxima of DV UMa (2002).

E	max ^a	error	$O - C^b$	N^c
0	52377.0138	0.0005	-0.0103	99
1	52377.1026	0.0004	-0.0101	145
2	52377.1928	0.0005	-0.0084	139
13	52378.1912	0.0021	0.0157	57
23	52379.0605	0.0020	-0.0006	73
24	52379.1648	0.0011	0.0151	43
57	52382.0744	0.0027	0.0021	100
61	52382.4312	0.0006	0.0046	34
95	52385.4362	0.0026	-0.0015	43
118	52387.4681	0.0008	-0.0066	49

^a BJD-2400000.^b Against $max = 2452377.0241 + 0.088564E$.^c Number of points used to determine the maximum.**Table 256.** Superhump maxima of DV UMa (2005).

E	max ^a	error	$O - C^b$	N^c
0	53413.2479	0.0006	-0.0102	165
11	53414.2300	0.0020	-0.0031	55
20	53415.0339	0.0002	0.0030	156
21	53415.1206	0.0003	0.0011	247
22	53415.2095	0.0003	0.0014	266
100	53422.1268	0.0012	0.0049	76
101	53422.2090	0.0040	-0.0016	68
102	53422.3133	0.0021	0.0140	68
111	53423.1032	0.0016	0.0062	181
112	53423.1906	0.0016	0.0050	159
113	53423.2692	0.0028	-0.0051	95
123	53424.1582	0.0008	-0.0025	144
168	53428.1363	0.0023	-0.0131	157

^a BJD-2400000.^b Against $max = 2453413.2581 + 0.088638E$.^c Number of points used to determine the maximum.**Table 257.** Superhump maxima of DV UMa (2007).

E	max ^a	error	$O - C^b$	N^c
0	54177.7552	0.0015	-0.0096	54
3	54178.0184	0.0004	-0.0124	237
4	54178.1104	0.0007	-0.0091	126
5	54178.1985	0.0005	-0.0097	197
11	54178.7343	0.0007	-0.0058	55
12	54178.8256	0.0008	-0.0032	38
21	54179.6333	0.0009	0.0065	10
22	54179.7248	0.0008	0.0094	13
23	54179.8096	0.0009	0.0056	13
26	54180.0746	0.0004	0.0045	118
27	54180.1700	0.0013	0.0113	60
30	54180.4252	0.0005	0.0005	211
31	54180.5147	0.0001	0.0013	744
32	54180.6016	0.0002	-0.0005	636
33	54180.6906	0.0003	-0.0001	316
48	54182.0254	0.0013	0.0048	98
49	54182.1176	0.0010	0.0082	108
50	54182.2056	0.0055	0.0076	47
61	54183.1792	0.0014	0.0058	72
116	54188.0485	0.0015	-0.0014	78
138	54189.9866	0.0020	-0.0139	101

^a BJD-2400000.^b Against $max = 2454177.7648 + 0.088664E$.^c Number of points used to determine the maximum.**Table 258.** Superhump maxima (1) of ER UMa (1995).

E	max ^a	error	$O - C^b$	N^c
0	49744.2521	0.0006	0.0027	16
1	49744.3196	0.0003	0.0045	31
14	49745.1720	0.0003	0.0022	21
15	49745.2371	0.0003	0.0015	23
16	49745.3010	0.0005	-0.0004	20
17	49745.3675	0.0002	0.0004	31
28	49746.0889	0.0004	-0.0014	30
29	49746.1560	0.0007	0.0000	22
31	49746.2860	0.0005	-0.0015	24
32	49746.3507	0.0003	-0.0025	30
43	49747.0719	0.0004	-0.0046	38
59	49748.1244	0.0017	-0.0040	18
60	49748.1906	0.0064	-0.0036	17
62	49748.3257	0.0016	0.0000	22
90	49750.1636	0.0012	-0.0030	21
91	49750.2351	0.0015	0.0028	31
107	49751.2878	0.0021	0.0035	21
121	49752.2090	0.0041	0.0042	24
122	49752.2798	0.0051	0.0094	25
123	49752.3260	0.0053	-0.0102	14

^a BJD-2400000.^b Against $max = 2449744.2494 + 0.065747E$.^c Number of points used to determine the maximum.

The 2007 superoutburst was caught by chance at $V = 14$. Judging from the superhump maxima (table 264), there was a clear decrease in the superhump period. In conjunction with the faintness, we probably observed the late stage of a superoutburst associated with a stage B-C transition. The nominal value $P_{\text{dot}} = -16.0(6.5) \times 10^{-5}$ would not be a good representative period derivative.

The 2009 superoutburst was well-observed during the middle-to-late stages (table 265). The $O - C$ diagram clearly depicts the presence of stages B and C. The first ($E = 0$ epoch probably corresponds to the stage A. Although orbital humps emerged after the rapid decline from the superoutburst plateau, no prominent traditional late superhumps were recorded (cf. the 2000 superoutburst, Patterson et al. 2000a).

A combined $O - C$ diagram drawn from all the superoutburst is presented in figure 154. The combined diagram appears to show stage B lasting for ~ 120 cycles with a positive P_{dot} . The duration of the stage B is com-

Table 259. Superhump maxima (2) of ER UMa (1995).

E	max ^a	error	$O - C^b$	N^c
58	49748.0946	0.0004	0.0319	15
59	49748.1542	0.0035	0.0257	15
60	49748.2242	0.0033	0.0300	15
61	49748.2885	0.0010	0.0285	14
62	49748.3510	0.0008	0.0253	22
76	49749.2744	0.0011	0.0282	16
90	49750.1782	0.0018	0.0115	18
91	49750.2561	0.0009	0.0237	16
120	49752.1620	0.0006	0.0230	42
121	49752.2282	0.0008	0.0234	24
167	49755.2366	0.0006	0.0074	31
168	49755.3038	0.0008	0.0089	30
183	49756.2848	0.0004	0.0037	31
184	49756.3525	0.0006	0.0057	31
197	49757.1990	0.0017	-0.0026	12
229	49759.2950	0.0005	-0.0105	22

^a BJD-2400000.^b Against $max = 2449744.2494 + 0.065747E$.^c Number of points used to determine the maximum.

patible that during the 2009 superoutburst, although the behavior of the 2009 $O - C$ looks slightly different from others during its early stage. The likely presence of a positive P_{dot} , then would suggest the similarity to NSV 4838 (Imada et al. 2009b). The lack of a positive P_{dot} in individual superoutbursts may have been a result from the deficiency of observations around the end of the stage B. Some of superoutbursts seem to show stage C superhumps while others tend to show humps resembling traditional late superhumps. Future observations of this object at these epochs will be particularly important.

6.132. *KS Ursae Majoris*

KS UMa (=SBS1017+533) was originally discovered as an emission-line object (Balayan 1997). In 1998, the object was found to be in outburst during a spectroscopic survey (P. Garnavich, vsnet-alert 1441). T. Vanmunster reported the detection of superhumps with a period of 0.069(1) d during this outburst (CVC 161, also in vsnet-alert 1448). Hazen, Garnavich (1999) surveyed historical outbursts. Jiang et al. (2000) also selected this CV from the ROSAT all-sky survey.

Olech et al. (2003) reported on the period variation of superhumps in KS UMa. We had more extensive data on the same superoutburst, notably covering the earlier stage than in Olech et al. (2003). Table 266 presents the combined list of times of superhump maxima, after adding a systematic difference of 0.003 d to Olech et al. (2003). The entire data now clearly show a sharp transition from a longer period in the early stage (before $E = 15$), stabilized segment with a slightly positive P_{dot} , and followed by a sharp transition to a shorter period after $E = 95$. The pattern of period change can be reasonably interpreted as stages A-C. The negative P_{dot} in Olech et al. (2003) was

Table 260. Superhump maxima of IY UMa (2000).

E	max ^a	error	$O - C^b$	N^c
0	51561.2170	0.0006	-0.0116	77
1	51561.2956	0.0003	-0.0089	120
2	51561.3719	0.0012	-0.0084	51
13	51562.2164	0.0007	0.0014	145
14	51562.2935	0.0011	0.0027	156
14	51562.2878	-	-0.0030	0
15	51562.3661	0.0010	-0.0006	157
15	51562.3646	-	-0.0021	0
16	51562.4414	0.0011	-0.0012	35
16	51562.4428	-	0.0003	0
17	51562.5173	0.0013	-0.0011	34
17	51562.5177	-	-0.0007	0
18	51562.5940	0.0018	-0.0003	34
18	51562.5955	-	0.0012	0
19	51562.6716	0.0010	0.0015	26
19	51562.6730	-	0.0028	0
22	51562.9033	0.0016	0.0056	13
23	51562.9797	0.0017	0.0061	19
23	51562.9758	-	0.0022	0
24	51563.0507	-	0.0012	0
27	51563.2799	0.0009	0.0027	149
28	51563.3557	0.0005	0.0027	135
33	51563.7371	-	0.0048	0
34	51563.8133	-	0.0051	0
35	51563.8874	-	0.0033	0
36	51563.9641	-	0.0041	0
37	51564.0385	-	0.0027	0
41	51564.3425	-	0.0032	0
42	51564.4130	-	-0.0022	0
42	51564.4133	0.0015	-0.0019	81
43	51564.4913	-	0.0003	0
43	51564.4929	0.0099	0.0018	36
44	51564.5680	0.0019	0.0011	31
44	51564.5738	-	0.0069	0
48	51564.8713	0.0015	0.0009	12
49	51564.9483	-	0.0020	0
59	51565.7068	-	0.0018	0
60	51565.7814	-	0.0006	0
69	51566.4643	0.0066	0.0006	23
72	51566.6989	-	0.0076	0
74	51566.8463	-	0.0033	0
75	51566.9216	-	0.0027	0
76	51566.9968	-	0.0020	0
77	51567.0729	-	0.0023	0
79	51567.2199	-	-0.0025	0
79	51567.2168	0.0044	-0.0056	19
80	51567.2977	-	-0.0005	0
80	51567.2957	0.0018	-0.0025	35
81	51567.3727	-	-0.0014	0
81	51567.3701	0.0015	-0.0041	49

^a BJD-2400000.^b Against $max = 2451561.22862 + 0.075870E$.^c Number of points used to determine the maximum. $N = 0$ refers to Patterson et al. (2000a).

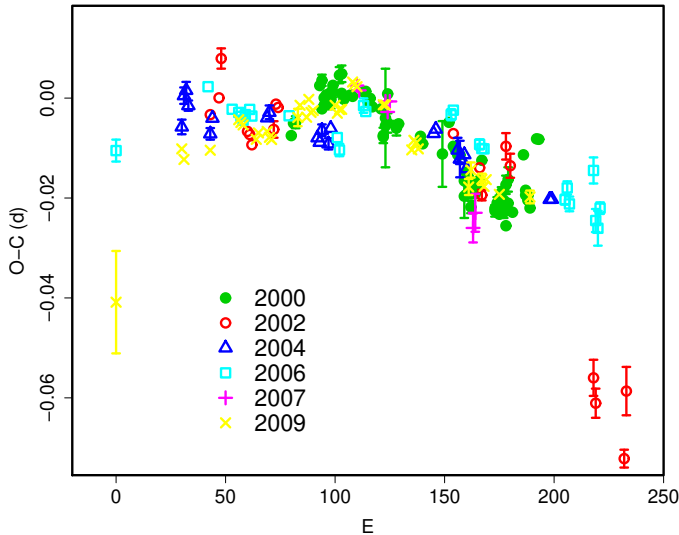


Fig. 154. Comparison of $O-C$ diagrams of IY UMa between different superoutbursts. A period of 0.07610 d was used to draw this figure. Approximate cycle counts (E) after the start of the superoutburst were used.

a result of the fit to the stages B and C together. Our data yielded $P_{\text{dot}} = +2.2(1.1) \times 10^{-5}$ for the stage B.

We also observed the 2007 superoutburst (table 267). The observation covered the middle-to-late plateau stage. Excluding the last point (taken during the rapid fading stage), we obtained $P_{\text{dot}} = +1.5(1.9) \times 10^{-5}$, probably corresponding to the stage B of the 2003 superoutburst.

The $O-C$ behavior was slightly different between the 2003 and 2007 superoutbursts (figure 155). This may have been a result of a longer duration of the 2003 superoutburst than the 2007 one.

6.133. *KV Ursae Majoris*

This object is a BHXT. The times of superhump maxima, a reanalysis of Uemura et al. (2002c), used for drawing figure 30 (subsection 4.11) are listed in table 268.

The $O-C$ diagram was composed of three stages as in SU UMa-type dwarf novae: stage A ($E \leq 124$) with a mean $P_{\text{SH}} = 0.17082(7)$ d, stage B for $124 \leq E \leq 348$ (mean $P_{\text{SH}} (P_1) = 0.17056(3)$ d and $P_{\text{dot}} = +0.9(0.6) \times 10^{-5}$) and stage C for $E \geq 238$ (mean $P_{\text{SH}} (P_2) = 0.17038(3)$ d). The global P_{dot} was $-0.43(0.05) \times 10^{-5}$.

6.134. *MR Ursae Majoris*

MR UMa = 1RXP J113123+4322.5 is an ROSAT-selected CV (Wei et al. 1997), which underwent the first secure recorded outburst in 2002 (vsnet-alert 7221). We observed the middle-to-late stage of the 2002 superoutburst (table 269, figure 7). The data clearly indicated a stage B–C transition around $E = 80$. The P_{dot} of the stage B was $+9.3(1.2) \times 10^{-5}$. The behavior was very similar during the 2003 and 2007 superoutbursts (tables 270, 271; figure 156), with $P_{\text{dot}} = +6.0(2.3) \times 10^{-5}$ (2003, $E \leq 84$) and $P_{\text{dot}} = +3.8(1.6) \times 10^{-5}$ (2007, $E \leq 79$). For more

Table 260. Superhump maxima of IY UMa (2000) (continued).

E	max	error	$O-C$	N
82	51567.4456	–	–0.0044	0
82	51567.4429	0.0012	–0.0070	88
83	51567.5234	–	–0.0025	0
83	51567.5235	0.0009	–0.0024	136
84	51567.5978	–	–0.0039	0
85	51567.6748	–	–0.0028	0
86	51567.7528	–	–0.0007	0
87	51567.8328	–	0.0035	0
93	51568.2798	–	–0.0048	0
93	51568.2793	0.0012	–0.0053	119
94	51568.3558	–	–0.0046	0
94	51568.3570	0.0012	–0.0035	158
95	51568.4308	–	–0.0055	0
95	51568.4331	0.0014	–0.0032	118
96	51568.5078	–	–0.0044	0
96	51568.5113	0.0010	–0.0009	70
97	51568.5858	–	–0.0022	0
97	51568.5834	0.0011	–0.0047	71
98	51568.6568	–	–0.0071	0
98	51568.6650	0.0018	0.0011	76
99	51568.7374	–	–0.0024	0
99	51568.7422	0.0024	0.0024	43
101	51568.8878	–	–0.0037	0
106	51569.2798	–	0.0089	0
107	51569.3488	–	0.0021	0
107	51569.3478	0.0008	0.0011	85
108	51569.4238	–	0.0012	0
108	51569.4229	0.0008	0.0003	86
109	51569.4975	0.0009	–0.0010	62
112	51569.7396	–	0.0135	0
113	51569.8156	–	0.0136	0

information of the 2003, 2004 and 2005 superoutbursts, see Tanabe, Koizumi (2007), although they did not distinguish different stages of period evolution.

6.135. *CU Velorum*

Although CU Vel had long been known as an SU UMa-type dwarf nova (Vogt 1980), the details of the reported superhump period (0.0799 d, Ritter 1984) was not reported in a solid publication. Mennickent, Diaz (1996) reported an orbital period of 0.0785 d.

We observed the 2002 superoutburst. The times of superhumps maxima are listed in table 272. The object clearly showed the stage A development with a longer period. Excluding this epoch ($E = 0$), we obtained $P_{\text{dot}} = -8.4(1.4) \times 10^{-5}$ for the stage B. A PDM analysis yielded a mean superhump period of 0.080789(5) d (figure 157).

6.136. *HS Virginis*

We reanalyzed the data in Kato et al. (1998b). Double-wave modulations were observed on 1996 March 18 (BJD 2450161) during the fading stage from the superoutburst plateau (the same feature was also recorded by Patterson

Table 261. Superhump maxima of IY UMa (2002).

E	\max^a	error	$O - C^b$	N^c
0	52405.7582	0.0005	-0.0105	50
4	52406.0660	0.0009	-0.0059	119
5	52406.1500	0.0020	0.0023	95
17	52407.0486	0.0004	-0.0083	423
18	52407.1241	0.0005	-0.0086	452
19	52407.1981	0.0009	-0.0103	189
29	52407.9622	0.0017	-0.0039	163
30	52408.0434	0.0005	0.0015	263
31	52408.1188	0.0005	0.0011	233
111	52414.2016	0.0005	0.0222	328
123	52415.1079	0.0009	0.0194	160
124	52415.1785	0.0011	0.0142	254
135	52416.0254	0.0026	0.0276	235
137	52416.1737	0.0024	0.0244	174
175	52419.0231	0.0036	-0.0056	193
176	52419.0941	0.0029	-0.0103	117
189	52420.0723	0.0018	-0.0171	75
190	52420.1619	0.0048	-0.0033	103
215	52422.0515	0.0024	-0.0079	117
228	52423.0235	0.0042	-0.0210	80

^a BJD-2400000.^b Against $\max = 2452405.7688 + 0.075771E$.^c Number of points used to determine the maximum.**Table 262.** Superhump maxima of IY UMa (2004).

E	\max^a	error	$O - C^b$	N^c
0	53332.4726	0.0015	-0.0043	31
1	53332.5550	0.0016	0.0020	33
2	53332.6321	0.0017	0.0032	22
3	53332.7052	0.0010	0.0002	35
13	53333.4605	0.0012	-0.0046	91
14	53333.5398	0.0002	-0.0013	137
39	53335.4423	0.0008	0.0009	62
40	53335.5195	0.0014	0.0021	35
62	53337.1886	0.0003	-0.0011	146
63	53337.2638	0.0006	-0.0019	192
64	53337.3424	0.0012	0.0006	136
67	53337.5679	0.0011	-0.0018	60
68	53337.6471	0.0007	0.0014	59
115	53341.2228	0.0004	0.0044	206
116	53341.2998	0.0003	0.0054	216
126	53342.0566	0.0025	0.0021	129
127	53342.1309	0.0037	0.0004	76
128	53342.2067	0.0003	0.0002	192
129	53342.2840	0.0004	0.0014	194
130	53342.3573	0.0007	-0.0013	122
168	53345.2429	0.0005	-0.0041	135
169	53345.3190	0.0006	-0.0040	134

^a BJD-2400000.^b Against $\max = 2453332.4769 + 0.076012E$.^c Number of points used to determine the maximum.**Table 263.** Superhump maxima of IY UMa (2006).

E	\max^a	error	$O - C^b$	N^c
0	53834.3769	0.0022	-0.0127	90
42	53837.5859	0.0003	0.0039	90
53	53838.4185	0.0001	0.0003	29
56	53838.6462	0.0002	-0.0001	72
57	53838.7215	0.0003	-0.0008	70
58	53838.7968	0.0003	-0.0014	72
59	53838.8740	0.0006	-0.0002	64
61	53839.0273	0.0006	0.0010	52
62	53839.1021	0.0004	-0.0002	91
79	53840.3958	0.0008	0.0013	48
101	53842.0657	0.0007	-0.0011	92
102	53842.1393	0.0012	-0.0035	87
113	53842.9852	0.0014	0.0064	85
114	53843.0602	0.0010	0.0053	92
153	53846.0274	0.0011	0.0081	80
154	53846.1044	0.0006	0.0091	111
166	53847.0108	0.0010	0.0033	38
167	53847.0860	0.0009	0.0026	76
168	53847.1621	0.0005	0.0026	214
205	53849.9676	0.0010	-0.0043	93
206	53850.0461	0.0013	-0.0018	90
207	53850.1190	0.0015	-0.0050	92
218	53850.9628	0.0026	0.0027	92
219	53851.0288	0.0023	-0.0072	147
220	53851.1034	0.0035	-0.0087	123
221	53851.1835	0.0012	-0.0046	84
259	53854.0846	0.0032	0.0081	98
312	53858.1018	0.0008	-0.0033	30

^a BJD-2400000.^b Against $\max = 2453834.3896 + 0.076011E$.^c Number of points used to determine the maximum.**Table 264.** Superhump maxima of IY UMa (2007).

E	\max^a	error	$O - C^b$	N^c
0	54134.2161	0.0002	-0.0017	179
1	54134.2913	0.0003	-0.0021	190
13	54135.2023	0.0006	0.0019	188
14	54135.2763	0.0006	0.0003	189
15	54135.3545	0.0007	0.0030	159
53	54138.2209	0.0029	-0.0025	102
54	54138.3001	0.0038	0.0011	134

^a BJD-2400000.^b Against $\max = 2454134.2178 + 0.075577E$.^c Number of points used to determine the maximum.

Table 265. Superhump maxima of IY UMa (2009).

E	\max^a	error	$O - C^b$	N^c
0	54934.6870	0.0102	-0.0346	51
30	54937.0007	0.0003	-0.0034	144
31	54937.0746	0.0003	-0.0055	201
43	54937.9897	0.0007	-0.0034	119
56	54938.9851	0.0003	0.0029	123
57	54939.0607	0.0002	0.0024	126
58	54939.1363	0.0003	0.0019	82
64	54939.5900	0.0007	-0.0009	84
65	54939.6674	0.0002	0.0004	122
69	54939.9721	0.0003	0.0008	83
70	54940.0470	0.0004	-0.0004	123
71	54940.1226	0.0007	-0.0008	108
83	54941.0402	0.0017	0.0038	104
84	54941.1188	0.0009	0.0063	97
87	54941.3447	0.0004	0.0039	55
88	54941.4244	0.0004	0.0075	70
89	54941.4979	0.0003	0.0049	69
90	54941.5743	0.0003	0.0053	73
100	54942.3364	0.0003	0.0065	58
101	54942.4109	0.0002	0.0050	144
102	54942.4877	0.0003	0.0057	142
103	54942.5639	0.0005	0.0058	68
108	54942.9499	0.0008	0.0113	53
109	54943.0255	0.0006	0.0109	88
110	54943.1011	0.0004	0.0104	62
122	54944.0107	0.0005	0.0070	86
123	54944.0868	0.0005	0.0070	88
135	54944.9910	0.0004	-0.0018	177
136	54945.0690	0.0003	0.0001	213
137	54945.1446	0.0006	-0.0004	79
138	54945.2195	0.0008	-0.0015	80
161	54946.9621	0.0016	-0.0088	44
162	54947.0416	0.0015	-0.0054	61
167	54947.4203	0.0011	-0.0071	72
168	54947.4950	0.0008	-0.0085	70
169	54947.5724	0.0008	-0.0072	64
175	54948.0261	0.0008	-0.0100	139
189	54949.0909	0.0013	-0.0103	191

^a BJD-2400000.

^b Against $\max = 2454934.7216 + 0.076083E$.

^c Number of points used to determine the maximum.

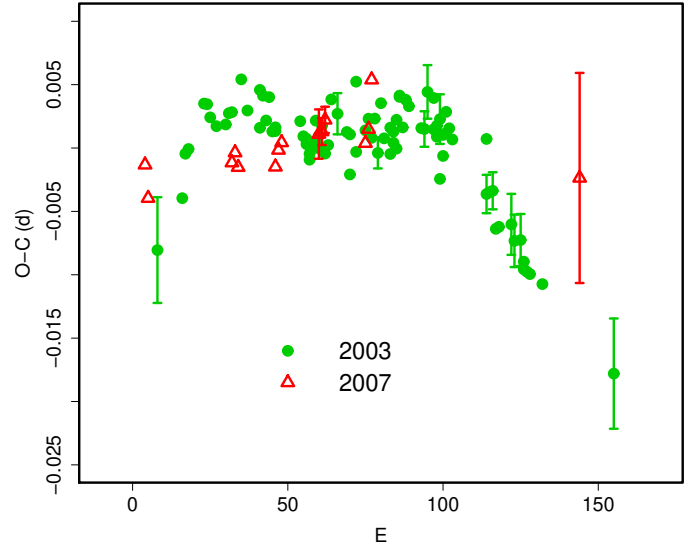


Fig. 155. Comparison of $O - C$ diagrams of KS UMa between different superoutbursts. A period of 0.07019 d was used to draw this figure. Approximate cycle counts (E) after the start of the superoutburst were used.

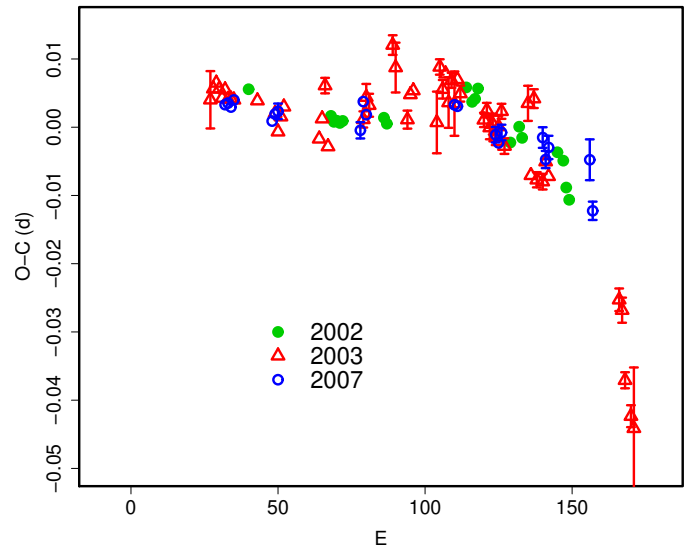


Fig. 156. Comparison of $O - C$ diagrams of MR UMa between different superoutbursts. A period of 0.06512 d was used to draw this figure. Approximate cycle counts (E) after the start of the 2007 superoutburst were used. Since the starts of the 2002 and 2003 superoutburst were not well constrained, we shifted the $O - C$ diagrams to best fit the 2007 one.

Table 266. Superhump maxima of KS UMa (2003).

E	max ^a	error	$O - C^b$	N^c
0	52690.0021	0.0042	-0.0128	129
8	52690.5677	0.0005	-0.0081	69
9	52690.6414	0.0003	-0.0045	114
10	52690.7120	0.0002	-0.0041	114
15	52691.0665	0.0002	-0.0001	153
16	52691.1366	0.0002	-0.0001	179
17	52691.2058	0.0002	-0.0011	217
19	52691.3455	0.0003	-0.0017	180
22	52691.5562	0.0002	-0.0013	78
23	52691.6273	0.0002	-0.0004	113
24	52691.6975	0.0002	-0.0002	115
27	52691.9107	0.0008	0.0026	75
29	52692.0486	0.0003	0.0003	126
33	52692.3280	0.0009	-0.0008	64
33	52692.331	-	0.0022	0
34	52692.4007	0.0004	0.0018	93
35	52692.4690	0.0003	-0.0001	167
36	52692.541	-	0.0018	0
37	52692.6085	0.0004	-0.0008	114
38	52692.6787	0.0003	-0.0007	115
38	52692.679	-	-0.0004	0
46	52693.241	-	0.0006	0
47	52693.310	-	-0.0005	0
48	52693.3796	0.0008	-0.0010	82
48	52693.380	-	-0.0006	0
49	52693.4485	0.0008	-0.0022	97
49	52693.449	-	-0.0017	0
50	52693.520	-	-0.0009	0
51	52693.5902	0.0006	-0.0008	139
51	52693.592	-	0.0010	0
52	52693.6600	0.0004	-0.0011	142
52	52693.661	-	-0.0001	0
53	52693.7320	0.0004	0.0008	117
54	52693.8000	0.0007	-0.0014	28
55	52693.8708	0.0008	-0.0006	32
56	52693.9446	0.0009	0.0030	30
58	52694.0839	0.0016	0.0020	96
61	52694.293	-	0.0008	0
62	52694.3598	0.0009	-0.0025	73
62	52694.363	-	0.0007	0
64	52694.5075	0.0009	0.0050	40
64	52694.502	-	-0.0005	0
67	52694.7143	0.0008	0.0014	32
68	52694.7854	0.0007	0.0024	32
69	52694.8541	0.0007	0.0009	33
70	52694.9258	0.0008	0.0025	32
71	52694.9932	0.0012	-0.0001	108
72	52695.0674	0.0005	0.0039	139
73	52695.1348	0.0008	0.0011	190
75	52695.2739	0.0007	0.0001	132
75	52695.276	-	0.0021	0

^a BJD-2400000.^b Against $max = 2452690.0148 + 0.070120E$.^c Number of points used to determine the maximum. $N = 0$ refers to Olech et al. (2003).**Table 266.** Superhump maxima of KS UMa (2003) (continued).

E	max	error	$O - C$	N
76	52695.3459	0.0005	0.0019	168
76	52695.345	-	0.0010	0
77	52695.4147	0.0008	0.0006	97
77	52695.417	-	0.0029	0
78	52695.4891	0.0004	0.0049	148
78	52695.489	-	0.0048	0
79	52695.5568	0.0006	0.0024	118
80	52695.6292	0.0005	0.0047	107
81	52695.6988	0.0006	0.0042	102
85	52695.9779	0.0008	0.0028	264
86	52696.0480	0.0014	0.0028	129
87	52696.1211	0.0021	0.0058	71
89	52696.2585	0.0008	0.0030	139
89	52696.261	-	0.0054	0
90	52696.3281	0.0005	0.0025	248
90	52696.329	-	0.0033	0
91	52696.3997	0.0020	0.0039	74
91	52696.395	-	-0.0008	0
92	52696.4687	0.0007	0.0027	73
92	52696.467	-	0.0011	0
93	52696.5407	0.0007	0.0046	71
93	52696.539	-	0.0030	0
94	52696.6096	0.0006	0.0034	93
95	52696.6789	0.0007	0.0026	92
106	52697.4467	0.0015	-0.0009	104
106	52697.451	-	0.0034	0
107	52697.517	-	-0.0007	0
108	52697.5873	0.0015	-0.0006	51
109	52697.6545	0.0008	-0.0035	102
110	52697.7248	0.0007	-0.0033	43
114	52698.0058	0.0024	-0.0028	34
115	52698.0747	0.0021	-0.0040	55
117	52698.2151	0.0021	-0.0038	220
118	52698.283	-	-0.0060	0
118	52698.2836	0.0007	-0.0054	306
119	52698.353	-	-0.0062	0
120	52698.423	-	-0.0063	0
124	52698.7030	0.0008	-0.0068	49
147	52700.3103	0.0044	-0.0123	27

Table 267. Superhump maxima of KS UMa (2007).

E	max ^a	error	$O - C^b$	N^c
0	54148.1875	0.0005	-0.0003	65
1	54148.2550	0.0003	-0.0030	97
28	54150.1530	0.0003	-0.0007	94
29	54150.2240	0.0003	0.0001	102
30	54150.2930	0.0007	-0.0011	59
42	54151.1353	0.0005	-0.0013	97
43	54151.2068	0.0005	-0.0000	101
44	54151.2776	0.0007	0.0005	33
56	54152.1206	0.0019	0.0010	42
57	54152.1909	0.0011	0.0012	103
58	54152.2621	0.0010	0.0021	83
71	54153.1727	0.0005	-0.0000	102
72	54153.2440	0.0006	0.0010	103
73	54153.3181	0.0009	0.0049	53
140	54158.0130	0.0083	-0.0042	103

^a BJD-2400000.

^b Against $max = 2454148.1878 + 0.070210E$.

^c Number of points used to determine the maximum.

Table 268. Superhump maxima of KV UMa (2000).

E	max ^a	error	$O - C^b$	N^c
0	51634.6924	0.0049	-0.0016	262
6	51635.6902	0.0076	-0.0269	269
7	51635.8547	0.0029	-0.0329	332
9	51636.2067	0.0026	-0.0219	339
11	51636.5675	0.0061	-0.0022	139
12	51636.7238	0.0016	-0.0163	322
13	51636.8721	0.0034	-0.0386	256
44	51642.1861	0.0060	-0.0106	216
47	51642.7033	0.0030	-0.0050	302
50	51643.2040	0.0035	-0.0159	319
67	51646.1234	0.0032	0.0047	301
68	51646.2830	0.0090	-0.0062	183
73	51647.1499	0.0029	0.0081	291
74	51647.3038	0.0084	-0.0085	204
79	51648.1637	0.0067	-0.0012	116
97	51651.2340	0.0034	-0.0002	303
124	51655.8592	0.0030	0.0209	91
143	51659.0872	0.0021	0.0091	207
157	51661.4826	0.0014	0.0172	423
168	51663.3514	0.0015	0.0103	329
169	51663.5266	0.0024	0.0150	258
170	51663.6969	0.0021	0.0148	325
174	51664.3556	0.0013	-0.0086	253
176	51664.7106	0.0021	0.0054	414
192	51667.4434	0.0016	0.0099	255
196	51668.1256	0.0022	0.0100	339
197	51668.2866	0.0059	0.0005	169
198	51668.4571	0.0048	0.0005	136
208	51670.1646	0.0110	0.0027	200
225	51673.0836	0.0022	0.0230	336
231	51674.0974	0.0025	0.0137	330
288	51683.8159	0.0039	0.0126	213
301	51686.0379	0.0036	0.0178	317
302	51686.2179	0.0144	0.0273	159
313	51688.0759	0.0041	0.0096	330
319	51689.1095	0.0027	0.0201	341
325	51690.1186	0.0049	0.0061	325
348	51694.0587	0.0025	0.0242	268
366	51697.1087	0.0167	0.0049	73
383	51700.0164	0.0016	0.0138	342
384	51700.1707	0.0033	-0.0024	191
389	51701.0352	0.0018	0.0095	249
395	51702.0577	0.0018	0.0089	340
401	51703.0799	0.0019	0.0080	327
448	51711.0806	0.0053	-0.0058	273
471	51715.0013	0.0033	-0.0070	283
524	51724.0308	0.0039	-0.0150	249
565	51731.0189	0.0108	-0.0181	249
571	51732.0578	0.0068	-0.0024	178
606	51737.9900	0.0041	-0.0383	160
641	51743.9930	0.0062	-0.0034	256
647	51744.9802	0.0184	-0.0394	232

^a BJD-2400000.

^b Against $max = 2451634.6939 + 0.170519E$.

^c Number of points used to determine the maximum.

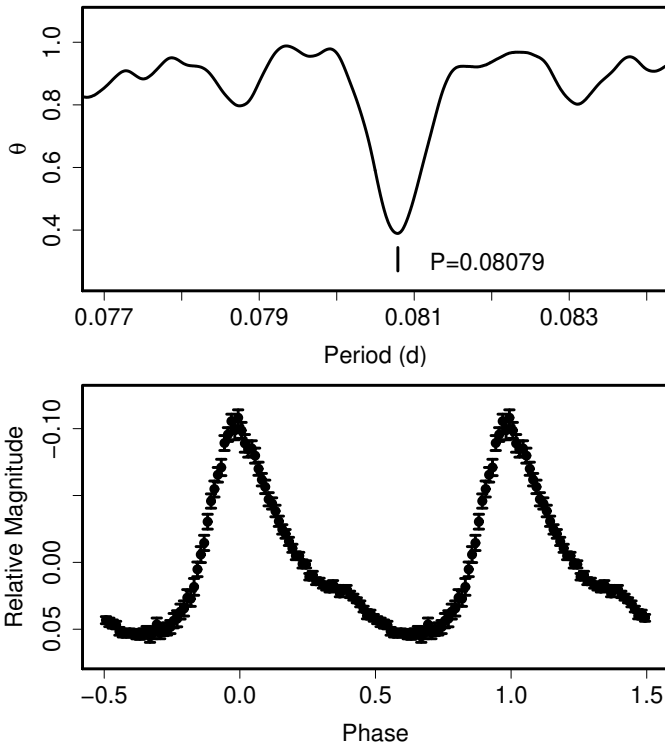


Fig. 157. Superhumps in CU Vel (2002). (Upper): PDM analysis. (Lower): Phase-averaged profile.

Table 269. Superhump maxima of MR UMa (2002).

E	max ^a	error	$O - C^b$	N^c
0	52340.2579	0.0002	0.0003	123
28	52342.0774	0.0003	-0.0013	150
29	52342.1416	0.0003	-0.0021	166
30	52342.2069	0.0002	-0.0019	277
31	52342.2717	0.0002	-0.0021	333
32	52342.3371	0.0004	-0.0018	122
46	52343.2493	0.0003	-0.0002	329
47	52343.3135	0.0003	-0.0010	203
74	52345.0771	0.0007	0.0065	120
76	52345.2052	0.0006	0.0045	76
77	52345.2708	0.0007	0.0050	125
78	52345.3374	0.0006	0.0066	121
89	52346.0458	0.0006	-0.0004	74
92	52346.2435	0.0007	0.0022	120
93	52346.3070	0.0007	0.0006	117
105	52347.0863	0.0006	-0.0006	109
107	52347.2153	0.0007	-0.0016	118
108	52347.2765	0.0006	-0.0055	115
109	52347.3398	0.0005	-0.0072	89

^a BJD-2400000.^b Against $max = 2452340.2576 + 0.065041E$.^c Number of points used to determine the maximum.

et al. 2003). These modulations were probably associated with the manifestation of traditional late superhumps. We listed times of maxima of ordinary superhumps in table 273 and secondary maxima in table 274. The agreement of periods independently determined from these two sets strengthens the identification of the latter as being traditional late superhumps. Since Kato et al. (1998b) did not take into account the present knowledge in period variation and late superhumps, their period was contaminated by these phenomena. The mean P_{SH} for $23 \leq E \leq 99$ was 0.08006(3) d, giving a fractional period excess of 4.1 %, slightly smaller than the previous estimate. The global P_{dot} was $-18.3(3.8) \times 10^{-5}$, which is apparently affected by the stage A evolution ($E \leq 23$).

The analysis of the 2008 superoutburst (table 275) during its middle-to-late stage yielded a period of 0.08003(3) d, in good agreement with the above analysis of the 1996 superoutburst.

6.137. HV *Virginis*

Analyses of superhumps of this WZ Sge-type dwarf nova have been well documented (Kato et al. 2001d; Ishioka et al. 2003). We present our new observation of the 2008 superoutburst. Only ordinary superhumps are treated here (table 276). The $O - C$ diagram resembles those of many systems with short superhump periods, consisting of stages A-C (note, however, these stages were preceded by a stage of early superhumps in this object). The P_{dot} of the stage B was $+7.1(1.9) \times 10^{-5}$ ($18 \leq E \leq 157$). The value is in good agreement with those obtained during previous superoutbursts: $+7(1) \times 10^{-5}$ (Ishioka et al. 2003)

Table 270. Superhump maxima of MR UMa (2003).

E	max ^a	error	$O - C^b$	N^c
0	52711.9773	0.0042	-0.0067	75
1	52712.0441	0.0003	-0.0049	250
2	52712.1100	0.0002	-0.0039	424
3	52712.1743	0.0002	-0.0046	456
4	52712.2381	0.0004	-0.0058	209
5	52712.3044	0.0007	-0.0044	166
6	52712.3681	0.0006	-0.0056	96
7	52712.4333	0.0003	-0.0054	66
8	52712.4983	0.0005	-0.0053	51
16	52713.0191	0.0006	-0.0041	108
22	52713.4080	0.0005	-0.0049	80
23	52713.4704	0.0004	-0.0075	59
24	52713.5377	0.0004	-0.0051	63
25	52713.6043	0.0007	-0.0035	64
37	52714.3810	0.0007	-0.0061	68
38	52714.4491	0.0007	-0.0030	68
39	52714.5191	0.0011	0.0020	61
40	52714.5753	0.0006	-0.0067	57
52	52715.3607	0.0012	-0.0007	68
53	52715.4291	0.0019	0.0027	68
54	52715.4930	0.0017	0.0017	39
62	52716.0228	0.0014	0.0119	79
63	52716.0846	0.0036	0.0088	82
67	52716.3375	0.0013	0.0018	43
68	52716.4062	0.0008	0.0057	94
69	52716.4719	0.0003	0.0064	79
77	52716.9882	0.0045	0.0031	105
78	52717.0615	0.0011	0.0114	104
79	52717.1233	0.0014	0.0083	134
80	52717.1907	0.0006	0.0108	187
81	52717.2516	0.0037	0.0067	122
82	52717.3200	0.0011	0.0101	134
83	52717.3817	0.0047	0.0069	69
84	52717.4504	0.0006	0.0106	68
85	52717.5134	0.0012	0.0087	67
93	52718.0305	0.0010	0.0062	230
94	52718.0971	0.0011	0.0078	150
95	52718.1596	0.0017	0.0054	154
96	52718.2253	0.0015	0.0061	185
97	52718.2884	0.0011	0.0043	235
98	52718.3552	0.0016	0.0061	94
99	52718.4225	0.0011	0.0085	67
100	52718.4825	0.0011	0.0036	68
108	52719.0098	0.0026	0.0112	157
109	52719.0643	0.0009	0.0008	114
110	52719.1407	0.0014	0.0122	120
111	52719.1939	0.0011	0.0005	100
113	52719.3239	0.0011	0.0006	191
114	52719.3919	0.0007	0.0037	130
115	52719.4549	0.0005	0.0017	130
139	52720.9997	0.0017	-0.0123	68
140	52721.0633	0.0018	-0.0136	100
141	52721.1181	0.0012	-0.0237	68
143	52721.2431	0.0016	-0.0287	110
144	52721.3065	0.0089	-0.0303	107

^a BJD-2400000.^b Against $max = 2452711.9840 + 0.064949E$.^c Number of points used to determine the maximum.

Table 271. Superhump maxima of MR UMa (2007).

E	\max^a	error	$O - C^b$	N^c
0	54207.5744	0.0004	-0.0008	26
1	54207.6398	0.0005	-0.0005	34
2	54207.7043	0.0003	-0.0010	34
3	54207.7705	0.0006	0.0001	23
16	54208.6139	0.0006	-0.0021	34
17	54208.6801	0.0008	-0.0010	34
18	54208.7456	0.0011	-0.0006	21
46	54210.5662	0.0012	-0.0014	30
47	54210.6355	0.0007	0.0028	39
48	54210.6987	0.0009	0.0010	29
78	54212.6537	0.0007	0.0045	38
79	54212.7186	0.0007	0.0043	40
92	54213.5610	0.0011	0.0010	34
93	54213.6250	0.0008	-0.0001	39
94	54213.6916	0.0011	0.0015	35
108	54214.6025	0.0015	0.0017	44
109	54214.6644	0.0013	-0.0014	44
110	54214.7313	0.0017	0.0004	39
124	54215.6412	0.0030	-0.0005	43
125	54215.6989	0.0013	-0.0079	44

^a BJD-2400000.^b Against $\max = 2454207.5752 + 0.065052E$.^c Number of points used to determine the maximum.**Table 272.** Superhump maxima of CU Vel (2002).

E	\max^a	error	$O - C^b$	N^c
0	52620.2188	0.0003	-0.0205	239
22	52622.0161	0.0007	-0.0012	20
35	52623.0687	0.0002	0.0007	192
36	52623.1495	0.0002	0.0006	408
37	52623.2310	0.0003	0.0013	295
49	52624.2007	0.0002	0.0011	146
50	52624.2806	0.0004	0.0002	155
51	52624.3687	0.0003	0.0075	124
59	52625.0117	0.0003	0.0040	173
60	52625.0935	0.0004	0.0049	220
61	52625.1785	0.0003	0.0091	158
72	52626.0623	0.0002	0.0038	304
73	52626.1437	0.0002	0.0044	456
74	52626.2257	0.0002	0.0056	506
75	52626.3052	0.0003	0.0043	197
97	52628.0777	0.0002	-0.0013	111
98	52628.1591	0.0002	-0.0007	184
109	52629.0445	0.0003	-0.0044	281
110	52629.1249	0.0002	-0.0048	427
111	52629.2062	0.0002	-0.0043	301
122	52630.0946	0.0006	-0.0049	116
123	52630.1752	0.0005	-0.0051	113

^a BJD-2400000.^b Against $\max = 2452620.2393 + 0.080822E$.^c Number of points used to determine the maximum.**Table 273.** Superhump maxima of HS Vir (1996).

E	\max^a	error	$O - C^b$	N^c
0	50153.3417	0.0006	-0.0158	89
12	50154.3201	0.0007	0.0002	88
23	50155.2087	0.0018	0.0067	52
35	50156.1718	0.0006	0.0073	124
36	50156.2465	0.0008	0.0018	49
37	50156.3324	0.0006	0.0074	73
98	50161.2147	0.0020	-0.0024	142
99	50161.2922	0.0021	-0.0052	125

^a BJD-2400000.^b Against $\max = 2450153.3575 + 0.080201E$.^c Number of points used to determine the maximum.**Table 274.** Secondary Maxima of HS Vir (1996).

E	\max^a	error	$O - C^b$	N^c
0	50161.1697	0.0016	-0.0003	86
1	50161.2506	0.0014	0.0003	147
26	50163.2594	0.0006	-0.0000	95

^a BJD-2400000.^b Against $\max = 2450161.1700 + 0.080361E$.^c Number of points used to determine the maximum.and $+5.7(0.6) \times 10^{-5}$ (Kato et al. 2001d).

The $O - C$ diagrams after the appearance of ordinary superhumps were similar between superoutburst (figure 158), although the delay before the appearance of ordinary superhumps was shorter in a fainter superoutburst in 2002 (subsection 5.4).

6.138. *OU Virginis*

OU Vir was a CV discovered through a survey for quasars (Berg et al. 1992). Vanmunster et al. (2000b) established that the object is an eclipsing SU UMa-type dwarf nova, but their superhump period was rather poorly determined. Patterson et al. (2005) presented an analysis of the 2003 superoutburst and reported a superhump period of 0.0751(1) d. They did not give times of superhump maxima.

We present the analysis of the 2003 superoutburst, the data partly overlapping those in Patterson et al. (2005).

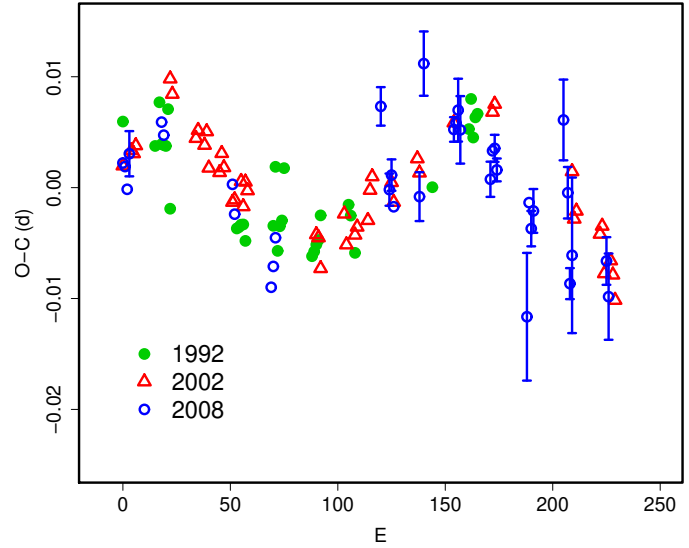
Table 275. Superhump maxima of HS Vir (2008).

E	\max^a	error	$O - C^b$	N^c
0	54619.0407	0.0006	0.0016	130
11	54619.9184	0.0006	-0.0010	106
12	54619.9983	0.0005	-0.0010	87
62	54624.0011	0.0072	0.0004	66

^a BJD-2400000.^b Against $\max = 2454619.0390 + 0.080028E$.^c Number of points used to determine the maximum.

Table 276. Superhump maxima of HV Vir (2008).

E	max ^a	error	$O - C^b$	N^c
0	54517.1492	0.0005	0.0001	103
1	54517.2071	0.0007	-0.0003	146
2	54517.2634	0.0009	-0.0023	60
3	54517.3248	0.0020	0.0009	61
18	54518.2019	0.0003	0.0040	239
19	54518.2590	0.0003	0.0029	219
51	54520.1195	0.0008	-0.0010	99
52	54520.1751	0.0005	-0.0037	103
69	54521.1593	0.0007	-0.0100	102
70	54521.2194	0.0010	-0.0081	92
71	54521.2803	0.0009	-0.0055	60
120	54524.1479	0.0017	0.0072	103
124	54524.3735	0.0015	-0.0002	58
125	54524.4331	0.0014	0.0011	65
126	54524.4885	0.0010	-0.0018	50
138	54525.1888	0.0022	-0.0006	389
140	54525.3173	0.0029	0.0114	302
154	54526.1273	0.0011	0.0057	96
155	54526.1862	0.0008	0.0063	130
156	54526.2456	0.0028	0.0075	55
157	54526.3021	0.0030	0.0057	55
171	54527.1136	0.0016	0.0015	36
172	54527.1744	0.0005	0.0041	178
173	54527.2329	0.0012	0.0043	135
174	54527.2893	0.0010	0.0024	70
188	54528.0919	0.0058	-0.0106	32
189	54528.1605	0.0009	-0.0003	59
190	54528.2164	0.0016	-0.0026	60
191	54528.2763	0.0020	-0.0010	44
205	54529.1004	0.0036	0.0074	37
207	54529.2104	0.0023	0.0009	58
208	54529.2605	0.0014	-0.0073	60
209	54529.3214	0.0070	-0.0047	58
225	54530.2533	0.0021	-0.0050	38
226	54530.3084	0.0039	-0.0082	61

^a BJD-2400000.^b Against $max = 2454517.1491 + 0.058263E$.^c Number of points used to determine the maximum.**Fig. 158.** Comparison of $O - C$ diagrams of HV Vir between different superoutbursts. A period of 0.05828 d was used to draw this figure. Approximate cycle counts (E) after the appearance of the ordinary superhumps were used.

Observations outside the eclipses, as described in V2051 Oph, were used in analysis. The mean superhump period with the PDM method was 0.074950(7) d (figure 159). The times of superhump maxima are listed in table 277. The $O - C$'s showed a slight signature of a discontinuous change around $E = 50$, but its nature remained uncertain because of the relatively large scatter in the data. Although we determined a global P_{dot} of $-1.8(0.6) \times 10^{-5}$, this value apparently needs to be verified by a detailed future study since eclipsing SU UMa-type dwarf novae are often associated with more or less complexity in analysis. The early stage of the 2008 superoutburst was also observed (table 278).

6.139. QZ Virginis

We reanalyzed the data in Kato (1997). The refined times of superhump maxima, together with those in Lemm et al. (1993), are listed in table 279. The earliest part ($E \leq 1$) showed large deviations from the nominal superhump period, as discussed in Kato (1997). A strongly negative $O - C$ at $E = 9$ may be interpreted as early development with a longer period (stage A). Thanks to the improvement in determination of times of maxima, it has now become evident that the segment $15 \leq E \leq 101$ showed a positive P_{dot} (stage B). Disregarding the discrepant points $E = 34$ and $E = 50$, we obtained $P_{\text{dot}} = +7.0(1.4) \times 10^{-5}$.

This period derivative and the overall behavior is similar to those during the 2007 and 2008 superoutbursts (tables 281, 282; figure 160). The P_{dot} 's for the corresponding segment were $+4.5(7.6) \times 10^{-5}$ ($E \leq 53$, 2007) and $+4.7(1.9) \times 10^{-5}$ ($E \leq 85$, 2008). A fragmentary observation of the 2005 superoutburst is also given (table 280). The negative P_{dot} in Lemm et al. (1993) probably

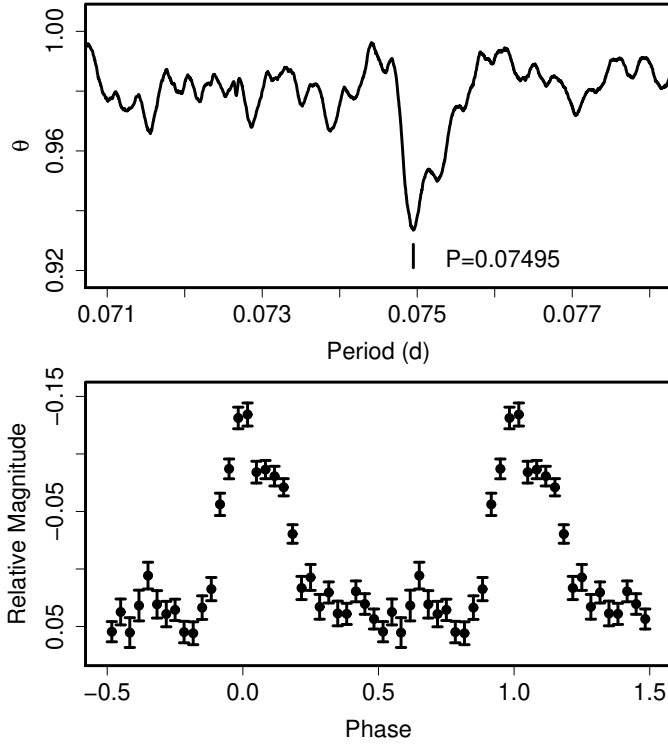


Fig. 159. Superhumps in OU Vir (2003). (Upper): PDM analysis. (Lower): Phase-averaged profile.

Table 277. Superhump maxima of OU Vir (2003).

E	\max^a	error	$O - C^b$	N^c
0	52764.9749	0.0019	-0.0033	197
1	52765.0514	0.0007	-0.0017	230
2	52765.1208	0.0004	-0.0072	309
4	52765.2722	0.0015	-0.0056	157
33	52767.4449	0.0020	-0.0054	84
34	52767.5222	0.0016	-0.0030	50
43	52768.2004	0.0012	0.0010	84
44	52768.2699	0.0026	-0.0045	100
46	52768.4237	0.0068	-0.0004	29
47	52768.5053	0.0014	0.0062	70
48	52768.5829	0.0014	0.0090	48
59	52769.4050	0.0013	0.0070	71
60	52769.4777	0.0012	0.0048	69
61	52769.5518	0.0016	0.0040	70
72	52770.3765	0.0024	0.0046	89
73	52770.4489	0.0013	0.0022	155
99	52772.3966	0.0015	0.0021	65
100	52772.4674	0.0026	-0.0020	58
209	52780.6333	0.0026	-0.0015	32
216	52781.1498	0.0058	-0.0094	264
217	52781.2372	0.0043	0.0031	185

^a BJD-2400000.

^b Against $\max = 2452764.9782 + 0.074912E$.

^c Number of points used to determine the maximum.

Table 278. Superhump maxima of OU Vir (2008).

E	\max^a	error	$O - C^b$	N^c
0	54556.4839	0.0006	0.0000	102
1	54556.5565	0.0010	-0.0023	107
2	54556.6333	0.0030	-0.0005	54
11	54557.3122	0.0030	0.0038	47
21	54558.0646	0.0063	0.0065	105
22	54558.1318	0.0009	-0.0012	99
23	54558.2049	0.0014	-0.0031	141
24	54558.2797	0.0019	-0.0032	64

^a BJD-2400000.

^b Against $\max = 2454556.4839 + 0.074962E$.

^c Number of points used to determine the maximum.

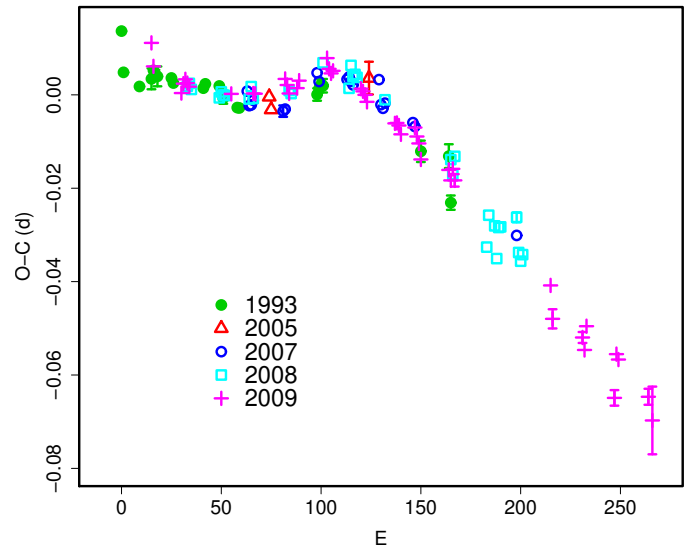


Fig. 160. Comparison of $O - C$ diagrams of QZ Vir between different superoutbursts. A period of 0.06038 d was used to draw this figure. Approximate cycle counts (E) after the start of the superoutburst were used. The start of the 2008 superoutburst was missed. The $O - C$ analysis suggests that the superoutburst started two days before the initial detection. The $O - C$ diagram was shifted by this value.

resulted from a stage A-B transition and sparse sampling.

The 2009 superoutburst was particularly well observed (table 283). This superoutburst was preceded by a distinct precursor and followed by a rebrightening. Despite the presence of a precursor, the P_{dot} during the stage B ($E \leq 91$) was positive with $+11.4(1.8) \times 10^{-5}$. The stage C superhumps had a period of 0.06000(1) before $E = 152$, then the period slightly shortened to 0.05992(7) d. These late-stage superhumps apparently endured during the period of the rebrightening.

Further detailed analysis will be presented in Ohshima et al. (2009).

Table 279. Superhump maxima of QZ Vir (1993).

E	max ^a	error	$O - C^b$	N^c
0	48990.3101	0.0008	0.0053	138
1	48990.3617	0.0006	-0.0034	134
9	48990.8417	-	-0.0054	0
15	48991.2056	0.0022	-0.0030	55
16	48991.2678	0.0006	-0.0010	99
17	48991.3273	0.0010	-0.0019	89
18	48991.3873	0.0021	-0.0021	22
25	48991.8096	-	-0.0015	0
26	48991.8689	-	-0.0025	0
34	48992.3636	0.0050	0.0102	49
41	48992.7735	-	-0.0017	0
42	48992.8348	-	-0.0006	0
49	48993.2570	0.0003	-0.0002	121
50	48993.3249	0.0016	0.0074	97
51	48993.3751	0.0012	-0.0026	74
c58	48993.7958	-	-0.0037	0
59	48993.8561	-	-0.0036	0
98	48996.2138	0.0013	0.0042	124
99	48996.2755	0.0007	0.0056	136
100	48996.3367	0.0011	0.0066	131
101	48996.3968	0.0014	0.0064	71
150	48999.3414	0.0023	-0.0014	71
164	49000.1857	0.0025	-0.0006	79
165	49000.2361	0.0015	-0.0105	138

^a BJD-2400000.^b Against $max = 2448990.3048 + 0.060253E$.^c Number of points used to determine the maximum.
 $N = 0$ refers to Lemm et al. (1993).**Table 280.** Superhump maxima of QZ Vir (2005).

E	max ^a	error	$O - C^b$	N^c
0	53678.2944	0.0005	0.0014	178
1	53678.3520	0.0005	-0.0014	143
50	53681.3174	0.0035	0.0000	45

^a BJD-2400000.^b Against $max = 2453678.2930 + 0.060488E$.^c Number of points used to determine the maximum.**Table 281.** Superhump maxima of QZ Vir (2007).

E	max ^a	error	$O - C^b$	N^c
0	54111.1604	0.0005	-0.0031	137
1	54111.2177	0.0002	-0.0061	428
2	54111.2782	0.0004	-0.0058	338
3	54111.3396	0.0003	-0.0047	299
18	54112.2430	0.0012	-0.0052	89
19	54112.3038	0.0010	-0.0046	45
35	54113.2777	0.0009	0.0052	88
36	54113.3362	0.0004	0.0035	269
50	54114.1820	0.0004	0.0057	137
51	54114.2428	0.0003	0.0063	149
52	54114.3023	0.0002	0.0055	321
53	54114.3619	0.0002	0.0049	289
66	54115.1480	0.0007	0.0077	168
67	54115.2030	0.0003	0.0024	426
68	54115.2626	0.0003	0.0018	326
69	54115.3241	0.0003	0.0030	322
83	54116.1652	0.0008	0.0006	67
84	54116.2248	0.0007	-0.0001	131
135	54119.2808	0.0006	-0.0170	133

^a BJD-2400000.^b Against $max = 2454111.1636 + 0.060254E$.^c Number of points used to determine the maximum.

6.140. *RX Volantis*

Although RX Vol was listed as a possible SU UMa-type dwarf nova with a maximum of magnitude 16 (Kholopov et al. 1985), little had been known until 2003. The first-ever outburst since the discovery, at an exceptional brightness of 14.7, was reported on 2003 May 4 (R. Stubbings, vsnet-outburst 5482). This outburst turned out to be a superoutburst (vsnet-outburst 5502). The mean superhump period with the PDM method was 0.061348(7) d (figure 161). The times of superhump maxima are listed in table 284. The object clearly showed positive superhump derivative except for the earliest part. P_{dot} was $+5.8(0.8) \times 10^{-5}$ for ($E \geq 12$). Schmidtobreick et al. (2005) summarized the history of this object and presented a spectrum in quiescence.

6.141. *TY Vulpeculae*

Kato, Uemura (1999) suggested the SU UMa-type nature of this object based on the observation of the 1999 September short outburst. The SU UMa-type nature of TY Vul was established by Vanmunster et al. (aavso-photometry message on 2003 December 7)²¹, who reported a period of 0.0809(2) d. We observed the same superoutburst and obtained the times of superhump maxima after incorporating the AAVSO data (table 285). The period of 0.08048(7) d can satisfactorily expressed the maxima, and the period was in agreement with the one by Vanmunster et al. The resultant $O - C$ diagram showed a large negative period derivative $P_{\text{dot}} = -14.8(3.0) \times 10^{-5}$

²¹ <<http://www.aavso.org/pipermail/aavso-photometry/2003-December/000153.html>>.

Table 282. Superhump maxima of QZ Vir (2008).

E	\max^a	error	$O - C^b$	N^c
0	54470.2452	0.0002	-0.0075	346
1	54470.3062	0.0004	-0.0067	322
2	54470.3653	0.0006	-0.0078	214
16	54471.2088	0.0004	-0.0065	114
17	54471.2705	0.0002	-0.0050	307
18	54471.3302	0.0002	-0.0055	598
19	54471.3905	0.0002	-0.0054	206
31	54472.1143	0.0006	-0.0035	107
32	54472.1773	0.0004	-0.0006	105
33	54472.2352	0.0003	-0.0029	107
51	54473.3237	0.0010	0.0027	213
52	54473.3834	0.0007	0.0023	237
68	54474.3561	0.0004	0.0123	281
81	54475.1356	0.0004	0.0097	253
82	54475.2009	0.0005	0.0148	273
83	54475.2589	0.0002	0.0127	334
84	54475.3197	0.0004	0.0133	287
85	54475.3794	0.0003	0.0129	254
99	54476.2200	0.0004	0.0112	106
132	54478.1997	0.0006	0.0055	114
133	54478.2569	0.0008	0.0026	115
134	54478.3211	0.0005	0.0067	115
150	54479.2678	0.0008	-0.0093	108
151	54479.3350	0.0006	-0.0022	115
154	54479.5139	0.0005	-0.0039	65
155	54479.5672	0.0007	-0.0106	105
156	54479.6343	0.0005	-0.0038	103
157	54479.6948	0.0006	-0.0034	111
165	54480.1799	0.0011	0.0004	118
166	54480.2327	0.0007	-0.0069	127
167	54480.2912	0.0004	-0.0086	232
168	54480.3530	0.0004	-0.0070	229

^a BJD-2400000.^b Against $\max = 2454470.2527 + 0.060162E$.^c Number of points used to determine the maximum.

for the entire span of observations. This large variation can be attributed to a stage B-C transition. The parameters based on this interpretation are given in table 2. The object may be similar to AX Cap and SDSS J1627 in the evolution of the superhump period (see subsection 4.10).

6.142. DO Vulpeculae

Although DO Vul had long been known as a dwarf nova (Baade 1928), the identification was only recently known (Skiff 1997; Henden et al. 2001).

Vanmunster reported the detection of superhumps with a period of 0.065 d during the 2005 outburst.

Observations of the 2008 superoutburst yielded a mean period of 0.058286(14) d (PDM analysis, figure 162) and a P_{dot} of $+9.9(2.1) \times 10^{-5}$ (table 286).

Table 283. Superhump maxima of QZ Vir (2009).

E	\max^a	error	$O - C^b$	N^c
0	54856.1944	0.0006	-0.0097	118
1	54856.2497	0.0003	-0.0144	118
15	54857.0893	0.0004	-0.0159	38
16	54857.1517	0.0002	-0.0136	213
17	54857.2130	0.0003	-0.0124	158
18	54857.2726	0.0002	-0.0129	223
19	54857.3322	0.0003	-0.0134	168
40	54858.5987	0.0002	-0.0086	120
51	54859.2629	0.0002	-0.0053	340
52	54859.3232	0.0001	-0.0050	562
67	54860.2321	0.0003	0.0026	268
68	54860.2912	0.0007	0.0016	285
69	54860.3498	0.0008	0.0001	247
73	54860.5924	0.0004	0.0024	112
74	54860.6544	0.0004	0.0043	116
88	54861.5045	0.0004	0.0133	143
89	54861.5626	0.0003	0.0113	143
90	54861.6220	0.0003	0.0107	143
91	54861.6830	0.0004	0.0115	142
105	54862.5245	0.0002	0.0119	261
106	54862.5843	0.0003	0.0116	259
107	54862.6439	0.0004	0.0111	149
108	54862.7028	0.0004	0.0099	142
122	54863.5435	0.0004	0.0095	143
123	54863.6040	0.0004	0.0099	143
124	54863.6638	0.0005	0.0097	143
125	54863.7223	0.0003	0.0081	135
132	54864.1464	0.0008	0.0116	348
133	54864.2049	0.0002	0.0100	391
134	54864.2638	0.0003	0.0088	384
135	54864.3207	0.0005	0.0057	384
149	54865.1638	0.0009	0.0076	97
150	54865.2219	0.0004	0.0057	189
151	54865.2848	0.0004	0.0084	193
152	54865.3427	0.0013	0.0063	116
200	54868.2184	0.0009	-0.0019	94
201	54868.2717	0.0021	-0.0088	111
216	54869.1734	0.0012	-0.0083	64
217	54869.2311	0.0006	-0.0107	153
218	54869.2965	0.0005	-0.0053	132
232	54870.1265	0.0017	-0.0165	56
233	54870.1963	0.0005	-0.0068	62
234	54870.2555	0.0007	-0.0076	62
249	54871.1532	0.0017	-0.0111	224
251	54871.2689	0.0072	-0.0156	157

^a BJD-2400000.^b Against $\max = 2454856.2040 + 0.060082E$.^c Number of points used to determine the maximum.

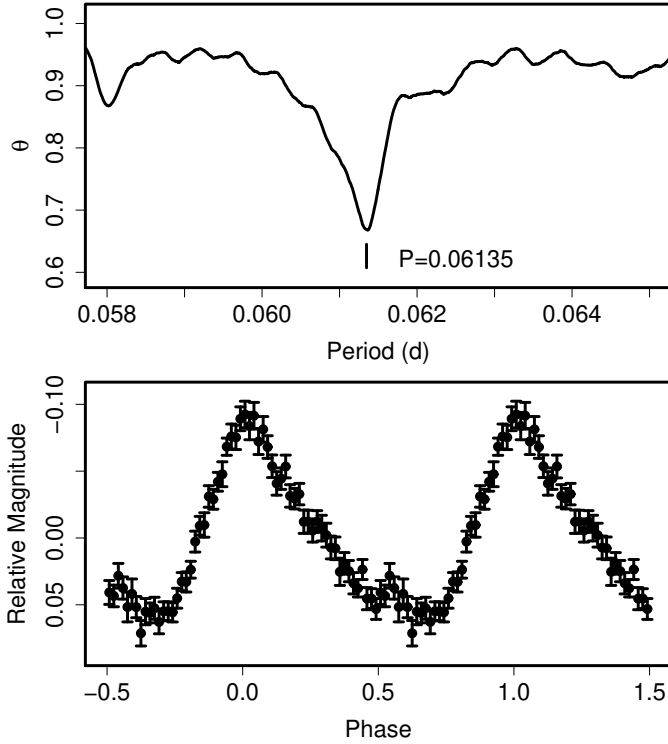


Fig. 161. Superhumps in RX Vol (2003). (Upper): PDM analysis. (Lower): Phase-averaged profile.

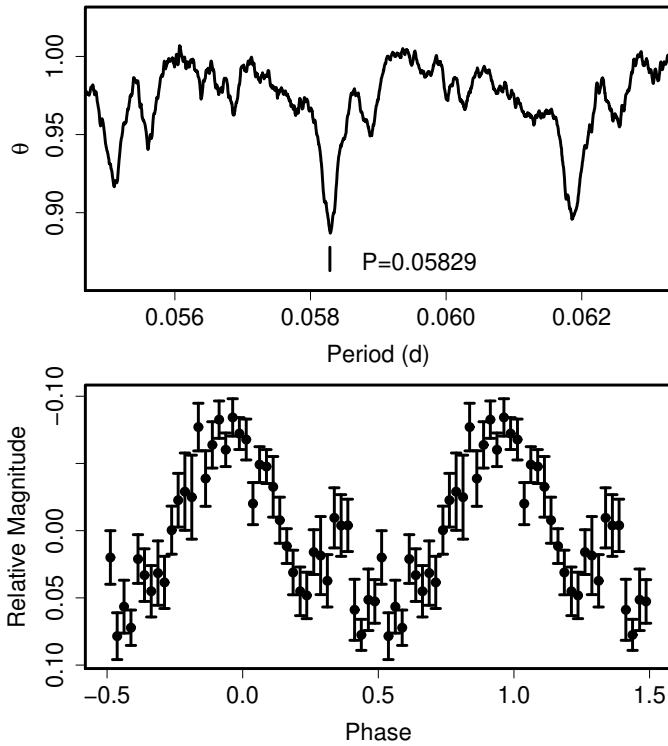


Fig. 162. Superhumps in DO Vul (2008). (Upper): PDM analysis. (Lower): Phase-averaged profile.

Table 284. Superhump maxima of RX Vol (2003).

E	\max^a	error	$O - C^b$	N^c
0	52764.0491	0.0009	0.0029	110
1	52764.1074	0.0008	-0.0001	100
12	52764.7858	0.0005	0.0032	159
13	52764.8466	0.0004	0.0026	270
14	52764.9077	0.0004	0.0023	204
15	52764.9688	0.0004	0.0021	204
16	52765.0301	0.0004	0.0020	205
19	52765.2143	0.0006	0.0022	62
20	52765.2770	0.0007	0.0035	66
21	52765.3368	0.0008	0.0019	70
22	52765.3954	0.0009	-0.0008	70
31	52765.9479	0.0009	-0.0006	161
36	52766.2529	0.0006	-0.0024	57
37	52766.3164	0.0006	-0.0003	61
38	52766.3728	0.0012	-0.0053	68
52	52767.2333	0.0010	-0.0039	72
53	52767.2934	0.0012	-0.0051	71
54	52767.3553	0.0011	-0.0046	58
68	52768.2145	0.0010	-0.0045	72
69	52768.2757	0.0017	-0.0046	71
70	52768.3399	0.0012	-0.0018	71
85	52769.2619	0.0019	-0.0003	71
86	52769.3237	0.0016	0.0002	69
101	52770.2446	0.0027	0.0006	70
133	52772.2127	0.0013	0.0050	71
134	52772.2747	0.0027	0.0057	71

^a BJD-2400000.

^b Against $\max = 2452764.0462 + 0.061364E$.

^c Number of points used to determine the maximum.

6.143. NSV 4838

The times of superhump maxima during the 2005 and 2007 superoutbursts are listed in tables 287 and 288. The observations used here partly include the data in Imada et al. (2009b). The P_{dot} for the 2007 superoutburst ($0 \leq E \leq 101$, stage B) was $+7.4(1.9) \times 10^{-5}$. The 2005 superoutburst was apparently observed during the stage C. The period of 0.06960(3) d obtained by the PDM analysis confirmed the $O - C$ analysis. The object underwent another superoutburst in 2009 February.

6.144. NSV 5285

NSV 5285 was originally discovered as a blue eruptive object that underwent an outburst at $B = 14.5$ (Kowal et al. 1976). The object remained bright at least for five days and faded to $B \sim 20$ thereafter. Kowal et al. (1976) suggested that this object is probably a quasar which underwent a 5.5-mag outburst. Duszynowicz (2008) detected an outbursting variable star, which turned out to be identical with NSV 5285. Subsequent photometric observations established that this is an superoutburst of an SU UMa-type dwarf nova (vsnet-alert 10726). The times of superhump maxima are given in table 289. The mean P_{SH} using the PDM method was 0.08082(3) d.

Table 285. Superhump maxima of TY Vul (2003).

E	\max^a	error	$O - C^b$	N^c
0	52976.8787	0.0017	-0.0213	115
1	52976.9653	0.0036	-0.0153	139
7	52977.4546	0.0012	-0.0088	45
8	52977.5447	0.0008	0.0008	67
9	52977.6266	0.0019	0.0022	37
12	52977.8734	0.0009	0.0075	110
13	52977.9471	0.0015	0.0007	148
14	52978.0234	0.0037	-0.0035	45
42	52980.2944	0.0023	0.0140	112
50	52980.9377	0.0024	0.0134	119
51	52981.0194	0.0032	0.0147	72
54	52981.2534	0.0011	0.0072	104
55	52981.3292	0.0018	0.0025	97
63	52981.9853	0.0044	0.0147	115
67	52982.2998	0.0010	0.0073	89
68	52982.3786	0.0019	0.0057	49
70	52982.5368	0.0061	0.0029	61
79	52983.2488	0.0006	-0.0095	43
80	52983.3292	0.0022	-0.0096	43
116	52986.2255	0.0014	-0.0107	37
120	52986.5434	0.0051	-0.0148	20

^a BJD-2400000.^b Against $\max = 2452976.9001 + 0.080484E$.^c Number of points used to determine the maximum.**Table 286.** Superhump maxima of DO Vul (2008).

E	\max^a	error	$O - C^b$	N^c
0	54671.1058	0.0070	0.0170	83
19	54672.1978	0.0060	0.0032	58
33	54673.0010	0.0030	-0.0085	76
34	54673.0668	0.0008	-0.0009	107
50	54673.9948	0.0015	-0.0041	67
51	54674.0489	0.0003	-0.0082	125
52	54674.1111	0.0004	-0.0043	96
71	54675.2216	0.0027	0.0004	82
120	54678.0700	0.0025	-0.0032	29
121	54678.1308	0.0045	-0.0006	22
137	54679.0580	0.0030	-0.0046	120
138	54679.1190	0.0015	-0.0019	124
155	54680.1195	0.0075	0.0092	84
156	54680.1748	0.0018	0.0063	119

^a BJD-2400000.^b Against $\max = 2454671.0887 + 0.058204E$.^c Number of points used to determine the maximum.**Table 287.** Superhump maxima of NSV 4838 (2005).

E	\max^a	error	$O - C^b$	N^c
0	53528.4392	0.0046	-0.0040	39
14	53529.4228	0.0016	0.0042	92
15	53529.4787	0.0020	-0.0095	42
28	53530.3987	0.0015	0.0048	86
29	53530.4660	0.0006	0.0024	162
43	53531.4406	0.0014	0.0016	75
44	53531.5142	0.0052	0.0056	27
86	53534.4297	0.0018	-0.0050	55

^a BJD-2400000.^b Against $\max = 2453528.4432 + 0.069668E$.^c Number of points used to determine the maximum.**Table 288.** Superhump maxima of NSV 4838 (2007).

E	\max^a	error	$O - C^b$	N^c
0	54139.1208	0.0011	-0.0018	176
1	54139.1858	0.0004	-0.0066	233
2	54139.2561	0.0004	-0.0061	208
3	54139.3275	0.0004	-0.0045	185
58	54143.1687	0.0007	-0.0021	155
59	54143.2408	0.0006	0.0001	249
73	54144.2176	0.0009	-0.0002	250
74	54144.2898	0.0010	0.0022	208
101	54146.1839	0.0015	0.0117	60
115	54147.1579	0.0008	0.0086	117
116	54147.2293	0.0007	0.0101	146
117	54147.2975	0.0014	0.0085	91
129	54148.1327	0.0005	0.0062	123
130	54148.2021	0.0007	0.0057	257
131	54148.2710	0.0009	0.0049	217
157	54150.0767	0.0017	-0.0041	148
158	54150.1483	0.0012	-0.0024	149
159	54150.2179	0.0012	-0.0025	133
171	54151.0560	0.0007	-0.0020	140
172	54151.1248	0.0010	-0.0031	128
185	54152.0349	0.0037	-0.0003	141
186	54152.0939	0.0017	-0.0111	116
187	54152.1749	0.0041	0.0001	117
188	54152.2372	0.0085	-0.0074	124
189	54152.3104	0.0025	-0.0040	127

^a BJD-2400000.^b Against $\max = 2454139.1226 + 0.069798E$.^c Number of points used to determine the maximum.

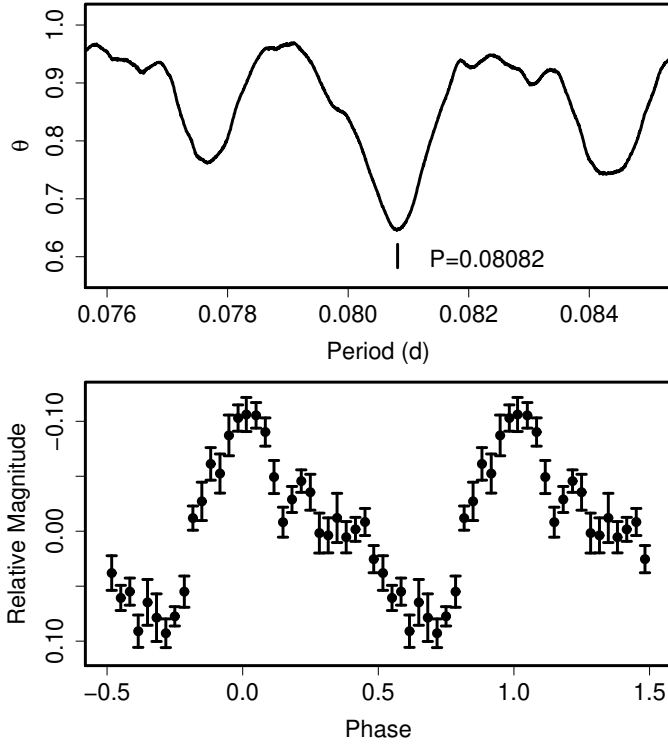


Fig. 163. Superhumps in NSV 5285 (2008). (Upper): PDM analysis. (Lower): Phase-averaged profile.

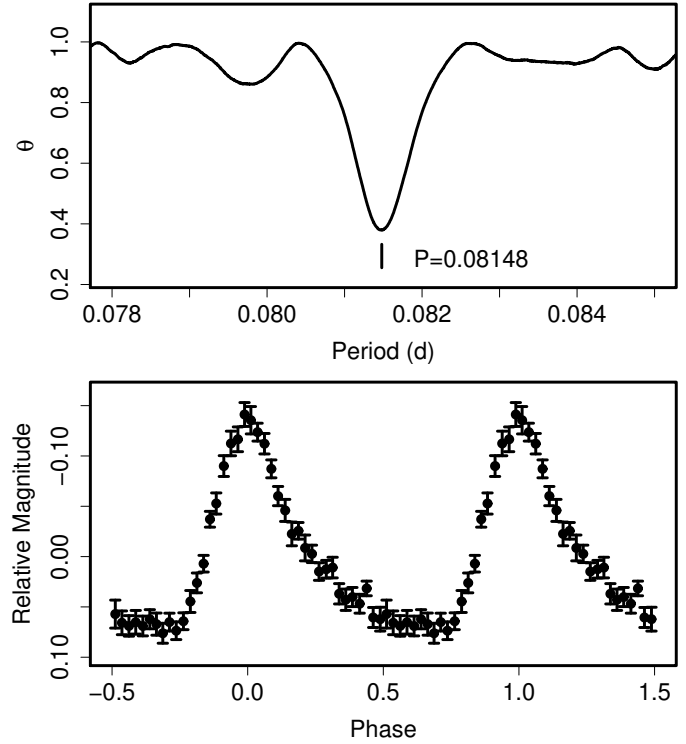


Fig. 164. Superhumps in NSV 14652 (2004). (Upper): PDM analysis. (Lower): Phase-averaged profile.

Table 289. Superhump maxima of NSV 5285 (2008).

E	\max^a	error	$O - C^b$	N^c
0	54791.3043	0.0013	0.0019	52
11	54792.2686	0.0008	-0.0015	94
12	54792.3566	0.0009	-0.0014	97
34	54794.2945	0.0008	0.0010	179

^a BJD-2400000.

^b Against $\max = 2454791.3024 + 0.087973E$.

^c Number of points used to determine the maximum.

6.145. NSV 14652

NSV 14652 was discovered by Reinmuth (1930) as a variable star (AN 254.1930). The object was positively recorded twice in 1901 and 1904. The object was identified with a ROSAT source (vsnet-chat 3314). T. Kinnunen detected the object in outburst on a Palomar Observatory Sky Survey scan (cf. vsnet-alert 5203, 5205).

We present times of superhump maxima during a superoutburst in 2004 September (table 290). The mean P_{SH} with the PDM method was 0.08148(1) d (figure 164). The $O - C$ diagram showed a stage B-C transition around $E = 50$. The P_{dot} during the stage B was close to zero, $-3.0(3.6) \times 10^{-5}$. The other parameters are listed in table 2.

Table 290. Superhump maxima of NSV 14652 (2004).

E	\max^a	error	$O - C^b$	N^c
0	53251.4459	0.0006	-0.0016	79
1	53251.5282	0.0007	-0.0008	82
2	53251.6107	0.0010	0.0003	64
12	53252.4245	0.0008	-0.0005	69
13	53252.5057	0.0016	-0.0007	59
36	53254.3814	0.0007	0.0015	68
37	53254.4646	0.0008	0.0032	56
38	53254.5438	0.0008	0.0010	52
48	53255.3602	0.0011	0.0028	69
49	53255.4397	0.0007	0.0008	67
50	53255.5212	0.0008	0.0009	63
60	53256.3308	0.0007	-0.0041	53
61	53256.4137	0.0015	-0.0027	35

^a BJD-2400000.

^b Against $\max = 2453251.4475 + 0.081457E$.

^c Number of points used to determine the maximum.

6.146. 1RXS J023238.8-371812

In 2007 October, K. Malek (“Pi of the Sky”²²) reported a possible nova outburst (vsnet-alert 9622) close to the location of 1RXS J023238.8–371812 (hereafter 1RXS J0232). T. Kato suggested that the object can be identified with a 6dF Galactic object and that it is most likely a large-amplitude dwarf nova (vsnet-alert 9620). This suggestion was later confirmed by the detection of superhumps (vsnet-alert 9634). The superoutburst was unusual in that it had both a “dip”, characteristic to type-A superoutbursts (subsection 5.3), during the superoutburst plateau and four distinct post-superoutburst rebrightenings, characteristic to type-B superoutbursts (figure 165).

The times of superhump maxima during the main superoutburst are listed in table 291. The resultant P_{dot} was $-1.7(0.7) \times 10^{-5}$. Since the only later portion of the superoutburst was observed, this value may have been affected by a possible stage B–C transition. The only small variation of the P_{SH} , however, may be associated with the extreme WZ Sge-type nature of this object.

The period analyses and superhump profiles are presented in figures 166 and 167. The analysis during the rebrightening phase follows the same way as in SDSS J0804 (Kato et al. 2009). The mean P_{SH} during the main superoutburst was 0.066191(4) d. During the rebrightening phase, two candidate periods were present: 0.066963(4) d and 0.065851(4) d. Since the former period is 1.2 % longer than the P_{SH} during the main superoutburst, it appears to be slightly too long for a superhump period at this stage (see subsection 5.1). The latter period, 0.5 % shorter than the P_{SH} , which might represent the orbital period. The phase-averaged profile also resembles that of orbital humps rather than superhumps (cf. Kato et al. 2009). If this identification of the period is confirmed, the small ϵ would place 1RXS J0232 similar to EG Cnc. Since the periodicity can be very complex during rebrightenings (Kato et al. 2009) and since the coverage of the rebrightening phase was not sufficient, further observations are needed to correctly identify the periods.

6.147. 1RXS J042332+745300

1RXS J042332+745300 (=HS 0417+7445, hereafter 1RXS J0423) is a CV (Wu et al. 2001) selected from the ROSAT catalog and also selected spectroscopically (Aungwerojwit et al. 2006). Although Aungwerojwit et al. (2006) detected superhumps during the 2001 superoutburst, the period was not precisely determined.

We observed the 2008 superoutburst and identified the correct P_{SH} . Combined with the AAVSO observations, we obtained a mean P_{SH} of 0.078320(6) d. Among candidate P_{orb} given in Aungwerojwit et al. (2006), the period of 0.07632 d best fits our P_{SH} , and gives a fractional superhump excess of 2.6 %. The times of superhump maxima are listed in table 292.

This outburst was associated with a precursor ($E \leq 2$, figure 169). A longer period was observed for $E \leq 30$ during the developmental stage of superhumps. This dura-

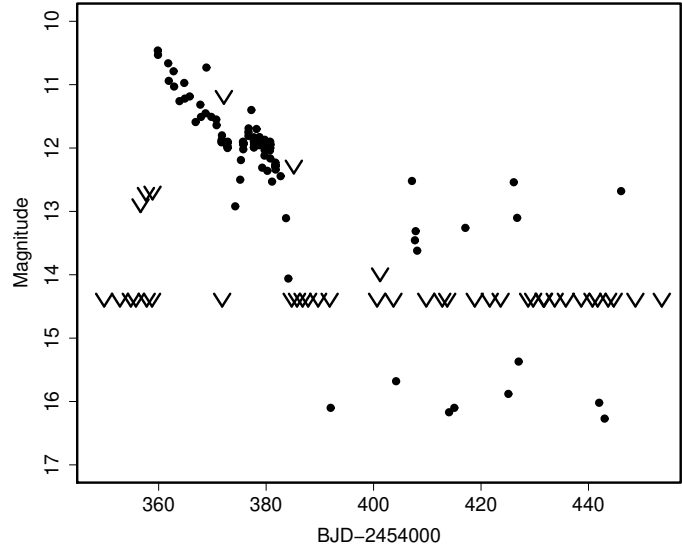


Fig. 165. Superoutburst of 1RXS J0232 in 2007. The data are a combination of our observations, VSNET, ASAS-3 and “Pi of the Sky” observations. The “V”-marks indicate upper limits. There was a “dip” during the superoutburst plateau (around BJD 2454374). Four post-superoutburst rebrightenings were recorded.

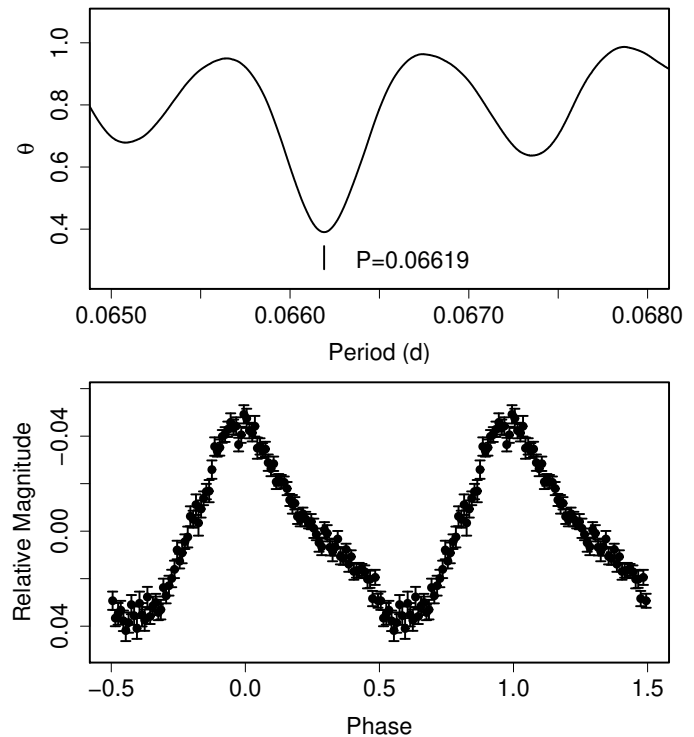


Fig. 166. Superhumps in 1RXS J0232 during the main superoutburst. (Upper): PDM analysis. (Lower): Phase-averaged profile.

²² <<http://grb.fuw.edu.pl/pi/index.html>>.

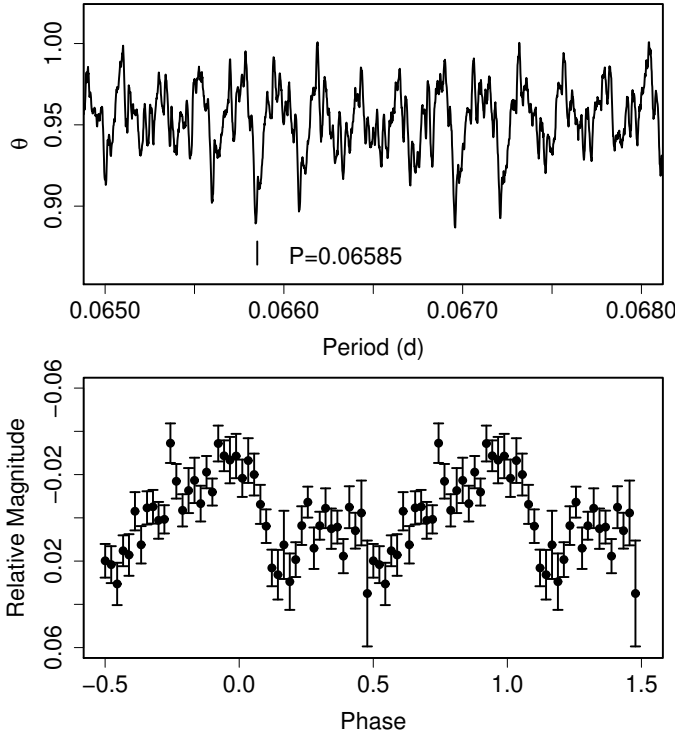


Fig. 167. Hump features in 1RXS J0232 during the re-brightening phase. (Upper): PDM analysis. A period of 0.065850(4) is selected by a comparison with the superhump period (see text). Another potential period is 0.066963(4) d. (Lower): Phase-averaged profile at the period of 0.065850 d.

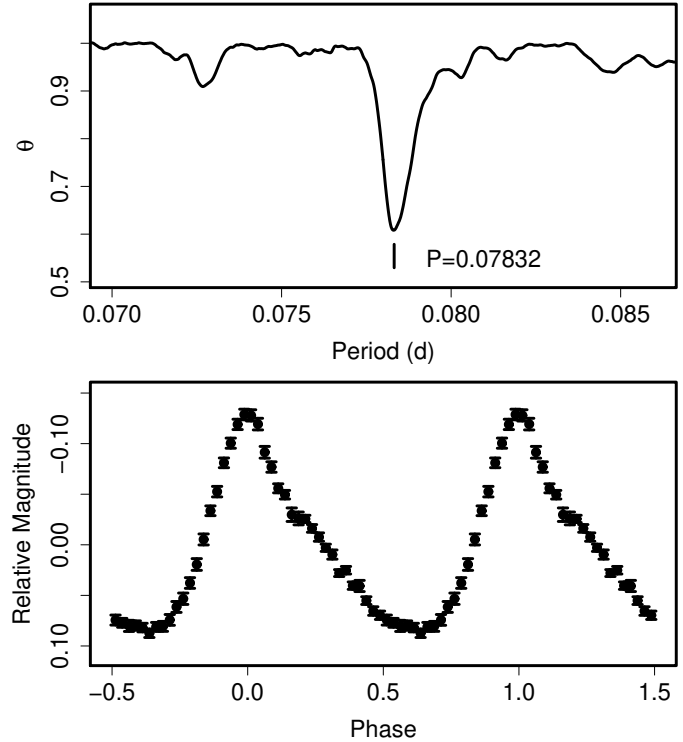


Fig. 168. Ordinary superhumps in 1RXS J0423 (2008). (Upper): PDM analysis. (Lower): Phase-averaged profile.

Table 291. Superhump maxima of 1RXS J0232 (2007).

E	\max^a	error	$O - C^b$	N^c
0	54376.0443	0.0003	-0.0020	191
1	54376.1127	0.0002	0.0002	285
46	54379.0904	0.0003	0.0005	66
47	54379.1566	0.0003	0.0005	68
48	54379.2231	0.0003	0.0009	65
49	54379.2886	0.0004	0.0001	68
50	54379.3550	0.0003	0.0004	69
60	54380.0178	0.0004	0.0015	287
61	54380.0835	0.0005	0.0010	337
62	54380.1487	0.0004	0.0001	339
63	54380.2149	0.0003	0.0001	68
64	54380.2811	0.0003	0.0002	69
65	54380.3467	0.0003	-0.0004	69
75	54381.0065	0.0005	-0.0023	160
106	54383.0589	0.0005	-0.0010	152

^a BJD-2400000.

^b Against $\max = 2454376.0463 + 0.066166E$.

^c Number of points used to determine the maximum.

tion of stage A was thus rather unusually long. Although there was a slight indication of a stage B–C transition around $E = 68$, the change in the period was smaller than in other systems with similar superhump periods. The periods listed in table 2 are based on this interpretation. The presence of a precursor and the relatively short (~ 10 d) duration of this superoutburst might signify a “borderline” superoutburst as observed in BZ UMa in 2007 (subsection 6.126), which may be responsible for the unusual development of superhumps. Further investigation of this object is still needed.

The light curve became double-humped during the post-superoutburst stage. The three maxima of secondary humps ($E = 153$, the first one of $E = 166$, and $E = 167$) were excluded in the period analysis presented in table 2.

6.148. 1RXS J053234.9+624755

This object (hereafter 1RXS J0532) was discovered as a dwarf nova by Bernhard et al. (2005). Kapusta, Thorstensen (2006) provided a radial-velocity study and yielded an orbital period of 0.05620(4) d. (See also Kapusta, Thorstensen 2006 for the history of superhump observation). Parimucha, Dubovsky (2006) observed the 2006 July superoutburst and reported a period of 0.05707(12) d. We report on the 2005 and 2008 superoutbursts. The 2005 superoutburst (data from Imada et al. 2009a, a combination of our data and the AAVSO observations) showed a prominent precursor outburst associated with superhumps. This behavior was very similar

Table 292. Superhump maxima of 1RXS J0423 (2008).

E	\max^a	error	$O - C^b$	N^c
0	54530.3689	0.0019	-0.0412	247
1	54530.4581	0.0008	-0.0302	294
2	54530.5199	0.0016	-0.0466	195
15	54531.5647	0.0021	-0.0186	86
16	54531.6461	0.0003	-0.0155	167
17	54531.7271	0.0002	-0.0127	163
18	54531.8075	0.0002	-0.0105	158
24	54532.2842	0.0002	-0.0031	155
25	54532.3641	0.0002	-0.0014	158
26	54532.4432	0.0002	-0.0005	163
27	54532.5204	0.0002	-0.0016	168
28	54532.6013	0.0004	0.0011	328
29	54532.6814	0.0004	0.0030	164
30	54532.7615	0.0002	0.0049	205
31	54532.8376	0.0005	0.0027	85
35	54533.1552	0.0003	0.0075	239
36	54533.2294	0.0010	0.0035	147
37	54533.3123	0.0003	0.0082	495
38	54533.3916	0.0002	0.0093	378
39	54533.4680	0.0002	0.0075	591
40	54533.5478	0.0003	0.0090	278
41	54533.6247	0.0004	0.0076	129
45	54533.9369	0.0005	0.0071	165
46	54534.0140	0.0003	0.0059	173
50	54534.3272	0.0004	0.0062	213
51	54534.4050	0.0002	0.0058	343
52	54534.4882	0.0002	0.0108	262
53	54534.5648	0.0002	0.0092	121
59	54535.0365	0.0005	0.0115	150
63	54535.3475	0.0003	0.0097	338
64	54535.4280	0.0003	0.0120	212
65	54535.5042	0.0004	0.0100	193
66	54535.5828	0.0004	0.0104	293
67	54535.6624	0.0004	0.0118	104
68	54535.7439	0.0006	0.0150	51
72	54536.0504	0.0008	0.0087	160
73	54536.1253	0.0006	0.0053	161
77	54536.4406	0.0004	0.0077	99
78	54536.5177	0.0005	0.0066	101
79	54536.5986	0.0003	0.0093	167
80	54536.6770	0.0003	0.0094	165
81	54536.7533	0.0003	0.0075	149
82	54536.8352	0.0007	0.0112	98
103	54538.4714	0.0006	0.0048	108
104	54538.5501	0.0003	0.0053	137
105	54538.6310	0.0003	0.0080	102
106	54538.7092	0.0008	0.0080	82
107	54538.7881	0.0004	0.0087	69
153	54542.3301	0.0009	-0.0473	102
166	54543.3462	0.0038	-0.0481	61
166	54543.4001	0.0022	0.0058	54
167	54543.4535	0.0008	-0.0189	65
168	54543.5606	0.0018	0.0099	18
169	54543.6203	0.0037	-0.0086	18
170	54543.7092	0.0036	0.0020	18
171	54543.7824	0.0014	-0.0029	18

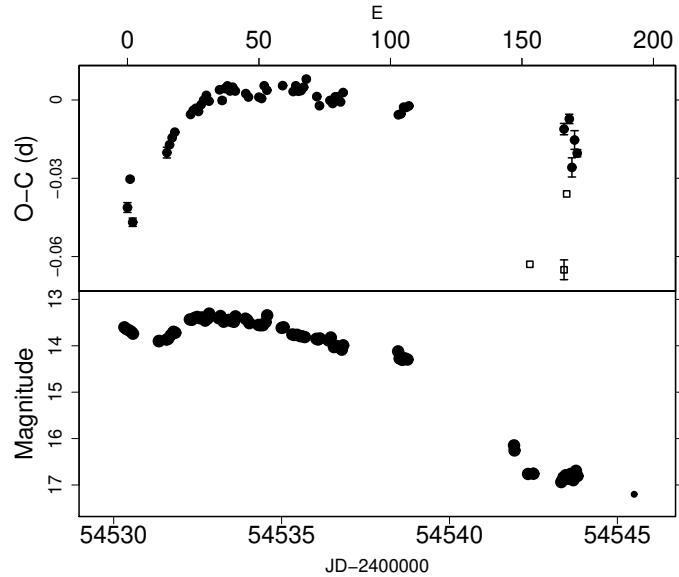
^a BJD-2400000.^b Against $\max = 2454530.4101 + 0.078218E$.^c Number of points used to determine the maximum.

Fig. 169. $O - C$ of superhumps 1RXS J0423 (2008). (Upper): $O - C$ diagram. The $O - C$ values were against the global mean period of 0.078320 d. Open squares represent likely secondary hump maxima. (Lower): Light curve. The last pre-outburst observation was on BJD 2454525.5 at magnitude 17.4.

to QZ Vir (=T Leo) in 1993 (Kato 1997). The mean superhump period with the PDM method was 0.057120(6) d (figure 170). The times of superhump maxima are listed in table 293. The $O - C$ diagram showed a stage B-C transition (figure 171). The behavior in the period during the transition from the precursor outburst was quite different from the one in QZ Vir in 1993 (Kato 1997). The P_{dot} in the former interval ($E \leq 162$) was $+5.7(0.8) \times 10^{-5}$. The 2008 superoutburst was observed except for the late stage (table 294). The $O - C$ behavior was similar to that of the 2005 one, giving $P_{\text{dot}} = +10.2(0.8) \times 10^{-5}$ ($E \leq 138$). Since there was no clear precursor at the onset of the 2008 superoutburst, the P_{dot} does not seem to show very strong dependence on the presence of a precursor, on the contrary to Uemura et al. (2005). The development of the superhumps during the 2005 superoutburst, however, may have been earlier by ~ 26 superhump cycles compared to the 2008 one (figure 172).

6.149. 2QZ J021927.9-304545

Imada et al. (2006b) reported the 2005 superoutburst of this object (hereafter 2QZ J0219). We also observed the 2009 superoutburst during its middle-to-late stage. The mean superhump period with the PDM method was 0.08100(1) d, in good agreement with that of stage C superhumps during the 2005 superoutburst. The times of superhump maxima are listed in table 295.

6.150. ASAS J002511+1217.2

ASAS J002511+1217.2 (hereafter ASAS J0025) is a dwarf nova discovered by the ASAS-3 (Pojmanski 2002)

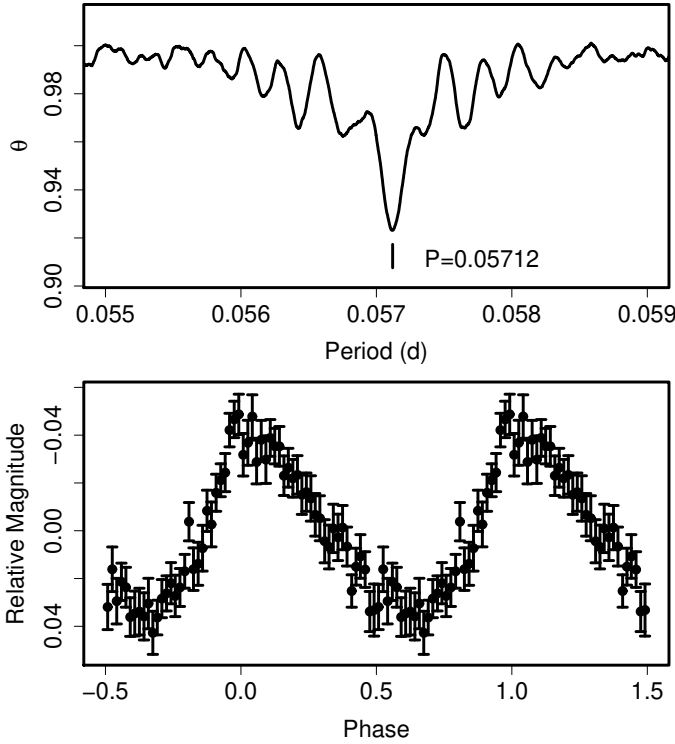


Fig. 170. Superhumps in 1RXS J0532 (2005). (Upper): PDM analysis. (Lower): Phase-averaged profile.

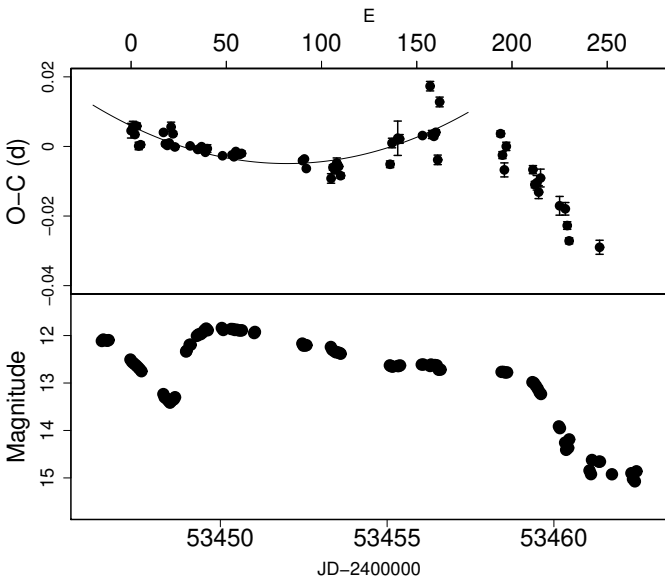


Fig. 171. $O - C$ of superhumps 1RXS J0532 (2005). (Upper): $O - C$ diagram. The curve represents a quadratic fit to $E \leq 162$. (Lower): Light curve. The superoutburst was preceded by a precursor.

Table 293. Superhump maxima of 1RXS J0532 (2005).

E	max^a	error	$O - C^b$	N^c
0	53447.3252	0.0021	0.0014	34
1	53447.3834	0.0016	0.0025	44
2	53447.4384	0.0006	0.0004	34
3	53447.4980	0.0009	0.0028	29
4	53447.5494	0.0011	-0.0028	33
5	53447.6069	0.0008	-0.0024	33
17	53448.2963	0.0005	0.0018	36
18	53448.3502	0.0006	-0.0014	133
19	53448.4069	0.0004	-0.0018	161
20	53448.4648	0.0004	-0.0010	174
21	53448.5265	0.0014	0.0036	66
22	53448.5817	0.0006	0.0017	33
23	53448.6351	0.0007	-0.0020	23
31	53449.0926	0.0004	-0.0013	93
35	53449.3202	0.0004	-0.0020	111
36	53449.3776	0.0002	-0.0018	143
37	53449.4354	0.0002	-0.0011	143
38	53449.4920	0.0004	-0.0016	32
39	53449.5481	0.0004	-0.0026	28
40	53449.6063	0.0011	-0.0015	19
48	53450.0615	0.0003	-0.0031	104
53	53450.3475	0.0004	-0.0026	33
54	53450.4041	0.0004	-0.0031	33
55	53450.4628	0.0005	-0.0015	34
56	53450.5191	0.0006	-0.0023	33
57	53450.5762	0.0004	-0.0022	33
58	53450.6337	0.0007	-0.0019	30
90	53452.4606	0.0006	-0.0021	68
91	53452.5182	0.0004	-0.0016	99
92	53452.5727	0.0003	-0.0043	80
105	53453.3128	0.0014	-0.0064	52
106	53453.3732	0.0008	-0.0032	178
107	53453.4296	0.0008	-0.0038	171
108	53453.4888	0.0014	-0.0018	159
109	53453.5449	0.0004	-0.0027	81
110	53453.5994	0.0008	-0.0053	58
136	53455.0887	0.0010	-0.0006	179
137	53455.1520	0.0014	0.0056	107
140	53455.3248	0.0049	0.0072	81
141	53455.3818	0.0013	0.0070	103
153	53456.0686	0.0005	0.0087	176
157	53456.3115	0.0014	0.0231	34
158	53456.3547	0.0012	0.0093	37
159	53456.4114	0.0007	0.0088	37
160	53456.4697	0.0008	0.0100	38
161	53456.5189	0.0014	0.0021	37
162	53456.5927	0.0014	0.0188	37
194	53458.4126	0.0008	0.0115	26
195	53458.4636	0.0010	0.0054	38
196	53458.5165	0.0020	0.0012	37
197	53458.5804	0.0012	0.0081	38
211	53459.3739	0.0012	0.0022	40

^a BJD-2400000.

^b Against $max = 2453447.3238 + 0.057099E$.

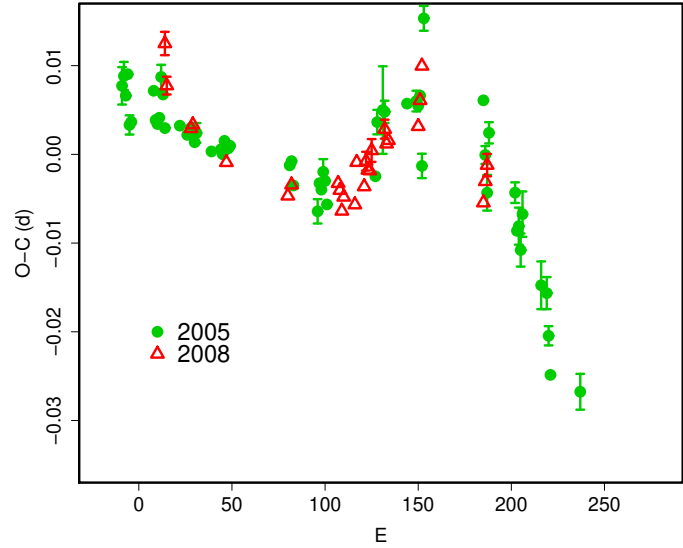
^c Number of points used to determine the maximum.

Table 293. Superhump maxima of 1RXS J0532 (2005) (continued).

E	\max^a	error	$O - C^b$	N^c
212	53459.4268	0.0009	-0.0021	39
213	53459.4844	0.0021	-0.0015	39
214	53459.5389	0.0019	-0.0041	39
215	53459.6001	0.0026	-0.0000	39
225	53460.1637	0.0027	-0.0074	160
228	53460.3343	0.0018	-0.0081	73
229	53460.3866	0.0011	-0.0129	70
230	53460.4394	0.0009	-0.0172	61
246	53461.3520	0.0020	-0.0181	39

Table 294. Superhump maxima of 1RXS J0532 (2008).

E	\max^a	error	$O - C^b$	N^c
0	54474.1642	0.0013	0.0093	102
1	54474.2167	0.0010	0.0046	37
14	54474.9549	0.0003	0.0002	80
15	54475.0125	0.0002	0.0006	108
33	54476.0371	0.0002	-0.0030	121
66	54477.9196	0.0004	-0.0057	98
68	54478.0352	0.0005	-0.0044	92
93	54479.4644	0.0004	-0.0034	108
94	54479.5208	0.0005	-0.0041	110
95	54479.5756	0.0004	-0.0064	114
96	54479.6343	0.0004	-0.0048	117
102	54479.9764	0.0008	-0.0055	90
103	54480.0383	0.0005	-0.0007	107
107	54480.2642	0.0005	-0.0033	110
108	54480.3243	0.0011	-0.0004	117
109	54480.3804	0.0003	-0.0014	117
110	54480.4375	0.0005	-0.0014	117
111	54480.4970	0.0013	0.0009	79
118	54480.8995	0.0011	0.0036	107
119	54480.9550	0.0007	0.0019	96
120	54481.0125	0.0009	0.0024	108
136	54481.9287	0.0008	0.0045	87
137	54481.9888	0.0009	0.0074	108
138	54482.0498	0.0008	0.0113	92
171	54483.9207	0.0006	-0.0030	261
172	54483.9802	0.0005	-0.0005	385
173	54484.0392	0.0013	0.0013	185

^a BJD-2400000.^b Against $\max = 2454474.1550 + 0.057127E$.^c Number of points used to determine the maximum.**Fig. 172.** Comparison of $O - C$ diagrams of 1RXS J0532 between different superoutbursts. A period of 0.05716 d was used to draw this figure. Approximate cycle counts (E) after the start of the 2008 superoutburst were used. The $O - C$ diagram of the 2005 superoutburst bet fits the 2008 one by assuming an earlier development of the superhumps by ~ 26 superhump cycles.**Table 295.** Superhump maxima of 2QZ J0219 (2009)

E	\max^a	error	$O - C^b$	N^c
0	54841.9576	0.0010	0.0015	94
12	54842.9286	0.0004	0.0002	395
24	54843.8982	0.0006	-0.0023	253
25	54843.9810	0.0006	-0.0005	271
49	54845.9290	0.0011	0.0032	260
50	54846.0001	0.0011	-0.0068	127
61	54846.9029	0.0014	0.0049	224
62	54846.9821	0.0012	0.0030	267
74	54847.9480	0.0017	-0.0032	189

^a BJD-2400000.^b Against $\max = 2454841.9562 + 0.081014E$.^c Number of points used to determine the maximum.

survey (cf. Price et al. 2004b; for more information see e.g. Golovin et al. 2005 and Templeton et al. 2006).

Golovin et al. (2005) presented a preliminary period analysis and an $O-C$ diagram showing the presence of a variation in the superhump period. Templeton et al. (2006) claimed that the object belongs to WZ Sge-type subclass based on their findings in the period variation and the presence of a rebrightening. The claim by Templeton et al. (2006), however, led to a rather misguided conclusion because they compared the portions of different stages (ordinary superhumps in ASAS J0025 and early superhumps in WZ Sge), thereby resulting an inadequate period selection in drawing the $O-C$ diagram. We used combined data set used in Templeton et al. (2006) and ours, and determined superhump maxima during the superoutburst plateau and subsequent rapid fading (table 296). The object showed a clear positive period derivative before the terminal brightening (this agrees with the general tendency in Golovin et al. 2005). The P_{dot} in this interval ($E \leq 151$) was $+8.7(0.4) \times 10^{-5}$. The mean periods for the initial part ($E \leq 30$) and the last part ($165 \leq E \leq 219$) were 0.05682(5) d and 0.05686(3) d, respectively, while the mean period during the entire plateau was 0.057109(7) d.

The superhumps in this object showed complex behavior (see figure 34). After the termination of the main superoutburst, the superhumps became doubly humped. One the maxima (peak 1, dots in figure 34) of these double waves, which are listed in table 297, are on a smooth extension of the times of maxima listed in table 296 (filled circles in figure 34), but had a shorter period. The other (peak 2, open squares in figure 34) are on a smooth extension of the times of the maxima during the post-rebrightening stage (table 298). The mean periods of two components of the humps between the termination of the main superoutburst and rebrightening were 0.056833(12) d (peak 1) and 0.056829(21) d (peak 2), respectively. These periods almost exactly match the mean period during initial and last parts of the superoutburst plateau.

The mean period of the superhumps during the post-rebrightening stage (corresponding to $347 \leq E \leq 661$) was 0.057000(6) d. This period, longer than some of observed (super)hump periods at earlier times, is unlikely the orbital period. Furthermore, the humps during the post-rebrightening stage ($347 \leq E \leq 661$) appear to be on a smooth extension of the superhumps at late stage of the superoutburst plateau ($165 \leq E \leq 219$). The combined set of them yielded a mean period of 0.056995(3) d. The stability of the period and phase for such a long interval ($166 \leq E \leq 661$, 28 d) is surprising. These humps bear strong resemblance to post-superoutburst superhumps in some of well-observed WZ Sge-type dwarf novae (Kato et al. 2008; subsection 5.1). Following the same procedure as in Kato et al. (2008), the mean period of these post-superoutburst superhumps was found to be 0.3 % longer than the superhump period near the onset of the superoutburst (see discussion in Kato et al. 2008 for this selection), which is close to the universal ~ 0.5 % excess

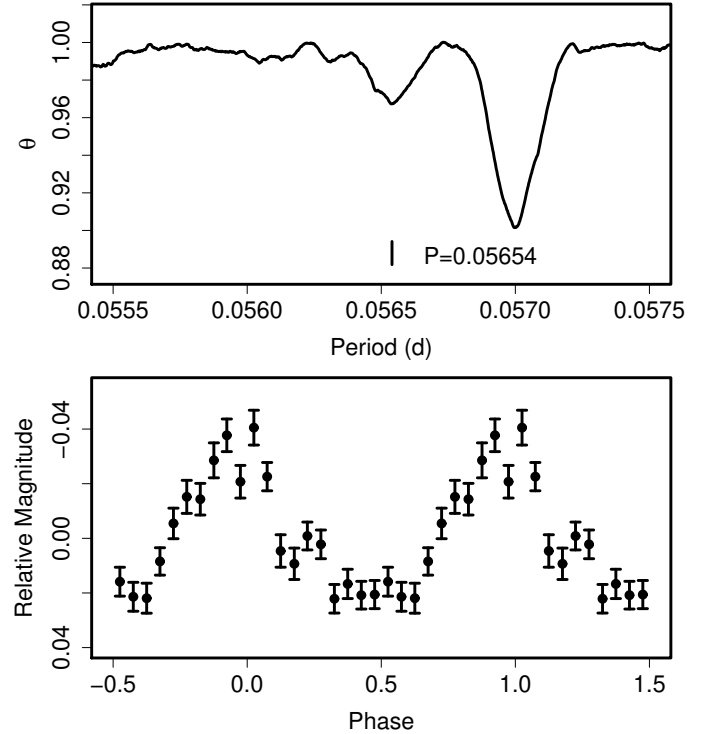


Fig. 173. Candidate orbital period after subtracting the superhump signal. (Upper): PDM analysis. The tick denotes the candidate orbital period. The strong signal around $P = 0.0570$ d is the residual superhump signal. (Lower): Phase-averaged profile.

described in Kato et al. (2008).

We also performed a period analysis of the post-superoutburst stage (BJD after 2453282) after subtracting fitted superhump signals (figure 173). The candidate P_{dot} was found with a period of 0.056540(3) d. Although further spectroscopic confirmation is required, this period gives ϵ of 1.0 %.

6.151. ASAS J023322–1047.0

ASAS J023322–1047.0 (hereafter ASAS J0233) is a dwarf nova detected by ASAS-3 on 2006 January 20 ($V = 12.1$, vsnet-alert 8801). Early superhumps were immediately detected (vsnet-alert 8815), and ordinary superhumps developed eight days after the outburst detection (vsnet-alert 8825). Vanmunster et al. (2006) summarized this outburst and reported period analyses. The data was a combination of ours and the AAVSO data, as utilized in Vanmunster et al. (2006). The mean periods of early and ordinary superhumps determined with the PDM method were 0.054895(23) d (figure 174) and 0.055970(9) d (figure 175), respectively. The times of ordinary superhump maxima are listed in table 299. The $O-C$ diagram (cf. figure 4) clearly demonstrates the presence of the early development stage (stage A, $E \leq 2$), stage B with a positive period derivative, and the final transition to a shorter period (stage C). The P_{dot} for the stage B ($7 \leq E \leq 216$) was $+4.9(0.5) \times 10^{-5}$.

Table 296. Superhump maxima of ASAS J0025 (2004).

E	\max^a	error	$O - C^b$	N^c
0	53264.3302	0.0007	0.0120	46
1	53264.3810	0.0005	0.0057	41
2	53264.4408	0.0002	0.0084	160
3	53264.4971	0.0001	0.0076	238
4	53264.5544	0.0002	0.0078	160
9	53264.8371	0.0001	0.0050	159
10	53264.8950	0.0001	0.0058	170
11	53264.9512	0.0001	0.0049	170
12	53265.0123	0.0004	0.0089	180
13	53265.0656	0.0002	0.0051	465
14	53265.1215	0.0002	0.0039	389
15	53265.1825	0.0004	0.0078	207
16	53265.2352	0.0005	0.0034	262
17	53265.2921	0.0005	0.0032	296
18	53265.3500	0.0002	0.0040	181
19	53265.4064	0.0003	0.0033	116
20	53265.4635	0.0003	0.0033	143
21	53265.5198	0.0002	0.0025	91
30	53266.0316	0.0003	0.0004	90
31	53266.0893	0.0002	0.0010	114
32	53266.1455	0.0002	0.0001	285
33	53266.2010	0.0003	-0.0015	351
34	53266.2594	0.0003	-0.0002	227
35	53266.3164	0.0006	-0.0003	72
37	53266.4306	0.0006	-0.0003	64
40	53266.6011	0.0003	-0.0011	30
41	53266.6573	0.0002	-0.0020	37
42	53266.7141	0.0003	-0.0023	37
44	53266.8279	0.0002	-0.0026	162
47	53266.9947	0.0023	-0.0072	109
48	53267.0575	0.0004	-0.0015	90
49	53267.1131	0.0004	-0.0030	68
50	53267.1682	0.0005	-0.0050	85
51	53267.2240	0.0003	-0.0063	89
53	53267.3428	0.0004	-0.0016	110
54	53267.3979	0.0002	-0.0037	216
55	53267.4559	0.0002	-0.0028	278
56	53267.5123	0.0002	-0.0035	247
57	53267.5692	0.0003	-0.0037	129
58	53267.6253	0.0002	-0.0047	170
59	53267.6830	0.0002	-0.0041	256
60	53267.7406	0.0002	-0.0036	247
61	53267.8010	0.0006	-0.0002	392
62	53267.8549	0.0009	-0.0035	314
64	53267.9652	0.0013	-0.0073	101
65	53268.0262	0.0004	-0.0035	329
66	53268.0833	0.0003	-0.0035	177
67	53268.1378	0.0004	-0.0061	172
68	53268.1921	0.0017	-0.0089	85
69	53268.2518	0.0006	-0.0063	232
70	53268.3121	0.0004	-0.0031	98
71	53268.3691	0.0005	-0.0031	63
72	53268.4264	0.0008	-0.0030	103
73	53268.4792	0.0015	-0.0073	61

^a BJD-2400000.^b Against $\max = 2453264.3182 + 0.057099E$.^c Number of points used to determine the maximum.**Table 296.** Superhump maxima of ASAS J0025 (2004) (continued).

E	\max	error	$O - C$	N
75	53268.5953	0.0003	-0.0054	158
76	53268.6533	0.0003	-0.0045	461
77	53268.7070	0.0004	-0.0078	292
78	53268.7731	0.0005	0.0012	309
79	53268.8248	0.0003	-0.0043	405
80	53268.8804	0.0003	-0.0058	162
81	53268.9356	0.0005	-0.0077	187
82	53268.9989	0.0009	-0.0014	296
83	53269.0551	0.0003	-0.0024	515
84	53269.1111	0.0011	-0.0035	181
85	53269.1649	0.0005	-0.0068	287
86	53269.2266	0.0005	-0.0021	215
88	53269.3348	0.0004	-0.0082	61
91	53269.5104	0.0009	-0.0039	68
92	53269.5645	0.0006	-0.0069	53
96	53269.7960	0.0011	-0.0038	314
97	53269.8540	0.0015	-0.0028	393
98	53269.9110	0.0002	-0.0030	280
99	53269.9732	0.0009	0.0022	106
100	53270.0234	0.0006	-0.0048	212
101	53270.0828	0.0005	-0.0024	244
102	53270.1390	0.0005	-0.0034	218
103	53270.1979	0.0006	-0.0015	245
104	53270.2542	0.0004	-0.0024	235
108	53270.4826	0.0012	-0.0023	26
109	53270.5399	0.0014	-0.0021	41
110	53270.5973	0.0025	-0.0019	25
111	53270.6553	0.0006	-0.0010	39
112	53270.7129	0.0007	-0.0005	38
113	53270.7708	0.0011	0.0004	311
114	53270.8243	0.0007	-0.0032	366
115	53270.8836	0.0003	-0.0010	162
116	53270.9407	0.0003	-0.0011	162
128	53271.6280	0.0016	0.0010	266
130	53271.7378	0.0010	-0.0033	231
131	53271.8054	0.0014	0.0072	478
132	53271.8597	0.0009	0.0044	151
135	53272.0370	0.0013	0.0103	203
136	53272.0847	0.0013	0.0010	117
141	53272.3738	0.0021	0.0045	59
142	53272.4346	0.0009	0.0083	147
143	53272.4867	0.0007	0.0033	162
144	53272.5497	0.0017	0.0092	59
148	53272.7788	0.0007	0.0099	445
149	53272.8355	0.0006	0.0095	217
150	53272.8921	0.0005	0.0089	152
151	53272.9467	0.0005	0.0065	100
165	53273.7524	0.0008	0.0128	248
166	53273.8051	0.0004	0.0084	300
167	53273.8622	0.0004	0.0084	155
168	53273.9187	0.0002	0.0078	156
169	53273.9776	0.0003	0.0096	86
176	53274.3737	0.0007	0.0060	73
177	53274.4309	0.0007	0.0061	47
184	53274.8282	0.0003	0.0037	156
185	53274.8866	0.0003	0.0050	152

Table 296. Superhump maxima of ASAS J0025 (2004) (continued).

E	max	error	$O - C$	N
186	53274.9414	0.0003	0.0027	155
197	53275.5699	0.0008	0.0031	179
198	53275.6251	0.0007	0.0013	194
199	53275.6807	0.0008	-0.0003	198
200	53275.7391	0.0005	0.0010	219
201	53275.7959	0.0004	0.0007	264
202	53275.8520	0.0003	-0.0003	262
203	53275.9072	0.0005	-0.0022	251
204	53275.9699	0.0011	0.0035	206
205	53276.0252	0.0035	0.0016	67
206	53276.0874	0.0016	0.0067	169
210	53276.3114	0.0011	0.0023	71
216	53276.6502	0.0016	-0.0015	77
217	53276.7020	0.0012	-0.0068	78
218	53276.7573	0.0018	-0.0086	387
219	53276.8210	0.0018	-0.0019	208
233	53277.6047	0.0023	-0.0177	53
236	53277.7781	0.0023	-0.0156	38

Table 297. Superhump maxima of ASAS J0025 (secondary).

E	max ^a	error	$O - C$ ^b	N ^c
233	53277.6047	0.0023	-0.0196	53
236	53277.7781	0.0023	-0.0175	38
250	53278.5726	0.0015	-0.0224	24
251	53278.6297	0.0018	-0.0224	19
252	53278.6842	0.0015	-0.0250	20
253	53278.7424	0.0003	-0.0239	171
254	53278.7987	0.0005	-0.0247	158
258	53279.0230	0.0010	-0.0288	123
259	53279.0847	0.0011	-0.0242	129
260	53279.1406	0.0013	-0.0254	56
261	53279.1955	0.0005	-0.0276	60
262	53279.2567	0.0013	-0.0235	60
263	53279.3078	0.0014	-0.0295	62
264	53279.3643	0.0008	-0.0301	73
265	53279.4231	0.0011	-0.0284	104
266	53279.4825	0.0010	-0.0261	89
267	53279.5426	0.0011	-0.0231	19
268	53279.5945	0.0008	-0.0283	31
269	53279.6508	0.0015	-0.0291	39
270	53279.7072	0.0006	-0.0298	40
271	53279.7660	0.0006	-0.0281	98
272	53279.8204	0.0004	-0.0307	39
273	53279.8787	0.0003	-0.0296	38
274	53279.9317	0.0019	-0.0337	39
275	53279.9928	0.0008	-0.0297	81
276	53280.0481	0.0005	-0.0315	146
277	53280.1072	0.0007	-0.0295	57
288	53280.7305	0.0004	-0.0343	163
289	53280.7868	0.0003	-0.0351	173
290	53280.8454	0.0003	-0.0336	13
291	53280.9008	0.0008	-0.0353	13
292	53280.9558	0.0013	-0.0374	14
294	53281.0744	0.0025	-0.0330	67
295	53281.1286	0.0006	-0.0359	78
296	53281.1862	0.0009	-0.0354	30
297	53281.2434	0.0004	-0.0353	29
300	53281.4104	0.0021	-0.0396	60
301	53281.4667	0.0011	-0.0404	65
302	53281.5246	0.0012	-0.0396	64
306	53281.7553	0.0005	-0.0373	13
307	53281.8106	0.0004	-0.0391	13
309	53281.9226	0.0057	-0.0413	13
313	53282.1501	0.0003	-0.0422	80
314	53282.2111	0.0015	-0.0383	20
315	53282.2727	0.0033	-0.0338	21
320	53282.5523	0.0018	-0.0397	90
336	53283.4611	0.0015	-0.0445	64
338	53283.5737	0.0018	-0.0461	18
339	53283.6312	0.0008	-0.0457	20
340	53283.6758	0.0039	-0.0582	19
342	53283.7987	0.0029	-0.0495	13
343	53283.8649	0.0045	-0.0404	13
344	53283.9182	0.0023	-0.0442	13
345	53283.9693	0.0018	-0.0502	11
346	53284.0245	0.0004	-0.0521	18
347	53284.0832	0.0014	-0.0505	25

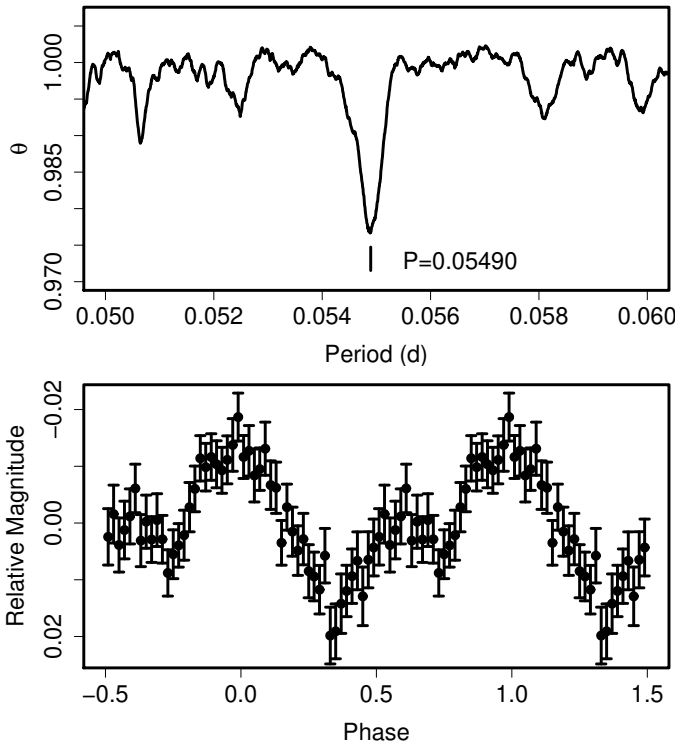
^a BJD-2400000.^b Against $max = 2453264.3200 + 0.057100E$.^c Number of points used to determine the maximum.**Fig. 174.** Early superhumps in ASAS J0233 (2006). (Upper): PDM analysis. (Lower): Phase-averaged profile.

Table 298. Superhump maxima of ASAS J0025 (late stage).

E	\max^a	error	$O - C^b$	N^c
250	53278.5472	0.0009	-0.0478	70
251	53278.5962	0.0032	-0.0559	20
252	53278.6610	0.0010	-0.0482	19
253	53278.7125	0.0011	-0.0538	19
254	53278.7774	0.0027	-0.0460	158
258	53278.9998	0.0019	-0.0520	85
259	53279.0531	0.0007	-0.0558	136
260	53279.1227	0.0065	-0.0433	95
261	53279.1790	0.0042	-0.0441	60
262	53279.2317	0.0017	-0.0485	60
263	53279.2859	0.0018	-0.0514	61
264	53279.3427	0.0025	-0.0517	59
265	53279.3939	0.0042	-0.0576	90
266	53279.4544	0.0011	-0.0542	90
267	53279.5112	0.0061	-0.0545	87
268	53279.5736	0.0019	-0.0492	20
269	53279.6345	0.0019	-0.0454	44
270	53279.6803	0.0005	-0.0567	43
271	53279.7349	0.0013	-0.0592	186
272	53279.7884	0.0011	-0.0628	29
273	53279.8433	0.0056	-0.0650	34
274	53279.9020	0.0013	-0.0634	38
275	53279.9595	0.0020	-0.0630	72
276	53280.0178	0.0038	-0.0618	112
277	53280.0731	0.0011	-0.0636	115
278	53280.1385	0.0012	-0.0553	28
289	53280.7640	0.0007	-0.0579	174
290	53280.8171	0.0014	-0.0619	20
291	53280.8733	0.0058	-0.0628	13
292	53280.9369	0.0025	-0.0563	13
294	53281.0452	0.0016	-0.0622	33
295	53281.1093	0.0031	-0.0552	65
296	53281.1566	0.0016	-0.0650	48
297	53281.2198	0.0010	-0.0589	37
298	53281.2851	0.0062	-0.0507	29
300	53281.3864	0.0005	-0.0636	64
301	53281.4422	0.0015	-0.0649	64
302	53281.5187	0.0014	-0.0455	64
303	53281.5615	0.0112	-0.0598	52
306	53281.7292	0.0017	-0.0634	12
307	53281.7853	0.0008	-0.0644	13
308	53281.8391	0.0012	-0.0677	13
309	53281.8952	0.0014	-0.0687	13
310	53281.9526	0.0003	-0.0684	91
312	53282.0689	0.0004	-0.0663	33
313	53282.1250	0.0003	-0.0673	94
314	53282.1787	0.0011	-0.0707	27
315	53282.2343	0.0013	-0.0722	20
316	53282.2921	0.0015	-0.0715	13
319	53282.5229	0.0022	-0.0120	73
320	53282.5825	0.0037	-0.0095	40
321	53282.6361	0.0030	-0.0131	35

^a BJD-2400000.^b Against $\max = 2453264.3200 + 0.057100E$.^c Number of points used to determine the maximum.**Table 298.** Superhump maxima of ASAS J0025 (late stage, continued).

E	\max	error	$O - C$	N
322	53282.6940	0.0043	-0.0122	20
329	53283.0874	0.0011	-0.0185	111
330	53283.1498	0.0046	-0.0132	29
333	53283.3209	0.0007	-0.0134	91
334	53283.3801	0.0023	-0.0113	83
335	53283.4307	0.0016	-0.0178	50
336	53283.4890	0.0010	-0.0166	63
337	53283.5459	0.0026	-0.0168	47
338	53283.6062	0.0018	-0.0136	19
339	53283.6640	0.0023	-0.0129	19
340	53283.7158	0.0014	-0.0182	24
341	53283.7745	0.0013	-0.0166	23
342	53283.8296	0.0012	-0.0186	13
343	53283.8839	0.0035	-0.0214	11
354	53284.5242	0.0056	-0.0092	8
355	53284.5778	0.0024	-0.0127	15
356	53284.6310	0.0008	-0.0166	15
357	53284.6888	0.0039	-0.0159	15
360	53284.8582	0.0011	-0.0178	14
361	53284.9206	0.0029	-0.0125	14
362	53284.9771	0.0231	-0.0131	38
363	53285.0282	0.0027	-0.0191	84
364	53285.0842	0.0005	-0.0202	53
366	53285.2073	0.0014	-0.0113	49
367	53285.2684	0.0063	-0.0073	46
370	53285.4228	0.0014	-0.0242	20
371	53285.4786	0.0012	-0.0255	19
372	53285.5398	0.0009	-0.0214	20
373	53285.5988	0.0035	-0.0195	20
385	53286.2793	0.0010	-0.0242	24
386	53286.3371	0.0012	-0.0235	32
387	53286.4023	0.0034	-0.0154	32
388	53286.4559	0.0019	-0.0189	31
393	53286.7365	0.0018	-0.0238	160
394	53286.7980	0.0092	-0.0194	123
402	53287.2410	0.0017	-0.0332	32
403	53287.3080	0.0021	-0.0233	33
404	53287.3638	0.0049	-0.0246	32
405	53287.4223	0.0009	-0.0232	32
406	53287.4793	0.0021	-0.0233	31
407	53287.5323	0.0016	-0.0274	25
426	53288.6193	0.0014	-0.0253	15
427	53288.6787	0.0029	-0.0230	15
428	53288.7304	0.0013	-0.0284	9
430	53288.8398	0.0095	-0.0332	9
431	53288.9068	0.0031	-0.0233	14
432	53288.9730	0.0059	-0.0142	7
437	53289.2404	0.0013	-0.0323	15
440	53289.4162	0.0011	-0.0278	15
441	53289.4720	0.0012	-0.0291	15
442	53289.5446	0.0012	-0.0136	15
443	53289.5998	0.0033	-0.0155	15
444	53289.6469	0.0043	-0.0255	15
447	53289.8176	0.0022	-0.0261	7
448	53289.8722	0.0019	-0.0286	9

Table 298. Superhump maxima of ASAS J0025 (late stage, continued).

E	max	error	$O - C$	N
449	53289.9291	0.0017	-0.0288	72
450	53289.9885	0.0018	-0.0265	59
452	53290.1029	0.0011	-0.0263	60
453	53290.1585	0.0003	-0.0278	55
455	53290.2744	0.0008	-0.0261	30
456	53290.3270	0.0011	-0.0306	30
458	53290.4338	0.0005	-0.0380	30
465	53290.8337	0.0200	-0.0378	15
466	53290.8986	0.0023	-0.0300	11
467	53290.9596	0.0008	-0.0261	13
469	53291.0679	0.0007	-0.0320	16
473	53291.3023	0.0023	-0.0260	12
474	53291.3581	0.0021	-0.0273	19
475	53291.4106	0.0010	-0.0319	19
482	53291.8093	0.0015	-0.0329	13
483	53291.8712	0.0013	-0.0281	14
484	53291.9256	0.0009	-0.0308	71
485	53291.9818	0.0006	-0.0317	59
486	53292.0430	0.0010	-0.0276	72
487	53292.0926	0.0010	-0.0351	47
491	53292.3158	0.0006	-0.0403	40
492	53292.3818	0.0009	-0.0314	38
493	53292.4401	0.0010	-0.0302	38
508	53293.2965	0.0045	-0.0303	15
509	53293.3562	0.0120	-0.0277	14
510	53293.4054	0.0013	-0.0356	19
511	53293.4661	0.0034	-0.0320	20
512	53293.5218	0.0018	-0.0334	20
519	53293.9220	0.0034	-0.0329	58
520	53293.9750	0.0010	-0.0370	68
521	53294.0282	0.0009	-0.0409	110
525	53294.2583	0.0010	-0.0392	43
544	53295.3481	0.0011	-0.0343	32
545	53295.4075	0.0011	-0.0320	32
546	53295.4561	0.0019	-0.0405	32
560	53296.2596	0.0005	-0.0364	28
561	53296.3127	0.0012	-0.0404	29
568	53296.7112	0.0013	-0.0416	146
601	53298.5985	0.0009	-0.0386	158
622	53299.7986	0.0013	-0.0376	16
623	53299.8454	0.0059	-0.0479	16
624	53299.9045	0.0010	-0.0459	16
626	53300.0194	0.0021	-0.0452	47
627	53300.0728	0.0024	-0.0489	58
638	53300.7013	0.0016	-0.0485	14
639	53300.7655	0.0022	-0.0414	14
640	53300.8217	0.0103	-0.0423	17
641	53300.8770	0.0051	-0.0441	15
642	53300.9418	0.0095	-0.0364	13
661	53302.0138	0.0039	-0.0493	34
747	53306.9570	0.0024	-0.0167	35
748	53306.9952	0.0016	-0.0356	50
904	53315.9164	0.0016	-0.0220	29

Table 299. Superhump maxima of ASAS J0233 (2006).

E	max ^a	error	$O - C$ ^b	N ^c
0	53763.8972	0.0009	-0.0004	135
1	53763.9533	0.0004	-0.0003	252
2	53764.0095	0.0006	-0.0001	251
7	53764.2952	0.0004	0.0056	51
8	53764.3509	0.0005	0.0053	53
12	53764.5774	0.0002	0.0078	83
13	53764.6310	0.0003	0.0054	74
14	53764.6880	0.0002	0.0064	105
18	53764.9097	0.0004	0.0040	216
19	53764.9660	0.0004	0.0044	310
20	53765.0212	0.0020	0.0036	105
25	53765.2996	0.0003	0.0019	56
26	53765.3557	0.0004	0.0021	55
30	53765.5790	0.0002	0.0013	93
31	53765.6340	0.0002	0.0003	93
32	53765.6897	0.0003	0.0001	93
48	53766.5841	0.0003	-0.0016	58
49	53766.6425	0.0011	0.0008	59
61	53767.3092	0.0006	-0.0045	45
66	53767.5893	0.0022	-0.0045	45
73	53767.9802	0.0007	-0.0056	79
79	53768.3155	0.0005	-0.0062	54
84	53768.5961	0.0003	-0.0057	53
85	53768.6508	0.0004	-0.0070	58
86	53768.7066	0.0012	-0.0072	33
91	53768.9892	0.0028	-0.0046	42
120	53770.6146	0.0005	-0.0033	58
121	53770.6683	0.0006	-0.0056	58
126	53770.9530	0.0026	-0.0009	288
127	53770.9957	0.0023	-0.0142	129
137	53771.5623	0.0015	-0.0076	108
138	53771.6199	0.0007	-0.0060	102
139	53771.6825	0.0018	0.0006	54
143	53771.9139	0.0040	0.0080	166
144	53771.9557	0.0015	-0.0062	156
161	53772.9160	0.0019	0.0021	18
214	53775.8936	0.0058	0.0115	46
216	53776.0035	0.0035	0.0094	51
244	53777.5705	0.0018	0.0083	45
245	53777.6248	0.0019	0.0066	58
246	53777.6714	0.0053	-0.0028	57
263	53778.6282	0.0012	0.0020	58
264	53778.6805	0.0017	-0.0018	58
280	53779.5786	0.0011	0.0003	49
281	53779.6327	0.0023	-0.0016	58

^a BJD-2400000.^b Against $max = 2453763.8976 + 0.056003E$.^c Number of points used to determine the maximum.

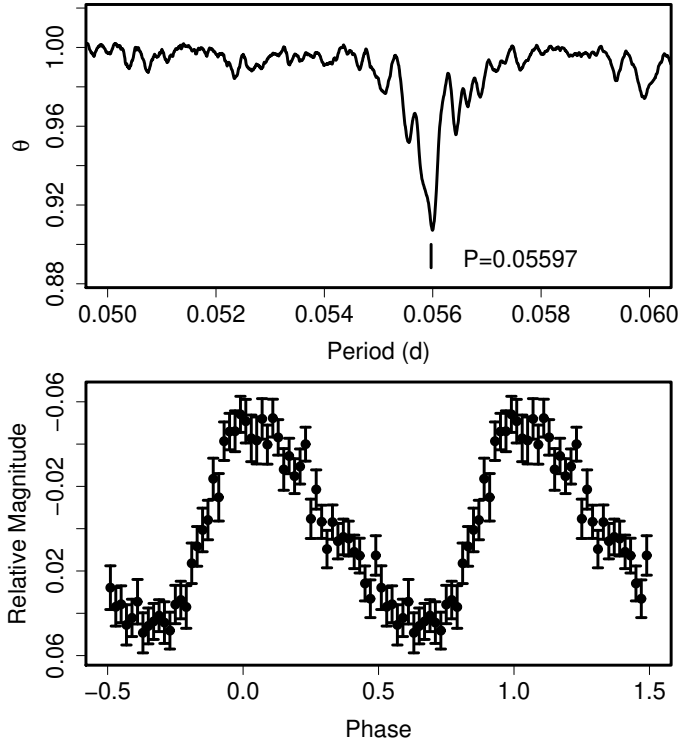


Fig. 175. Ordinary superhumps in ASAS J0233 (2006). (Upper): PDM analysis. (Lower): Phase-averaged profile.

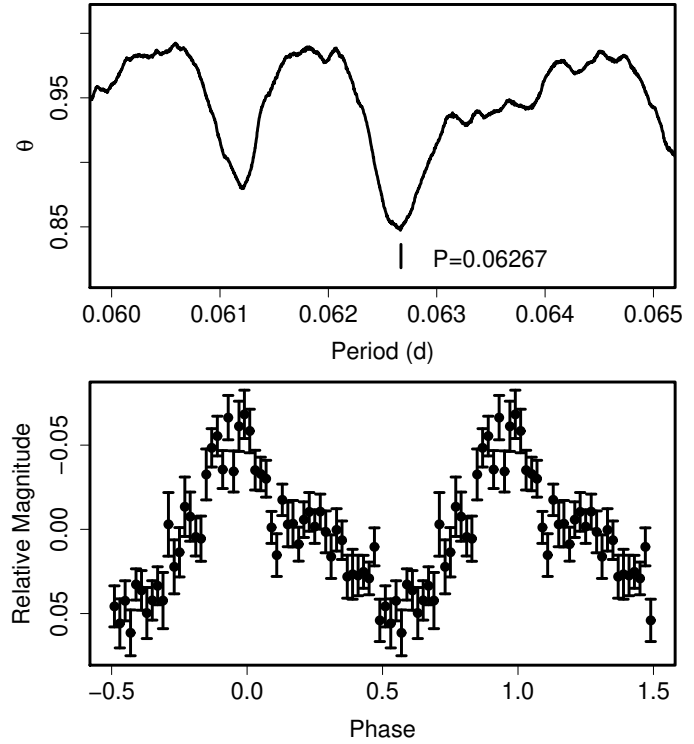


Fig. 176. Superhumps in ASAS J0918 (2005). (Upper): PDM analysis. (Lower): Phase-averaged profile.

6.152. ASAS J091858–2942.6 = Dwarf nova in Pyxis 2005

This object (hereafter ASAS J0918) was independently discovered by G. Pojmanski and K. Haseda (Pojmanski et al. 2005). Follow-up spectroscopy revealed that the object was not a nova, but a dwarf nova in outburst (Kawabata et al. 2005). We undertook time-series photometry soon after the discovery announcement.

A PDM analysis yielded a mean superhump period of 0.06267(2) d (figure 176). The times of superhump maxima are listed in table 300. Although we can derive a global $P_{\text{dot}} = -15.6(4.3) \times 10^{-5}$, this value should not be regarded as the representative period derivative of this system since the object showed a remarkable terminal rebrightening before $E = 78$ and the observed $O - C$'s most likely reflected a shortening of the superhump period between stage B and C. The period derivative for the stage B was not significantly determined from a short segment $E \leq 32$. Future observations starting from the early epoch of a superoutburst are necessary to determine the period derivative, although continuous monitoring by ASAS-3 has not detected any further outburst.

6.153. ASAS J102522–1542.4

ASAS J102522–1542.4 (hereafter ASAS J1025) is a dwarf nova detected by ASAS-3 on 2006 January 26 ($V = 12.2$, vsnet-alert 8821). The detection of early superhumps (vsnet-alert 8824; figure 177, period 0.06136(6) d) and ordinary superhumps (vsnet-alert 8843; figure 178,

Table 300. Superhump maxima of ASAS J0918 (2005).

E	max ^a	error	$O - C^b$	N^c
0	53448.0457	0.0011	-0.0049	275
1	53448.1088	0.0020	-0.0044	171
14	53448.9300	0.0021	0.0025	58
15	53448.9939	0.0016	0.0037	91
16	53449.0527	0.0041	-0.0002	107
17	53449.1128	0.0037	-0.0027	93
30	53449.9332	0.0014	0.0033	62
31	53449.9968	0.0007	0.0043	84
32	53450.0583	0.0007	0.0031	236
78	53452.9311	0.0020	-0.0055	63
79	53453.0001	0.0013	0.0008	63

^a BJD–2400000.

^b Against $\text{max} = 2453448.0506 + 0.062642E$.

^c Number of points used to determine the maximum.

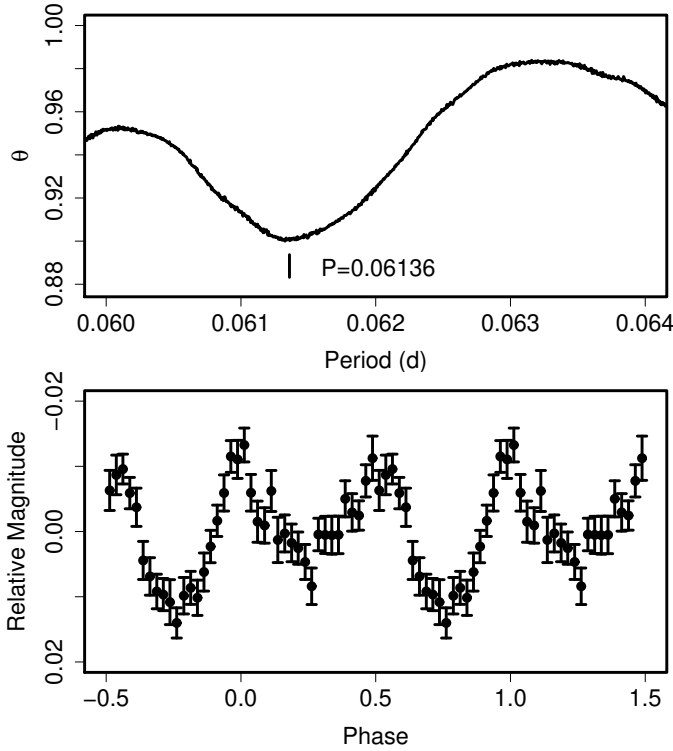


Fig. 177. Early superhumps in ASAS J1025 (2006). (Upper): PDM analysis. (Lower): Phase-averaged profile.

mean period 0.063314(5) d led to a likely classification as a WZ Sge-type dwarf nova. Vanmunster et al. (2006) provided a provisional analysis.

The times of superhump maxima (excluding early superhumps) are listed in table 301. The $O-C$ diagram (cf. figure 4) consisted of three stages A–C. We obtained $P_{\text{dot}} = +10.9(0.6) \times 10^{-5}$ (stage B, $27 \leq E \leq 142$). The stage C superhumps persisted until the start of the rebrightening.

The fractional superhump excess determined from the period of early and ordinary superhumps was 3.2(1) %, which is unusually large for a WZ Sge-type dwarf nova. Combined with the large P_{dot} and the short delay before ordinary superhumps emerged, the object appears to be a “borderline” long- P_{SH} WZ Sge-like dwarf nova similar to BC UMa (Patterson et al. 2003) and ASAS J1600 (Soejima et al. 2009). The exact identification of the P_{orb} , however, should await further observation because the period of early superhumps was determined from a short baseline.

6.154. ASAS J153616–0839.1

ASAS J153616–0839.1 (hereafter ASAS J1536) is a dwarf nova detected by ASAS-3 on 2004 February 2 ($V = 11.54$). A predisccovery observation by K. Haseda on 2004 January 31 ($m_{\text{pg}} = 11.2$) was reported (vsnet-alert 7986, 7987; see also Schmidtobreick et al. 2004). The object showed a relatively smooth fading until February 7, then followed by a ~ 0.2 mag rise associated with prominent superhumps. The object underwent four post-superoutburst

Table 301. Superhump maxima of ASAS J1025 (2006).

E	max ^a	error	$O - C^b$	N^c
0	53764.0703	0.0014	−0.0134	190
1	53764.1397	0.0010	−0.0073	400
2	53764.1957	0.0007	−0.0146	402
3	53764.2511	0.0006	−0.0225	535
4	53764.3255	0.0016	−0.0114	345
7	53764.5218	0.0011	−0.0050	43
8	53764.5815	0.0010	−0.0085	52
9	53764.6420	0.0011	−0.0114	61
11	53764.7765	0.0003	−0.0035	135
12	53764.8409	0.0004	−0.0024	137
13	53764.9058	0.0004	−0.0008	133
14	53764.9707	0.0004	0.0008	120
15	53765.0315	0.0012	−0.0016	42
16	53765.0984	0.0009	0.0020	97
17	53765.1591	0.0003	−0.0007	214
18	53765.2227	0.0004	−0.0004	197
19	53765.2869	0.0003	0.0006	193
23	53765.5426	0.0002	0.0030	169
24	53765.6074	0.0002	0.0045	188
25	53765.6687	0.0004	0.0025	64
27	53765.7982	0.0001	0.0054	135
28	53765.8604	0.0001	0.0044	135
29	53765.9231	0.0001	0.0038	135
30	53765.9855	0.0001	0.0029	134
31	53766.0484	0.0006	0.0025	64
32	53766.1121	0.0003	0.0029	76
33	53766.1743	0.0003	0.0017	145
34	53766.2385	0.0004	0.0027	140
42	53766.7449	0.0002	0.0027	94
43	53766.8074	0.0001	0.0019	127
44	53766.8706	0.0002	0.0018	121
45	53766.9335	0.0002	0.0014	122
46	53766.9956	0.0002	0.0002	107
63	53768.0702	0.0003	−0.0013	255
64	53768.1324	0.0002	−0.0024	393
65	53768.1955	0.0002	−0.0026	419
66	53768.2587	0.0002	−0.0026	417
67	53768.3223	0.0002	−0.0023	333
68	53768.3866	0.0002	−0.0014	106
74	53768.7653	0.0003	−0.0024	116
75	53768.8290	0.0002	−0.0020	117
76	53768.8909	0.0004	−0.0034	117
77	53768.9539	0.0002	−0.0037	106
78	53769.0191	0.0007	−0.0018	53
80	53769.1449	0.0006	−0.0025	30
81	53769.2077	0.0005	−0.0031	33
82	53769.2748	0.0004	0.0007	20
84	53769.3993	0.0002	−0.0014	129
85	53769.4626	0.0003	−0.0014	144
86	53769.5259	0.0003	−0.0014	144
87	53769.5891	0.0003	−0.0015	144

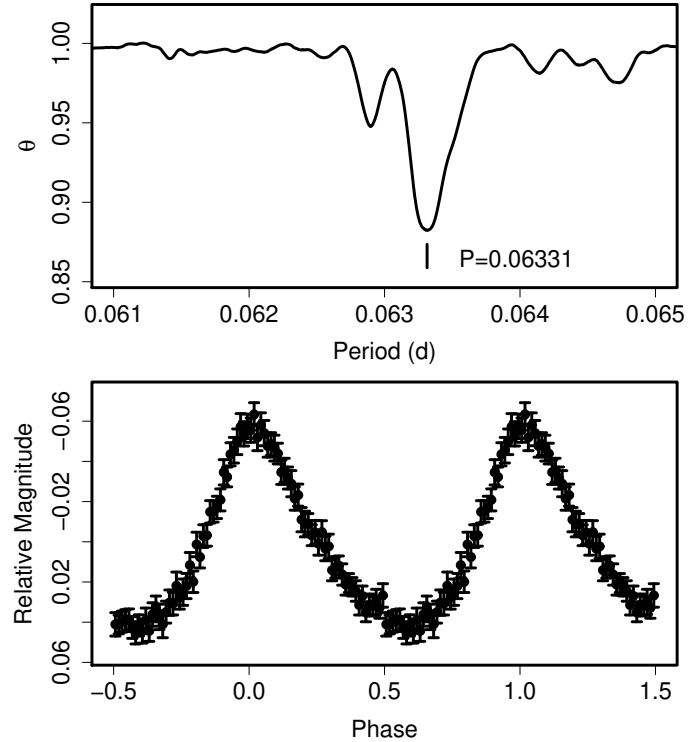
^a BJD−2400000.

^b Against $max = 2453764.0837 + 0.063297E$.

^c Number of points used to determine the maximum.

Table 301. Superhump maxima of ASAS J1025 (2006) (continued).

E	max	error	$O - C$	N
93	53769.9692	0.0005	-0.0011	43
94	53770.0338	0.0005	0.0002	89
95	53770.0970	0.0009	0.0000	78
97	53770.2257	0.0018	0.0022	77
98	53770.2854	0.0006	-0.0014	261
99	53770.3491	0.0027	-0.0010	108
105	53770.7347	0.0005	0.0047	45
106	53770.7976	0.0005	0.0044	66
107	53770.8635	0.0016	0.0070	92
108	53770.9233	0.0005	0.0035	65
109	53770.9879	0.0009	0.0048	46
110	53771.0466	0.0039	0.0002	137
111	53771.1150	0.0004	0.0053	195
112	53771.1778	0.0004	0.0048	194
113	53771.2407	0.0004	0.0044	193
114	53771.3039	0.0008	0.0043	193
121	53771.7517	0.0005	0.0091	57
122	53771.8117	0.0014	0.0057	79
123	53771.8797	0.0006	0.0105	65
124	53771.9424	0.0007	0.0099	51
127	53772.1339	0.0006	0.0115	242
128	53772.1954	0.0004	0.0096	237
129	53772.2566	0.0008	0.0075	138
141	53773.0222	0.0011	0.0136	24
142	53773.0864	0.0007	0.0144	14
158	53774.0871	0.0040	0.0024	56
159	53774.1543	0.0014	0.0064	90
160	53774.2209	0.0005	0.0097	134
161	53774.2833	0.0005	0.0088	135
173	53775.0398	0.0005	0.0057	21
174	53775.1067	0.0007	0.0093	233
175	53775.1704	0.0008	0.0097	250
176	53775.2300	0.0007	0.0060	218
177	53775.2919	0.0009	0.0046	134
188	53775.9848	0.0013	0.0012	12
189	53776.0482	0.0011	0.0013	237
190	53776.1181	0.0009	0.0079	336
191	53776.1781	0.0009	0.0046	230
192	53776.2426	0.0008	0.0059	142
193	53776.3006	0.0013	0.0005	133
205	53777.0572	0.0031	-0.0024	81
206	53777.1187	0.0015	-0.0042	134
207	53777.1802	0.0016	-0.0060	133
208	53777.2431	0.0017	-0.0065	133
209	53777.3080	0.0062	-0.0048	99
223	53778.1895	0.0057	-0.0095	33
232	53778.7589	0.0008	-0.0097	65
233	53778.8201	0.0012	-0.0118	66
234	53778.8824	0.0014	-0.0129	66
235	53778.9464	0.0011	-0.0122	63
249	53779.8286	0.0021	-0.0161	65
250	53779.8939	0.0012	-0.0141	64
251	53779.9557	0.0017	-0.0156	56

**Fig. 178.** Ordinary superhumps in ASAS J1025 (2006). (Upper): PDM analysis. (Lower): Phase-averaged profile.

rebrightenings (figure 179).

The times of superhump maxima are listed in table 302. There was a clear stage A–B transition around $E = 30$. The P_{dot} of the stage B was $+2.4(2.1) \times 10^{-5}$. We know little information whether the object had already developed superhumps or early superhumps before the start of our observation. We, however, adopted this value as the representative period derivative of this system since the object is likely a WZ Sge-type dwarf nova with multiple rebrightenings and a rise associated with prominent superhumps can be better interpreted as a signature of emergence of ordinary superhumps (cf. Patterson et al. 1998). Following this interpretation, the epoch of our observation corresponds to the middle plateau stage of the superoutburst rather than its final stage. We present a representative averaged light curve of superhumps (figure 180).

The object showed a weaker superhump signal during the rebrightening and post-superoutburst stages (figure 181). The period, 0.06473(1) d, appears to be longer than the P_{SH} during the superoutburst plateau, analogous to other WZ Sge-type dwarf novae (subsection 5.1).

6.155. ASAS J160048–4846.2

Imada, Monard (2006) and Soejima et al. (2009) reported a detailed report of the 2005 superoutburst. We further analyzed the data in combination with the AAVSO observations. The times of superhump maxima are listed in table 303. The result basically confirmed the analy-

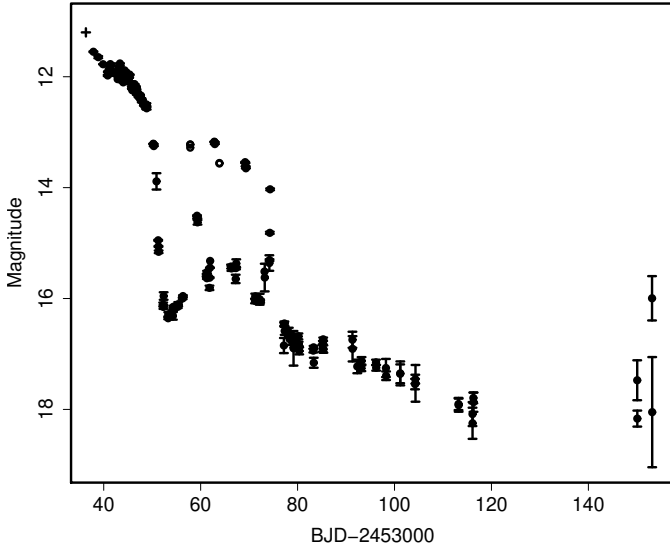


Fig. 179. Light curve of ASAS J1536 (2004). The filled circles, open circles and a cross represent CCD observations used here and ASAS-3 *V* data, and Haseda's prediscovery photographic observation, respectively.

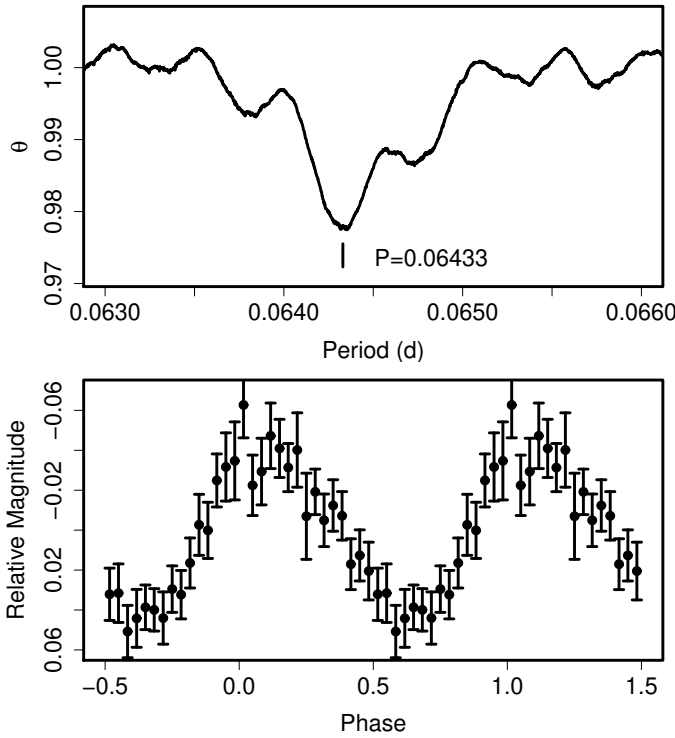


Fig. 180. Ordinary superhumps in ASAS J1536 (2004) after BJD 2453043 (Upper): PDM analysis. (Lower): Phase-averaged profile.

Table 302. Superhump maxima of ASAS J1536 (2004).

E	\max^a	error	$O - C^b$	N^c
0	53041.3165	0.0019	-0.0206	189
15	53042.3057	0.0009	-0.0017	200
16	53042.3627	0.0024	-0.0094	85
30	53043.2831	0.0005	0.0053	89
31	53043.3509	0.0006	0.0084	71
39	53043.8620	0.0079	0.0020	10
42	53044.0604	0.0005	0.0064	115
43	53044.1220	0.0003	0.0032	106
45	53044.2550	0.0003	0.0068	204
46	53044.3178	0.0005	0.0050	205
54	53044.8268	0.0026	-0.0036	20
58	53045.0914	0.0004	0.0024	133
59	53045.1546	0.0003	0.0008	125
61	53045.2840	0.0005	0.0008	205
62	53045.3527	0.0006	0.0048	163
69	53045.8043	0.0023	0.0036	16
70	53045.8644	0.0073	-0.0009	20
73	53046.0600	0.0003	0.0005	125
74	53046.1224	0.0006	-0.0017	81
76	53046.2592	0.0009	0.0057	191
77	53046.3184	0.0008	0.0002	189
78	53046.3816	0.0010	-0.0013	57
82	53046.6400	0.0006	-0.0016	59
84	53046.7845	0.0029	0.0134	16
85	53046.8407	0.0086	0.0050	19
89	53047.0923	0.0005	-0.0022	106
90	53047.1578	0.0003	-0.0014	118
92	53047.2875	0.0008	-0.0011	219
93	53047.3481	0.0009	-0.0051	176
98	53047.6728	0.0010	-0.0039	42
100	53047.8029	0.0049	-0.0031	16
101	53047.8652	0.0062	-0.0055	18
108	53048.3228	0.0007	-0.0008	111
115	53048.7757	0.0093	-0.0007	13
116	53048.8331	0.0169	-0.0080	16
138	53050.2659	0.0010	0.0017	151
139	53050.3257	0.0015	-0.0032	159

^a BJD-2400000.

^b Against $\max = 2453041.3371 + 0.0646895E$.

^c Number of points used to determine the maximum.

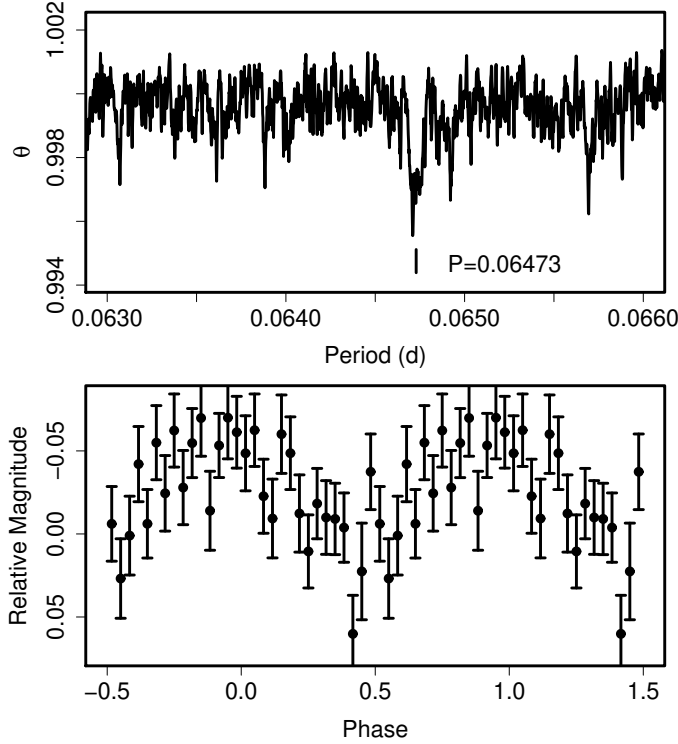


Fig. 181. Superhumps in ASAS J1536 (2004) during the rebrightenings and post-superoutburst stage. (Upper): PDM analysis. (Lower): Phase-averaged profile.

Table 303. Superhump maxima of ASAS J1600 (2005).

E	max ^a	error	$O - C^b$	N^c
0	53533.4285	0.0011	-0.0240	147
1	53533.4925	0.0006	-0.0250	147
2	53533.5648	0.0007	-0.0176	147
8	53533.9619	0.0009	-0.0101	107
9	53534.0332	0.0008	-0.0038	111
10	53534.0990	0.0009	-0.0029	90
13	53534.2960	0.0003	-0.0006	145
14	53534.3632	0.0002	0.0016	147
15	53534.4283	0.0003	0.0017	147
16	53534.4932	0.0002	0.0017	145
17	53534.5604	0.0002	0.0040	147
18	53534.6229	0.0004	0.0016	84
28	53535.2765	0.0001	0.0058	146
29	53535.3418	0.0002	0.0062	146
30	53535.4064	0.0001	0.0058	147
31	53535.4711	0.0002	0.0056	146
32	53535.5359	0.0002	0.0054	147
45	53536.3752	0.0003	0.0005	86
46	53536.4410	0.0002	0.0014	146
47	53536.5059	0.0002	0.0014	132
48	53536.5699	0.0003	0.0005	95
59	53537.2848	0.0002	0.0011	148
60	53537.3490	0.0002	0.0004	148
61	53537.4139	0.0002	0.0003	148
62	53537.4787	0.0002	0.0002	144
63	53537.5452	0.0004	0.0017	117
73	53538.1946	0.0003	0.0018	123
74	53538.2590	0.0003	0.0012	144
75	53538.3240	0.0003	0.0013	147
76	53538.3890	0.0003	0.0014	140
77	53538.4533	0.0003	0.0008	146
78	53538.5195	0.0003	0.0020	146
79	53538.5843	0.0006	0.0019	87
89	53539.2362	0.0003	0.0044	144
90	53539.3009	0.0004	0.0042	144
91	53539.3654	0.0003	0.0038	144
92	53539.4313	0.0004	0.0047	144
93	53539.4970	0.0004	0.0055	144
104	53540.2136	0.0004	0.0078	147
105	53540.2786	0.0004	0.0079	147
106	53540.3421	0.0003	0.0064	147
107	53540.4072	0.0003	0.0065	147
108	53540.4723	0.0004	0.0067	147
109	53540.5376	0.0003	0.0071	132
119	53541.1813	0.0018	0.0014	90
120	53541.2491	0.0005	0.0042	147
121	53541.3134	0.0005	0.0036	146
122	53541.3777	0.0004	0.0031	146
123	53541.4407	0.0005	0.0010	147
124	53541.5058	0.0005	0.0013	146
125	53541.5711	0.0007	0.0016	111

^a BJD-2400000.

^b Against $max = 2453533.4525 + 0.064936E$.

^c Number of points used to determine the maximum.

sis by Soejima et al. (2009). The maxima for $E \geq 243$ were humps observed during the rebrightening. Since the $O - C$'s of these humps were not on a smooth extension of the stage C superhumps, these humps are less likely persisting superhumps.

6.156. CTCV J0549-4921

The identification of this object (hereafter CTCV J0549) as an SU UMa-type dwarf nova was reported by Imada et al. (2008a). As in KK Tel (Kato et al. 2003d), Imada et al. (2008a) failed to identify the correct P_{SH} and P_{dot} due to the large variation in P_{SH} . In table 304, we listed updated times of superhump maxima, measured from the data reported in Imada et al. (2008a). Following the stage A period evolution ($E \leq 1$), the P_{SH} varied strongly as in UV Gem and KK Tel. The identified periods are given in table 2. After an examination of ASAS-3 light curve (Pojmanski 2002), we detected a number of outbursts (table 305). The object appears to be more active than inferred by Imada et al. (2008a). The typical length of supercycle is 750-800 d.

6.157. Ha 0242-2802

Ha 0242-2802 (hereafter Ha 0242) was discovered as a CV selected by H α emission (Howell et al. 2002). Woudt et al. (2004) presented time-resolved photometry in quiescence and established its eclipsing nature. Mason, Howell (2005) reported phase-resolved spectroscopy. We observed

Table 303. Superhump maxima of ASAS J1600 (2005). (continued)

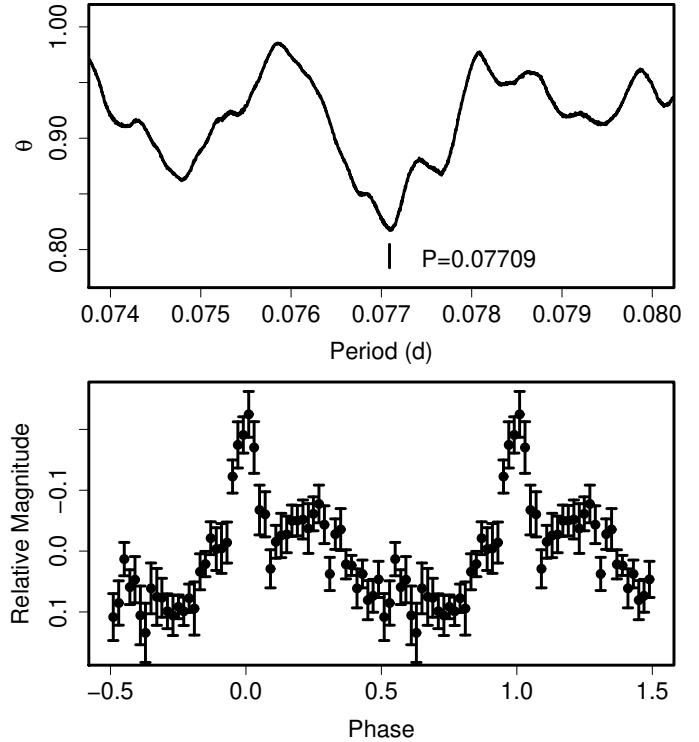
E	max	error	$O - C$	N
135	53542.2184	0.0008	-0.0004	144
136	53542.2824	0.0006	-0.0014	122
137	53542.3457	0.0004	-0.0031	147
138	53542.4114	0.0005	-0.0022	147
139	53542.4741	0.0008	-0.0045	147
140	53542.5399	0.0008	-0.0037	147
182	53545.2514	0.0016	-0.0194	86
243	53549.2366	0.0043	0.0046	106
244	53549.2939	0.0027	-0.0030	128
245	53549.3520	0.0033	-0.0098	115
246	53549.4149	0.0022	-0.0118	73

Table 304. Superhump maxima of CTCV J0549 (2006).

E	max ^a	error	$O - C$ ^b	N ^c
0	53828.2560	0.0017	-0.0251	188
1	53828.3308	0.0027	-0.0349	183
23	53830.2389	0.0004	0.0126	105
24	53830.3275	0.0005	0.0166	123
35	53831.2610	0.0002	0.0197	193
36	53831.3448	0.0004	0.0189	99
47	53832.2610	0.0003	0.0048	189
48	53832.3513	0.0010	0.0106	98
118	53838.2499	0.0003	-0.0111	190
119	53838.3334	0.0008	-0.0122	98

^a BJD-2400000.^b Against $max = 2453828.2811 + 0.084575E$.^c Number of points used to determine the maximum.**Table 305.** Outbursts of CTCV J0549.

JD-2400000	V max	Duration (d)	Type
51952.5	13.5	>9	Super
52172.9	13.7	1	Normal
52578.7	14.0	1	Normal
53025.6	13.6	>10	Super
53489.5	13.8	1	Normal
53740.6	13.6	2	Normal
53813.7	15.0	1	Normal
53830.5	13.3	>6	Super
54216.5	13.8	1	Normal
54301.9	13.8	1	Normal
54440.7	14.3	1	Normal
54586.5	13.1	>8	Super
54705.9	14.4	1	Normal

**Fig. 182.** Superhumps in Ha 0242 (2002). (Upper): PDM analysis. (Lower): Phase-averaged profile.**Table 306.** Superhump maxima of Ha 0242 (2006).

E	max ^a	error	$O - C$ ^b	N ^c
0	53742.3224	0.0023	-0.0047	102
8	53742.9480	0.0028	0.0048	166
9	53743.0219	0.0016	0.0017	128
29	53744.5569	0.0041	-0.0035	28
30	53744.6442	0.0012	0.0068	47
31	53744.7095	0.0022	-0.0050	26
42	53745.5612	0.0006	-0.0005	53
43	53745.6392	0.0005	0.0006	59

^a BJD-2400000.^b Against $max = 2453742.3271 + 0.077013E$.^c Number of points used to determine the maximum.

the 2006 superoutburst and established its SU UMa-type nature. The times of superhump maxima, measured from observations outside the eclipses, are listed in table 306. Due to the overlapping eclipses, it is difficult to clearly determine the period variation. The mean P_{SH} with the PDM method was 0.07709(2) d (figure 182), 3.3 % longer than the P_{orb} (updated using eclipse timings in Krajci 2006). This P_{SH} was adopted in table 2.

6.158. SDSSp J013701.06-091234.9

This object (hereafter SDSS J0137) was extensively studied by Imada et al. (2006a). We have reanalyzed the data and obtained improved and newly measured times

Table 307. Superhump maxima of SDSS J0137 (2003–2004).

E	max ^a	error	$O - C^b$	N^c
0	52996.8751	0.0007	-0.0022	64
1	52996.9288	0.0005	-0.0051	164
2	52996.9846	0.0008	-0.0059	134
8	52997.3246	0.0001	-0.0056	129
9	52997.3819	0.0002	-0.0049	128
10	52997.4397	0.0004	-0.0037	86
18	52997.8883	0.0010	-0.0080	59
19	52997.9478	0.0003	-0.0051	127
20	52998.0052	0.0005	-0.0043	107
21	52998.0612	0.0004	-0.0049	89
37	52998.9728	0.0005	0.0009	101
38	52999.0291	0.0005	0.0006	100
53	52999.8745	0.0035	-0.0031	41
54	52999.9370	0.0005	0.0027	57
55	52999.9940	0.0009	0.0032	38
67	53000.6751	0.0015	0.0049	61
71	53000.9011	0.0004	0.0044	96
72	53000.9591	0.0006	0.0058	136
73	53001.0153	0.0005	0.0055	159
74	53001.0708	0.0005	0.0043	154
96	53002.3202	0.0002	0.0083	119
97	53002.3770	0.0002	0.0085	126
98	53002.4356	0.0007	0.0104	75
106	53002.8862	0.0005	0.0082	77
107	53002.9404	0.0004	0.0058	90
108	53002.9965	0.0004	0.0053	75
109	53003.0512	0.0009	0.0033	61
125	53003.9561	0.0004	0.0025	86
126	53004.0132	0.0005	0.0030	80
127	53004.0674	0.0017	0.0006	65
131	53004.2942	0.0003	0.0009	128
132	53004.3502	0.0002	0.0004	102
166	53006.2671	0.0009	-0.0076	41
195	53007.9059	0.0005	-0.0105	93
197	53008.0251	0.0020	-0.0045	29
231	53009.9404	0.0015	-0.0139	83

^a BJD–2400000.^b Against $max = 2452996.8773 + 0.056611E$.^c Number of points used to determine the maximum.**Table 308.** Superhump maxima of SDSS J0137 (2009).

E	max ^a	error	$O - C^b$	N^c
0	54867.9004	0.0038	-0.0099	35
18	54868.9285	0.0009	0.0017	36
36	54869.9520	0.0006	0.0087	111
53	54870.9071	0.0008	0.0038	49
124	54874.9091	0.0017	-0.0038	53
160	54876.9456	0.0020	-0.0004	35

^a BJD–2400000.^b Against $max = 2454867.9103 + 0.056473E$.^c Number of points used to determine the maximum.**Table 309.** Superhump maxima of SDSS J0310 (2004).

E	max ^a	error	$O - C^b$	N^c
0	53198.5967	0.0009	0.0031	154
1	53198.6602	0.0012	-0.0020	98
14	53199.5511	0.0086	-0.0034	83
15	53199.6279	0.0013	0.0048	155
44	53201.6086	0.0023	-0.0050	154
49	53201.9664	0.0066	0.0097	73
78	53203.9367	0.0019	-0.0105	137
160	53209.5801	0.0116	0.0047	87
161	53209.6427	0.0084	-0.0013	134

^a BJD–2400000.^b Against $max = 2453198.5936 + 0.068637E$.^c Number of points used to determine the maximum.

6.159. SDSS J031051.66–075500.3

This object (hereafter SDSS J0310) is a CV selected during the course of the SDSS (Szkody et al. 2003). B. Monard detected an outburst in 2004 July and reported the presence of superhumps (vsnet-alert 8236, 8239). We analyzed the observation of this superoutburst. The best superhump period based on the first three nights was 0.06866(6) d (figure 183), supporting the identification by D. Nogami (vsnet-alert 8240). The times of superhump maxima based in this period identification are listed in table 309. We obtained a global P_{dot} of $+2.0(2.7) \times 10^{-5}$, which is probably a mixture of different stages of period evolution. The object underwent another superoutburst in 2009 January–February (vsnet-alert 10995). Further observations are absolutely needed to better qualify the period evolution.

6.160. SDSS J033449.86–071047.8

SDSS J033449.86–071047.8 (hereafter SDSS J0334) is a CV selected during the course of the SDSS (Szkody et al. 2007), who reported the classification as a dwarf nova and an orbital period of 0.079 d. The 2009 outburst was detected by H. Maehara (vsnet-alert 10967). The detection of superhumps qualified this object as an SU UMA-type dwarf nova (vsnet-alert 10973). The best superhump period determined from the observations was 0.07485(3) d (figure 184). The times of superhump maxima are listed

of superhump maxima (table 307). The P_{dot} for $E \leq 98$ (before the remarkable period shortening as described in Imada et al. 2006a) was $+2.3(1.7) \times 10^{-5}$.

The 2009 superoutburst was detected during its rising stage (vsnet-alert 10994). Only the stage C superhumps were recorded (table 308). The mean superhump period with the PDM method was 0.056443(8) d. We adopted this value rather than the one from the times of maxima because of fragmentary visibility of superhumps due to the unfavorable seasonal condition. The relatively low frequency of superoutburst (once in three to five years) appears to be confirmed.

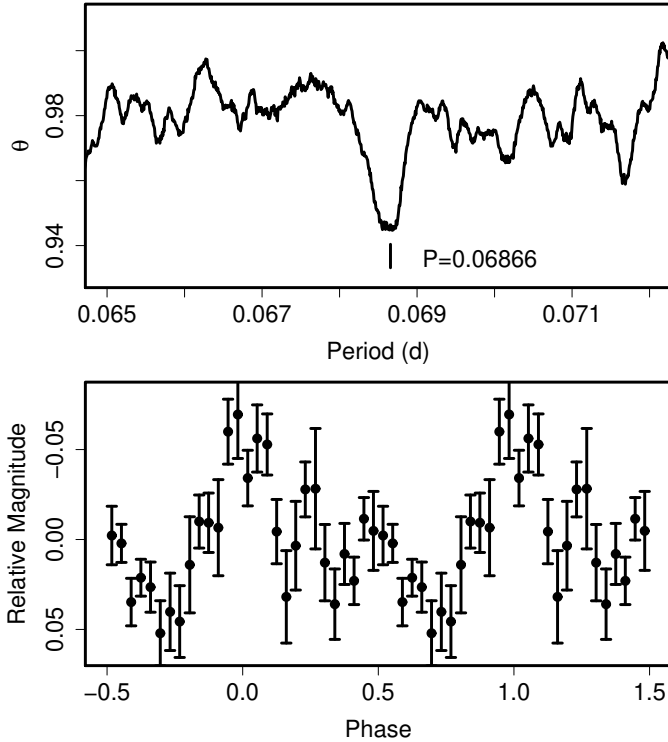


Fig. 183. Superhumps in SDSS J0310 (2004). (Upper): PDM analysis. (Lower): Phase-averaged profile.

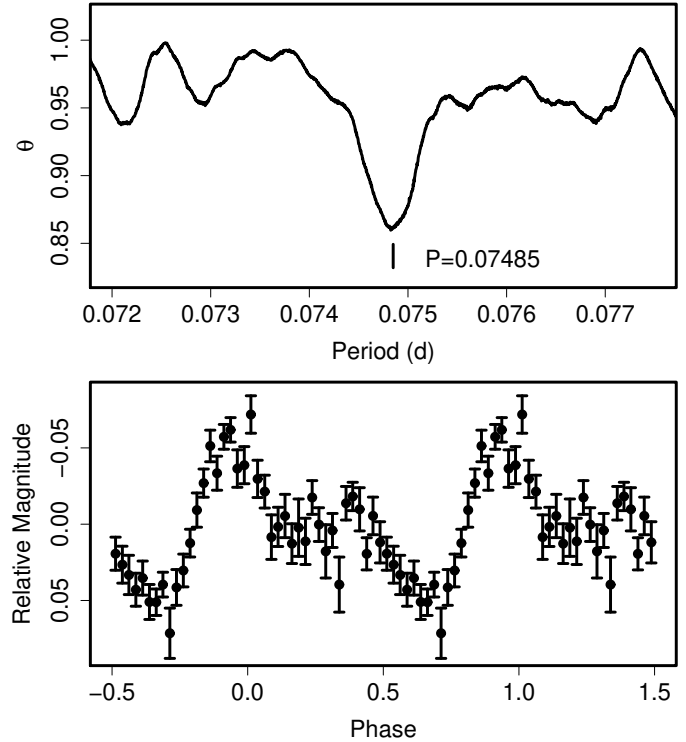


Fig. 184. Superhumps in SDSS J0334 (2009). (Upper): PDM analysis. (Lower): Phase-averaged profile.

Table 310. Superhump maxima of SDSS J0334 (2009).

E	\max^a	error	$O - C^b$	N^c
0	54856.0144	0.0009	-0.0041	160
1	54856.0945	0.0024	0.0012	89
12	54856.9133	0.0015	-0.0025	73
13	54856.9924	0.0014	0.0019	207
14	54857.0689	0.0023	0.0036	127
39	54858.9403	0.0014	0.0056	136
40	54859.0062	0.0022	-0.0032	166
52	54859.9067	0.0024	-0.0000	145
53	54859.9821	0.0015	0.0006	189
54	54860.0531	0.0037	-0.0031	113

^a BJD-2400000.

^b Against $\max = 2454856.0185 + 0.074773E$.

^c Number of points used to determine the maximum.

in table 310.

6.161. *SDSS J074640.62+173412.8*

SDSS J074640.62+173412.8 (hereafter SDSS J0746) is a CV selected during the course of the SDSS (Szkody et al. 2006), who suggested the dwarf nova-type classification based on its variability. J. Shears reported an outburst of this object in 2009 January (cvnet-outburst 2949). The detection of superhumps led to a classification as an SU UMA-type dwarf nova (vsnet-alert 11069). The mean superhump period with the PDM method was

0.066761(15) d (figure 185). The times of superhump maxima are listed in table 311. There was a stage B-C transition around $E = 78$. Excluding $E = 30$, we obtained $P_{\text{dot}} = +9.3(2.5) \times 10^{-5}$, fairly common for this P_{SH} .

6.162. *SDSS J081207.63+131824.4*

SDSS J081207.63+131824.4 (hereafter SDSS J0812) is a CV selected during the course of the SDSS (Szkody et al. 2007). The 2008 superoutburst detected by K. Itagaki (Yamaoka et al. 2008g) led to the classification as a long- P_{orb} SU UMA-type dwarf nova. The mean superhump period with the PDM method was 0.08432(1) d (figure 186). The times of superhump maxima are listed in table 312. We obtained a global P_{dot} of $-24.0(5.2) \times 10^{-5}$, a value similar to the one in UV Gem having a similar P_{SH} .

6.163. *SDSSp J082409.73+493124.4*

SDSSp J082409.73+493124.4 (hereafter SDSS J0824) is a CV selected during the course of the SDSS (Szkody et al. 2002) (see Boyd et al. 2008b for the history of observation). Boyd et al. (2008b) reported the detection of superhumps with a mean period of 0.06954(5). Boyd et al. (2008b) interpreted an apparent phase transition in the late course of the superoutburst as being the transition to late superhumps. Their data, however, had a gap in the middle stage of the superoutburst. Our own observations happened to fill the gap. We used a combined data set by ours and from the AAVSO database, the latter including the partial data in Boyd et al. (2008b). We used the data

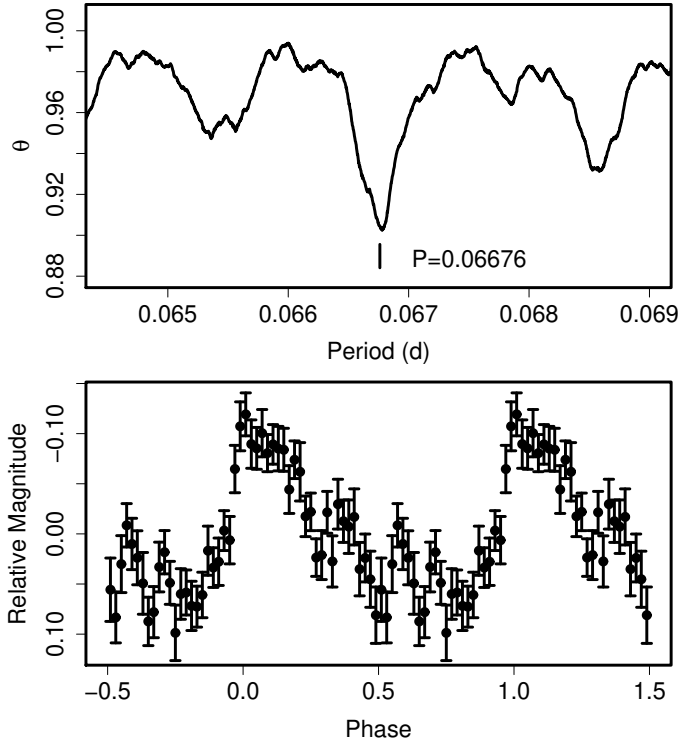


Fig. 185. Superhumps in SDSS J0746 (2009). (Upper): PDM analysis. (Lower): Phase-averaged profile.

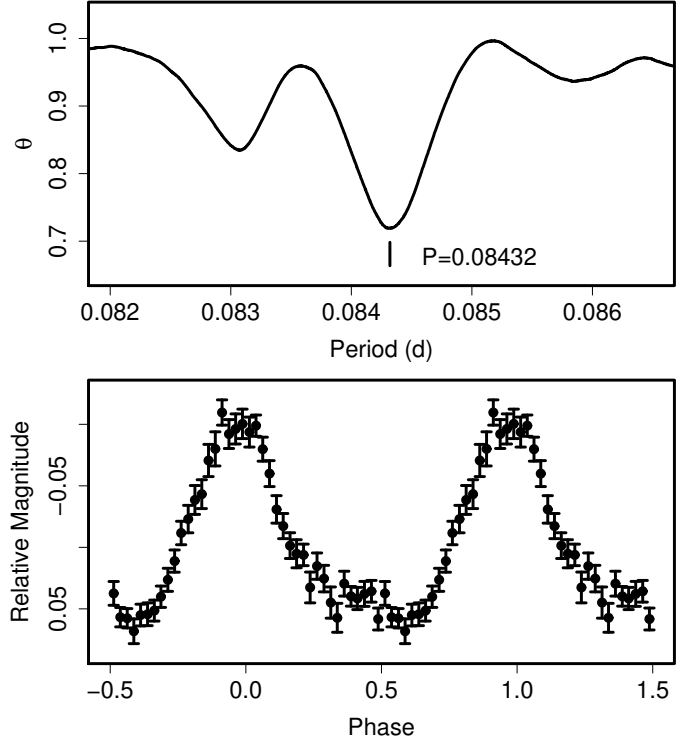


Fig. 186. Superhumps in SDSS J0812 (2008). (Upper): PDM analysis. (Lower): Phase-averaged profile.

Table 311. Superhump maxima of SDSS J0746 (2009).

E	\max^a	error	$O - C^b$	N^c
0	54874.9304	0.0011	0.0039	49
1	54874.9954	0.0019	0.0021	70
2	54875.0599	0.0015	-0.0001	42
30	54876.9158	0.0063	-0.0127	42
31	54876.9944	0.0026	-0.0009	70
32	54877.0607	0.0017	-0.0013	257
33	54877.1304	0.0015	0.0016	292
34	54877.1928	0.0023	-0.0027	119
76	54880.0014	0.0027	0.0031	232
77	54880.0711	0.0016	0.0061	314
78	54880.1387	0.0020	0.0069	182
90	54880.9367	0.0068	0.0042	64
91	54880.9988	0.0033	-0.0005	56
92	54881.0658	0.0019	-0.0003	42
93	54881.1409	0.0018	0.0081	60
94	54881.1859	0.0044	-0.0136	71
138	54884.1366	0.0039	0.0008	99
139	54884.1979	0.0044	-0.0046	74

^a BJD-2400000.

^b Against $\max = 2454874.9265 + 0.066734E$.

^c Number of points used to determine the maximum.

Table 312. Superhump maxima of SDSS J0812 (2008).

E	\max^a	error	$O - C^b$	N^c
0	54751.2800	0.0002	-0.0146	333
35	54754.2365	0.0036	-0.0002	75
36	54754.3234	0.0006	0.0027	154
47	54755.2555	0.0004	0.0101	299
48	54755.3309	0.0008	0.0014	188
59	54756.2661	0.0015	0.0120	216
60	54756.3402	0.0010	0.0020	120
71	54757.2698	0.0008	0.0070	319
83	54758.2727	0.0023	0.0012	88
95	54759.2586	0.0018	-0.0217	103

^a BJD-2400000.

^b Against $\max = 2454751.2946 + 0.084059E$.

^c Number of points used to determine the maximum.

Table 313. Superhump maxima of SDSS J0824 (2007).

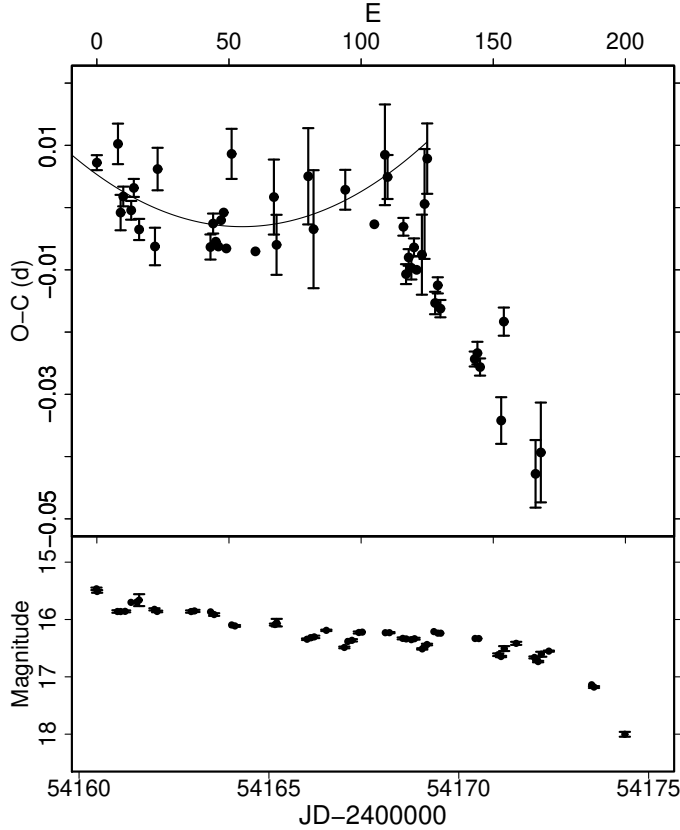


Fig. 187. $O-C$ of superhumps SDSS J0824. (Upper): $O-C$ diagram. The values of $O-C$'s are different from those listed in table 313 and were calculated from a linear fit for the times of superhumps for $E \leq 110$. The curve represents a quadratic fit with $P_{\text{dot}} = +8.0 \times 10^{-5}$. (Lower): Light curve.

common to the AAVSO database and those in Boyd et al. (2008b) to determine the systematic difference between our measurements and those by Boyd et al. (2008b).

Table 313 lists combined times of superhump maxima, after adding a systematic difference of 0.0035 d to Boyd et al. (2008b). The entire data now clearly show a sharp transition from the stage B with a slightly positive P_{dot} to the stage C after $E = 110$ (figure 187). The phase discontinuity reported in Boyd et al. (2008b) reflected this period variation rather than a transition to late superhumps. The P_{dot} of the first segment was $+8.0(2.5) \times 10^{-5}$.

Another likely superoutburst was observed in 2007 December (J. Shears, baavss-alert 1492), giving a supercycle length of ~ 300 d.

6.164. SDSSp J083845.23+491055.5

SDSSp J083845.23+491055.5 (hereafter SDSS J0838) was discovered as a CV having a typical spectrum of a dwarf novae (Szkody et al. 2002). We analyzed the AAVSO data during the 2007 October superoutburst (cf. baavss-alert 1383, 1386). The times of superhump maxima are listed in table 314.

The object underwent another superoutburst in 2009 (baavss-alert 1944). The observation of this superoutburst

E	max^a	error	$O-C^b$	N^c
0	54160.4661	0.0012	0.0001	45
8	54161.0272	0.0033	0.0044	101
9	54161.0860	0.0028	-0.0064	102
10	54161.1583	0.0016	-0.0037	103
13	54161.3654	0.0015	-0.0054	108
14	54161.4388	0.0014	-0.0017	118
16	54161.5716	0.0017	-0.0080	102
22	54161.9875	0.0030	-0.0098	79
23	54162.0697	0.0034	0.0028	74
43	54163.4526	0.0020	-0.0064	144
44	54163.5262	0.0016	-0.0025	120
45	54163.5930	-	-0.0053	0
46	54163.6620	-	-0.0059	0
47	54163.7360	-	-0.0015	0
48	54163.8070	-	-0.0001	0
49	54163.8710	-	-0.0057	0
51	54164.0257	0.0040	0.0098	69
60	54164.6380	-	-0.0044	0
67	54165.1351	0.0060	0.0055	79
68	54165.1972	0.0048	-0.0020	62
80	54166.0455	0.0077	0.0109	100
82	54166.1765	0.0095	0.0028	91
94	54167.0201	0.0032	0.0110	95
105	54167.7820	-	0.0073	0
109	54168.0722	0.0081	0.0191	134
110	54168.1384	0.0035	0.0157	139
116	54168.5491	0.0014	0.0087	23
117	54168.6112	0.0016	0.0012	17
118	54168.6837	0.0013	0.0041	23
119	54168.7518	0.0019	0.0026	21
120	54168.8248	0.0014	0.0060	23
121	54168.8910	-	0.0026	0
123	54169.0330	0.0064	0.0053	102
124	54169.1109	0.0088	0.0136	102
125	54169.1879	0.0057	0.0211	102
128	54169.3741	0.0018	-0.0016	75
129	54169.4467	0.0013	0.0014	61
130	54169.5127	0.0014	-0.0022	74
143	54170.4116	0.0012	-0.0082	77
144	54170.4823	0.0018	-0.0071	70
145	54170.5499	0.0014	-0.0092	55
153	54171.0994	0.0037	-0.0165	93
154	54171.1851	0.0023	-0.0004	42
166	54171.9979	0.0054	-0.0229	80
168	54172.1408	0.0080	-0.0191	79

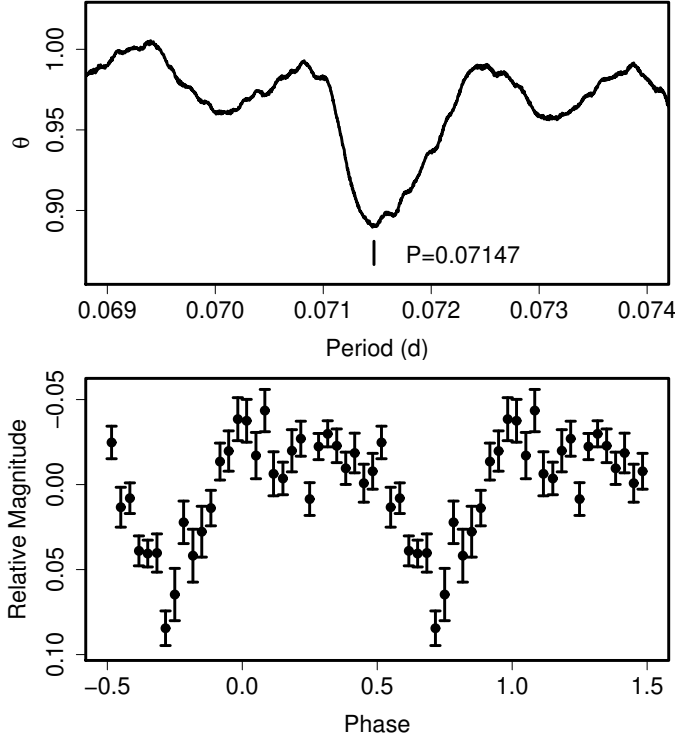
^a BJD-2400000.

^b Against $\text{max} = 2454160.4659 + 0.069607E$.

^c Number of points used to determine the maximum. $N = 0$ refers to Boyd et al. (2008b).

Table 315. Superhump maxima of SDSS J0838 (2009).

E	max ^a	error	$O - C^b$	N^c
0	54884.1135	0.0002	-0.0010	140
1	54884.1829	0.0005	-0.0034	69
2	54884.2575	0.0003	-0.0005	131
101	54891.3654	0.0010	0.0059	51
102	54891.4367	0.0009	0.0055	52
103	54891.5065	0.0010	0.0036	49
111	54892.0825	0.0010	0.0057	140
112	54892.1485	0.0010	-0.0000	151
123	54892.9322	0.0045	-0.0054	90
129	54893.3651	0.0027	-0.0029	51
131	54893.5091	0.0022	-0.0024	53
152	54895.0228	0.0031	0.0049	126
153	54895.0841	0.0038	-0.0055	137
154	54895.1732	0.0040	0.0118	146
155	54895.2169	0.0062	-0.0162	73

^a BJD-2400000.^b Against $max = 2454884.1145 + 0.071732E$.^c Number of points used to determine the maximum.**Fig. 188.** Superhumps in SDSS J0838 (2009, late stage). (Upper): PDM analysis. (Lower): Phase-averaged profile.**Table 314.** Superhump maxima of SDSS J0838 (2007).

E	max ^a	error	$O - C^b$	N^c
0	54396.5730	0.0008	0.0010	98
1	54396.6432	0.0007	-0.0020	101
2	54396.7194	0.0008	0.0010	57

^a BJD-2400000.^b Against $max = 2454396.5720 + 0.07316E$.^c Number of points used to determine the maximum.

finally led to an identification of the superhump period (vsnet-alert 11099). The times of superhump maxima are listed in table 315. Although the identification of the cycle number between $E = 2$ (stage B) and $E = 101$ was rather uncertain, the stage C superhumps with a mean period of 0.07147(2) d (PDM method, figure 188) were eventually identified.

6.165. SDSS J100515.39+191108.0

The 2009 outburst of this object (hereafter SDSS J1005) was reported S. Brady (cvnet-outburst 2859), which later turned out to be a superoutburst. We analyzed the available data of this outburst during its late stage and obtained a mean superhump period of 0.07747(2) d with the PDM method (figure 189). The times of superhump maxima are listed in table 316. These superhumps most likely correspond to stage C superhumps. J. Pietz reported a period of 0.0779 d (cvnet-outburst 2866).

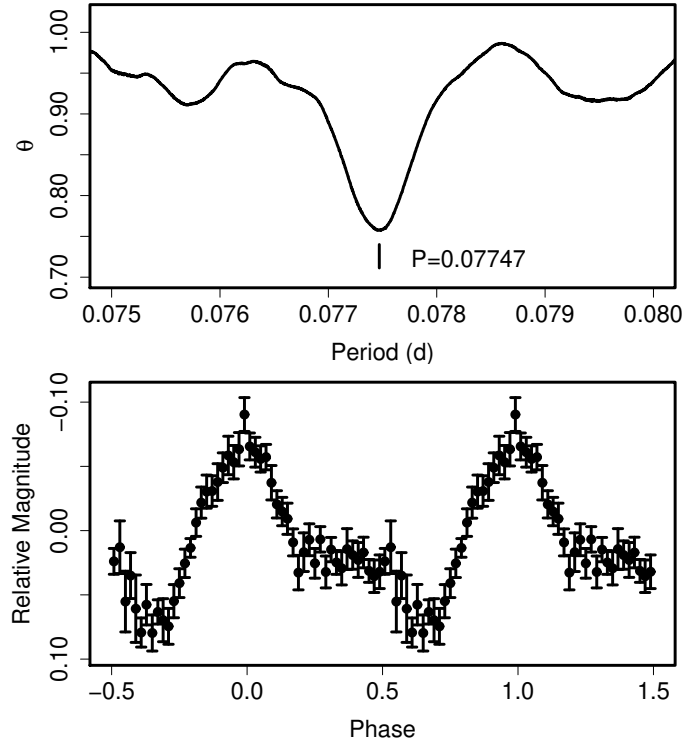
**Fig. 189.** Superhumps in SDSS J1005 (2009). (Upper): PDM analysis. (Lower): Phase-averaged profile.

Table 316. Superhump maxima of SDSS J1005 (2009).

E	\max^a	error	$O - C^b$	N^c
0	54838.5679	0.0004	-0.0016	106
1	54838.6471	0.0005	0.0002	140
10	54839.3442	0.0003	0.0007	166
16	54839.8075	0.0008	-0.0005	51
17	54839.8855	0.0004	0.0001	80
18	54839.9622	0.0006	-0.0006	40
36	54841.3606	0.0006	0.0046	112
41	54841.7439	0.0018	0.0009	54
42	54841.8201	0.0007	-0.0003	81
43	54841.8990	0.0007	0.0011	67
46	54842.1303	0.0054	0.0003	56
47	54842.2034	0.0014	-0.0041	142
48	54842.2891	0.0025	0.0043	149
49	54842.3570	0.0025	-0.0052	115

^a BJD-2400000.^b Against $\max = 2454838.5695 + 0.077404E$.^c Number of points used to determine the maximum.**Table 317.** Superhump maxima of SDSS J1100 (2009).

E	\max^a	error	$O - C^b$	N^c
0	54940.1283	0.0015	-0.0020	122
15	54941.1459	0.0045	0.0026	71
63	54944.3870	0.0014	0.0024	108
64	54944.4492	0.0027	-0.0030	61

^a BJD-2400000.^b Against $\max = 2454940.1303 + 0.067529E$.^c Number of points used to determine the maximum.6.166. *SDSS J110014.72+131552.1*

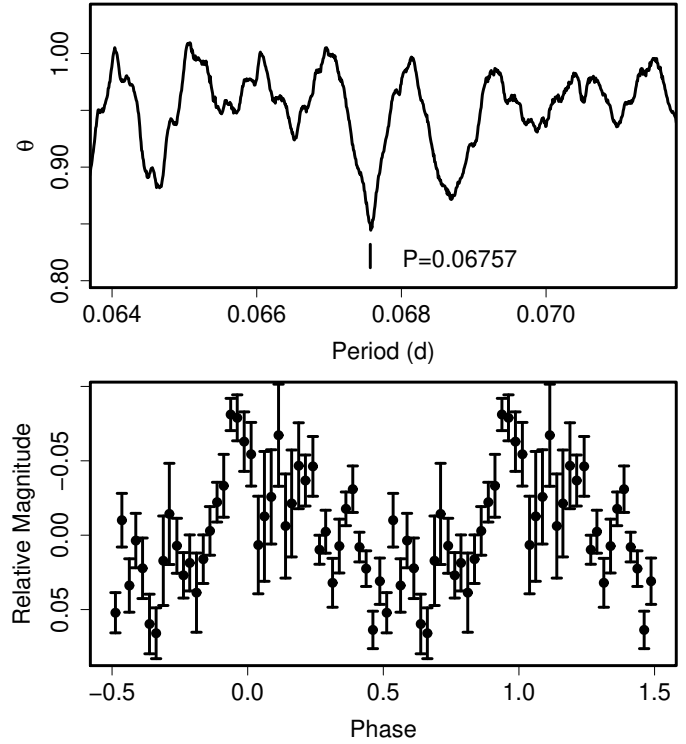
SDSS J110014.72+131552.1 (hereafter SDSS J1100) was selected as a CV during the course of the SDSS (Szkody et al. 2006). During the 2009 outburst detected by the CRTS (vsnet-alert 11188), superhumps were detected (vsnet-alert 11198, 11202). Although the short baseline of the observations makes alias selection slightly ambiguous, we present the $O - C$'s based on the period of 0.06757(2) d (PDM method).

6.167. *SDSS J122740.83+513925.0*

SDSS J122740.83+513925.0 (hereafter SDSS J1227) was selected as a high-inclination CV during the course of the SDSS (Szkody et al. 2004). Littlefair et al. (2008) reported parameters of eclipses. Shears et al. (2008b) reported the detection of superhumps and discussed on the variation of eclipses during the 2007 superoutburst. Using the times of eclipses published in Littlefair et al. (2008) and Shears et al. (2008b), we obtained the following updated ephemeris (equation 7).

$$\text{Min(BJD)} = 2453796.2478(4) + 0.06295835(5)E. \quad (7)$$

We analyzed the combined data set with ours, AAVSO data, and data extracted from figures in Shears et al.

**Fig. 190.** Superhumps in SDSS J1100 (2009). (Upper): PDM analysis. (Lower): Phase-averaged profile.

(2008b) which were not included in ours nor in the AAVSO data. The times of superhump maxima are listed in table 318. The first night of the observation either corresponded to the stage A or the complex profile disturbed the $O - C$'s. The period appears almost constant for the interval $33 \leq E \leq 124$, with a mean P_{SH} of 0.064552(21) d and $P_{\text{dot}} = +2.8(2.5) \times 10^{-5}$. This P_{dot} appears rather unusual for this P_{SH} . The positive $O - C$'s for $126 \leq E \leq 129$ may reflect the terminal stage of the stage B, when the P_{SH} usually lengthens. This identification seems to be supported by the apparent increase of the amplitudes of superhumps at this epoch. Using the entire interval for $33 \leq E \leq 129$, we obtained a mean P_{SH} of 0.064593(22) d and $P_{\text{dot}} = +6.1(2.1) \times 10^{-5}$. We adopted these values in table 2. The fractional superhump excesses for these periods are 2.5 % and 2.6 %, respectively.

6.168. *SDSS J152419.33+220920.0*

SDSS J152419.33+220920.0 (hereafter SDSS J1524) was suggested to be a high-inclination CV during the course of the SDSS (Szkody et al. 2009). The 2009 outburst of this object was detected by the CRTS (vsnet-alert 11133). Subsequent observations established the presence of superhumps and eclipses (cvnet-outburst 3029).

The times of eclipse minima, measured outside the eclipses as in V2051 Oph, are listed in table 319. The times for $E < 0$ were from the CRTS chance detections of eclipses. The times of these epochs have typical uncertainties of 0.001–0.002 d (approximately half duration of

Table 318. Superhump maxima of SDSS J1227 (2007).

E	\max^a	error	$O - C^b$	N^c
0	54256.4358	0.0012	-0.0237	-
1	54256.5064	0.0021	-0.0178	-
33	54258.6073	0.0004	0.0114	61
34	54258.6739	0.0003	0.0133	60
35	54258.7354	0.0008	0.0100	58
40	54259.0611	0.0010	0.0120	104
61	54260.4153	0.0032	0.0066	57
62	54260.4762	0.0006	0.0028	37
63	54260.5428	0.0004	0.0047	100
77	54261.4417	0.0012	-0.0028	103
78	54261.5105	0.0007	0.0012	98
80	54261.6421	0.0008	0.0034	31
81	54261.7047	0.0010	0.0012	33
82	54261.7706	0.0009	0.0024	35
86	54262.0316	0.0009	0.0044	49
101	54262.9979	0.0011	-0.0004	81
102	54263.0632	0.0014	0.0002	114
111	54263.6429	0.0016	-0.0028	34
112	54263.7045	0.0016	-0.0059	35
113	54263.7691	0.0024	-0.0060	35
114	54263.8314	0.0034	-0.0085	35
123	54264.4155	0.0026	-0.0070	74
124	54264.4887	0.0006	0.0014	68
126	54264.6177	0.0009	0.0009	41
127	54264.6816	0.0012	0.0001	39
128	54264.7449	0.0010	-0.0014	41
129	54264.8114	0.0026	0.0004	40

^a BJD-2400000.^b Against $\max = 2454256.4595 + 0.064740E$.^c Number of points used to determine the maximum.

the eclipse). The epochs for $E \geq 0$ were determined from time-resolved CCD observations; the typical uncertainty of the determination is ~ 0.001 d or less. The resultant orbital ephemeris is given in equation 8.

The times of superhump maxima are listed in table 320. A stage B-C transition around $E = 89$ was clearly detected. The mean P_{SH} and P_{dot} during the stage B were 0.067111(14) d (PDM method, figure 191) and $+8.2(2.6) \times 10^{-5}$, respectively. The fractional superhump excess for P_1 was 2.7 %.

$$\text{Min(BJD)} = 2454921.5937(1) + 0.0653187(1). \quad (8)$$

6.169. SDSS J155644.24-000950.2

SDSS J155644.24-000950.2 (hereafter SDSS J1556) was selected as a dwarf nova during the course of the SDSS (Szkody et al. 2002). Woudt et al. (2004) obtained 0.07408(1) d from quiescent orbital humps. During the 2006 March outburst, H. Maehara reported the detection of superhumps (vsnet-alert 9440).

We observed the 2007 superoutburst. A PDM analysis yielded a mean superhump period of 0.082853(5) d (figure 192, which corresponds to the longer one-day alias of Woudt et al. (2004). Both PDM analysis and superhump

Table 319. Eclipse Minima of SDSS J1524.

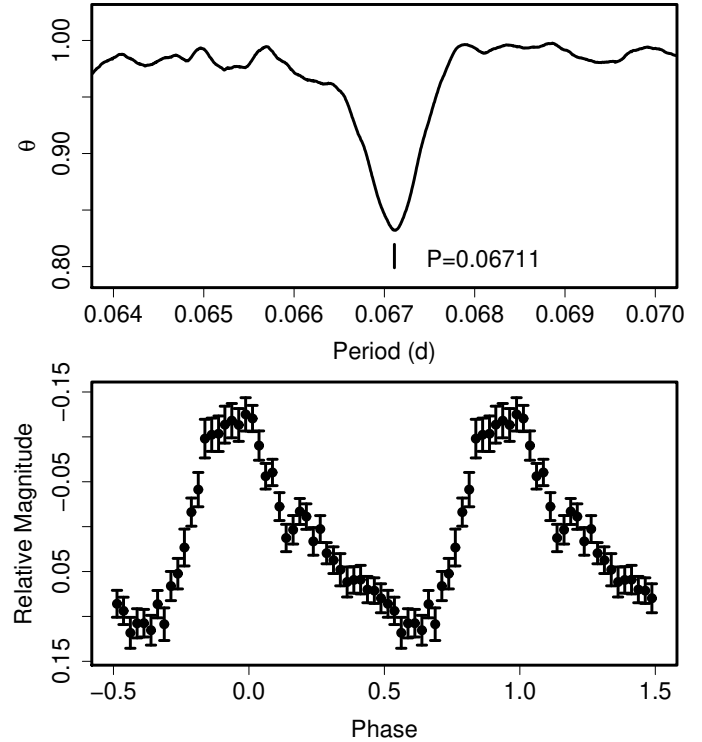
E	Minimum*	$O - C^\dagger$
-4528	54625.8317	0.0012
-4283	54641.8325	-0.0012
-134	54912.8405	-0.0005
-26	54919.8935	-0.0020
0	54921.5936	-0.0001
13	54922.4421	-0.0008
14	54922.5100	0.0018
15	54922.5743	0.0008
16	54922.6386	-0.0002
18	54922.7697	0.0003
19	54922.8351	0.0004
20	54922.9006	0.0006
29	54923.4880	0.0000
30	54923.5536	0.0003
33	54923.7502	0.0010
34	54923.8151	0.0006
35	54923.8804	0.0005
36	54923.9452	0.0000
40	54924.2054	-0.0011
41	54924.2702	-0.0015
43	54924.4011	-0.0013
45	54924.5342	0.0011
46	54924.5986	0.0002
48	54924.7293	0.0003
49	54924.7933	-0.0011
50	54924.8598	0.0002
51	54924.9250	0.0001
58	54925.3821	-0.0001
61	54925.5785	0.0003
74	54926.4259	-0.0014
75	54926.4927	0.0001
76	54926.5575	-0.0005
79	54926.7539	0.0000
80	54926.8193	0.0001
81	54926.8845	0.0000
85	54927.1457	-0.0001
86	54927.2111	0.0000
87	54927.2768	0.0004
105	54928.4527	0.0005
107	54928.5828	0.0000
110	54928.7792	0.0004
111	54928.8446	0.0005

*BJD-2400000.

†Against equation 8.

Table 320. Superhump maxima of SDSS J1524 (2009).

E	max ^a	error	$O - C^b$	N^c
0	54921.6110	0.0006	0.0018	59
13	54922.4789	0.0005	-0.0016	107
14	54922.5442	0.0005	-0.0034	100
15	54922.6118	0.0006	-0.0028	77
17	54922.7479	0.0005	-0.0008	58
18	54922.8117	0.0003	-0.0040	59
19	54922.8802	0.0005	-0.0025	58
20	54922.9478	0.0004	-0.0019	46
27	54923.4232	0.0019	0.0044	48
28	54923.4835	0.0010	-0.0024	115
29	54923.5508	0.0010	-0.0022	105
30	54923.6210	0.0012	0.0011	54
32	54923.7501	0.0017	-0.0040	58
33	54923.8221	0.0013	0.0011	57
34	54923.8854	0.0009	-0.0026	57
35	54923.9579	0.0014	0.0028	40
38	54924.1618	0.0021	0.0056	52
39	54924.2205	0.0015	-0.0027	63
40	54924.2899	0.0016	-0.0003	125
41	54924.3538	0.0060	-0.0035	32
42	54924.4186	0.0016	-0.0056	54
43	54924.4859	0.0014	-0.0054	61
44	54924.5569	0.0009	-0.0014	117
45	54924.6209	0.0008	-0.0045	76
47	54924.7562	0.0006	-0.0032	62
48	54924.8256	0.0008	-0.0008	69
49	54924.8926	0.0009	-0.0009	68
50	54924.9596	0.0010	-0.0009	57
56	54925.3620	0.0022	-0.0006	30
57	54925.4301	0.0009	0.0005	73
58	54925.4935	0.0007	-0.0032	134
59	54925.5578	0.0013	-0.0059	120
72	54926.4481	0.0022	0.0131	100
73	54926.5103	0.0042	0.0082	100
74	54926.5699	0.0022	0.0008	82
77	54926.7797	0.0020	0.0096	59
78	54926.8433	0.0011	0.0062	60
83	54927.1772	0.0018	0.0049	141
84	54927.2443	0.0021	0.0051	108
85	54927.3113	0.0010	0.0050	125
87	54927.4448	0.0020	0.0045	34
88	54927.5155	0.0009	0.0081	48
89	54927.5798	0.0010	0.0054	53
101	54928.3835	0.0043	0.0048	23
102	54928.4494	0.0018	0.0037	68
103	54928.5143	0.0009	0.0016	85
104	54928.5840	0.0015	0.0042	78
107	54928.7820	0.0010	0.0012	58
108	54928.8481	0.0023	0.0002	57
117	54929.4467	0.0082	-0.0044	58
118	54929.5129	0.0026	-0.0052	37
148	54931.5131	0.0037	-0.0158	50
163	54932.5228	0.0043	-0.0115	48

^a BJD-2400000.^b Against $max = 2454921.6092 + 0.067025E$.^c Number of points used to determine the maximum.**Fig. 191.** Superhumps in SDSS J1524 (2009) before BJD 2454928. (Upper): PDM analysis. (Lower): Phase-averaged profile.

$O - C$ analyses supported this alias selection. Using the one-day alias period 0.08001(1) calculated from Woudt et al. (2004), we obtained a reasonable fractional superhump excess of 3.6 %.

The times of superhump maxima are listed in table 321. The $O - C$ diagram (figure 4) showed a strong decrease in the superhump period. The global P_{dot} was $-8.7(1.1) \times 10^{-5}$, and was $-6.9(0.8) \times 10^{-5}$ excluding the initial stage of development (stage A, $E \leq 1$). We consider the latter value as being the representative period derivative.

Details of these and other observations and discussion will be presented in Maehara et al., in preparation.

6.170. SDSS J162718.39+120435.0

The 2008 outburst of SDSS J162718.39+120435.0 (hereafter SDSS J1627) was detected by S. Brady (cvnet-outburst 2421), which was subsequently proven to be a superoutburst (cvnet-outburst 2426). The observations presented here are a combination of Shears et al. (2008c) and the VSNET Collaboration. The times of superhump maxima (table 322) indicated a long P_{SH} with a strong global period variation of $P_{\text{dot}} = -20.0(2.5) \times 10^{-5}$. The $O - C$ diagram (figure 29) was clearly composed of all stages A-C. The abrupt period change between stages B and C was also noted in Shears et al. (2008c). The periods of each segments are listed in table 2.

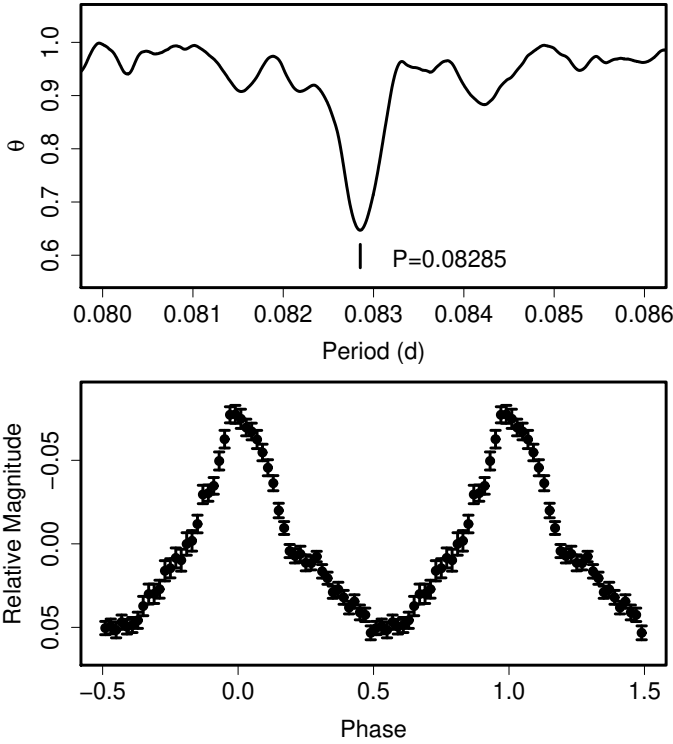


Fig. 192. Superhumps in SDSS J1556 (2007). (Upper): PDM analysis. (Lower): Phase-averaged profile.

Table 321. Superhump maxima of SDSS J1556 (2007).

E	\max^a	error	$O - C^b$	N^c
0	54311.9945	0.0003	-0.0114	204
1	54312.0754	0.0005	-0.0134	245
12	54313.0013	0.0002	0.0010	256
13	54313.0836	0.0003	0.0004	214
24	54313.9997	0.0002	0.0050	234
25	54314.0794	0.0004	0.0018	182
61	54317.0704	0.0015	0.0096	54
72	54317.9804	0.0005	0.0080	359
73	54318.0629	0.0004	0.0077	311
84	54318.9733	0.0002	0.0066	428
85	54319.0570	0.0005	0.0074	360
101	54320.3751	0.0004	-0.0003	83
121	54322.0285	0.0008	-0.0043	304
133	54323.0182	0.0008	-0.0090	365
145	54324.0123	0.0005	-0.0093	378

^a BJD-2400000.

^b Against $\max = 2454312.0059 + 0.082866E$.

^c Number of points used to determine the maximum.

Table 322. Superhump maxima of SDSS J1627.

E	\max^a	error	$O - C^b$
0	54617.7385	0.0016	-0.0659
2	54617.9384	0.0025	-0.0843
6	54618.4293	0.0047	-0.0303
7	54618.5422	0.0017	-0.0266
8	54618.6593	0.0011	-0.0186
9	54618.7619	0.0007	-0.0252
10	54618.8736	0.0004	-0.0227
15	54619.4453	0.0007	0.0029
16	54619.5581	0.0006	0.0065
17	54619.6670	0.0003	0.0063
18	54619.7794	0.0003	0.0095
19	54619.8891	0.0002	0.0100
26	54620.6590	0.0002	0.0155
27	54620.7679	0.0002	0.0151
28	54620.8776	0.0003	0.0156
33	54621.4239	0.0004	0.0159
33	54621.4241	0.0004	0.0161
34	54621.5389	0.0004	0.0218
35	54621.6439	0.0011	0.0175
36	54621.7584	0.0004	0.0228
37	54621.8668	0.0003	0.0220
38	54621.9815	0.0004	0.0275
49	54623.1727	0.0005	0.0175
50	54623.2884	0.0012	0.0239
52	54623.5010	0.0005	0.0182
54	54623.7199	0.0003	0.0187
55	54623.8292	0.0003	0.0188
56	54623.9345	0.0004	0.0149
60	54624.3742	0.0006	0.0178
71	54625.5686	0.0005	0.0110
79	54626.4409	0.0005	0.0096
80	54626.5494	0.0005	0.0090
86	54627.1992	0.0008	0.0035
98	54628.5042	0.0006	-0.0019
109	54629.7014	0.0005	-0.0059
110	54629.8139	0.0007	-0.0026
111	54629.9205	0.0010	-0.0052
117	54630.5779	0.0009	-0.0030
118	54630.6836	0.0013	-0.0065
119	54630.7940	0.0012	-0.0054
120	54630.9006	0.0010	-0.0080
127	54631.6609	0.0008	-0.0121
128	54631.7746	0.0010	-0.0075
149	54634.0514	0.0099	-0.0239
150	54634.1522	0.0082	-0.0324

^a BJD-2400000.

^b Against $\max = 2454617.8043 + 0.109202E$.

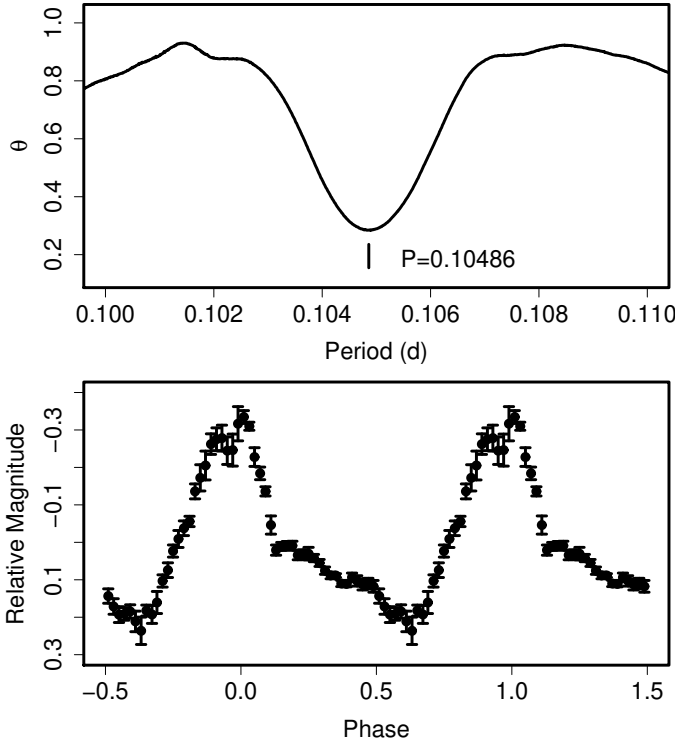


Fig. 193. Superhumps in SDSS J1702 before BJD 2453652. (Upper): PDM analysis. (Lower): Phase-averaged profile.

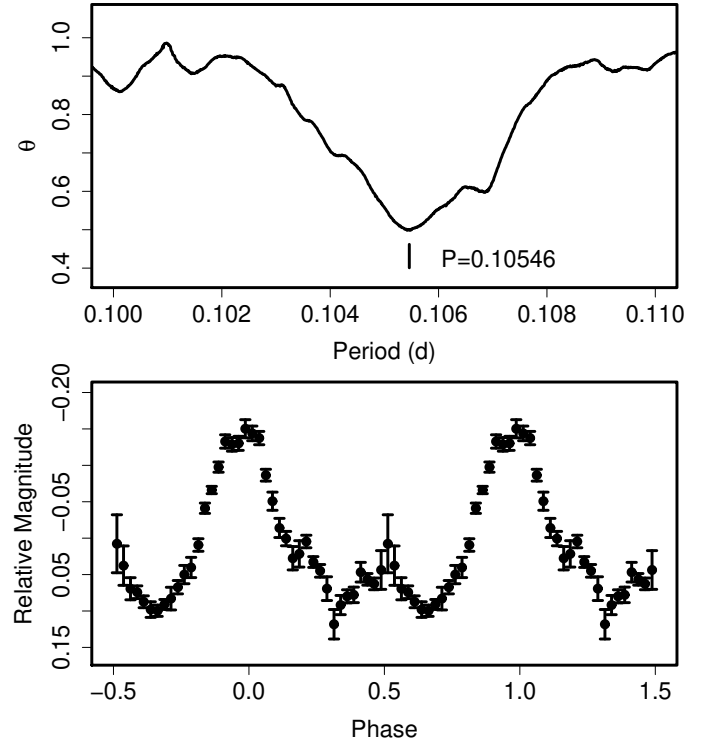


Fig. 194. Superhumps in SDSS J1702 after BJD 2453652. (Upper): PDM analysis. (Lower): Phase-averaged profile.

6.171. *SDSS J170213.26+322954.1*

This object (hereafter SDSS J1702) was discovered as a high-inclination CV by Szkody et al. (2004). Littlefair et al. (2006) identified this object as an eclipsing CV in the period gap and suggested that it has an evolved secondary. Boyd et al. (2006) observed the 2005 superoutburst of this object and established its SU UMa-type nature. We used the AAVSO data which includes the data used in Boyd et al. (2006). Using the eclipse ephemeris by Boyd et al. (2006), we extracted the times of superhump maxima outside the eclipses (table 323). Although our analysis basically confirmed the P_{SH} , the periods before $E \leq 20$ and $E \geq 38$ appears to show a discontinuous change. The mean periods determined with the PDM method were 0.10486(3) d before BJD 2453652 (figure 193) and 0.10546(3) d after BJD 2453652 (figure 194), respectively. Although the timing of $E = 38$ maximum was affected by an eclipse, the $O - C$ analysis also supports the same tendency. These periods correspond to fractional superhump excesses of 4.8 % and 5.4 %, respectively.

It is very unusual for such a long P_{SH} -system to show an increase in the P_{SH} during the middle-to-late stage of a superoutburst (cf. V725 Aql, subsection 6.8). Although the effect of the overlapping orbital variation can not be excluded, this object deserves further detailed study for evolution of superhump periods.

Table 323. Superhump maxima of SDSS J1702 (2005).

E	max ^a	error	$O - C^b$	N^c
0	53648.3842	0.0003	0.0045	152
2	53648.5926	0.0018	0.0027	14
9	53649.3267	0.0009	0.0014	215
18	53650.2729	0.0002	0.0020	178
19	53650.3820	0.0008	0.0060	93
38	53652.3560	0.0033	-0.0163	39
47	53653.3115	0.0005	-0.0063	263
48	53653.4184	0.0008	-0.0045	105
56	53654.2611	0.0007	-0.0023	146
57	53654.3672	0.0006	-0.0012	204
66	53655.3154	0.0011	0.0014	225
85	53657.3228	0.0038	0.0125	85

^a BJD-2400000.

^b Against $max = 2453648.3797 + 0.105066E$.

^c Number of points used to determine the maximum.

6.172. *SDSSp J173008.38+624754.7*

SDSSp J173008.38+624754.7 (hereafter SDSS J1730) was selected as a dwarf nova during the course of the SDSS (Szkody et al. 2002). Szkody et al. (2002) obtained an orbital period of 117(5) m (0.081(3) d) from radial-velocity study, which made the object a good candidate for an SU UMa-type dwarf nova.

We observed the 2001 October superoutburst, soon after the discovery announcement of this object, 2002 February-March and 2004 March superoutbursts. We first analyzed the best sampled superoutburst in 2004 (table 324). The mean P_{SH} and the global P_{dot} was 0.07948(2) d and $-7.7(3.5) \times 10^{-5}$. This P_{dot} was likely from a stage B-C transition around $E = 10$. The mean periods before and after this epoch were 0.08007(24) d and 0.07946(2) d, respectively.

The times of superhump maxima for the 2001 superoutburst are listed in table 325. The last two superhumps ($E = 108$ and $E = 109$) have large $O - C$'s. These superhumps may have been traditional late superhumps, or the period had largely changed before these observations. We disregarded these maxima and obtained a mean P_{SH} of 0.07941(10) d, which likely reflects stage C superhumps.

The 2002 February-March superoutburst (table 326) was probably observed during the stage C. The mean P_{SH} was 0.07939(5) d, with an insignificant P_{dot} of $+2.0(3.5) \times 10^{-5}$.

We derived a mean supercycle of 109(1) d from the times of these four superoutbursts and the 2002 September one.

The variation of superhump period has generally been small in this system. In conjunction with the long superhump period, the object resembles BF Ara and HV Aur. The shortness of the cycle length of normal outbursts (9–10 d) and supercycle also resembles BF Ara (cf. Kato et al. 2003a). The lack of period variation, though, may be a result of the lack of observations during the early stage (cf. the 2004 superoutburst). This possibility should be resolved by future observations.

6.173. *SDSS J210014.12+004446.0*

This object (hereafter SDSS J2100) was selected as a CV during the course of the SDSS Szkody et al. (2004). Tramosch et al. (2005) reported the detection of superhumps with a period of 0.08746(8) d on two consecutive nights during the 2003 superoutburst. We observed the earliest stage of the 2007 superoutburst. Assuming that the first epoch observation was taken during the stage A development, we assigned E for superhumps (table 327). The mean period for $44 \leq E \leq 56$ was 0.08696(15) d.

6.174. *SDSS J225831.18–094931.7*

SDSS J225831.18–094931.7 (hereafter SDSS J2258) was selected as a CV during the course of the SDSS (Szkody et al. 2003). The SU UMa-type nature was established during the 2004 June superoutburst (vsnet-alert 8162; the reported period of 0.045 d referred to a half of P_{SH}). During its superoutburst in 2005 August,

Table 324. Superhump maxima of SDSS J1730 (2004).

E	max ^a	error	$O - C^b$	N^c
0	53082.5597	0.0005	-0.0042	34
1	53082.6414	0.0004	-0.0020	26
5	53082.9597	0.0002	-0.0016	155
6	53083.0432	0.0004	0.0024	83
7	53083.1241	0.0006	0.0038	201
8	53083.2008	0.0005	0.0010	158
9	53083.2791	0.0004	-0.0001	196
13	53083.5965	0.0010	-0.0006	21
30	53084.9505	0.0004	0.0022	159
31	53085.0284	0.0004	0.0006	158
50	53086.5388	0.0005	0.0008	65
51	53086.6178	0.0007	0.0004	61
61	53087.4123	0.0011	0.0000	54
62	53087.4894	0.0007	-0.0024	72
63	53087.5716	0.0005	0.0004	46
64	53087.6498	0.0024	-0.0009	25

^a BJD-2400000.

^b Against $max = 2453082.5639 + 0.079481E$.

^c Number of points used to determine the maximum.

Table 325. Superhump maxima of SDSS J1730 (2001).

E	max ^a	error	$O - C^b$	N^c
0	52205.3181	0.0004	0.0021	71
1	52205.4009	0.0004	0.0053	74
8	52205.9567	0.0010	0.0038	173
20	52206.9088	0.0009	0.0003	177
21	52206.9873	0.0010	-0.0007	173
35	52208.0953	0.0010	-0.0075	171
85	52212.0865	0.0124	0.0024	23
86	52212.1341	0.0234	-0.0295	130
108	52213.9347	0.0072	0.0194	129
109	52213.9994	0.0025	0.0044	120

^a BJD-2400000.

^b Against $max = 2452205.3160 + 0.079624E$.

^c Number of points used to determine the maximum.

Table 326. Superhump maxima of SDSS J1730 (2002).

E	max ^a	error	$O - C^b$	N^c
0	52326.2335	0.0010	0.0081	143
1	52326.3031	0.0021	-0.0016	150
26	52328.2777	0.0093	-0.0118	119
50	52330.1936	0.0010	-0.0013	228
51	52330.2749	0.0007	0.0007	280
52	52330.3621	0.0035	0.0085	219
115	52335.3449	0.0017	-0.0103	290
139	52337.2672	0.0024	0.0067	321
140	52337.3410	0.0094	0.0011	259

^a BJD-2400000.

^b Against $max = 2452326.2254 + 0.079390E$.

^c Number of points used to determine the maximum.

Table 327. Superhump maxima of SDSS J2100 (2007).

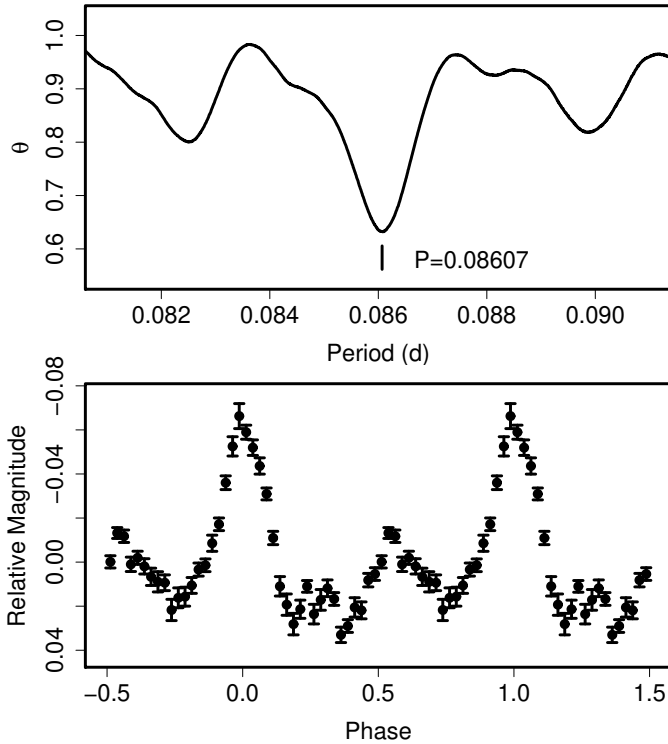
E	\max^a	error	$O - C^b$	N^c
0	54318.2574	0.0021	-0.0027	180
44	54322.1570	0.0038	0.0063	78
45	54322.2459	0.0024	0.0068	46
56	54323.2014	0.0033	-0.0104	77

^a BJD-2400000.^b Against $\max = 2454318.2601 + 0.088423E$.^c Number of points used to determine the maximum.**Table 328.** Superhump maxima of SDSS J2258 (2004).

E	\max^a	error	$O - C^b$	N^c
0	53159.5243	0.0004	-0.0031	368
1	53159.6148	0.0007	0.0015	211
12	53160.5599	0.0006	0.0016	379
13	53160.6464	0.0008	0.0023	290
20	53161.2446	0.0023	-0.0008	145
23	53161.5019	0.0073	-0.0012	224
24	53161.5887	0.0012	-0.0003	380

^a BJD-2400000.^b Against $\max = 2453159.5274 + 0.085900E$.^c Number of points used to determine the maximum.**Table 329.** Superhump maxima of SDSS J2258 (2008).

E	\max^a	error	$O - C^b$	N^c
0	54788.9460	0.0004	0.0023	178
1	54789.0298	0.0004	-0.0001	260
11	54789.8849	0.0019	-0.0064	77
12	54789.9817	0.0003	0.0042	389
13	54790.0657	0.0004	0.0021	423
23	54790.9250	0.0004	-0.0000	309
24	54791.0122	0.0003	0.0011	820
25	54791.0971	0.0013	-0.0002	286
34	54791.8713	0.0023	-0.0013	87
35	54791.9586	0.0005	-0.0001	260
36	54792.0410	0.0010	-0.0038	187
46	54792.9068	0.0011	0.0005	122
47	54792.9962	0.0012	0.0038	162
58	54793.9362	0.0007	-0.0037	289
59	54794.0250	0.0016	-0.0011	123
82	54796.0086	0.0022	0.0013	64
92	54796.8730	0.0034	0.0043	55
93	54796.9520	0.0015	-0.0029	81

^a BJD-2400000.^b Against $\max = 2454788.9438 + 0.086141E$.^c Number of points used to determine the maximum.**Fig. 195.** Superhumps in SDSS J2258 (2004). (Upper): PDM analysis. (Lower): Phase-averaged profile.

H. Maehara established a long P_{SH} of 0.083 d (vsnet-campaign-dn 4489).

The times of superhump maxima during the 2008 superoutburst are listed in table 329. This outburst was apparently detected during its late stage, since the object already started fading rapidly after six days. The mean superhump period with the PDM method was 0.08607(2) d (figure 195), which most likely refers to P_2 , with an almost zero P_{dot} of $+1.5(2.1) \times 10^{-5}$. The maxima for $82 \leq E \leq 93$ refer to the post-superoutburst stage. There was no apparent indication of a phase shift around the termination of the superoutburst.

The times of superhump maxima during the 2004 superoutburst are also given (table 328). The 2004 superoutburst was caught during its final stage. The 2005 observation is omitted because it was a single-night observation.

6.175. OT J004226.5+421537

This object (hereafter OT J0042) was discovered by K. Itagaki as a possible nova in M31 which reached a peak magnitude of 14.5 around 2008 November 28.6 UT (=M31N 2008-11b, Nakano et al. 2008). Multicolor photometry by S. Kiyota suggested that this object is a foreground dwarf nova rather than a nova in M31 (vsnet-alert 10747). The object was indeed spectroscopically confirmed as a dwarf nova (Kasliwal et al. 2008).

Until 2008 December 7, early superhumps were present (vsnet-alert 10747, 10763, 10786). The mean period of early superhumps was 0.05550(2) d (figure 196).

On December 10, ordinary superhump emerged (cvnet-outburst 2801, vsnet-alert 10818). The times of superhump maxima are listed in table 330. The mean P_{SH} determined with the PDM method was 0.05687(2) d (figure

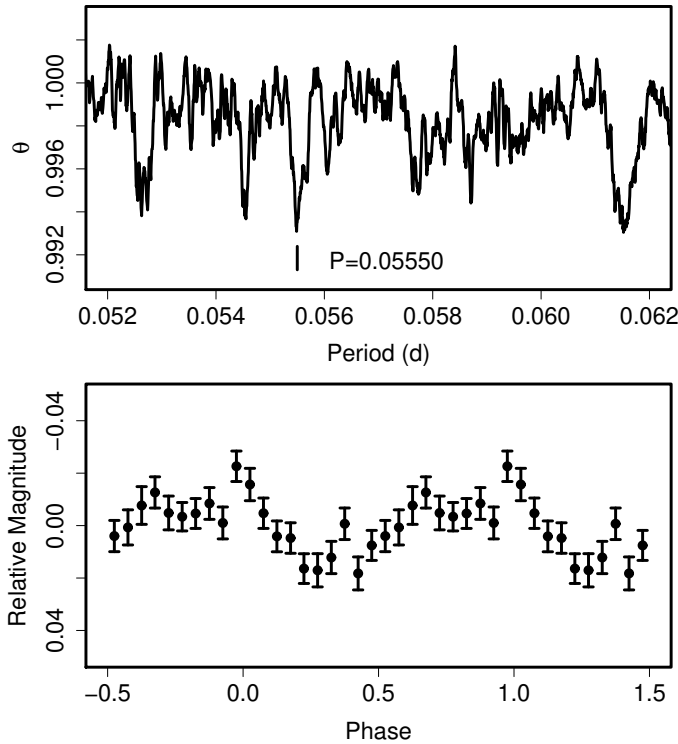


Fig. 196. Early superhumps in OT J0042 (2008). (Upper): PDM analysis. (Lower): Phase-averaged profile.

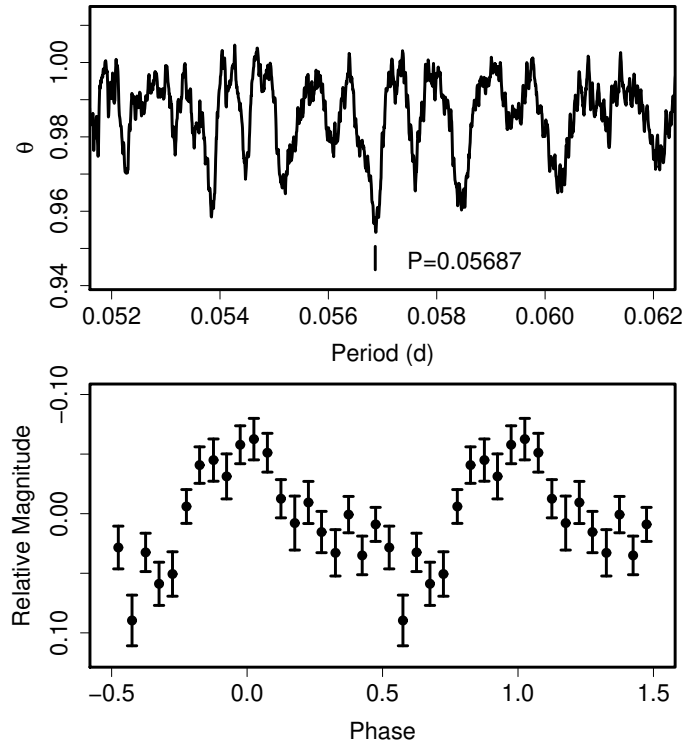


Fig. 197. Ordinary superhumps in OT J0042 (2008). (Upper): PDM analysis. (Lower): Phase-averaged profile.

197). The P_{dot} was slightly positive, $+4.0(1.8) \times 10^{-5}$. The fractional superhump excess is 2.5(1) %, which is slightly large for a WZ Sge-type dwarf nova. Since the amplitudes of early superhumps and ordinary superhumps were low, these period determinations may have been affected by non-ideal photometric conditions and the fractional superhump excess needs to be treated with caution.

6.176. OT J011306.7+215250

This object (=CSS080922:011307+215250, hereafter OT J0113) was discovered by the Catalina Real-time Transient Survey (CRTS, Drake et al. 2008b).²³ H. Maehara detected superhumps and identified this object as a long- P_{SH} SU UMa-type dwarf nova (vsnet-alert 10539). The observation was performed during the last stage of the superoutburst (table 331). The cycle count is based on period determination in Shafter et al. (2009).

6.177. OT J021110.2+171624

This object (=CSS080130:021110+171624, hereafter OT J0211) was discovered by the CRTS in 2008 January (Djorgovski et al. 2008a; Drake et al. 2009; cvnet-discussion 1106). The detection of superhumps led to a classification as an SU UMa-type dwarf nova (cvnet-discussion 1109). Djorgovski et al. (2008a) reported spectroscopic confirmation as a CV.

Table 330. Superhump maxima of OT J0042 (2008).

E	max ^a	error	$O - C^b$	N^c
0	54810.9649	0.0033	0.0052	43
1	54811.0200	0.0016	0.0034	128
2	54811.0747	0.0044	0.0013	98
3	54811.1324	0.0034	0.0021	78
4	54811.1963	0.0031	0.0091	43
34	54812.8911	0.0023	-0.0029	30
35	54812.9431	0.0040	-0.0077	28
36	54813.0008	0.0063	-0.0069	30
37	54813.0675	0.0029	0.0029	40
70	54814.9424	0.0034	0.0004	30
71	54814.9984	0.0041	-0.0005	95
72	54815.0529	0.0017	-0.0030	136
73	54815.1110	0.0014	-0.0017	119
74	54815.1668	0.0032	-0.0028	112
89	54816.0244	0.0020	0.0014	67
90	54816.0657	0.0023	-0.0142	18
158	54819.9633	0.0039	0.0148	30
160	54820.0728	0.0027	0.0105	127
161	54820.1130	0.0021	-0.0061	112
162	54820.1708	0.0087	-0.0053	61

^a BJD-2400000.

^b Against $max = 2454810.9596 + 0.056892E$.

^c Number of points used to determine the maximum.

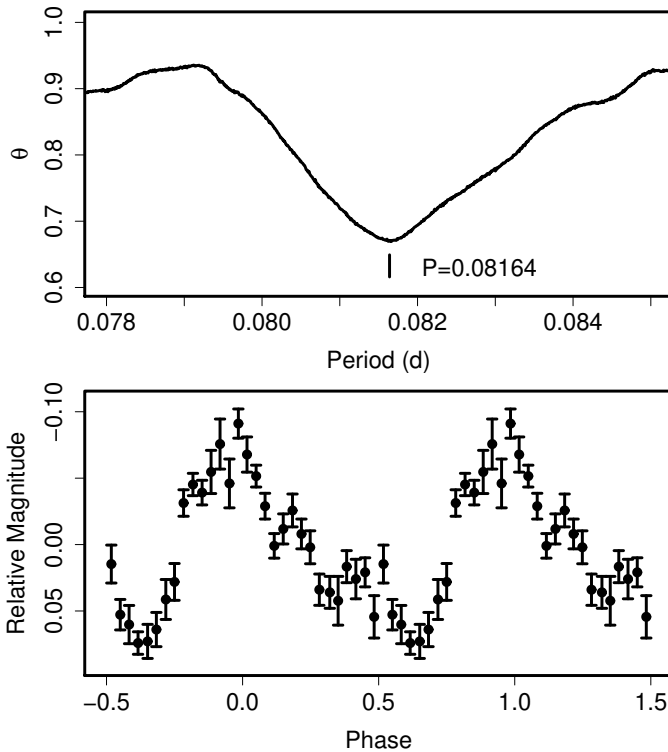
²³ <<http://nesssi.cacr.caltech.edu/catalina/>>. For the information of the individual Catalina CVs, see <<http://nesssi.cacr.caltech.edu/catalina/AllCV.html>>.

Table 331. Superhump maxima of OT J0113 (2008).

E	\max^a	error	$O - C^b$	N^c
0	54732.1975	0.0007	0.0016	187
21	54734.1751	0.0040	-0.0017	93
22	54734.2694	0.0032	-0.0016	129
43	54736.2535	0.0040	0.0016	51

^a BJD-2400000.^b Against $\max = 2454732.1959 + 0.094325E$.^c Number of points used to determine the maximum.**Table 332.** Superhump maxima of OT J0211.

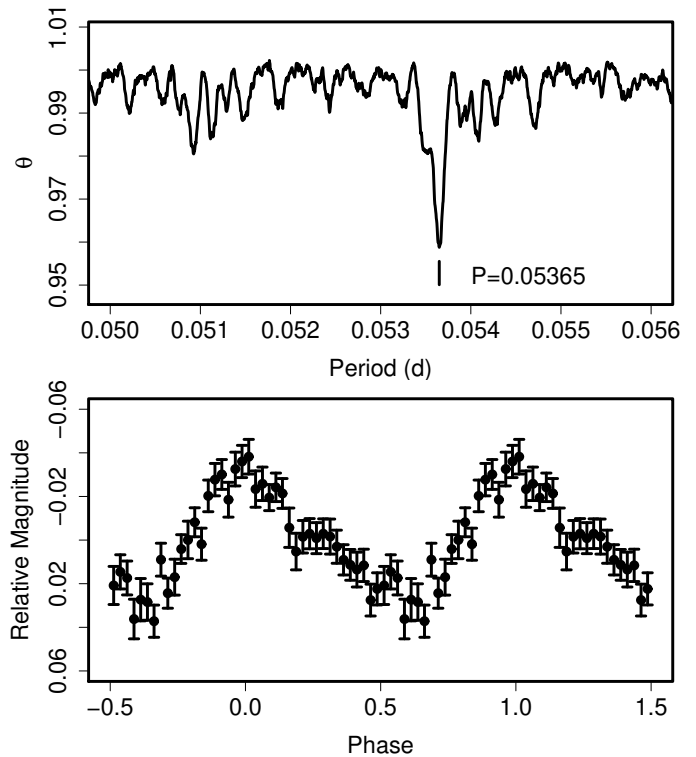
E	\max^a	error	$O - C^b$	N^c
0	54775.0286	0.0046	0.0006	89
1	54775.1098	0.0011	0.0001	129
12	54776.0016	0.0037	-0.0062	53
13	54776.0932	0.0009	0.0038	227
14	54776.1728	0.0013	0.0018	87

^a BJD-2400000.^b Against $\max = 2454775.0281 + 0.081643E$.^c Number of points used to determine the maximum.**Fig. 198.** Superhumps in OT J0211 (2008). (Upper): PDM analysis. (Lower): Phase-averaged profile.

We observed the 2008 November superoutburst (vsnet-alert 10663) and established the superhump period of 0.08164(6) d with the PDM method (figure 198). The times of superhump maxima are listed in table 332. The object appears to have a relatively short supercycle of ~ 280 d, typical for an SU UMa-type dwarf nova with a long P_{SH} .

6.178. OT J023839.1+355648

This object (=CSS081026:023839+355648, hereafter OT J0238) was discovered by the CRTS. H. Maehara suggested that this object may be a WZ Sge-type dwarf nova (vsnet-alert 10628). Superhumps were later detected (vsnet-alert 10667, figure 199). A reanalysis of the early data confirmed the presence of early superhumps (vsnet-alert 10686), confirming the suggested classification of the object as a WZ Sge-type dwarf nova with the shortest

**Fig. 199.** Ordinary superhumps in OT J0238 (2008). (Upper): PDM analysis. (Lower): Phase-averaged profile.

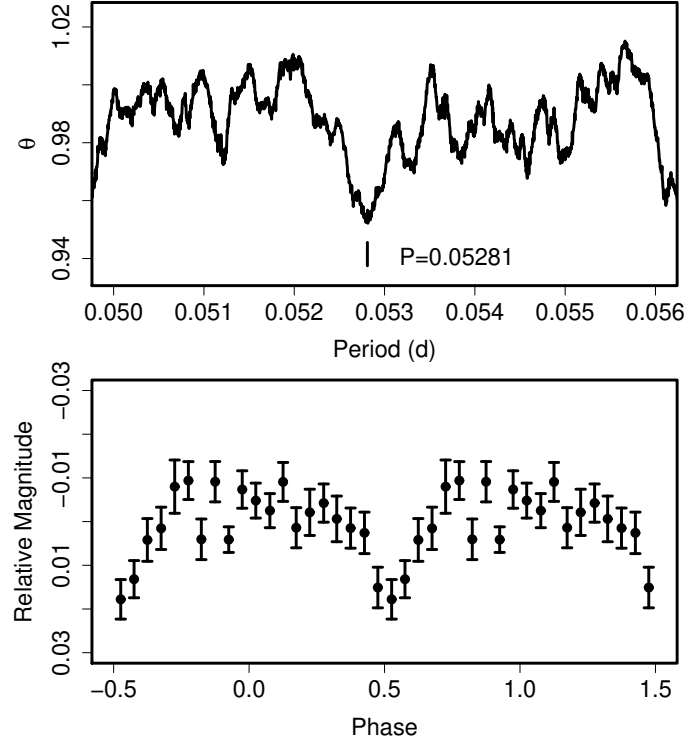
known P_{SH} . Shugarov et al. (2008) observed the same outburst and reported periods of 0.0531 d and 0.0537 d for early and ordinary superhumps. We used the combined data set with ours and Shugarov et al. (2008), after selecting the best-quality segment, and refined the period of early superhumps to be 0.05281(6) d (figure 200).

The times of superhump maxima are listed in table 333. The $O - C$ diagram clearly consists of A-C stages. The P_{dot} for the stage B ($67 \leq E \leq 350$, disregarding $E = 347$) was $+2.0(0.2) \times 10^{-5}$. The duration of the stage A (52 P_{SH} or longer) is longer than those of typical SU UMa-type dwarf novae (20–30 P_{SH}). This might be a signature of slow evolution of superhumps in this system.

The details will be presented by Maehara et al., in preparation.

Table 333. Superhump maxima of OT J0238 (2008).

E	max ^a	error	$O - C^b$	N^c
0	54772.4407	0.0023	-0.0347	22
1	54772.5024	0.0016	-0.0266	28
2	54772.5582	0.0007	-0.0245	27
3	54772.6087	0.0020	-0.0277	25
19	54773.4863	0.0011	-0.0089	24
32	54774.1946	0.0016	0.0016	25
37	54774.4622	0.0020	0.0009	21
50	54775.1666	0.0006	0.0075	110
51	54775.2196	0.0006	0.0068	133
52	54775.2751	0.0006	0.0087	88
67	54776.0801	0.0007	0.0085	110
68	54776.1354	0.0011	0.0101	118
69	54776.1896	0.0007	0.0107	19
70	54776.2396	0.0006	0.0070	22
71	54776.2947	0.0006	0.0085	28
72	54776.3480	0.0007	0.0080	22
73	54776.4018	0.0007	0.0082	21
74	54776.4552	0.0006	0.0079	22
75	54776.5091	0.0007	0.0082	22
91	54777.3662	0.0006	0.0064	19
92	54777.4206	0.0006	0.0072	23
93	54777.4725	0.0004	0.0053	24
94	54777.5256	0.0005	0.0048	21
95	54777.5826	0.0009	0.0082	15
107	54778.2241	0.0023	0.0055	13
108	54778.2773	0.0009	0.0050	17
109	54778.3303	0.0009	0.0044	18
110	54778.3824	0.0008	0.0028	12
114	54778.6007	0.0013	0.0065	12
115	54778.6509	0.0014	0.0029	8
127	54779.2962	0.0008	0.0041	39
145	54780.2584	0.0024	0.0002	99
146	54780.3128	0.0016	0.0009	45
147	54780.3642	0.0016	-0.0014	56
164	54781.2831	0.0015	0.0050	33
165	54781.3313	0.0008	-0.0005	41
166	54781.3868	0.0015	0.0014	20
167	54781.4351	0.0019	-0.0039	12
186	54782.4608	0.0029	0.0019	13
187	54782.5170	0.0031	0.0044	11
188	54782.5629	0.0034	-0.0033	15
189	54782.6141	0.0011	-0.0059	10
197	54783.0494	0.0096	0.0001	80
198	54783.0909	0.0033	-0.0120	105
199	54783.1512	0.0021	-0.0055	112
200	54783.2075	0.0018	-0.0028	99
201	54783.2606	0.0013	-0.0034	113
216	54784.0712	0.0054	0.0021	110
217	54784.1159	0.0068	-0.0069	107
256	54786.2136	0.0009	-0.0025	16
257	54786.2657	0.0013	-0.0042	9

^a BJD-2400000.^b Against $max = 2454772.4753 + 0.053675E$.^c Number of points used to determine the maximum.**Fig. 200.** Early superhumps in OT J0238 (2008) before BJD 2454769.5. (Upper): PDM analysis. The alias selection was based on P_{SH} . (Lower): Phase-averaged profile.**Table 333.** Superhump maxima of OT J0238 (2008). (continued)

E	max	error	$O - C$	N
258	54786.3234	0.0017	-0.0001	10
259	54786.3771	0.0038	-0.0000	13
260	54786.4285	0.0018	-0.0023	11
261	54786.4835	0.0036	-0.0010	14
301	54788.6365	0.0019	0.0050	16
310	54789.1212	0.0025	0.0066	92
311	54789.1727	0.0014	0.0045	112
312	54789.2210	0.0024	-0.0010	132
313	54789.2781	0.0046	0.0025	56
329	54790.1421	0.0047	0.0077	114
330	54790.1946	0.0024	0.0065	115
331	54790.2408	0.0035	-0.0009	114
347	54791.0835	0.0024	-0.0170	39
348	54791.1658	0.0035	0.0116	150
349	54791.2073	0.0025	-0.0006	153
350	54791.2693	0.0085	0.0077	100
384	54793.0858	0.0038	-0.0007	70
404	54794.1400	0.0025	-0.0201	97
405	54794.1981	0.0036	-0.0156	65

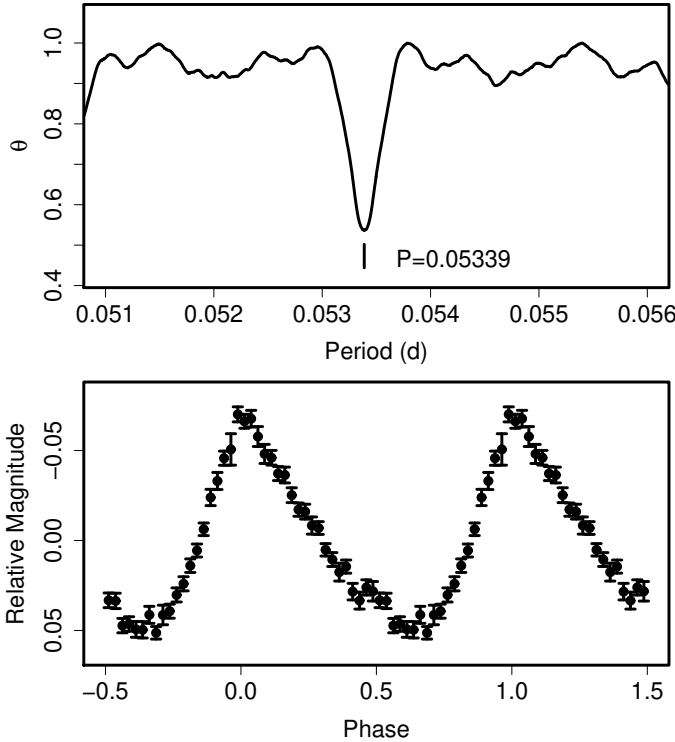


Fig. 201. Superhumps in OT J0329 (2006). (Upper): PDM analysis. (Lower): Phase-averaged profile.

6.179. OT J032912.3+125018

This object (also known as VS 0329+1250; hereafter OT J0329) was discovered by Skvarc, Palcic (2006). The detection of superhumps led to a classification as an SU UMa-type dwarf nova (Waagen et al. 2006). Shafter et al. (2007) reported a superhump period of 0.053394(7) d, the shortest record at that time among ordinary SU UMa-type dwarf novae. We used a combination of the photometric data by Shafter et al. (2007) and AAVSO observations and obtained times of superhump maxima (table 334; the times for superhumps were systematically different from those by Shafter et al. (2007) due to the difference in the method for determining the maxima). The mean P_{SH} with the PDM method was 0.053388(4) d (figure 201). The P_{dot} was $+2.8(0.3) \times 10^{-5}$ ($E \leq 139$, figure 202), confirming the positive P_{dot} reported in Shafter et al. (2007). Although there appears to have been a transition to stage C after $E = 139$, we could not measure P_2 because of the lack of observations.

According to the CRTS, this object (=CSS081025:032912+125018) has a magnitude of 21 in quiescence and experienced two further faint outbursts. The relatively small outburst amplitude for an extremely short P_{SH} and the presence of relatively frequent (approximately once per year) outbursts, combined with the relatively large P_{dot} , would place the object as a member of OT J0557 (group “X” in Uemura et al. 2009, though the P_{dot} is larger in OT J0557) rather than an extreme WZ Sge-type dwarf nova.

Table 334. Superhump maxima of OT J0329 (2006).

E	max ^a	error	$O - C^b$	N^c
0	54035.4296	0.0006	0.0017	27
1	54035.4833	0.0007	0.0019	28
2	54035.5343	0.0003	-0.0005	44
3	54035.5889	0.0004	0.0008	60
4	54035.6429	0.0004	0.0013	94
5	54035.6964	0.0004	0.0014	124
6	54035.7498	0.0003	0.0014	64
7	54035.8032	0.0004	0.0014	66
8	54035.8570	0.0004	0.0018	70
26	54036.8163	0.0003	-0.0002	58
44	54037.7764	0.0003	-0.0015	104
45	54037.8306	0.0002	-0.0006	112
46	54037.8845	0.0002	-0.0002	79
47	54037.9369	0.0003	-0.0012	56
48	54037.9900	0.0002	-0.0015	57
62	54038.7377	0.0003	-0.0015	56
63	54038.7914	0.0003	-0.0012	56
64	54038.8449	0.0003	-0.0011	57
65	54038.8977	0.0003	-0.0017	57
66	54038.9526	0.0006	-0.0003	33
75	54039.4305	0.0016	-0.0029	30
76	54039.4858	0.0008	-0.0010	52
77	54039.5417	0.0010	0.0014	52
78	54039.5931	0.0012	-0.0006	41
79	54039.6460	0.0009	-0.0011	41
80	54039.7009	0.0010	0.0004	61
81	54039.7528	0.0006	-0.0011	62
82	54039.8045	0.0009	-0.0029	64
83	54039.8587	0.0007	-0.0020	59
95	54040.5010	0.0007	-0.0006	87
96	54040.5541	0.0006	-0.0009	74
99	54040.7159	0.0008	0.0006	75
100	54040.7690	0.0006	0.0003	111
101	54040.8232	0.0007	0.0011	55
120	54041.8362	0.0014	-0.0005	38
121	54041.8929	0.0010	0.0028	57
138	54042.8018	0.0016	0.0037	66
139	54042.8544	0.0015	0.0029	56
263	54049.4722	0.0083	-0.0018	34
264	54049.5433	0.0070	0.0160	24
266	54049.6205	0.0083	-0.0136	20

^a BJD-2400000.

^b Against $max = 2454035.4280 + 0.053407E$.

^c Number of points used to determine the maximum.

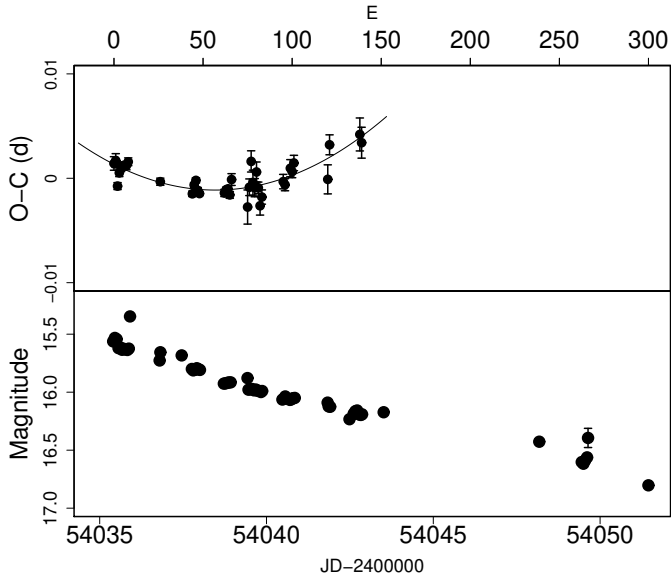


Fig. 202. $O - C$ of superhumps OT J0329 (2006). (Upper): $O - C$ diagram. The $O - C$ values were against the mean period for the stage B ($E \leq 139$, thin curve). Late-stage humps with large errors were omitted. (Lower): Light curve.

Table 335. Superhump maxima of OT J0406 (2008).

E	\max^a	error	$O - C^b$	N^c
0	54687.3825	0.0004	0.0005	151
11	54688.2619	0.0008	0.0005	350
24	54689.2989	0.0009	-0.0018	193
36	54690.2605	0.0007	0.0005	167
61	54692.2591	0.0013	0.0003	138

^a BJD-2400000.

^b Against $\max = 2454687.3820 + 0.079947E$.

^c Number of points used to determine the maximum.

6.180. OT J040659.8+005244

This object (hereafter OT J0406) was discovered by K. Itagaki (Yamaoka et al. 2008a). Subsequent observations confirmed the SU UMa-type nature of the object (vsnet-alert 10422). The mean superhump period with the PDM method was 0.07992(2) d (figure 203). The times of superhump maxima are listed in table 335. The period was almost constant with $P_{\text{dot}} = +2.8(3.4) \times 10^{-5}$. The outburst may have been detected during its late course, and the lack of period variation may be attributed to stage C superhumps.

6.181. OT J055718+683226

This object was discovered by Kloehr et al. (2006) and was extensively studied by Uemura et al. (2009). We present a supplementary analysis using the combined data with Uemura et al. (2009) and the AAVSO data (table 336). The P_{dot} for $E \leq 110$ (stage B) was $+9.0(2.1) \times 10^{-5}$. The relatively large P_{dot} with a very short P_{SH} strength-

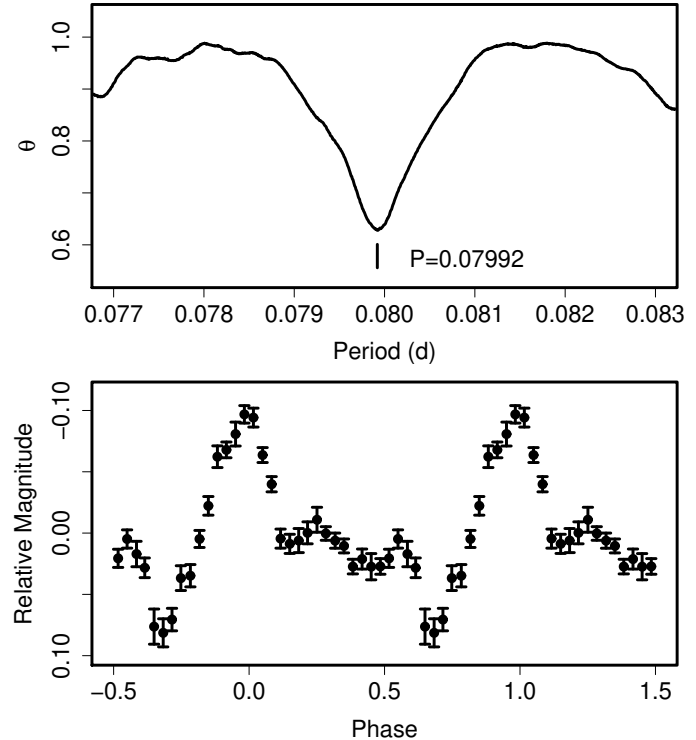


Fig. 203. Superhumps in OT J0406 (2008). (Upper): PDM analysis. (Lower): Phase-averaged profile.

ens the similarity to V844 Her, as suggested by Uemura et al. (2009).

6.182. OT J074727.6+065050

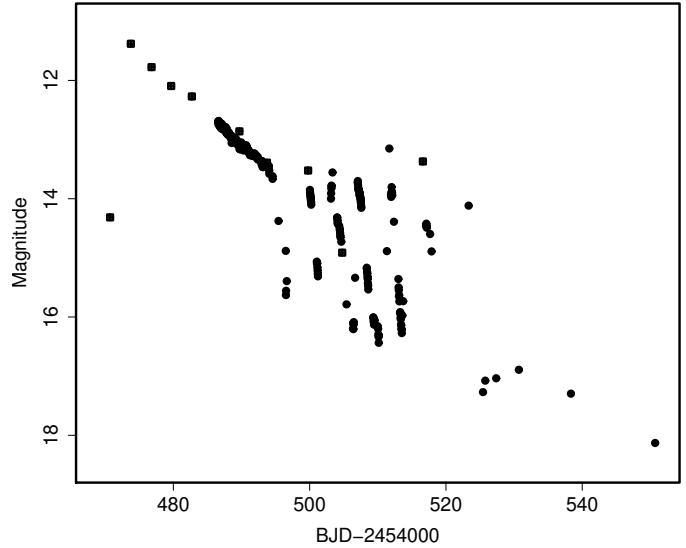
This object (hereafter OT J0747) was discovered by K. Itagaki (Yamaoka et al. 2008f). Soon after the discovery announcement and spectroscopic confirmation, this object was proposed to be a good candidate for a WZ Sge-type dwarf nova (vsnet-alert 9832). The detection of superhumps and later repeated rebrightenings confirmed this suggestion. The outburst behavior was very similar to those of EG Cnc or UZ Boo (figure 204). The post-superoutburst observations indicated that the final fading was on a smooth extension of the quiescence during the rebrightening phase, as in SDSS J0804 (for the implication, see Kato et al. 2009).

The times of superhump maxima during the main superoutburst are listed in table 337. The detection of the outburst was 11 d after the maximum ($V = 11.4$) retroactively measured with ASAS-3. The stage of early superhumps and early development of the ordinary superhumps were not recorded. The P_{dot} during the plateau stage was $+4.0(0.8) \times 10^{-5}$ ($E \leq 109$). Shears et al. (2009b) reported P_{dot} of $+4.4(0.9) \times 10^{-5}$ using a slightly different set of observations.

After removing the global trend of the outburst (the method is the same as in Kato et al. 2009), PDM analyses yielded mean superhump periods of 0.060750(7) d during the superoutburst (figure 205) and 0.060771(3) d during

Table 336. Superhump maxima of OT J0557 (2006).

E	max ^a	error	$O - C^b$	N^c
0	54087.2836	0.0005	-0.0005	155
1	54087.3365	0.0009	-0.0011	95
15	54088.0832	0.0005	-0.0017	99
16	54088.1373	0.0006	-0.0010	99
17	54088.1868	0.0012	-0.0049	99
19	54088.2976	0.0006	-0.0009	111
20	54088.3487	0.0005	-0.0032	100
34	54089.0971	0.0009	-0.0022	106
35	54089.1478	0.0009	-0.0049	132
36	54089.2019	0.0010	-0.0041	140
37	54089.2561	0.0010	-0.0033	105
38	54089.3088	0.0007	-0.0039	144
39	54089.3628	0.0005	-0.0033	177
40	54089.4162	0.0010	-0.0034	80
41	54089.4709	0.0013	-0.0021	55
42	54089.5255	0.0014	-0.0009	63
43	54089.5765	0.0007	-0.0032	121
49	54089.8967	0.0019	-0.0033	60
50	54089.9555	0.0012	0.0021	101
51	54090.0055	0.0011	-0.0013	100
52	54090.0576	0.0042	-0.0026	100
54	54090.1670	0.0031	0.0001	30
74	54091.2388	0.0019	0.0041	42
91	54092.1382	0.0026	-0.0039	167
92	54092.1956	0.0086	0.0001	65
97	54092.4736	0.0037	0.0112	44
98	54092.5204	0.0022	0.0045	43
99	54092.5738	0.0031	0.0046	79
100	54092.6371	0.0014	0.0145	35
109	54093.1147	0.0048	0.0116	110
110	54093.1708	0.0051	0.0143	113
143	54094.9264	0.0021	0.0082	93
144	54094.9808	0.0026	0.0092	67
180	54096.8984	0.0044	0.0050	62
183	54097.0587	0.0062	0.0051	111
185	54097.1442	0.0075	-0.0161	112
257	54100.9959	0.0024	-0.0081	100
258	54101.0637	0.0040	0.0063	57
259	54101.1063	0.0025	-0.0045	88
260	54101.1477	0.0021	-0.0165	42

^a BJD-2400000.^b Against $max = 2454087.2842 + 0.053385E$.^c Number of points used to determine the maximum.**Fig. 204.** Light curve of the 2008 superoutburst of OT J0747. The filled circles and filled squares represent CCD observations used here and ASAS-3 V data, respectively.

the rebrightening phase (figure 206). The superhump period during the rebrightening phase is 0.3 % longer than that during the superoutburst plateau. This behavior follows the general tendency in WZ Sge-type dwarf novae (subsection 5.1).

6.183. OT J080714.2+113812

This object (hereafter OT J0807) was discovered by K. Itagaki and was suggested to be a candidate WZ Sge-type dwarf nova (vsnet-newvar 2602, vsnet-alert 9721, 9731). The object was soon confirmed to exhibit superhumps. The outburst was associated with an unusual rebrightening following a one-day dip near the termination of the superoutburst (vsnet-alert 9745, 9746, figure 207). The mean superhump period with the PDM method was 0.060818(10) d (figure 208). The times of superhump maxima are listed in table 338. Judging from the light curve and the variation of the amplitude of superhumps, the outburst was probably detected during its middle-to-late course. The stage of early superhumps, if the object is indeed a WZ Sge-type dwarf nova, and early development of the ordinary superhumps thus were not recorded. The table includes the maxima during the rebrightening ($E = 218, 219$). The break in the $O - C$ diagram most likely reflected a transition to the stage C. We determined a relatively large $P_{\text{dot}} = +9.5(4.8) \times 10^{-5}$ for the earlier phase ($E \leq 89$). This behavior of period variation is similar to those observed in the stage B of short-period SU UMa-type dwarf novae or some WZ Sge-type dwarf novae. More detailed analysis will be reported by Maehara et al., in preparation.

6.184. OT J081418.9-005022

This object (=CSS080409:081419-005022, hereafter OT J0814) was discovered by the CRTS (Drake et al.

Table 337. Superhump maxima of OT J0747 (2008).

E	\max^a	error	$O - C^b$	N^c
0	54486.5762	0.0017	0.0016	6
1	54486.6361	0.0006	0.0007	8
2	54486.6980	0.0004	0.0019	7
3	54486.7587	0.0009	0.0019	8
4	54486.8186	0.0010	0.0010	8
7	54487.0016	0.0005	0.0019	154
8	54487.0616	0.0002	0.0011	338
9	54487.1224	0.0007	0.0012	170
16	54487.5446	0.0034	-0.0018	20
18	54487.6691	0.0006	0.0013	8
20	54487.7896	0.0012	0.0003	6
21	54487.8474	0.0017	-0.0027	6
24	54488.0330	0.0007	0.0008	68
25	54488.0928	0.0004	-0.0001	114
26	54488.1540	0.0004	0.0003	114
31	54488.4583	0.0011	0.0009	91
32	54488.5150	0.0013	-0.0031	95
40	54489.0066	0.0009	0.0026	56
41	54489.0653	0.0005	0.0006	125
42	54489.1229	0.0005	-0.0025	111
43	54489.1846	0.0005	-0.0016	113
44	54489.2463	0.0005	-0.0006	114
45	54489.3052	0.0006	-0.0024	110
52	54489.7309	0.0008	-0.0018	58
53	54489.7911	0.0005	-0.0024	76
54	54489.8517	0.0007	-0.0025	81
55	54489.9134	0.0024	-0.0015	76
62	54490.3446	0.0020	0.0045	58
63	54490.3991	0.0012	-0.0017	64
64	54490.4592	0.0010	-0.0024	63
68	54490.7028	0.0006	-0.0017	42
69	54490.7627	0.0005	-0.0026	58
70	54490.8245	0.0014	-0.0015	57
73	54491.0071	0.0008	-0.0011	174
74	54491.0708	0.0014	0.0020	121
75	54491.1264	0.0014	-0.0033	113
76	54491.1893	0.0016	-0.0011	115
77	54491.2520	0.0013	0.0009	85
83	54491.6146	0.0011	-0.0009	26
84	54491.6774	0.0017	0.0012	23
85	54491.7383	0.0022	0.0014	23
86	54491.8001	0.0021	0.0024	29
87	54491.8590	0.0014	0.0006	34
88	54491.9183	0.0011	-0.0009	30
92	54492.1609	0.0024	-0.0011	78
105	54492.9571	0.0014	0.0055	173
106	54493.0142	0.0010	0.0019	173
108	54493.1374	0.0019	0.0035	62
109	54493.1957	0.0018	0.0012	41
122	54493.9844	0.0006	0.0003	51
123	54494.0423	0.0009	-0.0025	56

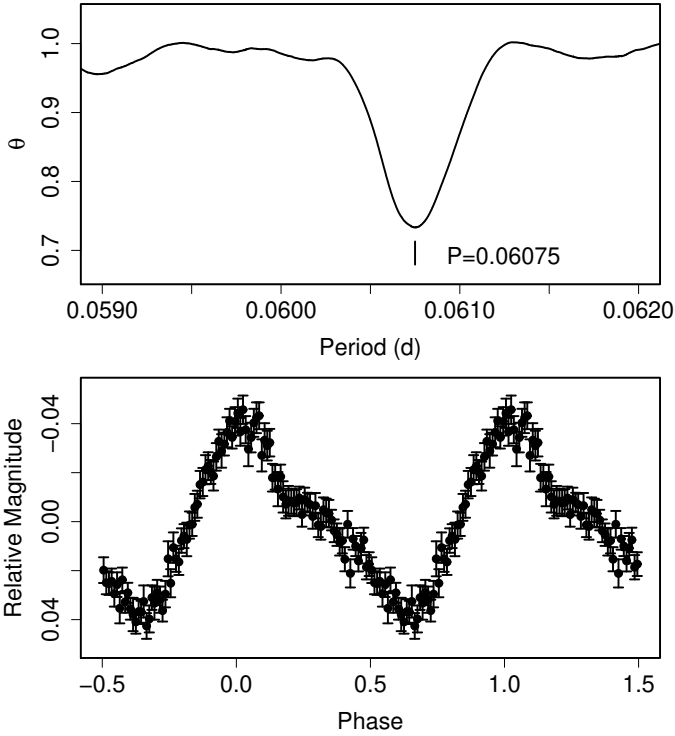
^a BJD-2400000.^b Against $\max = 2454486.5746 + 0.060733E$.^c Number of points used to determine the maximum.

Fig. 205. Superhumps in OT J0747 during the superoutburst plateau (2008). (Upper): PDM analysis. (Lower): Phase-averaged profile.

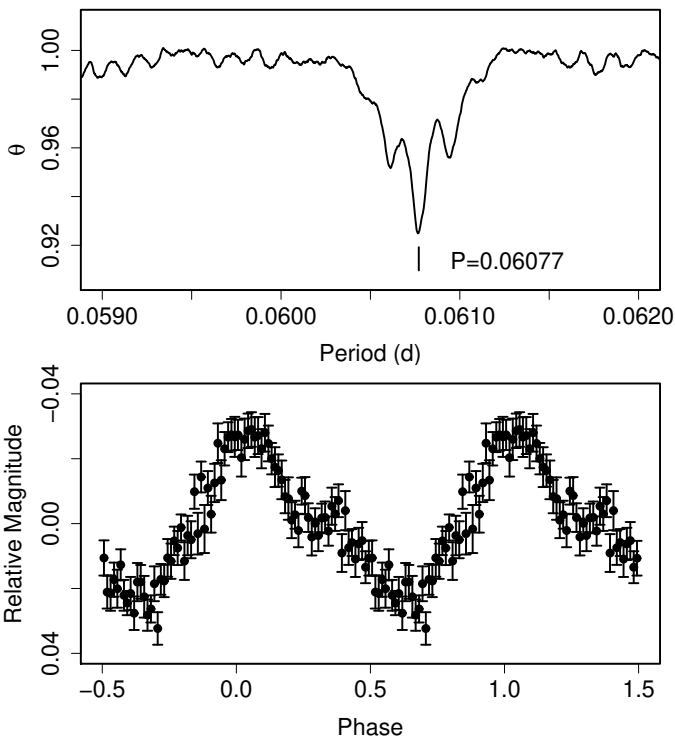


Fig. 206. Superhumps in OT J0747 during the rebrightening phase (2008). (Upper): PDM analysis. (Lower): Phase-averaged profile.

Table 338. Superhump maxima of OT J0807 (2007).

E	\max^a	error	$O - C^b$	N^c
0	54424.9170	0.0003	-0.0049	113
1	54424.9763	0.0003	-0.0064	113
4	54425.1594	0.0014	-0.0056	90
5	54425.2201	0.0004	-0.0057	368
6	54425.2808	0.0005	-0.0058	373
7	54425.3422	0.0005	-0.0052	296
16	54425.8931	0.0006	-0.0012	111
17	54425.9525	0.0009	-0.0026	102
18	54426.0110	0.0005	-0.0049	108
22	54426.2538	0.0012	-0.0053	220
23	54426.3192	0.0013	-0.0006	116
26	54426.5005	0.0014	-0.0017	121
27	54426.5581	0.0012	-0.0048	123
28	54426.6250	0.0013	0.0013	105
29	54426.6828	0.0013	-0.0017	116
37	54427.1660	0.0072	-0.0047	106
38	54427.2294	0.0010	-0.0021	66
39	54427.2906	0.0006	-0.0016	80
54	54428.2073	0.0013	0.0034	321
55	54428.2763	0.0069	0.0116	345
56	54428.3218	0.0024	-0.0037	267
70	54429.1825	0.0030	0.0062	129
71	54429.2575	0.0046	0.0204	131
72	54429.3205	0.0035	0.0226	123
89	54430.3462	0.0033	0.0150	37
153	54434.2262	0.0013	0.0052	123
154	54434.2872	0.0024	0.0054	123
155	54434.3496	0.0018	0.0071	132
169	54435.2044	0.0022	0.0111	147
170	54435.2615	0.0025	0.0073	204
187	54436.2838	0.0052	-0.0036	54
218	54438.1507	0.0030	-0.0208	188
219	54438.2086	0.0027	-0.0237	175

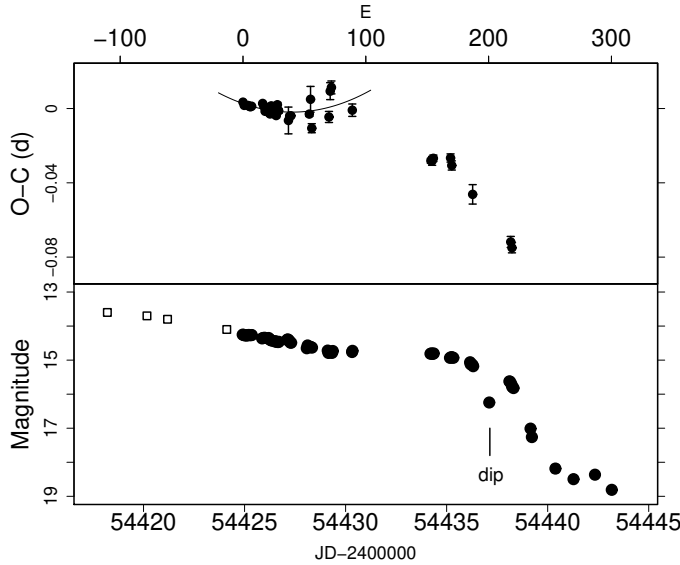
^a BJD-2400000.^b Against $\max = 2454424.9219 + 0.060778E$.^c Number of points used to determine the maximum.

Fig. 207. $O - C$ of superhumps OT J0807 (2007). (Upper): $O - C$ diagram. The $O - C$ values were against the mean period for the stage B ($E < 89$, thin curve) (Lower): Light curve. Large dots are our CCD observations and open squares are Itagaki's CCD observations.

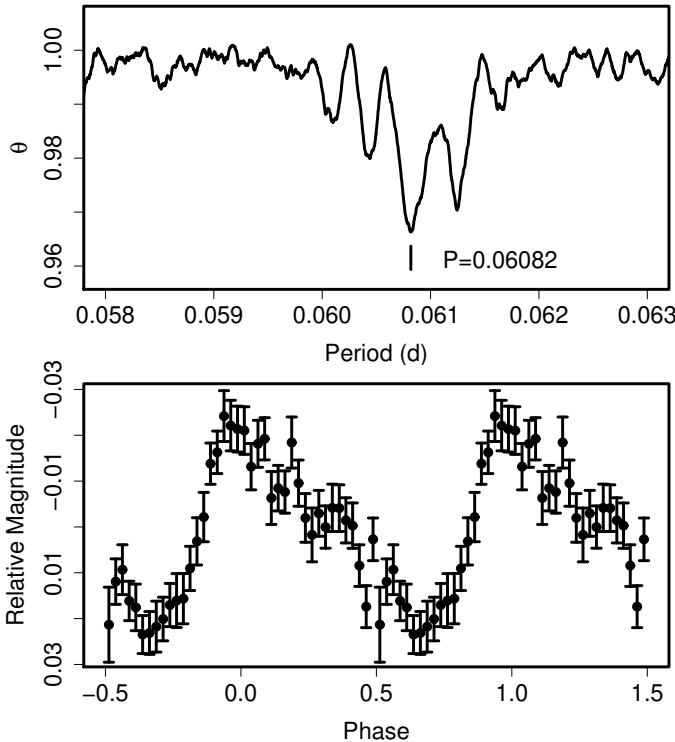


Fig. 208. Superhumps in OT J0807 (2007). (Upper): PDM analysis. (Lower): Phase-averaged profile.

2008a; Drake et al. 2009; vsnet-alert 10038). ASAS-3 detected a new outburst in 2008 October (vsnet-alert 10594), during which superhumps were detected (vsnet-alert 10603, 10630). Due to the short visibility of the object, it was difficult to uniquely determine P_{SH} . We adopted the most likely period (0.0763 d) that best express all the recorded superhumps. The times of superhump maxima are listed in table 339. There was likely a stage B-C transition.

6.185. OT J084555.1+033930

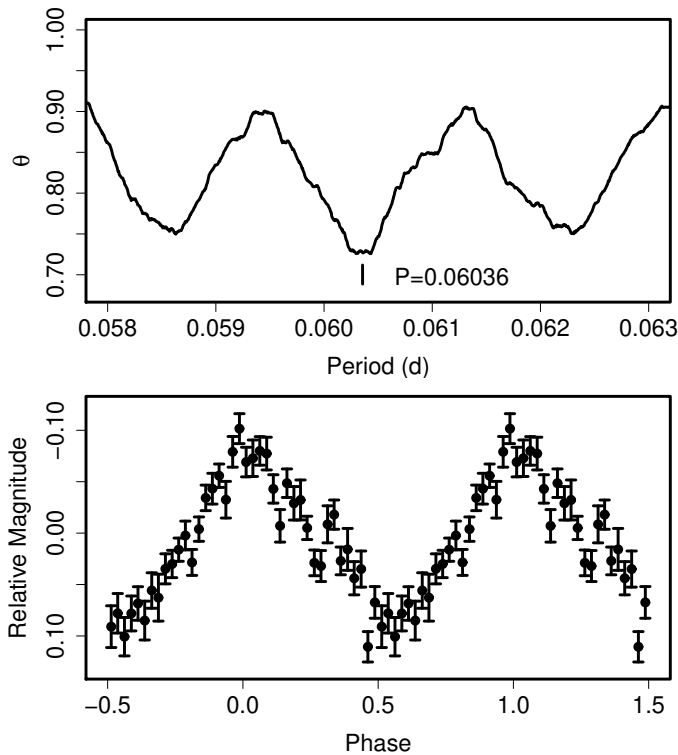
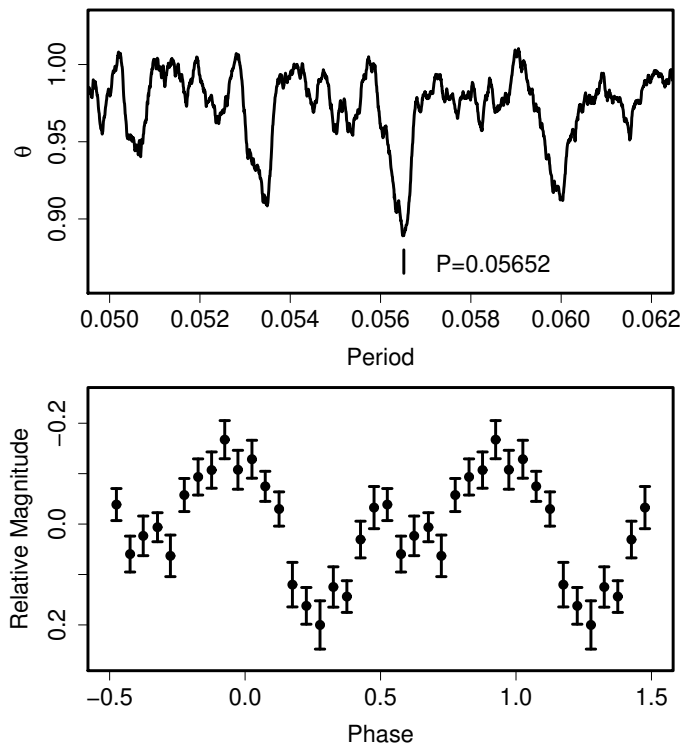
This object (hereafter OT J0845) was discovered by K. Itagaki (Yamaoka et al. 2008c; Honda et al. 2008). The mean superhump period with the PDM method was 0.06036(2) d (figure 209, excluding the first night). The times of superhump maxima are listed in table 340. The observation on the first night ($E = 0$) apparently

Table 339. Superhump maxima of OT J0814 (2008).

E	max ^a	error	$O - C^b$	N^c
0	54759.5713	0.0008	-0.0041	116
1	54759.6459	0.0009	-0.0058	95
79	54765.6153	0.0007	0.0148	149
101	54767.2901	0.0066	0.0116	81
141	54770.3126	0.0022	-0.0166	91

^a BJD-2400000.^b Against $max = 2454759.5754 + 0.076268E$.^c Number of points used to determine the maximum.**Table 340.** Superhump maxima of OT J0845 (2008).

E	max ^a	error	$O - C^b$	N^c
0	54487.1018	0.0032	-0.0004	100
66	54491.0961	0.0007	0.0023	208
67	54491.1548	0.0006	0.0006	114
68	54491.2181	0.0009	0.0034	110
69	54491.2735	0.0015	-0.0017	105
99	54493.0894	0.0016	-0.0001	168
100	54493.1443	0.0013	-0.0057	114
167	54497.2036	0.0043	0.0016	52

^a BJD-2400000.^b Against $max = 2454487.1022 + 0.060478E$.^c Number of points used to determine the maximum.**Fig. 209.** Superhumps in OT J0845 (2008) after BJD 2454491. (Upper): PDM analysis. (Lower): Phase-averaged profile.**Fig. 210.** Early superhumps in OT J0902 (2008). (Upper): PDM analysis. (Lower): Phase-averaged profile.

caught the evolutionary stage of superhumps (cf. vsnet-alert 9847). We used $E > 0$ data and obtained $P_{\text{dot}} = +6.7(3.4) \times 10^{-5}$. The object is likely a large-amplitude SU UMa-type dwarf nova rather than a typical WZ Sge-type star (vsnet-alert 9852).

6.186. OT J090239.7+052501

OT J090239.7+052501 (=CSS080304:090240+052501, hereafter OT J0902) is a transient discovered by the CRTS Drake et al. (2009). The object had a blue SDSS counterpart with $g = 23.17$, $g - r = +0.07$ (vsnet-alert 9945). Spectroscopic observation of the outbursting object revealed the presence of a broad HeII emission lines (Djorgovski et al. 2008b) which is suggestive of a WZ Sge-type outburst in a high-inclination system (vsnet-alert

9948; Imada et al. 2006c). Early superhumps were subsequently detected (vsnet-alert 9953, 9955, 9963). The object was still in outburst 27 d after the outburst detection (vsnet-alert 10011). Although we did not observe ordinary superhumps, we include this object for improving the statistics of WZ Sge-type dwarf novae. The mean period of early superhumps was 0.05652(3) d (figure 210). Uemura and Arai (vsnet-alert 9963) independently obtained the same period.

6.187. OT J102146.4+234926

This object (also called Var Leo 06, hereafter OT J1021) was discovered by Christensen (2006) in the course of

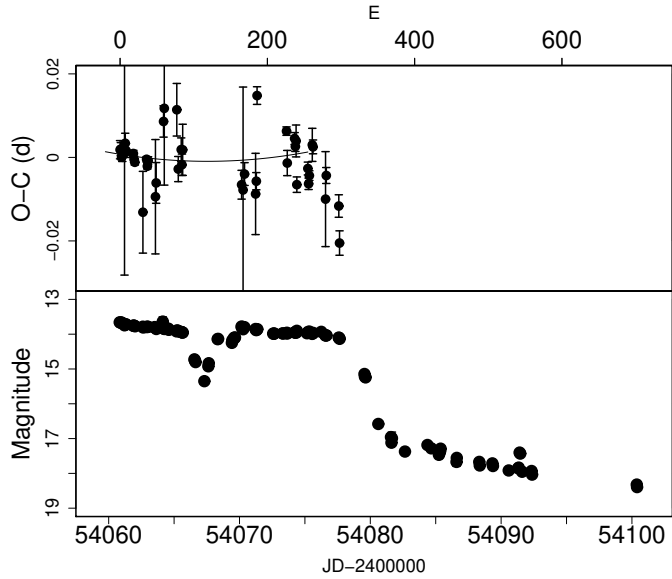


Fig. 211. $O - C$ of superhumps OT J1021 (2006). (Upper): $O - C$ diagram. The $O - C$ values were against the mean period for the stage B ($E \leq 240$, thin curve). (Lower): Light curve.

the Catalina Sky Survey (CSS). Golovin et al. (2007) and Uemura et al. (2008a) reported the detection of superhumps and classified the object as a WZ Sge-type dwarf nova. We reanalyzed the data for OT J1021 in Uemura et al. (2008a) in combination with the AAVSO data, and determined the superhump maxima during the plateau stage and the rebrightening stage (table 341). The maxima can be well expressed by a single period of 0.056295(10) d without a phase shift (figure 211). This lack of a phase shift, as well as the smooth continuation of the general fading trend before and after the “dip”, the dip phenomenon in this object can be better understood as a temporary cooling of the disk, and the plateau stage of the main superoutburst and the “rebrightening” comprise a continuous entity, rather than the complete termination of a superoutburst and a newly triggered superoutburst (see e.g. discussion for AL Com Nogami et al. 1997a). A similar phenomenon was also observed in 1RXS J0232 (subsection 6.146).

The $O - C$ apparently showed a break around $E = 240$ (corresponding to a stage B–C transition), rather than a phase shift as shown in Uemura et al. (2008a). The mean period and P_{dot} for $E \leq 240$ were 0.056312(12) d and $0.4(0.8) \times 10^{-5}$, respectively. The period after the transition was 0.056043(65), which is probably identical to the newly appeared period of 0.055988(15) d during the fading tail (Uemura et al. 2008a). Although Uemura et al. (2008a) attributed this period to a candidate orbital period, the above behavior agrees with a transition to a shorter superhump period, generally seen in SU UMa-type dwarf novae.

Table 341. Superhump maxima of OT J1021.

E	max ^a	error	$O - C$ ^b	N ^c
0	54060.8730	0.0022	0.0008	9
1	54060.9295	0.0015	0.0009	36
2	54060.9839	0.0006	-0.0010	60
3	54061.0404	0.0013	-0.0007	29
6	54061.2101	0.0292	0.0000	62
7	54061.2688	0.0024	0.0024	118
8	54061.3233	0.0017	0.0007	134
18	54061.8857	0.0008	0.0002	56
19	54061.9407	0.0007	-0.0012	58
20	54061.9963	0.0007	-0.0019	58
31	54062.6037	0.0098	-0.0136	40
36	54062.8980	0.0006	-0.0009	58
37	54062.9526	0.0007	-0.0025	58
38	54063.0103	0.0009	-0.0011	58
48	54063.5648	0.0137	-0.0096	41
49	54063.6244	0.0049	-0.0063	34
59	54064.2022	0.0038	0.0086	121
60	54064.2617	0.0184	0.0117	91
77	54065.2186	0.0063	0.0117	217
79	54065.3171	0.0030	-0.0025	108
83	54065.5470	0.0028	0.0023	33
84	54065.5997	0.0026	-0.0013	42
85	54065.6595	0.0061	0.0022	28
165	54070.1562	0.0034	-0.0047	66
167	54070.2676	0.0246	-0.0059	57
169	54070.3840	0.0027	-0.0021	68
184	54071.2239	0.0097	-0.0066	72
185	54071.2833	0.0021	-0.0035	193
186	54071.3601	0.0021	0.0170	204
226	54073.6041	0.0010	0.0092	21
227	54073.6527	0.0030	0.0016	24
237	54074.2217	0.0014	0.0076	167
238	54074.2761	0.0012	0.0057	317
239	54074.3338	0.0038	0.0071	235
240	54074.3796	0.0019	-0.0034	94
255	54075.2282	0.0015	0.0008	364
256	54075.2808	0.0014	-0.0029	300
257	54075.3391	0.0012	-0.0009	159
261	54075.5717	0.0040	0.0065	24
262	54075.6275	0.0017	0.0061	24
279	54076.5723	0.0114	-0.0062	32
280	54076.6343	0.0019	-0.0005	67
297	54077.5843	0.0027	-0.0075	7
298	54077.6318	0.0029	-0.0163	10

^a BJD-2400000.

^b Against $max = 2454060.8722 + 0.056295E$.

^c Number of points used to determine the maximum.

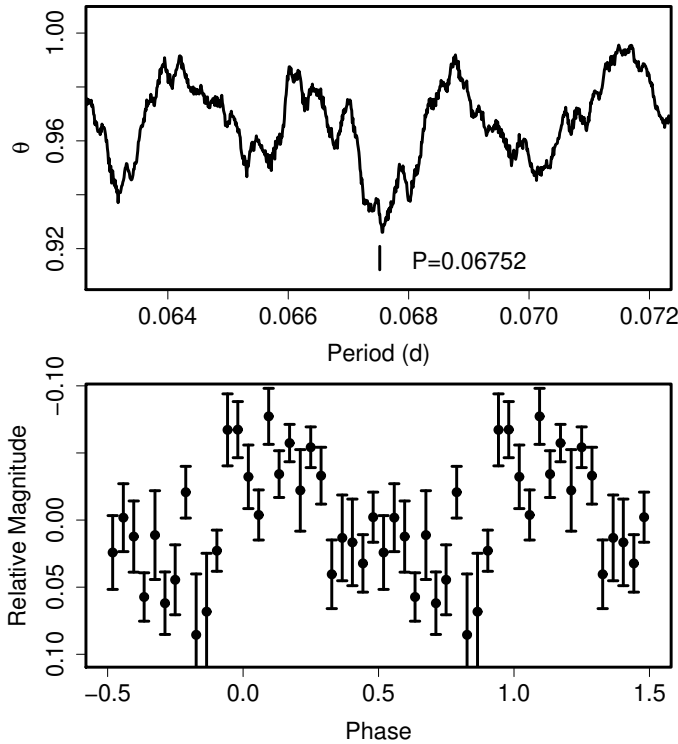


Fig. 212. Superhumps in OT J1026 (2009). (Upper): PDM analysis. (Lower): Phase-averaged profile.

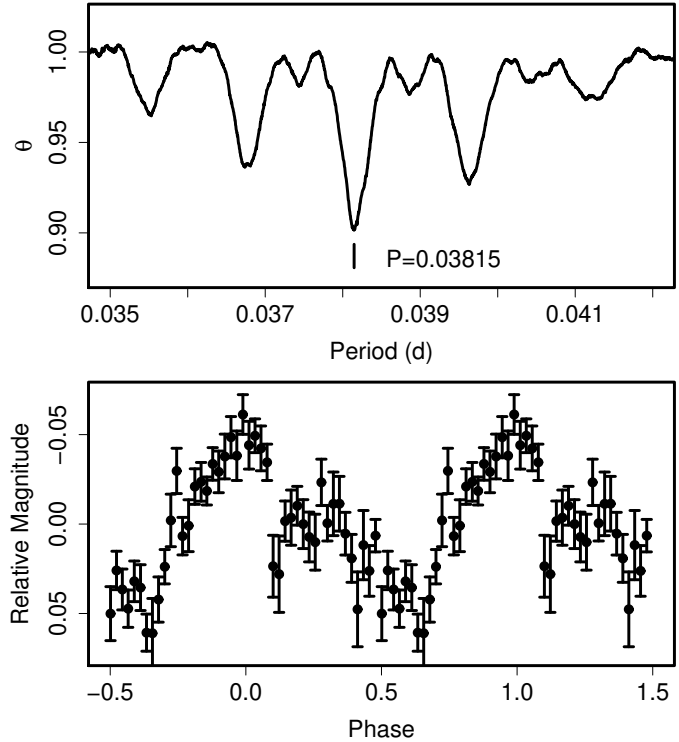


Fig. 213. Superhumps in OT J1028 (2009). (Upper): PDM analysis. (Lower): Phase-averaged profile.

Table 342. Superhump maxima of OT J1026 (2009).

E	max ^a	error	$O - C^b$	N^c
0	54835.1783	0.0137	-0.0180	40
1	54835.2703	0.0018	0.0064	72
2	54835.3407	0.0026	0.0092	61
28	54837.0918	0.0051	0.0034	28
29	54837.1526	0.0035	-0.0034	40
30	54837.2300	0.0039	0.0065	67
32	54837.3608	0.0019	0.0021	39
46	54838.2987	0.0076	-0.0061	71

^a BJD-2400000.

^b Against $max = 2454835.1963 + 0.067575E$.

^c Number of points used to determine the maximum.

6.188. OT J102637.0+475426

This object (hereafter OT J1026) was discovered by K. Itagaki (Yamaoka, Itagaki 2009). The SU UMa-type nature of this object was immediately clarified (vsnet-alert 10882). The object soon started fading, indicating that the outburst was caught during its final stage. A PDM analysis of the entire data set yielded a period of 0.06752(9) d (figure 212). This period presumably corresponds to P_2 . The times of superhump maxima are given in table 342.

6.189. OT J102842.9-081927

This transient (=CSS090331:102843-081927, hereafter OT J1028) was detected by the CRTS. The object soon turned out to be an ultrashort-period SU UMa-type dwarf nova (vsnet-alert 11149, 11158, 11164). An unusual $V - J$ color was reported (vsnet-alert 11163). A spectroscopic observation clarified its hydrogen-rich nature (vsnet-alert 11166), suggesting that the object is similar to V485 Cen and EI Psc.

The times of superhump maxima are listed in table 343. The outburst was apparently observed during the relatively late stage and the following decline phase. Although we included times of maxima after BJD 2454928 (decline phase) because of the continued detection of the periodicity after the decline, this part of the data suffered from the low signal-to-noise ratio. We thus restricted to $E \leq 59$ for determining parameters, yielding a marginally positive $P_{\text{dot}} = +11.6(8.5) \times 10^{-5}$. A PDM analysis of the same interval yielded a period of 0.038147(14) d (figure 213).

6.190. OT J111217.4-353829

This object (hereafter OT J1112) was detected by “Pi of the Sky” and its dwarf nova-type nature was confirmed (vsnet-alert 9764, 9767, 9769, 9770, 9771). The detection of early superhumps and ordinary superhumps led to a classification of a typical WZ Sge-type dwarf nova (vsnet-alert 9775, 9806). The presence of HeII and CIV emission lines in the spectrum was also very similar to WZ Sge (vsnet-alert 9782). The times of superhump maxima

Table 343. Superhump maxima of OT J1028 (2009).

E	max ^a	error	$O - C^b$	N^c
0	54922.9883	0.0016	0.0015	56
1	54923.0247	0.0009	-0.0001	72
2	54923.0621	0.0011	-0.0009	72
3	54923.0995	0.0010	-0.0015	72
4	54923.1380	0.0008	-0.0012	72
28	54924.0535	0.0021	0.0002	43
29	54924.0918	0.0020	0.0005	119
30	54924.1280	0.0010	-0.0014	120
31	54924.1655	0.0025	-0.0020	119
32	54924.2069	0.0017	0.0012	110
52	54924.9632	0.0058	-0.0042	42
53	54925.0118	0.0038	0.0063	71
54	54925.0446	0.0015	0.0010	71
55	54925.0860	0.0009	0.0043	72
56	54925.1237	0.0016	0.0039	71
57	54925.1616	0.0014	0.0037	72
58	54925.1983	0.0034	0.0023	70
59	54925.2356	0.0008	0.0015	67
134	54928.0912	0.0022	0.0005	62
135	54928.1210	0.0051	-0.0079	68
159	54929.0377	0.0060	-0.0053	50
188	54930.1368	0.0054	-0.0108	52
189	54930.1747	0.0066	-0.0110	66
213	54931.0986	0.0017	-0.0013	64
214	54931.1529	0.0071	0.0150	46
240	54932.1301	0.0032	0.0019	58
423	54939.1023	0.0029	0.0037	44

^a BJD-2400000.^b Against $max = 2454922.9868 + 0.038089E$.^c Number of points used to determine the maximum.

are listed are in table 344. The change in the superhump period was very small, $P_{\dot{ot}} = +0.5(0.3) \times 10^{-5}$, similar to WZ Sge itself. The mean periods of early and ordinary superhumps, determined with the PDM method, were 0.05847(2) d (figure 214) and 0.058965(9) d (figure 215), respectively. This P_{SH} is adopted in table 2. The fractional superhump excess was estimated to be 0.8(1) %, also very typical for a WZ Sge-type dwarf nova. More detailed analysis will be presented in Maehara et al., in preparation.

6.191. OT J130030.3+115101

This transient (=CSS080702:130030+115101, hereafter OT J1300) was detected by the CRTS. Independent detections by ASAS-3 suggested a superoutburst of an SU UMa-type dwarf nova (vsnet-alert 10300). Five days after the maximum, the object showed superhumps (vsnet-alert 10311). The mean superhump period with the PDM method was 0.06440(2) d (figure 216) The times of superhump maxima are listed in table 345. The epoch $E = 0$ corresponded to a growing stage of superhumps. Disregarding this epoch, we obtained $P_{\dot{ot}} = +14.4(1.5) \times 10^{-5}$.

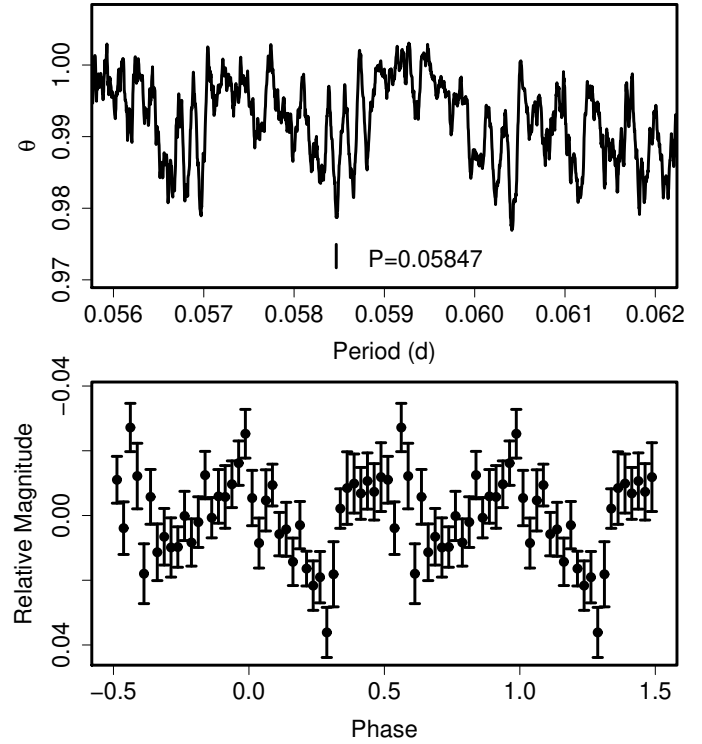


Fig. 214. Early superhumps in OT J1112 (2007). (Upper): PDM analysis. (Lower): Phase-averaged profile.

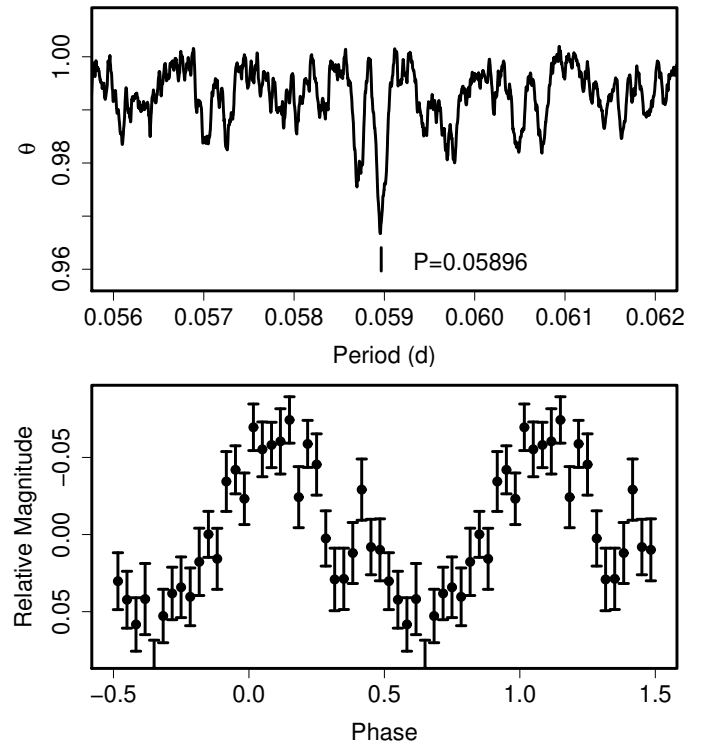


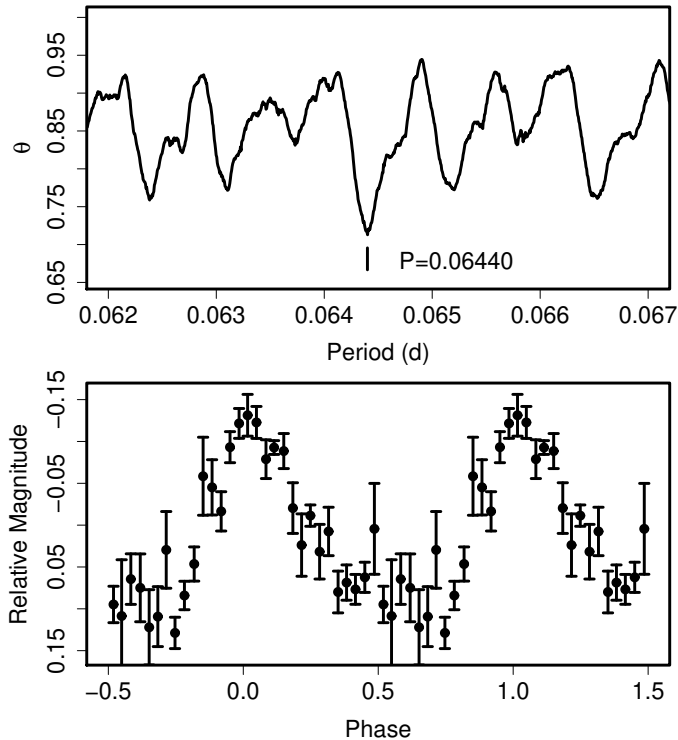
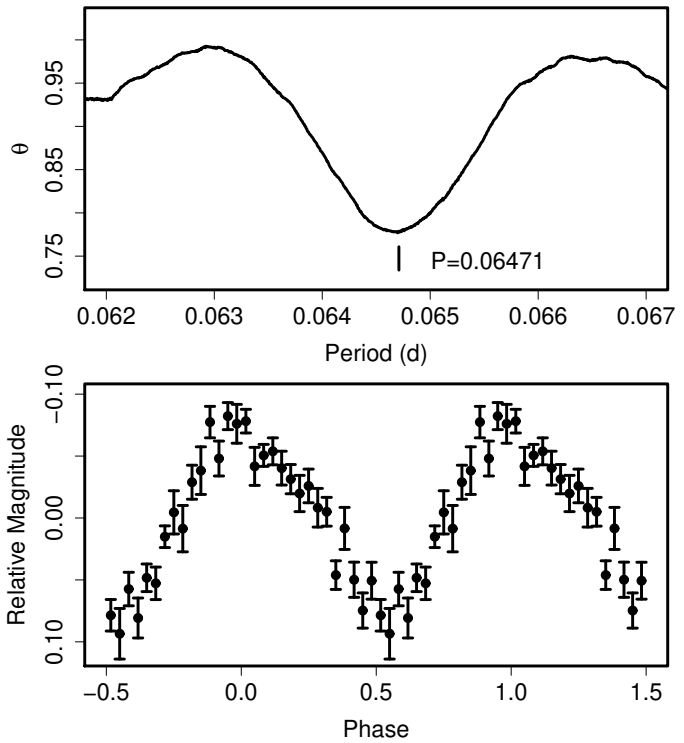
Fig. 215. Ordinary superhumps in OT J1112 (2007). (Upper): PDM analysis. (Lower): Phase-averaged profile.

Table 344. Superhump maxima of OT J1112 (2007–2008).

E	max ^a	error	$O - C^b$	N^c
0	54475.3297	0.0027	-0.0009	124
16	54476.2778	0.0010	0.0030	281
82	54480.1717	0.0008	0.0023	61
83	54480.2255	0.0019	-0.0029	96
84	54480.2868	0.0009	-0.0007	233
85	54480.3474	0.0019	0.0009	303
116	54482.1778	0.0010	0.0020	61
117	54482.2350	0.0014	0.0002	61
118	54482.2934	0.0007	-0.0004	61
119	54482.3517	0.0008	-0.0011	51
218	54488.1932	0.0080	-0.0016	39
219	54488.2539	0.0028	0.0001	61
220	54488.3062	0.0014	-0.0066	60
221	54488.3695	0.0024	-0.0023	33
253	54490.2588	0.0019	-0.0014	130
254	54490.3219	0.0042	0.0028	112
269	54491.2046	0.0021	0.0003	36
270	54491.2656	0.0036	0.0023	108
287	54492.2705	0.0014	0.0040	135

^a BJD-2400000.^b Against $max = 2454475.3306 + 0.059010E$.^c Number of points used to determine the maximum.**Table 345.** Superhump maxima of OT J1300 (2008).

E	max ^a	error	$O - C^b$	N^c
0	54653.0315	0.0007	-0.0016	120
14	54653.9374	0.0012	0.0027	44
15	54653.9998	0.0003	0.0007	108
16	54654.0645	0.0008	0.0011	88
77	54657.9847	0.0013	-0.0069	51
93	54659.0198	0.0039	-0.0021	43
108	54659.9915	0.0010	0.0037	80
109	54660.0547	0.0014	0.0024	50

^a BJD-2400000.^b Against $max = 2454653.0331 + 0.064396E$.^c Number of points used to determine the maximum.**Fig. 216.** Superhumps in OT J1300 (2008) after BJD 2454653.9. (Upper): PDM analysis. (Lower): Phase-averaged profile.**Fig. 217.** Superhumps in OT J1440 (2009). (Upper): PDM analysis. (Lower): Phase-averaged profile.*6.192. OT J144011.0+494734*

This transient (=CSS090530:144011+494734, hereafter OT J1440) was detected by the CRTS. The detection of superhumps confirmed the SU UMa-type classification (vsnet-outburst 10297, vsnet-alert 11283). The mean superhump period with the PDM method was 0.06471(5) d (figure 217). The times of superhump maxima are listed in table 346. Although there was a clear break in the $O - C$ diagram between $E = 1$ and $E = 15$, it was unclear whether this break is attributed to stage A–B or stage B–C transition. We adopted the latter interpretation because the period was almost constant after the break.

Table 346. Superhump maxima of OT J1440 (2009).

E	\max^a	error	$O - C^b$	N^c
0	54983.0238	0.0031	-0.0045	69
1	54983.0935	0.0121	0.0003	64
15	54984.0043	0.0016	0.0025	188
16	54984.0689	0.0011	0.0023	224
22	54984.4581	0.0005	0.0021	92
23	54984.5209	0.0009	-0.0001	101
24	54984.5867	0.0006	0.0009	74
37	54985.4313	0.0013	0.0018	73
38	54985.4918	0.0007	-0.0027	106
39	54985.5566	0.0009	-0.0027	104

^a BJD-2400000.^b Against $\max = 2454983.0283 + 0.064899E$.^c Number of points used to determine the maximum.**6.193. OT J144341.9-175550**

This transient (=CSS090418:144342-175550, hereafter OT J1443) was detected by the CRTS. The detection of superhumps confirmed the SU UMa-type classification (vsnet-alert 11193, 11195, 11196, 11199, 11219). The times of superhump maxima are listed in table 347. Thanks to the early detection of the outburst, all stages A-C were recorded. The P_{dot} during the stage B was $+11.0(1.3) \times 10^{-5}$ ($12 \leq E \leq 112$). Other parameters are listed in table 2. The mean P_{SH} over the entire superoutburst was 0.072065(10) d (PDM method, figure 218).

6.194. OT J163120.9+103134

This transient (=CSS080505:163121+103134, hereafter OT J1631) was discovered by the CRTS (Drake et al. 2009). Soon after the discovery announcement, past outbursts from ASAS-3 records and the ROSAT identification were noticed (cvnet-discussion 1136, vsnet-alert 10159). The detection of superhump led to secure classification of this object. Mahabal et al. (2008) presented a spectroscopical confirmation as a CV. The mean superhump period with the PDM method was 0.064129(5) d (figure 219). The times of superhump maxima are listed in table 348. The $O - C$ diagram showed a clear positive period derivative ($E \leq 96$) before a transition to the stage C, behavior typical for this superhump period (cf. figure 7). We obtained $P_{\text{dot}} = +12.5(1.3) \times 10^{-5}$ for the stage B.

6.195. OT J191443.6+605214

This transient (hereafter OT J1914) was detected by K. Itagaki (Yamaoka et al. 2008d). The SU UMa-type nature of this object was soon established (vsnet-alert 10558). The mean superhump period during the entire plateau phase was 0.071292(14) d (PDM method, figure 220). The times of superhump maxima are listed in table 349. A stage B-C transition was recorded around $E = 82$. The mean P_{SH} and P_{dot} during the stage B were 0.07134(3) d and $+9.7(2.6) \times 10^{-5}$, respectively. Boyd et al. (2009) reported $P_{\text{dot}} = +3.4(2.0) \times 10^{-5}$ using a slightly different treatment and data set.

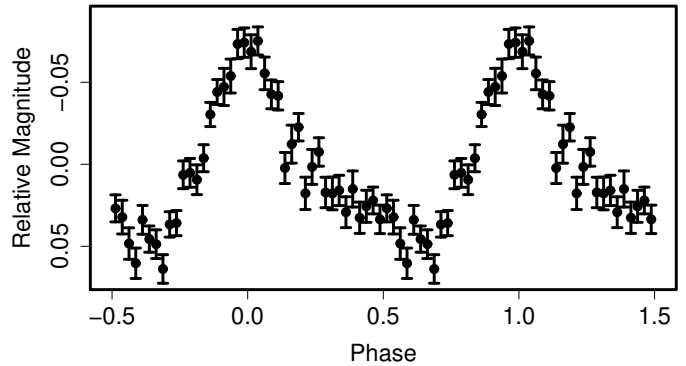
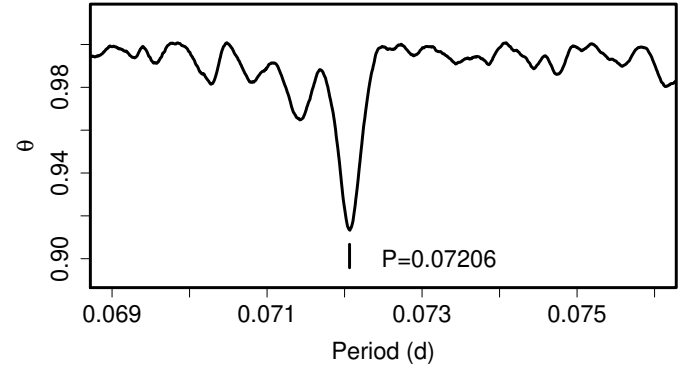
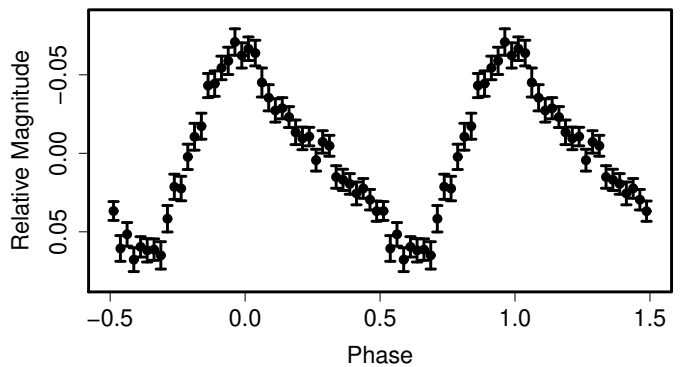
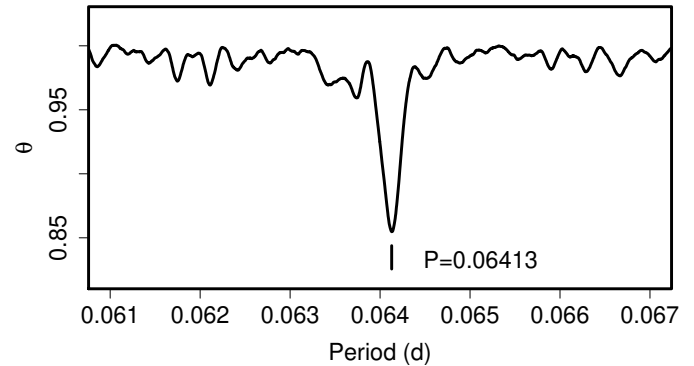
**Fig. 218.** Superhumps in OT J1443 (2009). (Upper): PDM analysis. (Lower): Phase-averaged profile.**Fig. 219.** Superhumps in OT J1631 (2008). (Upper): PDM analysis. (Lower): Phase-averaged profile.

Table 347. Superhump maxima of OT J1443 (2009).

E	max ^a	error	$O - C^b$	N^c
0	54940.1823	0.0024	-0.0308	134
1	54940.2643	0.0019	-0.0209	151
12	54941.0808	0.0009	0.0025	42
13	54941.1551	0.0009	0.0047	179
14	54941.2256	0.0004	0.0031	75
15	54941.2986	0.0009	0.0040	43
26	54942.0921	0.0004	0.0044	58
27	54942.1640	0.0004	0.0042	72
28	54942.2359	0.0004	0.0040	74
29	54942.3077	0.0003	0.0037	74
30	54942.3790	0.0004	0.0029	60
54	54944.1074	0.0004	0.0009	74
55	54944.1785	0.0005	-0.0001	75
56	54944.2504	0.0004	-0.0003	74
57	54944.3236	0.0007	0.0008	48
68	54945.1178	0.0006	0.0019	152
69	54945.1862	0.0006	-0.0017	261
70	54945.2608	0.0021	0.0007	146
95	54947.0691	0.0012	0.0066	119
110	54948.1540	0.0005	0.0100	115
111	54948.2340	0.0011	0.0178	120
112	54948.3033	0.0018	0.0150	71
123	54949.0852	0.0011	0.0038	141
124	54949.1598	0.0010	0.0064	246
125	54949.2346	0.0010	0.0090	184
137	54950.0927	0.0010	0.0019	151
138	54950.1625	0.0009	-0.0003	314
139	54950.2310	0.0015	-0.0040	260
151	54951.0961	0.0060	-0.0040	319
152	54951.1674	0.0009	-0.0048	393
153	54951.2305	0.0034	-0.0139	209
165	54952.1111	0.0063	0.0015	314
166	54952.1698	0.0037	-0.0119	242
179	54953.1123	0.0021	-0.0066	180
180	54953.1803	0.0021	-0.0107	285

^a BJD-2400000.^b Against $max = 2454940.2131 + 0.072099E$.^c Number of points used to determine the maximum.

Table 348. Superhump maxima of OT J1631 (2008).

E	max ^a	error	$O - C^b$	N^c
0	54592.4052	0.0004	0.0062	247
1	54592.4679	0.0005	0.0048	246
2	54592.5331	0.0014	0.0059	135
16	54593.4275	0.0004	0.0024	218
17	54593.4905	0.0005	0.0012	200
18	54593.5549	0.0006	0.0014	103
27	54594.1302	0.0012	-0.0005	66
28	54594.1947	0.0012	-0.0001	67
31	54594.3860	0.0006	-0.0013	184
32	54594.4492	0.0005	-0.0022	201
33	54594.5102	0.0006	-0.0054	156
46	54595.3437	0.0009	-0.0056	122
47	54595.4096	0.0009	-0.0039	204
48	54595.4725	0.0011	-0.0052	205
63	54596.4348	0.0009	-0.0049	84
64	54596.5012	0.0012	-0.0027	76
65	54596.5619	0.0060	-0.0061	52
77	54597.3381	0.0012	0.0004	105
78	54597.4012	0.0024	-0.0006	182
79	54597.4648	0.0011	-0.0011	193
80	54597.5281	0.0020	-0.0020	175
81	54597.5935	0.0010	-0.0007	70
89	54598.1132	0.0010	0.0058	126
90	54598.1716	0.0083	0.0001	86
91	54598.2398	0.0013	0.0042	137
94	54598.4314	0.0011	0.0033	83
95	54598.4930	0.0008	0.0008	82
96	54598.5581	0.0025	0.0018	47
109	54599.3918	0.0009	0.0017	72
110	54599.4507	0.0009	-0.0036	81
125	54600.4145	0.0034	-0.0019	76
137	54601.1945	0.0030	0.0084	185
138	54601.2497	0.0010	-0.0005	135

^a BJD-2400000.^b Against $max = 2454592.3989 + 0.064140E$.^c Number of points used to determine the maximum.

6.196. OT J195951.3+224232

This object (also called Var Vul 05, hereafter OT J1959) was discovered by J. Hanisch (vsnet-alert 8629; Renz et al. 2005). Subsequent observations confirmed the presence of superhumps (cvnet-outburst 543, vsnet-alert 8640). The large outburst amplitude (~ 8 mag, vsnet-alert 8654) makes the object an excellent candidate for a WZ Sge-type dwarf nova.

The object underwent another recorded outburst in 2008 April.²⁴ The recurrence time may be an order of ~ 1000 d.

We adopted a mean superhump period of 0.05990(3) d (figure 221). Although there was some hint of double-wave modulations suggesting early superhumps, the large amplitude of the modulations and the epoch of the observa-

²⁴ <<http://tech.groups.yahoo.com/group/VarVul05/message/98>>.

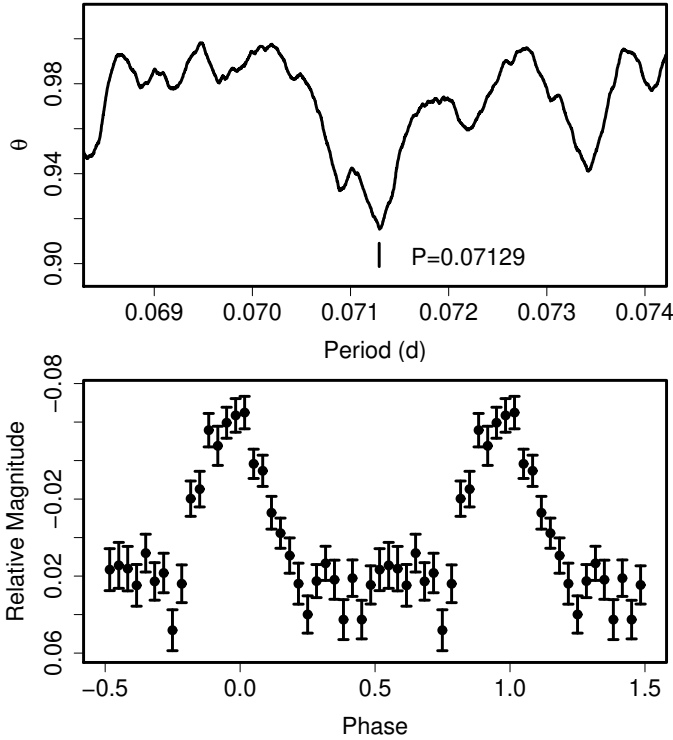


Fig. 220. Superhumps in OT J1914 (2008, plateau phase). (Upper): PDM analysis. (Lower): Phase-averaged profile.

tion (> 6 d after the outburst detection) suggest the identification of these humps as ordinary superhumps. The times of superhump maxima are listed in table 350. The resultant P_{dot} is virtually zero, $-0.7(5.2) \times 10^{-5}$.

Although this object is provisionally listed as a WZ Sge-type object based on its apparently large outburst amplitude and the long outburst duration (table 8), this object might resemble a borderline object such as BC UMa and RZ Leo. Future detection of early superhumps and accurate determination of P_{dot} are desired.

6.197. OT J213122.4–003937

This transient (hereafter OT J2131) was detected by K. Itagaki (Yamaoka et al. 2008e). Subsequent observations confirmed the SU UMa-type nature of this object (vsnet-alert 10830). Since the individual observations were not long enough, we could not uniquely select the superhump period among one-day aliases (e.g. 0.069 d, as in vsnet-alert 10830). In table 351, we list epochs based on the base period of 0.06463(3) d, a candidate superhump period. This selection of the alias needs to be verified by future observations.

6.198. OT J213701.8+071446

This transient (hereafter OT J2137) was detected by K. Itagaki (vsnet-alert 10670, 10671). The object was soon confirmed to be an SU UMa-type dwarf nova in the period gap (vsnet-alert 10674, 10677). The mean superhump period during the entire observation with the PDM method

Table 349. Superhump maxima of OT J1914.

E	\max^a	error	$O - C^b$	N^c
0	54743.0965	0.0021	-0.0093	128
1	54743.1697	0.0023	-0.0073	64
40	54745.9467	0.0013	-0.0050	152
41	54746.0178	0.0012	-0.0050	136
68	54747.9442	0.0013	0.0003	291
69	54748.0183	0.0010	0.0032	285
70	54748.0888	0.0011	0.0026	215
72	54748.2343	0.0006	0.0058	54
73	54748.3078	0.0012	0.0082	23
74	54748.3753	0.0016	0.0045	26
82	54748.9491	0.0010	0.0091	203
83	54749.0172	0.0015	0.0060	182
84	54749.0870	0.0013	0.0048	147
87	54749.3001	0.0019	0.0044	25
88	54749.3682	0.0039	0.0013	26
91	54749.5881	0.0012	0.0077	16
100	54750.2198	0.0017	-0.0008	28
101	54750.2931	0.0006	0.0013	49
105	54750.5809	0.0025	0.0045	15
111	54751.0003	0.0021	-0.0030	154
112	54751.0633	0.0065	-0.0111	31
116	54751.3613	0.0014	0.0023	25
117	54751.4338	0.0024	0.0036	25
119	54751.5767	0.0030	0.0043	16
124	54751.9109	0.0029	-0.0173	54
125	54752.0113	0.0058	0.0119	42
126	54752.0664	0.0054	-0.0041	29
138	54752.9118	0.0041	-0.0125	131
139	54752.9948	0.0031	-0.0007	302
140	54753.0569	0.0030	-0.0097	91

^a BJD–2400000.

^b Against $\max = 2454743.1058 + 0.071148E$.

^c Number of points used to determine the maximum.

Table 350. Superhump maxima of OT J1959 (2005).

E	\max^a	error	$O - C^b$	N^c
0	53606.3830	0.0012	0.0004	37
1	53606.4448	0.0017	0.0024	26
2	53606.4991	0.0023	-0.0033	33
44	53609.0202	0.0156	0.0012	42
45	53609.0786	0.0020	-0.0003	53
68	53610.4518	0.0022	-0.0052	36
69	53610.5220	0.0058	0.0051	20
93	53611.9546	0.0012	-0.0003	96

^a BJD–2400000.

^b Against $\max = 2453606.3825 + 0.059919E$.

^c Number of points used to determine the maximum.

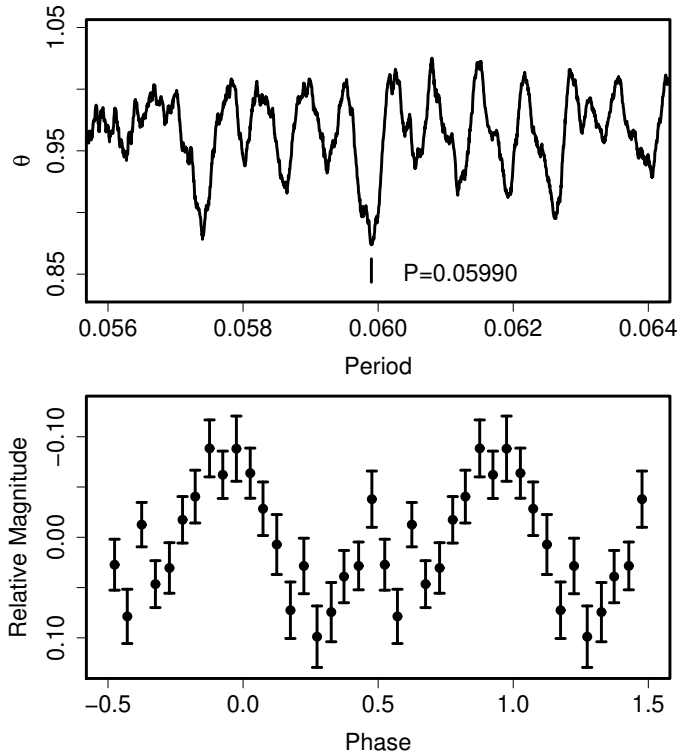


Fig. 221. Superhumps in OT J1959 (2005). (Upper): PDM analysis. (Lower): Phase-averaged profile.

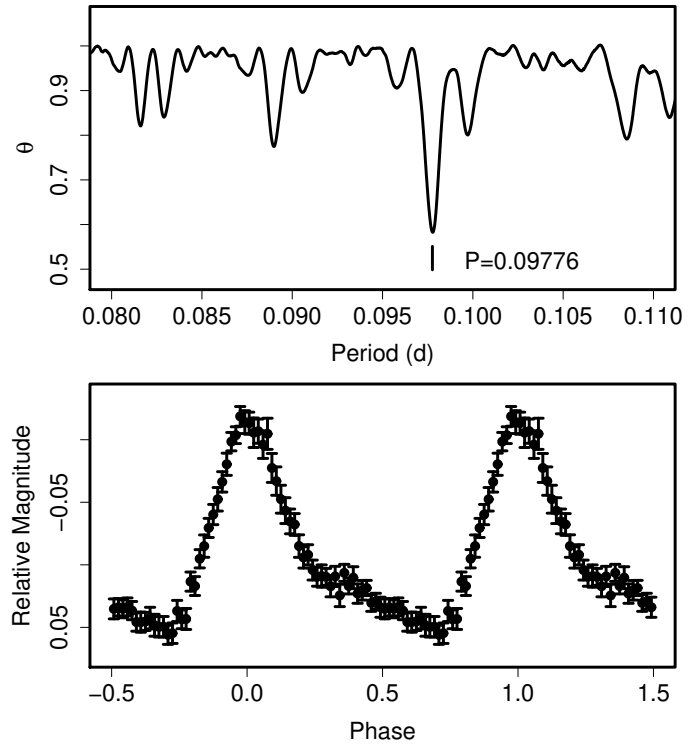


Fig. 222. Superhumps in OT J2137 (2008). (Upper): PDM analysis. (Lower): Phase-averaged profile.

Table 351. Superhump maxima of OT J2131 (2008).

E	\max^a	error	$O - C^b$	N^c
0	54819.8932	0.0028	-0.0020	179
15	54820.8670	0.0024	0.0030	84
16	54820.9282	0.0042	-0.0004	119
62	54823.8993	0.0011	-0.0006	245

^a BJD-2400000.

^b Against $\max = 2454819.8951 + 0.064593E$.

^c Number of points used to determine the maximum.

Table 352. Superhump maxima of OT J2137.

E	\max^a	error	$O - C^b$	N^c
0	54778.0721	0.0003	-0.0067	171
5	54778.5693	0.0019	0.0019	37
6	54778.6678	0.0007	0.0027	46
10	54779.0583	0.0002	0.0023	184
20	54780.0345	0.0003	0.0012	142
43	54782.2815	0.0074	0.0005	48
50	54782.9661	0.0005	0.0010	404
51	54783.0585	0.0011	-0.0043	194
53	54783.2597	0.0008	0.0014	95
60	54783.9419	0.0012	-0.0004	462
61	54784.0404	0.0009	0.0004	236

^a BJD-2400000.

^b Against $\max = 2454778.0788 + 0.097726E$.

^c Number of points used to determine the maximum.

was 0.097762(14) d (figure 222). The times of superhump maxima are listed in table 352. There was an apparent transition in the period between $E = 0$ and $E = 5$. After $E = 5$, the superhump period was almost constant ($P_{\text{SH}} = 0.09768(3)$ d, $P_{\text{dot}} = +2.3(4.7) \times 10^{-5}$). Since the object faded 6 d after this transition (vsnet-obs 62796), we probably observed the stage C superhumps, which could explain the lack of period variation. The object underwent a rebrightening (vsnet-alert 10708) 5 d after the fading. Such a rebrightening is rare in a long- P_{SH} system. The object may resemble V725 Aql in its period evolution of superhumps and in the presence of a rebrightening (Uemura et al. 2001; subsection 6.8).

Table 353. Superhump maxima of TSS J0222 (2005).

E	max ^a	error	$O - C^b$	N^c
0	53695.1319	0.0022	-0.0009	52
1	53695.1905	0.0052	0.0021	61
14	53695.9146	0.0041	0.0035	61
20	53696.2345	0.0028	-0.0103	88
37	53697.1953	0.0010	0.0054	105
38	53697.2488	0.0017	0.0033	88
74	53699.2534	0.0072	0.0064	58
88	53700.0250	0.0017	-0.0003	117
89	53700.0771	0.0014	-0.0039	110
90	53700.1366	0.0018	-0.0000	88
91	53700.1910	0.0015	-0.0011	82
92	53700.2465	0.0015	-0.0013	71
104	53700.9131	0.0038	-0.0019	66
125	53702.0762	0.0024	-0.0063	141
126	53702.1392	0.0024	0.0010	198
127	53702.1980	0.0116	0.0043	126
128	53702.2416	0.0054	-0.0077	34
159	53703.9711	0.0047	-0.0017	83
160	53704.0376	0.0052	0.0092	109
195	53705.9712	0.0075	-0.0031	81
196	53706.0327	0.0036	0.0028	57
197	53706.0861	0.0032	0.0006	59

^a BJD-2400000.^b Against $max = 2453695.1328 + 0.055598E$.^c Number of points used to determine the maximum.

6.199. TSS J022216.4+412260

The 2005 superoutburst of this WZ Sge-type dwarf nova was described in Imada et al. (2006c). We used the data used in Imada et al. (2006c) and determined times of superhump maxima during the plateau phase (table 353). The superhumps were likely growing before $E = 37$. We used the segment later than this epoch and obtained $P_{\text{dot}} = +2.2(1.5) \times 10^{-5}$.

7. Conclusion

We systematically surveyed period variations of superhumps in SU UMa-type dwarf novae based on newly obtained data and past publications. We found:

- In well-observed systems, the $O - C$ diagram of superhump maxima are usually composed of three distinct stages: early evolutionary stage with a longer superhump period (stage A), middle stage with systematically varying periods (stage B), and final stage with a shorter superhump period (stage C).
- During the stage B, the period derivative is strongly correlated to the orbital period, or, more likely, to the mass ratio of the system. Previously reported anomalously large period derivatives in EI Psc and V485 Cen were not confirmed.
- Upon transition to stage C, the superhump period generally decreases by 0.5–1.0 %.

- We generally did not find strong evidence that period derivatives vary between different superoutburst of the same object. No apparent correlation with the presence of a precursor outburst was recorded.
- The superhump period at the start of stage B is close to that in the stage C. The fractional superhump excesses of these periods are strongly correlated to the orbital period, or the mass ratio. This period is slightly shorter than that expected for the precession rate of single-particle dynamical 3:1 resonance.
- In systems with positive period derivatives, the maximum period at the end of stage B has a limit correlated to the mass ratio. We interpret that the lengthening of the period is a result of outward propagation of the eccentricity wave and this upper limit of the period corresponds to the radius near the tidal truncation.
- We interpreted that stage C superhumps are rejuvenated excitation of 3:1 resonance when the superhumps in the outer disk is effectively quenched.
- Traditional phase reversal in “late superhumps” was not recorded in many systems. We suggested that some of these observations misinterpreted stage C superhumps.
- In some systems, particularly WZ Sge-type dwarf novae and analogous systems, long-enduring superhump signals were recorded during the post-superoutburst stage. The $O - C$ analysis suggests that these superhumps evolved from superhumps in the stages B or C. The periods of these persisting superhumps are usually longer than the periods of superhumps during the main superoutburst by 0.2–0.5 %.
- The period variation in systems with long superhump periods vary from system to system. Some systems show a very large decrease in the superhump period. While some systems show a stepwise decrease as in short-period systems, some systems show a more continuous change.
- Some long-period systems apparently lack period variations, and there is even a hint of positive period derivatives in systems with very infrequent outbursts. The superoutbursts in these systems resemble those of short-period systems in the frequent presence of a rebrightening.
- The positive period derivatives appears to be confirmed in ER UMa-type dwarf novae. In ER UMa itself, the stage C superhumps seem to appear earlier than in other SU UMa-type dwarf nova accompanied by a phase ~ 0.5 offset.
- In WZ Sge-type dwarf novae, period derivatives are an excellent function of the fractional superhump excess or the mass-ratio.
- In WZ Sge-type dwarf novae, the type of rebrightening is correlated with the period variation. Superoutbursts with multiple rebrightenings or with a long-lasting rebrightening tend to have smaller period derivatives while superoutbursts with a single rebrightening tend to have larger period derivatives.

- The superhumps of at least one outburst of a black-hole X-ray binary (KV UMa) exhibited the same evolutionary sequence as in SU UMa-type dwarf novae, although the degree of period variation was an order of magnitude smaller.
- We refined the empirical relations between the fractional superhump excess and the mass ratio, and the fractional superhump excess and the superhump period.

The present survey has clarified the relation between general behavior of period variation of superhumps and the system mass ratio (or the superhump period). Although this would seem to indicate that SU UMa-type dwarf novae are “single parameter systems” regarding the period variation of superhumps, the difference in behavior between different objects with nearly equal superhump periods or mass ratios is much larger than the variation within the same system. This suggests the presence of a mechanism causing diversity in different systems; questions whether this diversity is related to outburst characteristics, or to the condition of the accretion disk, need to be answered by future investigations. There have also been indications of unusual development of superhumps in several systems, making future observations of superhumps in even well-observed objects still attractive. The early emergence of the stage C superhumps in ER UMa-type dwarf novae and some other systems, and the superhumps in WZ Sge-type dwarf novae, particularly the late-stage humps and transient enhancement of orbital humps, are still poorly understood. The study presents an alternative idea to the traditional picture of decreasing superhump period due to the shrinkage of the accretion disk from the radius of the 3:1 resonance, which anticipates novel theoretical progress in understanding the superhump phenomenon.

This work was supported by the Grant-in-Aid for the Global COE Program “The Next Generation of Physics, Spun from Universality and Emergence” from the Ministry of Education, Culture, Sports, Science and Technology (MEXT) of Japan. This work was partly supported by a Grant-in-Aid from the Ministry of Education, Culture, Sports, Science and Technology of Japan (19740104). Part of this work is supported by a Research Fellowship of the Japan Society for the Promotion of Science for Young Scientists (AI). The authors are grateful to observers of VSNET Collaboration and VSOLJ observers who supplied vital data. We also benefited from the data by Martin Nicholson, Achim Sucker, Paulo Cacella, T. Kryachko and his colleagues, Doug West, Oksana I. Dudka, and Masayuki Moriyama. We acknowledge with thanks the variable star observations from the AAVSO International Database contributed by observers worldwide and used in this research. This work is deeply indebted to outburst detections and announcement by a number of variable star observers worldwide, including participants of CVNET, BAA VSS alert and AVSON networks. We are grateful to Allen W. Shafter for providing observations of OT

J0329, and Artur Rutkowski for providing the times of superhump maxima for DI UMa. The CCD operation of the Bronberg Observatory is partly sponsored by the Center for Backyard Astrophysics. The CCD operation by Peter Nelson is on loan from the AAVSO, funded by the Curry Foundation. P. Schmeer’s observations were made with the Iowa Robotic Observatory, and he wishes to thank Robert Mutel and his students. We are grateful to the Catalina Real-time Transient Survey team for making their real-time detection of transient objects available to the public, and providing times of eclipses for SDSS J1524.

References

- Alksnis, A., & Zacs, L. 1981, *IBVS*, 1972
 Antipin, S. V. 1998, *IBVS*, 4578
 Antipin, S. V. 1999, *IBVS*, 4673
 Antipin, S. V., & Pavlenko, E. P. 2002, *A&A*, 391, 565
 Antipin, S. V., Samus, N. N., & Kroll, P. 2004, *IBVS*, 5544
 Araujo-Betancor, S., et al. 2005, *A&A*, 430, 629
 Argyle, R. W. 1983, *IAU Circ.*, 3878
 Aungwerojwit, A., et al. 2006, *A&A*, 455, 659
 Baade, W. 1928, *Astron. Nachr.*, 232, 65
 Baba, H., Kato, T., Nogami, D., Hirata, R., Matsumoto, K., & Sadakane, K. 2000, *PASJ*, 52, 429
 Bailey, J. 1979, *MNRAS*, 189, 41P
 Baily, C. D. 1992, *ApJ*, 391, 298
 Balayan, S. K. 1997, *Astrophysics*, 40, 211
 Baptista, R., Borges, B. W., Bond, H. E., Jablonski, F., Steiner, J. E., & Grauer, A. D. 2003, *MNRAS*, 345, 889
 Barwig, H., Kudritzki, R. P., Vogt, N., & Hunger, K. 1982, *A&A*, 114, L11
 Berg, C., Wegner, G., Foltz, C. B., Chaffee, Jr., F. H., & Hewett, P. C. 1992, *ApJS*, 78, 409
 Bernhard, K., Lloyd, C., Berthold, T., Kriebel, W., & Renz, W. 2005, *IBVS*, 5620
 Bohusz, E., & Udalski, A. 1979, *IBVS*, 1583
 Borges, B. W., & Baptista, R. 2005, *A&A*, 437, 235
 Boyd, D., Graham, K., Kato, T., Koff, R., Miller, I., Oksanen, A., Pickard, R., & Poyner, G. 2009, *J. British Astron. Assoc.*, in press (arXiv astro-ph/0905.0809)
 Boyd, D., Kracji, T., Shears, J., & Poyner, G. 2007, *J. British Astron. Assoc.*, 117, 198
 Boyd, D., et al. 2008a, *J. British Astron. Assoc.*, 118, 149
 Boyd, D., Oksanen, A., & Henden, A. 2006, *J. British Astron. Assoc.*, 116, 187
 Boyd, D., Shears, J., & Koff, R. 2008b, *J. British Astron. Assoc.*, 118, 199
 Busch, H., Häussler, K., & Splittgerber, E. 1979, *Veröff. Sternw. Sonneberg*, 9, 125
 Christensen, E. J. 2006, *CBET*, 746
 Djorgovski, S. G., et al. 2008a, *Astronomer’s Telegram*, 1416
 Djorgovski, S. G., et al. 2008b, *Astronomer’s Telegram*, 1411
 Downes, R. A. 1990, *AJ*, 99, 339
 Downes, R. A., Webbink, R. F., Shara, M. M., Ritter, H., Kolb, U., & Duerbeck, H. W. 2001, *PASP*, 113, 764
 Drake, A. J., et al. 2009, *ApJ*, 696, 870
 Drake, A. J., Mahabal, A., Djorgovski, S. G., Graham, M. J., Williams, R., Beshore, E. C., Larson, S. M., & Christensen, E. 2008a, *Astronomer’s Telegram*, 1479
 Drake, A. J., et al. 2008b, *Astronomer’s Telegram*, 1734
 Duerbeck, H. W. 1987, *Space Sci. Rev.*, 45, 1

- Duerbeck, H. W., Schmeer, P., Knapen, J. H., & Pollacco, D. 1999, *IBVS*, 4759
- Duszanowicz, G. 2008, *CBET*, 1574
- Erastova, L. K. 1973, *Astron. Tsirk.*, 774, 5
- Gao, W., Li, Z., Wu, X., Zhang, Z., & Li, Y. 1999, *ApJL*, 527, L55
- Gefner, H. 1974, *Mitteil. Veränderl. Sterne*, 6, 169
- Golovin, A., et al. 2007, *IBVS*, 5763
- Golovin, A., et al. 2005, *IBVS*, 5611
- Goranskij, V. P. 1972, *Astron. Tsirk.*, 696
- Green, R. F., Ferguson, D. H., Liebert, J., & Schmidt, M. 1982, *PASP*, 94, 560
- Grindlay, J., Cohn, H., Lugger, P., & Hertz, P. 1987, *IAU Circ.*, 4408
- Haefner, R. 1995, *IBVS*, 4178
- Haefner, R. 2004, *IBVS*, 5550
- Haefner, R., Schoembs, R., & Vogt, N. 1979, *A&A*, 77, 7
- Harlaftis, E., Collier, S., Horne, K., & Filippenko, A. V. 1999, *A&A*, 341, 491
- Harrison, T. E. 1991, *IAU Circ.*, 5233
- Harvey, D., Skillman, D. R., Patterson, J., & Ringwald, F. A. 1995, *PASP*, 107, 551
- Harvey, D. A., & Patterson, J. 1995, *PASP*, 107, 1055
- Haswell, C. A., King, A. R., Murray, J. R., & Charles, P. A. 2001, *MNRAS*, 321, 475
- Hawkins, M. R. S. 1983, *Nature*, 301, 688
- Hazen, M. L. 1993, *IBVS*, 3888
- Hazen, M. L., & Garnavich, P. M. 1999, *J. American Assoc. Variable Star Obs.*, 27, 19
- Heiser, A. M., & Henry, G. W. 1979, *IBVS*, 1559
- Hellier, C. 2001, *PASP*, 113, 469
- Henden, A. A., & Honeycutt, R. K. 1997, *PASP*, 109, 441
- Henden, A. A., Thorstensen, J. R., & Sumner, B. 2001, *IBVS*, 5141
- Hertz, P., Bailyn, C. D., Grindlay, J. E., Garcia, M. R., Cohn, H., & Lugger, P. M. 1990, *ApJ*, 364, 251
- Hessman, F. V., Mantel, K.-H., Barwig, H., & Schoembs, R. 1992, *A&A*, 263, 147
- Hirose, M., & Osaki, Y. 1990, *PASJ*, 42, 135
- Hirose, M., & Osaki, Y. 1993, *PASJ*, 45, 595
- Hoffmeister, C. 1966, *Astron. Nachr.*, 289, 139
- Hoffmeister, C. 1967a, *Astron. Nachr.*, 290, 43
- Hoffmeister, C. 1967b, *Astron. Nachr.*, 289, 205
- Honda, S., Kinugasa, K., & Yamaoka, H. 2008, *CBET*, 1229
- Howell, S. B., DeYoung, J. A., Mattei, J. A., Foster, G., Szkody, P., Cannizzo, J. K., Walker, G., & Fierce, E. 1996, *AJ*, 111, 2367
- Howell, S. B., & Kreidl, T. J. 1991, *IAU Circ.*, 5235
- Howell, S. B., Liebert, J., & Wagner, R. M. 1994, *IBVS*, 4074
- Howell, S. B., Mason, E., Huber, M., & Clowes, R. 2002, *A&A*, 395, L47
- Howell, S. B., Schmidt, R., DeYoung, J. A., Fried, R., Schmeer, P., & Gritz, L. 1993, *PASP*, 105, 579
- Hu, J.-Y., Qiu, Y.-L., Li, W.-D., Wei, J.-Y., & Esamdin, A. 1997, *IAU Circ.*, 6731
- Hurst, G. M., Isles, J., & McNaught, R. H. 1987, *IAU Circ.*, 4413
- Huth, H. 1962, *IBVS*, 16
- Iida, M., Kato, T., Nogami, D., & Baba, H. 1995a, *IBVS*, 4279
- Iida, M., Nogami, D., & Kato, T. 1995b, *IBVS*, 4208
- Imada, A., et al. 2009a, *PASJ*, in press
- Imada, A., et al. 2006a, *PASJ*, 58, 143
- Imada, A., Kato, T., Monard, L. A. G., Retter, A., Liu, A., & Nogami, D. 2006b, *PASJ*, 58, 383
- Imada, A., Kato, T., Monard, L. A. G. B., Stubbings, R., Uemura, M., Ishioka, R., & Nogami, D. 2008a, *PASJ*, 60, 267
- Imada, A., et al. 2005, *PASJ*, 57, 193
- Imada, A., Kubota, K., Kato, T., Nogami, D., Maehara, H., Nakajima, K., Uemura, M., & Ishioka, R. 2006c, *PASJ*, 58, L23
- Imada, A., & Monard, L. A. G. B. 2006, *PASJ*, 58, L19
- Imada, A., et al. 2008b, *PASJ*, 60, 1151
- Imada, A., et al. 2009b, *PASJ*, in press (arXiv astro-ph/0902.1013)
- Ishioka, R., et al. 2001, *PASJ*, 53, 905
- Ishioka, R., et al. 2003, *PASJ*, 55, 683
- Ishioka, R., et al. 2002, *A&A*, 381, L41
- Jablonski, F. J., & Steiner, J. E. 1987, *ApJ*, 313, 376
- Jiang, X. J., Engels, D., Wei, J. Y., Tesch, F., & Hu, J. Y. 2000, *A&A*, 362, 263
- Jurcevic, J. S., Honeycutt, R. K., Schlegel, E. M., & Webbink, R. F. 1994, *PASP*, 106, 481
- Kapusta, A. B., & Thorstensen, J. R. 2006, *PASP*, 118, 1119
- Kasliwal, M. M., Quimby, R., & Kulkarni, S. R. 2008, *CBET*, 1611
- Kato, T. 1991a, *IBVS*, 3671
- Kato, T. 1991b, *IAU Circ.*, 5379
- Kato, T. 1993, *PASJ*, 45, L67
- Kato, T. 1994, *IBVS*, 4136
- Kato, T. 1995a, *IBVS*, 4239
- Kato, T. 1995b, *IBVS*, 4242
- Kato, T. 1995c, *IBVS*, 4152
- Kato, T. 1996a, *IBVS*, 4369
- Kato, T. 1996b, *PASJ*, 48, 777
- Kato, T. 1997, *PASJ*, 49, 583
- Kato, T. 2001a, *IBVS*, 5122
- Kato, T. 2001b, *IBVS*, 5107
- Kato, T. 2002a, *PASJ*, 54, L11
- Kato, T. 2002b, *PASJ*, 54, 87
- Kato, T. 2004, *PASJ*, 56, S135
- Kato, T., Bolt, G., Nelson, P., Monard, B., Stubbings, R., Pearce, A., Yamaoka, H., & Richards, T. 2003a, *MNRAS*, 341, 901
- Kato, T., et al. 2002a, *A&A*, 396, 929
- Kato, T., Garradd, G., Stubbings, R., Pearce, A., & Nelson, P. 2001a, *IBVS*, 5117
- Kato, T., Hirata, R., & Mineshige, S. 1992, *PASJ*, 44, L215
- Kato, T., Ishioka, R., & Uemura, M. 2002b, *PASJ*, 54, 1029
- Kato, T., Kiyota, S., Novák, R., & Matsumoto, K. 1999a, *IBVS*, 4794
- Kato, T., & Kunjaya, C. 1995, *PASJ*, 47, 163
- Kato, T., Kunjaya, C., Okyudo, M., & Takahashi, A. 1994, *PASJ*, 46, L199
- Kato, T., Maehara, H., & Monard, B. 2008, *PASJ*, 60, L23
- Kato, T., & Matsumoto, K. 1999a, *IBVS*, 4776
- Kato, T., & Matsumoto, K. 1999b, *IBVS*, 4765
- Kato, T., & Matsumoto, K. 1999c, *IBVS*, 4763
- Kato, T., Matsumoto, K., Nogami, D., Morikawa, K., & Kiyota, S. 2001b, *PASJ*, 53, 893
- Kato, T., Matsumoto, K., & Stubbings, R. 1999b, *IBVS*, 4760
- Kato, T., Mineshige, S., & Hirata, R. 1995, *PASJ*, 47, 31
- Kato, T., et al. 2004a, *MNRAS*, 347, 861
- Kato, T., & Nogami, D. 1995, *IBVS*, 4260
- Kato, T., & Nogami, D. 1997a, *PASJ*, 49, 481
- Kato, T., & Nogami, D. 1997b, *PASJ*, 49, 341

- Kato, T., Nogami, D., Baba, H., & Matsumoto, K. 1998a, in ASP Conf. Ser. 137, *Wild Stars in the Old West*, ed. S. Howell, E. Kuulkers, & C. Woodward (San Francisco: ASP), 9
- Kato, T., Nogami, D., Baba, H., Matsumoto, K., Arimoto, J., Tanabe, K., & Ishikawa, K. 1996a, PASJ, 48, L21
- Kato, T., Nogami, D., Lockley, J. J., & Somers, M. 2001c, IBVS, 5116
- Kato, T., Nogami, D., & Masuda, S. 1996b, PASJ, 48, L5
- Kato, T., Nogami, D., & Masuda, S. 2003b, PASJ, 55, L7
- Kato, T., Nogami, D., Masuda, S., & Baba, H. 1998b, PASP, 110, 1400
- Kato, T., Nogami, D., Masuda, S., & Hirata, R. 1996c, PASJ, 48, 45
- Kato, T., Nogami, D., Matsumoto, K., & Baba, H. 2004b, PASJ, 56, S109
- Kato, T., Nogami, D., Moilanen, M., & Yamaoka, H. 2003c, PASJ, 55, 989
- Kato, T., et al. 2009, PASJ, in press (arXiv astro-ph/0903.1685)
- Kato, T., et al. 2003d, MNRAS, 339, 861
- Kato, T., & Schmeer, P. 1999, IBVS, 4757
- Kato, T., Sekine, Y., & Hirata, R. 2001d, PASJ, 53, 1191
- Kato, T., et al. 2002c, A&A, 395, 541
- Kato, T., & Uemura, M. 1999, IBVS, 4787
- Kato, T., & Uemura, M. 2000, IBVS, 4902
- Kato, T., & Uemura, M. 2001a, IBVS, 5158
- Kato, T., & Uemura, M. 2001b, IBVS, 5078
- Kato, T., Uemura, M., Ishioka, R., Matsumoto, K., & Tanabe, K. 2002d, IBVS, 5284
- Kato, T., Uemura, M., Ishioka, R., Nogami, D., Kunjaya, C., Baba, H., & Yamaoka, H. 2004c, PASJ, 56, S1
- Kato, T., Uemura, M., Ishioka, R., & Pietz, J. 2002e, PASJ, 54, 1017
- Kato, T., Uemura, M., Matsumoto, K., Kinnunen, T., Garradd, G., Masi, G., & Yamaoka, H. 2002f, PASJ, 54, 999
- Kato, T., et al. 2000, IAU Circ., 7343
- Kawabata, T., Kawabata, Y., Ayani, K., & Yamaoka, H. 2005, CBET, 120, 2
- Kazarovets, E. V., Samus, N. N., Durlevich, O. V., Kireeva, N. N., & Pastukhova, E. N. 2006, IBVS, 5721
- Kholopov, P. N. 1972, *Astron. Tsirk.*, 700
- Kholopov, P. N., et al. 1985, *General Catalogue of Variable Stars*, fourth edition (Moscow: Nauka Publishing House)
- Khruslov, A. V. 2005, *Perem. Zvezdy Pril.*, 5, 4
- Kiyota, S., & Kato, T. 1998, IBVS, 4644
- Kloehr, W., Torii, K., Maehara, H., Trontal, O., & Boyd, D. 2006, CBET, 777
- Kolotovkina, S. A. 1979, *Perem. Zvezdy Pril.*, 3, 665
- Kowal, C., Huchra, J., & Sargent, W. L. W. 1976, PASP, 88, 521
- Krajci, T. 2006, IBVS, 5690
- Kryachko, T. V. 2001, IBVS, 5058
- Krzeminski, W., & Vogt, N. 1985, A&A, 144, 124
- Kukarkin, B. V., et al. 1982, *New Catalogue of Suspected Variable Stars* (Moscow: Nauka Publishing House)
- Kunjaya, C., Kinugasa, K., Ishioka, R., Kato, T., Iwamatsu, H., & Uemura, M. 2001, IBVS, 5128
- Kurochkin, N. E. 1977, *Astron. Tsirk.*, 974, 4
- Kurochkin, N. E. 1984, *Astron. Tsirk.*, 1325, 5
- Kuulkers, E., Howell, S. B., & van Paradijs, J. 1996, ApJL, 462, L87
- Kwast, T., & Semeniuk, I. 1998, IBVS, 4654
- Lemm, K., Patterson, J., Thomas, G., & Skillman, D. R. 1993, PASP, 105, 1120
- Liller, M. H. 1983, IBVS, 2293
- Liller, W. 1996, IBVS, 4299
- Littlefair, S. P., Dhillon, V. S., Marsh, T. R., & Gänsicke, B. T. 2006, MNRAS, 371, 1435
- Littlefair, S. P., Dhillon, V. S., Marsh, T. R., Gänsicke, B. T., Southworth, J., Baraffe, I., Watson, C. A., & Copperwheat, C. 2008, MNRAS, 388, 1582
- Liu, Wu., Hu, J. Y., Li, Z. Y., & Cao, L. 1999, ApJS, 122, 257
- Lloyd, C. 2007, *Open European J. on Var. Stars*, 69, 1
- Lloyd, C., & Pickard, R. D. 2008, *Open European J. on Var. Stars*, 85, 1
- Loser, A. R. 1979, IBVS, 1661
- Lubbock, S., & McNaught, R. H. 1986, IAU Circ., 4209
- Lubow, S. H. 1991, ApJ, 381, 259
- McAdam, D., Huruhata, M., Bortle, J., Fujino, S., McNaught, R., Argyle, R. W., & Jones, D. H. P. 1983, IAU Circ., 3896
- Maehara, H., Hachisu, I., & Nakajima, K. 2007, PASJ, 59, 227
- Mahabal, A., et al. 2008, *Astronomer's Telegram*, 1520
- Mason, E., & Howell, S. B. 2005, A&A, 439, 301
- Mattei, J. A., et al. 1999, IAU Circ., 7340
- Maza, J., & Gonzalez, L. E. 1983, IAU Circ., 3856
- Maza, J., Gonzalez, L. E., Wischnjewsky, M., & Barrientos, F. 1992, PASP, 104, 1060
- McNaught, R. H. 1982, IBVS, 2232
- Meinunger, L. 1986, *Mitteil. Veränderl. Sterne*, 11, 1
- Mennickent, R. E., & Diaz, M. 1996, A&A, 309, 147
- Mennickent, R. E., Nogami, D., Kato, T., & Worraker, W. 1996, A&A, 315, 493
- Mennickent, R. E., Patterson, J., O'Donoghue, D., Unda, E., Harvey, D., Vanmuster, T., & Bolt, G. 1998, Ap&SS, 262, 1
- Misselt, K. A., & Shafter, A. W. 1995, AJ, 109, 1757
- Molnar, L. A., & Kobulnicky, H. A. 1992, ApJ, 392, 678
- Montgomery, M. M. 2001, MNRAS, 325, 761
- Motch, C., et al. 1998, A&AS, 132, 341
- Motch, C., Haberl, F., Guillout, P., Pakull, M., Reinsch, K., & Krautter, J. 1996, A&A, 307, 459
- Murray, J. R. 1998, MNRAS, 297, 323
- Murray, J. R. 2000, MNRAS, 314, 1P
- Nakano, S., Itagaki, K., & Kadota, K. 2008, CBET, 1588
- Nakano, S., et al. 2004, IAU Circ., 8363
- Nogami, D., Baba, H., Kato, T., & Novák, R. 1998a, PASJ, 50, 297
- Nogami, D., Baba, H., Matsumoto, K., & Kato, T. 2003a, PASJ, 55, 483
- Nogami, D., Buczynski, D., Baba, H., & Kato, T. 2001a, IBVS, 5157
- Nogami, D., Engels, D., Gänsicke, B. T., Pavlenko, E. P., Novák, R., & Reinsch, K. 2000, A&A, 364, 701
- Nogami, D., & Kato, T. 1995, IBVS, 4227
- Nogami, D., & Kato, T. 1997, PASJ, 49, 109
- Nogami, D., Kato, T., Baba, H., & Masuda, S. 1998b, PASJ, 50, L1
- Nogami, D., Kato, T., Baba, H., Matsumoto, K., Arimoto, J., Tanabe, K., & Ishikawa, K. 1997a, ApJ, 490, 840
- Nogami, D., Kato, T., Baba, H., Novák, R., Lockley, J. J., & Somers, M. 2001b, MNRAS, 322, 79
- Nogami, D., Kato, T., & Hirata, R. 1996, PASJ, 48, 607
- Nogami, D., Kato, T., & Masuda, S. 1998c, PASJ, 50, 411
- Nogami, D., Kato, T., Masuda, S., & Hirata, R. 1995a, IBVS, 4155

- Nogami, D., Kato, T., Masuda, S., & Hirata, R. 1995b, *IBVS*, 4163
- Nogami, D., Kato, T., Masuda, S., Hirata, R., Matsumoto, K., Tanabe, K., & Yokoo, T. 1995c, *PASJ*, 47, 897
- Nogami, D., & Masuda, S. 1997, *IBVS*, 4532
- Nogami, D., Masuda, S., & Kato, T. 1997b, *PASP*, 109, 1114
- Nogami, D., et al. 2004a, *PASJ*, 56, S99
- Nogami, D., Uemura, M., Ishioka, R., Kato, T., & Pietz, J. 2004b, *PASJ*, 56, S155
- Nogami, D., et al. 2003b, *A&A*, 404, 1067
- Novák, R., Vanmunster, T., Jensen, L. T., & Nogami, D. 2001, *IBVS*, 5108
- O'Donoghue, D., & Charles, P. A. 1996, *MNRAS*, 282, 191
- O'Donoghue, D., Chen, A., Marang, F., Mittaz, J. P. D., Winkler, H., & Warner, B. 1991, *MNRAS*, 250, 363
- Ohshima, T., et al. 2009, *PASJ*, in preparation
- Oizumi, S., et al. 2007, *PASJ*, 59, 643
- Olech, A. 1997, *Acta Astron.*, 47, 281
- Olech, A. 2003, *Acta Astron.*, 53, 85
- Olech, A., Cook, L. M., Złoczewski, K., Mularczyk, K., Kędzierski, P., Udalski, A., & Wisniewski, M. 2004a, *Acta Astron.*, 54, 233
- Olech, A., Mularczyk, K., Kędzierski, P., Złoczewski, K., Wiśniewski, M., & Szaruga, K. 2006, *A&A*, 452, 933
- Olech, A., Rutkowski, A., & Schwarzenberg-Czerny, A. 2007, *Acta Astron.*, 57, 331
- Olech, A., Schwarzenberg-Czerny, A., Kędzierski, P., Złoczewski, K., Mularczyk, K., & Wiśniewski, M. 2003, *Acta Astron.*, 53, 175
- Olech, A., Wisniewski, M., Złoczewski, K., Cook, L. M., Mularczyk, K., & Kędzierski, P. 2008, *Acta Astron.*, 58, 131
- Olech, A., Złoczewski, K., Cook, L. M., Mularczyk, K., Kędzierski, P., & Wisniewski, M. 2005, *Acta Astron.*, 55, 237
- Olech, A., Złoczewski, K., Mularczyk, K., Kędzierski, P., Wisniewski, M., & Stachowski, G. 2004b, *Acta Astron.*, 54, 57
- Osaki, Y. 1985, *A&A*, 144, 369
- Osaki, Y. 1989, *PASJ*, 41, 1005
- Osaki, Y. 1995a, *PASJ*, 47, L11
- Osaki, Y. 1995b, *PASJ*, 47, L25
- Osaki, Y. 1996, *PASP*, 108, 39
- Osaki, Y., & Meyer, F. 2002, *A&A*, 383, 574
- Osaki, Y., & Meyer, F. 2003, *A&A*, 401, 325
- Parimucha, S., & Dubovsky, P. 2006, *Open European J. on Var. Stars*, 52
- Pastukhova, E. N., & Samus, N. N. 2003, *IBVS*, 5448
- Patterson, J. 1979, *AJ*, 84, 804
- Patterson, J., Augusteijn, T., Harvey, D. A., Skillman, D. R., Abbott, T. M. C., & Thorstensen, J. 1996, *PASP*, 108, 748
- Patterson, J., Bond, H. E., Grauer, A. D., Shafter, A. W., & Mattei, J. A. 1993, *PASP*, 105, 69
- Patterson, J., Jablonski, F., Koen, C., O'Donoghue, D., & Skillman, D. R. 1995, *PASP*, 107, 1183
- Patterson, J., et al. 2005, *PASP*, 117, 1204
- Patterson, J., Kemp, J., Jensen, L., Vanmunster, T., Skillman, D. R., Martin, B., Fried, R., & Thorstensen, J. R. 2000a, *PASP*, 112, 1567
- Patterson, J., et al. 1998, *PASP*, 110, 1290
- Patterson, J., McGraw, J. T., Coleman, L., & Africano, J. L. 1981, *ApJ*, 248, 1067
- Patterson, J., et al. 2002, *PASP*, 114, 721
- Patterson, J., et al. 2003, *PASP*, 115, 1308
- Patterson, J., et al. 2000b, *PASP*, 112, 1584
- Pavlenko, E. P., Cook, L., Irsamambetova, T. R., A., Baklanov, & Dudka, O. 2002, in *ASP Conf. Ser.* 261, *The Physics of Cataclysmic Variables and Related Objects*, ed. B. T. Gänsicke, K. Beuermann, & K. Reinsch (San Francisco: ASP), 523
- Pavlov, M. V., & Shugarov, S. Yu. 1985, *Astron. Tsirk.*, 1373, 8
- Pearson, K. J. 2006, *MNRAS*, 371, 235
- Pinto, G., & Romano, G. 1972, *Mem. Soc. Astron. Ita.*, 43, 135
- Pojmanski, G. 2002, *Acta Astron.*, 52, 397
- Pojmanski, G., Yamaoka, H., Haseda, H., & Itagaki, K. 2005, *IAU Circ.*, 8495
- Price, A., et al. 2004a, *PASP*, 116, 1117
- Price, A., et al. 2004b, *IAU Circ.*, 8410
- Pych, W., & Olech, A. 1995, *Acta Astron.*, 45, 385
- Qiu, Y.-L., Qiao, Q.-Y., Hu, J.-Y., & Esamdin, A. 1997a, *IAU Circ.*, 6746
- Qiu, Y.-L., Qiao, Q. Y., Hu, J.-Y., & Esamdin, A. 1997b, *IAU Circ.*, 6772
- Quimby, R., et al. 2005, *Astronomer's Telegram*, 658
- Rajkov, A. A., & Yushchenko, A. V. 1987, *Astron. Tsirk.*, 1512, 6
- Reinmuth, K. 1930, *Astron. Nachr.*, 238, 333
- Renz, W., et al. 2005, *IAU Circ.*, 8591, 2
- Richter, G. A. 1983a, *IBVS*, 2332
- Richter, G. A. 1983b, *IBVS*, 2267
- Richter, G. A. 1986, *IBVS*, 2971
- Ringwald, F. A., & Thorstensen, J. R. 1990, *BAAS*, 22, 1291
- Ritter, H. 1984, *A&AS*, 57, 385
- Ritter, H., & Kolb, U. 2003, *A&A*, 404, 301
- Robertson, J. W., Honeycutt, R. K., & Turner, G. W. 1995, *PASP*, 107, 443
- Romano, G. 1964, *Mem. Soc. Astron. Ita.*, 35, 101
- Romano, G. 1969, *Mem. Soc. Astron. Ita.*, 40, 375
- Romano, G., & Minello, S. 1976, *IBVS*, 1140
- Rutkowski, A., Olech, A., Mularczyk, K., Boyd, D., Koff, R., & Wisniewski, M. 2007, *Acta Astron.*, 57, 267
- Rutkowski, A., Olech, A., Wiśniewski, M., Pietrukowicz, P., Pala, J., & Poleski, R. 2008, *A&A*, in press (arXiv astro-ph/0812.4043)
- Schmeer, P., & Duerbeck, H. W. 1999, *IBVS*, 4758
- Schmidtobreick, L., Galli, L., Whiting, A., & Tappert, C. 2004, *IBVS*, 5508
- Schmidtobreick, L., & Tappert, C. 2006, *A&A*, 455, 255
- Schmidtobreick, L., Tappert, C., Carver, A. J., Baes, M., & Vidal Perez, E. 2005, *IBVS*, 5604
- Semeniuk, I. 1980, *A&AS*, 39, 29
- Semeniuk, I., Nalezyty, M., Gembara, P., & Kwast, T. 1997a, *Acta Astron.*, 47, 299
- Semeniuk, I., Olech, A., Kwast, T., & Nalezyty, M. 1997b, *Acta Astron.*, 47, 201
- Shafter, A. W., et al. 2009, *American Astron. Soc. Meeting Abstracts*, 213, 491.08
- Shafter, A. W., Coelho, E. A., & Reed, J. K. 2007, *PASP*, 119, 388
- Shears, J., & Boyd, D. 2007, *J. British Astron. Assoc.*, 117, 25
- Shears, J., et al. 2009a, *J. British Astron. Assoc.*, in press (arXiv astro-ph/0905.1866)
- Shears, J., Boyd, D., Krajci, T., Koff, R., Thorstensen, J. R., & Poyner, G. 2008a, *J. British Astron. Assoc.*, 118, 95
- Shears, J., Boyd, D., & Poyner, G. 2006, *J. British Astron. Assoc.*, 116, 244

- Shears, J., et al. 2009b, *J. British Astron. Assoc.*, in press (arXiv astro-ph/0905.0061)
- Shears, J., Brady, S., Foote, J., Starkey, D., & Vanmunster, T. 2008b, *J. British Astron. Assoc.*, 118, 288
- Shears, J., Brady, S., Gaensicke, B., Krajci, T., Miller, I., Ogmen, Y., Pietz, J., & Staels, B. 2008c, *J. British Astron. Assoc.*, in press (arXiv astro-ph/0812.1295)
- Shears, J., Lloyd, C., Boyd, D., Brady, S., Miller, I., & Pickard, R. 2008d, *J. British Astron. Assoc.*, in press (arXiv astro-ph/0805.1591)
- Shears, J., Pickard, R., Krajci, T., & Poyner, G. 2008e, *J. British Astron. Assoc.*, 118, 145
- Sheets, H. A., Thorstensen, J. R., Peters, C. J., Kapusta, A. B., & Taylor, C. J. 2007, *PASP*, 119, 494
- Shugarov, S. Y., Volkov, I. M., & Chochol, D. 2008, *IBVS*, 5862
- Skiff, B. A. 1997, *IBVS*, 4459
- Skiff, B. A. 1999, *IBVS*, 4675
- Skillman, D. R., et al. 2002, *PASP*, 114, 630
- Skvarc, J., & Palcic, R. 2006, *CBET*, 701, 1
- Smith, A. J., Haswell, C. A., Murray, J. R., Truss, M. R., & Foulkes, S. B. 2007, *MNRAS*, 378, 785
- Soejima, Y., Imada, A., Nogami, D., Kato, T., & Monard, L. A. G. 2009, *PASJ*, 61, 395
- Soejima, Y., et al. 2009, *PASJ*, in press (arXiv astro-ph/0905.0348)
- Stellingwerf, R. F. 1978, *ApJ*, 224, 953
- Stepanian, J. A. 1982, *Perem. Zvezdy*, 21, 691
- Sterken, C., Vogt, N., Schreiber, M. R., Uemura, M., & Tuvikene, T. 2007, *A&A*, 463, 1053
- Stolz, B., & Schoembs, R. 1984, *A&A*, 132, 187
- Strohmeier, W. 1962, *IBVS*, 15
- Szkody, P., et al. 2002, *AJ*, 123, 430
- Szkody, P., et al. 2009, *AJ*, 137, 4011
- Szkody, P., & Feinswog, L. 1988, *ApJ*, 334, 422
- Szkody, P., et al. 2003, *AJ*, 126, 1499
- Szkody, P., et al. 2006, *AJ*, 131, 973
- Szkody, P., et al. 2004, *AJ*, 128, 1882
- Szkody, P., et al. 2007, *AJ*, 134, 185
- Tanabe, K., & Koizumi, M. 2007, in *ASP Conf. Ser.* 362, *The Seventh Pacific Rim Conference on Stellar Astrophysics*, ed. Y. W. Kang, H.-W. Lee, K.-C. Leung, & K.-S. Cheng (San Francisco: ASP), 207
- Targan, D. 1979, *IBVS*, 1539
- Templeton, M., et al. 2007, *CBET*, 1053
- Templeton, M. R., et al. 2006, *PASP*, 118, 236
- Thorstensen, J. R., & Fenton, W. H. 2003, *PASP*, 115, 37
- Thorstensen, J. R., Patterson, J. O., Kemp, J., & Vennes, S. 2002, *PASP*, 114, 1108
- Thorstensen, J. R., & Taylor, C. J. 1997, *PASP*, 109, 1359
- Tramposch, J., Homer, L., Szkody, P., Henden, A., Silvestri, N. M., Yirak, K., Fraser, O. J., & Brinkmann, J. 2005, *PASP*, 117, 262
- Udalski, A. 1990, *AJ*, 100, 226
- Udalski, A., & Pych, W. 1992, *Acta Astron.*, 42, 285
- Udalski, A., & Szymanski, M. 1988, *Acta Astron.*, 38, 215
- Uemura, M., et al. 2008a, *PASJ*, 60, 227
- Uemura, M., et al. 2009, *PASJ*, submitted
- Uemura, M., et al. 2008b, *IBVS*, 5815, 1
- Uemura, M., et al. 2004, *PASJ*, 56, S141
- Uemura, M., et al. 2002a, *PASJ*, 54, 599
- Uemura, M., et al. 2002b, *PASJ*, 54, L15
- Uemura, M., et al. 2002c, *PASJ*, 54, 285
- Uemura, M., et al. 2000, *PASJ*, 52, L9
- Uemura, M., Kato, T., Pavlenko, E., Baklanov, A., & Pietz, J. 2001, *PASJ*, 53, 539
- Uemura, M., Mennickent, R., & Stubbings, R. 2004, *IBVS*, 5569
- Uemura, M., et al. 2005, *A&A*, 432, 261
- van der Woerd, H., van der Klis, M., van Paradijs, J., Beuermann, K., & Motch, C. 1988, *ApJ*, 330, 911
- Vanmunster, T. 1997, *Odessa Astron. Publ.*, 10, 47
- Vanmunster, T. 2001, *IBVS*, 5031
- Vanmunster, T., et al. 2006, *Society for Astronom. Sciences Ann. Symp.*, 25, 77
- Vanmunster, T., & Sarneczky, K. 1997, *IAU Circ.*, 6740
- Vanmunster, T., Skillman, D. R., & Fried, R. 2000a, *IBVS*, 4940
- Vanmunster, T., Velthuis, F., & McCormick, J. 2000b, *IBVS*, 4955
- Vogt, N. 1974, *A&A*, 36, 369
- Vogt, N. 1980, *A&A*, 88, 66
- Vogt, N. 1983, *A&A*, 118, 95
- Vogt, N., & Semeniuk, I. 1980, *A&A*, 89, 223
- Waagen, E. O., Miles, R., Boyd, D., & Stanton, R. 2006, *CBET*, 701, 2
- Waagen, E. O., Schmeer, P., Stubbings, R., & Pearce, A. 2007, *IAU Circ.*, 8829
- Walker, A. D., & Olmsted, M. 1958, *PASP*, 70, 495
- Warner, B. 1983, *IBVS*, 2397
- Warner, B. 1985, in *Interacting Binaries*, ed. P. P. Eggleton, & J. E. Pringle (Dordrecht: D. Reidel Publishing Company), 367
- Warner, B., & O'Donoghue, D. 1988, *MNRAS*, 233, 705
- Warner, B., O'Donoghue, D., & Wargau, W. 1989, *MNRAS*, 238, 73
- Wei, J., Li, C., Xu, D., Hu, J., & Li, Q. 1997, *Acta Astrophys. Sinica*, 17, 107
- Wenzel, W. 1989, *IBVS*, 3405
- Wenzel, W. 1990, *IBVS*, 3440
- Wenzel, W. 1991, *IBVS*, 3626
- Wenzel, W. 1993, *IBVS*, 3829
- Whitehurst, R. 1988, *MNRAS*, 232, 35
- Wild, P. 1979, *IAU Circ.*, 3412
- Wolf, M., & Wolf, G. 1906, *Astron. Nachr.*, 170, 361
- Woudt, P. A., & Warner, B. 2001, *MNRAS*, 328, 159
- Woudt, P. A., Warner, B., & Pretorius, M. L. 2004, *MNRAS*, 351, 1015
- Wu, J.-H., Chen, Y., He, X.-T., Zhang, X.-Z., & Voges, W. 2001, *Chinese J. of Astron. and Astrophys.*, 1, 57
- Yamaoka, H., & Itagaki, K. 2009, *CBET*, 1644
- Yamaoka, H., Itagaki, K., Kaneda, H., Jacques, C., Pimentel, E., Maehara, H., & Bolt, G. 2008a, *CBET*, 1463
- Yamaoka, H., Itagaki, K., Korotkiy, S., & Samus, N. N. 2008b, *IAU Circ.*, 8971
- Yamaoka, H., Itagaki, K., Maehara, H., & Henden, A. 2008c, *CBET*, 1225
- Yamaoka, H., Itagaki, K., Maehara, H., & Nakano, S. 2008d, *CBET*, 1535
- Yamaoka, H., Itagaki, K., Miyashita, A., & Koff, R. A. 2008e, *CBET*, 1631
- Yamaoka, H., Itagaki, K., Naito, H., & Narusawa, S. 2008f, *CBET*, 1216
- Yamaoka, H., Itagaki, K., Schmeer, P., & Denisenko, D. 2008g, *CBET*, 1536
- Zhang, E.-H., Robinson, E. L., & Nather, R. E. 1986, *ApJ*, 305, 740
- Zharikov, S. V., et al. 2008, *A&A*, 486, 505

